Expanding the Scope of Nickel-Catalyzed C(sp^2)–N/O Cross-Coupling Reactions Using Tailored Ancillary Ligands

by

Joseph P. Tassone

Submitted in partial fulfilment of the requirements
for the degree of Doctor of Philosophy

at

Dalhousie University
Halifax, Nova Scotia
March 2020

"I loved the discovery chemistry offered. I loved the thrill of experiment, the challenge of trial and retrial. I loved the puzzle of it. I also will admit a somewhat foolish fondness toward the apparatus involved. The bottles and tubes. The acids and salts. The mercury and flame. There is something primal in chemistry, something that defies explication. Either you feel it or you don't."

- Patrick Rothfuss, The Wise Man's Fear

Table of Contents

List of Tables

List of Figures

List of Schemes

Abstract

The ubiquity of aryl C–N/O bonds in pharmaceuticals and natural products necessitates the development of robust and selective methodologies to construct such linkages efficiently. Palladium-catalyzed C(sp^2)–N/O cross-coupling has become a widely utilized method for the synthesis of aryl C–N/O bonds, however, the high cost and scarcity of palladium has spurred researchers to examine the use of inexpensive, Earth-abundant metals in these reactions. Though nickel has emerged as a suitable alternative to palladium in C(sp^2)–N cross-coupling, many nickel catalyst systems 'repurpose' ancillary ligands that demonstrated prior utility with palladium with limited success. Recently, the use of a tailored ancillary ligand, PAd-DalPhos, in nickel-catalyzed monoarylations of ammonia and primary alkylamines enabled an unprecedented scope of electrophiles to be cross-coupled at room temperature, demonstrating the power of applying tailored ancillary ligands in challenging nickel-catalyzed cross-coupling reactions.

Inspired by the success of the PAd-DalPhos ligand system, this thesis focused on the development of new nickel-catalyzed C(sp^2)–N/O cross-coupling reactions mediated by tailored ancillary ligands, with the goal of improving upon state-of-the-art metal-catalyzed procedures, or establishing reactivity with nickel that had not been observed previously. Chapter 2 details the nickel-catalyzed *N*-arylation of cyclopropylamine using **2-C3**, a pre-catalyst containing the tailored ancillary ligand CyPAd-DalPhos (**2-L3**). Using this pre-catalyst, the desired transformation was achieved for the first time, largely under mild conditions (3 mol % Ni, 25 °C), tolerating a variety of (hetero)aryl (pseudo)halide electrophiles. In Chapter 3, the first nickel-catalyzed C(sp^2)–O cross-coupling without recourse to photoredox catalysis is disclosed, where pre-catalysts **2-C3** and **2-C1**, containing **2-L3** and PAd-DalPhos (**2-L1**) respectively, facilitate the reaction of primary, secondary, and tertiary aliphatic alcohols with various (hetero)aryl electrophiles, including unprecedented reactivity with chlorides and pseudohalides. Finally, the nickel-catalyzed C(sp^2)–N cross-coupling of α,α,α-trisubstituted, primary alkylamines with (hetero)aryl halides using pre-catalyst **4-C1**, incorporating PhPAd-DalPhos (**4-L1**), is discussed in Chapter 4, expanding the scope of this transformation with nickel, and establishing room temperature reactivity for the first time with this class of nucleophile in metal-catalyzed cross-couplings.

List of Abbreviations and Symbols Used

OAc	acetate
Å	angstrom
bpy	2,2′-bipyridyl
dcype	1,2-bis(dicyclohexylphosphino)ethane
BINAP	2,2′-bis(diphenylphosphino)-1,1′-binaphthalene
XantPhos	4,5-bis(diphenylphosphino)-9,9-dimethylxanthene
DPEPhos	bis[(2-diphenylphosphino)phenyl] ether
dppf	1,1′-bis(diphenylphosphino)ferrocene
b.p.	boiling point
Anal. Calc'd.	combustion elemental analysis calculated
COSY	correlation spectroscopy
Cy	cyclohexyl
CPME	cyclopentyl methyl ether
cod	1,5-cyclooctadiene
DABCO	1,4-diazabicyclo[2.2.2]octane
dba	dibenzylideneacetone
DCM	dichloromethane
DFT	density functional theory
$OC(O)NEt_2$	diethylcarbamate
DMA	*N*,*N*-dimethylacetamide
DME	1,2-dimethoxyethane
Dipp	2,6-diisopropylphenyl
OSO_2NMe_2	dimethylsulfamate
DMSO	dimethylsulfoxide
dtbbpy	4,4′-di-*tert*-butyl-2,2′-bipyridine
equiv	equivalents
h	hour
HMRS-ESI	high-resolution mass spectrometry-electrospray ionization
HPLC-MS	high performance liquid chromatography-mass spectrometry
IR	infrared
LEDs	light-emitting diodes
OMs	mesylate
NMP	*N*-methyl-2-pyrrolidone
min	minute
NHC	*N*-heterocyclic carbene
NMR	nuclear magnetic resonance
o-tol/*o*-tolyl	*ortho*-tolyl
p-tolyl	*para*-tolyl
pin	pinacol

$^{13}C\{^{1}H\}$	proton-decoupled carbon
$^{19}F\{^{1}H\}$	proton-decoupled fluorine
$^{31}P\{^{1}H\}$	proton-decoupled phosphorus
PTFE	polytetrafluoroethylene
rac	racemic
RVC	reticulated vitreous carbon
temp./Temp.	temperature
Boc	*tert*-butyloxycarbonyl
t-Pent	*tert*-pentyl
THF	tetrahydrofuran
Ts	tosyl
OTs	tosylate
OTf	triflate

Acknowledgements

Pursuing a PhD is far from a solo undertaking, and there are many people I'd like to thank for their help over the course of my studies (in no particular order):

- My supervisor, Mark. I am very grateful for your unwavering guidance and support. You are an outstanding mentor; the things I've learned from you – about life and about chemistry – are too numerous to list, and I hope I can continue to seek out your advice long after the completion of my PhD. You have helped make these past four years among the most interesting, exciting, and memorable times of my life. Thank you for everything, Mark – keep rockin' on.
- Stradiotto group members, both past (Nick R.-L., Ryan S., Chris L., Preston, Jillian, Alex, Chris V., Carlos, Melody, Raymond, Sam, Julia, and Emma) and present (Kathleen, Connor, Nick B., Ryan M., and Casper). The support you've offered me over the past four years has been so greatly appreciated. Thank you for putting up with my quirks (my singing, and my talking to myself), and never making me feel bad about them. When we all get together, I know it's going to be a good time, and I won't soon forget some of the shenanigans we've been a part of. Thank you all so much.
- Members of the Dalhousie Department of Chemistry. I've been very fortunate to have worked with and gotten to know so many wonderful people during my PhD. I'm very thankful to have worked alongside Mark W. and Gianna in First Year Chemistry, but I am especially grateful to Jenn and Angela. You were both very supportive of my teaching aspirations, and working with you and learning from you has been so, so rewarding. To my fellow graduate students – you know who you are – I also say, "Thank you." Talking about our shared 'struggle' together has been a cathartic and enlightening experience. Getting to know all of you has been great, and I hope we can stay in touch. Take care.
- Greg. Finishing my PhD is bittersweet – I know you would be proud of my accomplishments, but I am so very sad that I'm unable to celebrate them with you. I can honestly say that I wouldn't be where I am today without you, and I will always be grateful for your guidance and friendship. Not a day goes by that I'm in the lab and I don't think about you. I miss you, Greg. Rest easy, my friend.
- My family and friends (back home). I appreciate your continued love and support. Every time I come home, it's like I never left (in the best possible way). I don't say it nearly enough, but I love you all, and I'm so very grateful for your presence in my life.
- Finally, most importantly, Mom, Papa, and Matthew. Being away from you has been tough – tougher than I ever thought it would be. I didn't quite appreciate that, when I was feeling down at home, there was always someone around to make me feel better. Or, if I was feeling good at home, that there was always someone around to share my happiness with. I know I generally present a calm, cool demeanour, regardless of how I'm actually feeling, so you'd never know how much I look forward to our weekly FaceTime calls, to seeing your faces, to hearing your voices. It's almost (not quite) like being back home – and it always makes me feel better. Your unconditional love and support are everything to me. I miss you and I love you, and I will always hold you in my heart, wherever my life takes me.

Chapter 1: Introduction

1.1 Ancillary Ligands in Homogeneous Transition Metal Catalysis

Catalysts play an important role in countless industrial processes.[1,2] While the synthesis of bulk chemicals, such as ammonia and polyethylene, are typically accomplished using heterogeneous catalysis,[1] fine chemicals, such as pharmaceuticals and agrochemicals, are largely prepared through homogeneous catalysis.[2] Among the classes of homogeneous catalysts that find application in industry, transition metal complexes are particularly prominent; the steric and electronic properties of these species can be modified by ancillary ligands, providing increased selectivity and reactivity compared to other homogeneous and heterogeneous catalysts. For example, changing the ligand from PPh_3 to $AsPh_3$ in the nickel-catalyzed polymerization of 1,3-butadiene dramatically alters the ratio of *cis*- and *trans*-1,4-polybutadiene produced (**Scheme 1.1**),[3] highlighting the profound effect ancillary ligands can have on the outcome of a metal-catalyzed reaction. Furthermore, the relative ease with which ancillary ligands can be introduced into the metal coordination sphere permits a versatile method for facilitating chemical transformations.

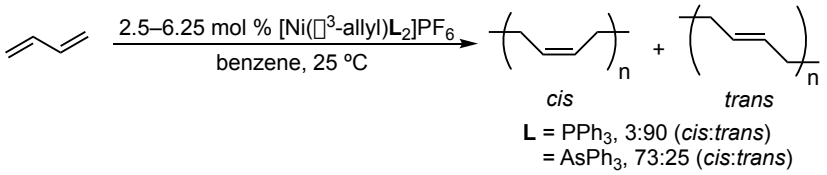

Scheme 1.1. The effect of altering the ligand on product distribution in the nickel-catalyzed polymerization of 1,3-butadiene.

The design of new ancillary ligands represents an important aspect of homogeneous transition metal catalysis.[4] Indeed, when poorly reactive substrates or substrates that exhibit unwanted reactivity patterns are employed in a catalytic reaction, or when a high degree of chemoselectivity, stereoselectivity, or enantioselectivity is important, the use of structurally simple ancillary ligands (e.g., PPh_3) is generally not sufficient to achieve desirable reaction outcomes.[5] For example, $RhCl(PPh_3)_3$ was among the first homogeneous pre-catalysts used in the hydrogenation of unsubstituted alkenes.[6] Despite its efficacy, the achiral nature of the pre-catalyst and its ancillary ligands precluded its application in the asymmetric hydrogenation of substituted olefins. To address this deficiency, Knowles and coworkers[7] developed the chiral monodentate phosphine CAMP, and a bidentate analogue

DiPAMP (**Figure 1.1**), to effect the rhodium-catalyzed asymmetric hydrogenation of α-acylaminocinnamic acids, such as the example shown in **Scheme 1.2**. The success of these systems prompted their use in the industrial synthesis of L-DOPA, a drug used in the treatment of Parkinson's disease,[6b] demonstrating the impact a thoughtfully designed ligand can have in directing the outcome of a challenging catalytic reaction.

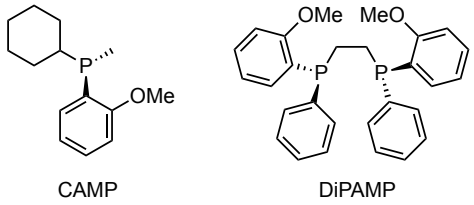

Figure 1.1. Structures of the CAMP and DiPAMP ligands.

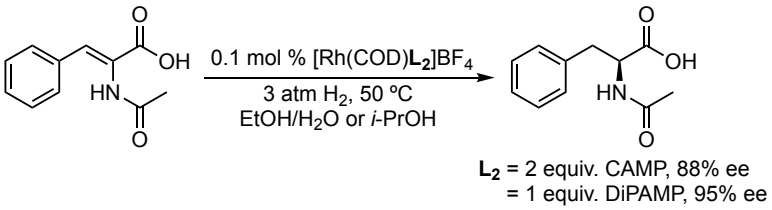

Scheme 1.2. Rhodium-catalyzed asymmetric hydrogenation using CAMP and DiPAMP ligands.

1.1.1 Phosphines as Ancillary Ligands in Homogeneous Transition Metal Catalysis

Phosphines ($:PR_3$) represent a ubiquitous class of ancillary ligands in homogeneous transition metal catalysis.[8] The attractiveness of phosphines stems from the variety of steric and electronic modifications that can be made to the basic ligand framework, providing a straightforward approach to tuning metal-centerd catalytic behaviour. Additionally, phosphines can be linked to other phosphorus or heteroatom donor groups to create ancillary ligands with varied denticities, permitting further opportunities for control over a chemical reaction. Since phosphorus-31 is NMR-active, phosphine-containing catalyst systems can be monitored spectroscopically, allowing real-time mechanistic studies of catalytic reactions.

The electronic properties of (monodentate) phosphines are typically evaluated by measuring the CO stretch(es) (ν_{CO}) of a metal complex containing the ligand of interest (e.g., $Ni(CO)_3L$ or *trans*-$RhCl(CO)L_2$) using IR spectroscopy.[2] The smaller the ν_{CO} value, the greater the electron-donating ability of the phosphine ligand.[2] Alternatively, the

phosphorus-selenium coupling constant ($^1J_{PSe}$), determined via $^{31}P\{^1H\}$ NMR spectroscopy, can be used as an indicator of phosphine donating-ability, with a smaller $^1J_{PSe}$ value corresponding to a more electron-releasing phosphine.[9]

Cone angle is commonly used to gauge the steric properties of phosphines.[10] This value is the measured angle of the imagined cone created by the outer edge of the substituents on a phosphorus atom when it is positioned 2.28 Å from a metal centre. Bidentate phosphines can be further compared using bite angle.[2] While the measured P–M–P angle of a ligand coordinated to a metal centre can be obtained from the solid-state structure of the complex, steric and/or electronic perturbations caused by the presence of other ligands may influence this value, precluding meaningful comparisons among different phosphines. Alternatively, finding ligand conformations in which the lone pairs on the phosphorus atoms of a bidentate phosphine are oriented toward a dummy metal atom, then fixing the dummy-P bond length for all ligands, allows the *natural* bite angle of a ligand to be calculated as a function of its non-bonded through-space P–P distance. The effect of ligand bite angle on catalytic performance is often quite pronounced; for example, Hayashi and coworkers[11] investigated two palladium pre-catalysts, containing either 1,1-bis(diphenylphosphino)ferrocene (dppf) or 1,3-bis(diphenylphosphino)propane (dppp), in the cross-coupling of bromobenzene and *sec*-butylmagnesium chloride (**Scheme 1.3**). It was found that the pre-catalyst incorporating dppf afforded a high yield of the coupled product, while the pre-catalyst incorporating dppp produced a mixture of the desired product and that arising from unwanted, β-hydrogen elimination. The reactivity differences were rationalized based on the larger bite angle of dppf versus dppp, which promotes faster reductive elimination to the desired product.

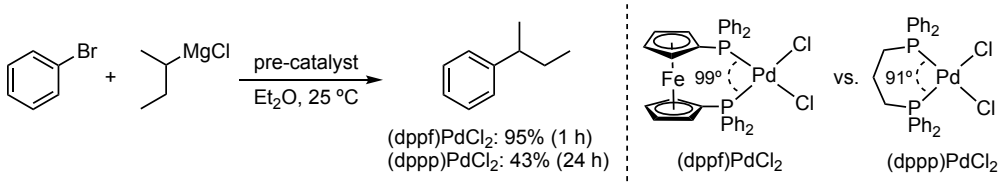

Scheme 1.3. The effect of ligand bite angle on pre-catalyst performance in the cross-coupling of bromobenzene and *sec*-butylmagnesium chloride.

1.2 Palladium-Catalyzed C(sp^2)–N Cross-Coupling: The Buchwald-Hartwig Amination Reaction

Palladium-catalyzed C(sp^2)–N (herein C–N) cross-coupling, also known as Buchwald-Hartwig amination (BHA), has become an established synthetic protocol for the preparation of *N*-arylamines in academia and industry, particularly in the synthesis of fine chemicals (e.g., pharmaceuticals or agrochemicals) and conjugated materials.[12] In BHA, a ligated palladium species mediates the cross-coupling of a (hetero)aryl (pseudo)halide with a nitrogen nucleophile to form a new aryl C–N bond (**Scheme 1.4**). The scope with respect to the aryl electrophile encompasses primarily aryl halides (chlorides, bromides, and iodides), as well as select phenol-derived electrophiles (tosylates, triflates, and mesylates).[10,13] Furthermore, a variety of nitrogen nucleophiles have been successfully employed in this reaction, including primary and secondary amines, ammonia, azoles, and amides.[10] The use of ammonia and amides as coupling partners is not trivial; ammonia can form catalytically inactive palladium dimers, and the generated products (i.e., anilines) can undergo further *N*-arylation,[14] while amides are only weakly nucleophilic and can circumvent desired reactivity by forming a κ^2-*N*,*O* palladium chelate.[15] Altogether, BHA serves as a practical alternative to conventional methods for the preparation of anilines, namely nucleophilic aromatic substitution, which typically requires harsh reaction conditions and highly activated substrates, and elimination-addition, which exhibits poor regioselectivity due to the intermediacy of aryne species.[16]

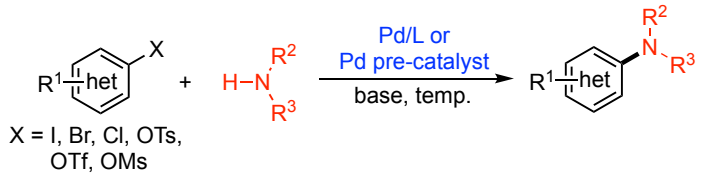

Scheme 1.4. The Buchwald-Hartwig amination reaction.

The general mechanism of BHA is similar to that of other palladium-catalyzed cross-coupling reactions, and is presented in **Figure 1.2**.[10] The active catalytic species is generally thought to be a mono- or bis-ligated Pd(0) complex, depending on the ancillary ligand employed. Firstly, the aryl electrophile undergoes oxidative addition to generate a Pd(II) aryl species (**I**). Next, the amine coordinates to palladium and is subsequently deprotonated, generating a Pd(II) amido complex (**II**). Alternatively, **I** may undergo

halogen exchange when alkoxide base is used, with protonation of the resulting Pd(II) alkoxide complex by the amine yielding **II**. Finally, reductive elimination furnishes the desired *N*-arylamine.

The steric and electronic properties of the ancillary ligand can have a significant impact on certain elementary steps of the catalytic cycle.[10] Strongly electron-donating ligands promote oxidative addition due to the increased electron density at the metal centre, enabling the use of more challenging electrophiles,[17] such as aryl chlorides or pseudohalides. Bulky ligands also enhance the rate of oxidative addition by favouring the formation of catalytically active, coordinatively unsaturated Pd(0) species.[10] The crowding of the metal centre through the use of sterically encumbered ligands additionally promotes reductive elimination, which is driven by the ensuing relief in steric congestion.

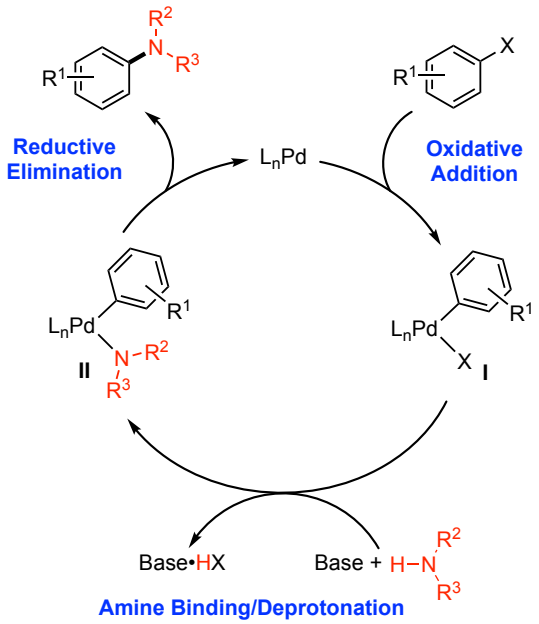

Figure 1.2. General mechanism of the Buchwald-Hartwig amination reaction.

1.2.1 Ancillary Ligands in the Buchwald-Hartwig Amination Reaction

Several classes of bulky, electron-rich ancillary ligands have found application in BHA. Catalyst systems incorporating biarylmonophosphine ligands developed by Buchwald and co-workers[18] (**Figure 1.3**) have effected C–N cross-couplings using a variety of (hetero)aryl electrophiles and nitrogen nucleophiles. The utility of this class of ancillary ligands stems from the highly modular design, which allows precise control over the steric and electronic environment of the metal centre through rational ligand

modification. For example, a pre-catalyst containing BrettPhos (see **Figure 1.3**) has demonstrated excellent activity in the coupling of (hetero)aryl chlorides, bromides, iodides with primary alkylamines, as well as substituted (heterocyclic) anilines, with the majority of reactions occurring with low catalyst loadings (0.05–2 mol % Pd) at elevated temperatures (85–110 °C).[19] Both coupling partners also featured a range of electron-donating and electron-withdrawing substituents, including alcohol, amide, ester, and nitrile functionalities. A related pre-catalyst system incorporating RuPhos (**Figure 1.3**) displayed comparably broad scope and reactivity in the coupling of secondary amines with (hetero)aryl chlorides. Other biarylmonophosphine ligands have been prepared for the cross-coupling of challenging nitrogen nucleophiles, including ammonia,[20] primary amides (*t*-BuBrettPhos, see **Figure 1.3**),[13b, 21] and secondary amides.[22]

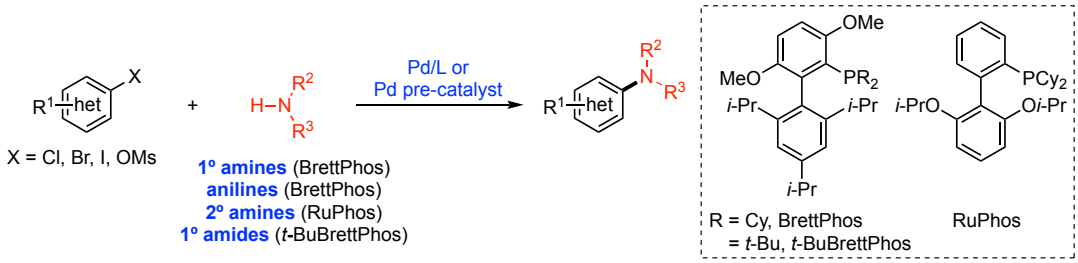

Figure 1.3. The utility of select biarylmonophosphine ligands used in BHA.

Bisphosphines have also been successfully applied as ancillary ligands in BHA. The advantage of bidentate ligands over monodentate ligands in this reaction arises from the lack of ligand dissociation enforced by chelation, which slows undesirable β-hydrogen elimination and promotes both oxidative addition and reductive elimination through increased steric crowding at the metal centre.[10] Notably, Hartwig and co-workers found that a catalyst system combining $Pd(OAc)_2$ and the bulky, electron-rich, bisphosphine JosiPhos ligand CyPF-*t*-Bu (**Figure 1.4**), from a family of ligands originally developed for use in asymmetric catalysis,[23] displayed excellent activity for BHA.[24] In particular, this catalyst system coupled a variety of substituted (hetero)aryl chlorides, bromides, and iodides with primary and secondary alkylamines using exceedingly low catalyst loadings (0.001–2 mol % Pd) at moderate to high temperatures (65–110 °C).[25] Furthermore, a $Pd[P(o\text{-tol})_3]_2$/CyPF-*t*-Bu catalyst system was among the first to effect the monoarylation of ammonia using (hetero)aryl (pseudo)halides (chlorides, bromides, iodides, and

tosylates).[26] These reactions were conducted at low catalyst loadings (0.1–2 mol % Pd) and displayed excellent functional group tolerance, with electrophiles bearing ester, trifluoromethyl, ketone, thiol, and nitrile moieties proceeding efficiently. Additionally, gaseous ammonia could be employed without noticeable loss of yield or selectivity.

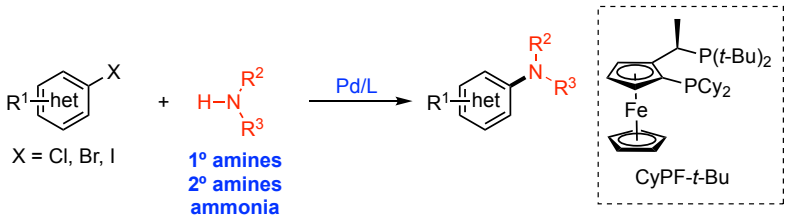

Figure 1.4. The utility of the CyPF-*t*-Bu ligand in BHA.

Whereas bidentate bisphosphines participate in effective chelation to a metal centre, the bonding of bidentate, hybrid phosphines, specifically those bearing P,N or P,O donor sets, is comparably weaker due to the repulsive interactions between the metal *d*-electrons and the lone pairs on the 'hard' heteroatom.[27] This type of bonding facilitates hemilability, the reversible coordination of a donor atom to a metal centre through various binding modes.[28] Such hemilabile ligands are well-suited to meet the dynamic electronic needs of the metal throughout the catalytic cycle by stabilizing low-coordinate intermediates, or by facilitating substrate coordination and/or product elimination, encouraging more efficient catalysis.[28]

The Me-DalPhos and Mor-DalPhos ligands (**Figure 1.5**) developed by Stradiotto and co-workers[29] are notable examples of P,N-hybrid ligands used in BHA. Catalyst mixtures of $[Pd(\eta^3\text{-allyl})Cl]_2$ or $[Pd(\eta^3\text{-cinnamyl})Cl]_2$ and Me-DalPhos demonstrated broad scope in the coupling of substituted (hetero)aryl chlorides with a range of nitrogen nucleophiles (ammonia, primary and secondary amines, and anilines), employing 0.5–2 mol % catalyst loadings at elevated temperatures (~110 °C).[30] Similarly, a catalyst system incorporating Mor-DalPhos effected the monoarylation of ammonia with deactivated (hetero)aryl chlorides and tosylates, exhibiting excellent chemoselectivity in the presence of other primary and secondary amines.[31] Furthermore, a (κ^2-*P*,*N*-Mor-DalPhos)Pd(Ph)Cl pre-catalyst facilitated the first examples of ammonia monoarylation using (hetero)aryl (pseudo)halides at room temperature.[31,32] The use of a $[Pd(cinnamyl)Cl]_2$/Mor-DalPhos catalyst system also enabled the coupling of (hetero)aryl chlorides and tosylates with hydrazine hydrate for the first time.[33] This transformation is particularly impressive

considering the potential drawbacks of using hydrazine as a coupling partner, namely metal-mediated N–N bond cleavage and the presence of multiple reactive N–H bonds.

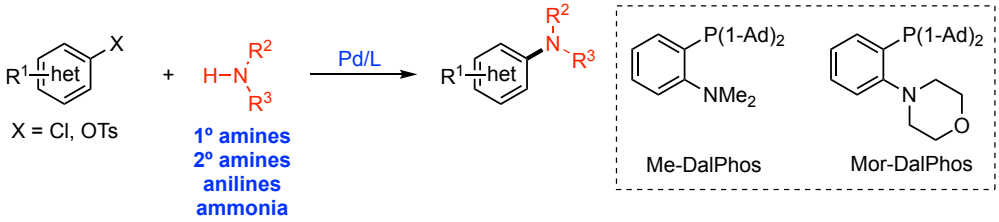

Figure 1.5. The utility of the Me-DalPhos and Mor-DalPhos ligands in BHA.

The use of NHCs as ancillary ligands for BHA has also been explored.[34] Like phosphines, the steric and electronic properties of NHCs can be tailored easily by altering the nitrogen and/or backbone substituents or the backbone saturation.[35] Indeed, palladium pre-catalysts developed by Nolan[34a, b] and Organ[34c, d] incorporating NHCs (**Figure 1.6**) have found particular success in BHA. For example, Nolan and co-workers[36] utilized the (SIPr)Pd(η^3-cinnamyl)Cl pre-catalyst to effect the coupling of sterically hindered aryl chlorides with primary and secondary amines at room temperature, whereas Organ and co-workers[37] employed the Pd-PEPPSI-IPr pre-catalyst (i.e., (IPr)$PdCl_2$(3-Cl-pyridine)) for the *N*-arylation of secondary dialkylamines and anilines using (hetero)aryl chlorides and bromides at moderate temperatures (25–80 °C). More recently, Organ and co-workers[38] have used the Pd-PEPPSI-IPent^{Cl} pre-catalyst (i.e., (IPent^{Cl})$PdCl_2$(3-Cl-pyridine)) to effect the monoarylation of primary amines with (hetero)aryl chlorides, including those bearing base-sensitive substituents, at moderate temperatures (60 °C).

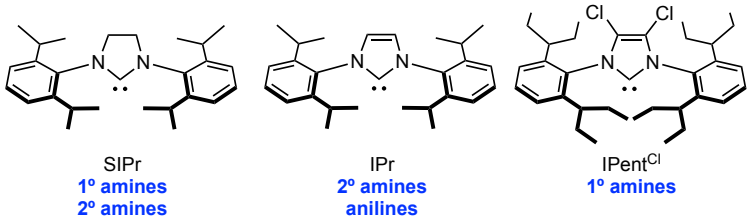

Figure 1.6. Structure and utility of select NHCs used by Nolan and Organ in BHA.

1.3 Nickel-Catalyzed C(sp^2)–N Cross-Coupling

Despite the efficacy of palladium-based catalyst systems for C–N cross-coupling, the high cost and low abundance of palladium has spurred researchers to examine the use of comparatively inexpensive and Earth-abundant metals in its place.[39] Whereas the copper-mediated Ullmann and Chan-Lam reactions represent alternatives to BHA for aryl amination,[40] harsh reaction conditions, high (10–50 mol %) or stoichiometric catalyst

loadings, and/or poor reactivity with aryl chlorides and pseudohalides, limit the general applicability of these methodologies for more challenging or selective transformations. Accordingly, nickel has recently emerged as a suitable alternative for palladium in C–N cross-coupling, providing similar or superior reactivity and versatility.[41]

1.3.1 Photoredox-/Electrochemically Mediated Nickel-Catalyzed C(sp^2)–N Cross-Coupling

Two divergent yet complementary strategies are typically employed to effect nickel-catalyzed C–N cross-coupling. The first approach involves the application of a photocatalyst in conjunction with a Ni(II) salt to mediate the desired transformation.[42] Many of these dual nickel/photoredox catalyst systems make use of 'hard', nitrogen-based ancillary ligands in order to stabilize Ni(I)/Ni(III) species thought to be present in the catalytic cycle; it has been proposed that the photocatalyst facilitates the oxidation of lower valent nickel intermediates formed during catalysis (e.g., Ni(II) to Ni(III)), enabling certain elementary steps (e.g., reductive elimination).[43] Alternatively, recent mechanistic studies suggest that the photocatalyst facilitates energy transfer to Ni(II)-amine intermediates, generating excited state Ni(II) species that enable C–N cross-coupling.[44]

MacMillan, Buchwald, and co-workers[43] reported the first examples of C–N cross-coupling using dual nickel/photoredox catalysis, with a catalyst system comprised of NiX_2(DME) (X = Br or Cl) and an iridium photocatalyst (**Ir-1**) allowing the cross-coupling of (hetero)aryl bromides with primary and secondary amines under blue light irradiation (**Scheme 1.5A**). Shortly thereafter, Oderinde, Johannnes, and co-workers[45] utilized a related system ($NiCl_2$(dtbbpy) and **Ir-1**) for the *N*-arylation of anilines using (hetero)aryl iodides (**Scheme 1.5B**). The synthesis of diarylanilines from (hetero)aryl iodides and anilines was similarly accomplished using a terpyridine-ligated, nickel pre-catalyst and a ruthenium photocatalyst.[46] Sulfonamides,[47] sulfamate esters,[48] and *NH*-sulfoximines[49] have also been employed as nucleophiles in dual nickel/photoredox-catalyzed C–N cross-coupling processes. In addition to precious metal photocatalysts, organic photocatalysts have demonstrated efficacy in facilitating this reaction.[50] Interestingly, Miyake and co-workers[51] recently reported a dual nickel/photoredox catalyst system for the C–N cross-

coupling of (hetero)aryl bromides with primary and secondary amines that proceeds without exogenous photocatalyst.

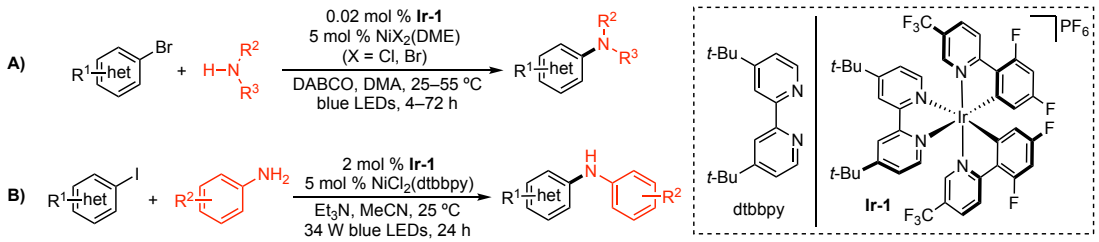

Scheme 1.5. Dual nickel/photoredox-catalyzed C–N cross-coupling developed by A) MacMillan and Buchwald, and B) Oderinde and Johannes.

Using a related approach to dual nickel/photoredox catalysis, Baran and co-workers[52] have disclosed protocols for electrochemically driven, nickel-catalyzed C–N cross-coupling (**Scheme 1.6**). Mechanistic studies indicate that a Ni(I)/N(III) catalytic cycle is enforced using electrochemical methods, with putative high spin nickel intermediates supported by 'hard' nitrogen-based ancillary ligands, as was seen in analogous light-driven, nickel-catalyzed C–N cross-coupling processes. The electrophile scope of this reaction largely encompasses (hetero)aryl bromides, with primary and secondary amines proving to be effective nucleophiles in this transformation.

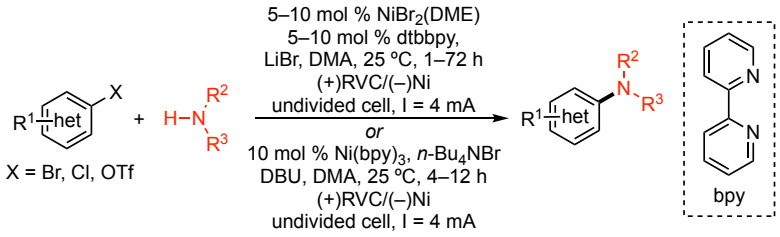

Scheme 1.6. Electrochemically driven, nickel-catalyzed C–N cross-coupling developed by Baran and co-workers.

1.3.2 Ancillary Ligand-Mediated Nickel-Catalyzed C(sp^2)–N Cross-Coupling

The second strategy used to facilitate nickel-catalyzed C–N cross-coupling involves the application of 'soft' ancillary ligands (i.e., phosphines and NHCs). Such ligands are thought to encourage nickel to traverse a catalytic cycle similar to that of BHA (see **Figure 1.2**), a view that is supported by the utility of Ni(0) and Ni(II) pre-catalysts in these reactions. However, as nickel can readily engage in single-electron chemistry,[39] discrepancies have arisen regarding the extent to which Ni(I) and Ni(III) species play a role in this transformation using 'soft' ancillary ligands.[53] For example, Hartwig and co-workers[54] discounted the presence of Ni(I)/Ni(III) species through radical trapping

experiments in a report detailing the nickel-catalyzed cross-coupling of ammonia and ammonium salts with (hetero)aryl chlorides and bromides using a pre-catalyst incorporating JosiPhos PhPF-*t*-Bu (*vide infra*). Furthermore, in their report on the nickel-catalyzed coupling of (hetero)aryl chlorides with primary alkylamines, Hartwig and co-workers[55] showed [(BINAP)Ni(μ-Cl)]$_2$ did not facilitate the desired transformation. Nevertheless, the catalytic competency of (L)NiCl species containing the bisphosphines PAd-DalPhos (*vide infra*) or dppf in the C–N cross-coupling of aryl chlorides with furfurylamine, ammonia, and morpholine has recently been demonstrated by Stradiotto and co-workers.[56] Thus, the formation and/or catalytic activity of Ni(I)/Ni(III) species in nickel-catalyzed C–N bond formation mediated by 'soft' ancillary ligands may be dependent upon a complex interplay of factors, including ancillary ligand and substrate employed, thereby complicating efforts to analyze the mechanism of this reaction.

Nickel-based catalyst systems incorporating 'soft' ancillary ligands, like analogous palladium-based systems used in BHA, are capable of effecting the cross-coupling of (hetero)aryl (pseudo)halides with primary amines, secondary amines, azoles, primary amides, and ammonia.[41, 57] The successful application of nickel in this reaction can be attributed, at least in part, to the more electropositive nature of the metal centre versus palladium, allowing comparably facile oxidative addition of challenging C(sp^2)–X bonds (X = Cl, OR).[39] Bidentate phosphines comprise a major class of ancillary ligands that have been employed in this transformation (**Figure 1.7**).[58] Hartwig and co-workers[55] established the utility of a nickel pre-catalyst incorporating *rac*-BINAP in the cross-coupling of (hetero)aryl chlorides with primary alkylamines at low catalyst loadings (1–4 mol %) and mild temperatures (50 °C). Similarly, Buchwald and co-workers[59] utilized a (dppf)Ni(*o*-tolyl)Cl pre-catalyst to effect the cross-coupling of (hetero)aryl chlorides, sulfamates, mesylates, and triflates with primary and secondary amines at 100–110 °C (5 mol % pre-catalyst loading). Notably, Stradiotto and Hartwig independently reported on the nickel-catalyzed monoarylation of ammonia using JosiPhos ligands; Stradiotto and co-workers[60] used a Ni(cod)$_2$/CyPF-Cy catalyst system to cross-couple ammonia with (hetero)aryl chlorides, bromides, and tosylates, additionally demonstrating the applicability of gaseous ammonia in this transformation, while Hartwig and co-workers[54] employed a nickel pre-catalyst containing PhPF-*t*-Bu to facilitate the monoarylation of ammonia and ammonium

salts using (hetero)aryl chlorides and bromides. Nickel pre-catalysts incorporating CyPF-Cy have also recently been shown to facilitate the monoarylation of ammonia and primary alkylamines with (hetero)aryl carbamates, sulfamates, and pivalates.[61]

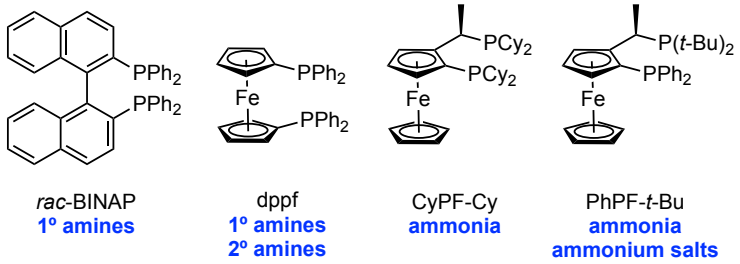

Figure 1.7. Select bidentate phosphines used in nickel-catalyzed C–N cross-coupling.

NHCs encompass another major class of ancillary ligands used in nickel-catalyzed C–N bond formation.[41b] Notably, Garg and co-workers[62] have employed $Ni(cod)_2$ or $NiCl_2(DME)$, in conjunction with SIPr•HCl (see **Figure 1.6**), to effect the cross-coupling of a variety of (hetero)aryl chlorides, carbamates, and sulfamates with anilines and secondary amines. Similarly, Nicasio and co-workers have used nickel pre-catalysts incorporating IPr (see **Figure 1.6**) to couple (hetero)aryl chlorides[63] and tosylates[64] with anilines and secondary amines. Furthermore, the nickel-catalyzed *N*-arylation of indoles and carbazoles with (hetero)aryl chlorides at 110 °C was accomplished by Nicasio and coworkers[65] using 5 mol % $(IPr)Ni(styrene)_2$.

Notwithstanding the success of the aforementioned nickel catalyst systems for C–N cross-coupling, the majority of ancillary ligands employed in such applications had previously demonstrated activity in facilitating BHA. While effective, this 'repurposing' of ligands does not account for the subtle, yet distinct, characteristics of nickel versus palladium.[39] Accordingly, there exist very few examples of ancillary ligands designed *specifically* for mediating nickel-catalyzed C–N bond formation.[66,67] This is in direct contrast to BHA, where ligand design enabled the development of highly active catalyst systems capable of tackling challenging coupling partners (e.g., (hetero)aryl pseudohalides, ammonia, amides, etc.), typically under mild conditions.[4-5] One notable example of a tailored ancillary ligand developed for nickel-catalyzed C–N cross-coupling is PAd-DalPhos (**Scheme 1.7**), prepared by Stradiotto and co-workers.[66] Since nickel can readily engage in oxidative addition chemistry, this ligand features phosphorus donor groups that possess relatively mild electron-donating capabilities (compared to the strongly

electron-releasing ligands employed in BHA), while maintaining steric bulk, with the aim of promoting reductive elimination (presumed to be more challenging for nickel versus palladium).[39] A nickel pre-catalyst incorporating PAd-DalPhos was thus able to effect the monoarylation of ammonia and primary alkylamines with an unprecedented scope of (hetero)aryl (pseudo)halides (chlorides, bromides, iodides, tosylates, and mesylates), largely under mild conditions (**Scheme 1.7**).[66, 68] Additionally, this pre-catalyst system facilitated the first examples of the nickel-catalyzed *N*-arylation of primary amides and lactams with (hetero)aryl (pseudo)halides.[57]

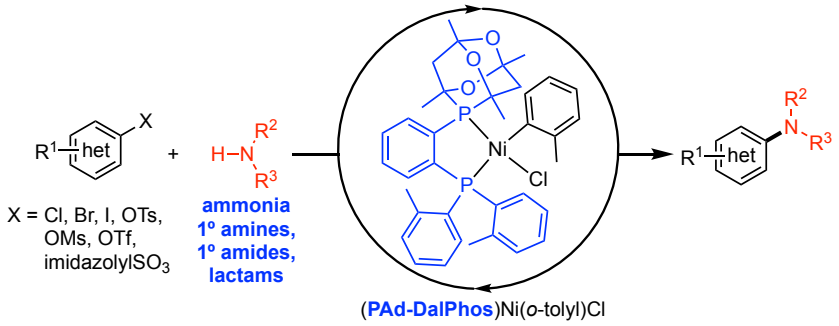

Scheme 1.7. The utility of a pre-catalyst containing the PAd-DalPhos ligand in nickel-catalyzed C–N cross-coupling reactions.

1.4 Thesis Research Focus

The development of more efficient catalytic methodologies, incorporating challenging substrates or employing milder reaction conditions, necessitates the use of more complex and/or thoughtfully designed ancillary ligands, as seen in the successful application of such ligands in BHA. However, despite the reactivity and economic benefits associated with the replacement of palladium with nickel in C–N cross-coupling reactions, there exists a stunning lack of new tailored ancillary ligands for such nickel-catalyzed processes. Indeed, the success of the PAd-DalPhos catalyst system in mediating nickel-catalyzed C–N bond formation with a broad range of (hetero)aryl electrophiles (chlorides, bromides, iodides, tosylates, and mesylates) and nitrogen nucleophiles (primary alkylamines, ammonia, primary amides, and lactams) highlights the advantages of using tailored ancillary ligands in this transformation. This further suggests that applying tailored ancillary ligands to other challenging nickel-catalyzed amination reactions, or those employing other heteroatom nucleophiles, would confer analogous reactivity benefits. Thus, the focus of this thesis will be to expand the scope of nickel-catalyzed C(sp^2)–N/O cross-coupling reactions through the use of tailored ancillary ligands. Such ligands will

likely feature a bidentate phosphine framework, given the established nature of this ligand scaffold in mediating nickel-catalyzed C–N bond formation (*vide supra*).[58] The exact nature of the phosphine substituents will be dictated by the reaction of interest. In addition to developing new and synthetically useful cross-coupling chemistry, the proposed studies will further advance the collective understanding of ancillary ligand effects on nickel catalysis.

Chapter 2 details the development of the nickel-catalyzed *N*-arylation of cyclopropylamine using a pre-catalyst incorporating CyPAd-DalPhos, a PAd-DalPhos variant. This pre-catalyst promotes the synthesis of *N*-arylcyclopropylamines using a broad scope of (hetero)aryl (pseudo)halide electrophiles, with the majority of reactions occurring at ambient temperatures. The nickel-catalyzed *N*-arylation of cyclopropanemethylamine hydrochloride and cyclobutylamine hydrochloride were also accomplished using this pre-catalyst system. Reaction monitoring and (pseudo)halide competition experiments revealed a pre-catalyst intolerance for deactivated electrophiles and a Cl > Br, OTs reactivity preference respectively.

Chapter 3 focuses on the development of a pre-catalyst system for nickel-catalyzed C(sp^2)–O cross-coupling without recourse to photoredox catalysis. Pre-catalysts containing CyPAd-DalPhos and PAd-DalPhos effect the cross-coupling of a wide range of (hetero)aryl (pseudohalides) with primary, secondary, and tertiary aliphatic alcohols. Notably, (hetero)aryl chloride and phenol-derived electrophiles are accommodated for the first time in this transformation with nickel. Competition experiments indicated a distinct preference for C–N vs. C–O cross-coupling using either pre-catalyst when equivalent amounts of amine and alcohol nucleophile are employed under optimized reaction conditions.

Finally, the development of a pre-catalyst system for the nickel-catalyzed C–N cross-coupling of α,α,α-trisubstituted, primary alkylamines is discussed in Chapter 4. This reaction is enabled by a pre-catalyst incorporating the tailored ancillary ligand PhPAd-DalPhos, enabling a broad scope of (hetero)aryl halide electrophiles to be accommodated for the first time with nickel. Furthermore, unprecedented room temperature reactivity with this class of nucleophile using any metal catalyst (palladium, nickel, or other) is accomplished with this pre-catalyst system. The PhPAd-DalPhos pre-catalyst did not

interact appreciably with carbamate electrophiles; this reactivity could be exploited in chemoselective transformations with electrophiles containing both chloride and carbamate moieties. Additionally, other hindered nucleophiles, including 2,6-disubstituted anilines and bulky alcohols, were successfully cross-coupled under optimized conditions.

Chapter 2: Nickel-Catalyzed *N*-Arylation of Cyclopropylamine and Related Ammonium Salts with (Hetero)aryl (Pseudo)halides at Room Temperature

2.1 Contributions

In this chapter, the nickel-catalyzed *N*-arylation of cyclopropylamine and related ammonium salts with (hetero)aryl (pseudo)halides under mild conditions is described. Preston M. MacQueen, a fellow PhD student, acted as a mentor to the author throughout the course of this project and provided some pseudohalide electrophiles for initial screening. Christopher M. Lavoie, another fellow PhD student, first synthesized **2-C4** and grew crystals of **2-C4** for X-ray crystallographic analysis. Dr. Robert McDonald and Dr. Michael J. Ferguson (University of Alberta) solved the solid-state structures for pre-catalysts **2-C3** to **2-C5**. The author was responsible for synthesizing and characterizing the new ligand and pre-catalysts, screening pre-catalysts for activity in the desired transformation, developing the scope of the reaction (including synthesizing pseudohalide coupling partners), and conducting supplementary experiments to explain trends in reactivity for this pre-catalyst system. The contributions of each author are noted throughout the text and are labelled as such throughout the chapter. This work has been published: ACS Catalysis, 2017, 7, 6048–6059.

2.2 Introduction

2.2.1 Synthesis of *N*-Arylcyclopropylamines

N-Arylcyclopropylamines[69] are an important core structure in several commercially available pharmaceuticals (**Figure 2.1**), including fluoroquinone antibiotics[70] (e.g., ciprofloxacin) and reverse transcriptase inhibitors[71] (e.g., abacavir and nevirapine), and have been used as mechanistic probes for biological processes (e.g., oxidation of amines by monoamine oxidase;[72] *N*-dealkylation of amines by cytochrome P450[73]) and organic reactions (e.g., the nitrosation of aromatic amines[74]). Because cyclopropyl halides are poorly reactive toward nucleophilic substitution by aromatic amines due to I-strain,[75] the development of alternative methods for preparing *N*-arylcyclopropylamines under mild conditions represents an important challenge. Conventional methods for the synthesis of *N*-arylcyclopropylamines include the reaction of 1-bromo-1-ethoxycyclopropane or (1-ethoxycyclopropoxy)trimethylsilane with anilines, followed by the reduction of the corresponding hemiaminals (**Scheme 2.1**),[76] as well as the base-mediated, Smiles

rearrangement of 2-aryloxy-*N*-cyclopropylacetamides (**Scheme 2.2**).[77] However, these approaches employ harsh conditions in two-step procedures and are generally unsuitable for heterocyclic substrates.

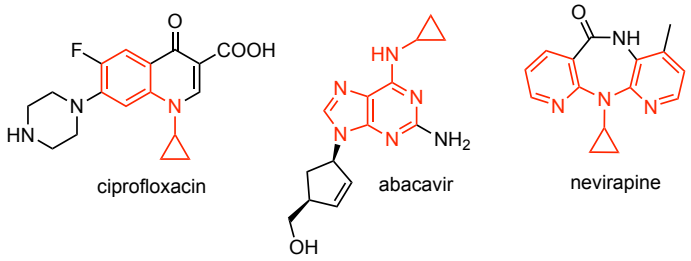

Figure 2.1. Structures of select pharmaceuticals containing an *N*-arylcyclopropylamine core.

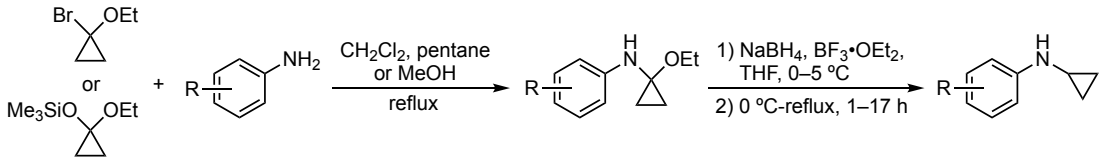

Scheme 2.1. Two-step synthesis of *N*-arylcyclopropylamines from 1-bromo-1-ethoxycyclopropane or (1-ethoxycyclopropoxy)trimethylsilane and anilines.

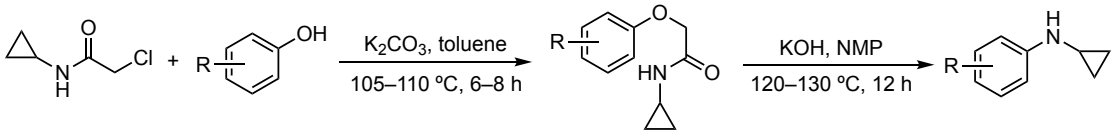

Scheme 2.2. Synthesis of *N*-arylcyclopropylamines using the Smiles rearrangement.

Whereas the application of ubiquitous copper[40c] or palladium[12b] catalyzed C–N cross-coupling methods employing cyclopropylamine and (hetero)aryl (pseudo)halides as substrates would appear to be well-suited to the assembly of *N*-arylcyclopropylamines, successful examples of such transformations are quite rare. Indeed, only a single entry in each of four isolated publications[78] employing copper catalysis with (hetero)aryl bromides and iodides have been disclosed.[79] Prior to 2016, the scope of such transformations achieved by use of palladium catalysis was also rather limited. Loeppky and co-workers[80] reported the first examples of the palladium-catalyzed *N*-arylation of cyclopropylamines with (hetero)aryl bromides using a $Pd_2(dba)_3$/BINAP catalyst system (**Scheme 2.3A**). Additionally, a related catalyst system incorporating (*R*)-Tol-BINAP or BrettPhos (see **Figure 1.3**) was developed by Zheng and co-workers[81] (**Scheme 2.3B**) to facilitate this transformation. However, both methodologies demonstrated only a narrow substrate scope.

Recently, the first broadly useful palladium-catalyzed *N*-arylation of cyclopropylamine was documented by Colacot and co-workers (**Scheme 2.3C**).[82] Pre-catalysts containing *t*-BuBrettPhos or BrettPhos effected the desired transformation at room temperature using (hetero)aryl bromides, and allowed the use of (hetero)aryl chlorides for the first time at elevated temperatures.

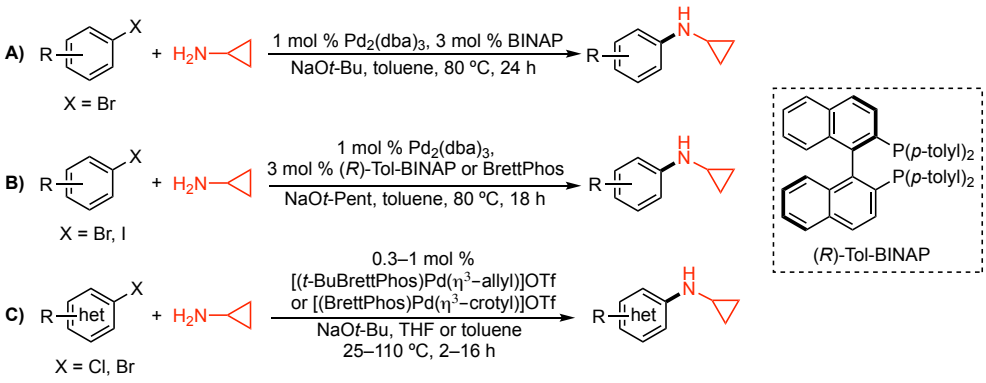

Scheme 2.3. Palladium-catalyzed *N*-arylation of cyclopropylamine reported by A) Loeppky, B) Zheng, and C) Colacot.

Given the lack of effective base metal-catalyzed procedures for the synthesis of *N*-arylcyclopropylamines, as well as the success of PAd-DalPhos (**2-L1**, **Figure 2.2**) in nickel-catalyzed C–N cross-coupling (*vide supra*), the question of whether this or related ancillary ligands might facilitate the nickel-catalyzed *N*-arylation of cyclopropylamine was posed. In particular, establishing broadly useful transformations that proceed at room temperature, in light of the low boiling point of cyclopropylamine (49–50 °C), was of interest. Furthermore, such an investigation could provide an opportunity to understand the ancillary ligand designs[4] that give rise to superior catalytic performance, particularly for challenging amine nucleophiles.

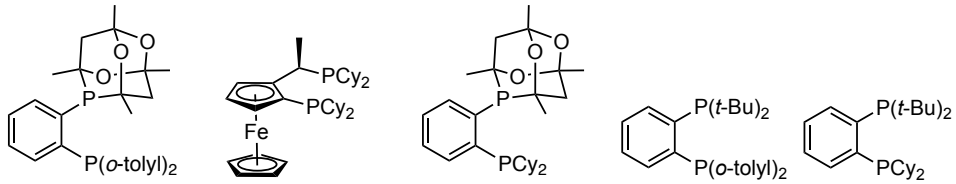

2-L1 (PAd-DalPhos) **2-L2** (CyPF-Cy) **2-L3** (CyPAd-DalPhos) **2-L4** **2-L5**

Figure 2.2. Ancillary ligands examined in this investigation.

Two major obstacles that could discourage the successful cross-coupling of cyclopropylamine with (hetero)aryl (pseudo)halides using nickel catalysis were anticipated. Firstly, the cyclopropylaminyl radical is known to undergo rapid ring opening (**Scheme 2.4**),[83] which, given the propensity for nickel to engage in radical chemistry,[39]

could lead to unwanted side reactions rather than the desired cross-coupled product. Additionally, the nickel-catalyzed ring opening of substituted cyclopropanes is well-documented,[84] further restricting the potential use of cyclopropylamine in this reaction. Notwithstanding such challenges, we anticipated that unwanted reactivity might be circumvented through the application of an appropriately tailored ancillary ligand.

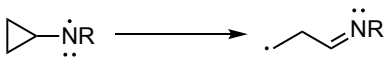

Scheme 2.4. Ring-opening of the cyclopropylaminyl radical.

2.3 Results and Discussion

2.3.1 Screening Pre-Catalysts 2-C1 and 2-C2 in the Nickel-Catalyzed *N*-Arylation of Cyclopropylamine

Pre-catalysts (**2-L1**)Ni(*o*-tolyl)Cl (**2-C1**)[66] and (**2-L2**)Ni(*o*-tolyl)Cl (**2-C2**)[61a, 68] were selected for use in a preliminary screen of the nickel-catalyzed *N*-arylation of cyclopropylamine (**Scheme 2.5**) employing three challenging (hetero)aryl chlorides under mild conditions (3 mol % Ni, 25 °C) that had previously proven effective for the cross-coupling of other primary alkylamines (e.g., furfurylamine) with **2-C1** or **2-C2**. Notably, only modest conversion to the desired *N*-(hetero)arylcyclopropylamine (≤50% conversion to **2-3a** to **2-3c**) was achieved in each case. However, the observation of negligible by-product formation in these test reactions suggested that unwanted side-reactions (e.g., cyclopropane ring-opening) are not dominant under the reaction conditions employed.

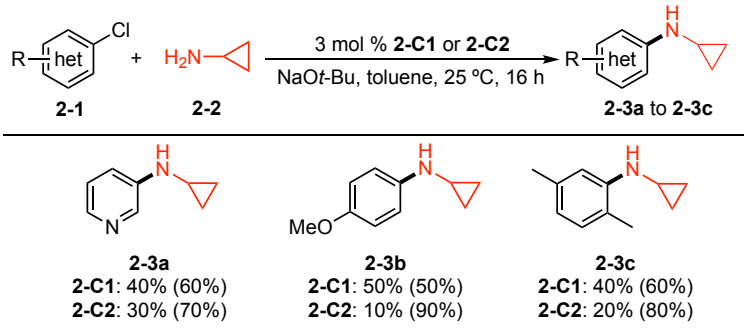

Scheme 2.5. Pre-catalyst screen of **2-C1** and **2-C2** for activity in the nickel-catalyzed *N*-arylation of cyclopropylamine. General conditions: (hetero)aryl chloride (1.0 equiv), cyclopropylamine (1.5 equiv), NaO*t*-Bu (1.5 equiv), in toluene. Conversions to product are estimated on the basis of GC data, and are reported as % **2-3a** to % **2-3c** (% **2-1a** to % **2-1c** remaining).

2.3.2 Synthesis of Pre-Catalysts 2-C3 to 2-C5

Encouraged by the clean, though modest, conversion to the desired *N*-(hetero)arylcyclopropylamines (**2-3a** to **2-3c**) achieved using **2-C1** and **2-C2** in the nickel-catalyzed *N*-arylation of cyclopropylamine, the question of whether variants of **2-C1** and **2-C2**, incorporating modified ancillary ligands similar to **2-L1** or **2-L2**, could promote the desired transformations more effectively was considered. As such, a selection of alternative ancillary ligands featuring pairings of sterically demanding, yet electronically varied, phosphine donor fragments were targeted (**2-L3** to **2-L5**, **Figure 2.2**). Substitution of the sterically hindered, but relatively electron poor, di-*o*-tolylphosphino donor fragment in **2-L1** for the similarly bulky, but comparatively more electron-releasing, dicyclohexylphosphino group gives rise to CyPAd-DalPhos (**2-L3**).[66] Alternatively, replacement of the phosphatrioxaadamantane moiety in **2-L1** with the more electron-rich and sterically similar[85] di-*tert*-butylphosphino group affords **2-L4**.[66] Finally, exchange of the phosphatrioxaadamantane cage in **2-L3** for a di-*tert*-butylphosphino group results in **2-L5**, whereby both phosphine donors are bulky and strongly electron-releasing, similar to **2-L2**.

While **2-L3** and **2-L4** had previously been synthesized,[66] **2-L5** had not been prepared prior to this work. Attempts to synthesize **2-L5** utilizing a C(sp^2)-P cross-coupling methodology were not successful (**Scheme 2.6**), irrespective of the catalyst system employed (i.e., $Pd(OAc)_2$/dippf[31, 86] or $Pd(PPh_3)_4$[66]). This is perhaps not surprising, considering the potential difficulties associated with oxidative addition of the sterically hindered (2-bromophenyl)dicyclohexylphosphine, as well as the association of the bulky HP(*t*-Bu)$_2$ nucleophile to the metal centre. Furthermore, both the substrate and desired product could act as ancillary ligands, coordinating to palladium and rendering it catalytically inactive. Subsequent attempts to synthesize **2-L5** focused on a lithium-halogen exchange procedure that had previously found success in the synthesis of **2-L1**, **2-L3**, and **2-L4**.[66] Gratifyingly, **2-L5** could be prepared via lithiation of (2-bromophenyl)di-*tert*-butylphosphine using *n*-BuLi, followed by quenching with $ClPCy_2$ (**Scheme 2.7**). Notably, whereas **2-L3** and **2-L4** are air-stable in the solid state, **2-L5** was found to be air-sensitive, requiring handling under inert atmosphere. Interestingly, complementary reactions involving the lithiation of (2-bromophenyl)dicyclohexylphosphine, followed by

quenching with ClP(*t*-Bu)$_2$ under identical conditions to the synthesis of **2-L5** did not yield the desired product, likely due to the greater steric bulk of ClP(*t*-Bu)$_2$ versus ClPCy$_2$ and the correspondingly more challenging nucleophilic substitution.

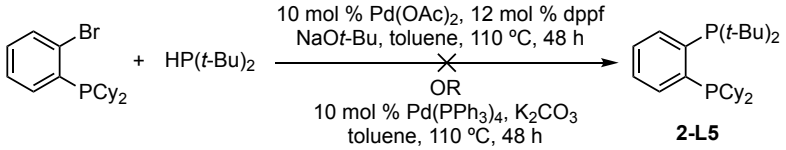

Scheme 2.6. Attempted synthesis of **2-L5** via C(sp^2)-P cross-coupling.

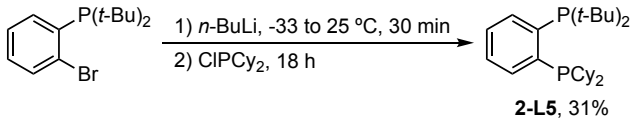

Scheme 2.7. Synthesis of **2-L5**.

Given the established efficacy of nickel pre-catalysts of the form L$_n$Ni(aryl)Cl in cross-coupling applications,[87] including C–N bond formation, (L)Ni(*o*-tolyl)Cl pre-catalysts incorporating **2-L3**-**L5** were developed in order to assess their catalytic competency in the *N*-arylation of cyclopropylamine. The desired complexes (**2-L3**)Ni(*o*-tolyl)Cl (**2-C3**), (**2-L4**)Ni(*o*-tolyl)Cl (**2-C4**), and (**2-L5**)Ni(*o*-tolyl)Cl (**2-C5**) were prepared in a two-step procedure adapted from the literature (**Scheme 2.8**).[66] Combination of each of **2-L3** to **2-L5** with NiCl$_2$(DME) in THF afforded the corresponding (L)NiCl$_2$ species, the identities of which were confirmed via spectroscopic and microanalytical analysis. Subsequent treatment with *o*-tolylmagnesium chloride in THF afforded after workup **2-C3** to **2-C5** as air-stable solids that were structurally characterized, including by use of single-crystal X-ray techniques (**Figure 2.3**). In all cases a distorted square planar geometry is observed ($\sum\angle \approx 360°$), and the Ni-P distance *trans* to the aryl group is longer than the analogous distance *trans* to chloride.

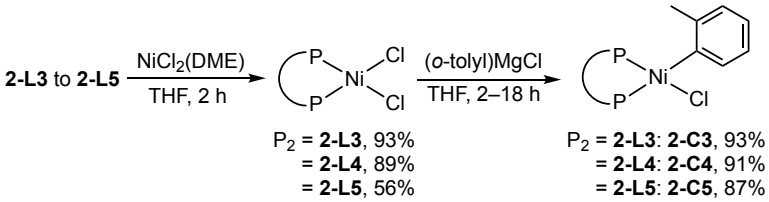

Scheme 2.8. Synthesis of pre-catalysts **2-C3** to **2-C5**.

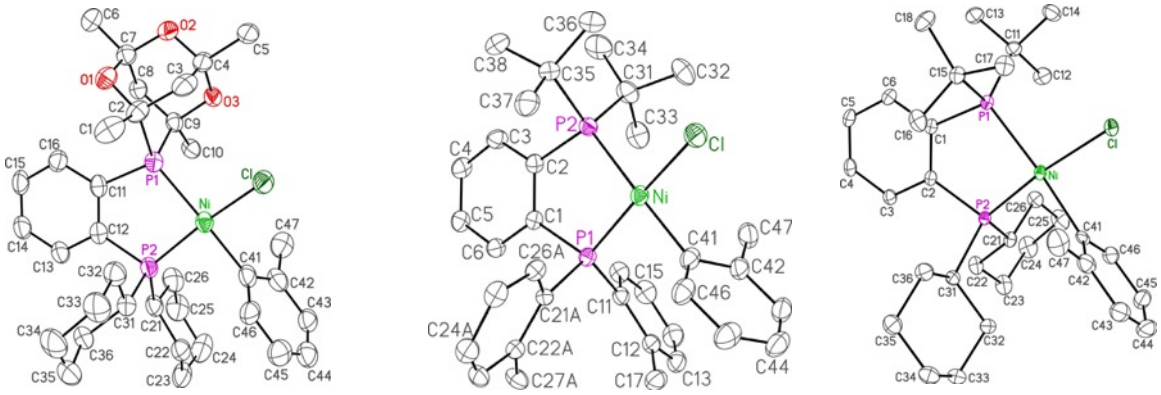

Figure 2.3. Single-crystal X-ray structures of **2-C3** (left), **2-C4** (middle), and **2-C5** (right), represented with thermal ellipsoids at the 30% probability level. Hydrogen atoms are omitted for clarity.

The behaviour of **2-C3** and **2-C4** in solution was more complex than initially anticipated, and warrants further discussion. The solution $^{31}P\{^{1}H\}$ NMR spectrum of bulk (as-prepared, amorphous) **2-C3** exhibits four pairs of doublets (**Figure 2.4A**), corresponding to four distinct species (**2-C3A** to **2-C3D**), as confirmed on the basis of ^{31}P-^{31}P COSY data (see **Figure A12** in the Appendices). Conversely, the solution $^{31}P\{^{1}H\}$ NMR spectrum of crystalline **2-C3** (**Figure 2.4B**) features only two pairs of doublets (~3:1 ratio) – a pattern that is similar to that of **2-C1**.[66] Given that the crystal structure of **2-C3** features the nickel-bound *o*-tolyl fragment *trans* to the chiral (racemic) phosphatrioxaadamantane cage (see **Figure 2.3**), the two pairs of doublets observed in **Figure 2.4B** were ascribed as arising from the presence of two Ni-C(aryl) rotational isomers (**2-C3A** and **2-C3B**) that differ on the basis of the relative orientation of the methyl group of the nickel-bound *o*-tolyl fragment above or below the square plane of the molecule. The emergence over time of the remaining two sets of doublets (**2-C3C** and **2-C3D**) in the solution $^{31}P\{^{1}H\}$ NMR spectrum of dissolved crystalline **2-C3** (see **Figure A13** in Appendix 3) suggests that **2-C3C** and **2-C3D** are structurally related to **2-C3A** and **2-C3B**. On the basis of these collective observations, the proposed identities of **2-C3A** to **2-C3D** are depicted in **Figure 2.5**: **2-C3A** and **2-C3B** are complexes in which the nickel-bound *o*-tolyl group is *trans* to the phosphatrioxaadamantane cage, while **2-C3C** and **2-C3D** are isomeric complexes in which the nickel-bound *o*-tolyl group is *trans* to the PCy_2 moiety. The chiral (racemic) nature of the phosphatrioxaadamantane cage, when paired with the relative orientation of the methyl group of the nickel-bound *o*-tolyl fragment above

or below the square plane, arising from hindered Ni-C(aryl) rotation, affords four diastereomers, in keeping with the solution $^{31}P\{^{1}H\}$ NMR spectrum of bulk **2-C3** (**Figure 2.4A**). Variable-temperature solution NMR experiments suggest that **2-C3A**/**B** to **2-C3C**/**D** isomerization is slow on the NMR timescale, with only slight changes in the relative $^{31}P\{^{1}H\}$ NMR peak intensities of **2-C3A** to **2-C3D** observed at elevated temperatures (see **Figure A14** in Appendix 3). This notion is further supported by $^{31}P\{^{1}H\}$ NMR saturation transfer experiments, in which chemical exchange was not observed between **2-C3A**/**B** and **2-C3C**/**D** at room temperature (see **Figure A15** in Appendix 3). Though experiments to determine the mechanism for this isomerization process were not conducted, the interconversion of **2-C3A**/**B** to **2-C3C**/**D** might occur through tetrahedral intermediates, or through dissociation of one phosphine donor atom of **2-L3** followed by rearrangement and subsequent re-chelation. Notably, only two diastereomers likely arising from rotamers of the nickel-bound *o*-tolyl group are observed in solution for **2-C1**.[66]

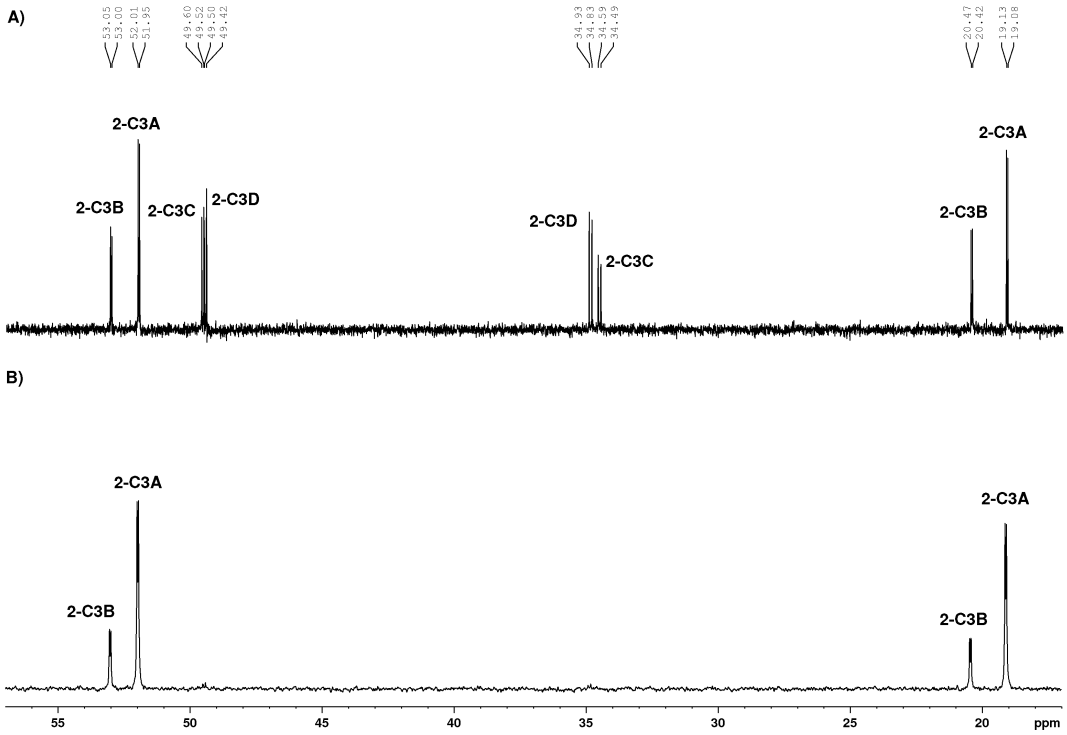

Figure 2.4. $^{31}P\{^{1}H\}$ NMR spectrum ($CDCl_3$) of A) bulk and B) recrystallized **2-C3**.

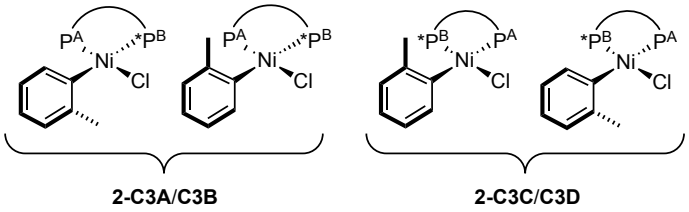

Figure 2.5. Proposed structures of the four diastereomers **2-C3A** to **2-C3D** (P^A = PCy_2; $^*P^B$ = chiral phosphatrioxaadamantane cage).

At first glance, it is tempting to rationalize the differing ancillary ligand binding selectivity within each of **2-C1** and **2-C3** as being attributable to the more closely matched *trans*-directing ability of the dialkylphosphino donor fragments in **2-C3** (leading to poor selectivity), versus the phosphatrioxaadamantane (superior) and P(*o*-tolyl)$_2$ (inferior) pairing in **2-C1**. However, the somewhat complex solution NMR behavior of **2-C4** (*vide infra*), featuring P(*o*-tolyl)$_2$ and P(*t*-Bu)$_2$ donors in analogy to **2-C1**, when contrasted with the observation of a *single* diastereomer in solution for **2-C5**, which features two dialkylphosphino donors similar to **2-C3**, suggests that the observed equilibrium distribution of isomers in pre-catalysts of this type may result from a complex interplay of factors.

The solution $^{31}P\{^1H\}$ NMR spectrum of **2-C4** (**Figure 2.6**) exhibits four distinct resonances that exhibit varying degrees of line-broadening. Compound **2-C4** is distinct from **2-C3** in that the orientation of the methyl group of the nickel-bound *o*-tolyl fragment above or below the square plane is rendered enantiotopic (rather than diastereotopic, as in **2-C3**) in the absence of a secondary chiral element. Variable-temperature solution $^{31}P\{^1H\}$ NMR studies of **2-C4** revealed coalescence to two broad signals at elevated temperatures (**Figure 2.7**). On this basis, the four $^{31}P\{^1H\}$ NMR resonances observed for **2-C4** were tentatively assigned as corresponding to two geometric isomers in which the nickel-bound *o*-tolyl group is *trans* to either the P(*o*-tolyl)$_2$ or P(*t*-Bu)$_2$ fragment. However, isomerism arising from hindered rotation involving the P(*o*-tolyl)$_2$ and Ni(*o*-tolyl) moieties, in addition to possible equilibria involving tetrahedral and square planar species,[88] is also likely contributing to the observed line broadening behavior. In keeping with such a scenario, the solution ^1H NMR spectrum of (**2-L4**)$NiCl_2$ is consistent with a C_1-symmetric structure arising from hindered rotation phenomena, whereas a C_S-symmetric structure is evident for (**2-L5**)$NiCl_2$.

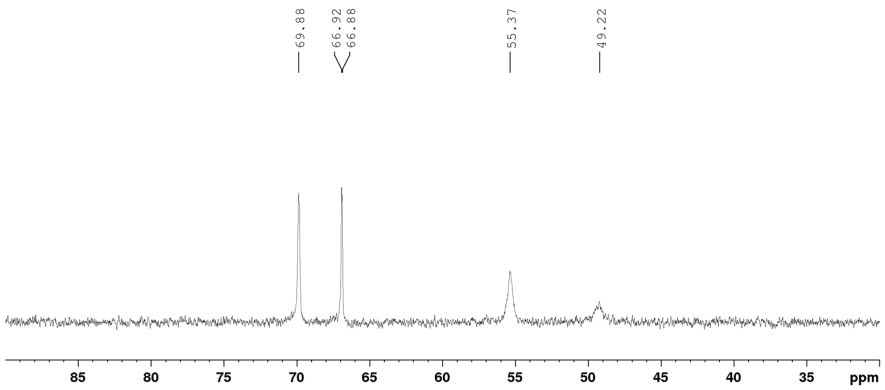

Figure 2.6. $^{31}P\{^{1}H\}$ NMR spectrum ($CDCl_3$) of **2-C4**.

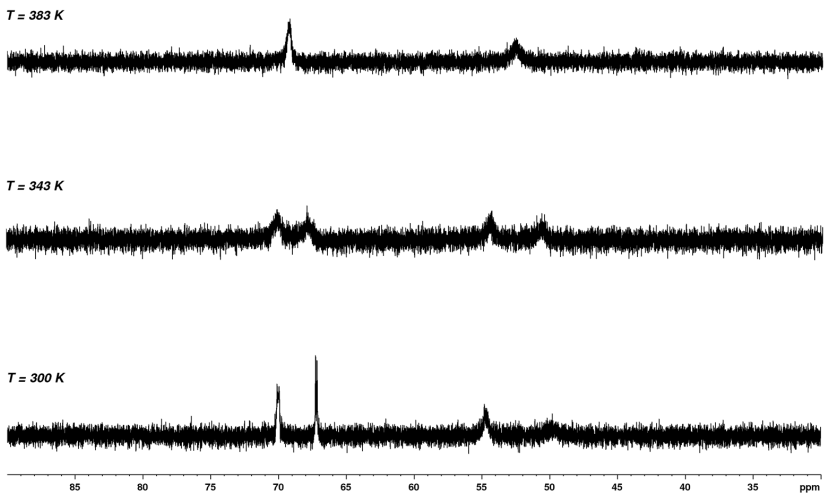

Figure 2.7. Elevated-temperature $^{31}P\{^{1}H\}$ NMR spectra ($C_2D_2Cl_4$) of **2-C4**.

2.3.3 Screening Pre-Catalysts 2-C3 to 2-C5 in the Nickel-Catalyzed *N*-Arylation of Cyclopropylamine

With the desired, new pre-catalysts in hand, **2-C3** to **2-C5** were screened for activity in the nickel-catalyzed C–N cross-coupling of cyclopropylamine (3 mol % Ni, 25 °C; **Scheme 2.9**), employing the same three challenging (hetero)aryl chlorides for which **2-C1** and **2-C2** had performed poorly (**Scheme 2.5**). Gratifyingly, both **2-C3** and **2-C5** demonstrated excellent performance in two of these test transformations, with almost quantitative conversion being observed when utilizing the heteroaryl or *ortho*-substituted aryl chloride **2-1a** or **2-1c** (leading to **2-3a** and **2-3c**, respectively). While **2-C4** performed comparatively poorly in transformations of **2-1a** or **2-1c**, this pre-catalyst proved superior

to **2-C3** or **2-C5** in the test transformation of electron-rich 4-chloroanisole (**2-1b**) leading to **2-3b**. Substituting weaker bases such as Cs_2CO_3 or K_3PO_4 for NaO*t*-Bu resulted in minimal conversion to the desired product (<5% conversion to **2-3a** when using **2-C3**). Furthermore, reducing the catalyst loading of **2-C3** below 3 mol % resulted in poorer conversions (e.g., 65% conversion to **2-3a** at 1 mol % catalyst loading). Given the similar reactivity profile of **2-C3** and **2-C5**, **2-C3** (and where appropriate, **2-C4**) was carried forward in subsequent catalytic applications on the basis of the practical consideration that **2-L3** (unlike **2-L5**) is not air-sensitive.

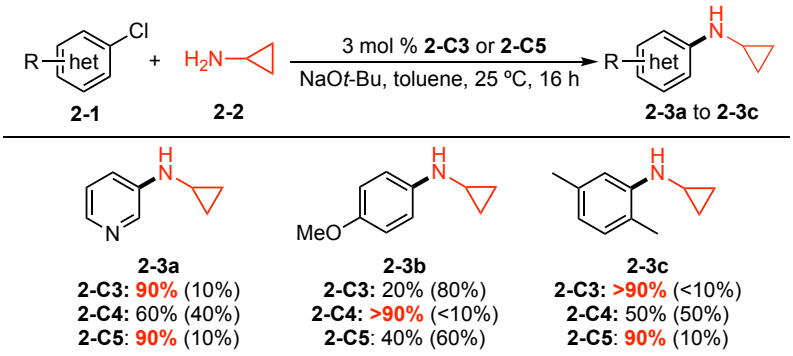

Scheme 2.9. Pre-catalyst screen of **2-C3** to **2-C5** in the nickel-catalyzed *N*-arylation of cyclopropylamine. General conditions: (hetero)aryl chloride (1.0 equiv), cyclopropylamine (1.5 equiv), NaO*t*-Bu (1.5 equiv), in toluene. Conversions to product are estimated on the basis of GC data, reported as % **2-3a** to % **2-3c** (% **2-1a** to % **2-1c** remaining).

From an ancillary ligand design perspective,[4] the similar performance of **2-C3** and **2-C5** in the successful formation of **2-3a** and **2-3c** indicates that the phosphatrioxaadamantane and P(*t*-Bu)$_2$ groups are interchangeable in terms of engendering desirable nickel catalysis in these particular transformations. Knowing that the phosphatrioxaadamantane cage is a poorer electron-donor versus P(*t*-Bu)$_2$, but that the two fragments possess a similar steric profile,[85] suggests that the selection of appropriate ancillary ligand sterics, rather than electronics, is a key design consideration in this particular reaction setting. However, such simple conclusions do not translate to the transformation leading to **2-3b**, whereby poor conversion to product was noted with the PAd-DalPhos (**2-L1**)-derived pre-catalyst **2-C1** featuring phosphatrioxaadamantane and P(*o*-tolyl)$_2$ ancillary ligand donor pairings, yet excellent conversion was achieved with the analogous pre-catalyst **2-C4**, which features P(*t*-Bu)$_2$ in place of the phosphatrioxaadamantane moiety. It is plausible that the successful formation of **2-3b** by

use of **2-C4** may arise in part from the more electron-rich nature of **2-L4** versus **2-L1**, resulting in more facile C(sp^2)–Cl activation of the electronically deactivated 4-chloroanisole substrate. However, the poor performance of **2-C2** or **2-C5** in the formation of **2-3b**, each featuring strongly electron-releasing phosphine donor fragments, supports the notion that a subtle balance of ancillary ligand steric and electronic properties must be achieved in order to engender desirable performance in nickel-catalyzed C–N cross-coupling of particular nucleophile and electrophile pairings. Indeed, while **2-L1** and **2-L2** proved inferior to **2-L3** and **2-L4** in the nickel-catalyzed *N*-arylation of cyclopropylamine, the inverse trend has been observed for the monoarylation of ammonia.[66, 68] As mentioned in Section 1.3, it must also be recognized that in contrast to the Pd(0)/Pd(II) cycle traversed in palladium-catalyzed C–N cross-coupling, the mechanistic scenario is likely more complex for nickel, whereby the ancillary ligand and substrates employed influence partitioning between Ni(0)/Ni(II) and Ni(I)/Ni(III) reaction manifolds of differing productivity.[56]

2.3.4 Scope of the Nickel-Catalyzed *N*-Arylation of Cyclopropylamine

The electrophile scope in the C–N cross-coupling of cyclopropylamine using **2-C3** was then surveyed (**Scheme 2.10**). A variety of (hetero)aryl (pseudo)halide coupling partners were successfully employed in this reaction, including those with electron-withdrawing (**2-3d** to **2-3g**) or *ortho*-substituents (**2-3c**, **2-3i** to **2-3k**). Heterocyclic electrophiles were also well-tolerated, including those featuring pyridine (**2-3a**), isoquinoline (**2-3j**), quinaldine (**2-3k**), quinoline (**2-3l**), quinoxaline (**2-3m**), pyrimidine (**2-3n** and **2-3o**), purine (**2-3p**), benzothiophene (**2-3q**), or benzothiazole (**2-3r**) frameworks. In conducting such transformations on an 8.5 mmol scale in (hetero)aryl chloride by use of **2-C3** (3 mol %), each of **2-3a** (1.004 g, 88%) and **2-3d** (1.223 g, 91%) were obtained in excellent yield. The use of **2-C3** enabled the *N*-arylation of cyclopropylamine using (hetero)aryl chlorides, bromides, and phenol-derived electrophiles (tosylate, sulfamate, and carbamate) at room temperature (3 mol % **2-C3**), as well as aryl triflate and aryl mesylate coupling partners, albeit at higher catalyst loadings (5 mol % **2-C3**) and elevated temperatures (110 °C). Use of **2-C4** in place of **2-C3** allowed the coupling of an electron-rich aryl chloride (**2-3b**) and aryl tosylate (**2-3h**) at room temperature. Control experiments performed in the absence of nickel showed no conversion to **2-3d** or **2-3i**, and only 10%

conversion to **2-3p** (as determined on the basis of GC analysis), highlighting the essential nature of the pre-catalyst in promoting this reaction. Notably, the transformations depicted in **Scheme 2.10** represent the first examples of room temperature C–N cross-couplings of cyclopropylamine employing (hetero)aryl chlorides, as well as the first examples of such cross-couplings involving phenol-derived electrophiles under any conditions.

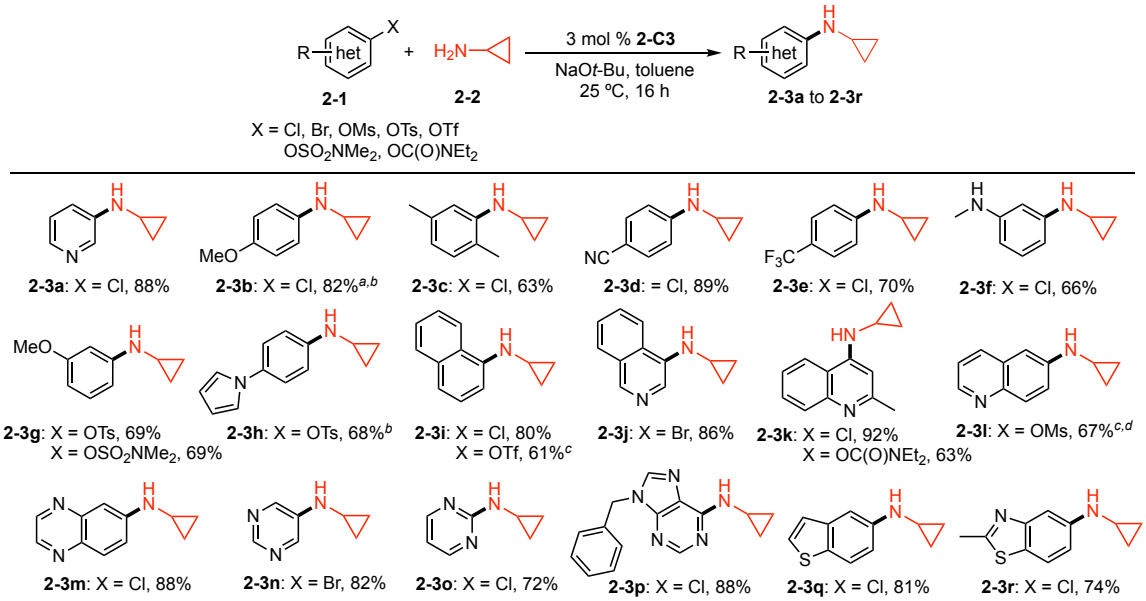

Scheme 2.10. Scope of the nickel-catalyzed *N*-arylation of cyclopropylamine. General conditions: (hetero)aryl (pseudo)halide (1.0 equiv), cyclopropylamine (1.5 equiv), NaO*t*-Bu (1.5 equiv), in toluene. Isolated yields reported. [a]Isolated as the corresponding *N*-acyl derivative. [b]Conducted using 3 mol % **2-C4**. [c]Conducted using 5 mol % **2-C3** and K_3PO_4 (3.0 equiv) at 110 °C. [d]1,4-dioxane used as solvent.

2.3.5 Limitations of the 2-C3 Pre-Catalyst System in the *N*-Arylation of Cyclopropylamine

While the scope of the nickel-catalyzed *N*-arylation of cyclopropylamine using **2-C3** with respect to (hetero)aryl (pseudo)halides was indeed broad, there exist notable limitations. Firstly, substrates containing carbonyl moieties, such as 4-bromopropiophenone and methyl 4-chlorobenzoate (**Figure 2.8**) provided negligible conversion to the desired cross-coupled product using this pre-catalyst system on the basis of GC analysis. This is likely due to the strongly basic conditions required to effect this transformation, which might favour competitive α-arylation or transesterification reactions respectively, in addition to the desired cross-coupling pathway. While the use of weaker bases such as Cs_2CO_3 and K_3PO_4 proved ineffective when used in place of NaO*t*-Bu in this reaction under the reported conditions (see **Scheme 2.10**), increasing the amount of weak

base added, as well as enhancing the solubility of such bases (e.g., by changing to a more polar solvent and/or increasing the reaction temperature) might permit access to base-sensitive substituents. Electron-rich, heteroaryl (pseudo)halides, including those comprising indole or benzodioxole cores, (**Figure 2.8**) also proved to be ineffective coupling partners when employing **2-C3** and/or **2-C4** in the nickel-catalyzed *N*-arylation of cyclopropylamine under the reported conditions. Increasing the reaction temperature may help to facilitate the more challenging oxidative addition needed to accommodate such deactivated substrates.

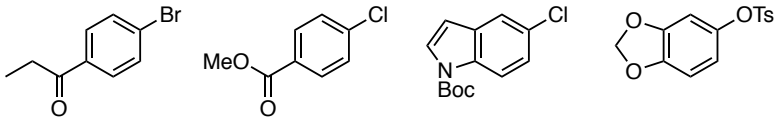

Figure 2.8. Representative (hetero)aryl (pseudo)halides that were not tolerated in the nickel-catalyzed *N*-arylation of cyclopropylamine using **2-C3**.

To demonstrate the practical utility of **2-C3** in facilitating the cross-coupling of (hetero)aryl (pseudo)halides and cyclopropylamine, the synthesis of nevirapine (see **Figure 2.1**) from **2-1s**[89] was attempted (**Scheme 2.11**). It was anticipated that the C(sp^2)–Cl bond adjacent to the electron-withdrawing carbonyl moiety would preferentially react with cyclopropylamine, given the deactivated nature of the other C(sp^2)–Cl bond (adjacent to the electron-donating amide nitrogen) and the poor capability of **2-C3** in engaging with such bonds (see **Scheme 2.9**). The resulting mono-arylated product (**2-3s**) could then be subjected to a second pre-catalyst system to facilitate the intramolecular C–N bond-forming reaction to furnish nevirapine. Unfortunately, the desired reaction did not proceed at room temperature or elevated temperatures (50 or 90 °C), even when switching to a more polar solvent (THF). The coordinating ability of the amide moiety may have impeded the success of this transformation by engaging with **2-C3** in a deleterious manner; the inability of **2-C3** in tolerating amide substituents was also seen when 4′-chloroacetanilide (containing a secondary amide) was used as a substrate, proving unreactive under the reported conditions.

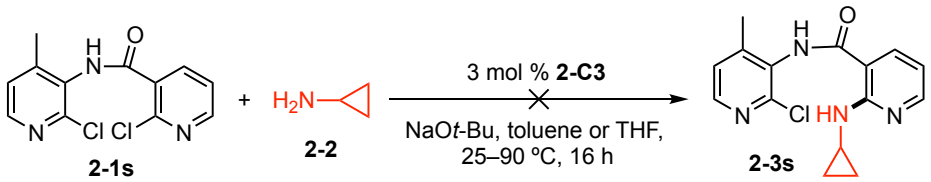

Scheme 2.11. Attempted synthesis of **2-3s** (en route to nevirapine) using **2-C3**.

2.3.6. (Pseudo)halide Competition Studies and Reaction Monitoring Experiments

Given that a variety of (hetero)aryl electrophiles proved to be viable coupling partners when using **2-C3**, a brief (pseudo)halide competition study with limiting cyclopropylamine to assess the relative preference of this pre-catalyst was conducted (**Scheme 2.12**). The aryl components of the electrophiles employed in the competition study were purposefully chosen to be sterically and electronically similar in order to minimize any reactivity bias, while still enabling rational analysis of the product mixtures. When an aryl chloride and bromide were used as competing cross-coupling partners, a modest preference for the aryl chloride was observed, with an overall 80% combined conversion to both products (**2-3t** and **2-3u**). In the case of the aryl chloride or bromide versus the aryl tosylate, a sizeable preference for the aryl halide was observed. However, the total conversion to **2-3t** and **2-3u** under these conditions was significantly lower (<50%), suggesting a potential inhibitory effect when the aryl tosylate engages with **2-C3**. Pre-catalyst **2-C2** displayed a similar intolerance to certain aryl electrophiles in the cross-coupling primary alkylamines.[68]

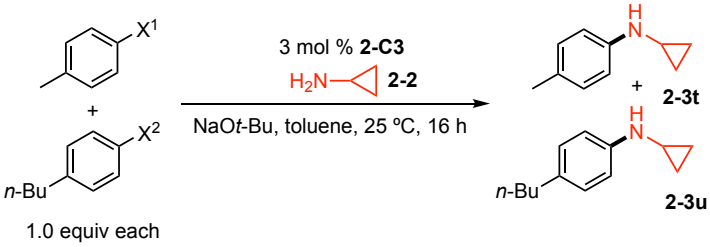

X^1	X^2	**2-3t**:**2-3u**	Total Conversion
Cl	Br	2:1	80%
Cl	OTs	4:1	45%
Br	OTs	5:1	25%

Scheme 2.12. Pseudohalide competition study employing **2-C3**. General conditions: cyclopropylamine (1.5 equiv), NaO*t*-Bu (1.5 equiv), in toluene. Reported product distributions and total conversions to **2-3t** and **2-3u** were estimated on the basis of calibrated GC data.

In the initial set of screening reactions using **2-C3** as a pre-catalyst for the room temperature cross-coupling of cyclopropylamine, the amination of 3-chloropyridine (**2-1a**) proceeded in high conversion to afford **2-3a** (**Scheme 2.9**). Conversely, the analogous cross-coupling using 4-chloroanisole (**2-1b**) afforded only modest amounts of the target *N*-

arylcyclopropylamine (**2-3b**) along with significant quantities (~80%) of unreacted **2-1b**. It is plausible that the poor performance of **2-1b** can be attributed to the inability of catalytic species derived from **2-C3** to engage in oxidative addition to the rather electron-rich and thus deactivated **2-1b**, and/or to subsequent catalyst inhibition pathways (e.g., slow transmetallation or reductive elimination; deleterious redox chemistry). In a preliminary examination of such phenomena, the otherwise successful cross-coupling of cyclopropylamine and **2-1a** to give **2-3a** by using **2-C3** was monitored over time in the presence of varying amounts of added **2-1b** (**Scheme 2.13** and **Figure A1** in Appendix 2). Evaluation of the conversion to **2-3a** after 40 minutes reaction time revealed that increasing the concentration of **2-1b** diminished the ability of **2-C3** to effect the otherwise facile conversion of **2-1a** to **2-3a**, and throughout, negligible amounts of **2-3b** were detected by use of GC methods. These preliminary observations suggest that **2-1b** engages with catalytic species derived from **2-C3** in such a way as to lead to suppression of catalytic activity.

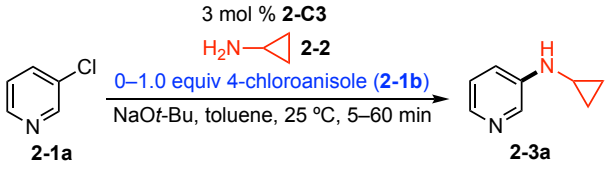

equiv **2-1b**	Conversion to **2-3a**[a]
0	85%
0.1	65%
1	50%

Scheme 2.13. Reaction monitoring of the formation **2-3a** using **2-C3** with varying amounts of **2-1b**. General conditions: **2-1a** (1.0 equiv) cyclopropylamine (1.5 equiv), NaO*t*-Bu (1.5 equiv), in toluene. Conversion to **2-3a** determined on the basis of calibrated GC data. [a]After 40 minutes reaction time.

2.3.7 Nickel-Catalyzed *N*-Arylation of Primary, Cyclic, Alkylammonium Salts

The utility of **2-C3** in facilitating the *N*-arylation of other primary cyclic alkylamines was then explored. Like cyclopropylamine, cyclopropanemethylamine and cyclobutylamine have rarely been used as nucleophiles in palladium- and copper-catalyzed C–N bond-forming processes,[90] and analogous nickel-catalyzed transformations employing these substrates were unknown prior to this work. Given that both amines are air and moisture sensitive, the more conveniently handled and commercially available hydrochloride salts of these substrates were employed in our catalytic survey. Notably, the use of alkyl ammonium salts in C–N cross-coupling chemistry is restricted to three reports concerning transformations of methylamine or ethylamine hydrochloride exclusively, employing palladium[91] or nickel[54, 66] catalysis.

Adapting the conditions employed for the *N*-arylation of cyclopropylamine (**Scheme 2.10**), the performance of **2-C3** in the *N*-arylation of cyclopropanemethylamine hydrochloride and cyclobutylamine hydrochloride with representative (hetero)aryl (pseudo)halides was assessed (**Scheme 2.14**). Desired amination products derived from electrophiles featuring *ortho*-substituents (**2-5a**, as well as **2-5b** using **2-C4**), an electron-withdrawing group (**2-6a**), or heterocyclic frameworks (**2-6b** and **2-6c**) were obtained successfully in this reaction, spanning (hetero)aryl chloride, bromide, and tosylate coupling partners. Notably, these transformations represent the first examples of the metal-catalyzed C–N cross-coupling of alkyl ammonium salts at room temperature.

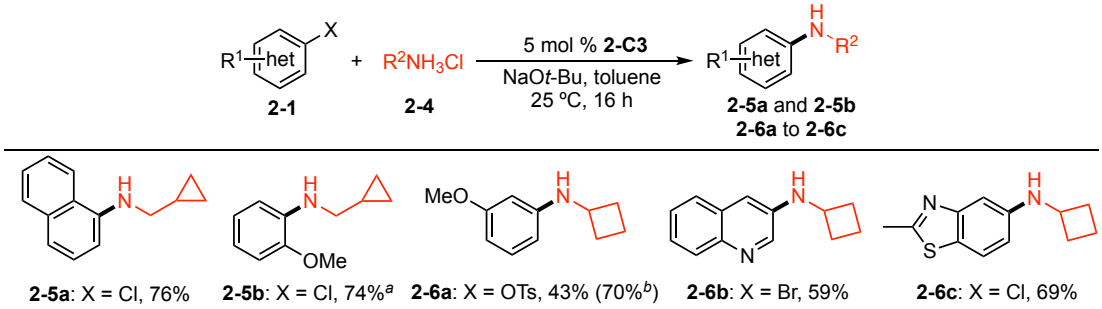

2-5a: X = Cl, 76% **2-5b**: X = Cl, 74%[a] **2-6a**: X = OTs, 43% (70%[b]) **2-6b**: X = Br, 59% **2-6c**: X = Cl, 69%

Scheme 2.14. The nickel-catalyzed *N*-arylation of cyclopropanemethylamine hydrochloride and cyclobutylamine hydrochloride. General conditions: (hetero)aryl (pseudo)halide (1.0 equiv), amine hydrochloride (1.1. equiv), NaO*t*-Bu (2.5 equiv), in toluene. Isolated yields reported. [a]Conducted using 5 mol % **2-C4**. [b]Yield estimated on the basis of calibrated GC data.

While cyclopropanemethylamine hydrochloride and cyclobutylamine hydrochloride were well-tolerated under these conditions, other related amine hydrochloride salts were not successful coupling partners using **2-C3** (**Figure 2.9**). When employing either ethyl 1-aminocyclopropanecarboxylate hydrochloride (**2-4c**) or *trans*-2-phenylcyclopropylamine hydrochloride (**2-4d**), only modest conversions (≤60%) to the desired *N*-arylated product were obtained on the basis of GC analysis, even when employing activated electrophiles (e.g., 4-chlorobenzotrifluoride or 4-chlorobenzonitrile). The ester moiety in **2-4c** appeared to react with the *tert*-butoxide base, yielding an apparent mixture of the desired *N*-arylated product (containing an ethyl ester) and an *N*-arylated product with a *tert*-butyl ester in many instances. Switching to a weaker base (e.g., Cs_2CO_3 and K_3PO_4) at elevated temperatures might ameliorate this problem. **2-4d** is thermally sensitive, and though it was stored at –33

°C, may not have reacted quickly enough before decomposing, even at ambient temperatures.

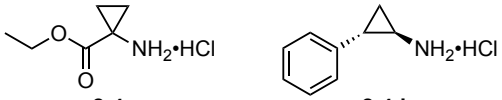

2-4c 2-4d

Figure 2.9. Structures of amine hydrochloride salts that were not successful coupling partners.

2.4 Summary

In summary, the first nickel-catalyzed C–N cross-couplings of cyclopropylamine, cyclopropanemethylamine hydrochloride, and cyclobutylamine hydrochloride have been developed. Subtle electronic modifications in the ancillary ligand framework were shown to be crucial for obtaining a highly effective pre-catalyst for such challenging transformations. In this regard, the reported protocol makes use of the air-stable pre-catalyst **2-C3**, in the majority of cases under mild conditions (3 mol % Ni, 25 °C), with the demonstrated electrophile scope spanning a diverse range of heteroaryl and (pseudo)halide motifs. Whereas **2-C3** was found to be less effective in combination with electron-rich aryl chlorides, pre-catalyst **2-C4**, featuring P(*o*-tolyl)$_2$ and P(*t*-Bu)$_2$ donor pairings, proved to be useful in promoting cross-couplings of these particular substrates. This reactivity trend was found to be consistent with the observation of catalyst inhibition in the otherwise efficient cross-coupling of cyclopropylamine and 3-chloropyridine using **2-C3**, upon addition of 4-chloroanisole. Competition studies involving **2-C3** revealed a (pseudo)halide reactivity preference (Cl > Br, OTs).

2.5 Experimental

2.5.1 General Considerations

Unless otherwise indicated, all experimental procedures were conducted in a nitrogen-filled, inert atmosphere glovebox using oven-dried glassware, with work-up procedures carried out on the benchtop in air. Toluene, and pentane used in the synthesis of **2-L5**, were purged with nitrogen, passed through a double column purification system containing alumina and copper-Q5 reactant, and stored over 4 Å molecular sieves in bulbs with Teflon taps prior to use. Diethyl ether, tetrahydrofuran (THF), and 1,4-dioxane were dried over Na/benzophenone, distilled under a nitrogen atmosphere, and stored in bulbs with Teflon taps over 4 Å molecular sieves. Dichloromethane used in the synthesis of **2-L5** was purged with nitrogen, and stored over 4 Å molecular sieves in a bulb with a Teflon

tap. $C_2D_2Cl_4$ was freeze-pump-thaw degassed three times and stored over 4 Å molecular sieves in a bulb with a Teflon tap in the glovebox. K_3PO_4 was dried under vacuum at 180 °C for 24 h, and stored under nitrogen in the glovebox prior to use. (2-bromophenyl)di-*tert*-butylphosphine,[92] **2-L3**,[66] **2-L4**,[66] **2-C1**,[66] **2-C2**,[68] 3-methoxyphenyl 4-methylbenzenesulfonate,[93] quinolin-6-yl methanesulfonate,[93] naphthalene-1-yl trifluoromethanesulfonate,[94] 3-methoxyphenyl dimethylsulfamate,[95] 2-methylquinolin-4-yl diethylcarbamate,[61a] and 9-benzyl-6-chloropurine[96] were prepared according to established literature procedures. Otherwise, all other solvents, reagents, and materials were used as received from commercial sources.

For General Procedures A and B, automated flash chromatography was carried out on a Biotage Isolera One automated flash purification system using 10 g Biotage SNAP KP-SIL (particle size 30-90 μm) or 12 g Silicycle Silia*Sep* (particle size 40–63 μm, 230–400 mesh) silica flash cartridges with a typical gradient of 2–4–2 column volumes and a flow rate of 10 mL/min. For General Procedure C, flash chromatography was carried out on silica gel using Silicycle Silia*Flash* 60 silica (particle size 40–63 μm; 230–400 mesh). Unless otherwise indicated, NMR spectra were recorded on a Bruker AV 300 MHz or Bruker AV 500 MHz spectrometer at 300 K, with chemical shifts (in ppm) referenced to residual protio solvent peaks (^{1}H), deuterated solvent peaks (^{13}C{^{1}H}), or external 85% H_3PO_4 (^{31}P{^{1}H}). Splitting patterns are indicated as follows: br, broad; app, apparent; s, singlet; d, doublet; t, triplet; q, quartet; sept, septet; dd, doublet of doublets; td, triplet of doublets; m, multiplet, with all coupling constants (*J*) reported in Hertz (Hz). In some cases, fewer than expected carbon resonances were observed despite prolonged acquisition times. Elemental analyses were performed by Galbraith Laboratories, Inc., Knoxville, TN. Mass spectra were obtained using ion trap electrospray ionization (ESI) instruments operating in positive mode. Gas chromatography (GC) data were obtained on an instrument equipped with a SGE BP-5 column (30 m, 0.25 mm i.d.).

2.5.2 Synthesis of 4-butylphenyl 4-methylbenzenesulfonate

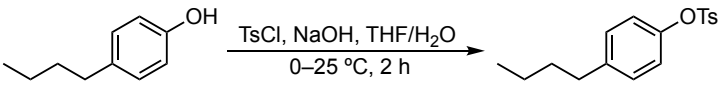

The following procedure was adapted from the literature.[97] In a 25-mL round-bottom flask containing a magnetic stir bar, 4-butylphenol (383 μL, 2.5 mmol) was dissolved in

THF (1.5 mL), to which was added a solution of NaOH (0.330 g, 8.25 mmol) in distilled, deionized water (1.9 mL), yielding a cloudy mixture. The mixture was then cooled to 0 °C, and a solution of TsCl (0.572 g, 3.0 mmol) in THF (3.5 mL) was added dropwise to the cooled, stirring mixture over ~15 min. After this time, the ice bath was removed, and the mixture was allowed to stir at room temperature for 2 h. Then, the mixture was diluted with EtOAc (20 mL) and separated. The retained organic layer was washed with distilled, deionized water (2 x 10 mL), dried using Na_2SO_4, and filtered. The volatiles were removed from the filtrate under reduced pressure, yielding a yellow oil. The oil was then dissolved in a minimal amount of CH_2Cl_2 and filtered over a short plug of silica gel, eluting with CH_2Cl_2 (~150 mL). The volatiles were removed from the clear, colorless filtrate under reduced pressure, yielding a pale-yellow oil (0.706 g, 93%). ^{1}H NMR (500 MHz, $CDCl_3$): δ 7.70 (d, *J* = 8.3 Hz, 2H), 7.30 (d, *J* = 8.1 Hz, 2H), 7.07 (d, *J* = 8.6 Hz, 2H), 6.87 (d, *J* = 8.6 Hz, 2H), 2.56 (t, *J* = 7.8 Hz, 2H), 2.45 (s, 3H), 1.58–1.52 (m, 2H), 1.32 (sextet, *J* = 7.4 Hz, 2H), 0.91 (t, *J* = 7.4 Hz, 3H). ^{13}C{^{1}H} NMR (126 MHz, $CDCl_3$): δ 147.7, 145.3, 142.0, 132.8, 129.8, 129.5, 128.7, 122.2, 35.1, 33.6, 22.4, 21.8, 14.0. HRMS-ESI (*m/z*): Calc'd for $C_{17}H_{20}NaO_3S$ $[M+Na]^+$: 327.1031. Found: 327.1025.

2.5.3 Synthesis of Ligand 2-L5 and Pre-Catalysts 2-C3 to 2-C5

Synthesis of di-*tert*-butyl(2-(dicyclohexyl)phosphino)phenyl)phosphine (2-L5). *All manipulations, including work-up, were performed in an inert atmosphere glovebox*. A glass vial was charged with (2-bromophenyl)di-*tert*-butylphosphine (0.138 g, 0.458 mmol), Et_2O (2 mL), and a magnetic stir bar, and the vial was placed in a –33 °C freezer for 20 min. After this time, the vial was removed from the freezer, magnetic stirring was initiated, and *n*-BuLi (275 μL of a 2.5 M solution in hexanes, 0.687 mmol) was added dropwise to the cooled, stirring solution, yielding a clear yellow solution. The solution was then allowed to stir at room temperature for 30 min., after which time a cold (–33 °C) solution of $ClPCy_2$ (106 μL, 0.481 mmol) in Et_2O (1 mL) was added dropwise to the stirring solution, yielding a cloudy yellow mixture upon complete addition. The mixture was allowed to stir at room temperature for 18 h (unoptimized), after which time CH_2Cl_2 (3 mL) was added, and the mixture was filtered through a Celite/silica plug (~1:1), eluting with CH_2Cl_2 (2 x 1 mL). The volatiles were removed from the clear, yellow filtrate under reduced pressure yielding a yellow-orange oil, which solidified under vacuum after several

hours. The solid residue was then washed with cold (–33 °C) pentane (3 x 1 mL), and was dried under reduced pressure to afford **2-L5**. Yield: 26.2 mg (14%). Additional **2-L5** could be isolated by removing the volatiles from the retained pentane washings, washing the resulting yellow solid with cold (–33 °C) pentane (2 x 1 mL), and drying under reduced pressure. Yield: 33.5 mg (17%). Combined Yield: 59.7 mg (31%). ^{1}H NMR (500 MHz, $CDCl_3$): δ 7.82-7.81 (m, 1H), 7.54 (br d, J = 5.8 Hz, 1H), 7.33–7.28 (m, 2H), 1.94–1.05 (m, 40H, overlapping Cy and *t*-Bu resonances, with the latter at 1.21, d, J_{PH} = 11.4 Hz). ^{13}C{^{1}H} NMR (126 MHz, $CDCl_3$): δ 146.3–145.6 (overlapping m), 135.7, 133.1 (d, J_{PC} = 6.9 Hz), 127.8, 126.7, 35.9 (dd, J_{PC} = 17.1, 5.0 Hz), 33.6 (dd, J_{PC} = 26.6, 4.1), 31.1 (d, J_{PC} = 14.7), 30.8 (d, J_{PC} = 16.2 Hz), 29.7 (d, J_{PC} = 9.4 Hz), 27.6–27.5 (overlapping d), 26.6. ^{31}P{^{1}H} NMR (203 MHz, $CDCl_3$): δ 17.9 (d, J_{PP} = 156.0 Hz), -9.9 (d, J_{PP} = 156.0 Hz). HRMS-ESI (*m/z*): Calc'd for $C_{26}H_{45}P_2$ $[M+H]^+$: 419.2996. Found: 419.2991.

Synthesis of (2-L3)NiCl$_2$. A glass vial was charged with $NiCl_2$(DME) (85.7 mg, 0.390 mmol), **2-L3** (200.0 mg, 0.409 mmol), THF (2 mL), and a magnetic stir bar. Stirring was initiated, affording initially a clear, dark orange solution. A red-brown precipitate formed after several minutes. The resulting mixture was stirred at room temperature for 2 hours, after which time the solid was collected on a glass filter frit in air and washed with cold (~0 °C) pentane (2 x 2 mL). The remaining solid was then dissolved off the frit using CH_2Cl_2 (10 mL), and the clear, dark red solution thus formed was collected. The volatiles were removed from the collected eluent solution under reduced pressure, yielding the target complex as a dark red-brown solid. Yield: 0.224 g (93%). ^{1}H NMR (500 MHz, $CDCl_3$): δ 8.32 (d, J = 7.6 Hz, 1H), 7.72 (d, J = 7.2 Hz, 1H), 7.68–7.62 (m, 2H), 4.02 (d, J = 13.5 Hz, 1H), 2.74–2.65 (m, 3H), 2.53 (d, J = 13.4 Hz, 1H), 2.31 (d, J = 14.0 Hz, 1H), 2.00–1.93 (m, 1H), 1.87–1.11 (overlapping m, 31H). ^{13}C{^{1}H} NMR (126 MHz, $CDCl_3$): δ 141.2, 139.0, 134.9, 132.4 (two signals), 131.8, 97.1 (d, J_{PC} = 64.7 Hz), 74.7, 53.6, 41.1, 40.2, 38.5, 37.3, 29.9 (d, J_{PC} = 13.6 Hz), 29.5, 28.9 (d, J_{PC} = 7.9 Hz), 27.6, 27.3–27.1 (m, overlapping signals), 26.8, 26.4, 25.8 (d, J_{PC} = 6.1 Hz). ^{31}P{^{1}H} NMR (203 MHz, $CDCl_3$): δ 75.8 (br s), 46.4 (br s). Anal. Calc'd. for $C_{28}H_{42}Cl_2NiO_3P_2$: C, 54.40; H, 6.85; N, 0. Found: C, 54.76; H, 6.72; N, <0.5.

Synthesis of (2-L3)Ni(*o*-tolyl)Cl, **2-C3**. A glass vial was charged with (**2-L3**)$NiCl_2$ (150.0 mg, 0.243 mmol), THF (2.5 mL), and a magnetic stir bar, yielding a clear, dark orange

solution. Stirring was initiated, then (*o*-tolyl)MgCl (277 μL of a 0.920 M solution in THF, 0.255 mmol) was added dropwise to the stirring solution over ~1-2 min., yielding a hazy, orange mixture upon complete addition. The mixture was allowed to stir at room temperature for 2 h, after which time the reaction mixture was quenched with MeOH (2 mL) in air. The volatiles were removed from the clear, orange solution under reduced pressure, yielding a pale-orange solid, which was dried under reduced pressure for ~1 h (unoptimized). The solid was then dissolved in CH_2Cl_2 (5 mL), cooled to ~0 °C, then filtered through Celite, eluting with cold (~0 °C) CH_2Cl_2 (2 x 3 mL). The volatiles were removed from the clear, orange filtrate under reduced pressure yielding the target complex as an orange solid. Yield: 0.153 g (93%). Anal. Calc'd. for $C_{35}H_{49}ClNiO_3P_2$: C, 62.38; H, 7.33; N, 0. Found: C, 62.71; H, 7.47; N, <0.5. A single crystal suitable for X-ray diffraction was obtained by slow evaporation of pentane into a toluene solution of **2-C3** at ~4 °C. As outlined in the text (**Figure 2.3** and **2.4**), complex **2-C3** (as prepared above) exists as four diastereomers in solution, whereas recrystallized samples, when dissolved in solution, initially feature only two of these diastereomers. Even in the latter case, the solution ^{1}H and $^{13}C\{^{1}H\}$ NMR spectra for **2-C3** are sufficiently complex so as to preclude meaningful assignment, given the C_1-symmetric nature of each diastereomer of **2-C3**; these and related spectra are provided for reference in the Appendices. Bulk **2-C3**: $^{31}P\{^{1}H\}$ NMR (203 MHz, $CDCl_3$): δ 53.0 (d, J_{PP} = 10.6 Hz), 52.0 (*d*, J_{PP} = 10.5 Hz), 49.55 (d, J_{PP} = 20.3 Hz), 49.47 (d, J_{PP} = 20.6 Hz), 34.9 (d, J_{PP} = 20.8 Hz), 34.5 (d, J_{PP} = 20.3 Hz), 20.4 (d, J_{PP} = 10.6 Hz), 19.1 (d, J_{PP} = 10.5 Hz). Recrystallized **2-C3**: $^{31}P\{^{1}H\}$ NMR (203 MHz, $CDCl_3$): δ 53.0 (d, J_{PP} = 10.4 Hz), 52.0 (d, J_{PP} = 10.2 Hz), 20.4 (d, J_{PP} = 10.4 Hz), 19.1 (d, J_{PP} = 10.3 Hz). Further spectroscopic experiments conducted on **2-C3** include: $^{31}P\{^{1}H\}$-$^{31}P\{^{1}H\}$ COSY (**Figure A12**), time-lapsed $^{31}P\{^{1}H\}$ NMR spectra of recrystallized **2-C3** (**Figure A13**), elevated-temperature $^{31}P\{^{1}H\}$ NMR (in $C_2D_2Cl_4$, **Figure A14)**, and $^{31}P\{^{1}H\}$ NMR saturation transfer experiments (**Figure A15**), which are discussed in Section 2.3.2.

Synthesis of (2-L4)$NiCl_2$. A glass vial was charged with THF (2.6 mL), $NiCl_2$(DME) (57.8 mg, 0.263 mmol), **2-L4** (200.0 mg, 0.276 mmol), and a magnetic stir bar, yielding a cloudy, purple mixture. The mixture was then stirred magnetically at room temperature for 2 hours, after which time the purple solid was collected on a glass filter frit in air and washed with cold (~0 °C) pentane (2 x 2 mL). The solid was dissolved off the frit using CH_2Cl_2 (15

mL), and was collected. The volatiles were removed from the clear, dark purple solution under reduced pressure, yielding the target complex a dark purple solid. Yield: 0.132 g (89%). ^{1}H NMR (500 MHz, $CDCl_3$): δ 8.03 (d, *J* = 7.6 Hz, 1H), 7.66 (t, *J* = 7.0 Hz, 1H), 7.56–7.53 (m, 1H), 7.47 (d, *J* = 7.0 Hz, 1H), 7.41–7.37 (m, 2H), 7.34 (d, *J* = 7.3 Hz, 1H), 7.24 (s, 1H), 7.21–7.18 (m, 1H), 7.15 (d, *J* = 7.4 Hz, 1H), 7.01 (t, *J* = 6.8 Hz, 1H), 6.31 (d, *J* = 6.1 Hz, 1H), 3.62 (br s, 3H), 2.55 (br s, 3H), 1.77 (br s, 9H), 1.30 (br s, 9H). ^{13}C{^{1}H} NMR (126 MHz, $CDCl_3$): δ 145.6, 142.9, 137.7, 136.0, 135.8, 133.8, 133.3, 132.6, 132.2, 131.94, 131.87, 131.7, 128.5, 126.7, 126.3, 126.0, 41.4, 39.7, 31.8, 31.0, 27.0, 23.9. ^{31}P{^{1}H} NMR (203 MHz, $CDCl_3$): δ 126.6 (br s), 90.7 (br s). Anal. Calc'd. for $C_{28}H_{36}Cl_2NiP_2$: C, 59.61; H, 6.43; N, 0. Found: C, 59.76; H, 6.01; N, <0.5.

Synthesis of (2-L4)Ni(*o*-tolyl)Cl, **2-C4**. A glass vial was charged with (**2-L4**)$NiCl_2$ (40.0 mg, 0.0709 mmol), THF (2 mL), and a magnetic stir bar, yielding a cloudy, purple mixture. Stirring was initiated, then (*o*-tolyl)MgCl (92.5 μL of a 0.920 M solution in THF, 0.0851 mmol) was added dropwise (~30 s/drop) to the stirring mixture, affording a clear, brown-orange solution upon complete addition. The solution was then allowed to stir at room temperature for 18 h (unoptimized), after which time the now darker-colored solution was quenched with MeOH (1.5 mL) in air. The volatiles were removed under reduced pressure, yielding a brown-orange solid residue, which was dried further under reduced pressure for ~1 h (unoptimized). CH_2Cl_2 (5 mL) was then added, and the cloudy, orange mixture was cooled to ~0 °C, and filtered through Celite, eluting with cold (~0 °C) CH_2Cl_2 (3 x 2 mL). The volatiles were removed from the clear, orange-brown filtrate under reduced pressure, yielding a brown-orange solid. The solid was washed with cold (~0 °C) pentane (2 x 1 mL) and dried under reduced pressure to afford the target complex. Yield: 0.040 g (91%). Anal. Calc'd. for $C_{34}H_{43}ClNiP_2$: C, 67.82; H, 6.99; N, 0. Found: C, 67.58; H, 7.04; N, <0.5. A single crystal suitable for X-ray diffraction was obtained by slow evaporation of pentane into a CH_2Cl_2 solution of **2-C4** at ~4 °C. As outlined in the text, complex **2-C4** exists in solution as two diastereomers, where temperature-dependent line broadening due to hindered rotation and/or dynamic equilibria involving tetrahedral and square planar species, is also apparent. As such, the solution ^{1}H and ^{13}C{^{1}H} NMR spectra for **2-C4** are sufficiently complex so as to preclude meaningful assignment; these spectra, as well as variable-temperature ^{31}P{^{1}H} NMR for **2-C4** (**Figure A22**), are provided for reference in

Appendix 3. $^{31}P\{^{1}H\}$ NMR (203 MHz, $CDCl_3$): δ 69.9 (s), 66.9 (d, J_{PP} = 8.9 Hz), 55.4 (br s), 49.2 (br s).

Synthesis of (2-L5)NiCl$_2$. A glass vial was charged with $NiCl_2$(DME) (30.0 mg, 0.137 mmol), **2-L5** (60.0 mg, 0.143 mmol), THF (1.5 mL), and a magnetic stir bar. Stirring was initiated, yielding a cloudy, red-orange mixture after several minutes. The mixture was allowed to stir at room temperature for 2 h, after which time the mixture was filtered onto a glass filter frit in air, and the collected orange solid was washed with cold (~0 °C) pentane (2 x 1 mL). The solid was washed off the frit using CH_2Cl_2 (10 mL), and the volatiles were removed from the slightly hazy, red-orange filtrate yielding an orange solid residue. The solid residue was dissolved in a minimal amount of CH_2Cl_2 and filtered through a short Celite plug. The volatiles were removed from the clear, red filtrate yielding the target complex as an orange solid. Yield 0.044 g (56%). ^{1}H NMR (500 MHz, $CDCl_3$): δ 7.95 (br d, J = 6.7 Hz, 1H), 7.70 (br d, J = 6.3 Hz, 1H), 7.61–7.57 (m, 2H), 2.64-2.57 (overlapping m, 4H), 1.86–1.77 (overlapping m, 8H), 1.70–1.67 (m, 2H), 1.63 (d, J_{PH} = 13.1 Hz, 18H), 1.57 (br s, 2H), 1.36-1.18 (overlapping m, 6H). $^{13}C\{^{1}H\}$ NMR (126 MHz, $CDCl_3$): δ 135.0, 132.2, 131.2, 130.7, 39.6 (d, J_{PC} = 13.2 Hz), 38.4 (d, J_{PC} = 26.7 Hz), 31.8, 30.7, 29.6, 27.5, 26.0. $^{31}P\{^{1}H\}$ NMR (203 MHz, $CDCl_3$): δ 91.9 (br s), 64.4 (br s). Anal. Calc'd. for $C_{26}H_{44}Cl_2NiP_2$: C, 56.97; H, 8.09; N, 0. Found: C, 56.69; H, 7.83; N, <0.5.

Synthesis of (2-L5)Ni(*o*-tolyl)Cl, **2-C5**. A glass vial was charged with (**2-L5**)$NiCl_2$ (35.0 mg, 0.0638 mmol), THF (1 mL), and a magnetic stir bar, yielding a cloudy, red-orange mixture. Stirring was initiated and (*o*-tolyl)MgCl (72.9 μL of a 0.920 M solution in THF, 0.0670 mmol) was then added dropwise (~30 s/drop) to the stirring solution, yielding a clear, orange solution upon complete addition. After several minutes, a yellow precipitate formed. The resulting cloudy, yellow mixture was then stirred at room temperature for 18 h (unoptimized), after which time the reaction was quenched with MeOH (2 mL) in air. The volatiles were removed under reduced pressure, yielding a yellow solid residue, which was dried further under vacuum for ~1.5 h. To the residue was added CH_2Cl_2 (5 mL), and the hazy, yellow mixture was cooled to ~0 °C, and filtered through Celite, eluting with cold (~0 °C) CH_2Cl_2 (2 x 3 mL). The volatiles were removed from the clear, orange-yellow filtrate, yielding the target complex as an orange-yellow solid. Yield: 0.034 g (87%). A single crystal suitable for X-ray diffraction was obtained by slow evaporation of a THF

solution of **2-C5** at room temperature. ^{1}H NMR (500 MHz, $CDCl_3$): δ 8.05–8.03 (m, 1H), 7.66–7.64 (m, 1H), 7.55–7.52 (m, 2H), 7.27-7.25 (overlapping m with $CHCl_3$, 1H), 6.87–6.85 (m, 1H), 6.79–6.75 (m, 2H), 3.13–3.11 (m, 1H), 3.05 (s, 3H), 2.65–2.58 (m, 1H), 2.22–2.14 (m, 1H), 1.86–1.77 (m, 3H), 1.72–1.69 (m, 2H), 1.64–1.58 (m, 10H), 1.53–1.49 (m, 14H), 1.43–1.40 (m, 1H), 1.20–1.00 (m, 6H), 0.41–0.33 (m, 1H). ^{13}C{^{1}H} NMR (126 MHz, $CDCl_3$): δ 144.1, 142.1, 135.4, 135.1 (d, J_{PC} = 12.1 Hz), 131.5 (d, J_{PC} = 14.3 Hz), 130.2, 129.6, 127.9, 124.3, 122.5, 37.5 (d, J_{PC} = 7.9 Hz), 37.1, 36.9, 33.8, 33.6, 32.1, 34.8 (d, J_{PC} = 4.2 Hz), 31.1 (d, J_{PC} = 4.4 Hz), 28.5, 27.7–27.5 (overlapping d), 26.3, 26.1 (d, J_{PC} = 11.4 Hz). ^{31}P{^{1}H} NMR (203 MHz, $CDCl_3$): δ 69.3 (d, J_{PP} = 15.5 Hz), 49.0 (d, J_{PP} = 15.3 Hz). Anal. Calc'd. for $C_{33}H_{51}ClNiP_2$: C, 65.64; H, 8.51; N, 0. Found: C, 65.27; H, 8.24; N, <0.5.

2.5.4 Procedures for the Nickel-Catalyzed *N*-Arylation of Cyclopropylamine

General Procedure for Pre-Catalyst Screening. In a nitrogen-filled glovebox, pre-catalyst (0.0036 mmol, 3 mol %), NaO*t*-Bu (17.3 mg, 0.18 mmol, 1.5 equiv), (hetero)aryl chloride (0.12 mmol, 1.0 equiv), toluene (1 mL), and cyclopropylamine (12.5 μL, 0.18 mmol, 1.5 equiv) were consecutively added to a 1 dram, screw-capped vial, followed by a magnetic stir bar. The vial was then sealed with a cap containing a PTFE septum and the reaction mixture was allowed to stir at room temperature for 16 h (unoptimized). After this time, the vial was removed from the glovebox, and an aliquot of the reaction mixture was filtered through a short Celite/silica plug, diluted with EtOAc (~1.5 mL), and subjected to GC analysis.

General Procedure for the *N*-Arylation of Cyclopropylamine Using (Hetero)aryl (Pseudo)halides at Room Temperature (GPA). In a nitrogen-filled glovebox, pre-catalyst (3 mol %), NaO*t*-Bu (1.5 equiv), (hetero)aryl (pseudo)halide (1.0 equiv), toluene, and cyclopropylamine (1.5 equiv) were consecutively added to a 4 dram, screw-capped vial, followed by a magnetic stir bar. The vial was then sealed with a cap containing a PTFE septum and the reaction mixture was allowed to stir at room temperature for 16 h (unoptimized). After this time, the vial was removed from the glovebox, and the crude reaction mixture was diluted with EtOAc or CH_2Cl_2 (10 mL) and filtered through Celite, eluting with additional solvent (2 x 10 mL). The volatiles were removed from the filtrate

under reduced pressure, and the resulting residue was purified by use of automated flash chromatography.

General Procedure for the *N*-Arylation of Cyclopropylamine Using (Hetero)aryl (Pseudo)halides at Elevated Temperatures (GPB). In a nitrogen-filled glovebox, **2-C3** (25.2 mg, 0.0375 mmol, 5 mol %), K_3PO_4 (3.0 equiv), (hetero)aryl (pseudo)halide (1.0 equiv), 1,4-dioxane or toluene, and cyclopropylamine (1.5 equiv) were consecutively added to a 4 dram, screw-capped vial, followed by a magnetic stir bar. The vial was then sealed with a cap containing a PTFE septum, removed from the glovebox, and placed in a temperature-controlled, aluminum heating block set to 110 °C. The mixture was stirred this temperature for 16 h (unoptimized), after which time the vial was removed from the heat source and allowed to cool to room temperature. The reaction mixture was then diluted with CH_2Cl_2 (10 mL) and filtered through Celite, eluting with additional CH_2Cl_2 (2 x 10 mL). The volatiles were removed from the filtrate under reduced pressure, and the resulting residue was purified by use of automated flash chromatography.

General Procedure for the *N*-Arylation of Small Cyclic Ammonium Salts Using Aryl (Pseudo)halides (GPC). In a nitrogen-filled glovebox, pre-catalyst (5 mol %), NaO*t*-Bu (2.5 equiv), solid (hetero)aryl (pseudo)halide (1.0 equiv), amine hydrochloride (1.1 equiv), and toluene were consecutively added to a 4 dram, screw-capped vial, followed by a magnetic stir bar. Liquid (hetero)aryl (pseudo)halides were added after the amine hydrochloride. The vial was then sealed with a cap containing a PTFE septum and allowed to stir at room temperature for 16 h (unoptimized). After this time, the vial was removed from the glovebox, and the crude reaction mixture was diluted with EtOAc or CH_2Cl_2 (10 mL) and filtered through Celite, eluting with additional solvent (2 x 10 mL). The volatiles were removed from the filtrate under reduced pressure and the resulting residue was purified by use of flash chromatography on silica gel.

General Procedure for the (Pseudo)halide Competition Studies. In a nitrogen-filled glovebox, **2-C3** (2.4 mg, 0.0036 mmol, 3 mol %), NaO*t*-Bu (17.3 mg, 0.18 mmol, 1.5 equiv), aryl halide 1 (1.0 equiv), aryl (pseudo)halide 2 (1.0 equiv), toluene (1 mL), and cyclopropylamine (12.5 μL, 0.18 mmol, 1.5 equiv) were consecutively added to a 1 dram, screw-capped vial, followed by a magnetic stir bar. The vial was then sealed with a cap containing a PTFE septum and the reaction mixture was allowed to stir at room temperature

for 16 h (unoptimized). After this time, the vial was removed from the glovebox, and a 367 μL aliquot of the reaction mixture was filtered through a short Celite/silica plug, diluted with EtOAc (~1.5 mL), and subjected to GC analysis.

Reaction Monitoring of the Nickel-Catalyzed *N*-Arylation of Cyclopropylamine. In a nitrogen-filled glovebox, **2-C3** (10.1 mg, 0.015 mmol, 5 mol %), NaO*t*-Bu (72.1 mg, 0.75 mmol, 1.5 equiv), 3-chloropyridine (47.5 μL, 0.5 mmol, 1.0 equiv), and toluene (4.17 mL) were consecutively added to a 4 dram, screw-capped vial, followed by a magnetic stir bar. 4-Chloroanisole (100 μL of a 0.5 M solution in toluene, 0.05 mmol, 10 mol % *or* 61.2 μL, 0.5 mmol, 1.0 equiv) was also added at this time, as appropriate. Finally, cyclopropylamine (52.0 μL, 0.75 mmol, 1.5 equiv) was added, and the vial was sealed with a cap containing a PTFE septum. The reaction was allowed to stir at room temperature for the indicated time, at which point 100 μL aliquots of the reaction mixture were taken, diluted with EtOAc, filtered through a short Celite/silica plug, and analyzed by use of GC methods employing dodecane as an internal standard.

2.5.5 Synthesis and Characterization of Cross-Coupled Products

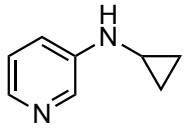

***N*-cyclopropylpyridin-3-amine** (**2-3a**). GPA was followed using **2-C3** (15.2 mg, 0.0225 mmol), NaO*t*-Bu (108.1 mg, 1.125 mmol), 3-chloropyridine (71.3 μL, 0.75 mmol), toluene (6.25 mL), cyclopropylamine (77.9 μL, 1.125 mmol), and CH_2Cl_2. After automated flash chromatography (50–100% EtOAc in hexanes), the title compound was obtained as an off-white solid (0.089 g, 88%). ^{1}H NMR (500 MHz, $CDCl_3$): δ 8.15 (br s, 1H), 7.99 (br s, 1H), 7.085–7.079 (br m, 2H), 4.20 (br s, 1H), 2.45-2.41 (app sept, 1H), 0.78-0.75 (m, 2H), 0.54–0.51 (m, 2H). ^{13}C{^{1}H} NMR (126 MHz, $CDCl_3$): δ 144.7, 139.4, 136.4, 123.7, 119.3, 25.0, 7.6. Spectroscopic data are consistent with those previously reported.[80]

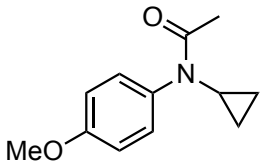

***N*-cyclopropyl-*N*-(4-methoxyphenyl)acetamide** (**2-3b**). GPA was followed using **2-C4** (13.9 mg, 0.0225 mmol), NaO*t*-Bu (108.1 mg, 1.125 mmol), 4-chloroanisole (91.9 μL, 0.75 mmol), toluene (6.25 mL), cyclopropylamine (77.9 μL, 1.125 mmol) and EtOAc. After 16 h, acetic anhydride (213 μL, 2.25 mmol) was added. The sealed reaction mixture was then removed from the glovebox and placed in a temperature-controlled, aluminum heating block set to 50 °C. The mixture was stirred at this temperature for 2 h, after which time the vial was removed from the heat source and allowed to cool to room temperature. The crude reaction mixture was then diluted with CH_2Cl_2 (10 mL) and filtered through Celite, eluting with additional CH_2Cl_2 (2 x 10 mL). The volatiles were removed from the filtrate under reduced pressure, and the resulting residue was purified by flash chromatography on silica gel (90% EtOAc in hexanes), affording the title compound as a light-purple oil (0.127 g, 82 %). ^{1}H NMR (300.1 MHz, $C_2D_2Cl_4$, 343 K): δ 7.02–6.98 (m, 2H), 6.94-6.90 (m, 2H), 3.84 (s, 3H), 3.22–3.14 (app sept, 1H), 1.98 (br s, 3H), 0.82–0.76 (m, 2H), 0.53-0.47 (m, 2H). ^{13}C{^{1}H} NMR (75.5 MHz, $C_2D_2Cl_4$, 343 K): δ 172.0, 158.4, 134.7, 128.8, 114.4, 55.4, 31.0, 23.1, 7.4. Spectroscopic data are consistent with those previously reported (in $CDCl_3$).[82]

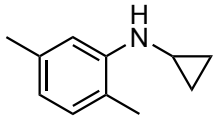

***N*-cyclopropyl-2,5-dimethylaniline** (**2-3c**). GPA was followed using **2-C3** (15.2 mg, 0.0225 mmol), NaO*t*-Bu (108.1 mg, 1.125 mmol), 2-chloro-1,4-dimethylbenzene (101 μL, 0.75 mmol), toluene (6.25 mL), cyclopropylamine (77.9 μL, 1.125 mmol), and EtOAc. After automated flash chromatography (0–5% EtOAc in hexanes), the title compound was obtained as pale-yellow oil (0.076 g, 63%). ^{1}H NMR (500 MHz, $CDCl_3$): δ 6.93 (d, J = 7.4 Hz, 1H), 6.87 (s, 1H), 6.52 (d, J = 7.4 Hz, 1H), 3.97 (br s, 1H), 2.46–2.42 (app sept, 1H), 2.33 (s, 3H), 2.06 (s, 3H), 0.78–0.75 (m, 2H), 0.56-0.53 (m, 2H). ^{13}C{^{1}H} NMR (126 MHz,

$CDCl_3$): δ 146.7, 136.7, 129.9, 118.8, 118.1, 112.1, 25.5, 21.7, 17.0 7.7. HRMS-ESI (*m/z*): Calc'd for $C_{11}H_{16}N$ $[M+H]^+$: 162.1283. Found: 162.1277.

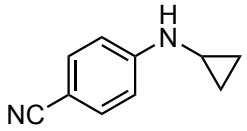

4-(cyclopropylamino)benzonitrile (**2-3d**). GPA was followed using **2-C3** (15.2 mg, 0.0225 mmol), NaO*t*-Bu (108.1 mg, 1.125 mmol), 4-chlorobenzonitrile (103.2 mg, 0.75 mmol), toluene (6.25 mL), cyclopropylamine (77.9 μL, 1.125 mmol), and EtOAc. After automated flash chromatography (0–5% EtOAc in hexanes), the title compound was obtained as a white solid (0.106 g, 89%). ^{1}H NMR (500 MHz, $CDCl_3$): δ 7.42 (d, J = 8.7 Hz, 2H), 6.74 (d, J = 8.7 Hz, 2H), 4.62 (br s, 1H), 2.48-2.44 (m, 1H), 0.82–0.79 (m, 2H), 0.56-0.53 (m, 2H). ^{13}C{^{1}H} NMR (126 MHz, $CDCl_3$): δ 152.1, 133.7, 120.6, 112.9, 99.5, 24.8, 7.7. Spectroscopic data are consistent with those previously reported.[81c]

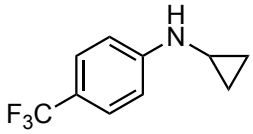

***N*-cyclopropyl-4-(trifluoromethyl)aniline** (**2-3e**). GPA was followed using **2-C3** (15.2 mg, 0.0225 mmol), NaO*t*-Bu (108.1 mg, 1.125 mmol), 4-chlorobenzotrifluoride (100 μL, 0.75 mmol), toluene (6.25 mL), cyclopropylamine (77.9 μL, 1.125 mmol), and CH_2Cl_2. After automated flash chromatography (0–5% EtOAc in hexanes), the title compound was obtained as a pale-yellow oil (0.106 g, 70%). ^{1}H NMR (500 MHz, $CDCl_3$): δ 7.43 (d, J = 8.5 Hz, 2H), 6.80 (d, J = 8.6 Hz, 2H), 4.45 (br s, 1H), 2.49-2.45 (app sept, 1H), 0.81–0.78 (m, 2H), 0.56–0.53 (m, 2H). ^{13}C{^{1}H} NMR (126 MHz, $CDCl_3$): δ 151.5, 126.7 (q, J_{CF} = 3.6 Hz), 125.3 (q, J_{CF} = 270.3 Hz), 119.6 (q, J_{CF} = 32.6 Hz), 112.6, 25.2 7.8. Spectroscopic data are consistent with those previously reported.[81a]

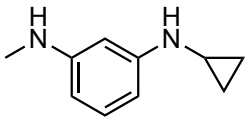

***N*^{1}-cyclopropyl-*N*^{3}-methylbenzene-1,3-diamine** (**2-3f**). GPA was followed using **2-C3** (15.2 mg, 0.0225 mmol), NaO*t*-Bu (108.1 mg, 1.125 mmol), *N*-methyl-3-chloroaniline (91.9 μL, 0.75 mmol), toluene (6.25 mL), cyclopropylamine (77.9 μL, 1.125 mmol), and

EtOAc. After automated flash chromatography (0–10% MeOH in CH_2Cl_2), the title compound was isolated as a yellow oil (0.080 g, 66%). ^{1}H NMR (500 MHz, $CDCl_3$): δ 7.03 (t, *J* = 8.0 Hz, 1H), 6.21-6.19 (m, 1H), 6.11 (t, *J* = 2.2 Hz, 1H), 6.08 (dd, *J* = 8.0, 1.6 Hz, 1H), 4.10 (br s, 1H), 3.66 (br s, 1H), 2.84 (s, 3H), 2.46–2.42 (app sept, 1H), 0.73–0.70 (m, 2H), 0.54–0.51 (m, 2H). ^{13}C{^{1}H} NMR (126 MHz, $CDCl_3$): δ 150.6, 150.0, 129.9, 103.3, 102.9, 97.3, 30.9, 25.4, 7.5. HRMS-ESI (*m/z*): Calc'd for $C_{10}H_{15}N_2$ $[M+H]^+$: 163.1235. Found: 163.1230.

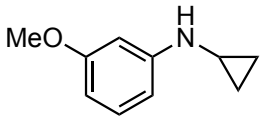

***N*-cyclopropyl-3-methoxyaniline** (**2-3g**). GPA was followed using **2-C3** (15.2 mg, 0.0225 mmol), NaO*t*-Bu (108.1 mg, 1.125 mmol), 3-methoxyphenyl 4-methylbenzenesulfonate (208.7 mg, 0.75 mmol), toluene (6.25 mL), cyclopropylamine (77.9 μL, 1.125 mmol), and EtOAc *or* **2-C3** (10.1 mg, 0.015 mmol), NaO*t*-Bu (72.1 mg, 0.75 mmol), 3-methoxyphenyl dimethylsulfamate (115.6 mg, 0.5 mmol), toluene (4.17 mL), cyclopropylamine (52.0 μL, 0.75 mmol), and CH_2Cl_2. With the aryl chloride, after automated flash chromatography (0-10% EtOAc in hexanes), the title compound was obtained as a yellow oil (0.085 g, 69%). With the aryl sulfamate, after automated flash chromatography (10–30% EtOAc in hexanes), the title compound was obtained as a pale-yellow oil (0.056 g, 69%). ^{1}H NMR (500 MHz, $CDCl_3$): δ 7.09 (t, *J* = 7.9 Hz, 1H), 6.40–6.39 (m, 2H), 6.33–6.31 (m, 1H), 4.45 (br s, 1H), 3.79 (s, 3H), 2.45–2.41 (app sept, 1H), 0.74–0.71 (m, 2H), 0.55–0.52 (m, 2H). ^{13}C{^{1}H} NMR (126 MHz, $CDCl_3$): δ 160.9, 150.3, 129.9, 106.5, 102.9, 99.3, 55.2, 25.3, 7.5. Spectroscopic data are consistent with those previously reported.[80]

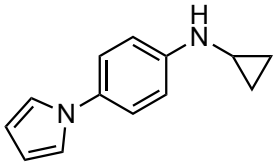

***N*-cyclopropyl-4-(1*H*-pyrrol-1-yl)aniline** (**2-3h**). GPA was followed using **2-C4** (13.9 mg, 0.0225 mmol), NaO*t*-Bu (108.1 mg, 1.125 mmol), 4-(1*H*-pyrrol-1-yl)phenyl 4-methylbenzenesulfonate (235.0 mg, 0.75 mmol), toluene (6.25 mL), cyclopropylamine (77.9 μL, 1.125 mmol), and CH_2Cl_2. After automated flash chromatography (20–50%

EtOAc in hexanes), the title compound was obtained as a brown-orange solid (0.101 g, 68%). ^{1}H NMR (500 MHz, $CDCl_3$): δ 7.25–7.22 (m, 2H), 6.99 (t, *J* = 2.2 Hz, 2H), 6.85–6.82 (m, 2H), 6.32 (t, *J* = 2.2 Hz, 2H), 4.30 (br s, 1H), 2.49-2.45 (app sept, 1H), 0.79–0.75 (m, 2H), 0.57-0.54 (m, 2H). ^{13}C{^{1}H} NMR (126 MHz, $CDCl_3$): δ 147.1, 132.4, 122.5, 119.9, 113.7, 109.4, 25.5, 7.6. HRMS-ESI (*m/z*): Calc'd for $C_{13}H_{15}N_2$ $[M+H]^+$: 199.1235. Found: 199.1230.

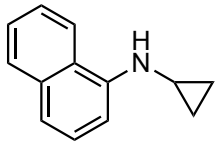

***N*-cyclopropylnaphthalen-1-amine** (**2-3i**). GPA was followed using **2-C3** (15.2 mg, 0.0225 mmol), NaO*t*-Bu (108.1 mg, 1.125 mmol), 1-chloronaphthalene (102 μL, 0.75 mmol), toluene (6.25 mL), cyclopropylamine (77.9 μL, 1.125 mmol), and EtOAc. After automated flash chromatography (0–5% EtOAc in hexanes), the title compound was obtained as a yellow oil (0.110 g, 80%). Additionally, GPB was followed using **2-C3** (15.2 mg, 0.0225 mmol), K_3PO_4 (286.6 mg, 1.35 mmol), napthalen-1-yl trifluoromethanesulfonate (124.3 mg, 0.45 mmol), toluene (7.5 mL), cyclopropylamine (46.8 μL, 0.675 mmol), and CH_2Cl_2. After automated flash chromatography, the title compound was obtained as an orange oil (0.050 g, 61%). ^{1}H NMR (500 MHz, $CDCl_3$): δ 7.80–7.78 (m, 1H), 7.72 (d, *J* = 8.2 Hz, 1H), 7.44–7.37 (m, 3H), 7.27 (d, *J* = 8.3 Hz, 1H), 7.07 (d, *J* = 7.5 Hz, 1H), 4.86 (br s, 1H), 2.61–2.57 (app sept, 1H), 0.87-0.83 (m, 2H), 0.66–0.63 (m, 2H). ^{13}C{^{1}H} NMR (126 MHz, $CDCl_3$): δ 144.0, 134.4, 128.8, 126.7, 126, 124.8, 123.4, 119.8, 117.9, 106.0, 25.6, 7.7. Spectroscopic data are consistent with those previously reported.[80]

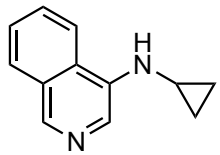

***N*-cyclopropylisoquinolin-4-amine** (**2-3j**). GPA was followed using **2-C3** (15.2 mg, 0.0225 mmol), NaO*t*-Bu (108.1 mg, 1.125 mmol), 4-bromoisoquinoline (156.0 mg, 0.75 mmol), toluene (6.25 mL), cyclopropylamine (77.9 μL, 1.125 mmol), and CH_2Cl_2. After automated flash chromatography (50–100% EtOAc in hexanes), the title compound was obtained as an off-white solid (0.119 g, 86%). ^{1}H NMR (500 MHz, $CDCl_3$): δ 8.73 (br s,

1H), 8.29 (br s, 1H), 7.90 (d, J = 8.1 Hz, 1H), 7.70 (d, J = 8.4 Hz, 1H), 7.63–7.60 (m, 1H), 7.55 (t, J = 7.1 Hz, 1H), 4.75 (br s, 1H), 2.64-2.60 (app sept, 1H), 0.89–0.86 (m, 2H), 0.67–0.64 (m, 2H). $^{13}C\{^{1}H\}$ NMR (126 MHz, $CDCl_3$): δ 142.7 138.2, 129.0, 128.5, 128.1, 126.9, 126, 125.1, 119.1, 25.4 7.9. HRMS-ESI (*m/z*): Calc'd for $C_{12}H_{13}N_2$ $[M+H]^+$: 185.1079. Found: 185.1073.

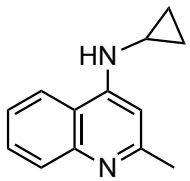

***N*-cyclopropyl-2-methylquinolin-4-amine** (**2-3k**). GPA was followed using **2-C3** (15.2 mg, 0.0225 mmol), NaO*t*-Bu (108.1 mg, 1.125 mmol), 4-chloroquinaldine (151 μL, 0.75 mmol), toluene (6.25 mL), cyclopropylamine (77.9 μL, 1.125 mmol), and CH_2Cl_2 *or* **2-C3** (10.1 mg, 0.015 mmol), NaO*t*-Bu (72.1 mg, 0.75 mmol), 2-methylquinolin-4-yl diethyl carbamate (129.2 mg, 0.5 mmol), toluene (4.17 mL), cyclopropylamine (52.0 μL, 0.75 mmol), and CH_2Cl_2. With the aryl chloride, after automated flash chromatography (50–100% EtOAc in hexanes), the obtained off-white solid was washed with EtOAc (3 x 1 mL) and dried under reduced pressure, affording the title compound as a white solid (0.108 g, 73%). The volatiles were removed from the retained washings, yielding a white-yellow solid. This solid was washed with cold (~0 °C) EtOAc (2 x 2 mL) and dried under reduced pressure, affording the title compound as a white solid (0.029 g, 19%). Total yield: 0.137 g (92%). With the aryl carbamate, after automated flash chromatography (0–10% MeOH in CH_2Cl_2), the title compound was obtained as an off-white solid (0.062 g, 63%). ^{1}H NMR (500 MHz, $CDCl_3$): δ 7.91 (d, J = 8.4 Hz, 1H), 7.61–7.57 (m, 2H), 7.36–7.33 (m, 1H), 6.76 (s, 1H), 5.29 (br s, 1H), 2.65 (s, 3H), 2.63–2.58 (m, 1H), 0.92–0.89 (m, 2H), 0.68–0.65 (m, 2H). $^{13}C\{^{1}H\}$ NMR (126 MHz, $CDCl_3$): δ 159.7, 150.4, 148.4, 129.4, 129.1, 124.0, 119.1, 117.4, 101.0, 26.0, 24.8, 7.7. HRMS-ESI (*m/z*): Calc'd for $C_{13}H_{15}N_2$ $[M+H]^+$: 199.1235. Found: 199.1230.

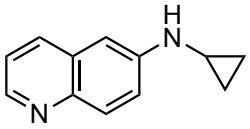

***N*-cyclopropylquinolin-6-amine** (**2-3l**). GPB was followed using **2-C3** (25.3 mg, 0.0375 mmol), K_3PO_4 (477.6 mg, 2.25 mmol), quinolin-6-yl methanesulfonate (167.4 mg, 0.75 mmol), 1,4-dioxane (6.25 mL), cyclopropylamine (77.9 μL, 1.125 mmol), and CH_2Cl_2. After automated flash chromatography (70–100% EtOAc in hexanes), the title compound was obtained as a yellow solid (0.092 g, 67%). ^{1}H NMR (500 MHz, $CDCl_3$): δ 8.62 (dd, *J* = 4.2, 1.5 Hz, 1H), 7.95 (d, *J* = 8.2 Hz, 1H), 7.88 (d, *J* = 9.0 Hz, 1H), 7.27–7.24 (m, 1H), 7.11 (dd, *J* = 9.0, 2.6 Hz, 1H), 7.02 (d, *J* = 2.5 Hz, 1H), 4.48 (br s, 1H), 2.55–2.51 (app sept, 1H), 0.83–0.79 (m, 2H), 0.59–0.56 (m, 2H). ^{13}C{^{1}H} NMR (126 MHz, $CDCl_3$): δ 146.8, 146.4, 143.6 134.1, 130.25, 130.17, 121.4, 121.2, 104.5, 25.4, 7.6. HRMS-ESI (*m/z*): Calc'd for $C_{12}H_{13}N_2$ $[M+H]^+$: 185.1079. Found: 185.1073.

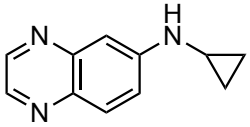

***N*-cyclopropylquinoxalin-6-amine** (**2-3m**). GPA was followed using **2-C3** (15.2 mg, 0.0225 mmol), NaO*t*-Bu (108.1 mg, 1.125 mmol), 6-chloroquinoxaline (123.4 mg, 0.75 mmol), toluene (6.25 mL), cyclopropylamine (77.9 μL, 1.125 mmol), and EtOAc. After automated flash chromatography (20–50% EtOAc in hexanes), the title compound was obtained as a yellow solid (0.122 g, 88%). ^{1}H NMR (500 MHz, $CDCl_3$): δ 8.64 (s, 1H), 8.51 (d, *J* = 1.5 Hz, 1H), 7.83 (d, *J* = 9.1 Hz, 1H), 7.31 (d, *J* = 2.5 Hz, 1H), 7.14 (dd, *J* = 9.1, 2.5 Hz, 1H), 4.72 (br s, 1H), 2.59–2.55 (app sept, 1H), 0.87–0.83 (m, 2H), 0.61–0.58 (m, 2H). ^{13}C{^{1}H} NMR (126 MHz, $CDCl_3$): δ 149.9, 145.4, 145.0, 140.6, 138.4, 130.1, 122.0, 105.3, 25.3, 7.7. HRMS-ESI (*m/z*): Calc'd for $C_{11}H_{12}N_3$ $[M+H]^+$: 186.1031. Found: 186.1026.

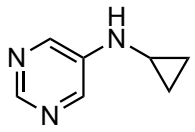

***N*-cyclopropylpyrimidin-5-amine** (**2-3n**). GPA was followed using **2-C3** (15.2 mg, 0.0225 mmol), NaO*t*-Bu (108.1 mg, 1.125 mmol), 5-bromopyrimidine (119.2 mg, 0.75

mmol), toluene (6.25 mL), cyclopropylamine (77.9 μL, 1.125 mmol), and CH_2Cl_2. After automated flash chromatography (50–100% EtOAc in hexanes), the title compound was obtained as a white solid (0.083 g, 82%). ^{1}H NMR (500 MHz, $CDCl_3$): δ 8.61 (s, 1H), 8.25 (s, 2H), 4.33 (br s, 1H), 2.47–2.43 (m, 1H), 0.82–0.79 (m, 2H), 0.56–0.53 (m, 2H). $^{13}C\{^1H\}$ NMR (126 MHz, $CDCl_3$): δ 149.2, 142.3, 141.4, 24.6, 7.7. Spectroscopic data are consistent with those previously reported.[82]

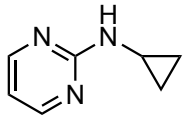

***N*-cyclopropylpyrimidin-2-amine** (**2-3o**). GPA was followed using **2-C3** (15.2 mg, 0.0225 mmol), NaO*t*-Bu (108.1 mg, 1.125 mmol) 2-chloropyrimidine (85.9 mg, 0.75 mmol), toluene (6.25 mL), cyclopropylamine (77.9 μL, 1.125 mmol), and CH_2Cl_2. After automated flash chromatography (5–50% EtOAc in hexanes), the title compound was obtained as a white solid (0.073 g, 72%). ^{1}H NMR (500 MHz, $CDCl_3$): δ 8.33 (br s, 2H), 6.58 (t, J = 4.6 Hz, 1H), 5.55 (br s, 1H), 2.79–2.74 (m, 1H), 0.85–0.82 (m, 2H), 0.57–0.53 (m, 2H). $^{13}C\{^1H\}$ NMR (126 MHz, $CDCl_3$): δ 163.5, 158.2, 111.2, 24.0, 7.5. Spectroscopic data are consistent with those previously reported.[98]

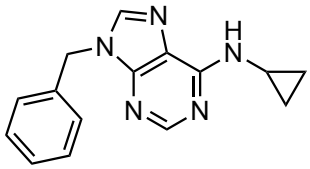

9-benzyl-*N*-cyclopropyl-9*H*-purin-6-amine (**2-3p**). GPA was followed using **2-C3** (15.2 mg, 0.0225 mmol), NaO*t*-Bu (108.1 mg, 1.125 mmol), 9-benzyl-6-chloropurine (183.5 mg, 0.75 mmol), toluene (6.25 mL), cyclopropylamine (77.9 μL, 1.125 mmol), and CH_2Cl_2. After automated flash chromatography (50–100% EtOAc in hexanes), the title compound was obtained as a white solid (0.166 g, 83%). Though this compound has been previously reported,[99] complete characterization data were not obtained. ^{1}H NMR (500 MHz, $CDCl_3$): δ 8.52 (s, 1H), 7.71 (s, 1H), 7.35–7.26 (m, 5H), 5.99 (br s, 1H), 5.36 (s, 2H). 3.05 (br s, 1H), 0.94–0.90 (m, 2H), 0.66–0.63 (m, 2H). $^{13}C\{^1H\}$ NMR (126 MHz, $CDCl_3$): δ 156.0, 153.6, 149.6, 139.9, 135.8, 129.2, 128.5, 127.9, 120.0, 47.3, 23.9, 7.6. HRMS-ESI (*m/z*): Calc'd for $C_{15}H_{16}N_5$ $[M+H]^+$: 266.1406. Found: 266.1400.

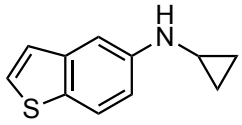

***N*-cyclopropylbenzo[*b*]thiophen-5-amine** (**2-3q**). GPA was followed using **2-C3** (15.2 mg, 0.0225 mmol), NaO*t*-Bu (108.1 mg, 1.125 mmol), 5-chlorobenzo[*b*]thiophene (126.5 mg, 0.75 mmol), toluene (6.25 mL), cyclopropylamine (77.9 μL, 1.125 mmol), and EtOAc. After automated flash chromatography (0–5% EtOAc in hexanes), the title compound was obtained as a pale-yellow oil (0.115 g, 81%). ^{1}H NMR (500 MHz, $CDCl_3$): δ 7.64 (d, J = 8.6 Hz, 1H), 7.38 (d, J = 5.4 Hz, 1H), 7.27 (d, J = 2.0 Hz, 1H), 7.20 (d, J = 5.4 Hz, 1H), 6.81 (dd, J = 8.6, 2.0 Hz, 1H), 4.21 (br s, 1H), 2.51–2.47 (app sept, 1H), 0.79–0.76 (m, 2H), 0.58–0.55 (m, 2H). ^{13}C{^{1}H} NMR (126 MHz, $CDCl_3$): δ 146.3, 141.1, 129.8, 126.9, 123.5, 122.8, 113.9, 105.7, 25.8, 7.6. HRMS-ESI (*m/z*): Calc'd for $C_{11}H_{12}NS$ $[M+H]^+$: 190.0690. Found: 190.0685.

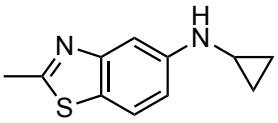

***N*-cyclopropyl-2-methylbenzo[*d*]thiazol-5-amine** (**2-3r**). GPA was followed using **2-C3** (15.2 mg, 0.0225 mmol), NaO*t*-Bu (108.1 mg, 1.125 mmol), 5-chloro-2-methylbenzothiazole (137.7 mg, 0.75 mmol), toluene (6.25 mL), cyclopropylamine (77.9 μL, 1.125 mmol), and CH_2Cl_2. After automated flash chromatography (0–30% EtOAc in hexanes), the title compound was isolated as an orange oil, which solidified under reduced pressure (0.114 g, 74%). ^{1}H NMR (500 MHz, $CDCl_3$): δ 7.52 (d, J = 8.6 Hz, 1H), 7.43 (d, J = 2.0 Hz, 1H), 6.76 (dd, J = 8.6, 2.0, 1H), 4.30 (br s, 1H), 2.77 (s, 3H), 2.48–2.44 (app sept, 1H), 0.76–0.73 (m, 2H), 0.54–0.52 (m, 2H). ^{13}C{^{1}H} NMR (126 MHz, $CDCl_3$): δ 167.6, 155.2, 148.0, 124.7, 121.5, 113.5, 105.2, 25.7, 20.3, 7.6. Spectroscopic data are consistent with those previously reported.[82]

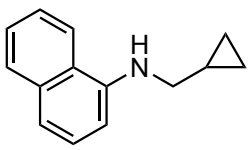

***N*-(cyclopropylmethyl)napthalen-1-amine** (**2-5a**). GPC was followed using **2-C3** (25.3 mg, 0.0375 mmol), NaO*t*-Bu (180.2 mg, 1.875 mmol) 1-chloronapthalene (102 μL, 0.75

mmol), cyclopropanemethylamine hydrochloride (88.8 mg, 0.825 mmol), toluene (6.25 mL), and EtOAc. After flash chromatography on silica gel (hexanes (150 mL), then 5% EtOAc in hexanes), the title compound was obtained as a yellow oil (0.113 g, 76%). ^{1}H NMR (500 MHz, $CDCl_3$): δ 7.90–7.88 (m, 1H), 7.81–7.79 (m, 1H), 7.48–7.44 (m, 2H), 7.35 (t, *J* = 7.9 Hz, 1H), 7.25 (d, *J* = 8.2 Hz, 1H), 6.60 (d, *J* = 7.5 Hz, 1H), 4.56 (br s, 1H), 3.13 (d, *J* = 7 Hz, 2H), 1.30–1.24 (m, 1H), 0.66–0.62 (m, 2H), 0.35–0.32 (m, 2H). ^{13}C{^{1}H} NMR (126 MHz, $CDCl_3$): δ 143.8, 134.4, 128.7, 126.7, 126, 124.7, 123.5, 120.0, 117.4, 104.5, 49.5, 10.9, 3.7. HRMS-ESI (*m/z*): Calc'd for $C_{14}H_{16}N$ $[M+H]^+$: 198.1283. Found: 198.1277.

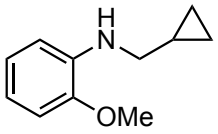

***N*-(cyclopropylmethyl)-2-methoxyaniline** (**2-5b**). GPC was followed using **2-C4** (23.2 mg, 0.0375 mmol), NaO*t*-Bu (180.2 mg, 1.875 mmol), 2-chloroanisole (95.2 μL, 0.75 mmol), cyclopropanemethylamine hydrochloride (88.8 mg, 0.825 mmol), toluene (6.26 mL), and EtOAc. After flash chromatography on silica (hexanes (200 mL), then 5% EtOAc in hexanes), the title compound was obtained as a yellow oil (0.098 g, 74%). ^{1}H NMR (500 MHz, $CDCl_3$): δ 6.87 (td, *J* = 7.7, 1.3 Hz, 1H), 6.78 (dd, *J* = 7.9, 1.2 Hz, 1H), 6.68 (td, *J* = 7.7, 1.5, 1H), 6.61 (dd, *J* = 7.8, 1.4 Hz, 1H), 4.41 (br s, 1H), 3.87 (s, 3H), 2.99 (d, *J* = 6.9 Hz, 2H), 1.19–1.11 (m, 1H), 0.59–0.55 (m, 2H), 0.28–0.25 (m, 2H). ^{13}C{^{1}H} NMR (126 MHz, $CDCl_3$): δ 147.0, 138.6, 121.4, 116.5, 110.1, 109.5, 55.5, 49.0, 11.0, 3.7. HRMS-ESI (*m/z*): Calc'd for $C_{11}H_{16}NO$ $[M+H]^+$: 178.1232. Found: 178.1226.

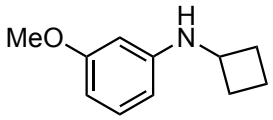

***N*-cyclobutyl-3-methoxyaniline** (**2-6a**). GPC was followed using **2-C3** (20.2 mg, 0.030 mmol), NaO*t*-Bu (144.2 mg, 1.5 mmol), 3-methoxyphenyl 4-methylbenzenesulfonate (167.0 mg, 0.6 mmol), cyclobutylamine hydrochloride (71.0 mg, 0.66 mmol), toluene (5.0 mL), and CH_2Cl_2. After flash chromatography on silica gel (10% EtOAc in hexanes), the title compound was obtained as a pale-yellow oil (0.046 g, 43%). ^{1}H NMR (500 MHz, $CDCl_3$): δ 7.08 (t, *J* = 8.1 Hz, 1H), 6.28 (dd, *J* = 8.1, 2.3 Hz, 1H), 6.19 (dd, *J* = 8.0, 2.0 Hz,

1H), 6.12 (t, J = 2.3 Hz, 1H), 3.95–3.86 (overlapping m, 2H), 3.78 (s, 3H), 2.46–2.41 (m, 2H), 1.87–1.76 (m, 4H). $^{13}C\{^{1}H\}$ NMR (126 MHz, $CDCl_3$): δ 161.0, 148.8, 130.1, 106.3, 102.6, 99.1, 55.2, 49.1, 31.4, 15.4. HRMS-ESI (*m/z*): Calc'd for $C_{11}H_{16}NO$ $[M+H]^+$: 178.1232. Found: 178.1226.

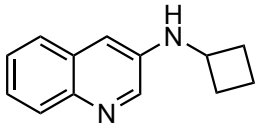

***N*-cyclobutylquinolin-3-amine** (**2-6b**). GPC was followed using **2-C3** (25.3 mg, 0.0375 mmol), NaO*t*-Bu (180.2 mg, 1.875 mmol), 3-bromoquinoline (101.8 μL, 0.75 mmol), cyclobutylamine hydrochloride (88.8 mg, 0.825 mmol), toluene (6.25 mL), and CH_2Cl_2. After flash chromatography on silica gel (20% EtOAc in hexanes (150 mL), then 50% EtOAc in hexanes (150 mL), then 70% EtOAc in hexanes), the title compound was obtained as a yellow solid (0.087 g, 59%). ^{1}H NMR (500 MHz, $CDCl_3$): δ 8.40 (d, J = 2.8 Hz, 1H), 7.94–7.92 (m, 1H), 7.61–7.59 (m, 1H), 7.43–7.38 (m, 2H), 6.93 (d, J = 2.7 Hz, 1H), 4.17 (br s, 1H), 4.03–3.99 (m, 1H), 2.55–2.50 (m, 2H), 1.96–1.83 (m, 4H). $^{13}C\{^{1}H\}$ NMR (126 MHz, $CDCl_3$): δ 143.4, 142.2, 140.6, 129.7, 129.1, 127.0, 126.0, 125.0, 110.8, 48.9, 31.0, 15.5. HRMS-ESI (*m/z*): Calc'd for $C_{13}H_{15}N_2$ $[M+H]^+$: 199.1235. Found: 199.1230.

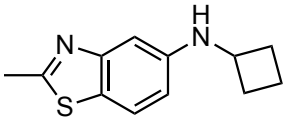

***N*-cyclobutyl-2-methylbenzo[*d*]thiazol-5-amine** (**2-6c**). GPC was followed using **2-C3** (25.3 mg, 0.0375 mmol), NaO*t*-Bu (180.2 mg, 1.875 mmol), 5-chloro-2-methylbenzothiazole (137.7 mg, 0.75 mmol), cyclobutylamine hydrochloride (88.8 mg, 0.825 mmol), toluene (6.25 mL), and EtOAc. After flash chromatography on silica gel (20% EtOAc in hexanes (150 mL), then 30% EtOAc in hexanes (100 mL), then 50% EtOAc in hexanes), the title compound was obtained as an orange solid (0.113 g, 69%). ^{1}H NMR (500 MHz, $CDCl_3$): δ 7.52 (d, J = 8.6 Hz, 1H), 7.07 (d, J = 2.3 Hz, 1H), 6.64 (dd, J = 8.6, 2.3 Hz, 1H), 3.98–3.95 (overlapping m, 2H), 2.77 (s, 3H), 2.50–2.45 (m, 2H), 1.89–1.80 (m, 4H). $^{13}C\{^{1}H\}$ NMR (126 MHz, $CDCl_3$): δ 167.6, 155.2, 146.4, 124.2, 121.6,

113.7, 104.7, 49.4, 31.2, 20.2, 15.5. HRMS-ESI (*m/z*): Calc'd for $C_{12}H_{15}N_2S$ $[M+H]^+$: 219.0956. Found: 219.0950.

2.5.6 Large-Scale Synthesis of 2-3a and 2-3d

Large-scale Synthesis of 2-3a. In a nitrogen-filled glovebox, an oven-dried 100 mL round-bottom flask was charged with **2-C3** (171.8 mg, 0.255 mmol), NaO*t*-Bu (1.225 g, 12.75 mmol), 3-chloropyridine (808 μL, 8.5 mmol), toluene (70 mL), and cyclopropylamine (883 μL, 12.75 mmol), followed by a magnetic stir bar. The flask was sealed with a rubber septum, and the reaction mixture was allowed to stir at room temperature for 16 h (unoptimized). After this time, the mixture was diluted with CH_2Cl_2 (120 mL) in air, and filtered through Celite, eluting with additional CH_2Cl_2 (2 x 100 mL). The filtrate was concentrated to ~20 mL under reduced pressure, and the resulting brown/orange mixture was purified by automated flash chromatography (100 g Biotage SNAP KP-SIL cartridge, 50–100% EtOAc in hexanes, 40 mL/min flow rate), affording the title compound as a white solid (1.004 g, 88%).

Large-scale Synthesis of 2-3d. In a nitrogen-filled glovebox, an oven-dried 100 mL round-bottom flask was charged with **2-C3** (171.8 mg, 0.255 mmol), NaO*t*-Bu (1.225 g, 12.75 mmol), 4-chlorobenzonitrile (1.169 g, 8.5 mmol), toluene (70 mL), and cyclopropylamine (883 μL, 12.75 mmol), followed by a magnetic stir bar. The flask was sealed with a rubber septum, and the reaction mixture was allowed to stir at room temperature for 16 h (unoptimized). After this time, the mixture was diluted with EtOAc (120 mL) in air, and filtered through Celite, eluting with additional EtOAc (2 x 100 mL). The filtrate was concentrated to ~20 mL under reduced pressure, and the resulting orange solution was purified by automated flash chromatography (100 g Biotage SNAP KP-SIL cartridge, 0–5% EtOAc in hexanes, 25–60 mL/min flow rate), affording the title compound as an off-white solid (1.223 g, 91%).

Chapter 3: Exploiting Ancillary Ligation to Enable Nickel-Catalyzed C(sp^2)–O Cross-Couplings of Aryl Electrophiles with Aliphatic Alcohols

3.1 Contributions

The nickel-catalyzed C(sp^2)–O cross-coupling of (hetero)aryl (pseudo)halides with aliphatic alcohols using pre-catalysts (PAd-DalPhos)Ni(*o*-tolyl)Cl (**2-C1**) and (CyPAd-DalPhos)Ni(*o*-tolyl)Cl (**2-C3**) is discussed in this chapter. Preston M. MacQueen, a fellow PhD student, conducted some of the catalytic experiments (including optimization) pertaining to primary aliphatic alcohols and the pre-catalyst competition experiments between linear, primary amines and primary alcohols. Carlos Diaz, a visiting PhD student, assisted Preston and the author in performing catalytic experiments using primary and secondary alcohols and phenols. Otherwise, the author was responsible for conducting the majority of the catalytic experiments (including optimization) pertaining to secondary alcohols, tertiary alcohols, and phenols, as well as the pre-catalyst competition experiments between primary and secondary aliphatic alcohols and between α-branched primary amines and secondary alcohols. The contributions of each author are noted throughout the text and are labelled as such throughout the chapter. This work has been published: J. Am. Chem. Soc., 2018, 140, 5023-5027.

3.2 Introduction

3.2.1 Palladium-Catalyzed C(sp^2)–O Cross-Coupling

Like C–N bonds, C(sp^2)–O (herein C–O) bonds, are common structural features in pharmaceuticals and natural products,[100] with C(sp^2)–O–C(sp^3) connections in particular appearing prevalently in such compounds. The nucleophilic substitution of alkyl halides with phenols through the Williamson ether synthesis[101] affords the desired C(sp^2)–O–C(sp^3) linkages, but complementary methodologies employing readily available (hetero)aryl halides and aliphatic alcohols can provide alternate disconnections that may be preferable in certain applications (e.g., when the alkyl halide is not commercially available or is difficult to prepare). Conventional methods that utilize such compounds include nucleophilic aromatic substitution reactions,[102] as well as copper catalysis (including the Ullman ether synthesis[103]),[104] but these procedures are generally limited to the use of activated (hetero)aryl bromide and iodide electrophiles under forcing reaction conditions. Thus, palladium-catalyzed C–O cross-coupling, like its C–N bond-forming

counterpart (see Section 1.2), has provided opportunities to expand the scope of this transformation, allowing the use of (hetero)aryl chlorides, under milder reaction conditions.

The mechanism of palladium-catalyzed cross-coupling of aryl halides and aliphatic alcohols (**Figure 3.1**)[105] is conceptually similar to that of BHA (see **Figure 1.2**). Firstly, oxidative addition of the aryl halide to a ligated Pd(0) species affords a Pd(II) aryl intermediate (**I**). Next, alcohol coordination followed by deprotonation generates a Pd(II) alkoxo complex (**II**), which undergoes reductive elimination to furnish the desired alkyl aryl ether. However, unlike in BHA, the rate of β-H elimination from the Pd(II) alkoxo intermediate **II** is competitive with product-forming reductive elimination, creating a possible equilibrium with a Pd(II) aryl hydride species (**III**). Reductive elimination from this intermediate affords the hydrodehalogenated product of the aryl halide (**IV**), while also liberating the carbonyl of the oxidized alcohol and regenerating catalytically active Pd(0).

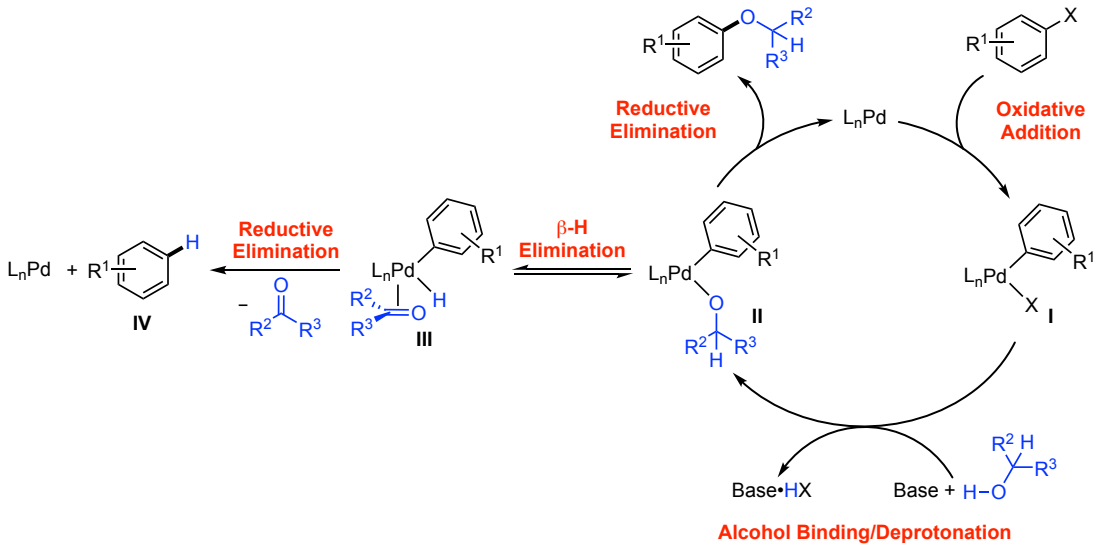

Figure 3.1. General mechanism of palladium-catalyzed C–O cross-coupling.

The potential for unproductive catalysis in palladium-catalyzed C–O cross-coupling has prompted the application of highly sterically encumbered ancillary ligands to promote C–O reductive elimination and minimize deleterious β-H elimination. Buchwald and co-workers[106] have developed several ancillary ligands that successfully facilitate this transformation. In particular, the use of a $[Pd(allyl)Cl]_2$/RockPhos catalyst system allowed for the cross-coupling of a variety of (hetero)aryl bromides and chlorides with both primary and secondary aliphatic alcohols at moderate temperatures (90 ºC; **Scheme 3.1A**).[106c] The

introduction of a methyl group at the C6-position of the upper aryl ring of the RockPhos ligand (vs. a methoxy group, cf. *t*-BuBrettPhos in **Figure 1.3**) was thought to enforce conformational rigidity of ligated palladium intermediates, enhancing the rate of reductive elimination. More recently, Buchwald and co-workers[106d] have disclosed palladium pre-catalysts incorporating *t*-BuBrettPhos and AdCyBrettPhos for the cross-coupling of primary aliphatic alcohols with (hetero)aryl bromides and chlorides under milder reaction temperatures (25–80 ºC; **Scheme 3.1B**).

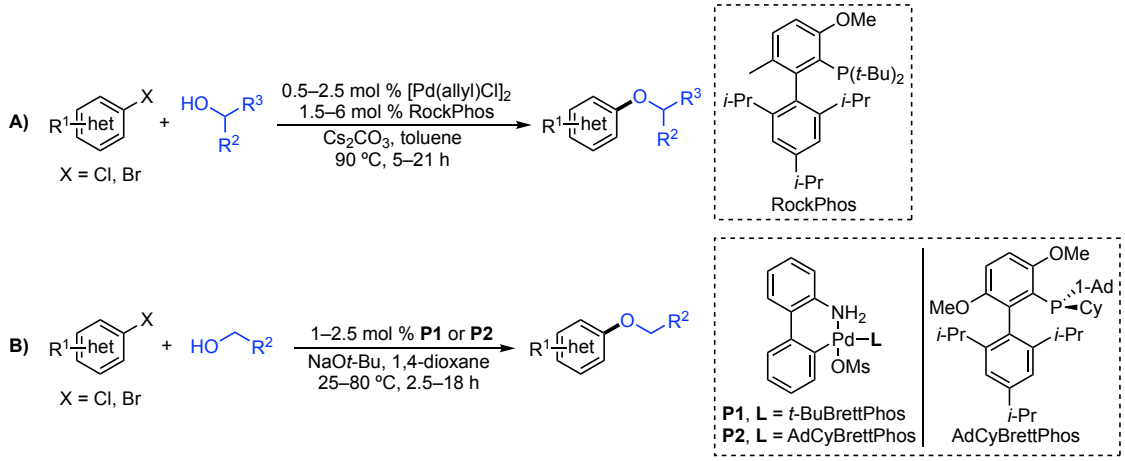

Scheme 3.1. Palladium-catalyzed C–O cross-couplings of primary and secondary alcohols developed by Buchwald and co-workers.

Another notable example of palladium-catalyzed cross-coupling of primary alcohols with (hetero)aryl bromides and chlorides was reported by Beller and co-workers.[105] A $Pd(OAc)_2$/Ad-BippyPhos catalyst system facilitated C–O cross-coupling under mild conditions (1 mol % Pd, 80 ºC), and tolerated various base-sensitive functional groups, including nitrile, ester, and aldehyde moieties. Notably, diols containing both primary and secondary or tertiary hydroxy groups could be employed in this reaction, with the primary site reacting preferentially with a high degree of chemoselectivity (99%).

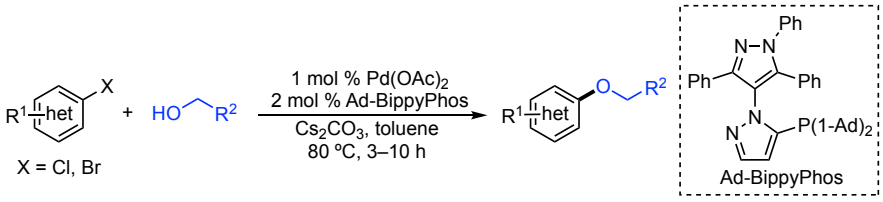

Scheme 3.2. Palladium-catalyzed C–O cross-coupling of primary aliphatic alcohols developed by Beller and co-workers.

Scientists at Merck have also disclosed a catalyst system for palladium-catalyzed C–O cross-coupling.[107] Mixtures of $Pd_2(dba)_3$ and CyPF-*t*-Bu (see **Figure 1.4**) effected the cross-coupling of activated (hetero)aryl chlorides and bromides with primary and secondary aliphatic alcohols at moderate to elevated temperatures (80–140 ºC), with quinoline, isoquinoline, pyrazolopyrimidine, and pyridine electrophiles being well-tolerated. Additionally, tertiary alcohols such as 1-adamantanol and 1-methylcyclopentanol could be employed in this transformation, reacting with 4-chloroquinaldine at 135 ºC using $[Pd(allyl)Cl]_2$ as the palladium source and THF as solvent.

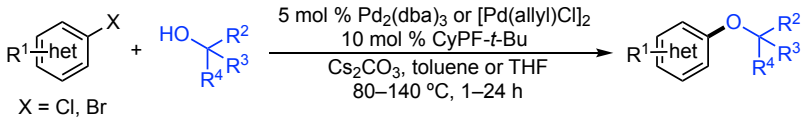

Scheme 3.3. Palladium-catalyzed C–O cross-coupling of primary, secondary, and tertiary alcohols developed by scientists at Merck.

3.2.2 Nickel-Catalyzed C(sp^2)–O Cross-Coupling

While the development of nickel-catalyzed alternatives to palladium-catalyzed cross-coupling reactions (including C–N cross-coupling reactions, see Section 1.3) has become increasingly of interest, reports of nickel-catalyzed C–O cross-coupling are exceedingly rare. MacMillan and co-workers[108] disclosed the first examples of nickel-catalyzed C–O cross-coupling in 2015, employing a dual nickel/photoredox catalysis strategy[42] to facilitate the desired transformation (see **Scheme 1.5** for the related C–N cross-coupling reaction). The rationale behind this methodology arises from seminal stoichiometric experiments conducted by Hillhouse and co-workers,[109] whereby C–O reductive elimination from a Ni(II) alkoxide could not be induced thermally; C–O reductive elimination was only observed to occur upon oxidation to a higher-valent Ni(III) alkoxide. Furthermore, computational studies on complexes of the form *cis*-$(PH_3)_2M(CH_3)(OH)$ (M = Ni, Pd, Pt) suggested that C–O reductive elimination from the Ni(II) alkoxide was thermodynamically unfavourable.[110] From these studies, MacMillan and co-workers hypothesized that, assuming an initial mechanism similar to that of palladium-catalyzed C–O cross-coupling (see **Figure 3.1**), oxidation of the putative Ni(II) aryl alkoxo intermediate to a Ni(III) aryl alkoxo species using an appropriate photocatalyst would engender facile C–O reductive elimination and enable nickel-catalyzed C–O cross-coupling (though Nocera and co-workers[111] later ruled out this mechanistic paradigm on

the basis of thorough spectroscopic and catalytic experiments). Thus, using a catalyst system comprised of $NiCl_2$(DME), dtbbpy, quinuclidine, and an Ir photocatalyst (**Ir-1**), a variety of (hetero)aryl bromides could be successfully cross-coupled with primary and secondary aliphatic alcohols at room temperature under blue light irradiation (**Scheme 3.4**). Light and **Ir-1** were crucial for the success of this reaction, as demonstrated in stoichiometric experiments examining reductive elimination from a (dtbbpy)Ni(aryl)(alkoxo) complex; product formation was not observed in the absence of light (with **Ir-1** present), nor in the absence of **Ir-1** under blue light irradiation.

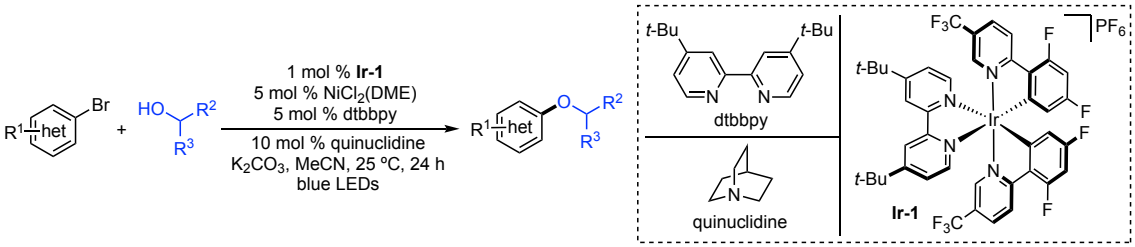

Scheme 3.4. Nickel/photoredox-catalyzed C–O cross-coupling developed by Macmillan and co-workers.

Following the study by MacMillan and co-workers, several other examples of C–O cross-coupling using dual nickel/photoredox catalysis have been reported. Xiao and co-workers[112] prepared phenolic glycosides from protected sugars and aryl bromides using catalyst mixtures of $NiCl_2$(DME), dtbbpy, and **Ir-1** (**Scheme 3.5A**), and accomplished the desymmetric intramolecular synthesis of chiral 1,4-benzodioxanes using a related catalyst system incorporating a dtbbpy variant with axial chirality (**Scheme 3.5B**).[113] Alternate photocatalysts have also been successfully applied in place of **Ir-1** to facilitate this transformation. The organic photocatalyst 4DPAIPN was used in conjunction with $NiBr_2$(DME) and dtbbpy by scientists at Merck to cross-couple primary and secondary alcohols with aryl bromide-containing, short-chain peptides under blue light irradiation.[114] This methodology could also be extended to the intramolecular macrocyclization of peptides (**Scheme 3.5C**). Heterogeneous and semi-heterogeneous photocatalysts, including CdS and a carbon nitride material prepared by polymerization of urea and oxamide (CN-OA-m), have been employed in cross-coupling reactions of (hetero)aryl bromides and primary and secondary aliphatic alcohols (**Scheme 3.5D**) by Xiao and co-workers[115] and Pieber and co-workers[116] respectively, demonstrating comparable scope to the initial system developed by MacMillan and co-workers.

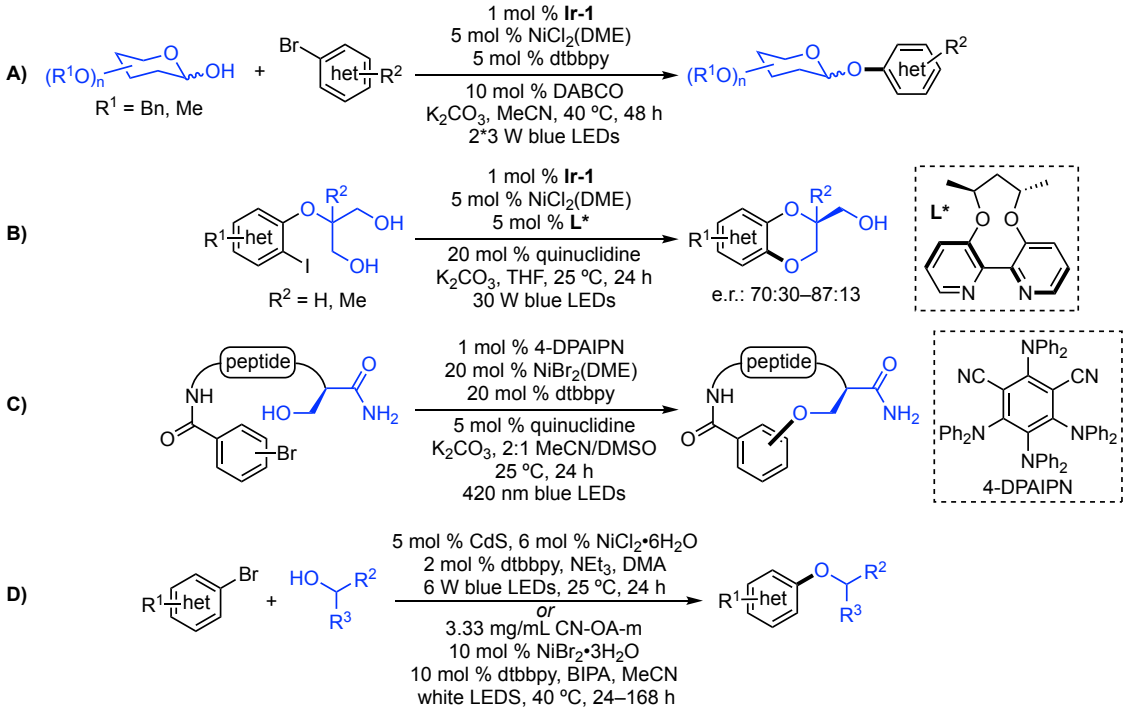

Scheme 3.5. Dual nickel/photoredox-catalyzed C–O cross-couplings reported by: A) and B) Xiao, C) Merck scientists, and D) Xiao/Pieber.

Despite the efficacy of such nickel/photoredox methodologies for C–O cross-coupling, all reported catalyst systems are limited to the use of activated (hetero)aryl bromide and/or iodide electrophiles. Furthermore, many of these systems utilize expensive, iridium photocatalysts, effectively negating the inherent sustainability and cost benefits of a base metal-catalyzed process. The previous success of PAd-DalPhos (**2-L1**, see Section 1.3.1) and CyPAd-DalPhos (**2-L3**, see Chapter 2) in mediating nickel-catalyzed C–N cross-coupling reactions suggested that these tailored ancillary ligands might also be suitable for effecting related C–O cross-couplings. In particular, the use of **2-L1**- and **2-L3**-ligated nickel pre-catalysts (**2-C1** and **2-C3** respectively) might allow for the use of inexpensive and readily available (hetero)aryl chloride and (pseudo)halide electrophiles in this transformation, providing complementary reactivity to existing nickel/photoredox systems

3.3 Results and Discussion

3.3.1 Screening Nickel Pre-Catalysts in the Cross-Coupling of 1-Chloronaphthalene and Isopropanol – Reaction Optimization

The investigation began by screening various nickel pre-catalysts in the cross-coupling of 1-chloronaphthalene (**3-1a**) and 2-propanol (**3-2a**) to form **3-3a** (**Table 3.1**).

The pre-catalysts of interest contained ligands that had previously proven effective for related C–N cross-coupling reactions, namely PAd-DalPhos (**2-L1**), CyPAd-DalPhos (**2-L3**), dppf (**3-L1**), and IPr (**3-L2**). (**2-L3**)Ni(*o*-tolyl)Cl (**2-C3**) provided the greatest conversion to **3-3a** using NaO*t*-Bu and toluene at 110 ºC (entry 2), while (**2-L1**)Ni(o-tolyl)Cl (**2-C1**), (**3-L1**)Ni(o-tolyl)Cl (**3-C1**), and (**3-L2**)Ni(styrene)$_2$ (**3-C2**) afforded negligible amounts of **3-3a** (entries 1, 3, and 4). Significant amounts of the hydrodehalogenated product, naphthalene ($C_{10}H_8$), were observed in these reactions; lowering the temperature to 80 ºC in an effort to mitigate hydrodehalogenation, while effective in the reactions using **2-C1** and **2-C3**, also reduced product formation (entries 5-8). Replacing NaO*t*-Bu with the weak base Cs_2CO_3, which had been successfully employed in palladium-catalyzed C–O cross-coupling (see **Section 3.2.1**), resulted in modest conversion to **3-3a** using **2-C1** (entry 9) at 110 ºC, but negligible C–O bond formation using the other pre-catalysts (entries 10–12). However, the use of Cs_2CO_3 decreased $C_{10}H_8$ formation significantly in all reactions.

Further optimization focused on improving conversion to **3-3a** using the optimal pre-catalyst **2-C3**. The addition of boron reagents such as PhB(OH)$_2$[117] or PhB(pin)[56] in related nickel-catalyzed cross-coupling reactions led to enhanced catalytic activity in prior reports, likely by converting off-cycle, odd-electron intermediates into those that are productive, but did not increase conversion to **3-3a** under these conditions (entries 13 and 14). Gratifyingly, increasing the amount of **3-2a** from 1.1 to 3.0 equivalents afforded greater conversion to **3-3a** (entry 15), likely due to the increased concentration of **3-2a** in solution (especially given its volatility (b.p. = 82 ºC) at 110 ºC), though this enhancement did not extend to the other pre-catalysts that were screened (entries 16-18). Increasing the catalyst loading of **2-C3** from 5 mol % to 7.5 or 10 mol % did not furnish **3-3a** in greater amounts (entries 19 and 20), but employing 5.0 equivalents of **3-2a** did improve conversion (entry 21).

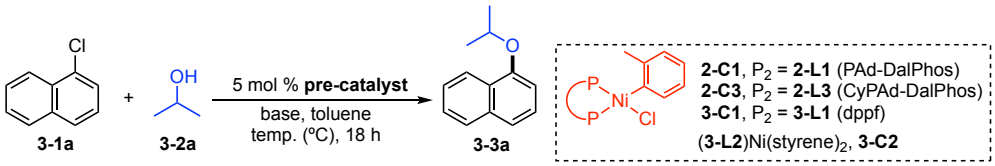

Entry	Pre-catalyst	Base	Temp. (°C)	Additive	**3-3a** (%)[a]	Remaining **3-1a** (%)[a]	$C_{10}H_8$ (%)[a]
1	**2-C1**	NaO*t*-Bu	110	-	<5	25	65
2	**2-C3**				45	10	35
3	**3-C1**				<5	<5	80
4	**3-C2**				<5	<5	80
5	**2-C1**	NaO*t*-Bu	80	-	<5	55	30
6	**2-C3**				<5	90	<5
7	**3-C1**				<5	<5	85
8	**3-C2**				<5	<5	75
9	**2-C1**	Cs_2CO_3	110	-	25	60	10
10	**2-C3**				<5	80	10
11	**3-C1**				<5	95	<5
12	**3-C2**				<5	80	20
13	**2-C3**	NaO*t*-Bu	110	$PhB(OH)_2$[b]	20	<5	55
14				PhB(pin)[b]	30	<5	60
15[c]	**2-C3**	NaO*t*-Bu	110	-	60	<5	30
16[c]	**2-C1**				10	<5	85
17[c]	**3-C1**				<5	15	80
18[c]	**3-C2**				<5	<5	80
19[c,d]	**2-C3**	NaO*t*-Bu	110	-	60	<5	30
20[c,e]					60	<5	30
21[f]					75	<5	20

Table 3.1. Optimization of the nickel-catalyzed cross-coupling of **3-1a** and **3-2a**. General conditions: pre-catalyst (5 mol %), base (1.5 equiv), **3-1a** (0.12 mmol, 1.0 equiv), **3-2a** (1.1 equiv), toluene (1 mL). [a]Estimated percent conversions on the basis of calibrated GC data, with the remaining mass balance attributed to unidentified byproducts. [b]0.15 equiv. [c]3.0 equiv **3-2a**. [d]7.5 mol % **2-C3**. [e]10 mol % **2-C3**. [f]5.0 equiv **3-2a**. $C_{10}H_8$ = naphthalene.

The difficulty of this nickel-catalyzed C–O cross-coupling was highlighted in reactions of **3-1a** and **3-2a** employing catalyst mixtures of $Ni(cod)_2$ and various ancillary ligands under optimized catalytic conditions (**Table 3.2**). Only **2-L3** successfully mediated the desired transformation to form **3-3a**, albeit with modest conversion (entry 1); other phosphine ligands (including **2-L1**), as well as ancillary ligands that had been used successfully in palladium-catalyzed C–O cross-coupling reactions (i.e., RockPhos, Ad-BippyPhos, and JosiPhos CyPF-*t*-Bu; see Section 3.2.1) furnished negligible conversion to **3-3a** (entries 2–7 and 8–10 respectively). Notably, the catalyst system developed by

MacMillan and co-workers (i.e., $NiCl_2$(DME), dtbbpy, and quinuclidine; see **Section 3.2.2**) was also not suitable for the desired transformation under these conditions (entry 11).

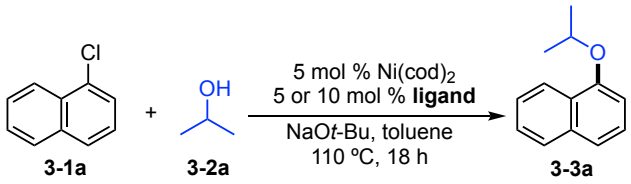

Entry	Ligand	**3-3a** (%)[a]	Remaining **3-1a** (%)[a]	$C_{10}H_8$ (%)[a]
1	**2-L3**	15	<5	70
2	**2-L1**	<5	<5	85
3	XantPhos	<5	<5	70
4	DPEPhos	<5	<5	85
5	*rac*-BINAP	<5	35	50
6	dcype	<5	<5	90
7	PCy_3[b]	<5	10	65
8	RockPhos	<5	<5	80
9	Ad-BippyPhos	<5	10	80
10	CyPF-*t*-Bu	<5	<5	85
11[c]	dtbbpy	<5	>95	<5

Table 3.2. Screening ancillary ligands in the nickel-catalyzed cross-coupling of **3-1a** and **3-2a**. General conditions: $Ni(cod)_2$ (5 mol %), ligand (5 mol %), NaO*t*-Bu (1.5 equiv), **3-1a** (0.12 mmol, 1.0 equiv), **3-2a** (3.0 equiv), toluene (1 mL). [a]Estimated percent conversions on the basis of calibrated GC data, with the remaining mass balance attributed to unidentified byproducts. [b]10 mol %.[c]5 mol % $NiCl_2$(DME) and 10 mol % quinuclidine used instead of $Ni(cod)_2$. $C_{10}H_8$ = naphthalene.

3.3.2 Screening Nickel Pre-Catalysts in the Cross-Coupling of 1-Chloronaphthalene and 4-Methyl-1-Pentanol – Reaction Optimization

Pre-catalysts **2-C1**, **2-C3**, **3-C1**, and **3-C2** were concurrently screened by Preston MacQueen in the nickel-catalyzed cross-coupling of **3-1a** and 4-methyl-1-pentanol (**3-2b**) to form **3-4a** (**Table 3.3**). As with reactions involving secondary alcohol **3-2a**, the use of **2-C3** afforded the greatest conversion to **3-4a** using NaO*t*-Bu and toluene at 110 °C (entry 1), though **2-C1** also provided **3-4a** in modest amounts (entry 2); reactions employing **3-C1** and **3-C2** resulted in significant hydrodehalogenation (entries 3 and 4). Exchanging NaO*t*-Bu for Cs_2CO_3 reduced conversion to product using **2-C3** (entry 5), however, comparable activity was achieved using **2-C1** (entry 6). K_2CO_3 also proved to be a suitable base in reactions involving **2-C1** (entry 7), while only modest conversion to **3-4a** was observed using K_3PO_4 (entry 8).

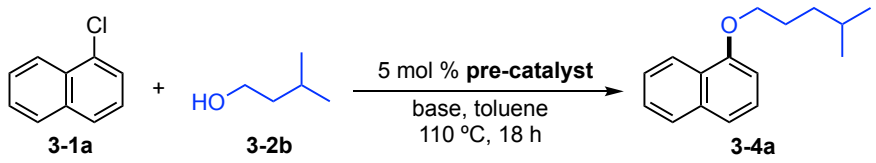

3-1a + **3-2b** → **3-4a**

Entry	Pre-catalyst	Base	**3-4a** (%)[a]	Remaining **3-1a** (%)[a]	$C_{10}H_8$[a]
1	**2-C3**	NaO*t*-Bu	80	<5	10
2	**2-C1**		50	<5	40
3	**3-C1**		<5	<5	75
4	**3-C2**		<5	<5	75
5	**2-C3**	Cs_2CO_3	10	65	5
6	**2-C1**		55	35	<5
7	**2-C1**	K_2CO_3	50	40	<5
8	**2-C1**	K_3PO_4	25	60	10

Table 3.3. Optimization of the nickel-catalyzed cross-coupling of **3-1a** and **3-2b**. General conditions: pre-catalyst (5 mol %), base (1.5 equiv), **3-1a** (0.12 mmol, 1.0 equiv), **3-2b** (1.1 equiv), toluene (1 mL). [a]Estimated percent conversions on the basis of calibrated GC data, with the remaining mass balance attributed to unidentified byproducts. $C_{10}H_8$ = naphthalene. Results obtained by Preston MacQueen.

3.3.3 Scope of the Nickel-Catalyzed Cross-Coupling of Aliphatic Alcohols with (Hetero)aryl (Pseudo)halides

Having established optimal reaction conditions, the scope of the nickel-catalyzed cross-coupling of aliphatic alcohols with (hetero)aryl (pseudo)halides was examined using pre-catalysts **2-C3** and **2-C1** (**Schemes 3.6** and **3.7**). The newly developed pre-catalyst system is competitive with state-of-the-art metal catalyzed C–O cross-coupling methodologies (palladium, nickel, or other). A variety of secondary alcohols were successful coupling partners in this reaction, including 2-propanol (**3-3a** to **3-3c**), 1-phenylethanol (**3-3d**), 1-methoxy-2-propanol (**3-3e**), 2-butanol (**3-3f**), 3,3-dimethyl-2-butanol (**3-3g**), 3-oxetanol (**3-3h**), cyclohexanol (**3-3i** and **3-3k**), and *trans*-4-methylcyclohexanol (**3-3j**). The first examples of tertiary alcohols as nucleophiles in nickel-catalyzed C–O cross-coupling were also achieved using 1-adamantanol (**3-3l**) and *tert*-butanol (**3-3m**). Additionally, various primary alcohols were effectively cross-coupled in this transformation, including 4-methyl-1-pentanol (**3-4a**), methanol (**3-4b** and **3-4c**), methanol-d_4 (**3-4c-*d*$_3$**), and 2-methyl-1-pentanol (**3-4d**), as well as those bearing chloro (**3-4e**), benzyl (**3-4f**), methylcyclopropyl (**3-4g**), amino (**3-4h**), thiophen-2-yl (**3-4i**), silyl (**3-4j**), 2-pyridyl (**3-4k**), and alkenyl (**3-4l**) substituents. Furthermore, 3-methyl-1,3-butanediol (**3-4m**) was cross-coupled selectively at the primary hydroxyl group.

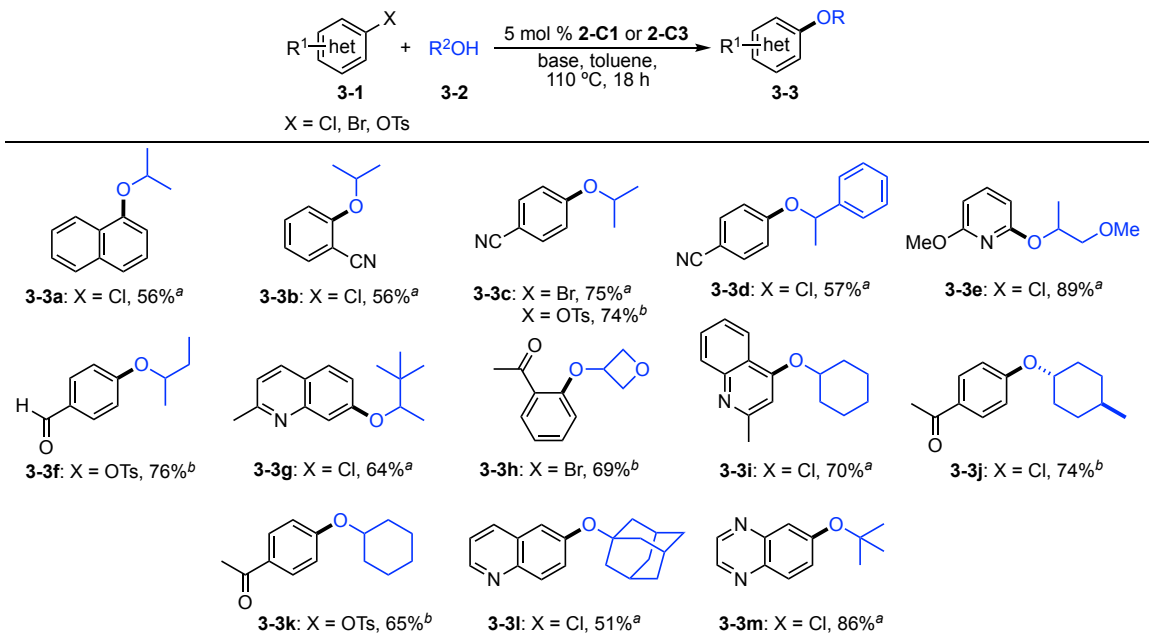

Scheme 3.6. Scope of the nickel-catalyzed cross-coupling of secondary and tertiary alcohols with (hetero)aryl (pseudo)halides. General conditions: (hetero)aryl (pseudo)halide (1.0 equiv), alcohol (1.1-5.0 equiv). Isolated yields reported. [a]Using **2-C3** (5 mol %) and NaO*t*-Bu (1.5 equiv). [b]Using **2-C1** (5 mol %) and Cs_2CO_3 (3.0 equiv). Compound **3-3i** isolated by Carlos Diaz.

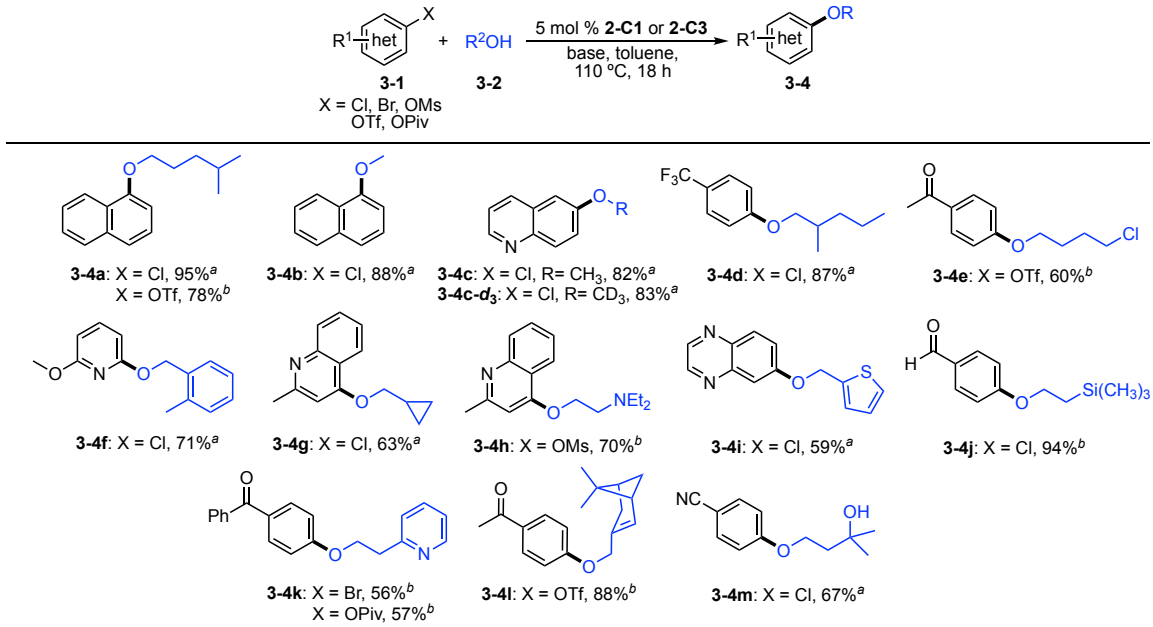

Scheme 3.7. Scope of the nickel-catalyzed cross-coupling of secondary and tertiary alcohols with (hetero)aryl (pseudo)halides. General conditions: (hetero)aryl (pseudo)halide (1.0 equiv), alcohol (1.1-5.0 equiv). Isolated yields reported. [a]Using **2-C3** (5 mol %) and NaO*t*-Bu (1.5 equiv). [b]Using **2-C1** (5 mol %) and Cs_2CO_3 (3.0 equiv). All compounds isolated by Preston MacQueen.

The scope of (hetero)aryl (pseudo)halides in this transformation encompasses activated chloride and phenol-derived electrophiles (i.e., tosylates, mesylates, triflates, and pivalates), representing the first cross-couplings of such substrates in nickel-catalyzed C–O cross-coupling. Electrophiles containing pyridine (**3-3e**, **3-4f**), quinaldine (**3-3g**, **3-3i**, **3-4g**, **3-4h**), quinoline (**3-3l**, **3-4c**), and quinoxaline (**3-3m**, **3-4i**) core structures, as well as those bearing nitrile, ether, aldehyde, ketone, and trifluoromethyl substituents (including in *ortho*-positions) were well-tolerated in this transformation. Additionally, the ability to conduct cross-couplings on synthetically useful scales was confirmed in the preparation of **3-3m** (1.09 g, 83%) from 6-chloroquinoxaline (6.5 mmol), and **3-4a** (0.89 g, 75%) from 1-chloronaphthlane (5.3 mmol). **2-C1** was generally employed with Cs_2CO_3 in reactions where **2-C3** and NaO*t*-Bu proved ineffective (e.g., with substrates bearing base-sensitive moieties). While certain substrates were effectively cross-coupled in the absence of pre-catalyst (see Section 3.3.4), control experiments in which **2-C3** or **2-C1** was omitted in the pairings presented in **Schemes 3.6** and **3.7** gave rise to <10% of cross-coupled product.

3.3.4 Limitations of the 2-C3/2-C1 Pre-Catalyst System in Nickel-Catalyzed C(sp^2)–O Cross-Coupling

While the scope of coupling partners in this transformation was generally quite broad, several classes of substrates were not compatible with the **2-C3** and **2-C1** pre-catalyst system under the reported conditions. Electrophiles bearing *meta*-substituents, e.g., 3-chloroanisole or 3-chlorotoluene, were not suitable substrates, largely giving rise to complex product mixtures regardless of the electronic character of the electrophile (**Figure 3.2A**). Heteroaryl halides in which the heteroatom and halogen exhibited a 1,3-relationship, such as 3-chloropyridine and 4-bromoisoquinoline, similarly resulted in poor conversion to product. The cause of the observed reactivity with these electrophiles is unclear, especially considering some of these substrates were successfully employed in reactions with cyclopropylamine using **2-C3** (see **Scheme 2.10**). Nicasio and co-workers[118] recently reported the formation of catalytically inactive nickel species when 3-chloropyridine was employed in the nickel-catalyzed *N*-arylation of indole using (**3-L2**)Ni(η^6-C_7H_8), which may account for the lack of activity when this electrophile was employed in nickel-catalyzed C–O cross-coupling. Additionally, electron-rich electrophiles, such as 4-bromoanisole (**Figure 3.2B**), and electrophiles whose core structures are sulfur-based

heterocycles, e.g., 5-chlorobenzothiophene and 2-methyl-5-chlorobenzothiazole (**Figure 3.2C**), were ineffective coupling partners in this transformation, perhaps due to the challenging oxidative addition of the C(sp^2)–X bond in these deactivated substrates. Reactions targeting certain highly activated electrophiles, e.g., 2-chloropyrimidine, 2-chlorobenzothiazole, or 2-chloroquinoline (**Figure 3.3**), often proceeded in the absence of nickel pre-catalyst irrespective of the corresponding alcohol nucleophile under the conditions employed, affording >70% conversion to the cross-coupled product in these instances.

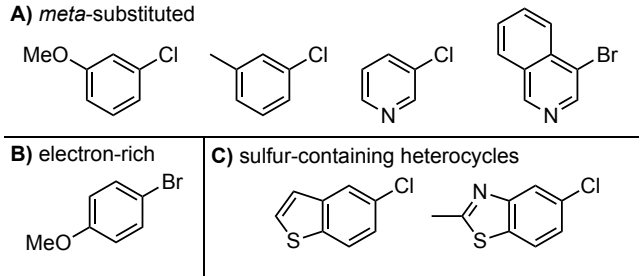

Figure 3.2. Representative (hetero)aryl electrophiles that were not tolerated in the nickel-catalyzed cross-coupling of aliphatic alcohols using **2-C3** or **2-C1**.

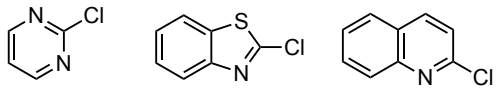

Figure 3.3. Representative electrophiles that reacted with alcohols in the absence of pre-catalyst under optimized reaction conditions.

Several secondary alcohols were ineffective nucleophiles in this reaction (**Figure 3.4**). 1,1,1-trifluoro-2-propanol was unreactive, perhaps due to its reduced nucleophilicity, while secondary alcohols possessing remote steric hindrance, such as (1*R*,2*S*,5*R*)-(-)-menthol or (-)-borneol, generally provided complex product mixtures. Reactions employing the tertiary alcohols 2-methyl-3-butyn-2-ol and ethyl α-hydroxyisobutyrate were also unsuccessful.

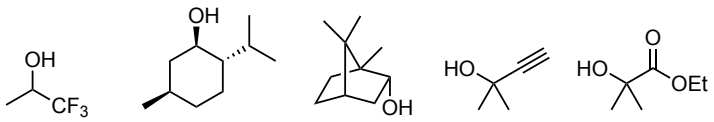

Figure 3.4. Representative secondary and tertiary alcohols that were not suitable nucleophiles in nickel-catalyzed C–O cross-coupling using **2-C3** or **2-C1**.

In order to demonstrate the synthetic utility of the **2-C3** pre-catalyst system, the preparation of fluoxetine (Prozac) via the cross-coupling of 4-chlorobenzotrifluoride and α-[2-(methylamino)ethyl]benzyl alcohol was attempted (**Scheme 3.8**). Despite the successful use of this electrophile in the preparation of **3-4d** (see **Scheme 3.7**), reactions conducted with α-[2-(methylamino)ethyl]benzyl alcohol largely furnished complicated mixtures of products on the basis of GC analysis. Increasing the catalyst loading of **2-C3** from 5.0 mol % to 7.5 or 10 mol %, employing the more reactive 4-bromobenzotrifluoride, or exchanging **2-C3**/NaO*t*-Bu for **2-C1**/Cs_2CO_3 did not improve reaction outcomes. Product mixtures likely arise from reactions at the pendant secondary amine; subsequent competition studies between alcohol and amine nucleophiles in reactions employing **2-C3** or **2-C1** demonstrated the preferential formation of the C–N vs C–O cross-coupled product (see **Scheme 3.9**).

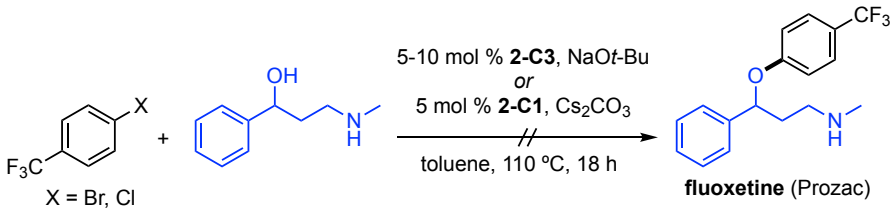

Scheme 3.8. Attempted synthesis of the anti-depressant drug fluoxetine using nickel-catalyzed C–O cross-coupling.

3.3.5 Screening Pre-Catalysts in the Nickel-Catalyzed C(sp^2)–O Cross-Coupling of Phenols

The success of the **2-C3**/**2-C1** pre-catalyst system in the nickel-catalyzed cross-coupling of aliphatic alcohols with (hetero)aryl (pseudo)halides prompted the examination of other oxygen nucleophiles that might also be suitable coupling partners in this transformation. Though there exist several reports of phenol cross-coupling using palladium[119] or copper[104b] catalysts, the preparation of diaryl ethers using nickel catalysis is relatively rare.[120] Thus, pre-catalysts **2-C3**, **2-C1**, **3-C1**, and **3-C2** were screened for activity in the reaction of 1-chloronaphthalene (**3-1a**) and phenol (**3-5a**) at 110 °C (**Table 3.4**). Unfortunately, negligible conversion to the cross-coupled product **3-6a** was observed under optimal conditions (i.e., NaO*t*-Bu/toluene) regardless of the pre-catalyst employed (entries 1–4). Exchanging NaO*t*-Bu for the weaker bases Cs_2CO_3 (entries 5–8) or K_3PO_4 (entries 9–12) afforded similar results.

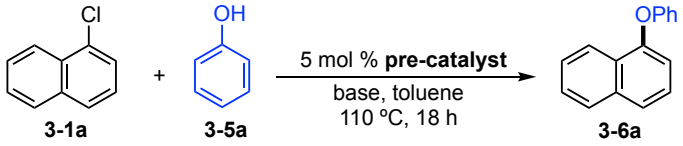

Entry	Pre-catalyst	Base	**3-6a** (%)[a]	Remaining **3-1a** (%)[a]
1	**2-C3**	NaO*t*-Bu	<5	>95
2	**2-C1**		<5	>95
3	**3-C1**		<5	>95
4	**3-C2**		<5	90
5	**2-C3**	Cs_2CO_3	<5	>95
6	**2-C1**		<5	>95
7	**3-C1**		<5	90
8	**3-C2**		<5	90
9	**2-C3**	K_3PO_4	<5	>95
10	**2-C1**		<5	>95
11	**3-C1**		<5	>95
12	**3-C2**		<5	>95

Table 3.4. Optimization of the nickel-catalyzed cross-coupling of **3-1a** and **3-5a**. General conditions: pre-catalyst (5 mol %), base (1.5 equiv), **3-1a** (0.12 mmol, 1.0 equiv), **3-5a** (1.1 equiv), toluene (1 mL). [a]Estimated percent conversions on the basis of calibrated GC data, with the remaining mass balance attributed to unidentified byproducts. Results jointly obtained by the author and Carlos Diaz.

It was postulated that **3-1a** and **3-5a** might not be ideal coupling partners for this study given the electron-neutral nature of each substrate. Thus, the pre-catalysts of interest were screened in the reaction of the more activated 4-chlorobenzonitrile (**3-1b**) and 4-methoxyphenol (**3-5b**). Pre-catalysts **2-C3**, **2-C1**, and **3-C2** furnished modest conversion to product **3-6b** using NaO*t*-Bu as base (entries 1, 2, and 4). However, substituting NaO*t*-Bu for Cs_2CO_3 (entries 5–8) or K_3PO_4 (entries 9–12), shut down the observed catalytic activity. While the addition of 0.15 equivalents of $PhB(OH)_2$ did not have a significant effect on the outcome of the reaction (entries 13–16), the same amount of PhB(pin) additive provided a slight increase in conversion to **3-6b** for each pre-catalyst (entries 17–20). However, product conversion remained at <50% in all cases. Thus, **3-1b** was replaced with the more activated 4-bromobenzonitrile (**3-1c**) in subsequent reactions.

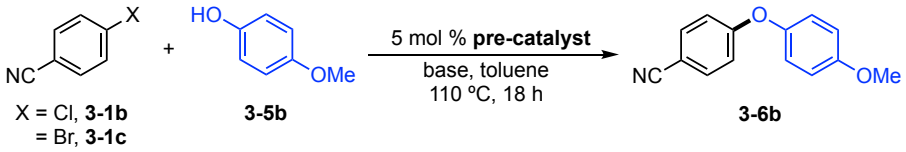

X = Cl, **3-1b**
= Br, **3-1c**

3-5b

3-6b

Entry	Pre-catalyst	X	Base	Additive	**3-6b** (%)[a]	Remaining **3-1** (%)[a]
1	**2-C3**	Cl	NaO*t*-Bu	-	30	65
2	**2-C1**				30	60
3	**3-C1**				0	>95
4	**3-C2**				20	70
5	**2-C3**	Cl	Cs_2CO_3	-	<5	95
6	**2-C1**				<5	85
7	**3-C1**				<5	85
8	**3-C2**				<5	90
9	**2-C3**	Cl	K_3PO_4	-	<5	80
10	**2-C1**				<5	90
11	**3-C1**				<5	>95
12	**3-C2**				<5	85
13	**2-C3**	Cl	NaO*t*-Bu	$PhB(OH)_2$[b]	25	60
14	**2-C1**				25	25
15	**3-C1**				5	70
16	**3-C2**				10	60
17	**2-C3**	Cl	NaO*t*-Bu	PhB(pin)[b]	45	45
18	**2-C1**				30	25
19	**3-C1**				15	70
20	**3-C2**				20	65
21	**2-C3**	Br	NaO*t*-Bu	-	70	30
22	**2-C1**				30	30
23	**3-C1**	Br	NaO*t*-Bu	-	<5	90
24	**3-C2**				15	75
25	**2-C3**	Br	NaO*t*-Bu	PhB(pin)[b]	45	40
26[c]				-	30	60
27[d]				-	60	40

Table 3.5. Optimization of the nickel-catalyzed cross-coupling of **3-1b**/**3-1c** and **3-5b**. General conditions: pre-catalyst (5 mol %), base (1.5 equiv), **3-1b**/**3-1c** (0.12 mmol, 1.0 equiv), **3-5b** (1.1 equiv), toluene (1 mL). [a]Estimated percent conversions on the basis of calibrated GC data, with the remaining mass balance attributed to unidentified byproducts. [b]0.15 equiv. [c]10 mol % **2-C3**. [d]48 h reaction time. Results jointly obtained by the author and Carlos Diaz.

Increased conversion to **3-6b** was observed using **2-C3** (entry 21) in this transformation, but a similar enhancement in conversion was not observed for the other pre-catalysts (entries 22–24). Attempts to further optimize the reaction with **2-C3** were unsuccessful; adding PhB(pin) (entry 25) or increasing the catalyst loading from 5 mol %

to 10 mol % (entry 26) resulted in poorer catalytic performance, while longer reaction times did not improve the reaction outcome (entry 27). Given the modest efficacy of **2-C3** in this transformation, as well as the existence of other, superior, base metal-catalyzed protocols for this reaction,[104b] an expanded investigation of the scope was not conducted. The differing reactivity of pre-catalyst **2-C3** in reactions employing phenols vs. those employing aliphatic alcohols may be due to an adverse interaction of the phenol or phenol cross-coupled product with the nickel centre resulting in catalyst deactivation. Alternatively, the putative nickel aryl phenoxide complex of **2-C3** may be more stable than the corresponding nickel aryl alkoxide species and thus is less inclined to participate in catalysis. The mass balance of material at the end of the reactions involving phenols can largely be attributed to electrophile and product exclusively (see **Tables 3.4** and **3.5**), suggesting that degradation of the starting material or product (when formed) is likely not occurring.

3.3.6 Competition Experiments in Nickel-Catalyzed C(sp^2)–O Cross-Couplings Using 2-C3 and 2-C1

Having established the scope of nickel-catalyzed cross-coupling of aliphatic alcohols with **2-C3** and **2-C1**, competition experiments were performed in order to elucidate any reactivity preferences (**Scheme 3.9**). Reactions employing excess amine and alcohol nucleophile with limiting electrophile revealed the preferential formation of the C–N cross-coupled product at 25 ºC and 110 ºC using either **2-C3** and **2-C1** (**Scheme 3.9A**), in keeping with the demonstrated utility of these pre-catalysts for the monoarylation of primary alkylamines (see Section 1.2.1 and Chapter 2). This preference for C–N cross-coupling was observed regardless of whether the nucleophiles were linear (**Scheme 3.9A**) or substituted at the α-position (**Scheme 3.9B**). Furthermore, the cross-coupled product **3-4a** arising from primary alcohol **3-2b** was obtained almost exclusively using **2-C3** and **2-C1** in reactions containing equimolar quantities of **3-2b** and 2-propanol (**3-2a**; **Scheme 3.9C**), reaffirming the chemoselectivity observed in the synthesis of **3-4m** (see **Scheme 3.7**).

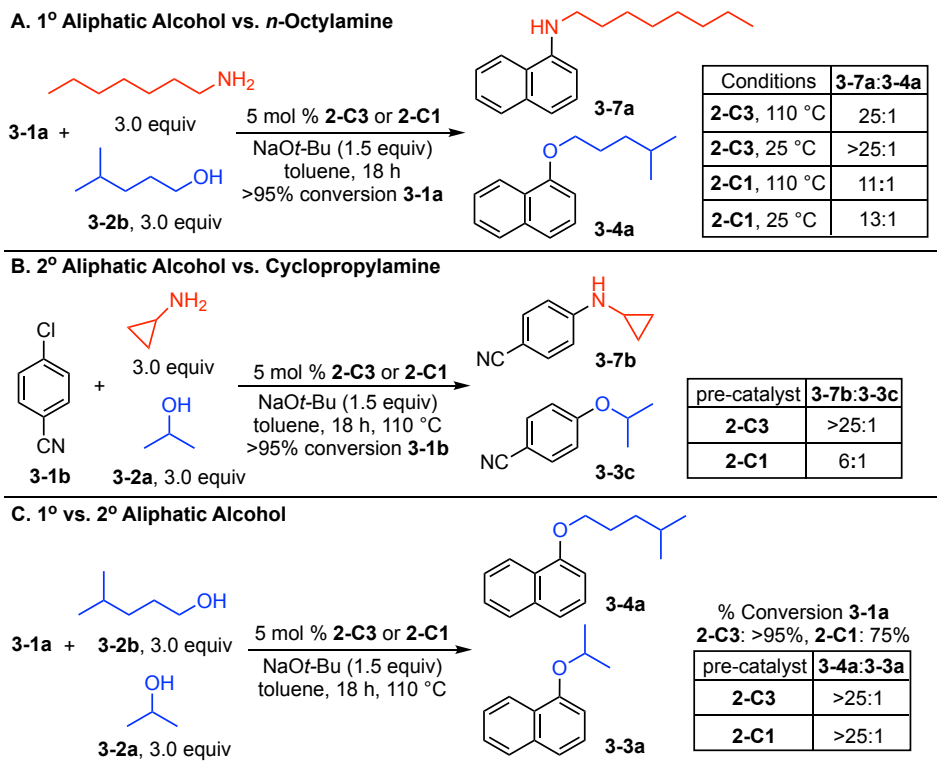

Scheme 3.9. Competition experiments in nickel-catalyzed C–O cross-couplings using **2-C3** and **2-C1**. Results in Scheme 3.9A obtained by Preston MacQueen.

3.4 Summary

This chapter details the development of a nickel-catalyzed C–O cross-coupling methodology enabled by pre-catalysts **2-C3** and **2-C1** containing tailored ancillary ligands **2-L3** (CyPAd-DalPhos) and **2-L1** (PAd-DalPhos). This pre-catalyst system tolerates a wide range of (hetero)aryl (pseudo)halides (bromides, chlorides, tosylates, mesylates, triflates, and pivalates) and aliphatic alcohols (primary, secondary, and tertiary), and is competitive with state-of-the-art palladium- and nickel-catalyzed procedures. Notably, the first examples of (hetero)aryl chlorides and phenol-derived electrophiles (sulfonates and pivalates) in nickel-catalyzed C–O bond formation were achieved using **2-C3** and **2-C1**. Furthermore, this methodology represents the only nickel-catalyzed C–O cross-coupling procedure that does not rely on dual nickel/photoredox catalysis, illustrating the efficacy of using tailored ancillary ligands to facilitate challenging nickel-catalyzed transformations.

3.5 Experimental

3.5.1 General Considerations

Unless otherwise indicated, all experimental procedures were conducted in a nitrogen-filled, inert-atmosphere glovebox using oven-dried glassware, with workup procedures carried out on the benchtop in air. Toluene was purged with nitrogen, passed through a double-column purification system containing alumina and copper-Q5 reactant, and stored over 4Å molecular sieves in bulbs fitted with Teflon taps prior to use. Methanol, *tert*-butanol, isopropanol, 2-butanol, and 1-phenylethanol were purged with nitrogen, and stored over 4 Å molecular sieves in bulbs fitted with Teflon taps. Cs_2CO_3 and K_3PO_4 were ground and dried under vacuum at 180 °C for 24 h, and stored under nitrogen in the glovebox prior to use. Pre-catalysts **2-C1**,[66] **2-C3** (see Section 2.5.3), **3-C1**,[121] **3-C2**,[64] aryl pivalates,[122] aryl triflates,[94] as well as aryl mesylates and tosylates,[97] were prepared according to established literature procedures. Otherwise, all other solvents, reagents, and materials were used as received from commercial sources. Automated flash chromatography was carried out on a Biotage Isolera One automated flash purification system using 10 g Biotage SNAP KP-SIL (particle size 30−90 μm) or 12 g Silicycle SiliaSep (particle size 40−63 μm, 230−400 mesh) silica flash cartridges with a typical gradient of 2−4−2 column volumes and a flow rate of 10 mL/min, unless otherwise indicated. Manual flash chromatography was carried out on silica gel using Silicycle SiliaFlash 60 silica (particle size 40−63 μm; 230−400 mesh). NMR spectra were recorded on a Bruker AV 500 MHz spectrometer at 300 K, with chemical shifts (in ppm) referenced to residual protio solvent peaks (^{1}H) or deuterated solvent peaks (^{13}C{^{1}H}). Splitting patterns are indicated as follows: br, broad; app, apparent; s, singlet; d, doublet; t, triplet; q, quartet; sept, septet; dd, doublet of doublets; m, multiplet. All coupling constants (*J*) are reported in hertz (Hz). In some cases, fewer than expected carbon resonances were observed despite prolonged acquisition times. Mass spectra were obtained using ion trap electrospray ionization (ESI) instruments operating in positive mode. Gas chromatography (GC) data were obtained on an instrument equipped with a SGE BP-5 column (30 m, 0.25 mm i.d.).

3.5.2 General Catalytic Procedures

General Procedure for Pre-Catalyst Screening and Reaction Optimization. In a nitrogen-filled glovebox, pre-catalyst (0.006 mmol, 5 mol %), NaO*t*-Bu (17.3 mg, 0.18 mmol, 1.5 equiv), 1-chloronapthalene (16.3 μL, 0.12 mmol, 1.0 equiv), toluene (1 mL), and 4-methyl-1-pentanol (0.18 mmol, 1.1 equiv) or isopropanol (27.6 μL, 0.12 mmol, 3.0 equiv) were consecutively added to a 1 dram, screw-capped vial, followed by a magnetic stir bar. The vial was then sealed with a cap containing a PTFE septum, removed from the glovebox, and placed in a temperature-controlled aluminum heating block set to 110 °C. The mixture was stirred at this temperature for 18 h (unoptimized), after which time the vial was removed from the heat source and cooled to room temperature. An aliquot of the reaction mixture was filtered through a short Celite/silica plug, diluted with CH_2Cl_2 or EtOAc (~1.5 mL), and subjected to GC analysis.

General Procedure for Ni(cod)$_2$/Ligand Reactions. In a nitrogen-filled glovebox, ligand (0.006 mmol, 5 mol %), NaO*t*-Bu (17.3 mg, 0.18 mmol, 1.5 equiv), Ni(cod)$_2$ (100μL of a 0.06 M solution in toluene, 0.006 mmol, 5 mol %), toluene (900 μL), 1-chloronapthalene (16.3 μL, 0.12 mmol, 1.0 equiv), and 2-propanol (27.6 μL, 0.12 mmol, 3.0 equiv) were consecutively added to a 1 dram, screw-capped vial, followed by a magnetic stir bar. The vial was then sealed with a cap containing a PTFE septum, removed from the glovebox, and placed in a temperature-controlled aluminum heating block set to 110 °C. The mixture was stirred at this temperature for 18 h (unoptimized), after which time the vial was removed from the heat source and cooled to room temperature. An aliquot of the reaction mixture was filtered through a short Celite/silica plug, diluted with CH_2Cl_2 or EtOAc (~1.5 mL), and subjected to GC analysis.

General Procedure for the Cross-Coupling of (Hetero)aryl Electrophiles and Aliphatic Alcohols (GPA). In a nitrogen-filled glovebox, **2-C3** or **3-C1** (5 mol %), NaO*t*-Bu (1.5 equiv) or Cs_2CO_3 (3.0 equiv), (hetero)aryl (pseudo)halide (1.0 equiv), toluene, and alcohol (1.1-5.0 equiv) were consecutively added to a 4 dram, screw-capped vial, followed by a magnetic stir bar. The vial was then sealed with a cap containing a PTFE septum, removed from the glovebox, and placed in a temperature-controlled aluminum heating block set to 110 °C. The mixture was stirred at this temperature for 18 h (unoptimized), after which time the vial was removed from the heat source and cooled to room

temperature. The crude reaction mixture was then diluted with EtOAc or diethyl ether (20 mL), washed with brine (2 x 10 mL), and separated. The aqueous layer was subsequently extracted with EtOAc or diethyl ether (2 x 10 mL), and separated. The organic fractions were combined, dried over Na_2SO_4, filtered, and concentrated under reduced pressure. The resulting residue was then purified by either flash chromatography on silica gel or automated flash chromatography, as indicated.

General Procedure for Pre-Catalyst Screening in Phenol Cross-Coupling. In a nitrogen-filled glovebox, pre-catalyst (5 mol %), base (0.18 mmol, 1.5 equiv), electrophile (0.12 mmol, 1.0 equiv), phenol (12.4 mg, 0.132 mmol, 1.1 equiv) or 4-methoxyphenol (16.4 mg, 0.132 mmol, 1.1 equiv), and toluene were consecutively added to a 1 dram, screw-capped vial, followed by a magnetic stir bar. The vial was then sealed with a cap containing a PTFE septum, removed from the glovebox, and placed in a temperature-controlled aluminum heating block set to 110 °C. The mixture was stirred at this temperature for 18 h (unoptimized), after which time the vial was removed from the heat source and cooled to room temperature. An aliquot of the reaction mixture was filtered through a short Celite/silica plug, diluted with CH_2Cl_2 or EtOAc (~1.5 mL), and subjected to GC analysis.

General Procedure for Competition Experiments. In a nitrogen-filled glovebox, pre-catalyst (0.006 mmol, 5 mol %), NaO*t*-Bu (17.3 mg, 0.18 mmol, 1.5 equiv), nucleophilic coupling partner 1 (3.0 equiv), nucleophilic coupling partner 2 (3.0 equiv), toluene (1 mL), aryl halide (0.12 mmol, 1.0 equiv) and dodecane or mesitylene (0.12 mmol, 1.0 equiv) were consecutively added to a 1 dram, screw capped vial, followed by a magnetic stir bar. The vial was then sealed with a cap containing a PTFE septum, removed from the glovebox, and placed in a temperature-controlled aluminum heating block set to 25 or 110 °C, as appropriate. The mixture was stirred at this temperature for 18 h (unoptimized), after which time the vial was removed from the heat source and cooled to room temperature. An aliquot of the reaction mixture was filtered through a short Celite/silica plug, diluted with EtOAc (~1.5 mL), and subjected to GC analysis.

3.5.3 Synthesis and Characterization of Cross-Coupled Products

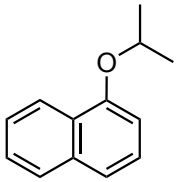

1-isopropoxynaphthalene (**3-3a**). GPA was followed using **2-C3** (25.3 mg, 0.0375 mmol), NaO*t*-Bu (108.1 mg, 1.125 mmol), 1-chloronaphthalene (102 μL, 0.75 mmol), 2-propanol (287 μL, 3.75 mmol), toluene (6.25 mL), and EtOAc. After flash chromatography on silica gel (hexanes), the title compound was obtained as a colourless oil (0.078 g, 56%). ^{1}H NMR (500 MHz, $CDCl_3$): δ 8.35 (d, J = 7.7 Hz, 1H), 7.84 (d, J = 8.6 Hz, 1H), 7.54–7.49 (m, 2H), 7.46–7.40 (m, 2H), 6.88 (d, J = 7.4 Hz, 1H), 4.78 (sept, J = 6.0 Hz, 1H), 1.51 (d, J = 6.1 Hz, 6H). ^{13}C{^{1}H} NMR (126 MHz, $CDCl_3$): δ 153.8, 134.9, 127.6, 126.7, 126.4, 126.0, 125.1, 122.5, 120.0, 106.5, 70.5, 22.3. Spectroscopic data are consistent with those previously reported.[123]

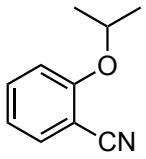

2-isoproproxybenzonitrile (**3-3b**). GPA was followed using **2-C3** (25.3 mg, 0.0375 mmol), NaO*t*-Bu (108.1 mg, 1.125 mmol), 2-chlorobenzonitrile (103.2 mg, 0.75 mmol), 2-propanol (172 μL, 2.25 mmol), toluene (6.25 mL), and diethyl ether. After flash chromatography on silica gel (100 mL hexanes, 100 mL 5% EtOAc in hexanes, 300 mL 10% EtOAc in hexanes, then 20% EtOAc in hexanes), the title compound was obtained as a yellow liquid (0.056 g, 56%). ^{1}H NMR (500 MHz, $CDCl_3$): δ 7.53–7.51 (m, 1H), 7.50–7.47 (m, 1H), 6.96–6.94 (m, 2H), 4.64 (sept, J = 6.1 Hz, 1H), 1.39 (d, J = 6.1 Hz, 6H). ^{13}C{^{1}H} NMR (126 MHz, $CDCl_3$): δ 160.0, 134.2, 134.0, 120.6, 116.8, 113.9, 103.1, 71.9, 21.9. Spectroscopic data are consistent with those previously reported.[124]

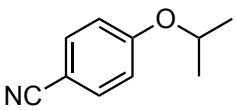

4-isoproproxybenzonitrile (**3-3c**). GPA was followed using **2-C3** (25.3 mg, 0.0375 mmol), NaO*t*-Bu (108.1 mg, 1.125 mmol), 4-bromobenzonitrile (136.5 mg, 0.75 mmol),

2-propanol (172 μL, 2.25 mmol), toluene (6.25 mL), and diethyl ether *or* GPA was followed using **2-C1** (25.9 mg, 0.0375 mmol), Cs_2CO_3 (733.1 mg, 2.25 mmol), 4-cyanophenyl 4-methylbenzenesulfonate (205.0 mg, 0.75 mmol), 2-propanol (172 μL, 2.25 mmol), toluene (6.25 mL), and diethyl ether. With the aryl bromide, after flash chromatography on silica gel (10% EtOAc in hexanes), the title compound was obtained as a pale-yellow liquid (0.091 g, 75%). With the aryl tosylate, after flash chromatography on silica gel (10 % EtOAc in hexanes), the title compound was obtained as a pale-yellow liquid (0.090 g, 74%). ^{1}H NMR (500 MHz, $CDCl_3$): δ 7.55 (d, J = 8.9 Hz, 2H), 6.91 (d, J = 8.9 Hz, 2H), 4.61 (sept, J = 6.1, 1H), 1.36 (d, J = 6.1 Hz, 6H). ^{13}C{^{1}H} NMR (126 MHz, $CDCl_3$): δ 161.5, 134.1, 119.4, 116.2, 103.5, 70.5, 21.9. Spectroscopic data are consistent with those previously reported.[125]

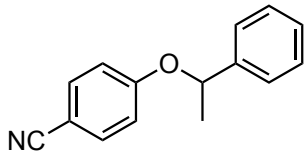

4-(1-phenylethoxy)benzonitrile (**3-3d**). GPA was followed using **2-C3** (25.3 mg, 0.0375 mmol), NaO*t*-Bu (108.1 mg, 1.125 mmol), 4-chlorobenzonitrile (103.2 mg, 0.75 mmol), 1-phenylethanol (272 μL, 2.25 mmol), toluene (6.25 mL), and EtOAc. After flash chromatography on silica gel (50 mL each of 5–9% EtOAc in hexanes, then 10% EtOAc in hexanes), the title compound was obtained as a yellow oil (0.095 g, 57%). Though this compound has been reported previously,[126] complete characterization data were not obtained. ^{1}H NMR (500 MHz, $CDCl_3$): δ 7.48 (d, J = 8.9 Hz, 2H), 7.37–7.33 (m, 4H), 7.30–7.27 (m, 1H), 6.90 (d, J = 8.9 Hz, 2H), 5.36 (q, J = 6.5 Hz, 1H), 1.67 (d, J = 6.4 Hz, 3H). ^{13}C{^{1}H} NMR (126 MHz, $CDCl_3$): δ 161.4, 142.0, 133.9, 129.0, 128.0, 125.5, 119.3, 116.6, 103.9, 76.7, 24.5. HRMS-ESI (*m*/*z*): Calc'd for $C_{15}H_{14}NNaO$ $[M+Na]^+$: 246.0895. Found: 246.0889.

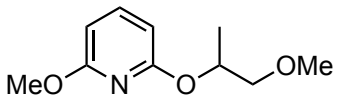

2-methoxy-6-((1-methoxypropan-2-yl)oxy)pyridine (**3-3e**). GPA was followed using **2-C3** (25.3 mg, 0.0375 mmol), NaO*t*-Bu (108.1 mg, 1.125 mmol), 2-chloro-6-methoxypyridine (89.2 μL, 0.75 mmol), 1-methoxy-2-propanol (221 μL, 2.25 mmol),

toluene (6.25 mL), and EtOAc. After flash chromatography on silica gel (10% EtOAc in hexanes), the title compound was obtained as a pale-yellow liquid (0.131 g, 89%). ^{1}H NMR (500 MHz, $CDCl_3$): δ 7.44 (t, J = 7.9 Hz, 1H), 6.29 (d, J = 7.9 Hz, 1H), 6.26 (d, J = 7.9 Hz, 1H), 5.36–5.30 (m, 1H), 3.87 (s, 3H), 3.62–3.49 (m, 2H), 3.40 (s, 3H), 1.34 (d, J = 6.4 Hz, 3H). ^{13}C{^{1}H} NMR (126 MHz, $CDCl_3$): δ 163.1, 162.3, 141.1, 102.3, 101.1, 75.7, 70.2, 59.4, 53.4, 17.0. Calc'd for $C_{10}H_{15}NNaO_3$ $[M+Na]^+$: 220.0950. Found: 220.0944.

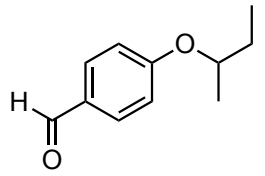

4-(*sec*-butoxy)benzaldehyde (**3-3f**). GPA was followed using **2-C1** (25.9 mg, 0.0375 mmol), Cs_2CO_3 (733.1 mg, 2.25 mmol), 4-formylphenyl 4-methylbenzenesulfonate (207.2 mg, 0.75 mmol), 2-butanol (206 μL, 2.25 mmol), toluene (6.25 mL), and EtOAc. After flash chromatography on silica gel (20% EtOAc in hexanes), the title compound was obtained as a yellow liquid (0.102 g, 76%). Though this compound has been reported previously,[127] complete characterization data were not obtained. ^{1}H NMR (500 MHz, $CDCl_3$): δ 9.85 (s, 1H), 7.80 (d, J = 8.8 Hz, 2H), 6.96 (d, J = 8.7 Hz, 2H), 4.41 (app sextet, J = 6.1 Hz, 1H), 1.80–1.60 (m, 2H), 1.32 (d, J = 6.1 Hz, 3H), 0.97 (t, J = 7.5 Hz, 3H). ^{13}C{^{1}H} NMR (126 MHz, $CDCl_3$): δ 190.8, 163.7, 132.2, 129.7, 115.8, 75.5, 29.2, 19.2, 9.8. HRMS-ESI (*m*/*z*): Calc'd for $C_{11}H_{14}NaO_2$ $[M+Na]^+$: 201.0891. Found: 201.0886.

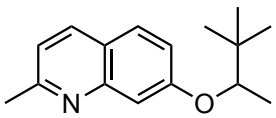

7-((3,3-dimethylbutan-2-yl)oxy)-2-methylquinoline (**3-3g**). GPA was followed using **2-C3** (25.3 mg, 0.0375 mmol), NaO*t*-Bu (108.1 mg, 1.125 mmol), 7-chloroquinaldine (133.2 mg, 0.75 mmol), 3,3-dimethyl-2-butanol (283 μL, 2.25 mmol), toluene (6.25 mL), and EtOAc. After flash chromatography on silica gel (30% EtOAc in hexanes), the title compound was obtained as a yellow liquid (0.116 g, 64%). ^{1}H NMR (500 MHz, $CDCl_3$): δ 7.92 (d, J = 8.3 Hz, 1H), 7.62 (d, J = 8.9 Hz, 1H), 7.36 (d, J = 2.4 Hz, 1H), 7.12–7.10 (m, 2H), 4.25 (q, J = 6.3 Hz, 1H), 2.70 (s, 3H), 1.29 (d, J = 6.3 Hz, 3H), 1.01 (s, 9H). ^{13}C{^{1}H}

NMR (126 MHz, $CDCl_3$): δ 160.1, 159.2, 149.8, 135.9, 128.6, 121.5, 120.0, 119.6, 108.4, 81.5, 35.2, 26.0, 25.4, 14.0. Calc'd for $C_{16}H_{22}NO$ $[M+H]^+$: 244.1701. Found: 244.1696.

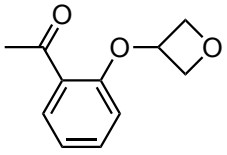

1-(2-(oxetan-3-yloxy)phenyl)ethan-1-one (**3-3h**). GPA was followed using **2-C1** (25.9 mg, 0.0375 mmol), Cs_2CO_3 (733.1 mg, 2.25 mmol), 2′-bromoacetophenone (101 μL, 0.75 mmol), 3-hydroxyoxetane (143 μL, 2.25 mmol), toluene (6.25 mL), and diethyl ether. After automated flash chromatography (10–30% EtOAc in hexanes), the title compound was obtained as an off-white solid (0.100 g, 69%). ^{1}H NMR (500 MHz, $CDCl_3$): δ 7.76 (dd, *J* = 7.7, 1.8 Hz, 1H), 7.42–7.38 (m, 1H), 7.05–7.02 (m, 1H), 6.45 (d, *J* = 8.3 Hz, 1H), 5.32–5.28 (app pent, 1H), 5.02 (t, *J* = 7.0 Hz, 2H), 4.82–4.79 (m, 2H), 2.67 (s, 3H). ^{13}C{^{1}H} NMR (126 MHz, $CDCl_3$): δ 199.4, 155.8, 133.8, 131.1, 128.7, 121.7, 112.2, 77.9, 70.8, 32.1. Spectroscopic data are consistent with those previously reported.[128]

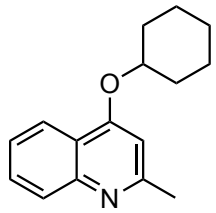

4-(cyclohexyloxy)-2-methylquinoline (**3-3i**). GPA was followed using **2-C3** (20.2 mg, 0.030 mmol), NaO*t*-Bu (86.5 mg, 0.9 mmol), 4-chloroquinaldine (121 μL, 0.6 mmol), cyclohexanol (190 μL, 1.8 mmol), toluene (5.0 mL), and EtOAc. The resulting residue was dissolved in a minimal amount of EtOAc, and then silica was added. The mixture was concentrated under reduced pressure, and the so-formed silica dry pack was then loaded onto a 25 g Biotage SNAP KP-SIL cartridge and purified via automated flash chromatography (0–10% MeOH in CH_2Cl_2, 20 mL/min flow rate), affording the title compound as a yellow oil (0.102 g, 70%), which solidified under reduced pressure. ^{1}H NMR (500 MHz, $CDCl_3$): δ 8.18–8.16 (m, 1H), 7.92 (d, *J* = 8.5 Hz, 1H), 7.65–7.61 (m, 1H), 7.42–7.39 (m, 1H), 6.60 (s, 1H), 4.59–4.55 (m, 1H), 2.68 (s, 3H), 2.06–2.02 (m, 2H), 1.89–1.85 (m, 2H), 1.76–1.70 (m, 2H), 1.62–1.59 (m, 1H), 1.50–1.42 (m, 3H). ^{13}C{^{1}H} NMR (126 MHz, $CDCl_3$): δ 160.6, 160.1, 149.3, 129.7, 128.2, 124.6, 122.1, 120.8, 101.9,

75.4, 31.4, 26.1, 25.7, 23.6. HRMS-ESI (*m*/*z*): Calc'd for $C_{16}H_{20}NO$ $[M+H]^+$: 242.1545. Found: 242.1539.

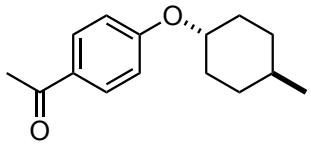

1-(4-(((1*r*,4*r*)-4-methylcyclohexyl)oxy)phenyl)ethan-1-one (**3-3j**). GPA was followed using **2-C1** (20.7 mg, 0.030 mmol), Cs_2CO_3 (586.5 mg, 1.8 mmol), 4′-chloroacetophenone (77.8 μL, 0.6 mmol), *trans*-4-methylcyclohexanol (113 μL, 0.9 mmol), toluene (5.0 mL), and EtOAc. After automated flash chromatography (0–10% EtOAc in hexanes), the title compound was obtained as an off-white solid (0.103 g, 74%). ^{1}H NMR (500 MHz, $CDCl_3$): δ 7.91 (d, *J* = 8.8 Hz, 2H), 6.90 (d, *J* = 8.9 Hz, 2H), 4.27–4.21 (m, 1H), 2.54 (s, 3H), 2.15–2.11 (m, 2H), 1.82–1.79 (m, 2H), 1.50–1.42 (m, 3H), 1.12–1.03 (m, 2H), 0.94 (d, *J* = 6.6 Hz, 3H). ^{13}C{^{1}H} NMR (126 MHz, $CDCl_3$): δ 196.9, 162.2, 130.7, 130.1, 115.3, 76.7, 33.2, 32.0, 31.9, 26.4, 22.0. HRMS-ESI (*m*/*z*): Calc'd for $C_{15}H_{20}NaO_2$ $[M+Na]^+$: 255.1361. Found: 255.1356.

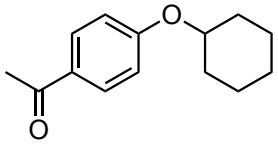

1-(4-(cyclohexyloxy)phenyl)ethan-1-one (**3-3k**). GPA was followed using **2-C1** (20.7 mg, 0.030 mmol), Cs_2CO_3 (586.5 mg, 1.8 mmol), 4-acetylphenyl 4-methylbenzenesulfonate (174.2 mg, 0.6 mmol), cyclohexanol (95.1 μL, 0.9 mmol), toluene (5.0 mL), and EtOAc. After automated flash chromatography (0–10% EtOAc in hexanes), the title compound was obtained as a white solid (0.085 g, 65%). ^{1}H NMR (500 MHz, $CDCl_3$): δ 7.91 (d, *J* = 8.8 Hz, 2H), 6.91 (d, *J* = 8.8 Hz, 2H), 4.37–4.32 (m, 1H), 2.54 (s, 3H), 2.00–1.97 (m, 2H), 1.82–1.80 (m, 2H), 1.61–1.52 (m, 3H), 1.43–1.32 (m, 3H). ^{13}C{^{1}H} NMR (126 MHz, $CDCl_3$): δ 196.8, 162.1, 130.7, 130.1, 115.3, 75.6, 31.7, 26.4, 25.6, 23.8. Spectroscopic data are consistent with those previously reported.[108]

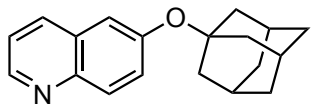

6-((adamantan-1-yl)oxy)quinoline (**3-3l**). GPA was followed using **2-C3** (20.2 mg, 0.030 mmol), NaO*t*-Bu (86.5 mg, 0.9 mmol), 6-chloroquinoline (98.2 mg, 0.6 mmol), 1-adamantanol (274.0 mg, 1.8 mmol), toluene (5.0 mL), and EtOAc. ~1 M aqueous KOH solution was used in place of brine during work-up. After flash chromatography on silica gel (30% EtOAc in hexanes), a yellow oil was obtained. A minimal amount of hexanes was added, and the volatiles were removed under reduced pressure, yielding an off-white solid. The solid was washed with 3 x 1 mL cold (~ 0 °C) hexanes and dried under reduced pressure. Yield: 0.086 g (51%). ^{1}H NMR (500 MHz, $CDCl_3$): δ 8.83 (dd, J =4.2, 1.4 Hz, 1H), 8.06 (d, J = 8.3 Hz, 1H), 8.00 (d, J = 9.0 Hz, 1H), 7.41 (dd, J = 9.0, 2.5 Hz, 1H), 7.37–7.34 (m, 2H), 2.20 (br s, 3H), 1.96 (d, J = 2.0 Hz, 6H), 1.63 (q, J = 12.2 Hz, 6H). ^{13}C{^{1}H} NMR (126 MHz, $CDCl_3$): δ 152.6, 149.2, 145.8, 135.5, 130.1, 129.2, 128.9, 121.2, 120.5, 79.0, 43.1, 36.3, 31.1. Calc'd for $C_{19}H_{22}NO$ $[M+H]^+$: 280.1701. Found: 280.1696

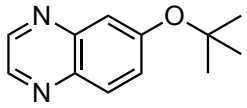

6-(*tert*-butoxy)quinoxaline (**3-3m**). GPA was followed using **2-C3** (25.3 mg, 0.0375 mmol), NaO*t*-Bu (108.1 mg, 1.125 mmol), 6-chloroquinoxaline (123.4 mg, 0.75 mmol), *tert*-butanol (215 μL, 2.25 mmol), toluene (6.25 mL), and EtOAc. After flash chromatography on silica gel (40% EtOAc in hexanes), the title compound was obtained as a yellow oil (0.131 g, 86%). ^{1}H NMR (500 MHz, $CDCl_3$): δ 8.72 (d, J = 1.8 Hz, 1H), 8.67 (d, J = 1.9 Hz, 1H), 7.94 (d, J = 9.1 Hz, 1H), 7.58 (d, J = 2.7 Hz, 1H), 7.38 (dd, J = 9.2, 2.6 Hz, 1H), 1.46 (s, 9H). ^{13}C{^{1}H} NMR (126 MHz, $CDCl_3$): δ 157.3, 144.9, 144.1, 143.0, 139.8, 130.0, 128.5, 117.7, 80.0, 28.9. HRMS-ESI (*m*/*z*): Calc'd for $C_{12}H_{15}N_2O$ $[M+H]^+$: 203.1184. Found: 203.1179.

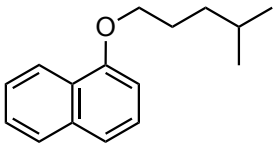

1-((4-methylpentyl)oxy)naphthalene (3-4a). GPA was followed using **2-C3** (16.8 mg, 0.025 mmol), NaO*t*-Bu (72.1 mg, 0.75 mmol), 1-chloronaphthalene (68.1 μL, 0.5 mmol), toluene (4.2 mL), 4-methyl-1-pentanol (68.4 μL, 0.55 mmol), and EtOAc *or* GPA was followed using **2-C1** (16.8 mg, 0.025 mmol), Cs_2CO_3 (488.7 mg, 1.5 mmol), 1-naphthyltrifluoromethanesulfonate (0.138 g, 0.5 mmol), toluene (4.2 mL), 4-methyl-1-pentanol (68.4 μL, 0.55 mmol), and EtOAc. With the aryl chloride, after flash chromatography on silica gel (hexanes), the title compound was obtained as a pale-yellow oil (0.108 g, 95%). With the aryl triflate, after flash chromatography on silica gel (hexanes), the title compound was obtained as a pale-yellow oil (0.089 g, 78%). ^{1}H NMR (500 MHz, $CDCl_3$): δ 8.34–8.32 (m, 1H), 7.84–7.82 (m, 1H), 7.52–7.49 (m, 2H), 7.45–7.44 (m, 1H), 7.42–7.39 (m, 1H), 6.85–6.83 (d, J = 7.4 Hz, 1H), 4.18–4.16 (m, 2H), 2.01–1.95 (m, 2H), 1.76–1.68 (m, 1H), 1.52–1.47 (m, 2H), 1.00 (d, J = 6.6 Hz, 6H). ^{13}C{^{1}H} NMR (126 MHz, $CDCl_3$): δ 155.2, 134.7, 127.6, 126.5, 126.1, 126.0, 125.3, 122.3, 120.2, 104.7, 68.7, 35.7, 28.1, 27.4, 22.8. HRMS-ESI (*m/z*): Calc'd for $C_{16}H_{20}NaO$ $[M+Na]^+$: 251.1412. Found 251.1406.

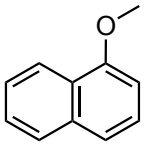

1-methoxynaphthalene (**3-4b**). GPA was followed using **2-C3** (23.6 mg, 0.035 mmol), NaO*t*-Bu (100.9 mg, 1.05 mmol), 1-chloronaphthalene (95.3 mg, 0.7 mmol), toluene (5.8 mL), methanol (141.7 μL, 3.5 mmol), and EtOAc. After automated flash chromatography (hexanes), the title compound was obtained as a clear oil (0.098 g, 88%). ^{1}H NMR (500 MHz, $CDCl_3$): δ 8.31–8.30 (m, 1H), 7.85–7.83 (m, 1H), 7.55–7.49 (m, 2H), 7.48–7.41 (m, 2H), 6.87–6.86 (m, 1H), 4.05 (s, 3H). ^{13}C{^{1}H} NMR (126 MHz, $CDCl_3$): δ 155.7, 134.7, 127.7, 126.6, 126.0, 126, 125.4, 122.2, 120.4, 104.0, 55.7. Spectroscopic data are consistent with those previously reported.[129]

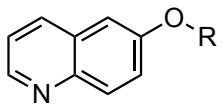

6-methoxyquinoline (**3-4c**) and **6-(methoxy-*d*$_3$)quinoline** (**3-4c-*d*$_3$**). GPA was followed using **2-C3** (23.6 mg, 0.035 mmol), NaO(*t*-Bu) (100.9 mg, 1.05 mmol), 6-chloroquinoline (114.5 mg, 0.7 mmol), toluene (5.8 mL), methanol (141.7 μL, 3.5 mmol) *or* methanol-d_4 (142.1 μL, 3.5 mmol), and EtOAc. After automated flash chromatography (0–20% EtOAc in hexanes), **3-4c** was obtained as a pale-yellow oil (0.093 g, 82%). After automated flash chromatography (0–20% EtOAc in hexanes), **3-4c-*d*$_3$,** was obtained as a pale-yellow oil (0.094 g, 83%). For **3-4c**: ^{1}H NMR (500 MHz, $CDCl_3$): δ 8.81–8.80 (m, 1H), 8.09–8.07 (m, 1H), 8.04–8.03 (m, 1H), 7.42–7.37 (m, 2H), 7.11–7.10 (m, 1H), 3.97 (s, 3H). For **3-4c**: $^{13}C\{^1H\}$ NMR (126 MHz, $CDCl_3$): δ 158.0, 148.2, 144.7, 135.0, 131.1, 129.5, 122.5, 121.6, 105.4, 55.7. Spectroscopic data are consistent with those previously reported.[130]

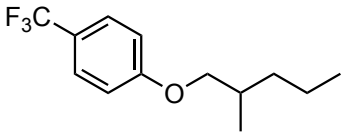

1-((2-methylpentyl)oxy)-4-(trifluoromethyl)benzene (**3-4d**). GPA was followed using **2-C3** (20.2 mg, 0.03 mmol), NaO*t*-Bu (86.5 mg, 0.9 mmol), 4-chlorobenzotrifluoride (80.1 μL, 0.6 mmol), toluene (5.0 mL), 2-methyl-1-pentanol (81.8 μL, 0.66 mmol), and EtOAc. After automated flash chromatography (100% hexanes), the title compound was obtained as a pale-yellow oil (0.127 g, 87%). ^{1}H NMR (500 MHz, $CDCl_3$): δ 7.57–7.55 (m, 2H), 6.99–6.98 (m, 2H), 3.90–3.87 (m, 1H), 3.81–3.78 (m, 1H), 2.05–1.96 (m, 1H), 1.55–1.35 (m, 3H), 1.30–1.24 (m, 1H), 1.07 (d, J = 6.7 Hz, 3H), 0.97 (t, J = 7.2 Hz, 3H). $^{13}C\{^1H\}$ NMR (126 MHz, $CDCl_3$): δ 162.0, 127.0 (d, J_{CF} = 3.5 Hz), 126, 123.7, 122.8 (q, J_{CF} = 65.0 Hz), 114.7, 73.6, 35.9, 33.0, 20.2, 17.2, 14.5.

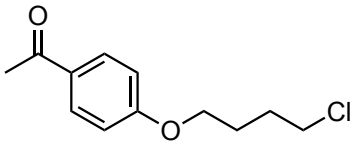

1-(4-(4-chlorobutoxy)phenyl)ethan-1-one (**3-4e**). GPA was followed using **2-C1** (20.7 mg, 0.03 mmol), Cs_2CO_3 (586.4 mg, 1.8 mmol), 4-acetylphenyl trifluoromethanesulfonate (161.0 mg, 0.6 mmol), toluene (5.0 mL), 4-chloro-1-butanol (65.8 μL, 0.66 mmol), and

EtOAc. After flash chromatography on silica gel (60–70% CH_2Cl_2 in hexanes), the title compound was obtained as a yellow oil (0.082 g, 60%). ^{1}H NMR (500 MHz, $CDCl_3$): δ 7.97–7.96 (m, 2H), 6.96–6.95 (m, 2H), 4.12–4.09 (m, 2H), 3.67–3.65 (m, 2H), 2.59 (s, 3H), 2.03–2.01 (m, 4H). ^{13}C{^{1}H} NMR (126 MHz, $CDCl_3$): δ 196.9, 163.0, 130.8, 130.6, 114.3, 67.5, 44.8, 29.4, 26.7, 26.5. HRMS-ESI (*m/z*): Calc'd for $C_{12}H_{15}ClNaO_2$ $[M+Na]^+$: 249.0658. Found: 249.0653.

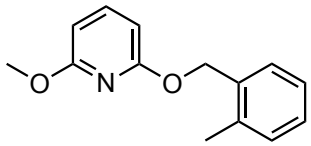

2-methoxy-6-((2-methylbenzyl)oxy)pyridine (**3-4f**). GPA was followed using **2-C3** (20.2 mg, 0.03 mmol), NaO*t*-Bu (86.5 mg, 0.9 mmol), 2-chloro-6-methoxypyridine (71.3 μL, 0.6 mmol), toluene (5.0 mL), 2-methylbenzyl alcohol (80.6 mg, 0.66 mmol), and EtOAc. After flash chromatography on silica gel (0–2% EtOAc in hexanes), the title compound was obtained as a pale-yellow oil (0.096 g, 71%). ^{1}H NMR (500 MHz, $CDCl_3$): δ 7.54–7.51 (m, 1H), 7.46–7.45 (m, 1H), 7.27–7.22 (m, 3H), 6.40–6.38 (m, 1H), 6.35–6.34 (m, 1H), 5.40 (s, 2H), 3.59 (s, 3H), 2.49 (s, 3H). ^{13}C{^{1}H} NMR (126 MHz, $CDCl_3$): δ 163.3, 162.8, 141.2, 137.2, 135.6, 130.5, 129.3, 128.3, 126.1, 101.9, 101.3, 66.3, 53.7, 19.2. HRMS-ESI (*m/z*): Calc'd for $C_{14}H_{15}NNaO_2$ $[M+Na]^+$: 252.1000. Found: 252.0995.

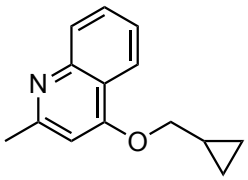

4-cyclopropylmethoxy-2-methylquinoline (**3-4g**). GPA was followed using **2-C3** (20.2 mg, 0.03 mmol), NaO*t*-Bu (86.5 mg, 0.9 mmol), 4-chloroquinaldine (121.0 μL, 0.6 mmol), toluene (5.0 mL), cyclopropanemethanol (53.4 μL, 0.66 mmol), and EtOAc. After flash chromatography on silica gel (60% EtOAc in hexanes), the title compound was obtained as a white solid (0.081 g, 63%). ^{1}H NMR (500 MHz, $CDCl_3$): δ 8.26–8.24 (m, 1H), 7.98–7.96 (m, 1H), 7.70–7.67 (m, 1H), 7.49–7.46 (m, 1H), 6.61 (s, 1H), 4.07 (d, J = 6.9 Hz, 2H), 2.71 (s, 3H), 1.46–1.40 (m, 1H), 0.77–0.74 (m, 2H), 0.50–0.47 (m, 2H). ^{13}C{^{1}H} NMR (126 MHz, $CDCl_3$): δ 161.9, 160.3, 149.1, 129.9, 128.3, 124.9, 122.1, 120.2, 101.3, 73.1,

26.2, 10.2, 3.5. HRMS-ESI (*m/z*): Calc'd for $C_{14}H_{16}NO$ $[M+H]^+$: 214.1232. Found: 214.1226.

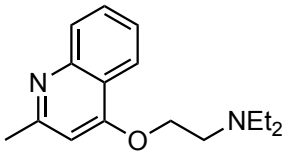

***N*,*N*-diethyl-2-((2-methylquinolin-4-yl)oxy)ethan-1-amine** (**3-4h**). GPA was followed using **2-C1** (20.7 mg, 0.03 mmol), Cs_2CO_3 (586.4 mg, 1.8 mmol), 2-methylquinolin-4-yl methanesulfonate (142.4 mg, 0.6 mmol), toluene (5.0 mL), 2-(diethylamino)ethanol (87.5 μL, 0.66 mmol), and EtOAc. After automated flash chromatography (0–5% MeOH in CH_2Cl_2), the title compound was obtained as a white solid (0.108 g, 70%). ^{1}H NMR (500 MHz, $CDCl_3$): δ 8.18–8.16 (m, 1H), 7.98–7.96 (m, 1H), 7.70–7.67 (m, 1H), 7.48–7.45 (m, 1H), 6.67 (s, 1H), 4.29 (t, *J* = 6.1 Hz, 2H), 3.09 (t, *J* = 6.1 Hz, 2H), 2.76–2.72 (m, 7H), 1.16 (t, *J* = 7.1 Hz, 6H). ^{13}C{^{1}H} NMR (126 MHz, $CDCl_3$): δ 161.8, 160.3, 149.1, 129.9, 128.3, 124.9, 121.9, 120.1, 101.4, 67.5, 51.6, 48.3, 26.2, 12.3. HRMS-ESI (*m/z*): Calc'd for $C_{16}H_{23}N_2O$ $[M+H]^+$: 259.1810. Found: 259.1805.

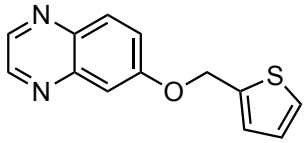

6-(thiophen-2-ylmethoxy)quinoxaline (**3-4i**). GPA was followed using **2-C3** (20.2 mg, 0.03 mmol), NaO*t*-Bu (86.5 mg, 0.9 mmol), 6-chloroquinoxaline (98.8 mg, 0.6 mmol), toluene (5.0 mL), 2-thiophenemethanol (62.5 μL, 0.66 mmol), and EtOAc. After flash chromatography on silica gel (EtOAc), the title compound was obtained as a pale-brown solid (0.086 g, 59%). ^{1}H NMR (500 MHz, $CDCl_3$): δ 8.81–8.80 (m, 1H), 8.75–8.74 (m, 1H), 8.05–8.03 (m, 1H), 7.53–7.51 (m, 2H), 7.41–7.40 (m, 1H), 7.25–7.24 (m, 1H), 7.09–7.07 (m, 1H), 5.43 (s, 2H). ^{13}C{^{1}H} NMR (126 MHz, $CDCl_3$): δ 159.5, 145.2, 144.7, 142.9, 139.6, 138.3, 130.9, 127.8, 127.2, 126.9, 124.0, 108.2, 65.6. HRMS-ESI (*m/z*): Calc'd for $C_{13}H_{10}N_2NaOS$ $[M+Na]^+$: 265.0412. Found: 265.0406.

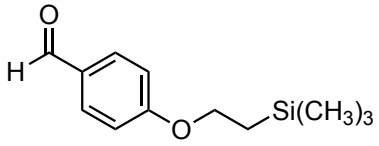

4-(2-(trimethylsilyl)ethoxy)benzaldehyde (**3-4j**). GPA was followed using **2-C1** (20.7 mg, 0.03 mmol), Cs_2CO_3 (586.4 mg, 1.8 mmol), 4-chlorobenzaldehyde (84.3 mg, 0.6 mmol), toluene (5.0 mL), 2-(trimethylsilyl)ethanol (94.6 μL, 0.66 mmol), and EtOAc. After flash chromatography on silica gel (0–2% EtOAc in hexanes), the title compound was obtained as a pale-yellow oil (0.117 g, 94%). ^{1}H NMR (500 MHz, $CDCl_3$): δ 9.91 (s, 1H), 7.87–7.85 (m, 2H), 7.02–7.00 (m, 2H), 4.20 (t, *J* = 8.0 Hz, 2H), 1.20 (t, *J* = 8.0 Hz, 2H), 0.13 (s, 9H). ^{13}C{^{1}H} NMR (126 MHz, $CDCl_3$): δ 191.0, 164.3, 132.2, 129.9, 115.0, 66.3, 17.8, -1.1. Spectroscopic data are consistent with those previously reported.[131]

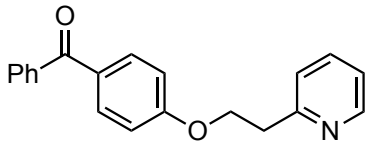

Phenyl(4-(2-(pyridin-2-yl)ethoxy)-phenyl)methanone (**3-4k**). GPA was followed using **2-C1** (17.3 mg, 0.025 mmol), Cs_2CO_3 (488.7 mg, 1.5 mmol), 4-bromobenzophenone (156.7 mg, 0.5 mmol), toluene (4.2 mL), 2-pyridineethanol (62.0 μL, 0.55 mmol), and EtOAc *or* GPA was followed using **2-C1** (12.1 mg, 0.0175 mmol), Cs_2CO_3 (342.1 mg, 3 mmol), 4-benzophenone pivalate (98.8 mg, 0.35 mmol), toluene (2.9 mL), 2-pyridineethanol (43.4 μL, 0.385 mmol), and EtOAc. With the aryl bromide, after flash chromatography on silica gel (20–30% EtOAc in hexanes), the title compound was obtained as a pale-yellow solid (0.084 g, 56%). With the aryl pivalate, after automated flash chromatography (30–50% EtOAc in hexanes), the title compound was obtained as a pale-yellow solid (0.060 g, 57%). ^{1}H NMR (500 MHz, $CDCl_3$): δ 8.61–8.60 (m, 1H), 7.85–7.82 (m, 2H), 7.79–7.77 (m, 2H), 7.69–7.65 (m, 1H), 7.61–7.58 (m, 1H), 7.52–7.49 (m, 2H), 7.32–7.30 (m, 1H), 7.22–7.19 (m, 1H), 7.02–6.99 (m, 2H), 4.51 (t, *J* = 6.7 Hz, 2H), 3.34 (t, *J* = 6.7 Hz, 2H). ^{13}C{^{1}H} NMR (126 MHz, $CDCl_3$): δ 195.8, 162.7, 158.3, 149.7, 138.6, 136.7, 132.8, 132.1, 130.4, 129.9, 128.4, 124.0, 121.9, 114.4, 67.6, 38.1. HRMS-ESI (*m/z*): Calc'd for $C_{20}H_{18}NO$ $[M+H]^{+\cdot}$: 304.1338. Found: 304.1332.

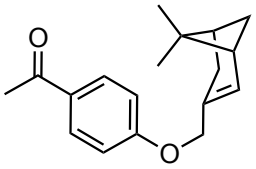

1-(4-(6,6-dimethyl-bicyclo[3.1.1]hept-2-en-3-ylmethoxy)-phenyl)ethan-1-one (**3-4l**). GPA was followed using **2-C1** (20.7 mg, 0.03 mmol), Cs_2CO_3 (586.4 mg, 1.8 mmol), 4-acetylphenyl trifluoromethanesulfonate (160.9 mg, 0.6 mmol), toluene (5.0 mL), (1*R*)-(-)-myrtenol (105.3 μL, 0.66 mmol), and EtOAc. After flash chromatography on silica gel (5–10% EtOAc in hexanes), the title compound was obtained as a white solid (0.143 g, 88%). ^{1}H NMR (500 MHz, $CDCl_3$): δ 7.96–7.94 (m, 2H), 6.98–6.96 (m, 2H), 5.66–5.65 (m, 1H), 4.50–4.49 (m, 2H), 2.59 (s, 3H), 2.48–2.44 (m, 1H), 2.40–2.36 (m, 1H), 2.33–2.29 (m, 1H), 2.27–2.24 (m, 1H), 2.18–2.16 (m, 1H), 1.34 (s, 3H), 1.24–1.23 (m, 1H), 0.87 (s, 3H). ^{13}C{^{1}H} NMR (126 MHz, $CDCl_3$): δ 197.0, 163.1, 143.5, 130.7, 130.5, 121.2, 114.8, 71.0, 43.5, 41.1, 38.3, 31.7, 31.5, 26.5, 26.4, 21.3. HRMS-ESI (*m/z*): Calc'd for $C_{18}H_{22}NaO_2$ $[M+Na]^+$: 293.1517. Found: 293.1512.

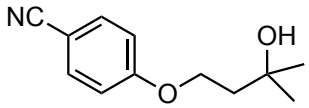

4-(3-hydroxy-3-methylbutoxy)benzonitrile (**3-4m**). GPA was followed using **2-C3** (20.2 mg, 0.03 mmol), NaO*t*-Bu (86.5 mg, 0.9 mmol), 4-chlorobenzonitrile (82.5 mg, 0.6 mmol), toluene (5.0 mL), 3-methyl-1,3-butanediol (70.4 μL, 0.66 mmol), and EtOAc. After flash chromatography on silica gel (40% EtOAc in hexanes), the title compound was obtained as an orange oil (0.082 g, 67%). ^{1}H NMR (500 MHz, $CDCl_3$): δ 7.63–7.61 (m, 2H), 7.01–6.98 (m, 2H), 4.25 (t, *J* = 6.5 Hz, 2H), 2.05 (t, *J* = 6.5 Hz, 2H), 1.74 (s, 1H), 1.36 (s, 6H). ^{13}C {^{1}H} NMR (126 MHz, $CDCl_3$): δ 162.2, 134.2, 119.4, 115.4, 104.4, 70.4, 65.5, 41.8, 30.0. HRMS-ESI (*m/z*): Calc'd for $C_{12}H_{15}NNaO_2$ $[M+Na]^+$: 228.1000. Found: 228.0995.

3.5.4 Large-Scale Synthesis of 3-3m and 3-4a

Large-Scale Synthesis of 3-3m. In a nitrogen-filled glovebox, an oven-dried 100 mL round-bottom Schlenk flask was charged with **2-C3** (219.0 mg, 0.325 mmol), NaO*t*-Bu (0.937 g, 9.75 mmol), 6-chloroquinoxaline (1.070 g, 6.5 mmol), toluene (54 mL), and *tert*-butanol (1.875 mL, 19.5 mmol), followed by a magnetic stir bar. The flask was sealed with

a rubber septum, removed from the glovebox and placed in a pre-heated oil bath. The reaction vessel was attached to a reflux condenser under a positive pressure of nitrogen. The reaction mixture was then stirred at 110 °C for 18 h (unoptimized). After this time, the mixture was diluted with EtOAc (200 mL), washed with brine (2 x 100 mL), and separated. The aqueous layer was then extracted with EtOAc (2 x 100 mL). The organic fractions were combined, dried over Na_2SO_4, and concentrated under reduced pressure. The resulting brown-orange mixture was purified by automated flash chromatography (100 g Biotage SNAP KP-SIL cartridge, 0–40% EtOAc in hexanes, 40 mL/min flow rate), affording the title compound as a yellow oil (1.094 g, 83%).

Large-Scale Synthesis of 3-4a. In a nitrogen-filled glovebox, an oven-dried 300 mL round-bottom Schlenk flask was charged with **2-C3** (178.6 mg, 0.265 mmol), NaO*t*-Bu (0.764 g, 7.95 mmol), 1-chloronaphthalene (722 μL, 5.3 mmol), toluene (45 mL), and 4-methyl-1-pentanol (726 μL, 5.83 mmol), followed by a magnetic stir bar. The flask was sealed with a rubber septum, removed from the glovebox and placed in a pre-heated oil bath. The reaction vessel was attached to a reflux condenser under a positive pressure of nitrogen. The reaction mixture was then stirred at 110 °C for 18 h (unoptimized). After this time, the mixture was diluted with EtOAc, washed with brine (25 mL), and separated. The aqueous layer was then extracted with ethyl acetate (2 x 25 mL). The organic fractions were combined, dried over Na_2SO_4, and concentrated under reduced pressure. The resulting brown-orange mixture was purified by automated flash chromatography (100 g Biotage SNAP KP-SIL cartridge, 0−5% EtOAc in hexanes, 20 mL/min flow rate), affording the title compound as a yellow oil (0.891 g, 75%).

Chapter 4: PhPAd-DalPhos – Ligand-Enabled, Nickel-Catalyzed Cross-Coupling of (Hetero)aryl Electrophiles with Bulky, Primary Alkylamines

4.1 Contributions

This chapter details the application of a nickel pre-catalyst containing PhPAd-DalPhos (**4-L1**) in the cross-coupling of (hetero)aryl electrophiles with α,α,α-trisubstituted, primary alkylamines. Emma V. England, an undergraduate student, conducted all of the catalytic experiments pertaining to 2,6-disubstituted anilines (including isolating **4-6a** to **4-6d**). Preston M. MacQueen, a fellow PhD student, conducted the pre-catalyst screening reactions using **2-C1** and **2-C2** (**Table 4.1**, entries 1 and 2). Dr. Michael J. Ferguson (University of Alberta) solved the solid-state structures for pre-catalysts **4-C1** and **4-C2**. The author was responsible for synthesizing and characterizing the new pre-catalysts, screening all other pre-catalysts for activity in the desired transformation, developing the scope of the bulky, primary alkylamine reaction, conducting the aryl chloride vs. aryl carbamate selectivity studies, and performing the nickel-catalyzed C–O cross-couplings using **4-C1**. The contributions of each author are noted throughout the text and are labelled as such throughout the chapter. This work has been published: Angew. Chem. Int. Ed. 2019, 58, 2485-2489.

4.2 Introduction

4.2.1 Palladium-Catalyzed C(sp^2)–N Cross-Coupling of α,α,α-Trisubstituted, Primary Alkylamines

The introduction of large, hydrocarbon functionalities (e.g., adamantane) into a drug generally increases its lipophilicity, resulting in changes in absorption or membrane permeability that can positively modulate its activity.[132] Such modifications could potentially be accomplished using metal-catalyzed C(sp^2)–N (herein C–N) cross-coupling reactions with α,α,α-trisubstituted, primary alkylamines, but few catalyst systems effectively promote this transformation.[133] Recently, Buchwald and co-workers[134] disclosed a palladium pre-catalyst system incorporating tailored biarylmonophosphines that effects the cross-coupling of (hetero)aryl bromides and chlorides with α,α,α-trisubstituted, primary alkylamines at elevated temperatures (80–120 ºC; **Scheme 4.1A**). Reaction progress kinetic analysis was used to identify the optimal ancillary ligand design, allowing for a wide range of electrophiles, containing carboxylic acid, ester, amide, and

nitrile moieties, to be employed in this reaction. Additionally, César and co-workers[135] applied pre-catalysts incorporating backbone-decorated NHCs in cross-coupling reactions of (hetero)aryl chlorides and α,α,α-trisubstituted, primary alkylamines at moderate temperatures (40–60 ºC; **Scheme 4.1B**). In each report, ancillary ligand design was crucial in engendering the desired reactivity, giving rise to broad electrophile scope at elevated temperatures (Buchwald) or milder reaction temperatures with aryl chlorides (César).

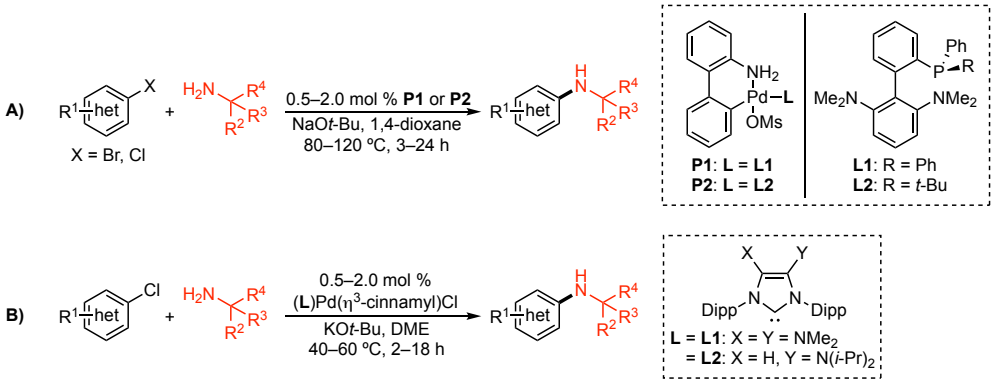

Scheme 4.1. Palladium-catalyzed C–N cross-couplings of α,α,α-trisubstituted, primary alkylamines reported by A) Buchwald and B) César.

4.2.2. Nickel-Catalyzed C(sp^2)–N Cross-Coupling of α,α,α-Trisubstituted, Primary Alkylamines

Examples of nickel-catalyzed C–N cross-coupling reactions using α,α,α-trisubstituted, primary alkylamines are scarce, with the groups of Tu,[136] Montgomery,[137] Baran,[52b] and Sawamura[138] each reporting one or two entries in which *tert*-butylamine and/or 1-adamantylamine is employed in the context of a broader nickel-catalyzed C–N cross-coupling survey (**Scheme 4.2**). Sawamura and coworkers[139] also developed a polystyrene cross-linked bisphosphine ligand that facilitated nickel-catalyzed C–N cross-coupling with aryl chlorides in combination with $Ni(cod)_2$ (**Scheme 4.3**). 1-Adamantylamine, *tert*-octylamine, and cumylamine were reacted with either 4-chlorotoluene or 4-chloroanisole, requiring elevated temperatures (120 ºC) in order to proceed efficiently.

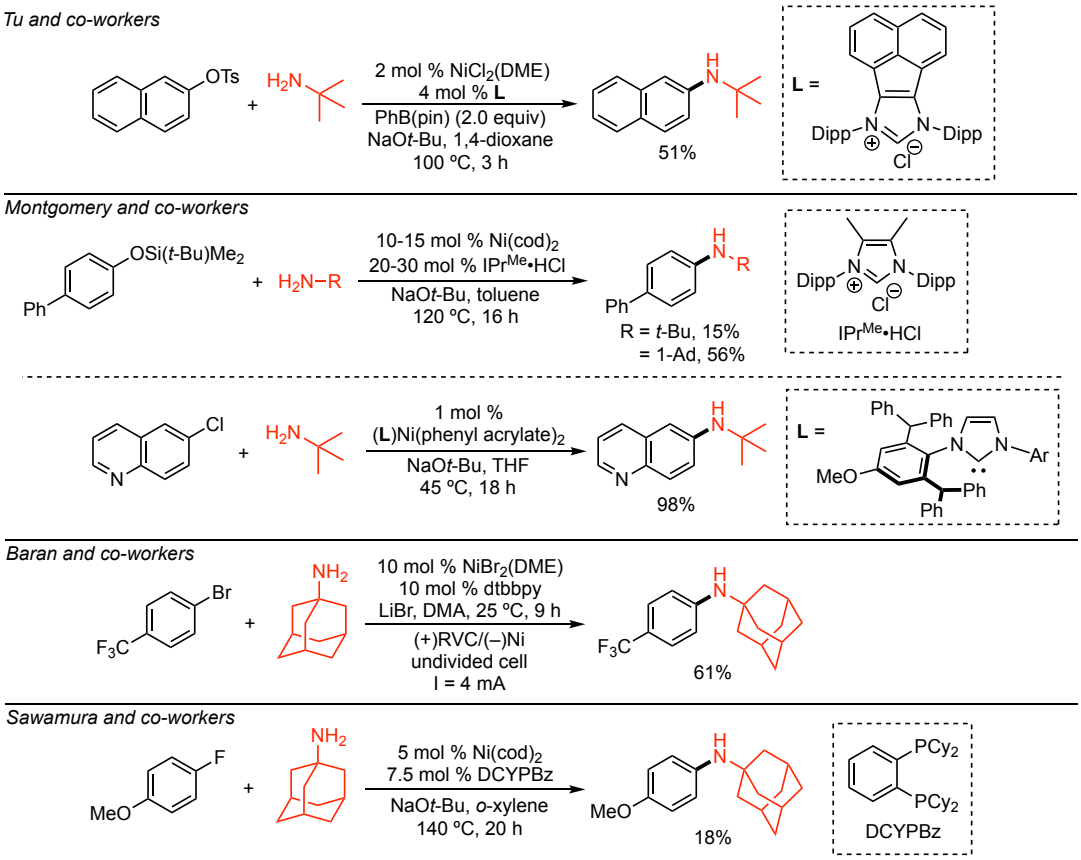

Scheme 4.2. The use of bulky, primary alkylamines in the context of broader nickel-catalyzed C–N cross-coupling surveys.

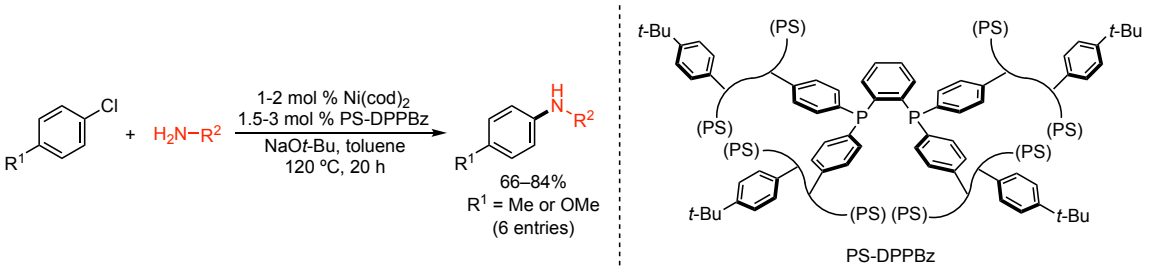

Scheme 4.3. Nickel-catalyzed C–N cross-coupling of α,α,α-trisubstituted, primary alkylamines facilitated by a polystyrene-linked bisphosphine ligand.

4.3 Results and Discussion

4.3.1 Screening Nickel Pre-Catalysts in the C(sp^2)–N Cross-Coupling of α,α,α-Trisubstituted, Primary Alkylamines

Given the limited extent of the nickel-catalyzed C–N cross-coupling of α,α,α-trisubstituted, primary alkylamines, it was hypothesized that applying a tailored ligand design strategy[4] might address the apparent challenges associated with this transformation. Thus, nickel pre-catalysts of the form (L)Ni(*o*-tolyl)Cl[87] were screened in the *N*-arylation

of 1-adamantylamine (**4-2a**) with three challenging (hetero)aryl chlorides (**4-1a** to **4-1c**) at 110 ºC (**Table 4.1**). Pre-catalysts that had previously promoted the cross-coupling of primary alkylamines, namely **2-C1**[57, 66] and **2-C2**,[61a, 68] incorporating PAd-DalPhos (**2-L1**) and JosiPhos CyPF-Cy (**2-L2**) respectively, were not competent in this transformation, with **2-C1** providing poor conversion to **4-3a** to **4-3c** (entry 1) and **2-C2** proving unreactive under these conditions (entry 2). Pre-catalyst **3-C1**, containing dppf (**3-L1**), also did not afford significant conversion to the desired products (entry 3), despite effecting the cross-coupling of secondary alkylamines in prior reports.[59, 140] Next, nickel pre-catalysts containing CyPAd-DalPhos (**2-L3**) and an electron-rich PAd-DalPhos variant (**2-L4**), **2-C3** and **2-C4** respectively, were screened for activity in the desired transformation, as both pre-catalysts had previously facilitated the cross-coupling of α-branched cyclopropylamine (see **Chapter 2**). While **2-C3** provided modest conversion to **4-3a** and **4-3b** (entry 4), **2-C4** did not furnish appreciable amounts of the desired products (entry 5).

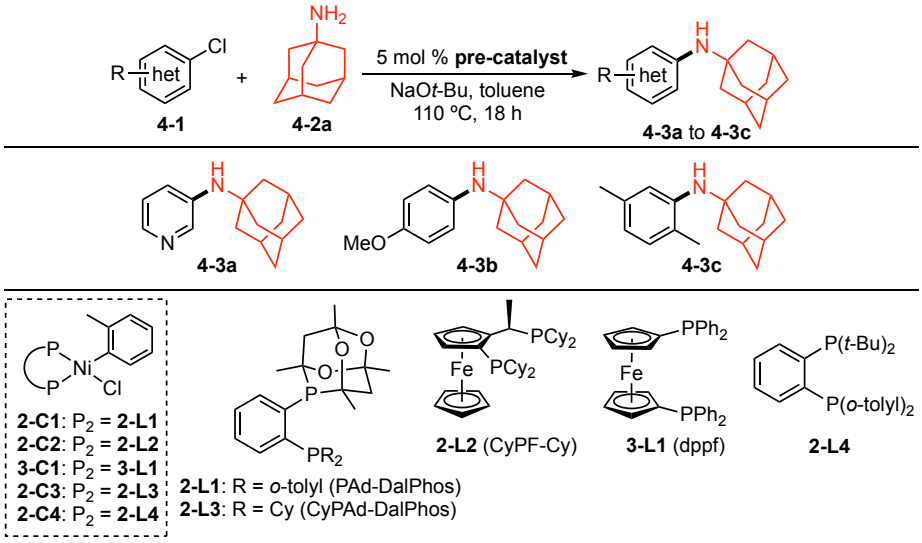

Entry	Pre-catalyst	Yield **4-3a** (%)[a]	Yield **4-3b** (%)[a]	Yield **4-3c** (%)[a]
1	**2-C1**	<5	11	19
2	**2-C2**	<5	<5	<5
3	**3-C1**	<5	<5	<5
4	**2-C3**	68	48	19
5	**2-C4**	<5	8	6

Table 4.1. Pre-catalyst screening for the nickel-catalyzed cross-coupling of **4-1a** to **4-1c** and **4-2a**. Reaction conditions: pre-catalyst (5 mol %), NaO*t*-Bu (1.5 equiv), **4-1a** to **4-1c** (0.12 mmol, 1.0 equiv), **4-2a** (1.1 equiv), and toluene (1 mL, [ArCl] = 0.12 M) at 110 ºC. [a]Conversions to product are estimated on the basis of calibrated GC data.

4.3.2 Synthesis of Pre-catalysts 4-C1 and 4-C2

Based on the results of this initial screen, it was anticipated that the steric bulk of **4-2a** might necessitate a less sterically hindered ancillary ligand in order to improve catalytic activity. Thus, pre-catalysts containing PAd-DalPhos variants in which the P(*o*-tolyl)$_2$ group was replaced with a PPh$_2$ or P(*i*-Pr)$_2$ moiety (**4-L1** and **4-L2** respectively) were subsequently examined. While the syntheses of **4-L1** and **4-L2** are known,[66] corresponding (L)Ni(*o*-tolyl)Cl pre-catalysts had not yet been prepared. **4-C1** and **4-C2**, containing **4-L1** and **4-L2** respectively, were synthesized as air-stable solids according to an adapted literature procedure (**Scheme 4.4**),[66] exhibiting similar spectroscopic and solid-state features to related (L)Ni(*o*-tolyl)Cl pre-catalysts (see **Figure 4.1**).

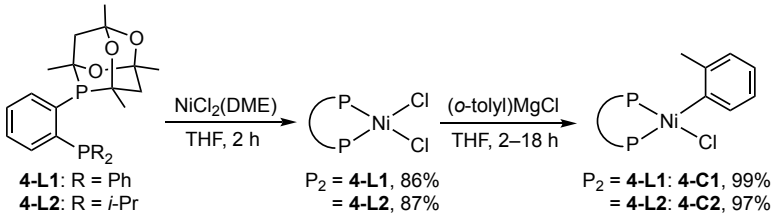

Scheme 4.4. Synthesis of pre-catalysts **4-C1** and **4-C2**.

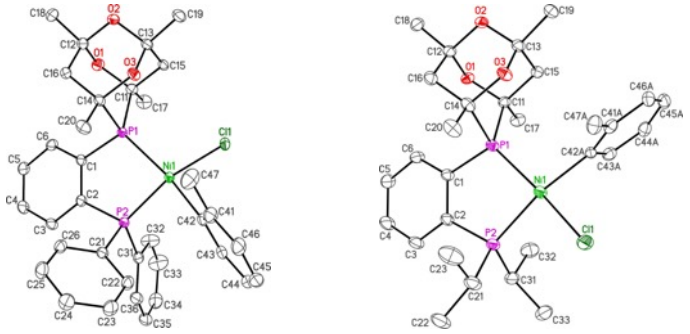

Figure 4.1. Single-crystal X-ray structures of **4-C1** (left) and **4-C2** (right; major orientation of disordered tolyl group shown), represented with thermal ellipsoids at the 30% probability level. Hydrogen atoms and the CH_2Cl_2 solvent molecule for **4-C2** omitted for clarity. Selected interatomic distances (Å): for **4-C1**, Ni–P1 2.2471(5), Ni–P2 2.1185(5), Ni–Cl1 2.2071(5), Ni–C42 1.9356(19); for **4-C2**, Ni–P1 2.1661(8), Ni–P2 2.2047(8), Ni–Cl1 2.1986(9), Ni–C42A 1.943(4).

4.3.3. Screening Pre-Catalysts 4-C1 and 4-C2 in the Nickel-Catalyzed C(sp^2)–N Cross-Coupling of α,α,α-Trisubstituted, Primary Alkylamines

With the new pre-catalysts in hand, **4-C1** and **4-C2** were screened in the cross-coupling of **4-1a** to **4-1c** and **4-2a** (**Table 4.2**). The use of **4-C1** afforded good conversions to **4-3a** and **4-3b** (entry 1), while only modest conversion to the desired products was

observed using **4-C2** (entry 2). As **2-C3** and **4-C1** provided similar conversions to **4-3a** and **4-3c** (see **Table 4.1**, entry 4), the temperature was lowered to 80 ºC to elucidate more significant differences in catalytic activity. At this temperature, **4-C1** emerged as the superior pre-catalyst, providing greater conversion to **4-3a** and **4-3b** when compared to **2-C3** (entries 4 and 5). The temperature could be further reduced to 60 ºC, with **4-C1** demonstrating excellent conversion to **4-3a** and **4-3c** while maintaining moderate conversion to **4-3b** (entry 5). However, reactions conducted at room temperature resulted in poorer conversion to the desired products (entry 6). Increasing the reaction concentration (entry 7), increasing the equivalents of **4-2a** (entry 8), or lowering the catalyst loading to 4 mol % (entry 9) did not improve conversion to **4-3a**.

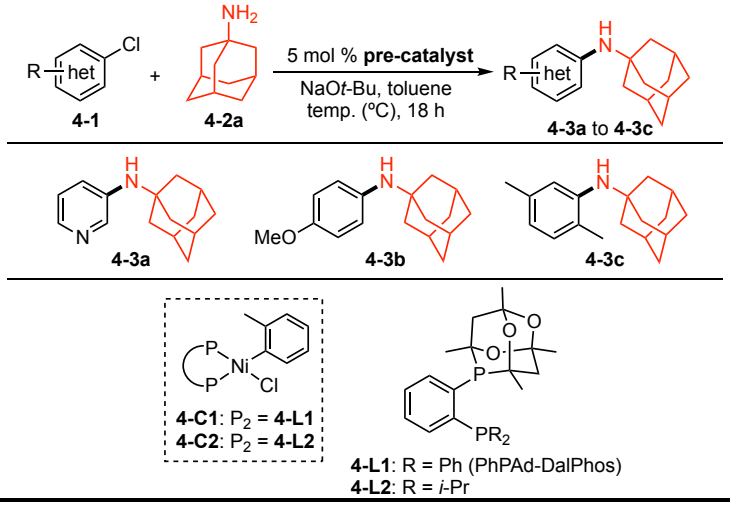

Entry	Pre-catalyst	Temp. (ºC)	Yield **4-3a** (%)[a]	Yield **4-3b** (%)[a]	Yield **4-3c** (%)[a]
1	**4-C1**	110	65	83	32
2	**4-C2**	110	27	27	27
3	**2-C3**	80	54	47	57
4	**4-C1**	80	91	66	49
5	**4-C1**	60	90	49	81
6	**4-C1**	25	73	9	56
7[b]	**4-C1**	60	86	-	-
8[c]	**4-C1**	60	77	-	-
9[d]	**4-C1**	60	70	-	-

Table 4.2. Pre-catalyst screening for the nickel-catalyzed cross-coupling of **4-1a** to **4-1c** and **4-2a**. Reaction conditions: pre-catalyst (5 mol %), NaO*t*-Bu (1.5 equiv), **4-1a** to **4-1c** (0.12 mmol, 1.0 equiv), **4-2a** (1.1 equiv), and toluene (1 mL, [ArCl] = 0.12 M) at the indicated temperature. [a]Conversions to product are estimated on the basis of calibrated GC data, with the remaining mass balance largely attributed to remaining **4-1a** to **4-1c** (see **Tables A6**–**A8** in Appendix 6 for more details). [b]1.5 equiv **4-2a**. [c]Toluene (0.5 mL, [ArCl] = 0.24 M). [d]4 mol % **4-C1**.

Additional screening was performed to ascertain the effects of solvent (**Table 4.3**) and base (**Table 4.4**) on the outcome of the reaction. 1,4-Dioxane proved to be a suitable solvent for this transformation (**Table 4.3**, entry 2), providing **4-3a** and **4-3b** in comparable amounts as when the reactions were conducted in toluene (entry 1). However, the use of other polar solvents such as CPME or THF resulted in reduced conversion to the desired products (entries 3 and 4). NaO*t*-Bu proved to be the ideal base in this reaction, regardless of solvent (**Table 4.4**, entries 1 and 7); the use of LiO*t*-Bu or KO*t*-Bu provided inferior conversion to **4-3a** in toluene (entries 2 and 3), though comparable conversion to **4-3b** was achieved with LiO*t*-Bu in dioxane (entry 8). Weak bases such as Cs_2CO_3, K_3PO_4, and DBU were not effective in this transformation, affording negligible conversion to product in either toluene or 1,4-dioxane (entries 4-6 and 10-12). Thus, the results of this additional screening revealed the conditions in entry 5 of **Table 4.2** to be optimal.

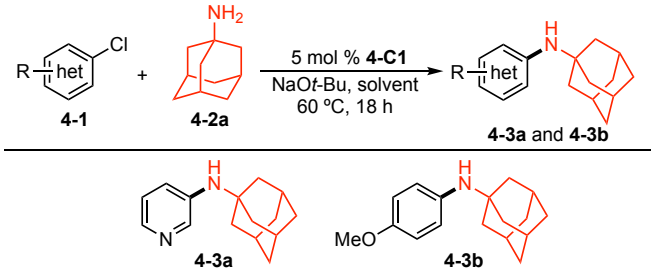

Entry	Solvent	Yield **4-3a** (%)[a]	Yield **4-3b** (%)[a]
1	toluene	90	49
2	1,4-dioxane	90	44
3	CPME	75	33
4	THF	20	20

Table 4.3. Solvent optimization for the nickel-catalyzed cross-coupling of **4-1a** and **4-1b** with **4-2a** using **4-C1**. Reaction conditions: **4-C1** (5 mol %), NaO*t*-Bu (1.5 equiv), **4-1a** and **4-1b** (0.12 mmol, 1.0 equiv), **4-2a** (1.1 equiv), and solvent (1 mL, [ArCl] = 0.12 M). [a]Conversions to product and remaining starting material are estimated on the basis of calibrated GC data, with the remaining mass balance largely attributed to remaining **4-1a** and **4-1b** (see **Tables A9** and **A10** in Appendix 6 for more details).

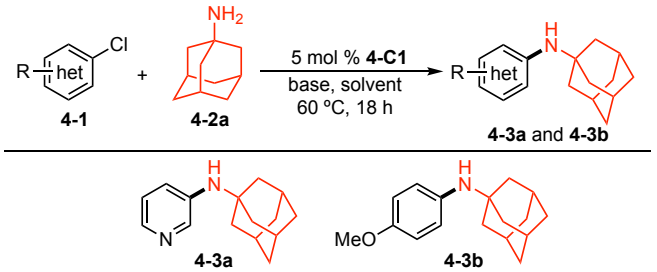

Entry	Solvent	Base	Yield **4-3a** (%)[a]	Yield **4-3b** (%)[a]
1	toluene	NaO*t*-Bu	90	49
2		LiO*t*-Bu	37	5
3		KO*t*-Bu	14	5
4		Cs_2CO_3[b]	<5	<5
5		K_3PO_4[b]	<5	<5
6		DBU[c]	<5	<5
7	1,4-dioxane	NaO*t*-Bu	90	44
8		LiO*t*-Bu	67	46
9		KO*t*-Bu	7	<5
10		Cs_2CO_3[b]	<5	<5
11		K_3PO_4[b]	<5	<5
12		DBU[c]	<5	<5

Table 4.4. Base optimization for the nickel-catalyzed cross-coupling of **4-1a** and **4-1b** with **4-2a** using **4-C1**. Reaction conditions: **4-C1** (5 mol %), base (1.5 equiv), **4-1a** and **4-1b** (0.12 mmol, 1.0 equiv), **4-2a** (1.1 equiv), and solvent (1 mL, [ArCl] = 0.12 M). [a]Conversions to product and remaining starting material are estimated on the basis of calibrated GC data, with the remaining mass balance largely attributed to remaining **4-1a** and **4-1b** (see **Tables A11** and **A12** in Appendix 6 for more details). [b]3.0 equiv. [c]2.0 equiv.

4.3.4 Scope of the Nickel-Catalyzed C(sp^2)–N Cross-Coupling of α,α,α-Trisubstituted, Primary Alkylamines

Having identified optimized reaction conditions using **4-C1**, the scope of the cross-coupling of (hetero)aryl halides with α,α,α-trisubstituted, primary alkylamines was then surveyed (**Scheme 4.5**). Various electrophiles were effective coupling partners in this transformation, including those with electron-donating (**4-3b** and **4-3d**) and electron-withdrawing (**4-3e**; **4-3j** to **4-3l**) substituents (e.g., ether, fluoro, nitrile, and ketone moieties), or substituents in the *ortho*-position (**4-3c** and **4-3d**; **4-3h** and **4-3i**). Reactions with heteroaryl halides containing pyridine (**4-3a** and **4-3m**), quinoline (**4-3f** and **4-3n**), benzodioxole (**4-3g**), benzothiophene (**4-3h**), quinaldine (**4-3o**), and quinoxaline (**4-3p**) cores also proceeded efficiently. Several α,α,α-trisubstituted, primary alkylamines could be used, including 1-adamantylamine (**4-3a** to **4-3c**; **4-3g** and **4-3h**), cumylamine (**4-3d, 4-3f**, **4-3m**, and **4-3n**), *tert*-octylamine (**4-3e** and **4-3l**), and *tert*-butylamine (**4-3i** to **4-3l**; **4-**

3o and **4-3p**). The reaction conditions also proved scalable, with 1.049 g (95%) of **4-3p** being produced on a 5.5 mmol scale. While the majority of the reactions employed (hetero)aryl chlorides, cross-couplings with (hetero)aryl bromides (**4-3f** and **4-3k**) and an aryl tosylate (**4-3i**) were also successful. Control reactions in the absence of **4-C1** provided <5% conversion (GC) to **4-3a**, **4-3l**, **4-3m**, **4-3p**. Notably, the first examples of room temperature C–N cross-coupling reactions of (hetero)aryl halides with α,α,α-trisubstituted, primary amines using any metal catalyst (palladium, nickel, or other) were achieved with a diverse set of electrophiles (**4-3i** to **4-3p**) using **4-C1**.

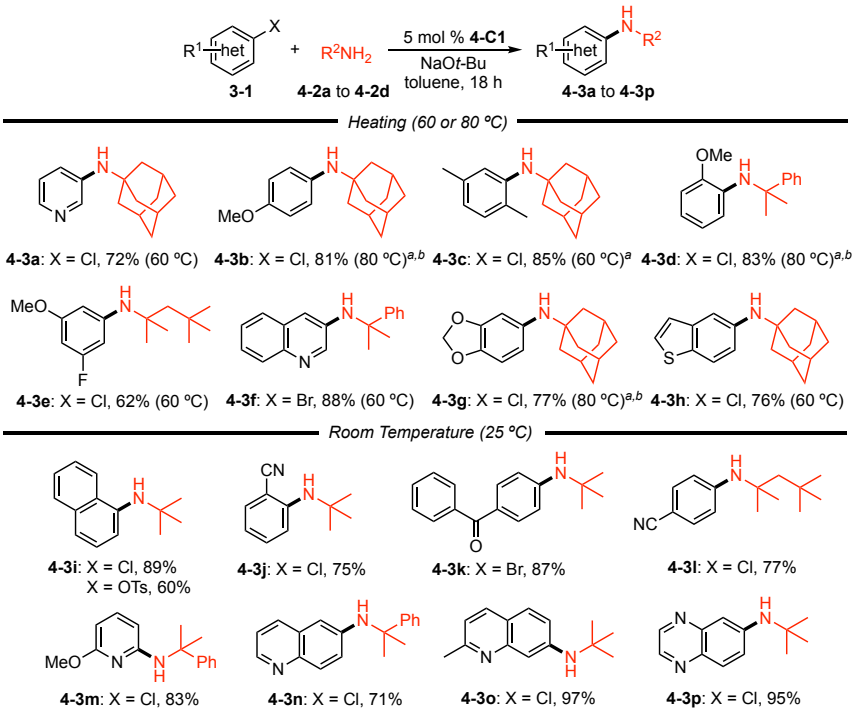

Scheme 4.5. Scope of the nickel-catalyzed cross-coupling of (hetero)aryl halides with α,α,α-trisubstituted, primary alkylamines using **4-C1**. Reaction conditions: **4-C1** (5 mol %), NaO*t*-Bu (1.5 equiv), **4-1** (0.5 mmol, 1.0 equiv), **4-2a** to **4-2d** (1.1 or 3.0 equiv), and toluene (4.17 mL, [ArX] = 0.12 M) at the indicated temperature. Isolated yields reported. [a]**4-C1** (6 mol %). [b]Toluene (2.08 mL, [ArCl = 0.24 M]).

4.3.5 Limitations of the 4-C1 Pre-Catalyst System for the Nickel-Catalyzed C(sp^2)–N Cross-Coupling of α,α,α-Trisubstituted, Primary Alkylamines

While the scope of the nickel-catalyzed C–N cross-coupling of α,α,α-trisubstituted, primary alkylamines using **4-C1** was generally quite broad, certain electrophiles and nucleophiles were not suitable coupling partners. (Hetero)aryl triflates, mesylates, or carbamates (**Figure 4.2A**) were generally unreactive under optimized reaction conditions; increasing the reaction temperature (110 °C) or making use of weak base conditions that

were previously effective for such substrates (see **Figure 2.10**) did not improve conversion to the desired products. The incompatibility of these substrates with **4-C1** may arise from the relatively poor electron-donating ability of **4-L1**, resulting in a metal centre that is unable to perform the challenging C(sp^2)–OR oxidative addition. The use of triphenylmethylamine (**Figure 4.2B**) in this transformation generally provided negligible conversion to product, even when paired with highly activated substrates (e.g., 4-chlorobenzonitrile), likely due to its considerable steric bulk. Additionally, reactions employing a 2-amino-2-methyl-1-propanol derivative (**Figure 4.2B**) were largely unsuccessful, likely due to the presence of the pendant silyl ether.

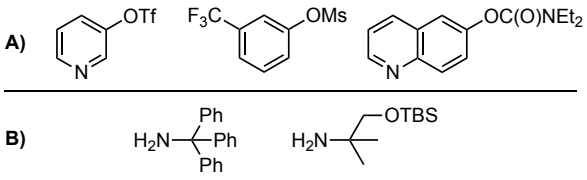

Figure 4.2. Representative A) electrophiles and B) nucleophiles that were not suitable coupling partners in the nickel-catalyzed C–N cross-coupling of α,α,α-trisubstituted, primary alkylamines using **4-C1**.

4.3.6 Chloride versus Carbamate Selectivity Studies

Given that (hetero)aryl carbamates were unsuccessful coupling partners under optimized reaction conditions, experiments were conducted to identify whether these substrates were simply unreactive or acted as catalyst poisons (**Scheme 4.6A**). Addition of one equivalent of quinolin-6-yl diethylcarbamate (**4-4**) to the otherwise successful reaction of 1-chloronaphthalene (**3-1a**) and *tert*-butylamine (**4-2d**) mediated by **4-C1** did not hinder conversion to product **4-3i**, suggesting additive **4-4** is not inhibitory. This reactivity pattern was then exploited in chemoselective cross-couplings of substrates **4-1q** and **4-1r**, whereby the aryl chloride reacted preferentially with α,α,α-trisubstituted, primary alkylamines using **4-C1**, even at elevated temperatures (**Scheme 4.6B**). Such chemoselectivity could potentially be leveraged in sequential reactions, with **4-C1** effecting the cross-coupling of an aryl chloride and an α,α,α-trisubstituted, primary alkylamine in the presence of a carbamate functionality, followed by directed metalation[141] or the introduction of a second nucleophile in a subsequent cross-coupling reaction[61, 142] involving the carbamate moiety.

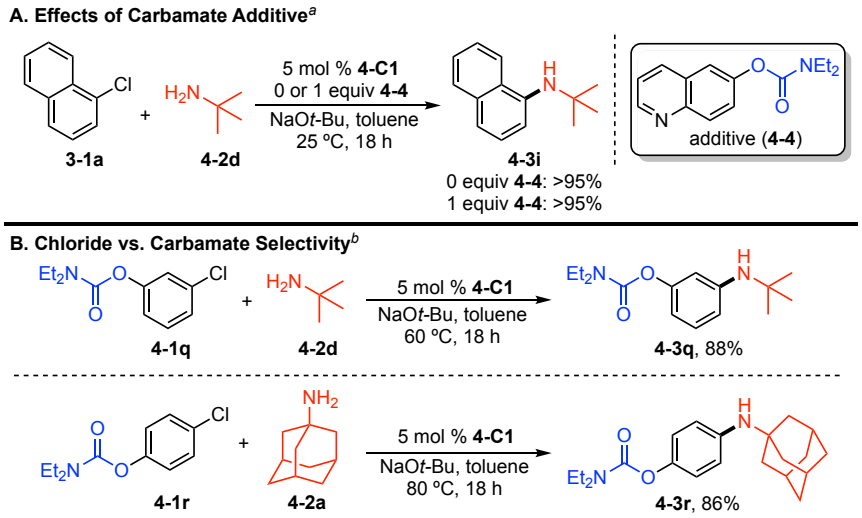

Scheme 4.6. A) Exploring the effect of a carbamate additive on the nickel-catalyzed cross-coupling of 1-chloronaphthalene and *tert*-butylamine. B) Chemoselective cross-coupling reactions. [a]Reaction conditions: **4-C1** (5 mol %), NaO*t*-Bu (1.5 equiv), **3-1a** (0.12 mmol, 1.0 equiv), **4-2d** (3.0 equiv), and toluene (1 mL, [ArCl] = 0.12 M). Conversion to **4-3i** determined on the basis of calibrated GC data. [b]Reaction conditions: **4-C1** (5 mol %), NaO*t*-Bu (1.5 equiv), **4-1q** and **4-1r** (0.5 mmol, 1.0 equiv), **4-2a** or **4-2d** (1.1 or 3.0 equiv), and toluene (4.17 mL, [ArCl] = 0.12 M) at the indicated temperature. Isolated yields reported.

4.3.7 Scope of the Nickel-Catalyzed C(sp^2)–N Cross-Coupling of Other, Sterically Hindered Nucleophiles

The scope of the nickel-catalyzed cross-coupling of (hetero)aryl halides and other bulky nucleophiles using **4-C1** was then briefly explored (**Scheme 4.7**). Electrophiles containing electron-donating or electron-withdrawing substituents, including in *ortho*-positions, were cross-coupled successfully, along with heteroaryl halides featuring benzothiophene (**4-6c**), quinoline (**4-6d**), or quinoxaline (**3-3m**) cores. Reactions with 2,6-dimethyl substituted anilines (**4-6a** to **4-6d**) proceeded efficiently at room temperature (**Scheme 4.7A**), but the bulkier 2,6-diisopropylaniline was not a suitable nucleophile, even at 110 ºC. Additionally, sterically hindered primary alcohols 3,3-dimethyl-2-butanol (**4-8a**) and *tert*-butanol (**4-8b**) were well-tolerated (**Scheme 4.7B**), albeit using increased catalyst loadings (7.5 mol %) and temperatures (60 ºC). Notably, these latter two entries represent only the second example of nickel-catalyzed C–O cross-coupling not mediated by photoredox catalysis (see Chapter 3). Furthermore, **4-C1** promoted this transformation at significantly reduced temperatures (60 ºC) compared to the previous state-of-the-art

nickel catalyst system, **2-C3** (110 ºC; see **Figure 3.6**), with **2-C3** providing minimal conversion to **3-3m** (15%) compared to **4-C1** (>95%) under these conditions.

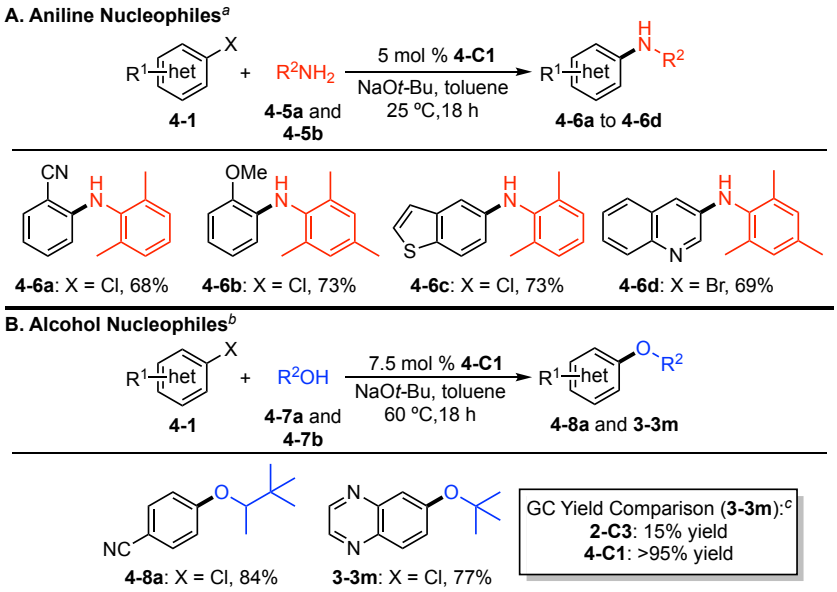

Scheme 4.7. Nickel-catalyzed cross-coupling reactions of A) anilines and B) alcohols using **4-C1**. [a]Reaction conditions: **4-C1** (5 mol %), NaO*t*-Bu (1.5 equiv), **4-1** (0.5 mmol, 1.0 equiv), **4-5a** or **4-5b** (1.1 equiv), and toluene (4.17 mL, [ArCl] = 0.12 M) at 25 ºC. Isolated yields reported. [b]Reaction conditions: **4-C1** (7.5 mol %), NaO*t*-Bu (1.5 equiv), **4-1** (0.5 mmol, 1.0 equiv), **4-7a** or **4-7b** (3.0 equiv), and toluene (4.17 mL, [ArCl] = 0.12 M) at 60 ºC. Isolated yields reported. [c]Conversion to **3-3m** determined on the basis of calibrated GC data.

4.3.8 Nickel-Catalyzed C(sp^2)–N Cross-Coupling of α,α,α-Trisubstituted, Primary Alkylamines with 1,8-Naphthalimide Electrophiles – Fluorescence Applications

4.3.8.1 Introduction

Following publication of the preceding study, a collaboration was established with scientists at the Walter and Eliza Hall Institute of Medical Research in Australia. The incorporation of α,α,α-trisubstituted, primary alkylamines (e.g., *tert*-butylamine) into rhodamine fluorophores had previously been shown to prevent oxidative photobluing,[143] a mechanism that reduces the stability and efficacy of fluorescent probes in biological applications. The collaborators were interested in determining whether a similarly beneficial effect could be observed with related 1,8-naphthalimide fluorophores, which have found application in anion sensing,[144] cellular imaging,[145] and DNA intercalation.[146] Amine-substituted 1,8-naphthalimides can be prepared via nucleophilic aromatic substitution of the corresponding bromo-[147] or nitro-substituted precursors,[148] but these

methodologies are generally limited in amine scope. Thus, recent efforts have focused on the development of more robust cross-coupling protocols using palladium[149] or copper[150] catalysts to access the desired compounds. However, α,α,α-trisubstituted, primary alkylamines had not previously been employed in these methods. Given the success of the **4-C1** pre-catalyst system in the nickel-catalyzed cross-coupling of α,α,α-trisubstituted, primary alkylamines, the researchers were interested in applying this base metal-catalyzed procedure to prepare corresponding amine-substituted 1,8-naphthalimides and assess the fluorescent properties of these compounds.

4.3.8.2 Screening Pre-Catalysts in the C(sp^2*)–N Cross-Coupling of Naphthalimide **4-9** and* tert-*Butylamine*

Initially, pre-catalysts of the form (L)Ni(*o*-tolyl)Cl[87] were screened in the cross-coupling of 1,8-napthalimide **4-9** with *tert*-butylamine (**4-2d**) under optimized catalytic conditions (see **Scheme 4.5**; **Table 4.5**). Pre-catalyst **4-C1**, incorporating PhPAd-DalPhos (**4-L1**) provided minimal conversion to the desired product **4-10a** (entry 1), despite being the optimal pre-catalyst for the cross-coupling of similar (hetero)aryl chlorides. Pre-catalysts **2-C1**, **2-C3**, and **3-C1**, incorporating PAd-DalPhos (**2-L1**), CyPAd-DalPhos (**2-L3**), and dppf (**3-C1**) respectively, were also ineffective for the desired transformation, affording negligible conversion to **4-10a** (entries 2–4).

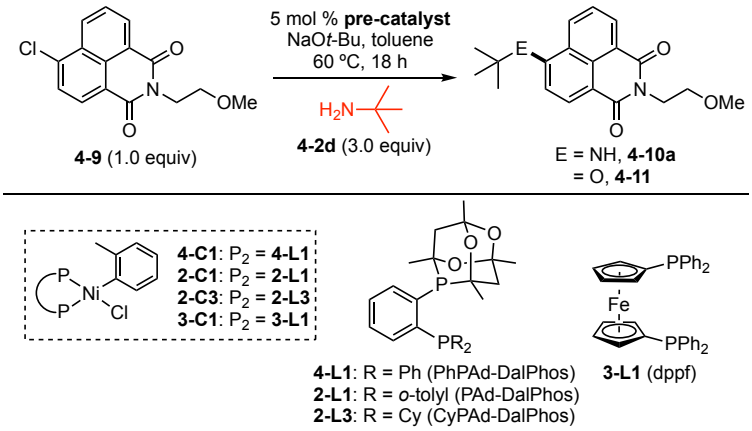

Entry	Pre-catalyst	Yield **4-10a** (%)[a]	Remaining **4-9** (%)[a]
1	**4-C1**	13	80
2	**2-C1**	<5	78
3	**2-C3**	<5	78
4	**3-C1**	8	63

Table 4.5. Pre-catalyst screen for the nickel-catalyzed cross-coupling of **4-9** with *tert*-butylamine (**4-2d**). Reaction conditions: pre-catalyst (5 mol %), NaO*t*-Bu (1.5 equiv), **4-9** (0.12 mmol, 1.0 equiv), **4-2d** (3.0 equiv), and toluene (1.0 mL, [**4-9**] = 0.12 M). [a]Conversion to **4-10a** and remaining **4-9** are estimated on the basis of calibrated GC data, with the remaining mass balance attributed to the –O*t*-Bu cross-coupled product of **4-9** (**4-11**). See **Table A13** in Appendix 6 for more details.

*4.3.8.3 Ligand Screening in the C(*sp^2*)–N Cross-Coupling of Naphthalimide **4-9** and* tert*-Butylamine*

Notwithstanding the low conversion to **4-10a**, the formation of product when employing **4-C1** was nonetheless encouraging. Therefore, an expanded optimization protocol using Ni(cod)$_2$/ligand catalyst mixtures (10 mol % each) was conducted at 80 ºC for 18 h (**Table 4.6**). Modest conversion to **4-10a** was observed when employing **4-L1** under these conditions (entry 1), while the related ligands **2-L1** and **2-L3** provided only minimal conversion to product (entries 2 and 3). Wide bite-angle bisphosphines proved to be suitable ligands for the desired transformation, with dppf (**3-L1**), XantPhos (**4-L3**), and *N*-XantPhos (**4-L4**) affording good conversion to **3-10a** (entries 4–6). DPEPhos (**4-L5**), which was employed in the nickel-catalyzed C–N cross-coupling of secondary amines and azoles with (hetero)aryl halides in a prior report,[117] furnished excellent conversion to **3-10a** (entry 7). The NHC ligand IPr (**3-L2**) proved to be equally as effective as **4-L5** in the desired transformation (entry 8), while its saturated analogue SIPr (**4-L6**) exhibited reduced activity (entry 9). While nickel-catalyzed C–N cross-coupling reactions facilitated

by catalyst systems incorporating IPr are well-known,[41b] the successful use of bulky, primary alkylamine nucleophiles in this chemistry has not been disclosed previously.

Halving the $Ni(cod)_2$ catalyst loading to 5 mol % in reactions employing **4-L5** (DPEPhos) and **3-L2** (IPr) confirmed the latter as the superior ligand; diminished activity was observed under these conditions using **4-L5** (entry 10), while **3-L2** maintained excellent conversion to **4-10a** (entry 11). Further optimization revealed that the reaction could be conducted at ambient temperature (entry 12 and 13) using 4 mol % $Ni(cod)_2$/8 mol % **3-L2** (entry 14). However, lowering the catalyst loading further resulted in decreased conversion to the desired product (entry 15). Cs_2CO_3 could also be employed as a base in this reaction, but required 1,4-dioxane as solvent, higher temperatures (60 ºC), and increased catalyst loadings (10 mol % $Ni(cod)_2$/20 mol % **3-L2**) and amine equivalents in order to proceed efficiently (see **Table A15** in Appendix 6). Control experiments in which either $Ni(cod)_2$ or **3-L2** were omitted from the reaction indicated the importance of each component to the observed activity (entry 16 and 17). Interestingly, catalyst mixtures of 5 mol % $Ni(cod)_2$/5 mol % **3-L1** (dppf), using LiO*t*-Bu as base and 1,4-dioxane as solvent, were also found to effect the desired transformation at room temperature (see **Table A16** in Appendix 6). However, comparing **3-L1** (dppf) and **3-L2** (IPr) in the Ni-catalyzed cross-coupling of **4-9** and 1-adamantylamine (**4-2a**; see **Scheme 4.8**) showed that the **3-L2** catalyst system provided the desired amine cross-coupled product **4-10b** exclusively, while the **3-L1** catalyst system afforded appreciable amounts of the unwanted –O*t*-Bu cross-coupled product of **4-9** (**4-11**, see below), as confirmed by ^1H NMR spectroscopy (~3:1 ratio of **4-10b**:**4-11**; see **Figure A128** in Appendix 7. On the basis of these collective optimization results, **3-L2** was selected as the optimal ligand for this transformation.

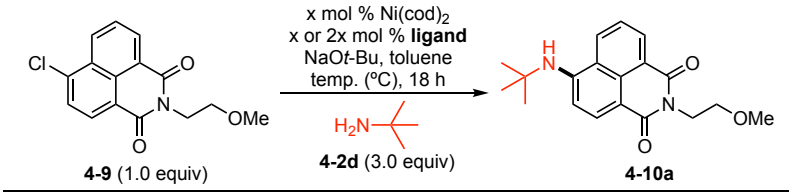

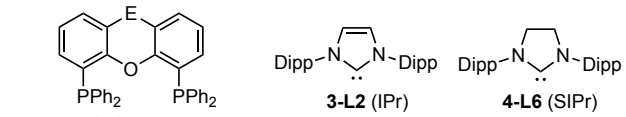

4-L3: E = $C(CH_3)_2$ (XantPhos)
4-L4: E = NH (*N*-XantPhos)
4-L5: E = nothing (DPEPhos)

Entry	x	Ligand	Temp. (ºC)	Yield **4-10a** (%)[a]	Remaining **4-9** (%)[a]
1	10	**4-L1**	80	55	25
2		**2-L1**		10	63
3		**2-L3**		15	55
4		**3-L1**		71	29
5	10	**4-L3**	80	51	23
6		**4-L4**		68	28
7		**4-L5**		>95	<5
8		**3-L2**		95	<5
9		**4-L6**		71	<5
10	5	**4-L5**	80	65	32
11		**3-L2**		>95	<5
12	5	**3-L2**	60	>95	<5
13		**3-L2**	25	>95	<5
14	4	**3-L2**	25	>95	<5
15	3	**3-L2**	25	83	17
16	5	-	25	<5	53
17[b]	5	**3-L2**	25	<5	59
18[b]	-	-	25	<5	47

Table 4.6. Ligand screen and optimization for the Ni-catalyzed cross-coupling of **4-9** with *tert*-butylamine (**4-2d**). Reaction conditions: $Ni(cod)_2$ (x mol %), ligand (x mol %; **3-L2** and **4-L6** = 2x mol %), NaO*t*-Bu (1.5 equiv), **4-9** (0.12 mmol, 1.0 equiv), **4-2d** (3.0 equiv), and toluene (1.0 mL, [**4-9**] = 0.12 M). [a]Conversion to **4-10a** and remaining **4-9** are estimated on the basis of calibrated GC data, with the remaining mass balance largely attributed to unidentified byproducts. See **Table A14** in Appendix 6 more details. [b]$Ni(cod)_2$ omitted from the reaction.

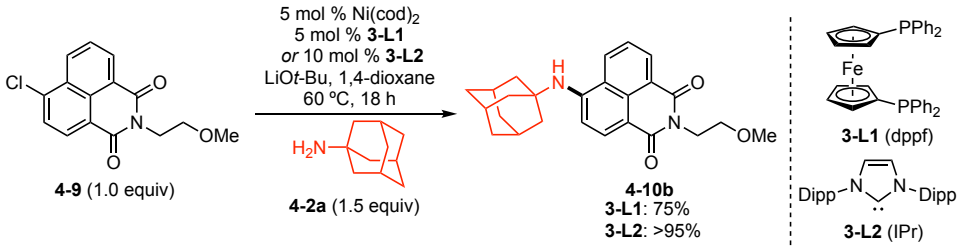

Scheme 4.8. Comparison of **3-L1** and **3-L2** in the nickel-catalyzed cross-coupling of **4-9** and 1-adamantylamine (**4-2a**). Yield of **4-10b** estimated on the basis of crude ^{1}H NMR data.

*4.3.8.4 Scope of the Nickel-Catalyzed C(*sp^2*)–N Cross-Coupling of Naphthalimide **9** with α,α,α-Trisubstituted, Primary Alkylamines*

With optimized reaction conditions in hand, the nickel-catalyzed cross-coupling of **4-9** with various α,α,α-trisubstituted, primary alkylamines was examined (**Scheme 4.9A**). While 4 mol % Ni(cod)$_2$/8 mol % **3-L2** could be used successfully with *tert*-butylamine (see **Table 4.6**), 5 mol % Ni(cod)$_2$/10 mol % **3-L2** was employed in scope exploration to ensure sufficient activity for more challenging coupling partners. Several bulky, primary alkylamines were well-tolerated in this reaction, including *tert*-butylamine (**4-10a**), 1-adamantylamine (**4-10b**), 2,2,2-trifluoro-1,1-dimethyl-ethylamine (**4-10c**), cumylamine (**4-10d**), and *tert*-octylamine (**4-10e**). Notably, the newly developed Ni(cod)$_2$/**3-L2** catalyst system is among the few systems capable of effecting the nickel-catalyzed cross-coupling of bulky, primary alkylamines,[52b, 136-139] and represents only the second example of such cross-couplings at room temperature with any metal catalyst, the first being the **4-C1** pre-catalyst system detailed earlier in this chapter.

Given the propensity for Ni(cod)$_2$/**3-L1** catalyst mixtures to furnish the –O*t*-Bu cross-coupled product of **4-9** (**4-11**, see above), this compound was prepared deliberately from **9** and *tert*-butanol using **3-C1** under conditions adapted from the literature (**Scheme 4.9B**).[59] Examples of nickel-catalyzed C(*sp*^{2})–O cross-coupling of (hetero)aryl electrophiles and aliphatic alcohols without recourse to photoredox catalysis[108, 113-116, 151] or electrochemistry,[52a] methods that are generally ineffective for transformations involving aryl chlorides, are limited to the studies discussed earlier in this thesis, employing either **2-C3** and **2-C1** (Chapter 3), or **4-C1** (Chapter 4), further emphasizing the potential of ancillary ligands to enable such challenging nickel-catalyzed cross-couplings.

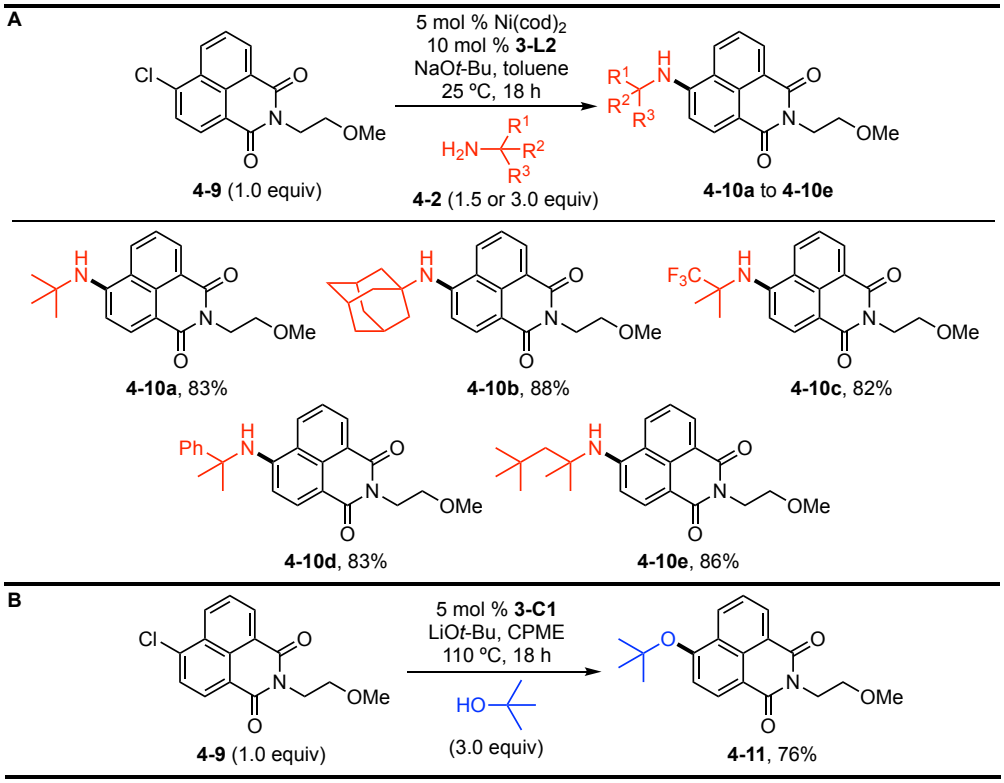

Scheme 4.9. A) Ni-catalyzed cross-coupling of **4-9** with bulky, primary alkylamines using Ni(cod)$_2$/**3-L2**. B) Ni-catalyzed cross-coupling of **4-9** with *tert*-butanol using **3-C1**. Reaction conditions: A) Ni(cod)$_2$ (5 mol %), **3-L2** (10 mol %), NaO*t*-Bu (1.5 equiv), **4-9** (0.4 mmol, 1.0 equiv), **4-2** (1.5 or 3.0 equiv), and toluene (3.33 mL, [**4-9**] = 0.12 M). B) **3-C1** (5 mol %), LiO*t*-Bu (1.5 equiv), **4-9** (0.45 mmol, 1.0 equiv), *tert*-butanol (3.0 equiv), and CPME (1.875 mL, [**4-9**] = 0.24 M). Isolated yields reported.

4.4 Summary

In conclusion, a new, nickel pre-catalyst **4-C1**, containing tailored ancillary ligand **4-L1** (PhPAd-DalPhos) was developed for the cross-coupling of α,α,α-trisubstituted, primary alkylamines and related hindered nucleophiles with (hetero)aryl halides. The use of **4-C1** allowed the first nickel-catalyzed C–N cross-couplings of α,α,α-trisubstituted, primary alkylamines with a substrate scope competitive to that achieved by palladium catalysis, as well as the first examples of room temperature reactivity with (hetero)aryl chlorides employing either palladium or nickel catalysis. Aryl chloride versus aryl carbamate selectivity could also be leveraged in chemoselective cross-coupling reactions. Additionally, a Ni(cod)$_2$/**3-L2** (IPr) catalyst system was developed for the synthesis of substituted 1,8-naphthalimides containing α,α,α-trisubstituted, primary alkylamines.

4.5 Experimental

4.5.1 General Considerations

Unless otherwise indicated, all experimental procedures were conducted in a nitrogen-filled, inert atmosphere glovebox, with work-up procedures carried out on the benchtop in air as indicated. Toluene was purged with nitrogen, passed through a double column purification system containing alumina and copper-Q5 reactant, and stored over 4 Å molecular sieves in bulbs fitted with PTFE taps prior to use. THF and CPME were dried over Na/benzophenone, distilled under a nitrogen atmosphere, and stored over 4 Å molecular sieves in bulbs fitted with PTFE taps. Anhydrous 1,4-dioxane was transferred to a bulb with a PTFE tap, sparged with nitrogen, and stored over 4 Å molecular sieves. Cs_2CO_3 and K_3PO_4 were dried under vacuum at 180 °C for 24 h, and stored under nitrogen in the glovebox prior to use. **2-L1**, **2-L3**, and **4-L1**,[66] **2-C1**,[66] **2-C2**,[68] **3-C1**,[59] **2-C3** (see Section 2.5.2), **2-C4** (see Section 2.5.2), (**4-L1**)$NiCl_2$,[152] **4-L2**,[66] naphthalen-1-yl 4-methylbenzenesulfonate,[97] quinolin-6-yl diethylcarbamate,[95] 3-chlorophenyl diethylcarbamate,[153] and 4-chlorophenyl diethylcarbamate[153] were prepared according to established literature procedures. Otherwise, all other solvents, reagents, and materials were used as received from commercial sources.

For General Procedures A-C, flash chromatography was carried out on silica gel using Silicycle Silia*Flash* 60 silica (particle size 40–63 μm; 230–400 mesh) or activated, neutral alumina (Brockmann I), as indicated. For the synthesis of **4-6c**, automated flash chromatography was carried out on a Biotage Isolera One automated flash purification system using a 12 g Silicycle Silia*Sep* (particle size 40–63 μm, 230–400 mesh) silica flash cartridge with a gradient of 2-4-2 column volumes and a flow rate of 10 mL/min. For General Procedure D, was carried out on activated, neutral alumina.

NMR spectra were recorded on a Bruker AV 500 MHz spectrometer at 300 K, with chemical shifts (in ppm) referenced to residual protio solvent peaks (^1H), deuterated solvent peaks ($^{13}C\{^1H\}$), external $CFCl_3$ ($^{19}F\{^1H\}$), or external 85% H_3PO_4 ($^{31}P\{^1H\}$). Splitting patterns are indicated as follows: br, broad; s, singlet; d, doublet; t, triplet; q, quartet; dd, doublet of doublets; m, multiplet, with all coupling constants (*J*) reported in Hertz (Hz). Elemental analyses were performed by Galbraith Laboratories, Inc., Knoxville, TN. Mass spectra were obtained using ion trap electrospray ionization (ESI) instruments operating in

positive mode. Gas chromatography (GC) data were obtained on an instrument equipped with an SGE BP-5 column (30 m, 0.25 mm i.d.).

4.5.2 Synthesis of Pre-Catalysts 4-C1 and 4-C2

Synthesis of (4-L1)Ni(*o*-tolyl)Cl, 4-C1. In an inert-atmosphere glovebox, (**4-L1**)$NiCl_2$ (500.0 mg, 0.825 mmol) was added to a 4 dram vial with a magnetic stir bar, followed by THF (16 mL). The red mixture was then cooled in a –33 ºC freezer for 15 min. After this time, the vial was removed from the freezer, magnetic stirring was initiated, and (*o*-tolyl)MgCl (990 µL of a 1.0 M solution in THF, 0.990 mmol) was added dropwise to the cooled, stirring solution, yielding a clear, orange solution upon complete addition. The solution was allowed to stir at ambient temperature for 4 h, after which time the vial was removed from the glovebox and MeOH (2 mL) was added in air. The volatiles were removed from the clear, orange solution under reduced pressure and the resulting orange solid was dried under vacuum. Then, CH_2Cl_2 (30 mL) was added and the resulting cloudy, orange mixture was cooled to ~0 ºC. The cooled mixture was then quickly filtered through Celite, washing the Celite pad with cold (~0 ºC) CH_2Cl_2 (2 x 10 mL). The volatiles were removed from the clear, orange filtrate, yielding the title compound as an orange solid, which in turn was washed with pentane (2 x 1 mL) and dried under reduced pressure. Yield: 0.545 g (99%). Anal. Calc'd for $C_{35}H_{37}ClNiO_3P_2$: C, 63.52; H, 5.64; N, 0. Found: C, 63.77; H, 5.34; N, <0.3. $^{31}P\{^1H\}$ NMR (203 MHz, $CDCl_3$): δ 49.5 (d, J_{PP} = 6.0 Hz), 48.8 (s), 35.9 (s), 35.2 (s), 21.9 (d, J_{PP} = 6.1 Hz), 21.4 (s). The $^{31}P\{^1H\}$ NMR spectrum of **4-C1** (see **Figure A131** in Appendix 8) displays a similar pattern of four major signals as seen in the $^{31}P\{^1H\}$ NMR spectrum of **2-C1**.[66] These signals (δ 49.5, 48.8, 21.9, and 21.4) are attributed to two rotational isomers of **4-C1** in which the methyl group of the nickel-bound *o*-tolyl fragment, *trans* to the chiral, racemic phosphadamantane cage (based on the X-ray crystal structure, **Figure 4.1**) is positioned above or below the square plane of **4-C1**. Minor signals at δ 35.9 and 35.2 may arise from other dynamic phenomena occurring in solution, perhaps due to reorientation of the ligand **4-L1** such that the phosphadamantane cage is now *trans* to the chloride ligand, as had previously been observed in the $^{31}P\{^1H\}$ NMR spectrum of **2-C3**.[154] Due to the presence of at least two diastereomers of **4-C1** in solution (each possessing C_1 symmetry, and in some cases exhibiting second-order coupling and/or line-broadening), the ^1H and $^{13}C\{^1H\}$ NMR spectra of **4-C1** (**Figures A129** and **A130** in

Appendix 8, respectively) are sufficiently complex so as to preclude meaningful assignment.

Synthesis of (4-L2)NiCl$_2$. In an inert-atmosphere glovebox, THF (5 mL) was added to a 4 dram vial containing NiCl$_2$(DME) (115.3 mg, 0.525 mmol) and **4-L2** (225.0 mg, 0.551 mmol), yielding a cloudy, brown mixture. A magnetic stir bar was added, the vial was sealed, and magnetic stirring was initiated. After several minutes, an orange precipitate formed. The resulting mixture was allowed to stir at ambient temperature for 2 h, after which time the vial was removed from the glovebox and the precipitated brown-orange solid was collected on a glass filter frit, washing the solid with cold (~0 ºC) pentane (2 x 1 mL). The collected solid was then washed off the frit using CH_2Cl_2 (15 mL). The volatiles were removed from the corresponding clear, red-orange solution, yielding the title compound as a dark red-brown solid, which was dried under reduced pressure. Yield: 0.245 g (87%). ^{1}H NMR (500 MHz, $CDCl_3$): δ 8.33 (br s, 1H, ArH), 7.69 (br s, 3H, ArH), 4.00 (apparent br d, J = 13.4 Hz, 1H, PCg -C*H*H), 2.97–2.93 (br m, 2H, 2 x *i*-Pr -C*H*), 2.31 (apparent br d, J = 13.9 Hz, 1H, PCg -C*H*H), 1.84–1.79 (m, 2H, 2 x PCg -C*H*H), 1.74 (s, 3H, PCg -CH_3), 1.58–1.46 (m, 18H, 3 x PCg -CH_3 + -CH(CH_3)$_2$ + -CH(CH_3)(CH_3)), 1.22 (br d, J = 5.1 Hz, 3H, -CH(CH_3)(CH_3)). ^{13}C{^{1}H} NMR (126 MHz, $CDCl_3$): δ 140.9 (br s, ArC-P), 139.1 (br s, ArC-P), 135.0 (s, ArC), 132.6 (s, ArC), 132.5 (s, ArC), 131.6 (s, ArC), 97.4 (s, CgP), 96.9 (s, CgP), 77.6 (s, CgP), 74.7 (s, CgP), 41.1 (s, CgP), 40.2 (s, CgP), 29.1 (br s, -*C*H(CH_3)$_2$), 29.0, (s, -*C*H(CH_3)$_2$), 27.7 (s, CgP), 26.8 (s, CgP), 26.4 (s, CgP), 20.0 (d, $J_{C\text{-}P}$ = 6.6 Hz, CgP), 19.2 (s, -CH(*C*H_3)$_2$), 18.4 (s, -CH(*C*H_3)$_2$). ^{31}P{^{1}H} NMR (203 MHz, $CDCl_3$): δ 82.5 (br s), 47.6 (br s). Anal. Calc'd for $C_{22}H_{34}Cl_2NiO_3P_2$: C, 49.11; H, 6.37; N, 0. Found: C, 49.28; H, 6.49; N, <0.3.

Synthesis of (4-L2)Ni(*o*-tolyl)Cl, 4-C2. In an inert-atmosphere glovebox, (**4-L2**)NiCl$_2$ (150.0 mg, 0.279 mmol) was added to a 4 dram vial with a magnetic stir bar, followed by THF (5 mL). The red-brown mixture was then cooled in a –33 ºC freezer for 15 min. After this time, the vial was removed from the freezer, magnetic stirring was initiated, and (*o*-tolyl)MgCl (335 µL of a 1.0 M solution in THF, 0.335 mmol) was added dropwise to the cooled, stirring solution, yielding a clear, red-orange solution upon complete addition. The solution was allowed to stir at ambient temperature for 4 h, after which time the now clear, orange solution was removed from the glovebox and MeOH (2 mL) was added. The

volatiles were removed from the clear, orange solution under reduced pressure and the resulting orange solid was dried under reduced pressure. Then, CH_2Cl_2 (10 mL) was added and the resulting cloudy, orange mixture was cooled to ~0 ºC. The cooled mixture was then quickly filtered through Celite, washing the Celite pad with cold (~0 ºC) CH_2Cl_2 (2 x 10 mL). The volatiles were removed from the clear, orange filtrate, yielding the title compound as an orange solid. The solid was washed with pentane (2 x 1 mL) and dried under reduced pressure. Yield: 0.162 g (97%). Anal. Calc'd for $C_{29}H_{41}ClNiO_3P_2$: C, 58.67; H, 6.96; N, 0. Found: C, 58.49; H, 6.88; N, <0.3. $^{31}P\{^1H\}$ NMR (203 MHz, $CDCl_3$): δ 59.1 (d, J_{PP} = 10.3 Hz), 57.5 (d, J_{PP} = 10.1 Hz), 55.2 (d, J_{PP} = 20.3 Hz), 54.8 (d, J_{PP} = 20.8 Hz), 35.1 (d, J_{PP} = 20.9 Hz), 34.7 (d, J_{PP} = 20.1 Hz), 20.7 (d, J_{PP} = 10.3 Hz), 19.1 (d, J_{PP} = 10.2 Hz). The $^{31}P\{^1H\}$ NMR spectrum of **4-L2** (see **Figure A137** in Appendix 8) exhibits four pairs of doublets, similar to those seen in the $^{31}P\{^1H\}$ NMR spectrum of **2-C3** (see **Figure 2.4** in **Section 2.3.2**). We ascribe the signals to four sets of diastereomers: two with the nickel-bound *o*-tolyl fragment *trans* to the phosphaadamantane cage, with the methyl group of this *o*-tolyl group oriented above or below the square plane of the molecule; and two with the nickel-bound *o*-tolyl fragment *trans* to the P(*i*-Pr)$_2$ group, with similar restricted rotation about the nickel-bound *o*-tolyl group. Due to the presence of these four diastereomers of **4-C2** in solution (each possessing C_1 symmetry, and in some cases exhibiting second-order coupling and/or line-broadening), the ^1H and $^{13}C\{^1H\}$ NMR spectra of **4-C2** (**Figures A135** and **A136** in Appendix 8, respectively) are sufficiently complex so as to preclude meaningful assignment.

4.5.3 Synthesis of 6-chloro-2-(2-methoxyethyl)-1*H*-benzo[*de*]isoquinoline-1,3(2*H*)-dione (4-9)

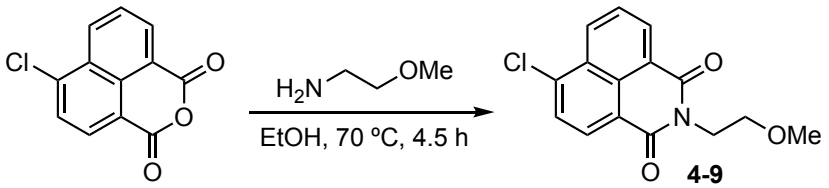

The following procedure was adapted from the literature.[149d] 4-Chloro-1,8-naphthalic anhydride (0.930 g, 4.0 mmol, 1.0 equiv) and 2-methoxyethylamine (351 µL, 4.04 mmol, 1.01 equiv) were combined in a 100 mL round-bottom flask with a magnetic stir bar. EtOH (20 mL) was added, and the resulting mixture was placed in a pre-heated,

70 ºC oil bath, and magnetic stirring was initiated. A cloudy, yellow-orange mixture formed after several minutes. The reaction was stirred at 70 ºC for 4.5 h, after which time the now cloudy white-orange mixture was cooled to room temperature and diluted with distilled water (25 mL). The mixture was placed in a 4 ºC fridge for ~60 min, after which time a solid was collected by vacuum filtration, washing with distilled water (3 x 5 mL), affording the title compound as an off-white solid. The product was then dried under reduced pressure at 65 ºC overnight. Yield: 1.046 g (90%). ^{1}H NMR ($CDCl_3$, 500 MHz): δ 8.64 (dd, *J* = 1.1, 7.3 Hz, 1H), 8.56 (dd, *J* = 1.1, 8.5 Hz, 1H), 8.48 (d, *J* = 7.9 Hz, 1H), 7.83 (dd, *J* = 7.4, 8.5 Hz, 1H), 7.79 (d, *J* = 7.9 Hz, 1H), 4.43 (t, *J* = 5.9 Hz, 2H), 3.73 (t, *J* = 5.9 Hz, 2H), 3.37 (s, 3H). ^{13}C NMR (126 MHz, $CDCl_3$,): δ 163.9, 163.7, 139.2, 132.2, 131.3, 130.7, 129.4, 129.3, 127.9, 127.5, 123.2, 121.7, 69.7, 58.9, 39.5. Spectroscopic data are consistent with those previously reported.[155]

4.5.4 General Procedures for the Nickel-Catalyzed C(*sp*^{2})–N Cross-Coupling of α,α,α-Trisubstituted, Primary Alkylamines

General Procedure for Pre-Catalyst Screening, Solvent Optimization, and Base Optimization. In a nitrogen-filled glovebox, pre-catalyst (0.006 mmol, 5 mol %), base (0.18 or 0.36 mmol, 1.5 or 3.0 equiv), (hetero)aryl chloride (0.12 mmol, 1 equiv), solvent (1 mL, [ArCl] = 0.12 M), and 1-adamantylamine (20.0 g, 0.132 mmol, 1.1 equiv) were consecutively added to a 1 dram vial with a magnetic stir bar. The vial was sealed with a cap containing a PTFE septum, removed from the glovebox, and placed in a temperature-controlled aluminum heating block set to the indicated temperature. Magnetic stirring was initiated. The reaction was allowed to stir at this temperature for 18 h (unoptimized), after which time the vial was removed from the heating block and allowed to cool to room temperature. An aliquot of the reaction mixture was then filtered through a short Celite/silica plug (1:1), diluted with EtOAc (~1.5 mL), and analyzed by GC.

General Procedure for the Cross-Coupling of (Hetero)aryl Halides with α,α,α-Trisubstituted, Primary Alkylamines at 60 or 80 ºC (GPA). In a nitrogen-filled glovebox, **4-C1** (0.025 mmol. 5 mol %), NaO*t*-Bu (0.75 mmol, 1.5 equiv), (hetero)aryl halide (0.5 mmol, 1 equiv), toluene, and amine (0.55 or 1.5 mmol, 1.1 or 3.0 equiv) were consecutively added to a 4 dram vial with a magnetic stir bar. 1-Adamantylamine was added prior to addition of toluene. The vial was sealed with a cap containing a PTFE

septum, removed from the glovebox, and placed in a temperature-controlled aluminum heating block set to the indicated temperature (60 or 80 ºC). Magnetic stirring was initiated. The reaction was allowed to stir at this temperature for 18 h (unoptimized), after which time the vial was removed from the heating block and allowed to cool to room temperature. The reaction mixture was diluted with EtOAc (20 mL) and filtered through Celite, rinsing the Celite plug with additional EtOAc (2 x 10 mL). The volatiles were removed from the collected filtrated under reduced pressure, and the resulting residue was purified via flash chromatography on silica gel or automated flash chromatography, as indicated.

General Procedure for the Cross-Coupling of (Hetero)aryl Halides with α,α,α-Trisubstituted, Primary Alkylamines and Anilines at Room Temperature (GPB). In a nitrogen-filled glovebox, **4-C1** (0.025 mmol. 5 mol %), NaO*t*-Bu (0.75 mmol, 1.5 equiv), (hetero)aryl halide (0.5 mmol, 1 equiv), toluene, and amine or aniline (0.55 or 1.5 mmol, 1.1 or 3.0 equiv) were consecutively added to a 4 dram vial with a magnetic stir bar. The vial was sealed with a cap containing a PTFE septum and magnetic stirring was initiated. After 18 h (unoptimized), the vial was removed from the glovebox. The reaction mixture was then diluted with EtOAc (20 mL) and filtered through Celite, rinsing the Celite plug with additional EtOAc (2 x 10 mL). The volatiles were removed from the collected filtrated under reduced pressure, and the resulting residue was purified via flash chromatography on silica gel or automated flash chromatography, as indicated.

General Procedure for the Cross-Coupling of (Hetero)aryl Chlorides with Bulky Alcohols (GPC). In a nitrogen-filled glovebox, **4-C1** (0.0375 mmol. 7.5 mol %), NaO*t*-Bu (0.75 mmol, 1.5 equiv), (hetero)aryl halide (0.5 mmol, 1 equiv), toluene, and alcohol (1.5 mmol, 3.0 equiv) were consecutively added to a 4 dram vial with a magnetic stir bar. The vial was sealed with a cap containing a PTFE septum, removed from the glovebox, and placed in a temperature-controlled aluminum heating block set 60 ºC. Magnetic stirring was initiated. The reaction mixture was allowed to stir at this temperature for 18 h (unoptimized), after which time the vial was removed from the heating block and allowed to cool to room temperature. The reaction mixture was diluted with EtOAc (20 mL), washed with brine (2 x 10 mL), and separated. The aqueous layer was then extracted with EtOAc (2 x 10 mL) and separated. The combined organic layers were then dried over

Na_2SO_4, filtered, and concentrated under reduced pressure. The resulting residue was purified via flash chromatography on silica gel.

Examining the Effects of (Pseudo)halide Addition on the Cross-Coupling of 1-Chloronapthalene and *tert*-Butylamine. In a nitrogen-filled glovebox, **4-C1** (4.0 mg, 0.006 mmol, 5 mol %), NaO*t*-Bu (17.3 mg, 0.18 mmol, 1.5 equiv), 1-chloronapthalene (16.3 μL, 0.12 mmol, 1 equiv), toluene (1 mL, [ArCl] = 0.12 M), and *tert*-butylamine (37.8 μL, 0.36 mmol, 3.0 equiv) were consecutively added to a 1 dram vial with a magnetic stir bar. Quinolin-6-yl diethylcarbamate (29.3 mg, 0.12 mmol, 1.0 equiv) was added after the 1-chloronapthalene, as appropriate. Magnetic stirring was initiated. The vial was sealed with a cap containing a PTFE septum and allowed to stir at ambient temperature for 18 h. After this time, the vial was removed from the glovebox and mesitylene (16.7 μL, 0.12 mmol, 1.0 equiv) was added as an internal standard. An aliquot of the reaction mixture was then filtered through a short Celite/silica plug (1:1), diluted with EtOAc (~1.5 mL), and analyzed by GC.

General Procedure for Screening Pre-catalysts in the Cross-Coupling of 4-9 and *tert*-Butylamine (4-2d). In a nitrogen-filled glovebox, pre-catalyst (5 mol %), NaO*t*-Bu (8.6 mg, 1.5 equiv), **4-9** (17.4 mg, 0.06 mmol, 1.0 equiv), toluene (500 μL), and **4-2d** (18.9 μL, 0.18 mmol, 3.0 equiv) were consecutively added to a 1 dram vial with a magnetic stir bar. The vial was sealed with a cap containing a PTFE septum, removed from the glovebox, and placed in a temperature-controlled, aluminum heating block set to 60 ºC. Magnetic stirring was initiated, and the reaction was allowed to stir at 60 ºC for 18 h (unoptimized). After this time, the reaction was removed from the heating block and allowed to cool to ambient temperature. An aliquot of the reaction mixture was then diluted with 10% MeOH in CH_2Cl_2, filtered through Celite, and analyzed by use of GC methods.

General Procedure for Ligand Screening and Optimization Using Ni(cod)$_2$ in the Cross-Coupling of 4-9 and *tert*-Butylamine (4-2d). In a nitrogen-filled glovebox, ligand (0.006 or 0.012 mmol, 10 or 20 mol %), base (0.09 or 0.18 mmol, 1.5 or 3.0 equiv), **4-9** (17.4 mg, 0.06 mmol, 1.0 equiv), solvent (400 or 450 μL), **4-2d** (18.9 μL, 0.18 mmol, 3.0 equiv), and Ni(cod)$_2$ (50 or 100 μL of a 0.06 M solution, 0.003 or 0.006 mmol, 5 or 10 mol %; total volume: 500 μL) were consecutively added to a 1 dram vial with a magnetic stir bar. The vial was sealed with a cap containing a PTFE septum and either allowed to react

at ambient temperature, or removed from the glovebox and placed in a temperature-controlled, aluminum heating block set to the indicated temperature. Magnetic stirring was initiated, and the reaction was allowed to stir for 18 h (unoptimized). After this time, the reaction was removed from the heating block and allowed to cool to ambient temperature or removed the glovebox (as necessary), and an aliquot of the reaction mixture was diluted with 10% MeOH in CH_2Cl_2, filtered through Celite, and analyzed by use of GC methods.

General Procedure for the Cross-Coupling of 4-9 with α,α,α-Trisubstituted, Primary Alkylamines (GPD). In a nitrogen-filled glovebox, **3-L2** (15.5 mg, 0.04 mmol, 10 mol %), NaO*t*-Bu (57.7 mg, 0.6 mmol, 1.5 equiv), **4-9** (115.9 mg, 0.4 mmol, 1.0 equiv), toluene (1.33 mL), and nucleophile (0.6 or 1.2 mmol, 1.5 or 3.0 equiv), were consecutively added to a 4 dram vial with a magnetic stir bar. 1-Adamantylamine was added prior to addition of toluene. Separately, $Ni(cod)_2$ (5.5 mg, 0.02 mmol, 5 mol %) was added to a 1 dram vial, and transferred to the reaction mixture using toluene (4 x 0.5 mL; total volume: 3.33 mL). The 4 dram vial was sealed with a cap containing a PTFE septum and allowed to react at ambient temperature under the influence of magnetic stirring for 18 h (unoptimized). After this time, the reaction was removed the glovebox, diluted with CH_2Cl_2 (~50 mL) and filtered through Celite. The resulting solution was concentrated by about half under reduced pressure, and activated neutral alumina was added. The volatiles were removed from the resulting heterogeneous mixture, and the so-formed alumina dry pack was placed on a column of activated, neutral alumina and purified by flash chromatography.

4.5.5 Synthesis and Characterization of Cross-Coupled Products

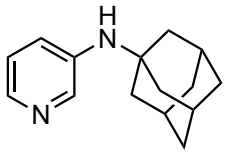

***N*-(adamantan-1-yl)pyridine-3-amine** (**4-3a**). GPA was followed using **4-C1** (16.5 mg, 0.025 mmol), NaO*t*-Bu (72.1 mg, 0.75 mmol), 3-chloropyridine (47.5 μL, 0.5 mmol), 1-admantylamine (83.2 mg, 0.55 mmol), and toluene (4.17 mL) at 60 ºC. After flash chromatography on silica gel (EtOAc), the title compound was obtained as a white solid (0.082 g, 72%). ^{1}H NMR (500 MHz, $CDCl_3$): δ 8.13 (d, J = 2.3 Hz, 1H), 8.00 (d, J = 4.1 Hz, 1H), 7.10–7.08 (m, 1H), 7.05–7.03 (m, 1H), 3.35 (br s, 1H), 2.12 (br s, 3H), 1.87 (d, J = 2.5 Hz, 6H), 1.72_1.64 (m, 6H). ^{13}C{^{1}H} NMR (126 MHz, $CDCl_3$): 142.4, 140.9, 140.2,

124.6, 123.3, 52.5, 43.4, 36.5, 29.8. Spectroscopic data are consistent with those previously reported.[135]

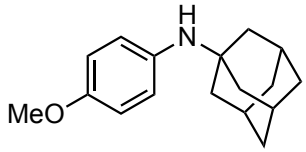

***N*-(4-methoxyphenyl)adamantan-1-amine** (**4-3b**). GPA was followed using **4-C1** (19.9 mg, 0.030 mmol), NaO*t*-Bu (72.1 mg, 0.75 mmol), 4-chloroanisole (61.2 μL, 0.5 mmol), 1-admantylamine (83.2 mg, 0.55 mmol), and toluene (2.08 mL) at 80 ºC. After flash chromatography on silica gel (20% EtOAc in hexanes), the title compound was obtained as a white solid (0.104 g, 81%). ^{1}H NMR (500 MHz, $CDCl_3$): δ 6.84–6.80 (m, 2H), 6.77–6.74 (m, 2H), 3.76 (s, 3H), 2.77 (br s, 1H), 2.08 (br s, 3H), 1.75 (d, *J* = 2.5 Hz, 6H), 1.67–1.59 (m, 6H). ^{13}C{^{1}H} NMR (126 MHz, $CDCl_3$): 154.9, 138.5, 124.3, 114.0, 55.6, 52.7, 43.92, 43.87, 36.6, 29.9. Spectroscopic data are consistent with those previously reported.[135]

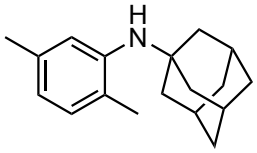

***N*-(2,5-dimethylphenyl)adamantan-1-amine** (**4-3c**). GPA was followed using **4-C1** (19.9 mg, 0.030 mmol), NaO*t*-Bu (72.1 mg, 0.75 mmol), 2-chloro-1,4-dimethylbenzene (67.0 μL, 0.5 mmol), 1-admantylamine (83.2 mg, 0.55 mmol), and toluene (4.17 mL) at 60 ºC. After flash chromatography on silica gel (5% EtOAc in hexanes), the title compound was obtained as a white solid (0.109 g, 85%). This yield reflects a 5% impurity (by mole) of pre-catalyst activation product, *N*-(*o*-tolyl)adamatan-1-amine (**4-3c´**),[135] that could not be removed via column chromatography. ^{1}H NMR (500 MHz, $CDCl_3$): δ 6.95 (d, *J* = 7.5 Hz, 1H), 6.81 (s, 1H), 6.51 (d, *J* = 7.5 Hz), 3.24 (br s, 1H), 2.29 (s, 3H), 2.13–2.12 (m, 6H), 1.96 (d, *J* = 2.7 Hz, 6H), 1.74–1.68 (m, 6H). ^{13}C{^{1}H} NMR (126 MHz, $CDCl_3$): δ 144.5, 136.0, 130.4, 121.9, 118.8, 117.8, 52.4, 43.7, 36.7, 30.0, 21.7, 18.0. HRMS-ESI (*m*/*z*): Calc'd for $C_{18}H_{26}N$ $[M+H]^+$: 256.2060. Found: 256.2069.

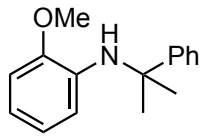

2-methoxy-*N*-(2-phenylpropan-2-yl)aniline (**4-3d**). GPA was followed using **4-C1** (19.9 mg, 0.030 mmol), NaO*t*-Bu (72.1 mg, 0.75 mmol), 2-chloroanisole (63.5 μL, 0.5 mmol), cumylamine (79.1 μL, 0.55 mmol), and toluene (2.08 mL) at 80 ºC. After flash chromatography on silica gel (2% EtOAc in hexanes), the title compound was obtained as a colourless oil (0.100 g, 83%). ^{1}H NMR (500 MHz, $CDCl_3$): δ 7.52_7.50 (m, 2H), 7.34_7.31 (m, 2H), 7.24–7.21 (m, 1H), 6.77 (dd, J = 7.2, 2.1 Hz, 1H), 6.59–6.53 (overlapping m, 2H), 6.03 (dd, J = 7.3, 2.2 Hz,1H), 4.73 (br s, 1H), 3.89 (s, 3H), 1.67 (s, 6H). ^{13}C{^{1}H} NMR (126 MHz, $CDCl_3$): δ 147.8, 147.3, 135.9, 128.6, 126.3, 126, 120.6, 116.1, 113.8, 109.5, 55.6, 55.5, 30.8. HRMS-ESI (*m*/*z*): Calc'd for $C_{16}H_{19}NNaO$ $[M+H]^+$: 264.1359. Found: 264.1352.

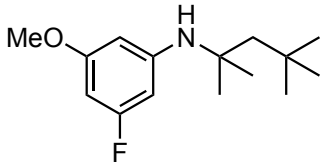

3-fluoro-5-methoxy-*N*-(2,4,4-trimethylpentan-2-yl)aniline (**4-3e**). GPA was followed using **4-C1** (16.5 mg, 0.025 mmol), NaO*t*-Bu (72.1 mg, 0.75 mmol), 3-chloro-5-fluoroanisole (63.5 μL, 0.5 mmol), *tert*-octylamine (88.3 μL, 0.55 mmol), and toluene (4.17 mL) at 60 ºC. After flash chromatography on silica gel (5% EtOAc in hexanes), the title compound was obtained as a yellow oil (0.078 g, 62%). ^{1}H NMR (500 MHz, $CDCl_3$): δ 6.02–5.99 (m, 1H), 5.98–5.96 (m, 2H), 3.74 (s, 3H), 3.70 (br s, 1H), 1.69 (s, 2H), 1.40 (s, 6H), 1.02 (s, 9H). ^{13}C{^{1}H} NMR (126 MHz, $CDCl_3$): δ 164.6 (d, J_{CF} = 240 Hz), 161.4 (d, J_{CF} = 14.2 Hz), 149.0 (d, J_{CF} = 13.6 Hz), 97.3 (d, J_{CF} = 1.8 Hz), 95.4 (d, J_{CF} = 25.7 Hz), 90.2 (d, J_{CF} = 26.2 Hz), 55.40, 55.37, 52.7, 31.9, 31.7, 30.6. ^{19}F{^{1}H} NMR (470.4 MHz, $CDCl_3$): δ –112.3. HRMS-ESI (*m*/*z*): Calc'd for $C_{15}H_{25}FNO$ $[M+H]^+$: 254.1915. Found: 254.1911.

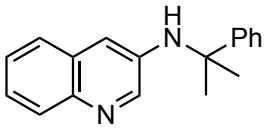

***N*-(2-phenylpropan-2-yl)quinoline-3-amine** (**4-3f**). GPA was followed using **4-C1** (16.5 mg, 0.025 mmol), NaO*t*-Bu (72.1 mg, 0.75 mmol), 3-bromoquinoline (67.9 μL, 0.5 mmol), cumylamine (79.1 μL, 0.55 mmol), and toluene (4.17 mL) at 60 ºC. After flash chromatography on silica gel (100 mL each of 10%, 20%, 30%, 40%, 50% EtOAc in hexanes, then 60% EtOAc in hexanes), the title compound was obtained as an off-white solid (0.115 g, 88%). ^{1}H NMR (500 MHz, $CDCl_3$): δ 8.40 (d, J = 2.9 Hz, 1H), 7.88 (d, J = 8.2 Hz, 1H), 7.52 (d, J = 7.6 Hz, 2H), 7.37–7.32 (m, 3H), 7.32–7.30 (m, 2H), 7.27–7.24 (m, 1H), 6.51 (d, J = 2.8 Hz, 1H), 4.43 (br s, 1H), 1.73 (s, 6H). ^{13}C{^{1}H} NMR (126 MHz, $CDCl_3$): δ 146.1, 144.6, 141.9, 139.2, 129.0, 128.9, 126.9, 126.7, 126.2, 125.6, 125.0, 113.8, 56.3, 30.4. HRMS-ESI (*m*/*z*): Calc'd for $C_{18}H_{19}N_2$ $[M+H]^+$: 263.1543. Found: 163.1548.

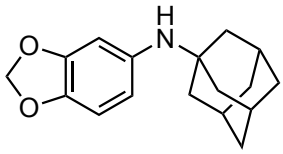

***N*-(adamantan-1-yl)benzo[*d*][1,3]dioxol-5-amine** (**4-3g**). GPA was followed using **4-C1** (19.9 mg, 0.030 mmol), NaO*t*-Bu (72.1 mg, 0.75 mmol), 5-chloro-1,3-benzodioxole (58.4 μL, 0.5 mmol), 1-admantylamine (83.2 mg, 0.55 mmol), and toluene (2.08 mL) at 80 ºC. After flash chromatography on silica gel (15% EtOAc in hexanes), the title compound was obtained as a white solid (0.104 g, 77%). ^{1}H NMR (500 MHz, $CDCl_3$): δ 6.63 (d, J = 8.2 Hz, 1H), 6.46 (d, J = 2.2 Hz, 1H), 6.30 (dd, J = 8.2, 2.1 Hz, 1H), 5.89 (s, 2H), 2.89 (br s, 1H), 2.08 (br s, 3H), 1.75 (d, J = 2.5 Hz, 6H), 1.68–1.60 (m, 6H). ^{13}C{^{1}H} NMR (126 MHz, $CDCl_3$): δ 147.7, 142.5, 140.1, 115.1, 108.0, 104.8, 100.9, 52.9, 43.9, 36.6, 29.9. Spectroscopic data are consistent with those previously reported.[156]

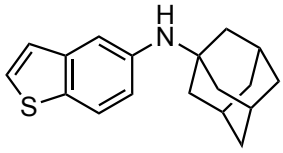

***N*-(adamantan-1-yl)benzo[*b*]thiophen-5-amine** (**4-3h**). GPA was followed using **4-C1** (19.9 mg, 0.030 mmol), NaO*t*-Bu (72.1 mg, 0.75 mmol), 5-chlorobenzothiophene (84.3

mg, 0.5 mmol), 1-admantylamine (83.2 mg, 0.55 mmol), and toluene (4.17 mL) at 60 ºC. After flash chromatography on silica gel (10% EtOAc in hexanes), the title compound was obtained as a white solid (0.106 g, 76%). ^{1}H NMR (500 MHz, $CDCl_3$): δ 7.64 (d, J = 8.6 Hz, 1H), 7.37 (d, J = 5.4 Hz, 1H), 7.28 (d, J = 2.1 Hz, 1H), 7.19 (d, J = 5.6 Hz, 1H), 6.89 (dd, J = 8.6, 2.2 Hz, 1H), 3.22 (br s, 1H), 2.12 (s, 3H), 1.88 (d, J = 2.6 Hz), 1.71–1.64 (m, 6H). ^{13}C{^{1}H} NMR (126 MHz, $CDCl_3$): δ 142.9, 140.6, 132.1, 126.8, 123.6, 122.4, 120.5, 114.3, 52.8, 43.8, 36.6, 29.9. HRMS-ESI (*m*/*z*): Calc'd for $C_{18}H_{22}NS$ $[M+H]^+$: 284.1467. Found: 284.1460.

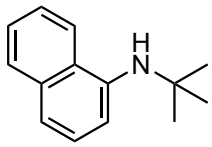

***N*-(*tert*-butyl)naphthalen-1-amine** (**4-3i**). GPB was followed using **4-C1** (16.5 mg, 0.025 mmol), NaO*t*-Bu (72.1 mg, 0.75 mmol), 1-chloronaphthalene (68.1 µL, 0.5 mmol) or naphthalen-1-yl methylbenzenesulfonate (149.2 mg, 0.5 mmol), *tert*-butylamine (158 µL, 1.5 mmol), and toluene (4.17 mL). With the aryl chloride, after flash chromatography on silica gel (5% EtOAc in hexanes), the title compound was obtained as a yellow oil (0.089 g, 89%). With the aryl tosylate, after flash chromatography on silica gel (5% EtOAc in hexanes), the title compound was obtained as a orange oil (0.060 g, 60%). ^{1}H NMR (500 MHz, $CDCl_3$): δ 7.86–7.80 (m, 2H), 7.47–7.44 (m, 2H), 7.37 (t, J = 7.9 Hz, 1H), 7.30–7.29 (m, 1H), 6.99–6.98 (m, 1H), 4.24 (br s, 1H), 1.51 (s, 9H). ^{13}C{^{1}H} NMR (126 MHz, $CDCl_3$): δ 141.9, 134.8, 129.0, 126.3, 125.61, 125.57, 124.8, 120.5, 118.0, 110.2, 51.8, 30.1. Spectroscopic data are consistent with those previously reported.[135]

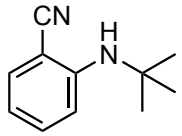

2-(*tert*-butylamino)benzonitrile (**4-3j**). GPB was followed using **4-C1** (16.5 mg, 0.025 mmol), NaO*t*-Bu (72.1 mg, 0.75 mmol), 2-chlorobenzonitrile (68.8 mg, 0.5 mmol), *tert*-butylamine (158 µL, 1.5 mmol), and toluene (4.17 mL). After flash chromatography on silica gel (5% EtOAc in hexanes), the title compound was obtained as a yellow oil (0.065 g, 75%). ^{1}H NMR (500 MHz, $CDCl_3$): δ 7.37 (dd, J = 7.7, 1.4 Hz, 1H), 7.35–7.31 (m, 1H), 6.93 (d, J = 8.6 Hz, 1H), 6.64 (t, J = 7.5 Hz, 1H), 4.54 (br s, 1H), 1.43 (s, 9H). ^{13}C{^{1}H}

NMR (126 MHz, $CDCl_3$): δ 149.4, 133.6, 133.2, 118.3, 116.3, 113.5, 97.4, 51.8, 29.8. Spectroscopic data are consistent with those previously reported.[157]

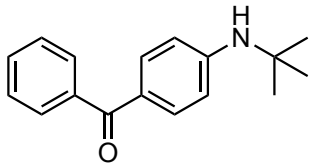

(4-(*tert*-butylamino)phenyl)(phenyl)methanone (**4-3k**). GPB was followed using **4-C1** (16.5 mg, 0.025 mmol), NaO*t*-Bu (72.1 mg, 0.75 mmol), 4-bromobenzophenone (130.6 mg, 0.5 mmol), *tert*-butylamine (158 μL, 1.5 mmol), and toluene (4.17 mL). After flash chromatography on silica gel (10% EtOAc in hexanes), the title compound was obtained as a yellow oil (0.110 g, 87%). ^{1}H NMR (500 MHz, $CDCl_3$): δ 7.73–7.70 (m, 4H), 7.53–7.50 (m, 1H), 7.46–7.43 (m, 2H), 6.66 (d, J = 8.8 Hz, 2H), 4.26 (br s, 1H), 1.43 (s, 9H). ^{13}C{^{1}H} NMR (126 MHz, $CDCl_3$): δ 195.2, 151.2, 139.4, 132.8, 131.2, 129.5, 128.1, 125.7, 113.6, 51.5, 29.8. Spectroscopic data are consistent with those previously reported.[158]

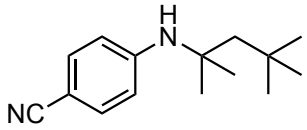

4-((2,4,4-trimethylpentan-2-yl)amino)benzonitrile (**4-3l**). GPB was followed using **4-C1** (16.5 mg, 0.025 mmol), NaO*t*-Bu (72.1 mg, 0.75 mmol), 4-chlorobenzonitrile (68.8 mg, 0.5 mmol), *tert*-octylamine (88.3 μL, 0.55 mmol), and toluene (4.17 mL). After flash chromatography on silica gel (100 mL each of 0–4% EtOAc in hexanes, then 5% EtOAc in hexanes), the title compound was obtained as a pale-yellow oil (0.089 g, 77%). ^{1}H NMR (500 MHz, $CDCl_3$): δ 7.36 (d, J = 8.8 Hz, 2H), 6.59 (d, J = 8.8 Hz, 2H), 4.19 (br s, 1H), 1.72 (s, 2H), 1.43 (s, 6H), 0.99 (s, 9H). ^{13}C{^{1}H} NMR (126 MHz, $CDCl_3$): δ 150.4, 133.5, 120.7, 114.3, 97.9, 55.5, 52.0, 31.9, 31.6, 30.4. HRMS-ESI (m/z): Calc'd for $C_{15}H_{22}N_2Na$ $[M+Na]^+$: 253.1675. Found: 253.1671.

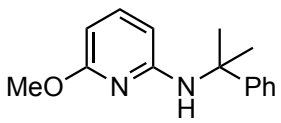

6-methoxy-*N*-(2-phenylpropan-2-yl)pyridin-2-amine (**4-3m**). GPB was followed using **4-C1** (16.5 mg, 0.025 mmol), NaO*t*-Bu (72.1 mg, 0.75 mmol), 2-chloro-6-

methoxypyridine (59.5 μL, 0.5 mmol), cumylamine (79.1 μL, 0.55 mmol), and toluene (4.17 mL). After flash chromatography on silica gel (5% EtOAc in hexanes), the title compound was obtained as a yellow oil (0.101 g, 83%). ^{1}H NMR (500 MHz, $CDCl_3$): δ 7.49 (d, *J* = 7.5 Hz, 2H), 7.31 (t, *J* = 7.7 Hz, 2H), 7.23–7.20 (m, 1H), 7.13 (t, *J* = 7.9 Hz, 1H), 5.95 (d, *J* = 7.9 Hz, 1H), 5.53 (d, *J* = 8.0 Hz, 1H), 4.91 (br s, 1H), 3.69 (s, 3H), 1.71 (s, 6H). ^{13}C{^{1}H} NMR (126 MHz, $CDCl_3$): δ 163.3, 156.1, 147.5, 139.5, 128.5, 126.3, 125.5, 99.9, 97.6, 55.4, 53.1, 30.6. HRMS-ESI (*m*/*z*): Calc'd for $C_{15}H_{19}N_2O$ $[M+H]^+$: 243.1492. Found: 243.1500.

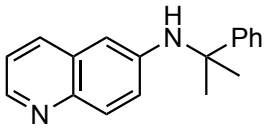

***N*-(2-phenylpropan-2-yl)quinolin-6-amine** (**4-3n**). GPB was followed using **4-C1** (16.5 mg, 0.025 mmol), NaO*t*-Bu (72.1 mg, 0.75 mmol), 6-chloroquinoline (81.8 mg, 0.5 mmol), cumylamine (79.1 μL, 0.55 mmol), and toluene (4.17 mL). After flash chromatography on silica gel (100 mL each of 10% EtOAc in hexanes, 20% EtOAc in hexanes, and 30% EtOAc in hexanes, then 40% EtOAc in hexanes), the title compound was obtained as a yellow oil (0.093 g, 71%). ^{1}H NMR (500 MHz, $CDCl_3$): δ 8.54 (d, *J* = 3.2 Hz, 1H), 7.79 (d, *J* = 9.1 Hz, 1H), 7.63 (d, *J* = 8.2 Hz, 1H), 7.54–7.52 (m, 2H), 7.35 (t, *J* = 7.7 Hz, 2H), 7.26–7.24 (m, 1H), 7.14 (dd, *J* = 8.2, 4.1, 1H), 6.99 (dd, *J* =9.1, 2.4, 1H), 6.26 (d, *J* = 2.2 Hz, 1H), 4.39 (br s, 1H), 1.72 (s, 6H). ^{13}C{^{1}H} NMR (126 MHz, $CDCl_3$): δ 146.7, 146.3, 143.9, 143.0, 134.1, 130.0, 129.7, 128.8, 126.7, 125.7, 122.8, 121.2, 107.0, 56.3, 30.7. HRMS-ESI (*m*/*z*): Calc'd for $C_{18}H_{19}N_2$ $[M+H]^+$: 263.1543. Found: 263.1533.

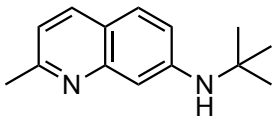

***N*-(*tert*-butyl)-2-methylquinolin-7-amine** (**4-3o**). GPB was followed using **4-C1** (16.5 mg, 0.025 mmol), NaO*t*-Bu (72.1 mg, 0.75 mmol), 7-chloroquinaldine (88.8 mg, 0.5 mmol), *tert*-butylamine (158 μL, 1.5 mmol), and toluene (4.17 mL). After flash chromatography on silica gel (850 mL 50% EtOAc in hexanes, then 75% EtOAc in hexanes), the title compound was obtained as a yellow oil, which solidified under reduced pressure (0.104 g, 97%). ^{1}H NMR (500 MHz, $CDCl_3$): δ 7.80 (d, *J* = 8.2 Hz, 1H), 7.46 (d,

J = 8.8 Hz, 1H), 7.19 (d, *J* = 2.3 Hz, 1H), 6.97 (d, *J* = 8.2 Hz, 1H), 6.76 (dd, *J* = 8.8, 2.4, 1H), 3.96 (br s, 1H), 2.66 (s, 3H), 1.46 (s, 9H). $^{13}C\{^{1}H\}$ NMR (126 MHz, $CDCl_3$): δ 159.0, 150.1, 147.7, 135.7, 128.1, 120.0, 119.7, 118.1, 107.6, 51.5, 29.6, 25.5. HRMS-ESI (*m*/*z*): Calc'd for $C_{14}H_{19}N_2$ $[M+H]^+$: 215.1543. Found: 215.1540.

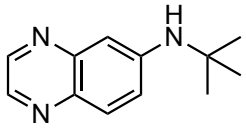

***N*-(*tert*-butyl)quinoxalin-6-amine** (**4-3p**). GPB was followed using **4-C1** (16.5 mg, 0.025 mmol), NaO*t*-Bu (72.1 mg, 0.75 mmol), 6-chloroquinoxaline (82.3 mg, 0.5 mmol), *tert*-butylamine (158 μL, 1.5 mmol), and toluene (4.17 mL). After flash chromatography on silica gel (40% EtOAc in hexanes), the title compound was obtained as a yellow oil (0.096 g, 95%). ^{1}H NMR (500 MHz, $CDCl_3$): δ 8.61 (d, *J* = 1.9 Hz, 1H), 8.48 (d, *J* = 1.9 Hz, 1H), 7.78 (d, *J* = 9.1 Hz, 1H), 7.15 (d, *J* = 2.7 Hz, 1H), 7.04 (dd, *J* = 9.1, 2.7 Hz, 1H), 4.23 (br s, 1H), 1.49 (s, 9H). $^{13}C\{^{1}H\}$ NMR (126 MHz, $CDCl_3$): δ 147.8, 145.4, 144.5, 140.3, 137.8, 130.0, 124.5, 106.0, 51.6, 29.4. HRMS-ESI (*m*/*z*): Calc'd for $C_{12}H_{16}N_3$ $[M+H]^+$: 202.1339. Found: 202.1334.

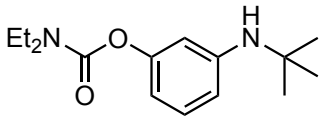

3-(*tert*-butylamino)phenyl diethylcarbamate (**4-3q**). GPA was followed using **4-C1** (16.5, 0.025 mmol), NaO*t*-Bu (72.1 mg, 0.75 mmol), 3-chlorophenyl diethylcarbamate (113.8 mg, 0.5 mmol), *tert*-butylamine (158 μL, 1.5 mmol), and toluene (4.17 mL) at 60 ºC. After flash chromatography on silica gel (20% EtOAc in hexanes), the title compound was obtained as a yellow oil (0.116 g, 88%). ^{1}H NMR (500 MHz, $CDCl_3$): δ 7.09 (t, *J* = 8.0 Hz, 1H), 6.54 (dd, *J* = 8.1, 2.1 Hz, 1H), 6.50 (t, *J* = 2.1 Hz, 1H), 6.48 (dd, *J* = 8.0, 2.0 Hz, 1H), 3.53 and 3.39 (overlapping br s, 1H+4H), 1.33 (s, 9H), 1.21 (br s, 6H). $^{13}C\{^{1}H\}$ NMR (126 MHz, $CDCl_3$): δ 154.4, 152.4, 148.1, 129.3, 113.6, 111.0, 110.3, 51.5, 42.2, 42.0, 30.1, 14.3, 13.5. HRMS-ESI (*m*/*z*): Calc'd for $C_{15}H_{24}N_2NaO_2$ $[M+Na]^+$: 287.1730. Found: 287.1738.

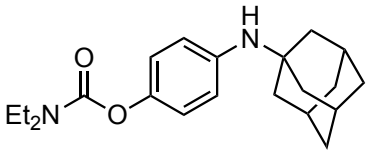

4-((adamantan-1-yl)amino)phenyl diethylcarbamate (**4-3r**). GPA was followed using **4-C1** (16.5, 0.025 mmol), NaO*t*-Bu (72.1 mg, 0.75 mmol), 3-chlorophenyl diethylcarbamate (113.8 mg, 0.5 mmol), 1-adamantylamine (83.2 mg, 0.55 mmol), and toluene (4.17 mL) at 80 ºC. After flash chromatography on silica gel (30% EtOAc in hexanes), the title compound was obtained as a yellow oil (0.148 g, 86%). ^{1}H NMR (500 MHz, $CDCl_3$): δ 6.92 (d, J = 8.8 Hz, 2H), 6.79 (d, J = 8.8 Hz, 2H), 3.39 (br s, 4H), 3.06 (br s, 1H), 2.09 (br s, 3H), 1.81 (d, J = 2.5 Hz, 6H), 1.68–1.61 (m, 6H), 1.21 (br s, 6H). ^{13}C{^{1}H} NMR (126 MHz, $CDCl_3$): δ 154.9, 145.3, 143.0, 121.9, 121.4, 52.7, 43.8, 42.3, 42.0, 36.6, 29.9, 14.3, 13.6. HRMS-ESI (*m*/*z*): Calc'd for $C_{21}H_{31}N_2O_2$ $[M+H]^+$: 343.2380. Found: 343.2379.

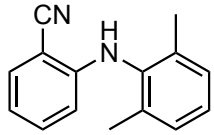

2-((2,6-dimethylphenyl)amino)benzonitrile (**4-6a**). GPB was followed using **4-C1** (16.5 mg, 0.025 mmol), NaO*t*-Bu (72.1 mg, 0.75 mmol), 2-chlorobenzonitrile (68.8 mg, 0.5 mmol), 2,6-dimethylaniline (67.7 μL, 0.55 mmol), and toluene (4.17 mL). After flash chromatography on silica gel (5% EtOAc in hexanes), the title compound was obtained as a white-orange solid (0.076 g, 68%). ^{1}H NMR (500 MHz, $CDCl_3$): δ 7.47 (dd, J = 7.8, 1.3 Hz, 1H), 7.26–7.23 (m, 1H), 7.16–7.15 (m, 3H), 6.72 (t, J = 7.5 Hz, 1H), 6.19 (d, J = 8.5 Hz, 1H), 5.92 (br s, 1H), 2.21 (s, 6H). ^{13}C{^{1}H} NMR (126 MHz, $CDCl_3$): δ 149.3, 137.0, 136.0, 134.4, 132.9, 128.9, 127.5, 118.0, 117.7, 112.1, 96.0, 18.3. Spectroscopic data are consistent with those previously reported.[157]

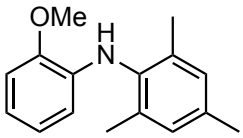

***N*-(2-methoxyphenyl)-2,4,6-trimethylaniline** (**4-6b**). GPB was followed using **4-C1** (16.5 mg, 0.025 mmol), NaO*t*-Bu (72.1 mg, 0.75 mmol), 2-chloroanisole (63.5 μL, 0.5 mmol), 2,4,6-trimethylaniline (77.2 μL, 0.55 mmol), and toluene (4.17 mL). After flash

chromatography on activated, neutral alumina (5% EtOAc in hexanes), the title compound was obtained as an orange solid (0.088 g, 73%). ^{1}H NMR (500 MHz, $CDCl_3$): δ 6.95 (br s, 2H), 6.86 (dd, *J* = 7.6, 1.6, 1H), 6.74–6.67 (m, 2H), 6.13 (dd, *J* = 7.6, 1.8, 1H), 5.58 (br s, 1H), 3.95 (s, 3H), 231 (s, 3H), 2.17 (s, 6H). ^{13}C{^{1}H} NMR (126 MHz, $CDCl_3$): δ 146.9, 136.6, 136.2, 135.8, 135.4, 129.3, 121.3, 117.1, 111.1, 110.0, 55.8, 21.1, 18.2. Spectroscopic data are consistent with those previously reported.[159]

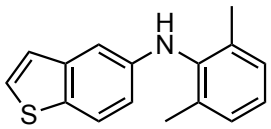

***N*-(2,6-dimethylphenyl)benzo[*b*]thiophen-5-amine** (**4-6c**). GPB was followed using **4-C1** (16.5 mg, 0.025 mmol), NaO*t*-Bu (72.1 mg, 0.75 mmol), 5-chlorobenzothiophene (84.3 mg, 0.5 mmol), 2,6-dimethylaniline (67.7 μL, 0.55 mmol), and toluene (4.17 mL). After automated flash chromatography (0–10% EtOAc in hexanes), the title compound was obtained as an orange oil (0.093 g, 73%). ^{1}H NMR (500 MHz, $CDCl_3$): δ 7.66 (d, *J* = 8.3 Hz, 1H), 7.35 (d, *J* = 5.4 Hz, 1H), 7.17–7.15 (m, 2H), 7.13–7.10 (m, 1H), 7.09 (d, *J* = 5.4 Hz, 1H), 6.77–6.75 (m, 2H), 5.24 (br s, 1H), 2.24 (s, 6H). ^{13}C{^{1}H} NMR (126 MHz, $CDCl_3$): δ 143.9, 141.1, 138.7, 135.9, 130.3, 128.8, 127.1, 126, 123.5, 123.1, 114.2, 106.4, 18.5. HRMS-ESI (*m*/*z*): Calc'd for $C_{16}H_{16}NS$ $[M+H]^+$: 254.0998. Found: 254.0999.

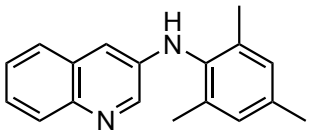

***N*-mesitylquinolin-3-amine** (**4-6d**). GPB was followed using **4-C1** (16.5 mg, 0.025 mmol), NaO*t*-Bu (72.1 mg, 0.75 mmol), 3-bromoquinoline (67.9 μL, 0.5 mmol), 2,4,6-trimethylaniline (77.2 μL, 0.55 mmol), and toluene (4.17 mL). After flash chromatography on silica gel (100 mL each of 10% and 20%, EtOAc in hexanes, 200 mL 30% EtOAc in hexanes, then 70% EtOAc in hexanes), the title compound was obtained as a yellow-brown solid (0.090 g, 69%). ^{1}H NMR (500 MHz, $CDCl_3$): δ 8.61 (d, *J* = 2.6 Hz, 1H), 7.96 (d, *J* = 8.2 Hz, 1H), 7.48–7.47 (m, 1H), 7.42–7.36 (m, 2H), 7.00 (s, 2H), 6.68 (d, *J* = 2.6 Hz, 1H), 5.44 (s, 1H), 2.35 (s, 3H), 2.20 (s, 6H). ^{13}C{^{1}H} NMR (126 MHz, $CDCl_3$): δ 143.1, 142.7, 140.2, 136.4, 136.0, 134.2, 129.6, 129.5, 129.2, 127.0, 126.1, 125.3, 111.6, 21.1, 18.3. Spectroscopic data are consistent with those previously reported.[160]

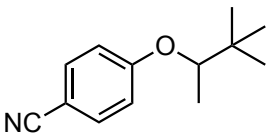

4-((3,3-dimethylbutan-2-yl)oxy)benzonitrile (**4-8a**). GPC was followed using **4-C1** (24.8 mg, 0.0375 mmol), NaO*t*-Bu (72.1 mg, 0.75 mmol), 4-chlorobenoznitrile (68.8 mg, 0.5 mmol), 3,3-dimethyl-2-butanol (189 μL, 1.5 mmol), and toluene (4.17 mL). After flash chromatography on silica gel (10% EtOAc in hexanes), the title compound was obtained as a yellow oil (0.085 g, 84%). ^{1}H NMR (500 MHz, $CDCl_3$): δ 7.55 (d, *J* = 8.9 Hz, 2H), 6.92 (d, *J* = 8.8 Hz, 2H), 4.09 (q, *J* = 6.3 Hz, 1H), 1.21 (d, *J* = 6.3 Hz, 3H), 0.98 (s, 9H). ^{13}C{^{1}H} NMR (126 MHz, $CDCl_3$): δ 162.3, 134.1, 119.5, 116.1, 103.3, 81.9, 35.2, 25.9, 14.1. HRMS-ESI (*m*/*z*): Calc'd for $C_{13}H_{17}NNaO$ $[M+Na]^+$: 226.1202 . Found: 226.1199.

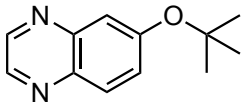

6-(*tert*-butoxy)quinoxaline (**3-3m**). GPC was followed using **4-C1** (24.8 mg, 0.0375 mmol), NaO*t*-Bu (72.1 mg, 0.75 mmol), 6-chloroquinoxaline (82.3 mg, 0.5 mmol), *tert*-butanol (143 μL, μL, 1.5 mmol), and toluene (4.17 mL). After flash chromatography on silica gel (40% EtOAc in hexanes), the title compound was obtained as a yellow oil (0.078 g, 77%). ^{1}H NMR (500 MHz, $CDCl_3$): δ 8.75 (br s, 1H), 8.71 (br s, 1H), 7.97 (d, *J* = 9.1 Hz, 1H), 7.61 (d, *J* = 2.5 Hz, 1H), 7.42 (dd, *J* = 9.1, 2.6 Hz, 1H), 1.50 (s, 9H). ^{13}C{^{1}H} NMR (126 MHz, $CDCl_3$): δ 157.4, 145.0, 144.1, 143.1, 139.9, 130.0, 128.6, 117.8, 80.1, 28.9. Spectroscopic data are consistent with those previously reported.

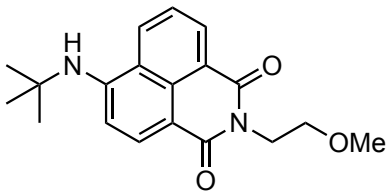

6-(*tert*-butylamino)-2-(2-methoxyethyl)-1*H*-benzo[*de*]isoquinoline-1,3(2*H*)-dione (**4-10a**). GPD was followed using *tert*-butylamine (126 μL, 0.12 mmol, 3.0 equiv). After flash chromatography (50% EtOAc in hexanes), the title compound was obtained as a yellow-orange solid (0.108 g, 83%). ^{1}H NMR (500 MHz, $CDCl_3$): δ 8.58 (dd, *J* = 1.0, 7.3 Hz, 1H), 8.43 (d, *J* = 8.6 Hz, 1H), 8.02 (dd, *J* = 8.5, 0.8 Hz, 1H), 7.60 (dd, *J* = 8.4, 7.4 Hz, 1H), 6.98

(d, J = 8.6 Hz, 1H), 5.28 (br s, 1H), 4.42 (t, J = 6.1 Hz, 2H), 3.72 (t, J = 6.1 Hz, 2H), 3.38 (s, 3H), 1.59 (s, 9H). $^{13}C\{^{1}H\}$ NMR (126 MHz, $CDCl_3$,): δ 164.9, 164.3, 148.2, 134.1, 131.3, 130.4, 125.9, 124.8, 123.4, 121.2, 109.9, 106.8, 70.0, 58.9, 52.3, 39.1, 29.6. HRMS-ESI (*m*/*z*): Calc'd for $C_{19}H_{22}N_2NaO_3$ $[M+Na]^+$: 349.1523 Found: 349.1535.

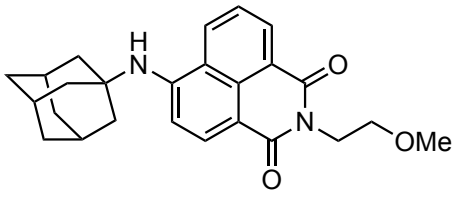

6-(adamantan-1-ylamino)-2-(2-methoxyethyl)-1*H*-benzo[*de*]isoquinoline-1,3(2*H*)-dione (**4-10b**). GPD was followed using 1-adamantylamine (90.9 mg, 0.6 mmol, 1.5 equiv). After flash chromatography (500 mL of 20% EtOAc in hexanes, 200 mL of 40% EtOAc in hexanes, then EtOAc), the title compound was obtained as an orange solid (0.142 g, 88%). ^{1}H NMR (500 MHz, $CDCl_3$): δ 8.56 (dd, J = 0.7, 7.3 Hz, 1H), 8.39 (d, J = 8.6 Hz, 1H), 8.02 (dd, J = 8.4 , 0.7 Hz, 1H), 7.58 (dd, J = 8.3, 7.4 Hz, 1H), 7.06 (d, J = 8.6 Hz, 1H), 5.15 (br s, 1H), 4.41 (t, J = 6.1 Hz, 2H), 3.71 (t, J = 6.1 Hz, 2H), 3.38 (s, 3H), 2.23 (br s, 3H), 2.171–2.167 (br m, 6H), 1.81–1.76 (br m, 6H). $^{13}C\{^{1}H\}$ NMR (126 MHz, $CDCl_3$,): δ 164.9, 164.2, 148.0, 134.0, 131.2, 130.4, 126.0, 124.7, 123.3, 121.3, 109.8, 107.7, 69.9, 58.9, 53.3, 42.4, 39.1, 36.5, 29.8. HRMS-ESI (*m*/*z*): Calc'd for $C_{25}H_{28}N_2NaO_3$ $[M+Na]^+$: 427.1992. Found: 427.1979.

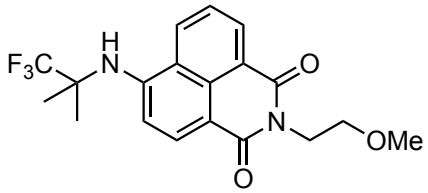

2-(2-methoxyethyl)-6-((1,1,1-trifluoro-2-methylpropan-2-yl)amino)-1H-benzo[*de*]isoquinoline-1,3(2*H*)-dione (**4-10c**). GPD was followed using 2,2,2-trifluoro-1,1-dimethyl-ethylamine (115.9 mg, 1.2 mmol, 3.0 equiv). After flash chromatography (20% EtOAc in hexanes), the title compound was obtained as a yellow-orange solid (0.125 g, 82%). ^{1}H NMR (500 MHz, $CDCl_3$): δ 8.59 (dd, J = 7.3, 0.6 Hz, 1H), 8.46 (d, J = 8.4 Hz, 1H), 8.11 (d, J = 8.3 Hz, 1H), 7.67 (dd, J = 8.4, 7.5 Hz, 1H), 7.18 (d, J = 8.4 Hz, 1H), 4.96 (br s, 1H), 4.42 (t, J = 6.0 Hz, 2H), 3.72 (t, J = 6.0 Hz, 2H), 3.38 (s, 3H), 1.73 (s, 6H). $^{13}C\{^{1}H\}$ NMR (126 MHz, $CDCl_3$,): δ 164.7, 164.1, 146.1, 133.4, 131.4, 129.9, 127.3 (q,

J_{CF} = 286 Hz), 126.2, 126, 123.5, 123.1, 113.6, 111.11–111.09 (m), 69.9, 58.9, 58.4 (q, J_{CF} = 28.1 Hz), 39.2, 22.7. $^{19}F\{^{1}H\}$ NMR (470 MHz, $CDCl_3$): δ -79.5. HRMS-ESI (*m*/*z*): Calc'd for $C_{19}H_{19}F_3N_2NaO_3$ $[M+Na]^+$: 403.1240. Found: 403.1247.

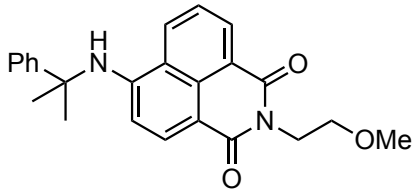

2-(2-methoxyethyl)-6-((2-phenylpropan-2-yl)amino)-1*H*-benzo[*de*]isoquinoline-1,3(2*H*)-dione (**4-10d**). GPD was followed using cumylamine (86.3 µL, 0.6 mmol, 1.5 equiv). After flash chromatography (40% EtOAc in hexanes), the title compound was obtained as a yellow-orange solid (0.129 g, 83%). ^{1}H NMR (500 MHz, $CDCl_3$): δ 8.60 (dd, *J* = 0.9, 7.4 Hz, 1H), 8.21 (d, *J* = 7.9 Hz, 1H), 8.14 (d, *J* = 8.5 Hz, 1H), 7.66 (dd, *J* = 8.4, 7.4 Hz), 7.46–7.44 (m, 2H), 7.36–7.33 (m, 2H), 7.29–7.27 (m, 1H), 6.21 (d, *J* = 8.6 Hz, 1H), 5.69 (br s, 1H), 4.39 (t, *J* = 6.0 Hz, 2H), 3.68 (t, *J* = 6.1 Hz, 2H), 3.35 (s, 3H), 1.86 (s, 6H). $^{13}C\{^{1}H\}$ NMR (126 MHz, $CDCl_3$,): δ 164.9, 164.2, 147.1, 145.2, 133.7, 131.2, 130.1, 129.2, 127.3, 126, 125.3, 124.9, 123.5, 121.0, 110.4, 108.7, 69.9, 58.9, 57.1, 39.1, 30.7. HRMS-ESI (*m*/*z*): Calc'd for $C_{24}H_{24}N_2NaO_3$ $[M+Na]^+$: 411.1679. Found: 411.1687.

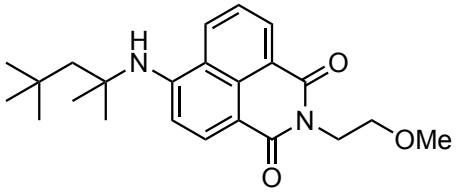

2-(2-methoxyethyl)-6-((2,4,4-trimethylpentan-2-yl)amino)-1*H*-benzo[*de*]isoquinoline-1,3(2*H*)-dione (**4-10e**). GPD was followed using *tert*-octylamine (96.3 µL, 0.6 mmol, 1.5 equiv). After flash chromatography (20% EtOAc in hexanes), the title compound was obtained as a yellow-orange solid (0.132, 86%). ^{1}H NMR (500 MHz, $CDCl_3$): δ 8.57 (dd, *J* = 0.9, 7.3 Hz, 1H), 8.43 (d, *J* = 8.6 Hz, 1H), 8.00 (dd, *J* = 8.5, 0.7 Hz, 1H), 7.59 (dd, *J* = 8.4, 7.4 1H), 6.97 (d, *J* = 8.6 Hz, 1H), 5.31 (br s, 1H), 4.42 (t, *J* = 6.1, 2H), 3.71 (t, *J* = 6.1 Hz, 2H), 3.38 (s, 3H), 1.93 (s, 2H), 1.63 (s, 6H), 1.04 (s, 9H). $^{13}C\{^{1}H\}$ NMR (126 MHz, $CDCl_3$,): δ 164.9, 164.3, 148.2, 134.1, 131.2, 130.4, 126, 124.8, 123.4, 121.2, 109.7, 107.0, 70.0, 58.9, 56.5, 52.1, 39.1, 32.1, 31.7, 30.3. HRMS-ESI (*m*/*z*): Calc'd for $C_{23}H_{30}N_2NaO_3$ $[M+Na]^+$: 405.2149. Found: 405.2156.

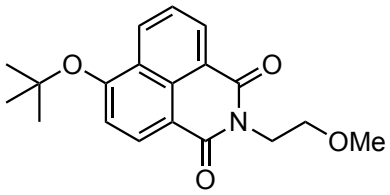

6-(*tert*-butoxy)-2-(2-methoxyethyl)-1H-benzo[*de*]isoquinoline-1,3(2*H*)-dione (**4-11**). In a nitrogen-filled glovebox, **3-C1** (16.6 mg, 0.0225 mmol, 5 mol %), LiO*t*-Bu (54.0 mg, 0.75 mmol, 1.5 equiv), **4-9** (130.4 mg, 0.45 mmol, 1.0 equiv), CPME (1.875 mL), and *tert*-butanol (129 µL, 1.35 mmol, 3.0 equiv), were consecutively added to a 1 dram vial with a magnetic stir bar. The vial was sealed with a cap containing a PTFE septum, removed from the glovebox, and placed in a temperature-controlled, aluminum heating block set to 110 ºC. Magnetic stirring was initiated, and the reaction was allowed to stir at 110 ºC for 18 h (unoptimized). After this time, the reaction was removed from the heating block and allowed to cool to room temperature. Then, the reaction was filtered through a Celite/silica plug (~2:1 ratio, ~1:0.5 x 4.5 cm), eluting with 10% MeOH in CH_2Cl_2 until the filtrate ran colourless (~50 mL). The resulting solution was concentrated by about half under reduced pressure, and activated neutral alumina was added. The volatiles were removed from the resulting heterogeneous mixture, and the so-formed alumina dry pack was placed on a column of activated, neutral alumina. After flash chromatography (10% EtOAc in hexanes), the title compound was obtained as yellow solid (0.112 g, 76%). ^{1}H NMR (500 MHz, $CDCl_3$): δ 8.63 (d, J = 7.2 Hz, 1H), 8.58–8.54 (m, 2H), 7.73–7.70 (m, 1H), 7.31–7.29 (m, 1H), 4.47 (t, J = 6.0 Hz, 2H), 3.76 (t, J = 6.0 Hz, 2H), 3.42 (s, 3H), 1.67 (s, 9H). ^{13}C{^{1}H} NMR (126 MHz, $CDCl_3$,): δ 164.8, 164.2, 158.6, 133.0, 131.7, 130.0, 129.9, 126.7, 125.9, 122.6, 115.4, 113.2, 81.8, 69.9, 58.9, 39.2, 29.1. HRMS-ESI (*m*/*z*): Calc'd for $C_{19}H_{21}NNaO_4$ $[M+Na]^+$: 350.1363. Found: 350.1372.

4.5.6 Large-Scale Synthesis of 4-3p

In a nitrogen-filled glovebox, **4-C1** (182.0 mg, 0.275 mmol), NaO*t*-Bu (792.8 mg, 8.25 mmol), 6-chloroquinoxaline (905.2 mg, 5.5 mmol), toluene (45.8 mL), and *tert*-butylamine (1.734 mL, 16.5 mmol) were consecutively added to a 100 mL round-bottom flask, followed by a magnetic stir bar. The flask was sealed with a septum, and magnetic stirring was initiated. After 18 h (unoptimized), the flask was removed from the glovebox. The reaction mixture was then diluted with EtOAc (50 mL) and filtered through Celite,

rinsing the Celite plug with additional EtOAc (3 x 25 mL). The resulting filtrate was concentrated to ~3-5 mL, and purified via automated flash chromatography (100 g Biotage® SNAP KP-SIL cartridge, 0–50% EtOAc in hexanes, 2–5–2 CV, 45 mL/min flow rate), affording the title compound as an orange oil (1.049 g, 95%). Spectroscopic data were consistent with those reported below.

Chapter 5: Research Summaries and Future Work

5.1 Chapter 2 Research Summary and Future Work

The newly developed **2-C3** pre-catalyst system, incorporating the tailored ancillary ligand CyPAd-DalPhos (**2-L3**), facilitated the first examples of the nickel-catalyzed *N*-arylation of cyclopropylamine. The scope of this transformation encompassed a wide variety of (hetero)aryl electrophiles (i.e., chlorides, bromides, and tosylates, with representative mesylate, triflate, carbamate, and sulfamate entries), with the majority of reactions proceeding at room temperature (see **Scheme 2.10**). Competition experiments established a reactivity preference for aryl chlorides vs. aryl bromides or tosylates (see **Scheme 2.12**). Additionally, reaction monitoring studies revealed that the addition of 4-chloroanisole had a deleterious effect on the outcome of a successful reaction (see **Scheme 2.13**). Finally, cyclopropanemethylamine hydrochloride and cyclobuytlmine hydrochloride were also effectively cross-coupled with representative (hetero)aryl (pseudo)halides at room temperature using **2-C3** (see **Scheme 2.14**).

The tendency of the **2-C3** pre-catalyst system to engage preferentially with aryl chlorides/bromides over corresponding aryl tosylates in the *N*-arylation of cyclopropylamine could be harnessed in chemoselective cross-couplings employing electrophiles bearing chloride/bromide and pseudohalide substituents (**Scheme 5.1A**). Though only a modest preference for the aryl chloride/bromide cross-coupled product was observed in competition experiments using **2-C3** (4:1 to 5:1; see **Scheme 2.13**), the use of heterocyclic electrophiles in which the halide is in an activated position compared to the pseudohalide moiety (e.g., substituted 2-halopyridines) may further enhance chemoselectivity (**Scheme 5.1B**). Judicious choice of pseudohalide may also encourage preferential reactivity at the halide; **2-C3** did not engage with a heteroaryl mesylate under optimized reaction conditions (see **2-3l** in **Scheme 2.10**), suggesting substrates incorporating a mesylate may be good candidates for this investigation. Ultimately, the resulting pseudohalide-containing, cross-coupled product could then be subjected to another nickel-catalyzed C–C[95, 122] or C–N[57, 59-62, 64, 66] cross-coupling reaction, allowing access to a diverse set of functionalized products.

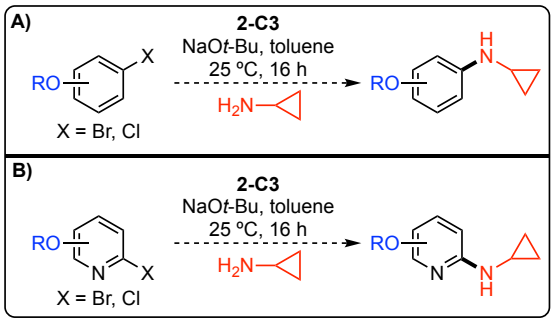

Scheme 5.1. Proposed chemoselective cross-couplings in the *N*-arylation of cyclopropylamine using **2-C3**.

2-C3 did not engage with electron-rich electrophiles efficiently, as evidenced in reaction monitoring experiments. The origin of this phenomenon could be further explored through stoichiometric experiments in an effort to overcome this deficiency. A (**2-L3**)Ni(*p*-anisyl)X complex could be prepared through the reaction of 4-methoxyphenyl magnesium bromide and (**2-L3**)$NiBr_2$, or through the addition of 4-chloroanisole to *in situ*-generated (**2-L3**)Ni(cod) (**Scheme 5.2A**). Addition of cyclopropylamine to a solution of either complex in the presence of base under optimized reaction conditions should initiate reductive elimination to form **2-3b** (**Scheme 5.2B**); monitoring the formation of **2-3b** could then allow insight into the feasibility of this process. Efficient generation of **2-3b** would suggest that reductive elimination is likely facile and not the source of poor reactivity with electron-rich substrates using **2-C3**.

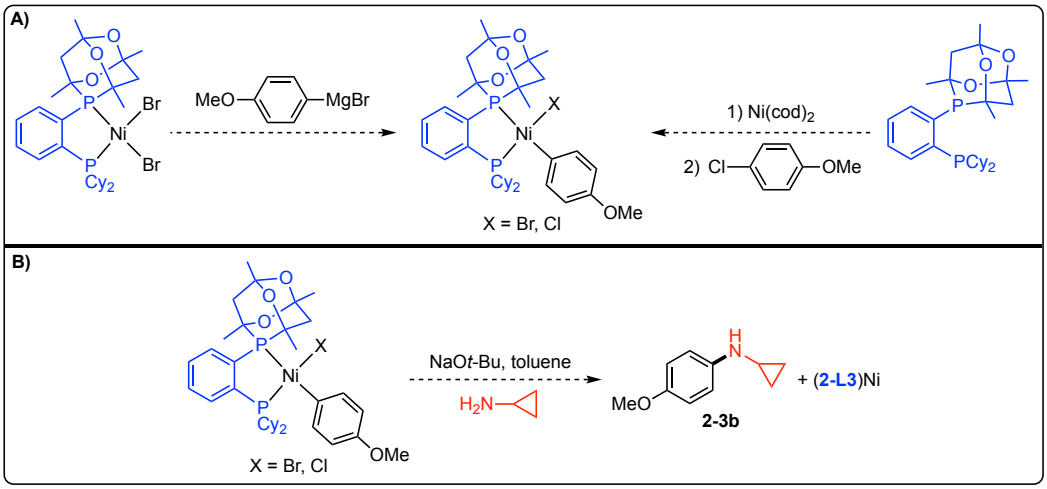

Scheme 5.2. A) Proposed synthesis of (**2-L3**)Ni(*p*-anisyl)X (X = Br, Cl). B) Stoichiometric reaction monitoring experiments using (**2-L3**)Ni(*p*-anisyl)X.

Recently, a nickel pre-catalyst containing a 3,4-disubstituted thiophenyl analogue of **2-L1**, ThioPAd-DalPhos, enabled nickel-catalyzed C–N cross-couplings of representative (hetero)aryl electrophiles and furfurylamine to proceed with unprecedentedly low catalyst loadings (0.125-2.5 mol %).[161] DFT calculations suggested that ThioPAd-DalPhos stabilizes key catalytic intermediates more effectively than **2-L1**, resulting in increased catalyst longevity and improving catalytic performance. Similarly, the application of a **2-L3** analogue, **5-L1**, wherein the 1,2-disubstituted phenylene backbone is replaced with a 3,4-disubstituted thiophenyl moiety (**Figure 5.1**), in the nickel-catalyzed *N*-arylation of cyclopropylamine might confer enhanced reactivity in the form of lower catalyst loadings and/or permit access to previously unsuccessful substrates (e.g., electron-rich electrophiles, or (hetero)aryl mesylates and/or triflates at room temperature). The activity of **5-L1** in this reaction might also provide further insight into the subtle steric and electronic ancillary ligand effects that appear to govern the success of this transformation (see Section 2.3.3).

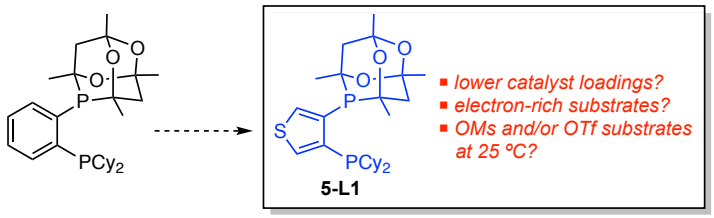

Figure 5.1. Proposed development of the thiophene-based, **2-L3** analogue, **5-L1**.

5.2 Chapter 3 Research Summary and Future Work

Pre-catalysts **2-C3** and **2-C1** were shown to effect nickel-catalyzed C–O cross-couplings of (hetero)aryl electrophiles with primary, secondary, and tertiary aliphatic alcohols. Previous examples of this transformation made use of (hetero)aryl bromides exclusively, relying on dual nickel/photoredox catalysis to facilitate product formation. The application of tailored ancillary ligands CyPAd-DalPhos (**2-L3**) and PAd-DalPhos (**2-L1**) in nickel-catalyzed C–O cross-coupling enabled access to inexpensive and abundant (hetero)aryl chlorides and (pseudo)halides (i.e., tosylates, mesylates, triflates, and pivalates) for the first time, without recourse to photoredox catalysis (**Schemes 3.6** and **3.7**). Efforts to extend the newly developed cross-coupling protocol to phenols were largely unsuccessful (see Section 3.3.5). Competition experiments revealed a marked preference for C–N vs. C–O bond formation using **2-C3** and **2-C1** when equimolar amounts of amine and alcohol nucleophile were employed under optimized reaction conditions with limiting

electrophile (**Scheme 3.9A** and **3.9B**). Furthermore, **2-C3** and **2-C1** preferentially formed the primary alcohol cross-coupled product **3-4a** in the presence of equivalent amounts of primary alcohol **3-3b** and secondary alcohol **3-2a** (**Scheme 3.9C**).

Because this investigation represents the first examples of nickel-catalyzed C–O cross-coupling facilitated by tailored ancillary ligands, stoichiometric and computational studies would provide mechanistic insight that could be used to inform the design of new ancillary ligands for this transformation. Firstly, the synthesis of Ni(II) alkoxide complexes containing **2-L3** and **2-L1** could be prepared from the reaction of pre-catalysts **2-C3** or **2-C1** and a suitable alkoxide source (i.e., pre-formed or commercially available metal alkoxides), or reacting **2-C3** or **2-C1** with an appropriate alcohol in the presence of base (i.e., NaO*t*-Bu or Cs_2CO_3) under pseudo-catalytic conditions (**Scheme 5.3**). The synthesis of these compounds at ambient temperatures would likely circumvent decomposition via C–O reductive elimination, as product formation was not observed at temperatures below 110 ºC using either pre-catalyst. However, the possibility of β-hydrogen elimination from these compounds may prohibit isolation and characterization.

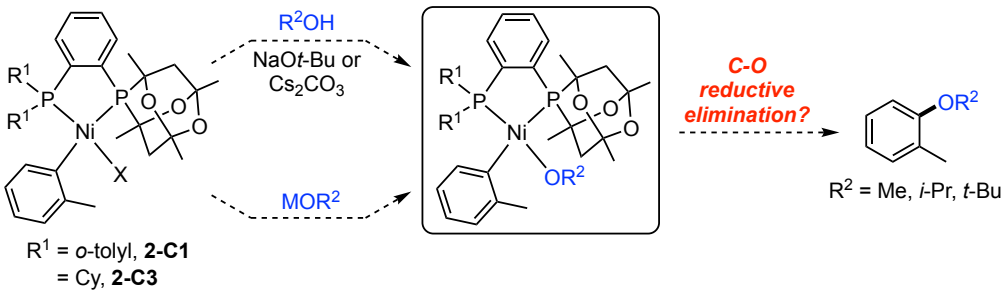

Scheme 5.3. Proposed synthesis of Ni(II) alkoxide complexes containing **2-L1** and **2-L3**, and subsequent reductive elimination studies.

With the (L)Ni(*o*-tolyl)OR complexes in hand, studies examining C–O reductive elimination could then be performed (**Scheme 5.3**). Reports by Hillhouse and co-workers[109] previously demonstrated that Ni(II) alkoxides required oxidation to higher valent nickel species in order to induce C–O reductive elimination. Thus, heating the (L)Ni(*o*-tolyl)OR species at 110 ºC (i.e., catalytic conditions) and monitoring the formation of alkyl aryl ether would provide insight into the feasibility of this process at Ni(II). Indeed, the use of tailored ancillary ligands **2-L3** and **2-L1** might enable this process such that higher nickel oxidation states are not necessary for C–O reductive elimination to occur.

Control experiments conducted in the absence of light would aid in the confirmation of a Ni(II) C–O reductive elimination pathway; Doyle and co-workers[151] recently showed that nickel pre-catalysts containing redox-active ligands can facilitate C–O cross-coupling via a Ni(I)/Ni(III) pathway under visible light irradiation in the absence of an exogenous photocatalyst. Examining C–O reductive elimination from Ni(II) alkoxide complexes derived from primary, secondary, and tertiary alcohols might also provide insight into the effects of sterics on this process. Computational studies exploring the feasibility of C–O reductive elimination from complexes of the form (L)Ni(*o*-tolyl)OR (L = **2-L3** or **2-L1**) might also corroborate experimental findings.

Examining the efficacy of Ni(I) pre-catalysts in facilitating C–O cross-coupling may also be of interest, particularly given the Ni(I)/Ni(III) catalytic cycles proposed by Doyle[151] and Nocera[111] in dual nickel/photoredox C–O cross-couplings. Ni(I) pre-catalysts incorporating **2-L1** (**5-C1**)[56] and **2-L3** (**5-C2**) can be prepared and screened for activity in the select test reactions, e.g., in the reaction of 1-chloronaphthalene (**3-1a**) and 4-methylpentanol (**3-2b**) or isopropanol (**3-2a**; **Scheme 5.4**), thus allowing direct comparison to corresponding Ni(II) pre-catalysts **2-C1** and **2-C3**. Screening Ni(I) pre-catalysts containing other tailored ancillary ligands, particularly those whose Ni(II) pre-catalysts were ineffective for this transformation, e.g., dppf (**3-L1**[53a, b]), may also be informative, given that significant differences in activity were observed between corresponding Ni(I) and Ni(II) pre-catalysts incorporating **3-L1** in the challenging *N*-arylation of a primary amide.[56] The aforementioned studies will thus help to illuminate whether oxidation state should be considered when developing new, nickel-catalyzed cross-coupling methodologies.

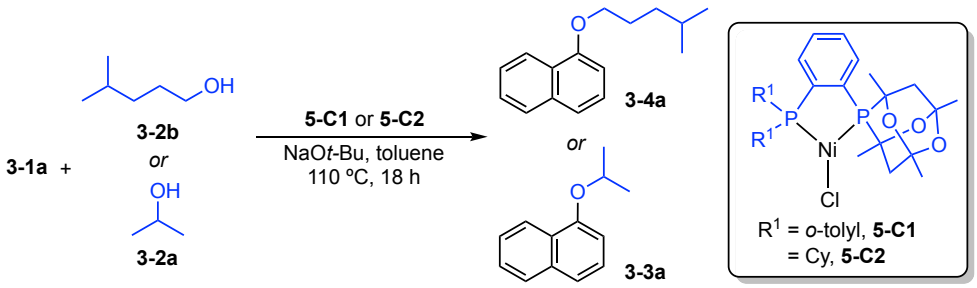

Scheme 5.4. Proposed screening of Ni(I) pre-catalysts incorporating **2-L1** and **2-L3** for activity in C–O cross-coupling reactions.

The formation of complex reaction mixtures when *meta*-substituted electrophiles were employed in nickel-catalyzed C–O cross-couplings using **2-C3** and **2-C1** warrants further investigation, particularly given the successful use of such substrates in analogous C–N cross-coupling reactions. Careful examination of the product mixtures resulting from reactions of *meta*-substituted electrophiles and aliphatic alcohols facilitated by **2-C3** and **2-C1** by HPLC-MS and/or NMR spectroscopy might help to elucidate the mechanism of decomposition that is occurring. Additionally, exploring the behaviour of **2-L3**- and **2-L1**-ligated, nickel oxidative addition complexes of representative *meta*-substituted electrophiles (e.g., 3-chlorotoluene and 3-chloroanisole) might also grant insight into the unusual reactivity of these substrates under catalytic conditions. Specifically, analyzing the products of stoichiometric reactions involving these complexes and aliphatic alcohols in the presence of base would reveal whether clean C–O cross-coupling is feasible with *meta*-substituted electrophiles (**Scheme 5.5**). If the C–O cross-coupled product is exclusively observed, other, deleterious pathways (e.g., comproportionation) might be the source of poor reactivity with these substrates, particularly if the corresponding homo-coupled, biaryl product is observed under these conditions.

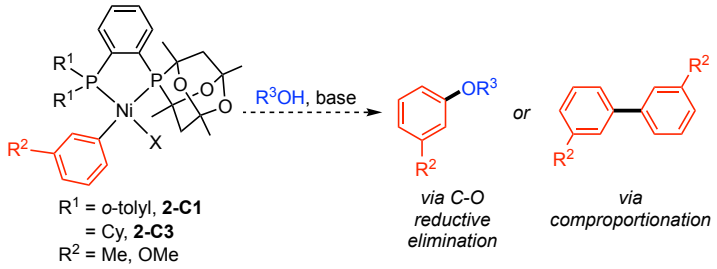

Scheme 5.5. Investigating the poor reactivity of *meta*-substituted electrophiles in nickel-catalyzed C–O cross-coupling.

Relatedly, the preparation of (**2-L3**)Ni(*o*-tolyl)OPh and (**2-L1**)Ni(*o*-tolyl)OPh complexes from reactions of **2-C3** and **2-C1** with a phenoxide source (e.g., NaOPh) may provide insight into the poor reactivity of phenols using these pre-catalysts. Attempts to induce C–O reductive elimination from such complexes would reveal whether this process is feasible (**Scheme 5.6A**). Additionally, given the electron-rich nature of phenols and diaryl ethers, it is possible that these species interact with a ligated Ni(0) complex to produce a highly stabilized intermediate that is catalytically inert. To test this hypothesis, complexes of the form (L)Ni(η^6-C_6H_5OH) (L = **2-L1**, **5-C3a**; L = **2-L3**, **5-C3b**) or

(L)Ni(η^6-C_6H_5OPh) (L = **2-L1**, **5-C4a**; L = **2-L3**, **5-C4b**) could be synthesized (e.g., from *in situ*-generated (L)Ni(cod) species, in a manner analogous to the synthesis of (IPr)Ni(η^6-C_7H_8)[162]). Then, these complexes could be screened for activity in C–N/O cross-couplings, comparing reaction outcomes to analogous reactions facilitated by **2-C3** and **2-C1** (**Scheme 5.6B**).

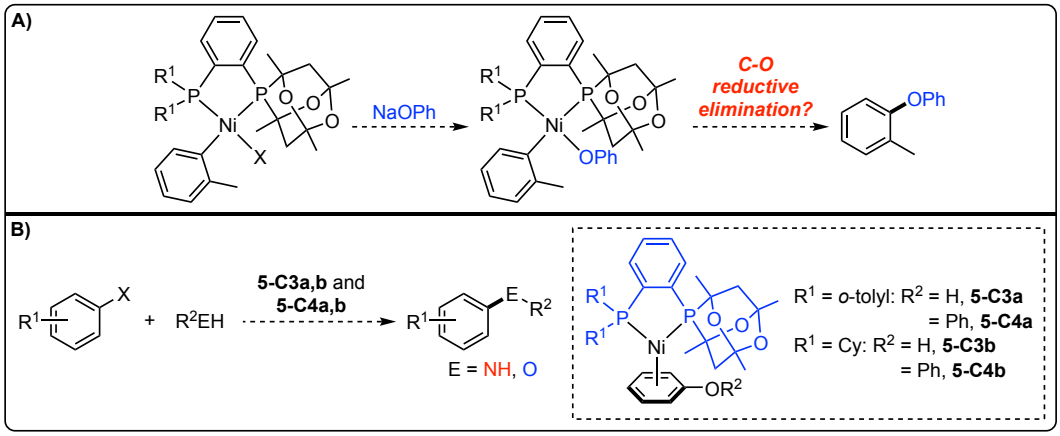

Scheme 5.6. A) Synthesis of Ni(II) phenoxide complexes containing **2-L1** and **2-L3**. B) Screening complexes **5-C3a,b** and **5-C4a,b** for activity in nickel-catalyzed C–N/O cross-coupling reactions.

The optimized catalytic conditions for the cross-coupling of aliphatic alcohols using **2-C3** and **2-C1** may find application in related reactions employing other oxygen-based nucleophiles. For example, the use of carboxylic acids in this chemistry to generate *O*-aryl esters may be of interest (**Scheme 5.7**). Current catalytic protocols for the *O*-arylation of carboxylic acids with nickel are limited to dual nickel/photoredox methodologies,[163] and utilize (hetero)aryl bromide and iodide electrophiles exclusively. The benefits conferred by the use of tailored ancillary ligands in the C–O cross-coupling of aliphatic alcohols, i.e., allowing access to (hetero)aryl chlorides and pseudohalides, may then transfer to reactions employing carboxylic acid nucleophiles.

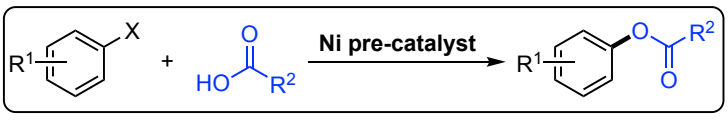

Scheme 5.7. Nickel-catalyzed C–O cross-coupling of carboxylic acids.

Finally, the marked preference for pre-catalysts **2-C3** and **2-C1** to engage in C–N cross-coupling vs. C–O cross-coupling, as evidenced by nucleophile competition experiments (see **Scheme 3.9C**), could be exploited in the chemoselective *N*-arylation of

alkanolamines (**Scheme 5.8**). Currently, there are no known nickel catalysts that facilitate this transformation. Numerous alkanolamines are commercially available, including chiral variants derived from amino acids, allowing access to a wide range of cross-coupled products. Given that chiral, *N*-arylated alkanolamines are of interest in the pharmaceutical industry,[164] the development of a nickel-catalyzed methodology for the *N*-arylation of alkanolamines would be of potential significant value.

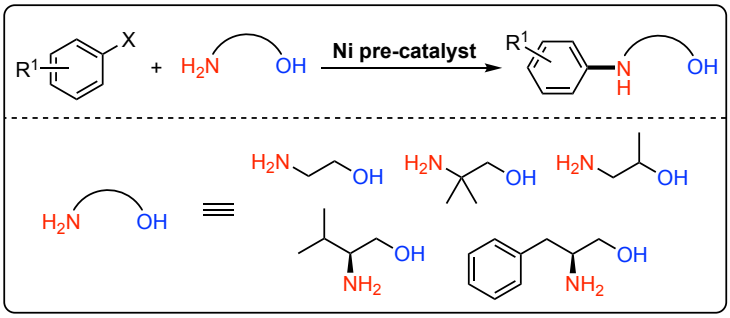

Scheme 5.8. Nickel-catalyzed *N*-arylation of alkanolamines.

5.3 Chapter 4 Research Summary and Future Work

Pre-catalyst **4-C1**, incorporating tailored ancillary ligand PhPAd-DalPhos (**4-L1**), effected nickel-catalyzed C–N cross-couplings of (hetero)aryl halides and α,α,α-trisubstituted, primary alkylamines, demonstrating broad electrophile scope with this class of nucleophile for the first time with nickel (**Scheme 4.5**). Furthermore, the first examples of room temperature reactivity with α,α,α-trisubstituted, primary alkylamines using any metal catalyst (palladium, nickel, or other) was achieved with **4-C1**. Carbamate electrophiles were generally unreactive with α,α,α-trisubstituted, primary alkylamines under optimized catalytic conditions using **4-C1**; this phenomenon was then exploited in chemoselective cross-coupling reactions employing electrophiles containing both chloride and carbamate moieties, with C–N bond formation occurring exclusively at the chloride substituent (**Scheme 4.6B**). The **4-C1** pre-catalyst system could also be applied in the nickel-catalyzed cross-couplings of other sterically hindered nucleophiles, including 2,6-disubstituted anilines (**Scheme 4.7A**) and bulky, aliphatic alcohols (**Scheme 4.7B**). As an extension of this chemistry, a newly developed $Ni(cod)_2$/IPr (**3-L2**) catalyst system was used to prepare 1,8-naphthalimide derivatives incorporating α,α,α-trisubstituted, primary alkylamine substituents in order to investigate the photochemical properties of such compounds (**Scheme 4.9**).

Triphenylmethylamine was not a suitable nucleophile in reactions involving **4-C1**, likely owing to its considerable steric bulk. Therefore, it might be interesting to see if this nucleophile could be accommodated in C–N cross-coupling reactions with a pre-catalyst containing an ancillary ligand whose steric properties were significantly reduced. The replacement of the PPh_2 moiety in **4-L1** with a PEt_2 moiety might produce an ancillary ligand with the appropriate sterics to test this hypothesis. The resulting ligand, **5-L2**, and its associated (L)Ni(*o*-tolyl)Cl pre-catalyst (**5-C5**) could be prepared in an analogous fashion to other **2-L1** and **2-C1** variants, respectively (**Scheme 5.9**). The use of **5-C5** in C–N cross-coupling reactions of triphenylmethylamine and other α,α,α-trisubstituted, primary alkylamines may offer insight into the effect of ligand sterics on the outcome of this transformation, particularly when compared with corresponding reactions utilizing **4-C1**. The increased electron-donating ability of **5-L2** vs. **4-L1** conferred by the PEt_2 moiety might also increase the electron density of the nickel centre in **5-C5** sufficiently such that it can engage in oxidative addition chemistry with pseudohalide electrophiles (e.g., triflates, mesylates, carbamates, and sulfamates) that could not be accessed using **4-C1**.

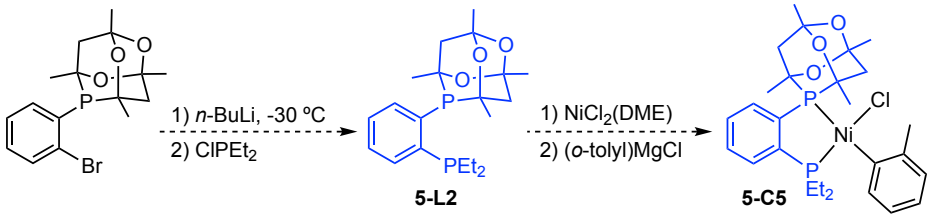

Scheme 5.9. Proposed synthesis of **5-L2** and **5-C5.**

In addition to α,α,α-trisubstituted, primary alkylamines, 2,6-disubstituted anilines, and bulky, aliphatic alcohols, another class of sterically hindered nucleophile that might be successfully accommodated in nickel-catalyzed cross-couplings using **4-C1** include α-branched secondary amines (**Scheme 5.10**). There are no known nickel catalysts that facilitate this transformation, and there exists only a single report using palladium catalysis with broad scope by Buchwald and co-workers[165] employing this class of nucleophile, emphasizing the need for highly active catalyst systems to overcome this synthetic challenge. The prevalence of *N*-arylated, α-branched secondary amines in biologically active molecules[166] further highlights the latent, practical value of this reaction.

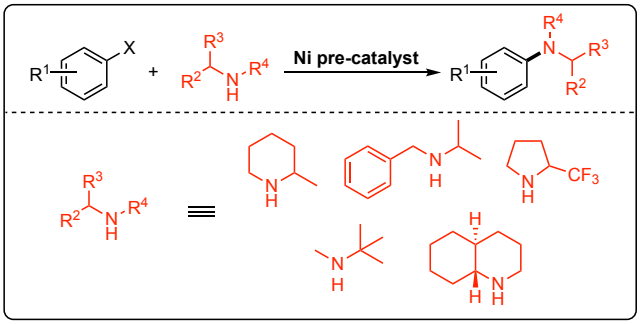

Scheme 5.10. Nickel-catalyzed *N*-arylation of α-branched secondary amines

The successful chemoselective cross-couplings of electrophiles containing chloride and carbamate substituents with α,α,α-trisubstituted, primary alkylamines using **4-C1** could be harnessed for sequential cross-coupling reactions in one pot employing two pre-catalysts. Initially, other pseudohalide electrophiles that do not interact well with **4-C1** could be identified in catalyst poisoning experiments similar to those displayed in **Scheme 4.6A**; (hetero)aryl sulfamates and pivalates are ideal candidates in these studies, owing to the many nickel-catalyzed C–C[95, 122] and C–N[57, 59-62, 64, 66] cross-coupling reactions that make use of such electrophiles.

With these synthetic handles identified, conditions for sequential cross-couplings in one pot employing two pre-catalysts can be established. As an example, **2-C2** effects the cross-coupling of (hetero)aryl carbamates and unhindered, primary alkylamines,[61a] but does not facilitate the C–N cross-coupling of α,α,α-trisubstituted, primary alkylamines and (hetero)aryl chlorides (see **Table 4.1**, entry 2), complementing the reactivity of **4-C1**. Thus, a viable sequential cross-coupling protocol involves the initial cross-coupling of an electrophile containing chloride and carbamate moieties with an α,α,α-trisubstituted, primary alkylamine *at the chloride substituent using **4-C1***, followed by a second cross-coupling reaction with an unhindered, primary alkylamine *at the carbamate substituent using **2-C2*** (**Scheme 5.11**). In order to test whether the second cross-coupling in the proposed reaction sequence is feasible, **4-3q** could be used in a cross-coupling reaction with an unhindered, primary alkylamine using **2-C2** (**Scheme 5.11A**). If this reaction is successful, then examining the ability of this sequence to occur in one pot would be of interest, that is, allowing the first reaction to proceed to completion, then adding the necessary materials (i.e., **2-C2** and unhindered, primary alkylamine) to the same reaction vessel to enable the second cross-coupling (**Scheme 5.11B**). Ideally, *all* materials for *both*

cross-coupling reactions should be added to the reaction vessel initially. However, in doing so, the selectivity of the reaction sequence may become compromised owing to the ability of **2-C2** to engage with (hetero)aryl chlorides in the C–N cross-coupling of unhindered, primary alkylamines.[68]

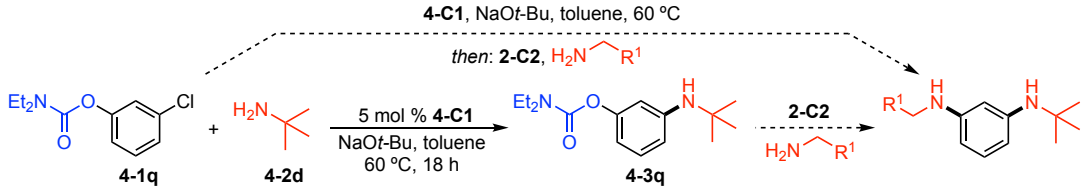

Scheme 5.11. Proposed two-step, one-pot cross-coupling sequence using **4-C1** and **2-C2**.

Given the potential applications of the amino-substituted 1,8-naphthalimides prepared in Section 4.3.8 as fluorescent probes in biological systems, it may be of interest to enhance the aqueous solubility of these compounds. Targeting 1,8-naphthalimide electrophiles that contain substituents on the imide nitrogen with highly polar functional groups, e.g., carboxylic acids or sulfonamides (**Figure 5.2**), in nickel-catalyzed C–N cross-couplings of α,α,α-trisubstituted, primary alkylamines may serve to increase the hydrophilicity of the desired products, enhancing their potential utility.

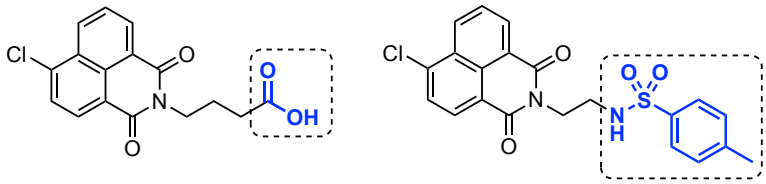

Figure 5.2. Representative 1,8-naphthalimide electrophiles containing polar functional groups to screen in the nickel-catalyzed C–N cross-coupling of α,α,α-trisubstituted, primary alkylamines using $Ni(cod)_2$/**3-L2**.

Chapter 6: Conclusions

The ubiquity of aryl C–N/O bonds in biologically active compounds, along with an increasing focus on developing more sustainable methodologies for industrial applications, requires innovative solutions to address current limitations in base metal-catalyzed processes. While many nickel-catalyzed C–N/O cross-coupling reactions proceed efficiently, little effort is being made to establish these processes as viable, greener alternatives to analogous transformations mediated by palladium. However, it is increasingly clear that the application of tailored ancillary ligands can help overcome existing challenges in this chemistry.

The focus of this thesis was to expand the scope of nickel-catalyzed C–N/O cross-coupling reactions using tailored ancillary ligands, in the hope that this approach would engender unprecedented reactivity with nickel, and develop catalyst systems that are comparable, or superior to, current, state-of-the-art catalytic procedures. In Chapter 2, a newly developed pre-catalyst, **2-C3**, incorporating **2-L3**, effected the first examples of the *N*-arylation of cyclopropylamine and related ammonium salts using nickel catalysis, and established unprecedented room temperature reactivity in this reaction for any metal catalyst (palladium, nickel, or other). Chapter 3 detailed the first examples of nickel-catalyzed C–O cross-coupling without recourse to photoredox catalysis, with pre-catalysts **2-C3** and **2-C1**, allowing a wide range of (hetero)aryl electrophiles, including, for the first time with nickel, chlorides and pseudohalides, to react with primary, secondary, and tertiary aliphatic alcohols. Finally, in Chapter 4, a pre-catalyst incorporating the tailored ancillary ligand **4-L1** facilitated the first nickel-catalyzed cross-couplings of bulky, primary alkylamines with broad electrophile scope, including the first examples of room temperature cross-couplings with this nucleophile class for any metal catalyst (palladium, nickel, or other).

Altogether, this study clearly demonstrates the profound, beneficial effects that tailored ancillary ligands can have on the outcome of challenging nickel-catalyzed cross-coupling reactions. Hopefully, the successful application of tailored ancillary ligands in these transformations will promote the utility of this approach in other reactions, and place such processes one step closer to becoming established, industrial protocols with enduring practicality.

References

1. Atkins, P. W. O., T. L.; Rourke, J. P.; Weller, M. T.; Armstrong, F. A. *Shriver & Atkins' Inorganic Chemistry*. 5th ed.; New York: W. H. Freeman and Co.: New York, 2010.

2. van Leeuwen, P. W. N. M. *Homogeneous Catalysis: Understanding the Art*. Kluwer Academic Publishers: Dordrecht; Boston, 2004.

3. Cornils, B.; Herrmann, W. A. *Applied Homogeneous Catalysis with Organometallic Compounds*. Wiley-VCH: Weinheim; Toronto, 2000.

4. Stradiotto, M.; Lundgren, R. J. *Ligand Design in Metal Chemistry: Reactivity and Catalysis*. John Wiley & Sons, Ltd: Chichester, West Sussex, UK, 2016.

5. Lundgren, R. J.; Stradiotto, M. *Chem. Eur. J.* **2012**, *18*, 9758-9769.

6. (a) Osborn, J. A.; Jardine, F. H.; Young, J. F.; Wilkinson, G. *J. Chem. Soc. A* **1966**, 1711-1732. (b) Knowles, W. S. *Acc. Chem. Res.* **1983**, *16*, 106-112.

7. (a) Knowles, W. S.; Sabacky, M. J.; Vineyard, B. D. *J. Chem. Soc., Chem. Commun.* **1972**, 10-11. (b) Vineyard, B. D.; Knowles, W. S.; Sabacky, M. J.; Bachman, G. L.; Weinkauff, D. J. *J. Am. Chem. Soc.* **1977**, *99*, 5946-5952.

8. J.A., G.; Zuidema, E.; Kamer, P. C. J.; van Leeuwen, P. W. N. M. Phosphorus Ligand Effects in Homogeneous Catalysis and Rational Catalyst Design. In *Phosphorus(III) Ligands in Homogeneous Catalysis: Design and Synthesis*, Kamer, P. C. J.; van Leeuwen, P. W. N. M., Eds. John Wiley & Sons, Ltd: Chichester, West Sussex, UK, 2012; pp 1-26.

9. Andersen, N. G.; Keay, B. A. *Chem. Rev.* **2001**, *101*, 997-1030.

10. Hartwig, J. F. *Organotransition Metal Chemistry: From Bonding to Catalysis*. University Science Books: Sausalito, Calif., 2010.

11. Hayashi, T.; Konishi, M.; Kobori, Y.; Kumada, M.; Higuchi, T.; Hirotsu, K. *J. Am. Chem. Soc.* **1984**, *106*, 158-163.

12. (a) Torborg, C.; Beller, M. *Adv. Synth. Catal.* **2009**, *351*, 3027-3043. (b) Ruiz-Castillo, P.; Buchwald, S. L. *Chem. Rev.* **2016**, *116*, 12564-12649.

13. (a) Fors, B. P.; Watson, D. A.; Biscoe, M. R.; Buchwald, S. L. *J. Am. Chem. Soc.* **2008**, *130*, 13552-13554. (b) Dooleweerdt, K.; Fors, B. P.; Buchwald, S. L. *Org.*

Lett. **2010**, *12*, 2350-2353. (c) Alsabeh, P. G.; Stradiotto, M. *Angew. Chem. Int. Ed.* **2013**, *52*, 7242-7246.

14. Aubin, Y.; Fischmeister, C.; Thomas, C. M.; Renaud, J.-L. *Chem. Soc. Rev.* **2010**, *39*, 4130-4145.

15. Fujita, K.-i.; Yamashita, M.; Puschmann, F.; Alvarez-Falcon, M. M.; Incarvito, C. D.; Hartwig, J. F. *J. Am. Chem. Soc.* **2006**, *128*, 9044-9045.

16. Paul, F.; Patt, J.; Hartwig, J. F. *J. Am. Chem. Soc.* **1994**, *116*, 5969-5970.

17. Yu, D.-G.; Li, B.-J.; Shi, Z.-J. *Acc. Chem. Res.* **2010**, *43*, 1486-1495.

18. Surry, D. S.; Buchwald, S. L. *Angew. Chem. Int. Ed.* **2008**, *47*, 6338-6361.

19. Maiti, D.; Fors, B. P.; Henderson, J. L.; Nakamura, Y.; Buchwald, S. L. *Chem. Sci.* **2011**, *2*, 57-68.

20. (a) Surry, D. S.; Buchwald, S. L. *J. Am. Chem. Soc.* **2007**, *129*, 10354-10355. (b) Cheung, C. W.; Surry, D. S.; Buchwald, S. L. *Org. Lett.* **2013**, *15*, 3734-3737.

21. Fors, B. P.; Dooleweerdt, K.; Zeng, Q.; Buchwald, S. L. *Tetrahedron* **2009**, *65*, 6576-6583.

22. Hicks, J. D.; Hyde, A. M.; Cuezva, A. M.; Buchwald, S. L. *J. Am. Chem. Soc.* **2009**, *131*, 16720-16734.

23. Togni, A.; Breutel, C.; Schnyder, A.; Spindler, F.; Landert, H.; Tijani, A. *J. Am. Chem. Soc.* **1994**, *116*, 4062-4066.

24. Hartwig, J. F. *Acc. Chem. Res.* **2008**, *41*, 1534-1544.

25. Shen, Q.; Ogata, T.; Hartwig, J. F. *J. Am. Chem. Soc.* **2008**, *130*, 6586-6596.

26. Vo, G. D.; Hartwig, J. F. *J. Am. Chem. Soc.* **2009**, *131*, 11049-11061.

27. Kwong, F. Y.; Chan, A. S. C. *Synlett* **2008**, *2008*, 1440-1448.

28. (a) Braunstein, P.; Naud, F. *Angew. Chem. Int. Ed.* **2001**, *40*, 680-699. (b) Bassetti, M. *Eur. J. Inorg. Chem.* **2006**, 4473-4482.

29. Stradiotto, M.; Lundgren, R.; Hesp, K. *Synlett* **2011**, *2011*, 2443-2458.

30. Lundgren, R. J.; Sappong-Kumankumah, A.; Stradiotto, M. *Chem. Eur. J.* **2010**, *16*, 1983-1991.

31. Lundgren, R. J.; Peters, B. D.; Alsabeh, P. G.; Stradiotto, M. *Angew. Chem. Int. Ed.* **2010**, *49*, 4071-4.

32. Alsabeh, P. G.; Lundgren, R. J.; McDonald, R.; Johansson Seechurn, C. C. C.; Colacot, T. J.; Stradiotto, M. *Chem. Eur. J.* **2013**, *19*, 2131-2141.

33. Lundgren, R. J.; Stradiotto, M. *Angew. Chem. Int. Ed.* **2010**, *49*, 8686-8690.

34. (a) Marion, N.; Nolan, S. P. *Acc. Chem. Res.* **2008**, *41*, 1440-1449. (b) Fortman, G. C.; Nolan, S. P. *Chem. Soc. Rev.* **2011**, *40*, 5151-5169. (c) Valente, C.; Çalimsiz, S.; Hoi, K. H.; Mallik, D.; Sayah, M.; Organ, M. G. *Angew. Chem. Int. Ed.* **2012**, *51*, 3314-3332. (d) Valente, C.; Pompeo, M.; Sayah, M.; Organ, M. G. *Org. Process Res. Dev.* **2014**, *18*, 180-190.

35. Kuhl, O. *Chem. Soc. Rev.* **2007**, *36*, 592-607.

36. Marion, N.; Navarro, O.; Mei, J.; Stevens, E. D.; Scott, N. M.; Nolan, S. P. *J. Am. Chem. Soc.* **2006**, *128*, 4101-4111.

37. Organ, M. G.; Abdel-Hadi, M.; Avola, S.; Dubovyk, I.; Hadei, N.; Kantchev, E. A. B.; O'Brien, C. J.; Sayah, M.; Valente, C. *Chem. Eur. J.* **2008**, *14*, 2443-2452.

38. Sharif, S.; Rucker, R. P.; Chandrasoma, N.; Mitchell, D.; Rodriguez, M. J.; Froese, R. D. J.; Organ, M. G. *Angew. Chem. Int. Ed.* **2015**, *54*, 9507-9511.

39. (a) Tasker, S. Z.; Standley, E. A.; Jamison, T. F. *Nature* **2014**, *509*, 299-309. (b) Ananikov, V. P. *ACS Catal.* **2015**, *5*, 1964-1971.

40. (a) Qiao, J. X.; Lam, P. Y. S. *Synthesis* **2011**, *2011*, 829-856. (b) Fischer, C.; Koenig, B. *Beilstein J. Org. Chem.* **2011**, *7*, 59-74. (c) Monnier, F.; Taillefer, M. Copper-Catalyzed C(aryl)–N Bond Formation. In *Amination and Formation of sp2 C–N Bonds*, Taillefer, M.; Ma, D., Eds. Springer Berlin Heidelberg: Berlin, Heidelberg, 2013; pp 173-204. (d) Sambiagio, C.; Marsden, S. P.; Blacker, A. J.; McGowan, P. C. *Chem. Soc. Rev.* **2014**, *43*, 3525-3550. (e) Coman, S. M.; Parvulescu, V. I. *Org. Process Res. Dev.* **2015**, *19*, 1327-1355.

41. (a) Marín, M.; Rama, R. J.; Nicasio, M. C. *Chem. Rec.* **2016**, *16*, 1819-1832. (b) Ritleng, V.; Henrion, M.; Chetcuti, M. J. *ACS Catal.* **2016**, *6*, 890-906.

42. Twilton, J.; Le, C.; Zhang, P.; Shaw, M. H.; Evans, R. W.; MacMillan, D. W. C. *Nat. Rev. Chem.* **2017**, *1*, 0052.

43. Corcoran, E. B.; Pirnot, M. T.; Lin, S.; Dreher, S. D.; DiRocco, D. A.; Davies, I. W.; Buchwald, S. L.; MacMillan, D. W. C. *Science* **2016**, *353*, 279.

44. Kudisch, M.; Lim, C.-H.; Thordarson, P.; Miyake, G. M. *J. Am. Chem. Soc.* **2019**, *141*, 19479-19486.

45. Oderinde, M. S.; Jones, N. H.; Juneau, A.; Frenette, M.; Aquila, B.; Tentarelli, S.; Robbins, D. W.; Johannes, J. W. *Angew. Chem. Int. Ed.* **2016**, *55*, 13219-13223.

46. Key, R. J.; Vannucci, A. K. *Organometallics* **2018**, *37*, 1468-1472.

47. Kim, T.; McCarver, S. J.; Lee, C.; MacMillan, D. W. C. *Angew. Chem. Int. Ed.* **2018**, *57*, 3488-3492.

48. Blackburn, J. M.; Gant Kanegusuku, A. L.; Scott, G. E.; Roizen, J. L. *Org. Lett.* **2019**, *21*, 7049-7054.

49. Wimmer, A.; König, B. *Org. Lett.* **2019**, *21*, 2740-2744.

50. Du, Y.; Pearson, R. M.; Lim, C.-H.; Sartor, S. M.; Ryan, M. D.; Yang, H.; Damrauer, N. H.; Miyake, G. M. *Chem. Eur. J.* **2017**, *23*, 10962-10968.

51. Lim, C.-H.; Kudisch, M.; Liu, B.; Miyake, G. M. *J. Am. Chem. Soc.* **2018**, *140*, 7667-7673.

52. (a) Kawamata, Y.; Vantourout, J. C.; Hickey, D. P.; Bai, P.; Chen, L.; Hou, Q.; Qiao, W.; Barman, K.; Edwards, M. A.; Garrido-Castro, A. F.; deGruyter, J. N.; Nakamura, H.; Knouse, K.; Qin, C.; Clay, K. J.; Bao, D.; Li, C.; Starr, J. T.; Garcia-Irizarry, C.; Sach, N.; White, H. S.; Neurock, M.; Minteer, S. D.; Baran, P. S. *J. Am. Chem. Soc.* **2019**, *141*, 6392-6402. (b) Li, C.; Kawamata, Y.; Nakamura, H.; Vantourout, J. C.; Liu, Z.; Hou, Q.; Bao, D.; Starr, J. T.; Chen, J.; Yan, M.; Baran, P. S. *Angew. Chem. Int. Ed.* **2017**, *56*, 13088-13093.

53. (a) Yin, G.; Kalvet, I.; Englert, U.; Schoenebeck, F. *J. Am. Chem. Soc.* **2015**, *137*, 4164-4172. (b) Guard, L. M.; Mohadjer Beromi, M.; Brudvig, G. W.; Hazari, N.; Vinyard, D. J. *Angew. Chem. Int. Ed.* **2015**, *54*, 13352-13356. (c) Mohadjer Beromi, M.; Nova, A.; Balcells, D.; Brasacchio, A. M.; Brudvig, G. W.; Guard, L. M.; Hazari, N.; Vinyard, D. J. *J. Am. Chem. Soc.* **2017**, *139*, 922-936. (d) Kalvet, I.; Guo, Q.; Tizzard, G. J.; Schoenebeck, F. *ACS Catal.* **2017**, *7*, 2126-2132.

54. Green, R. A.; Hartwig, J. F. *Angew. Chem. Int. Ed.* **2015**, *54*, 3768-3772.

55. Ge, S.; Green, R. A.; Hartwig, J. F. *J. Am. Chem. Soc.* **2014**, *136*, 1617-1627.

56. Lavoie, C. M.; McDonald, R.; Johnson, E. R.; Stradiotto, M. *Adv. Synth. Catal.* **2017**, *359*, 2972-2980.

57. Lavoie, C. M.; MacQueen, P. M.; Stradiotto, M. *Chem. Eur. J.* **2016**, *22*, 18752-18755.

58. Lavoie, C. M.; Stradiotto, M. *ACS Catal.* **2018**, *8*, 7228-7250.

59. Park, N. H.; Teverovskiy, G.; Buchwald, S. L. *Org. Lett.* **2014**, *16*, 220-223.

60. Borzenko, A.; Rotta-Loria, N. L.; MacQueen, P. M.; Lavoie, C. M.; McDonald, R.; Stradiotto, M. *Angew. Chem. Int. Ed.* **2015**, *54*, 3773-3777.

61. (a) MacQueen, P. M.; Stradiotto, M. *Synlett* **2017**, *28*, 1652-1656. (b) Schranck, J.; Furer, P.; Hartmann, V.; Tlili, A. *Eur. J. Org. Chem.* **2017**, *2017*, 3496-3500.

62. (a) Ramgren, S. D.; Silberstein, A. L.; Yang, Y.; Garg, N. K. *Angew. Chem. Int. Ed.* **2011**, *50*, 2171-2173. (b) Mesganaw, T.; Silberstein, A. L.; Ramgren, S. D.; Nathel, N. F. F.; Hong, X.; Liu, P.; Garg, N. K. *Chem. Sci.* **2011**, *2*, 1766-1771. (c) Hie, L.; Ramgren, S. D.; Mesganaw, T.; Garg, N. K. *Org. Lett.* **2012**, *14*, 4182-4185. (d) Fine Nathel, N. F.; Kim, J.; Hie, L.; Jiang, X.; Garg, N. K. *ACS Catal.* **2014**, *4*, 3289-3293.

63. Iglesias, M. J.; Prieto, A.; Nicasio, M. C. *Adv. Synth. Catal.* **2010**, *352*, 1949-1954.

64. Iglesias, M. J.; Blandez, J. F.; Fructos, M. R.; Prieto, A.; Álvarez, E.; Belderrain, T. R.; Nicasio, M. C. *Organometallics* **2012**, *31*, 6312-6316.

65. Rull, S. G.; Blandez, J. F.; Fructos, M. R.; Belderrain, T. R.; Nicasio, M. C. *Adv. Synth. Catal.* **2015**, *357*, 907-911.

66. Lavoie, C. M.; MacQueen, P. M.; Rotta-Loria, N. L.; Sawatzky, R. S.; Borzenko, A.; Chisholm, A. J.; Hargreaves, B. K. V.; McDonald, R.; Ferguson, M. J.; Stradiotto, M. *Nat. Commun.* **2016**, *7*, 11073.

67. Zhou, Y.-P.; Raoufmoghaddam, S.; Szilvási, T.; Driess, M. *Angew. Chem. Int. Ed.* **2016**, *55*, 12868-12872.

68. Clark, J. S. K.; Lavoie, C. M.; MacQueen, P. M.; Ferguson, M. J.; Stradiotto, M. *Organometallics* **2016**, *35*, 3248-3254.

69. (a) Salaün, J. Cyclopropane Derivatives and their Diverse Biological Activities. In *Small Ring Compounds in Organic Synthesis VI*, de Meijere, A., Ed. Springer Berlin Heidelberg: Berlin, Heidelberg, 2000; pp 1-67. (b) Wessjohann, L. A.; Brandt, W.; Thiemann, T. *Chem. Rev.* **2003**, *103*, 1625-1647.

70. Wang, J.; Sanchez-Rosello, M.; Acena, J. L.; del Pozo, C.; Sorochinsky, A. E.; Fustero, S.; Soloshonok, V. A.; Liu, H. *Chem. Rev.* **2014**, *114*, 2432-506.

71. Mandala, D.; Thompson, W. A.; Watts, P. *Tetrahedron* **2016**, *72*, 3389-3420.

72. Silverman, R. B. *Acc. Chem. Res.* **1995**, *28*, 335-342.

73. (a) Shaffer, C. L.; Harriman, S.; Koen, Y. M.; Hanzlik, R. P. *J. Am. Chem. Soc.* **2002**, *124*, 8268-8274. (b) Cerny, M. A.; Hanzlik, R. P. *J. Am. Chem. Soc.* **2006**, *128*, 3346-3354.

74. (a) Loeppky, R. N.; Singh, S. P.; Elomari, S.; Hastings, R.; Theiss, T. E. *J. Am. Chem. Soc.* **1998**, *120*, 5193-5202. (b) Loeppky, R. N.; Elomari, S. *J. Org. Chem.* **2000**, *65*, 96-103.

75. Brown, H. C.; Fletcher, R. S.; Johannesen, R. B. *J. Am. Chem. Soc.* **1951**, *73*, 212-221.

76. (a) Kang, J.; Kim, K. S. *J. Chem. Soc., Chem. Commun.* **1987**, 897-898. (b) Yoshida, Y.; Umezu, K.; Hamada, Y.; Atsumi, N.; Tabuchi, F. *Synlett* **2003**, 2139-2142.

77. Arava, V. R.; Bandatmakuru, S. R. *Synthesis* **2013**, *45*, 1039-1044.

78. (a) Zhang, Z.; Mao, J.; Zhu, D.; Wu, F.; Chen, H.; Wan, B. *Tetrahedron* **2006**, *62*, 4435-4443. (b) Liu, Z.-J.; Vors, J.-P.; Gesing, E. R. F.; Bolm, C. *Adv. Synth. Catal.* **2010**, *352*, 3158-3162. (c) Xie, R.; Fu, H.; Ling, Y. *Chem. Commun.* **2011**, *47*, 8976-8978. (d) Wang, Y.; Ling, J.; Zhang, Y.; Zhang, A.; Yao, Q. *Eur. J. Org. Chem.* **2015**, *2015*, 4153-4161.

79. (a) Gagnon, A.; St-Onge, M.; Little, K.; Duplessis, M.; Barabé, F. *J. Am. Chem. Soc.* **2007**, *129*, 44-45. (b) Benard, S.; Neuville, L.; Zhu, J. *Chem. Commun.* **2010**, *46*, 3393-3395.

80. Cui, W.; Loeppky, R. N. *Tetrahedron* **2001**, *57*, 2953-2956.

81. (a) Maity, S.; Zhu, M.; Shinabery, R. S.; Zheng, N. *Angew. Chem. Int. Ed.* **2012**, *51*, 222-226. (b) Nguyen, T. H.; Morris, S. A.; Zheng, N. *Adv. Synth. Catal.* **2014**, *356*, 2831-2837. (c) Nguyen, T. H.; Maity, S.; Zheng, N. *Beilstein J. Org. Chem.* **2014**, *10*, 975-980.

82. Gildner, P. G.; DeAngelis, A.; Colacot, T. J. *Org. Lett.* **2016**, *18*, 1442-1445.

83. Nonhebel, D. C. *Chem. Soc. Rev.* **1993**, *22*, 347-359.

84. (a) Sumida, Y.; Yorimitsu, H.; Oshima, K. *Org. Lett.* **2008**, *10*, 4677-4679. (b) Taniguchi, H.; Ohmura, T.; Suginome, M. *J. Am. Chem. Soc.* **2009**, *131*, 11298-11299. (c) Ogata, K.; Shimada, D.; Furuya, S.; Fukuzawa, S.-i. *Org. Lett.* **2013**, *15*, 1182-1185. (d) Martin, M. C.; Patil, D. V.; France, S. *J. Org. Chem.* **2014**, *79*, 3030-3039. (e) Hori, H.; Arai, S.; Nishida, A. *Adv. Synth. Catal.* **2017**, *359*, 1170-1176.

85. Pringle, P. G.; Smith, M. B. Phosphatrioxa-adamantane Ligands. In *Phosphorus(III) Ligands in Homogeneous Catalysis: Design and Synthesis*, Kamer, P. C. J.; van Leeuwen, P. W. N. M., Eds. John Wiley & Sons Ltd.: 2012; pp 391-404.

86. Murata, M.; Buchwald, S. L. *Tetrahedron* **2004**, *60*, 7397-7403.

87. Hazari, N.; Melvin, P. R.; Beromi, M. M. *Nat. Rev. Chem.* **2017**, *1*, 0025.

88. (a) Coussmak, C.; Hutchinson, M. H.; Sutton, L. E.; Mellor, J. R.; Venanzi, L. M. *J. Chem. Soc.* **1961**, 2705-2713. (b) Browning, M. C.; Venanzi, L. M.; Morgan, D. J.; Mellor, J. R.; Pratt, S. A. J.; Sutton, L. E. *J. Chem. Soc.* **1962**, 693-703. (c) Garton, G.; Henn, D. E.; Venanzi, L. M.; Powell, H. M. *J. Chem. Soc.* **1963**, 3625-3629.

89. Bernard, S.; Defoy, D.; Dory, Y. L.; Klarskov, K. *Bioorg. Med. Chem. Lett.* **2009**, *19*, 6127-6130.

90. (a) Yang, C.-T.; Fu, Y.; Huang, Y.-B.; Yi, J.; Guo, Q.-X.; Liu, L. *Angew. Chem. Int. Ed.* **2009**, *48*, 7398-7401. (b) Henderson, J. L.; Buchwald, S. L. *Org. Lett.* **2010**, *12*, 4442-4445. (c) Henderson, J. L.; McDermott, S. M.; Buchwald, S. L. *Org. Lett.* **2010**, *12*, 4438-4441. (d) Huang, Y.-B.; Yang, C.-T.; Yi, J.; Deng, X.-J.; Fu, Y.; Liu, L. *J. Org. Chem.* **2011**, *76*, 800-810. (e) Wang, J.; Zheng, N. *Angew. Chem. Int. Ed.* **2015**, *54*, 11424-11427.

91. Green, R. A.; Hartwig, J. F. *Org. Lett.* **2014**, *16*, 4388-4391.

92. Li, Y.-H.; Zhang, Y.; Ding, X.-H. *Inorg. Chem. Commun.* **2011**, *14*, 1306-1310.

93. Wilson, D. A.; Wilson, C. J.; Moldoveanu, C.; Resmerita, A.-M.; Corcoran, P.; Hoang, L. M.; Rosen, B. M.; Percec, V. *J. Am. Chem. Soc.* **2010**, *132*, 1800-1801.

94. Kwong, F. Y.; Lai, C. W.; Yu, M.; Tian, Y.; Chan, K. S. *Tetrahedron* **2003**, *59*, 10295-10305.

95. Quasdorf, K. W.; Riener, M.; Petrova, K. V.; Garg, N. K. *J. Am. Chem. Soc.* **2009**, *131*, 17748-17749.

96. Gundersen, L.-L.; Bakkestuen, A. K.; Aasen, A. J.; Øverås, H.; Rise, F. *Tetrahedron* **1994**, *50*, 9743-9756.

97. Lei, X.; Jalla, A.; Abou Shama, M. A.; Stafford, J. M.; Cao, B. *Synthesis* **2015**, *47*, 2578-2585.

98. Ho, L. A.; Raston, C. L.; Stubbs, K. A. *Eur. J. Org. Chem.* **2016**, *2016*, 5957-5963.

99. Kelley, J. L.; Krochmal, M. P.; Linn, J. A.; McLean, E. W.; Soroko, F. E. *J. Med. Chem.* **1988**, *31*, 606-612.

100. (a) Enthaler, S.; Company, A. *Chem. Soc. Rev.* **2011**, *40*, 4912-4924. (b) Evano, G.; Wang, J.; Nitelet, A. *Org. Chem. Front.* **2017**, *4*, 2480-2499.

101. (a) Williamson, A. *Justus Liebigs Annalen der Chemie* **1851**, *77*, 37-49. (b) Fuhrmann, E.; Talbiersky, J. *Org. Process Res. Dev.* **2005**, *9*, 206-211.

102. Liu, Q.; Lu, Z.; Ren, W.; Shen, K.; Wang, Y.; Xu, Q. *Chin. J. Chem* . **2013**, *31*, 764-772.

103. (a) Lindley, J. *Tetrahedron* **1984**, *40*, 1433-1456. (b) Monnier, F.; Taillefer, M. *Angew. Chem. Int. Ed.* **2009**, *48*, 6954-6971.

104. (a) Keerthi Krishnan, K.; Ujwaldev, S. M.; Sindhu, K. S.; Anilkumar, G. *Tetrahedron* **2016**, *72*, 7393-7407. (b) Bhunia, S.; Pawar, G. G.; Kumar, S. V.; Jiang, Y.; Ma, D. *Angew. Chem. Int. Ed.* **2017**, *56*, 16136-16179.

105. Gowrisankar, S.; Sergeev, A. G.; Anbarasan, P.; Spannenberg, A.; Neumann, H.; Beller, M. *J. Am. Chem. Soc.* **2010**, *132*, 11592-11598.

106. (a) Torraca, K. E.; Huang, X.; Parrish, C. A.; Buchwald, S. L. *J. Am. Chem. Soc.* **2001**, *123*, 10770-10771. (b) Vorogushin, A. V.; Huang, X.; Buchwald, S. L. *J. Am. Chem. Soc.* **2005**, *127*, 8146-8149. (c) Wu, X.; Fors, B. P.; Buchwald, S. L. *Angew.*

Chem. Int. Ed. **2011**, *50*, 9943-9947. (d) Zhang, H.; Ruiz-Castillo, P.; Buchwald, S. L. *Org. Lett.* **2018**, *20*, 1580-1583.

107. Maligres, P. E.; Li, J.; Krska, S. W.; Schreier, J. D.; Raheem, I. T. *Angew. Chem. Int. Ed. Engl.* **2012**, *51*, 9071-4.

108. Terrett, J. A.; Cuthbertson, J. D.; Shurtleff, V. W.; MacMillan, D. W. C. *Nature* **2015**, *524*, 330-334.

109. (a) Matsunaga, P. T.; Hillhouse, G. L.; Rheingold, A. L. *J. Am. Chem. Soc.* **1993**, *115*, 2075-2077. (b) Matsunaga, P. T.; Mavropoulos, J. C.; Hillhouse, G. L. *Polyhedron* **1995**, *14*, 175-185. (c) Han, R.; Hillhouse, G. L. *J. Am. Chem. Soc.* **1997**, *119*, 8135-8136.

110. Macgregor, S. A.; Neave, G. W.; Smith, C. *Faraday Discuss.* **2003**, *124*, 111-127.

111. Sun, R.; Qin, Y.; Ruccolo, S.; Schnedermann, C.; Costentin, C.; Nocera, D. G. *J. Am. Chem. Soc.* **2019**, *141*, 89-93.

112. Ye, H.; Xiao, C.; Zhou, Q.-Q.; Wang, P. G.; Xiao, W.-J. *J. Org. Chem.* **2018**, *83*, 13325-13334.

113. Zhou, Q.-Q.; Lu, F.-D.; Liu, D.; Lu, L.-Q.; Xiao, W.-J. *Org. Chem. Front.* **2018**, *5*, 3098-3102.

114. Lee, H.; Boyer, N. C.; Deng, Q.; Kim, H.-Y.; Sawyer, T. K.; Sciammetta, N. *Chem. Sci.* **2019**, *10*, 5073-5078.

115. Liu, Y.-Y.; Liang, D.; Lu, L.-Q.; Xiao, W.-J. *Chem. Commun.* **2019**, *55*, 4853-4856.

116. Cavedon, C.; Madani, A.; Seeberger, P. H.; Pieber, B. *Org. Lett.* **2019**, *21*, 5331-5334.

117. Sawatzky, R. S.; Ferguson, M. J.; Stradiotto, M. *Synlett* **2017**, *28*, 1586-1591.

118. Rull, S. G.; Funes-Ardoiz, I.; Maya, C.; Maseras, F.; Fructos, M. R.; Belderrain, T. R.; Nicasio, M. C. *ACS Catal.* **2018**, *8*, 3733-3742.

119. (a) Burgos, C. H.; Barder, T. E.; Huang, X.; Buchwald, S. L. *Angew. Chem. Int. Ed.* **2006**, *45*, 4321-4326. (b) Hu, T.; Schulz, T.; Torborg, C.; Chen, X.; Wang, J.; Beller, M.; Huang, J. *Chem. Commun.* **2009**, 7330-7332. (c) Salvi, L.; Davis, N. R.; Ali, S. Z.; Buchwald, S. L. *Org. Lett.* **2012**, *14*, 170-173. (d) Zhang, Y.; Ni, G.; Li,

C.; Xu, S.; Zhang, Z.; Xie, X. *Tetrahedron* **2015**, *71*, 4927-4932. (e) Zhang, T.; Tudge, M. T. *Tetrahedron Lett.* **2015**, *56*, 2329-2331.

120. (a) Takise, R.; Isshiki, R.; Muto, K.; Itami, K.; Yamaguchi, J. *J. Am. Chem. Soc.* **2017**, *139*, 3340-3343. (b) Ahanthem, D.; Laitonjam, W. S. *Asian J. Org. Chem.* **2017**, *6*, 1492-1497. (c) Zamiran, F.; Ghaderi, A. *J. Iran. Chem. Soc.* **2019**, *16*, 293-299.

121. Standley, E. A.; Smith, S. J.; Muller, P.; Jamison, T. F. *Organometallics* **2014**, *33*, 2012-2018.

122. Quasdorf, K. W.; Antoft-Finch, A.; Liu, P.; Silberstein, A. L.; Komaromi, A.; Blackburn, T.; Ramgren, S. D.; Houk, K. N.; Snieckus, V.; Garg, N. K. *J. Am. Chem. Soc.* **2011**, *133*, 6352-6363.

123. Balint, E.; Kovacs, O.; Drahos, L.; Keglevich, G. *Lett. Org. Chem.* **2013**, *10*, 330-336.

124. Crowley, V. M.; Khandelwal, A.; Mishra, S.; Stothert, A. R.; Huard, D. J. E.; Zhao, J.; Muth, A.; Duerfeldt, A. S.; Kizziah, J. L.; Lieberman, R. L.; Dickey, C. A.; Blagg, B. S. J. *J. Med. Chem.* **2016**, *59*, 3471-3488.

125. Hobson, A. D.; Harris, C. M.; van der Kam, E. L.; Turner, S. C.; Abibi, A.; Aguirre, A. L.; Bousquet, P.; Kebede, T.; Konopacki, D. B.; Gintant, G.; Kim, Y.; Larson, K.; Maull, J. W.; Moore, N. S.; Shi, D.; Shrestha, A.; Tang, X.; Zhang, P.; Sarris, K. K. *J. Med. Chem.* **2015**, *58*, 9154-9170.

126. Kato, T.; Matsuoka, S.-i.; Suzuki, M. *Chem. Commun.* **2016**, *52*, 8569-8572.

127. Musatov, D. M.; Starodubtseva, E. V.; Turova, O. V.; Kurilov, D. V.; Vinogradov, M. G.; Rakishev, A. K.; Struchkova, M. I. *Russ. J. Org. Chem.* **2010**, *46*, 1021-1028.

128. Yang, W.; Sun, J. *Angew. Chem. Int. Ed.* **2016**, *55*, 1868-1871.

129. Tolnai, G. L.; Pethő, B.; Králl, P.; Novák, Z. *Adv. Synth. Catal.* **2014**, *356*, 125-129.

130. Chen, S.; Wan, Q.; Badu-Tawiah, A. K. *Angew. Chem. Int. Ed.* **2016**, *55*, 9345-9349.

131. Dibakar, M.; Prakash, A.; Selvakumar, K.; Ruckmani, K.; Sivakumar, M. *Tetrahedron Lett.* **2011**, *52*, 5338-5341.

132. (a) Liu, J.; Obando, D.; Liao, V.; Lifa, T.; Codd, R. *Eur. J. Med. Chem.* **2011**, *46*, 1949-1963. (b) Wanka, L.; Iqbal, K.; Schreiner, P. R. *Chem. Rev.* **2013**, *113*, 3516-3604. (c) Johnson, T. W.; Gallego, R. A.; Edwards, M. P. *J. Med. Chem.* **2018**, *61*, 6401-6420.

133. (a) Berman, A. M.; Johnson, J. S. *J. Org. Chem.* **2006**, *71*, 219-224. (b) Barker, T. J.; Jarvo, E. R. *Angew. Chem. Int. Ed.* **2011**, *50*, 8325-8328. (c) Mailig, M.; Rucker, R. P.; Lalic, G. *Chem. Commun.* **2015**, *51*, 11048-11051. (d) Gui, J.; Pan, C.-M.; Jin, Y.; Qin, T.; Lo, J. C.; Lee, B. J.; Spergel, S. H.; Mertzman, M. E.; Pitts, W. J.; La Cruz, T. E.; Schmidt, M. A.; Darvatkar, N.; Natarajan, S. R.; Baran, P. S. *Science* **2015**, *348*, 886-891.

134. Ruiz-Castillo, P.; Blackmond, D. G.; Buchwald, S. L. *J. Am. Chem. Soc.* **2015**, *137*, 3085-92.

135. Zhang, Y.; Lavigne, G.; Lugan, N.; César, V. *Chem. Eur. J.* **2017**, *23*, 13792-13801.

136. Jiang, J.; Zhu, H.; Shen, Y.; Tu, T. *Org. Chem. Front.* **2014**, *1*, 1172-1175.

137. (a) Wiensch, E. M.; Montgomery, J. *Angew. Chem. Int. Ed.* **2018**, *57*, 11045-11049. (b) Nett, A. J.; Cañellas, S.; Higuchi, Y.; Robo, M. T.; Kochkodan, J. M.; Haynes, M. T.; Kampf, J. W.; Montgomery, J. *ACS Catal.* **2018**, *8*, 6606-6611.

138. Harada, T.; Ueda, Y.; Iwai, T.; Sawamura, M. *Chem. Commun.* **2018**, *54*, 1718-1721.

139. Iwai, T.; Harada, T.; Shimada, H.; Asano, K.; Sawamura, M. *ACS Catal.* **2017**, *7*, 1681-1692.

140. Clark, J. S. K.; Voth, C. N.; Ferguson, M. J.; Stradiotto, M. *Organometallics* **2017**, *36*, 679-686.

141. Snieckus, V. *Chem. Rev.* **1990**, *90*, 879-933.

142. (a) Li, B.-J.; Yu, D.-G.; Sun, C.-L.; Shi, Z.-J. *Chem. Eur. J.* **2011**, *17*, 1728-1759. (b) Rosen, B. M.; Quasdorf, K. W.; Wilson, D. A.; Zhang, N.; Resmerita, A.-M.; Garg, N. K.; Percec, V. *Chem. Rev.* **2011**, *111*, 1346-1416. (c) Tobisu, M.; Chatani, N. *Top. Organomet. Chem.* **2013**, *44*, 35-53.

143. Butkevich, A. N.; Bossi, M. L.; Lukinavičius, G.; Hell, S. W. *J. Am. Chem. Soc.* **2019**, *141*, 981-989.

144. Duke, R. M.; Veale, E. B.; Pfeffer, F. M.; Kruger, P. E.; Gunnlaugsson, T. *Chem. Soc. Rev.* **2010**, *39*, 3936-3953.

145. (a) Parkesh, R.; Clive Lee, T.; Gunnlaugsson, T. *Tetrahedron Lett.* **2009**, *50*, 4114-4116. (b) Zhu, B.; Zhang, X.; Li, Y.; Wang, P.; Zhang, H.; Zhuang, X. *Chem. Commun.* **2010**, *46*, 5710-5712. (c) Lee, M. H.; Kim, J. Y.; Han, J. H.; Bhuniya, S.; Sessler, J. L.; Kang, C.; Kim, J. S. *J. Am. Chem. Soc.* **2012**, *134*, 12668-12674. (d) Lee, M. H.; Han, J. H.; Kwon, P.-S.; Bhuniya, S.; Kim, J. Y.; Sessler, J. L.; Kang, C.; Kim, J. S. *J. Am. Chem. Soc.* **2012**, *134*, 1316-1322.

146. (a) Tan, S.; Yin, H.; Chen, Z.; Qian, X.; Xu, Y. *Eur. J. Med. Chem.* **2013**, *62*, 130-138. (b) Banerjee, S.; Kitchen, J. A.; Bright, S. A.; O'Brien, J. E.; Williams, D. C.; Kelly, J. M.; Gunnlaugsson, T. *Chem. Commun.* **2013**, *49*, 8522-8524.

147. Wu, A.; Xu, Y.; Qian, X.; Wang, J.; Liu, J. *Eur. J. Med. Chem.* **2009**, *44*, 4674-4680.

148. Grabchev, I.; Moneva, I.; Bojinov, V.; Guittonneau, S. *J. Mater. Chem.* **2000**, *10*, 1291-1296.

149. (a) Jiang, W.; Tang, J.; Qi, Q.; Wu, W.; Sun, Y.; Fu, D. *Dyes Pigm.* **2009**, *80*, 11-16. (b) Umeda, R.; Nishida, H.; Otono, M.; Nishiyama, Y. *Tetrahedron Lett.* **2011**, *52*, 5494-5496. (c) Fleming, C. L.; Ashton, T. D.; Pfeffer, F. M. *Dyes Pigm.* **2014**, *109*, 135-143. (d) Hearn, K. N.; Nalder, T. D.; Cox, R. P.; Maynard, H. D.; Bell, T. D. M.; Pfeffer, F. M.; Ashton, T. D. *Chem. Commun.* **2017**, *53*, 12298-12301.

150. (a) Wang, Q.; Li, C.; Zou, Y.; Wang, H.; Yi, T.; Huang, C. *Org. Biomol. Chem.* **2012**, *10*, 6740-6746. (b) Banerjee, S.; Kitchen, J. A.; Gunnlaugsson, T.; Kelly, J. M. *Org. Biomol. Chem.* **2013**, *11*, 5642-5655.

151. Shields, B. J.; Kudisch, B.; Scholes, G. D.; Doyle, A. G. *J. Am. Chem. Soc.* **2018**, *140*, 3035-3039.

152. Lavoie, C. M.; Tassone, J. P.; Ferguson, M. J.; Zhou, Y.; Johnson, E. R.; Stradiotto, M. *Organometallics* **2018**.

153. Feberero, C.; Suárez-Pantiga, S.; Cabello, Z.; Sanz, R. *Org. Lett.* **2018**, *20*, 2437-2440.

154. Tassone, J. P.; MacQueen, P. M.; Lavoie, C. M.; Ferguson, M. J.; McDonald, R.; Stradiotto, M. *ACS Catal.* **2017**, *7*, 6048-6059.

155. Sakayori, K.; Shibasaki, Y.; Ueda, M. *J. Polym. Sci., Part A: Polym. Chem.* **2005**, *43*, 5571-5580.

156. Dhayalan, V.; Knochel, P. *Synthesis* **2015**, *47*, 3246-3256.

157. Chen, C.-y.; Tang, G.; He, F.; Wang, Z.; Jing, H.; Faessler, R. *Org. Lett.* **2016**, *18*, 1690-1693.

158. Russell, G. A.; Yao, C.-F. *Heteroat. Chem* **1993**, *4*, 433-444.

159. Lan, X.-B.; Li, Y.; Li, Y.-F.; Shen, D.-S.; Ke, Z.; Liu, F.-S. *J. Org. Chem.* **2017**, *82*, 2914-2925.

160. Manna, S.; Serebrennikova, P. O.; Utepova, I. A.; Antonchick, A. P.; Chupakhin, O. N. *Org. Lett.* **2015**, *17*, 4588-4591.

161. Clark, J. S. K.; McGuire, R. T.; Lavoie, C. M.; Ferguson, M. J.; Stradiotto, M. *Organometallics* **2019**, *38*, 167-175.

162. Hoshimoto, Y.; Hayashi, Y.; Suzuki, H.; Ohashi, M.; Ogoshi, S. *Organometallics* **2014**, *33*, 1276-1282.

163. (a) Welin, E. R.; Le, C.; Arias-Rotondo, D. M.; McCusker, J. K.; MacMillan, D. W. C. *Science* **2017**, *355*, 380. (b) Lu, J.; Pattengale, B.; Liu, Q.; Yang, S.; Shi, W.; Li, S.; Huang, J.; Zhang, J. *J. Am. Chem. Soc.* **2018**, *140*, 13719-13725. (c) Zhu, D.-L.; Li, H.-X.; Xu, Z.-M.; Li, H.-Y.; Young, D. J.; Lang, J.-P. *Org. Chem. Front.* **2019**, *6*, 2353-2359. (d) Pieber, B.; Malik, J. A.; Cavedon, C.; Gisbertz, S.; Savateev, A.; Cruz, D.; Heil, T.; Zhang, G.; Seeberger, P. H. *Angew. Chem. Int. Ed.* **2019**, *58*, 9575-9580.

164. Sperry, J. B.; Price Wiglesworth, K. E.; Edmonds, I.; Fiore, P.; Boyles, D. C.; Damon, D. B.; Dorow, R. L.; Piatnitski Chekler, E. L.; Langille, J.; Coe, J. W. *Org. Process Res. Dev.* **2014**, *18*, 1752-1758.

165. Park, N. H.; Vinogradova, E. V.; Surry, D. S.; Buchwald, S. L. *Angew. Chem. Int. Ed.* **2015**, *54*, 8259-8262.

166. (a) Chu-Moyer, M. Y.; Ballinger, W. E.; Beebe, D. A.; Berger, R.; Coutcher, J. B.; Day, W. W.; Li, J.; Mylari, B. L.; Oates, P. J.; Weekly, R. M. *J. Med. Chem.* **2002**, *45*, 511-528. (b) Changelian, P. S.; Flanagan, M. E.; Ball, D. J.; Kent, C. R.; Magnuson, K. S.; Martin, W. H.; Rizzuti, B. J.; Sawyer, P. S.; Perry, B. D.; Brissette, W. H.; McCurdy, S. P.; Kudlacz, E. M.; Conklyn, M. J.; Elliott, E. A.; Koslov, E. R.; Fisher, M. B.; Strelevitz, T. J.; Yoon, K.; Whipple, D. A.; Sun, J.;

Munchhof, M. J.; Doty, J. L.; Casavant, J. M.; Blumenkopf, T. A.; Hines, M.; Brown, M. F.; Lillie, B. M.; Subramanyam, C.; Shang-Poa, C.; Milici, A. J.; Beckius, G. E.; Moyer, J. D.; Su, C.; Woodworth, T. G.; Gaweco, A. S.; Beals, C. R.; Littman, B. H.; Fisher, D. A.; Smith, J. F.; Zagouras, P.; Magna, H. A.; Saltarelli, M. J.; Johnson, K. S.; Nelms, L. F.; Des Etages, S. G.; Hayes, L. S.; Kawabata, T. T.; Finco-Kent, D.; Baker, D. L.; Larson, M.; Si, M.-S.; Paniagua, R.; Higgins, J.; Holm, B.; Reitz, B.; Zhou, Y.-J.; Morris, R. E.; Shea, J. J.; Borie, D. C. *Science* **2003**, *302*, 875. (c) Medina, J. R.; Becker, C. J.; Blackledge, C. W.; Duquenne, C.; Feng, Y.; Grant, S. W.; Heerding, D.; Li, W. H.; Miller, W. H.; Romeril, S. P.; Scherzer, D.; Shu, A.; Bobko, M. A.; Chadderton, A. R.; Dumble, M.; Gardiner, C. M.; Gilbert, S.; Liu, Q.; Rabindran, S. K.; Sudakin, V.; Xiang, H.; Brady, P. G.; Campobasso, N.; Ward, P.; Axten, J. M. *J. Med. Chem.* **2011**, *54*, 1871-1895. (d) DeGoey, D. A.; Randolph, J. T.; Liu, D.; Pratt, J.; Hutchins, C.; Donner, P.; Krueger, A. C.; Matulenko, M.; Patel, S.; Motter, C. E.; Nelson, L.; Keddy, R.; Tufano, M.; Caspi, D. D.; Krishnan, P.; Mistry, N.; Koev, G.; Reisch, T. J.; Mondal, R.; Pilot-Matias, T.; Gao, Y.; Beno, D. W. A.; Maring, C. J.; Molla, A.; Dumas, E.; Campbell, A.; Williams, L.; Collins, C.; Wagner, R.; Kati, W. M. *J. Med. Chem.* **2014**, *57*, 2047-2057.

Appendices

Appendix 1: Crystallographic Solution and Refinement Details for 2-C3, 2-C4, and 2-C5

2-C3. Crystallographic data for **2-C3**•0.5pentane were obtained at –100(±2) °C on a Bruker D8/APEX II CCD diffractometer using Cu Kα (λ = 1.54178 Å) microfocus source radiation, employing a sample that was mounted in inert oil and transferred to a cold gas stream on the diffractometer. Programs for diffractometer operation, data collection, data reduction, and absorption correction were supplied by Bruker. Gaussian integration (face-indexed) was employed as the absorption correction method. The structure of 2-**C3** was solved by use of intrinsic phasing methods, and refined by use of full-matrix least-squares procedures (on F^2) with R_1 based on $F_o^2 \geq 2\sigma(F_o^2)$ and wR_2 based on all data. Attempts to refine peaks of residual electron density as disordered or partial-occupancy solvent pentane carbon atoms were unsuccessful. The data were corrected for disordered electron density through use of the SQEEZE procedure as implemented in *PLATON*. A total solvent-accessible void volume of 417 Å^3 with a total electron count of 85 (consistent with 2 molecules of solvent pentane, or 0.5 molecules per formula unit of the nickel complex) was found in the unit cell. Anisotropic displacement parameters were employed for all the non-hydrogen atoms shown. Non-hydrogen atoms are represented by Gaussian ellipsoids at the 30% probability level.

2-C4. Crystallographic data for **2-C4** were obtained at –80(±2) °C on a Bruker PLATFORM/APEX II CCD diffractometer using graphite-monochromated Mo Kα (λ = 0.71073 Å) radiation, employing a sample that was mounted in inert oil and transferred to a cold gas stream on the diffractometer. Programs for diffractometer operation, data collection, data reduction, and absorption correction were supplied by Bruker. Gaussian integration (face-indexed) was employed as the absorption correction method. The structure of **2-C4** was solved by use of a Patterson/structure expansion, and refined by use of full-matrix least-squares procedures (on F^2) with R_1 based on $F_o^2 \geq 2\sigma(F_o^2)$ and wR_2 based on all data. Anisotropic displacement parameters were employed for all the non-hydrogen atoms shown. Non-hydrogen atoms are represented by Gaussian ellipsoids at the 30% probability level.

2-C5. Crystallographic data for **2-C5**•THF were obtained at –100(±2) °C on a Bruker D8/APEX II CCD diffractometer using Cu Kα (λ = 1.54178 Å) microfocus source radiation, employing a sample that was mounted in inert oil and transferred to a cold gas stream on the diffractometer. Programs for diffractometer operation, data collection, data reduction, and absorption correction were supplied by Bruker. Gaussian integration (face-indexed) was employed as the absorption correction method. The structure of **2-C5** was solved by use of intrinsic phasing methods, and refined by use of full-matrix least-squares procedures (on F^2) with R_1 based on $F_o^2 \geq 2\sigma(F_o^2)$ and wR_2 based on all data. The following distance restraints were applied to the disordered solvent tetrahydrofuran molecule: C–O, 1.430(2) Å; C–C, 1.500(2) Å (55:45 occupancy ratio). Anisotropic displacement parameters were employed for all the non-hydrogen atoms shown. Non-hydrogen atoms are represented by Gaussian ellipsoids at the 30% probability level.

Table A1. Crystallographic experimental details for **2-C3•**0.5pentane.

A. Crystal Data	
formula	$C_{37.50}H_{55}ClNiO_3P_2$
formula weight	709.91
crystal dimensions (mm)	0.18 × 0.13 × 0.04
crystal system	monoclinic
space group	$P2_1/n$ (an alternate setting of $P2_1/c$ [No. 14])
unit cell parameters	
a (Å)	10.0583 (2)
b (Å)	20.2200 (3)
c (Å)	18.7013 (3)
β (deg)	105.3145 (11)
V (Å^3)	3668.39 (11)
Z	4
ρcalcd (g cm^{-3})	1.285
μ (mm^{-1})	2.517
B. Data Collection and Refinement Conditions	
diffractometer	Bruker D8/APEX II CCD
radiation (λ [Å])	Cu Kα (1.54178) (microfocus source)
temperature (°C)	–100
scan type	ω and ϕ scans (1.0°) (10 s exposures)
data collection 2θ limit (deg)	136.78
total data collected	20374 (-12 ≤ h ≤ 12, -24 ≤ k ≤ 24, -22 ≤ l ≤ 22)
independent reflections	6631 (R_{int} = 0.0474)
number of observed reflections (*NO*)	4734 [$F_o^2 \geq 2\sigma(F_o^2)$]
structure solution method	intrinsic phasing (*SHELXT-2014*)
refinement method	full-matrix least-squares on F^2 (*SHELXL–2014*)
absorption correction method	Gaussian integration (face-indexed)
range of transmission factors	0.9716–0.6038
data/restraints/parameters	6631 / 0 / 380
goodness-of-fit (S) [all data]	1.027
final R indices	
R_1 [$F_o^2 \geq 2\sigma(F_o^2)$]	0.0571
wR_2 [all data]	0.1600
largest difference peak and hole	0.788 and –0.307 e Å^{-3}

Table A2. Crystallographic experimental details for **2-C4**.

A. Crystal Data	
formula	$C_{35}H_{43}ClNiP_2$
formula weight	619.79
crystal dimensions (mm)	0.21 × 0.20 × 0.13
crystal system	monoclinic
space group	$P2_1/c$ (No. 14)
unit cell parameters	
a (Å)	11.5868 (4)
b (Å)	18.0009 (6)
c (Å)	15.7031 (5)
β (deg)	104.9806 (5)
V (Å^3)	3163.93 (18)
Z	4
ρcalcd (g cm^{-3})	1.301
μ (mm^{-1})	0.821
B. Data Collection and Refinement Conditions	
diffractometer	Bruker PLATFORM/APEX II CCD
radiation (λ [Å])	graphite-monochromated Mo Kα (0.71073)
temperature (°C)	–80
scan type	ω scans (0.3°) (15 s exposures)
data collection 2θ limit (deg)	56.61
total data collected	30445 (-15 ≤ h ≤ 15, -23 ≤ k ≤ 23, -20 ≤ l ≤ 20)
independent reflections	7859 (R_{int} = 0.0332)
number of observed reflections (*NO*)	6158 [$F_o^2 \geq 2\sigma(F_o^2)$]
structure solution method	Patterson/structure expansion (*DIRDIF–2008*)
refinement method	full-matrix least-squares on F^2 (*SHELXL–2014*)
absorption correction method	Gaussian integration (face-indexed)
range of transmission factors	0.9721–0.8581
data/restraints/parameters	7859 / 0 / 419
goodness-of-fit (*S*) [all data]	1.028
final *R* indices	
R_1 [$F_o^2 \geq 2\sigma(F_o^2)$]	0.0374
wR_2 [all data]	0.1022
largest difference peak and hole	0.614 and –0.361 e Å^{-3}

Table A3. Crystallographic experimental details for **2-C5•**THF.

A. Crystal Data	
formula	$C_{37}H_{59}ClNiOP_2$
formula weight	675.94
crystal dimensions (mm)	0.35 × 0.28 × 0.08
crystal system	monoclinic
space group	$P2_1/c$ (No. 14)
unit cell parameters	
a (Å)	12.0390 (3)
b (Å)	20.9558 (4)
c (Å)	14.5762 (3)
β (deg)	104.2409 (8)
V (Å^3)	3564.38 (13)
Z	4
ρcalcd (g cm^{-3})	1.260
μ (mm^{-1})	2.517
B. Data Collection and Refinement Conditions	
diffractometer	Bruker D8/APEX II CCD
radiation (λ [Å])	Cu Kα (1.54178) (microfocus source)
temperature (°C)	–100
scan type	ω and ϕ scans (1.0°) (5 s exposures)
data collection 2θ limit (deg)	148.31
total data collected	25211 (-13 ≤ h ≤ 14, -26 ≤ k ≤ 26, -18 ≤ l ≤ 18)
independent reflections	6950 (R_{int} = 0.0274)
number of observed reflections (*NO*)	6784 [$F_o^2 \geq 2\sigma(F_o^2)$]
structure solution method	intrinsic phasing (*SHELXT-2014*)
refinement method	full-matrix least-squares on F^2 (*SHELXL–2014*)
absorption correction method	Gaussian integration (face-indexed)
range of transmission factors	0.9086–0.4640
data/restraints/parameters	6950 / 10 / 425
goodness-of-fit (S) [all data]	1.045
final R indices	
R_1 [$F_o^2 \geq 2\sigma(F_o^2)$]	0.0346
wR_2 [all data]	0.0955
largest difference peak and hole	0.541 and –0.482 e Å^{-3}

Appendix 2: Reaction Monitoring of the Formation of 2-3a Using 2-C3

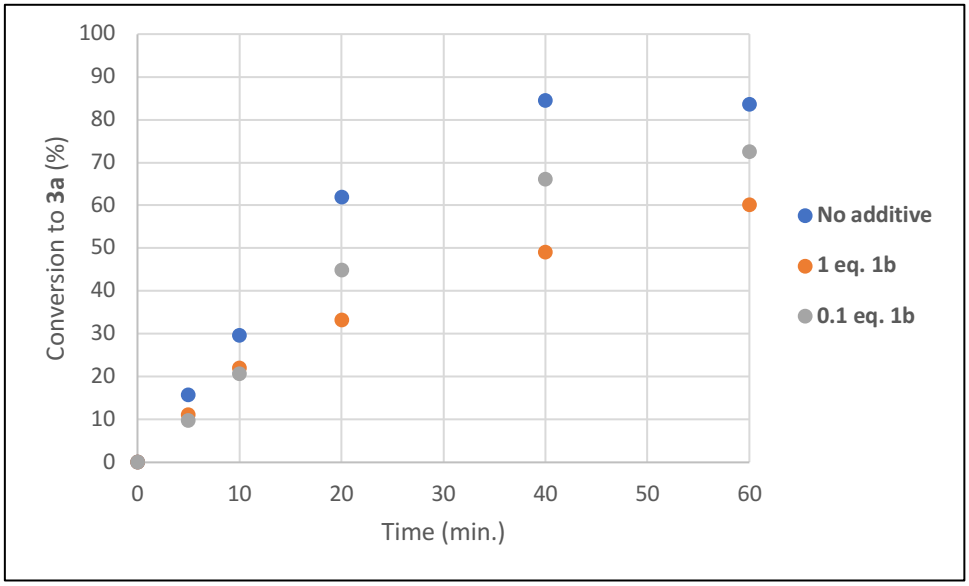

Figure A1. Reaction monitoring of the formation of **2-3a** using **2-C3** with varying amounts of 4-chloroanisole (**2-1b**).

Appendix 3: Chapter 2 NMR Spectra

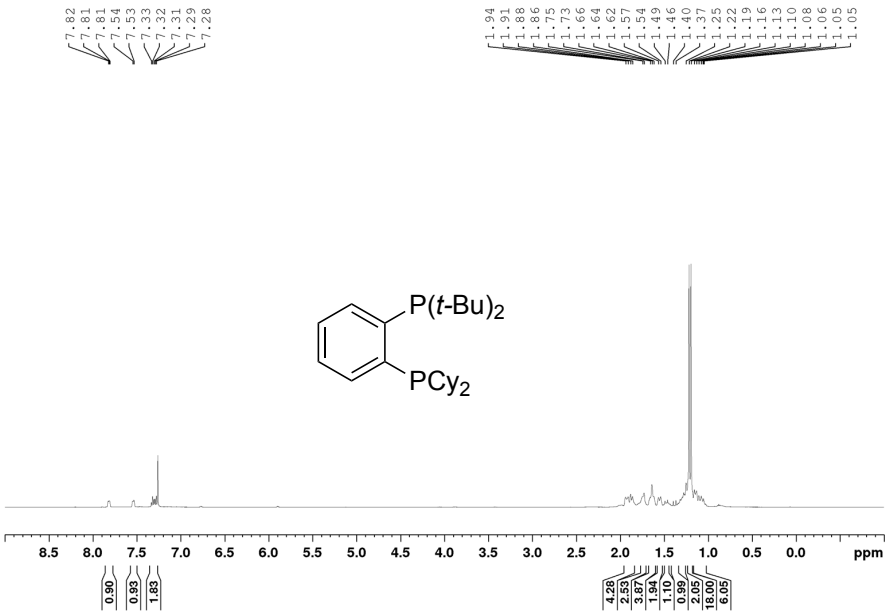

Figure A2. ^{1}H NMR spectrum of **2-L5** ($CDCl_3$, 500 MHz).

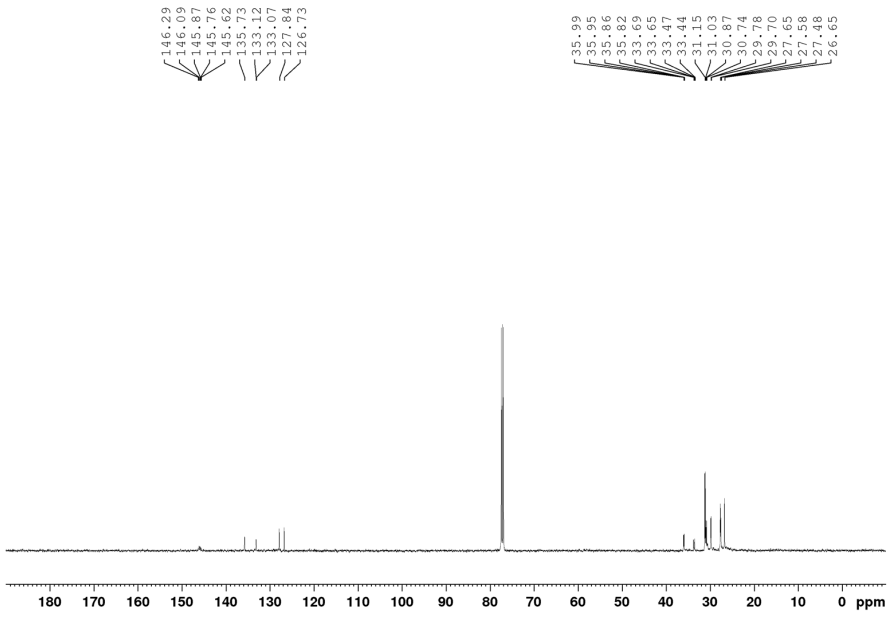

Figure A3. $^{13}C\{^{1}H\}$ NMR spectrum of **2-L5** ($CDCl_3$, 126 MHz).

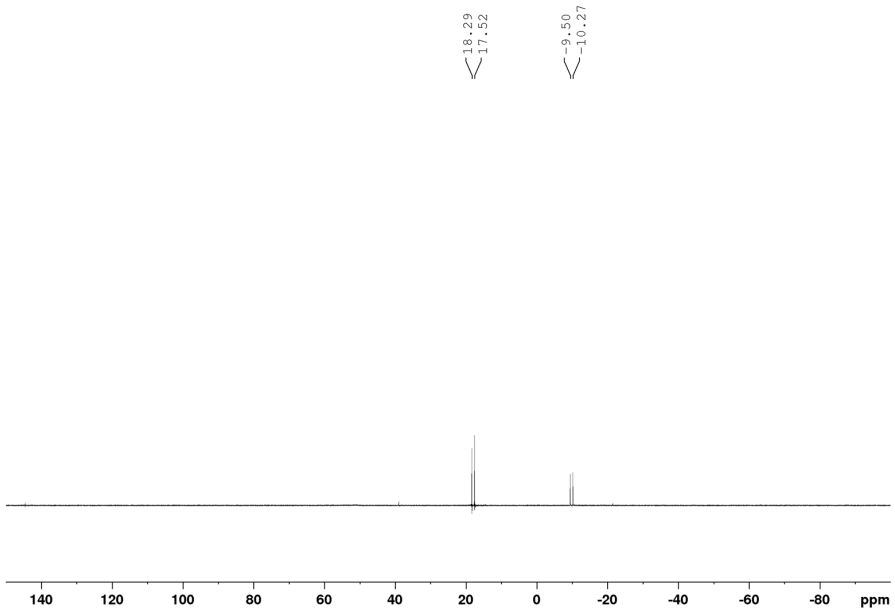

Figure A4. $^{31}P\{^{1}H\}$ NMR spectrum of **2-L5** ($CDCl_3$, 203 MHz).

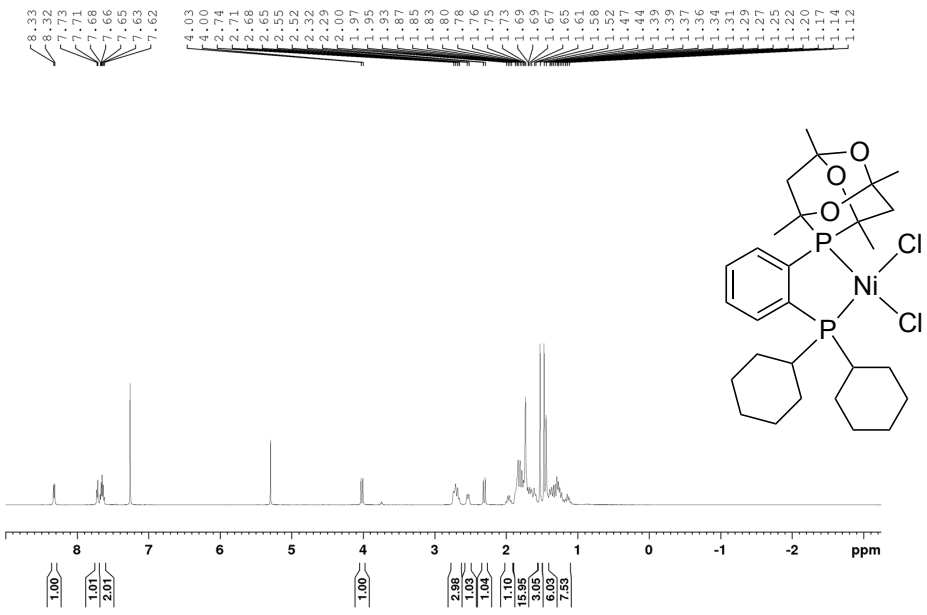

Figure A5. ^{1}H NMR spectrum of (**2-L3**)$NiCl_2$ ($CDCl_3$, 500 MHz).

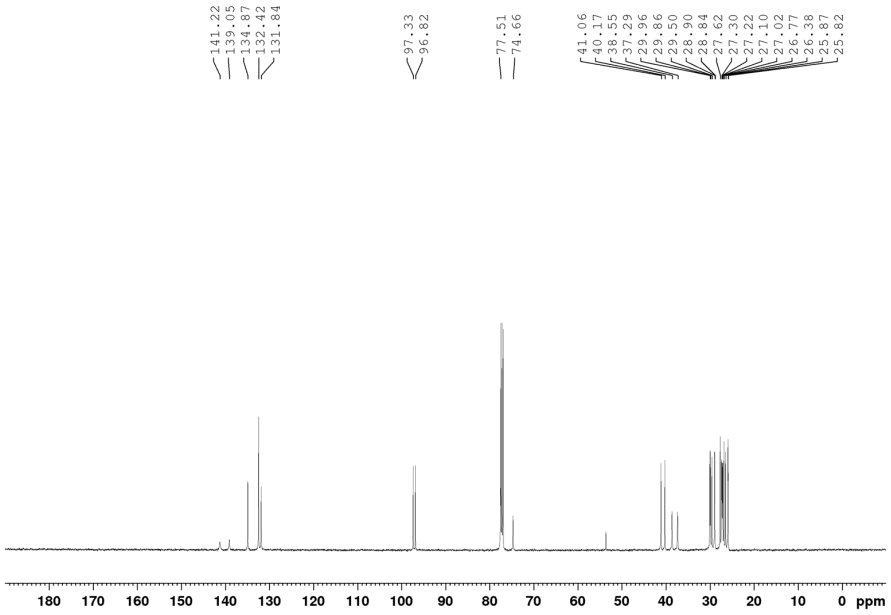

Figure A6. $^{13}C\{^{1}H\}$ NMR spectrum of (**2-L3**)$NiCl_2$ ($CDCl_3$, 126 MHz).

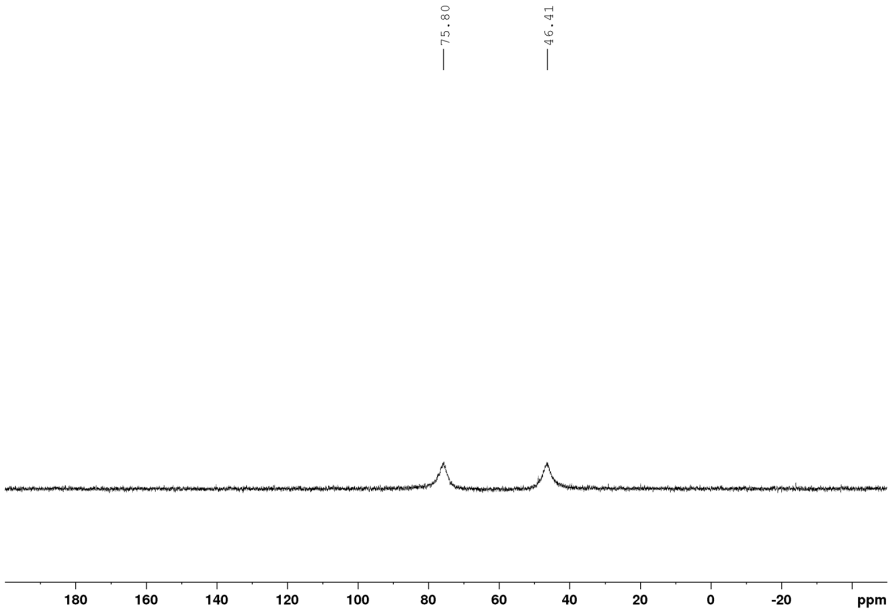

Figure A7. $^{31}P\{^{1}H\}$ NMR spectrum of (**2-L3**)$NiCl_2$ ($CDCl_3$, 203 MHz).

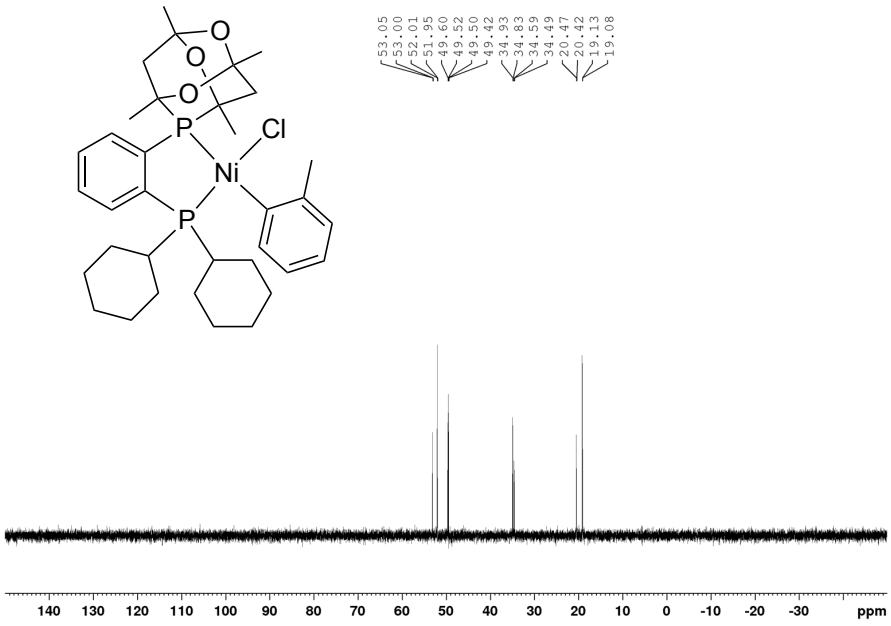

Figure A8. $^{31}P\{^{1}H\}$ NMR spectrum of **2-C3** ($CDCl_3$, 203 MHz).

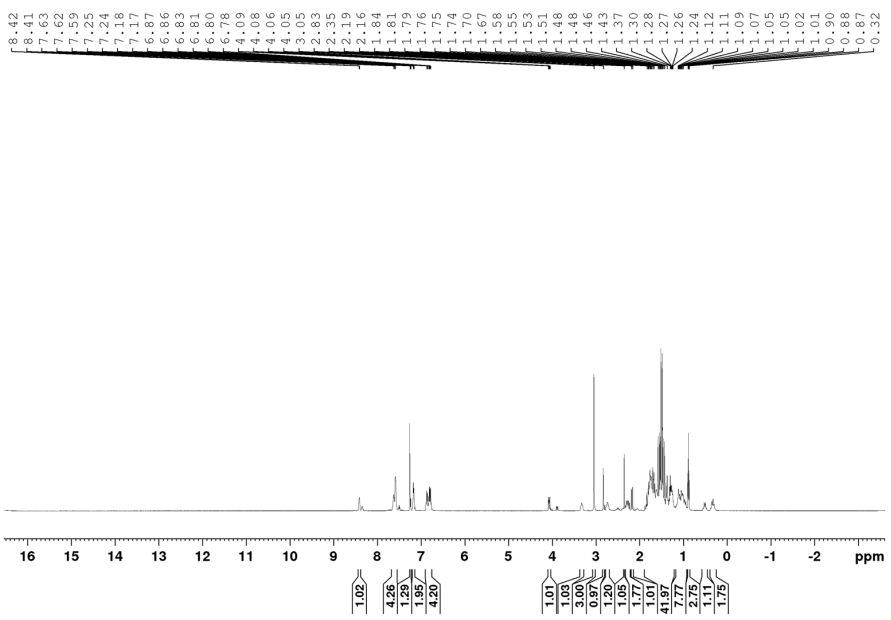

Figure A9. ^{1}H NMR spectrum of recrystallized **2-C3** ($CDCl_3$, 500 MHz).

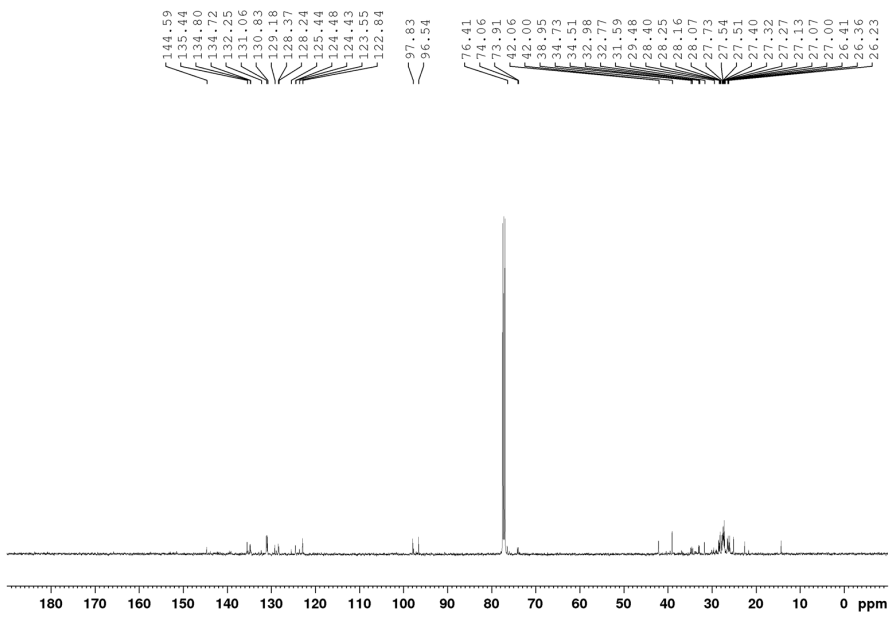

Figure A10. $^{13}C\{^{1}H\}$ NMR spectrum of recrystallized **2-C3** ($CDCl_3$, 126 MHz).

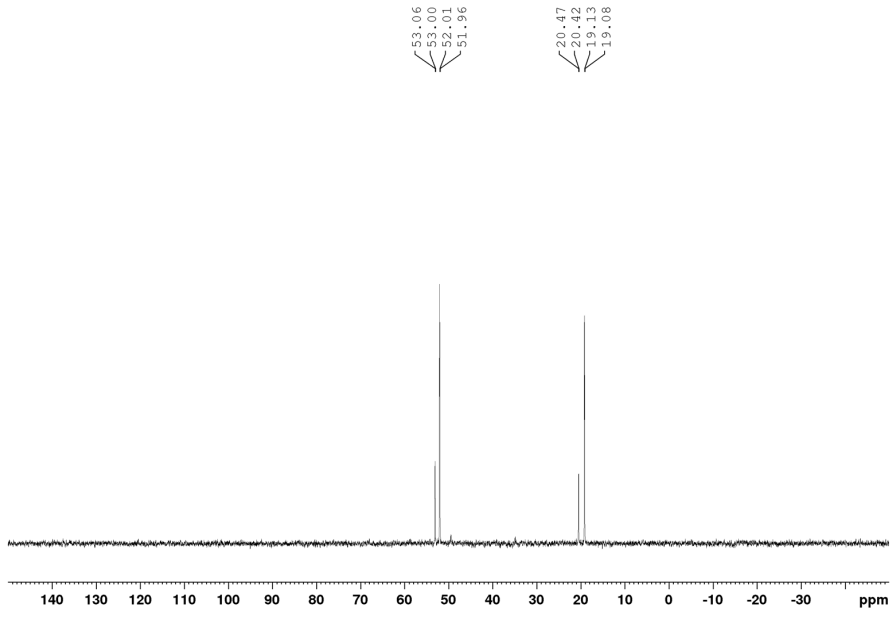

Figure A11. $^{31}P\{^{1}H\}$ NMR spectrum of recrystallized **2-C3** ($CDCl_3$, 203 MHz).

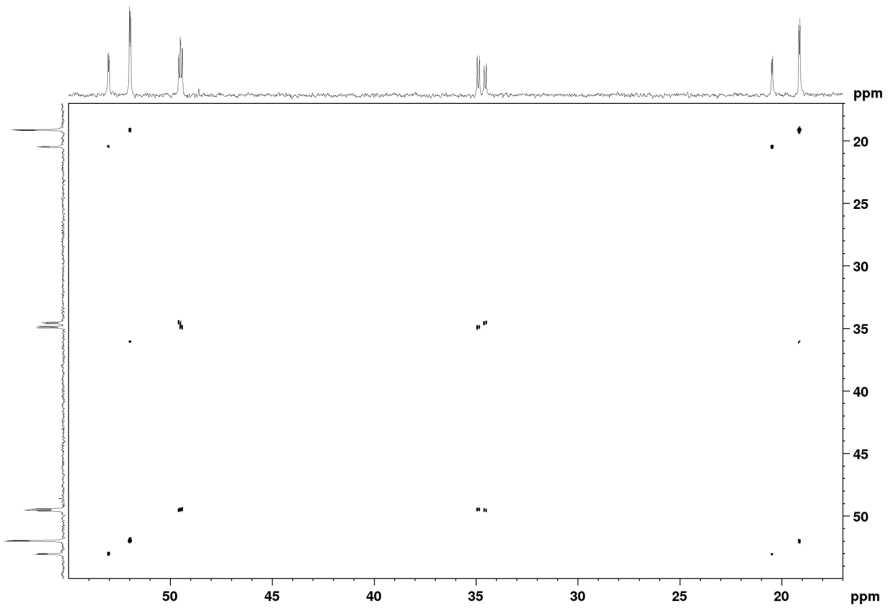

Figure A12. $^{31}P\{^{1}H\}$-$^{31}P\{^{1}H\}$ COSY spectrum of **2-C3** ($CDCl_3$, 203 MHz).

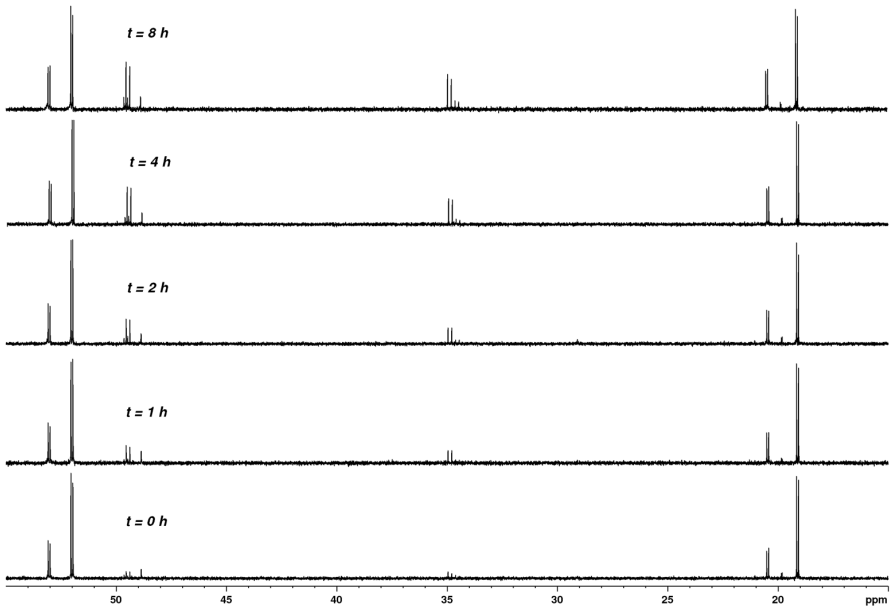

Figure A13. Time-lapsed $^{31}P\{^{1}H\}$ NMR spectra of recrystallized **2-C3** ($CDCl_3$, 121.5 MHz).

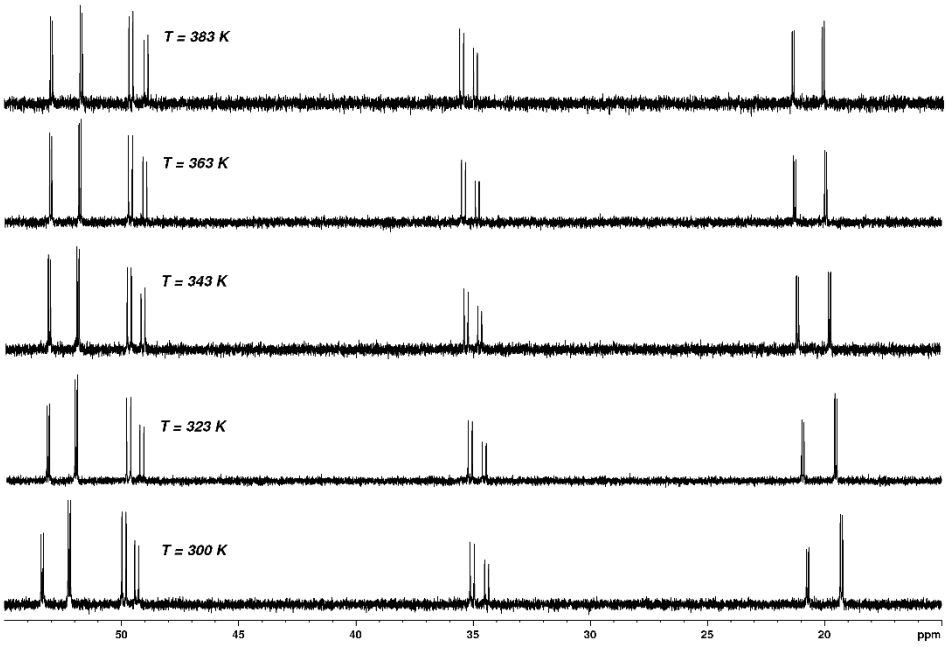

Figure A14. Elevated-temperature $^{31}P\{^{1}H\}$ NMR spectra of **2-C3** ($C_2D_2Cl_4$, 121.5 MHz).

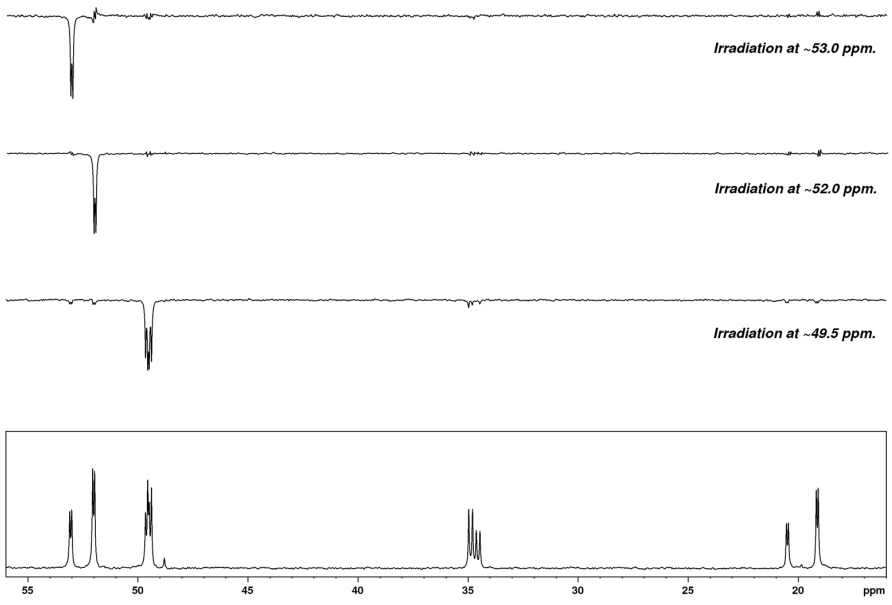

Figure A15. $^{31}P\{^{1}H\}$ saturation transfer spectra of **2-C3**, with difference spectra at the indicated irradiated frequencies shown and the parent spectrum boxed ($CDCl_3$, 121.5 MHz).

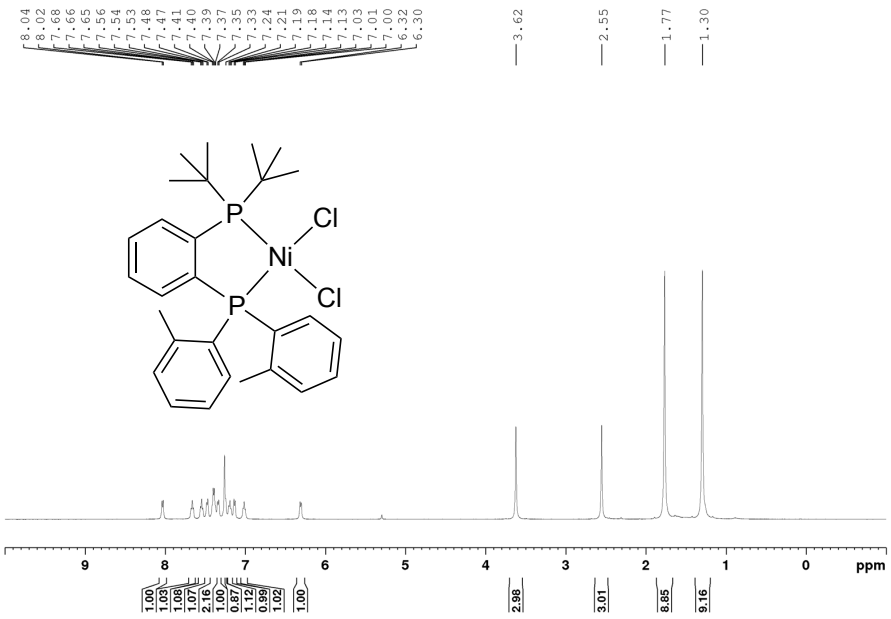

Figure A16. ^{1}H NMR spectrum of (**2-L4**)$NiCl_2$ ($CDCl_3$, 500 MHz).

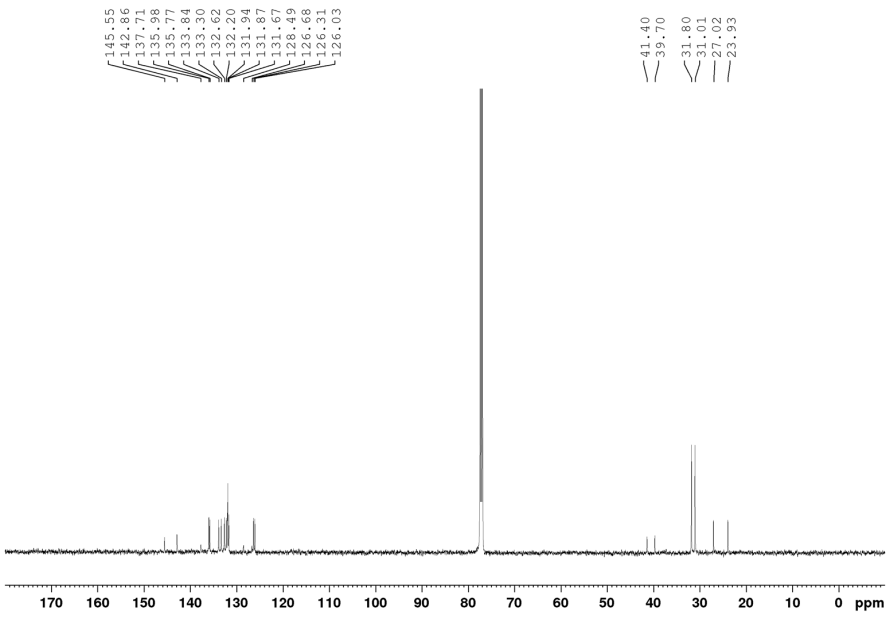

Figure A17. $^{13}C\{^{1}H\}$ NMR spectrum of (**2-L4**)$NiCl_2$ ($CDCl_3$, 126 MHz).

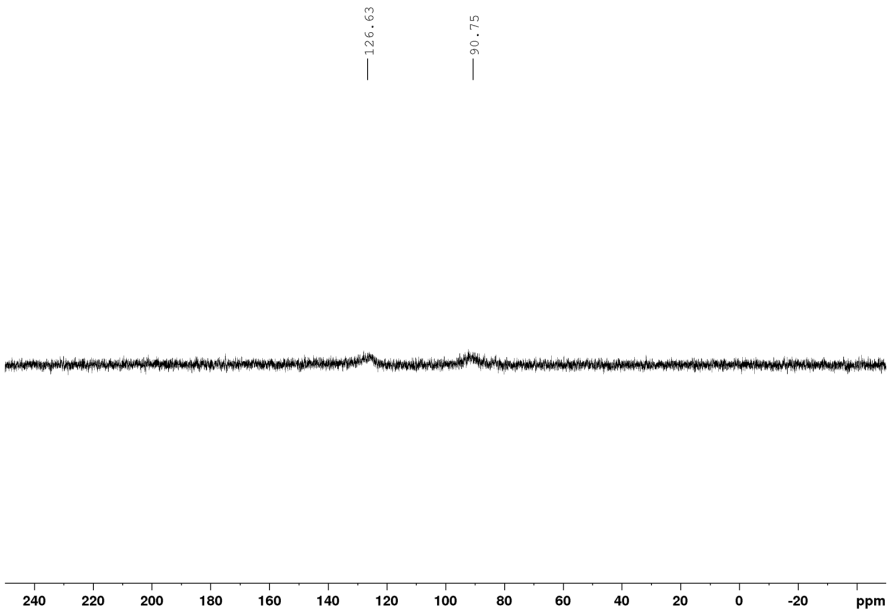

Figure A18. $^{31}P\{^{1}H\}$ NMR spectrum of (**2-L4**)$NiCl_2$ ($CDCl_3$, 203 MHz).

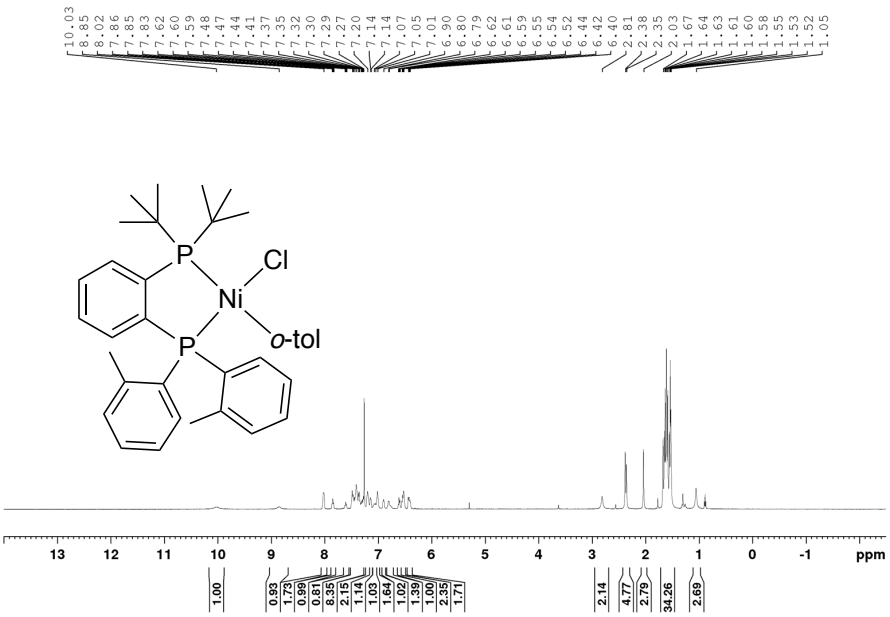

Figure A19. ^{1}H NMR spectrum of **2-C4** ($CDCl_3$, 500 MHz).

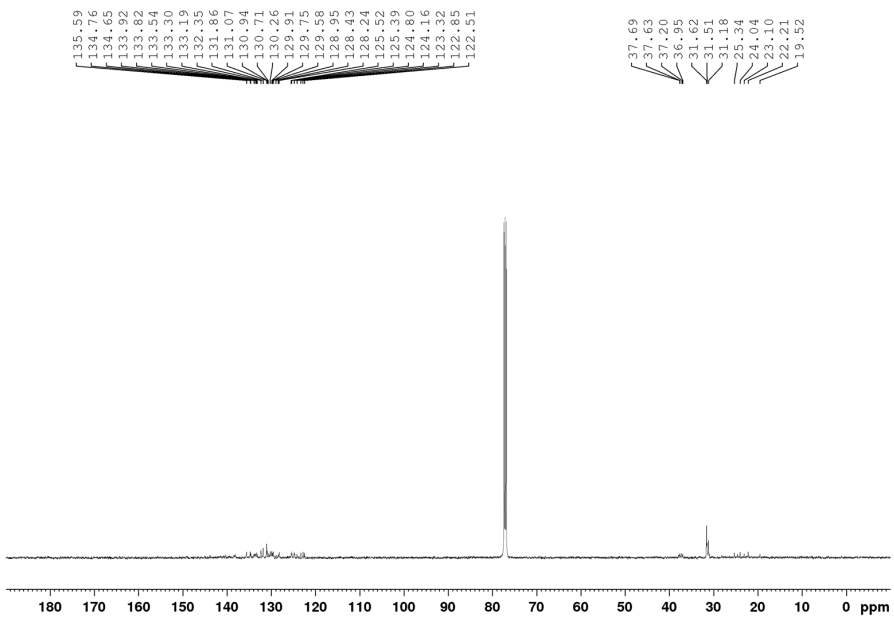

Figure A20. $^{13}C\{^{1}H\}$ NMR spectrum of **2-C4** ($CDCl_3$, 126 MHz).

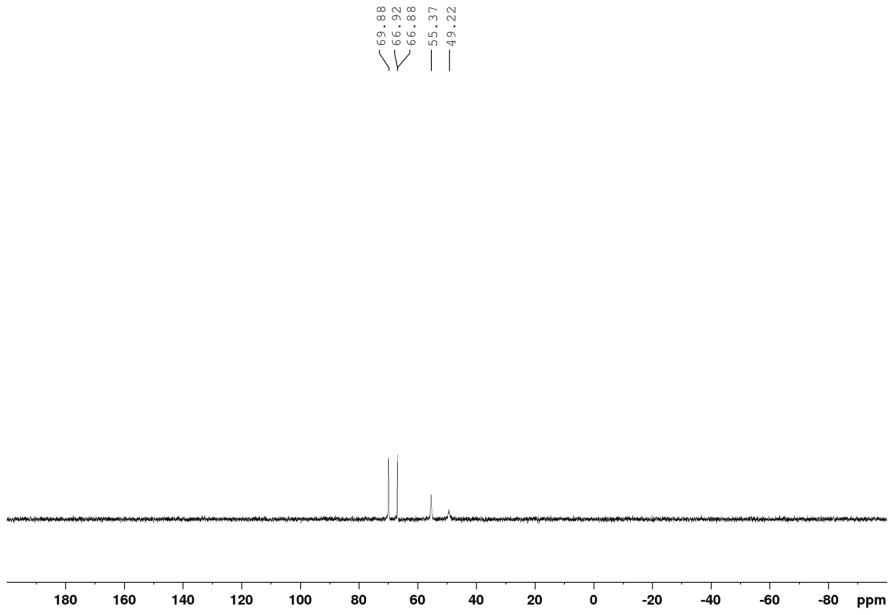

Figure A21. $^{31}P\{^{1}H\}$ NMR spectrum of **2-C4** ($CDCl_3$, 203 MHz).

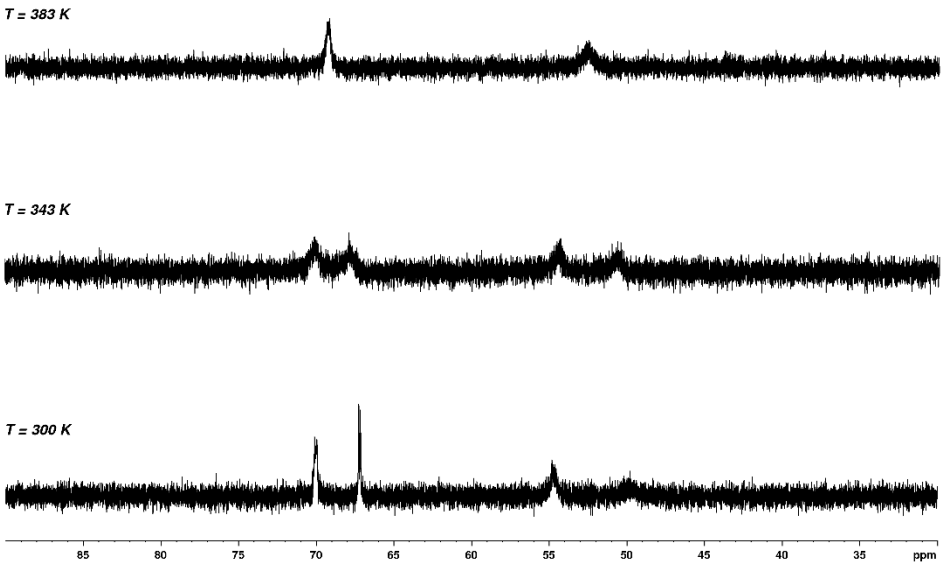

Figure A22. Elevated-temperature $^{31}P\{^{1}H\}$ NMR spectra of **2-C4** ($C_2D_2Cl_4$, 121.5 MHz).

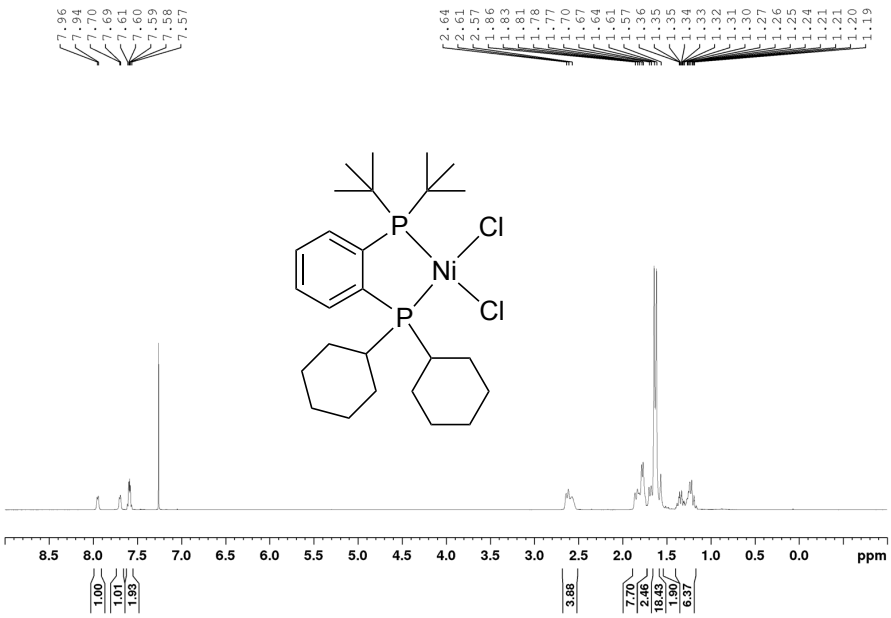

Figure A23. ^{1}H NMR spectrum of (**2-L5**)$NiCl_2$ ($CDCl_3$, 500 MHz).

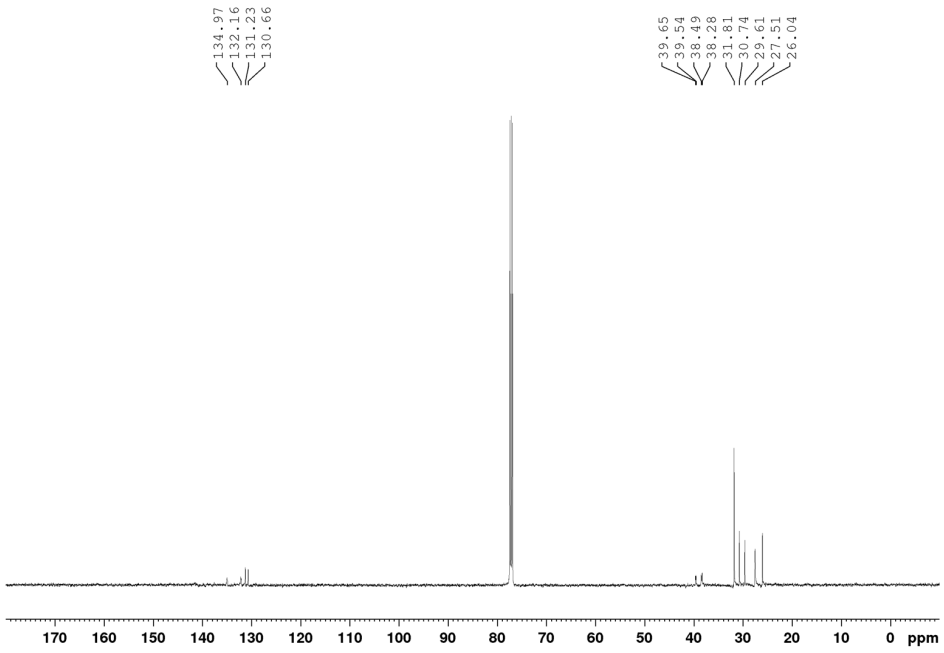

Figure A24. $^{13}C\{^{1}H\}$ NMR spectrum of (**2-L5**)$NiCl_2$ ($CDCl_3$, 126 MHz).

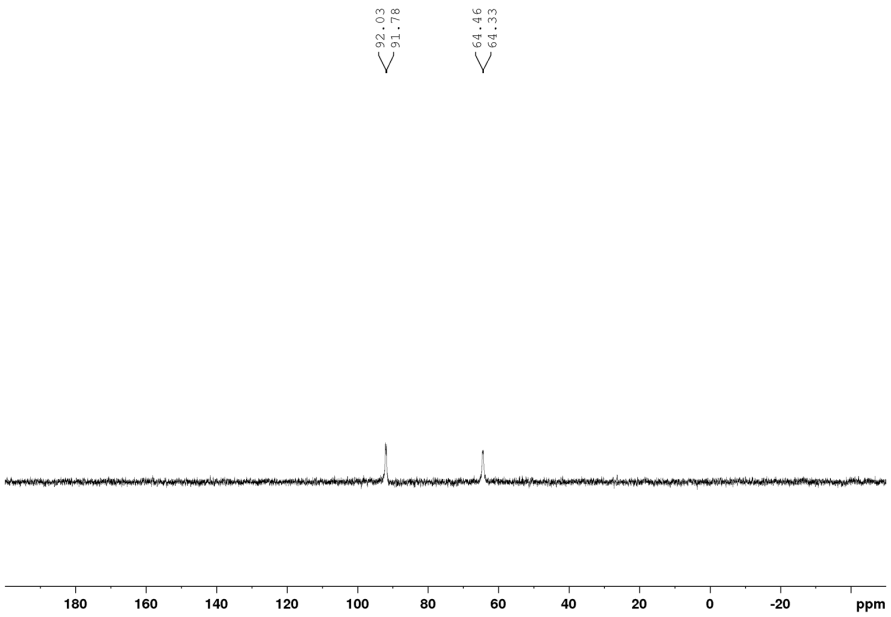

Figure A25. $^{31}P\{^{1}H\}$ NMR spectrum of (**2-L5**)$NiCl_2$ ($CDCl_3$, 203 MHz).

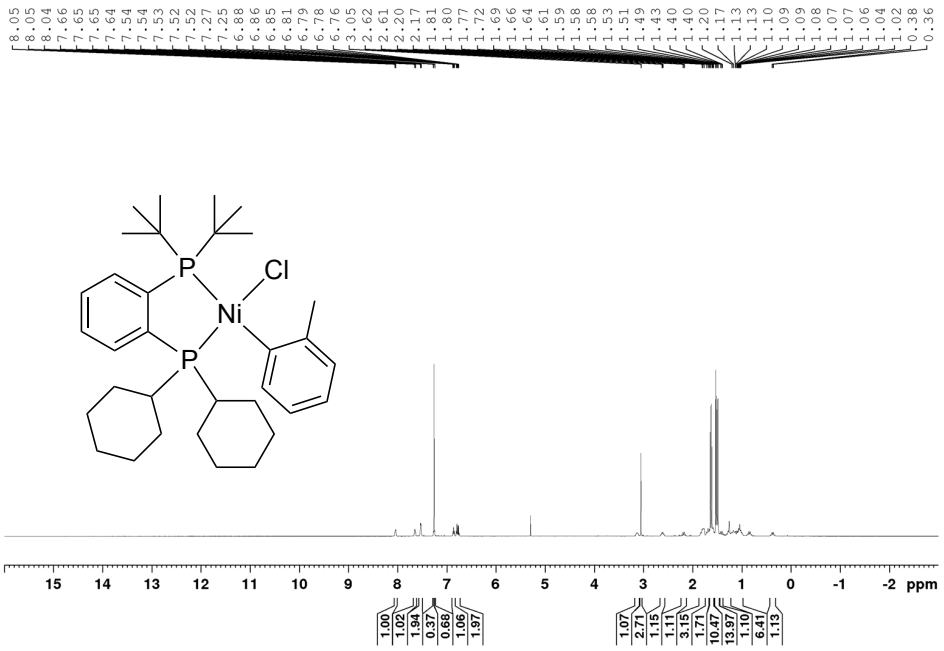

Figure A26. ^{1}H NMR spectrum of **2-C5** ($CDCl_3$, 500 MHz).

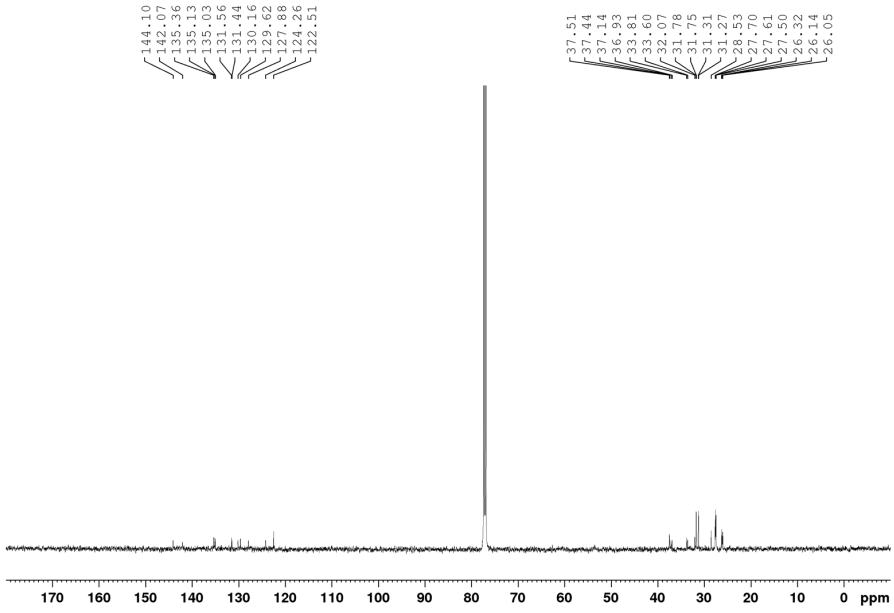

Figure A27. $^{13}C\{^{1}H\}$ NMR spectrum of **2-C5** ($CDCl_3$, 126 MHz).

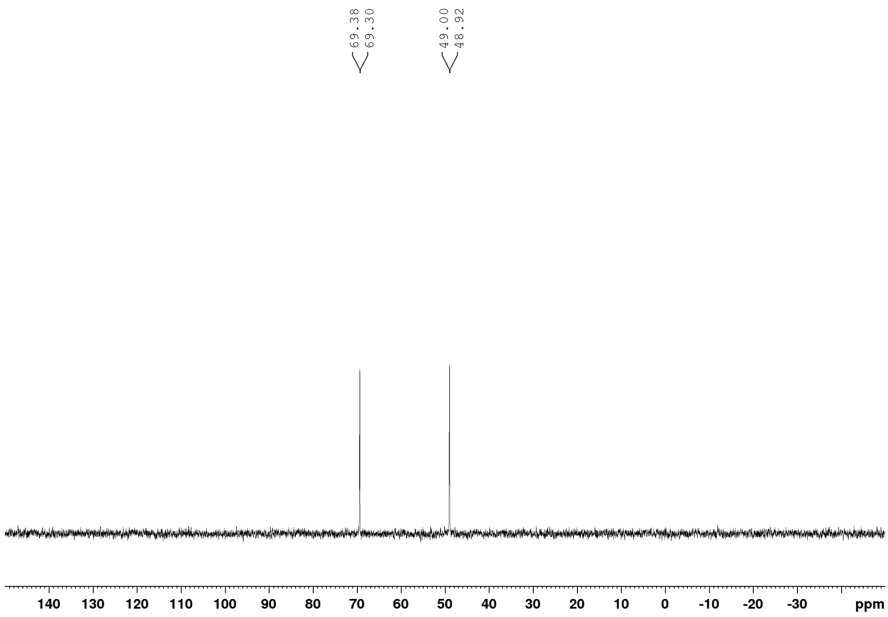

Figure A28. $^{31}P\{^{1}H\}$ NMR spectrum of **2-C5** ($CDCl_3$, 203 MHz).

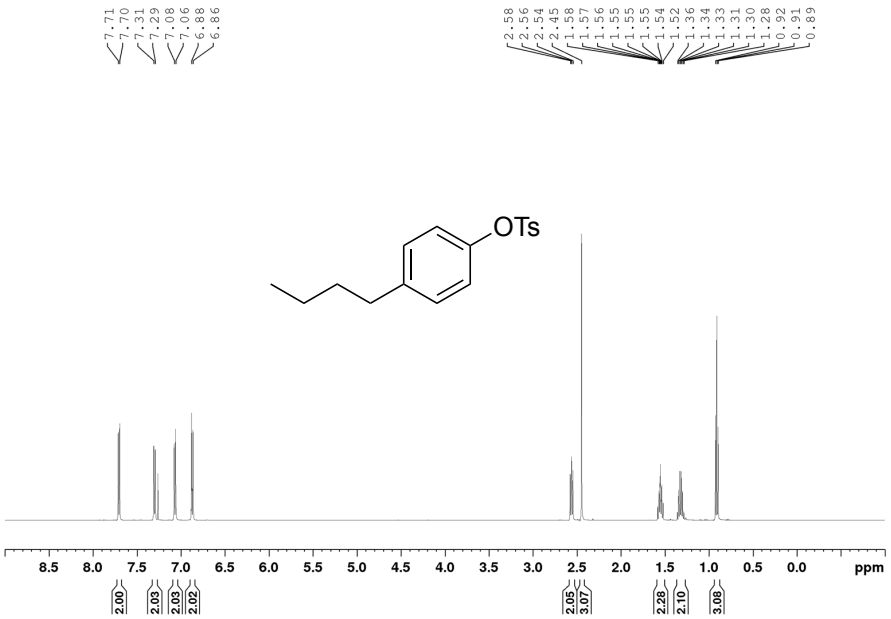

Figure A29. ^{1}H NMR spectrum of 4-butylphenyl 4-methylbenzenesulfonate ($CDCl_3$, 500 MHz).

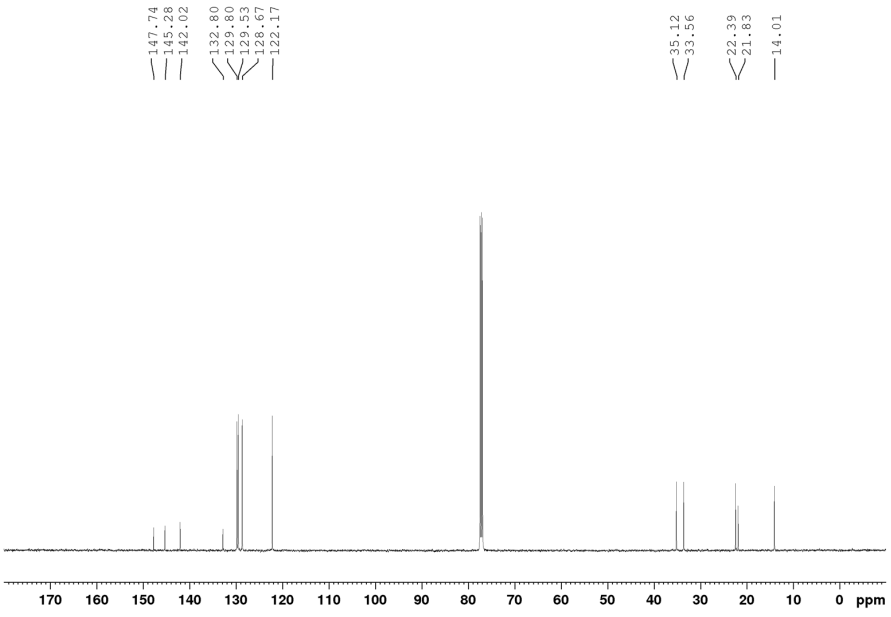

Figure A30. $^{13}C\{^{1}H\}$ NMR spectrum of 4-butylphenyl 4-methylbenzenesulfonate ($CDCl_3$, 126 MHz).

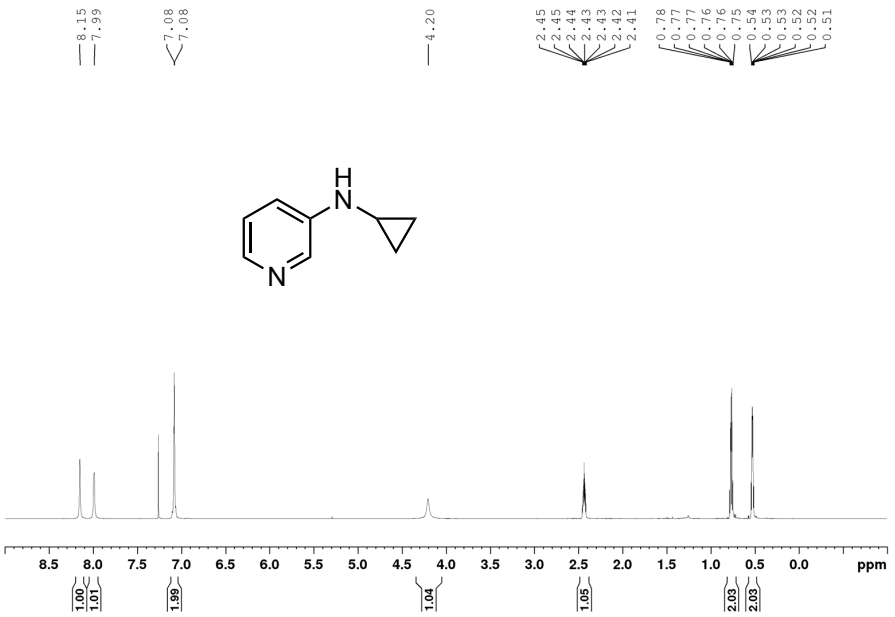

Figure A31. ^{1}H NMR spectrum of *N*-cyclopropylpyridin-3-amine, **2-3a** ($CDCl_3$, 500 MHz).

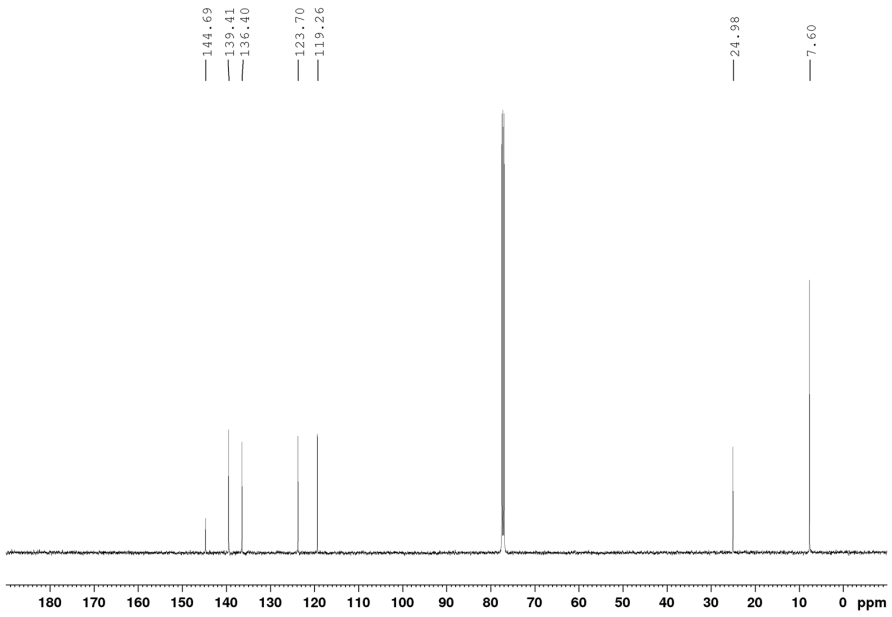

Figure A32. $^{13}C\{^{1}H\}$ NMR spectrum of *N*-cyclopropylpyridin-3-amine, **2-3a** ($CDCl_3$, 126 MHz).

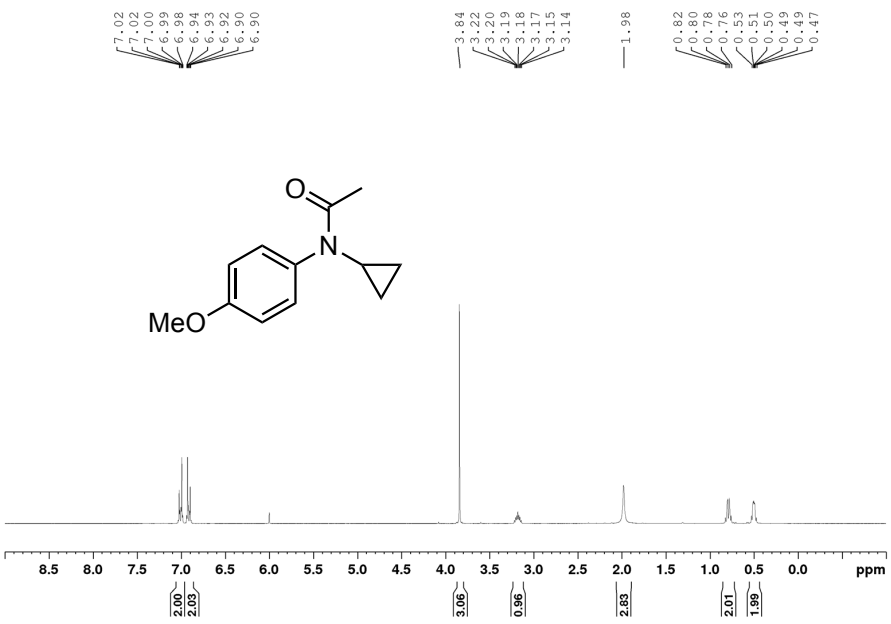

Figure A33. ^{1}H NMR spectrum of *N*-cyclopropyl-*N*-(4-methoxyphenyl)acetamide, **2-3b** ($C_2D_2Cl_4$, 300.1 MHz, 343 K).

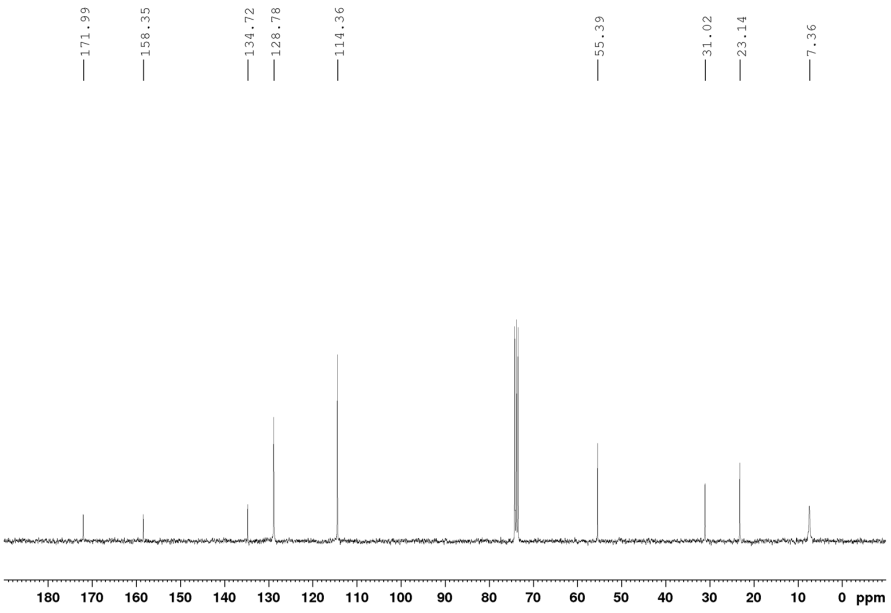

Figure A34. ^{13}C{^{1}H} NMR spectrum of *N*-cyclopropyl-*N*-(4-methoxyphenyl)acetamide, **2-3b** ($C_2D_2Cl_4$, 75.5 MHz, 343 K).

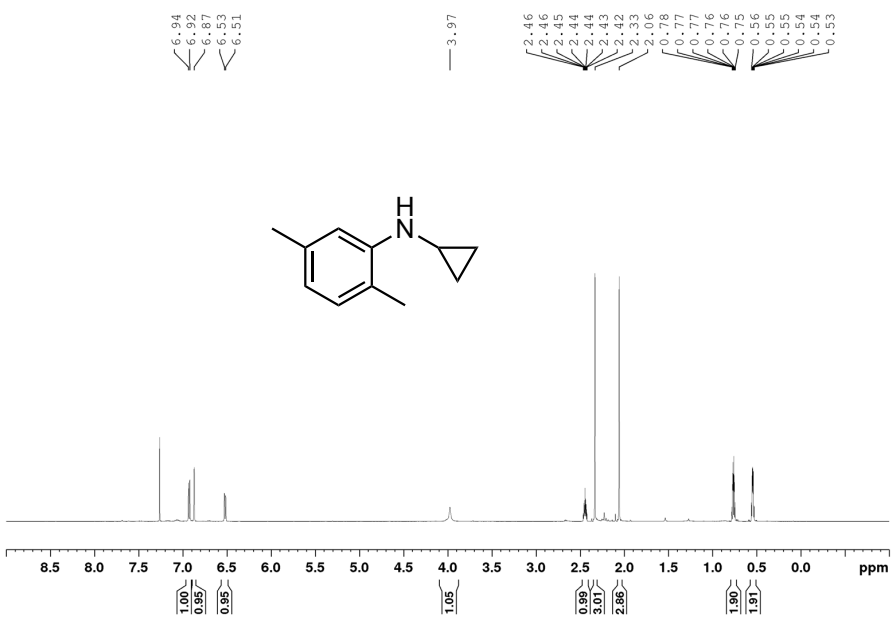

Figure A35. ^{1}H NMR spectrum of *N*-cyclopropyl-2,5-dimethylaniline, **2-3c** ($CDCl_3$, 500 MHz).

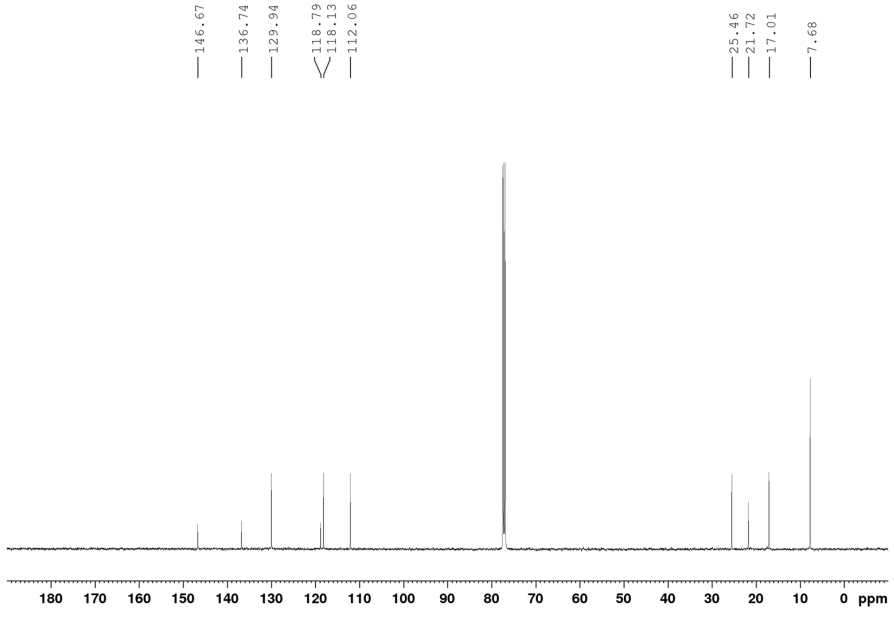

Figure A36. $^{13}C\{^{1}H\}$ NMR spectrum of *N*-cyclopropyl-2,5-dimethylaniline, **2-3c** ($CDCl_3$, 126 MHz).

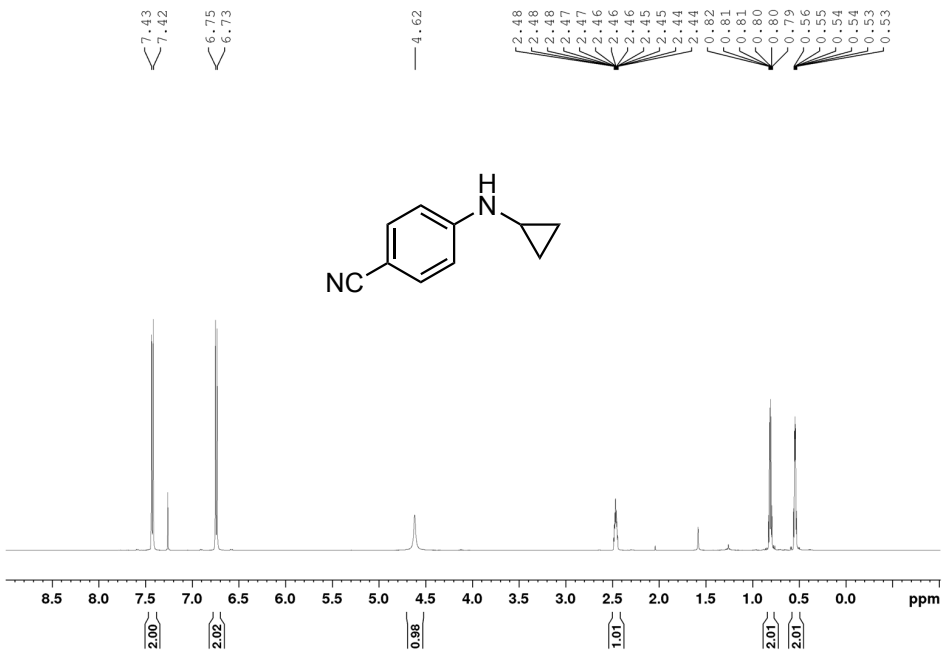

Figure A37. ^{1}H NMR spectrum of 4-(cyclopropylamino)benzonitrile, **2-3d** ($CDCl_3$, 500 MHz).

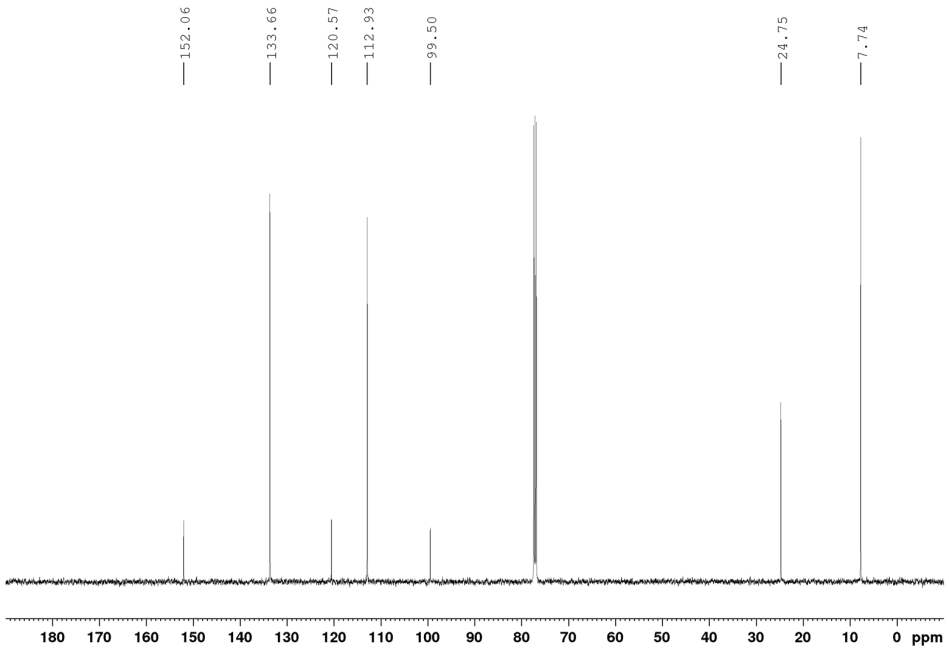

Figure A38. $^{13}C\{^{1}H\}$ NMR spectrum of 4-(cyclopropylamino)benzonitrile, **2-3d** ($CDCl_3$, 126 MHz).

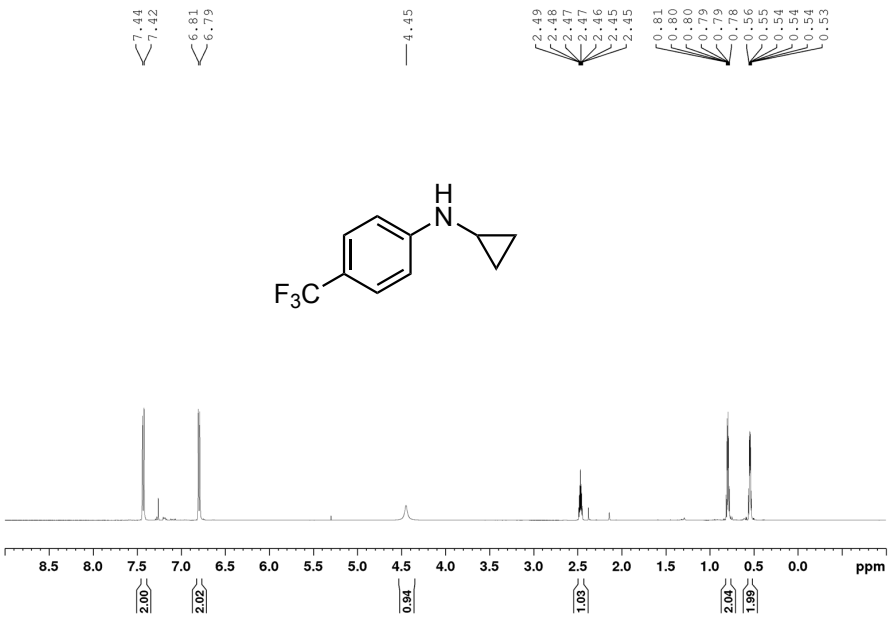

Figure A39. ^{1}H NMR spectrum of *N*-cyclopropyl-4-(trifluoromethyl)aniline, **2-3e** ($CDCl_3$, 500 MHz).

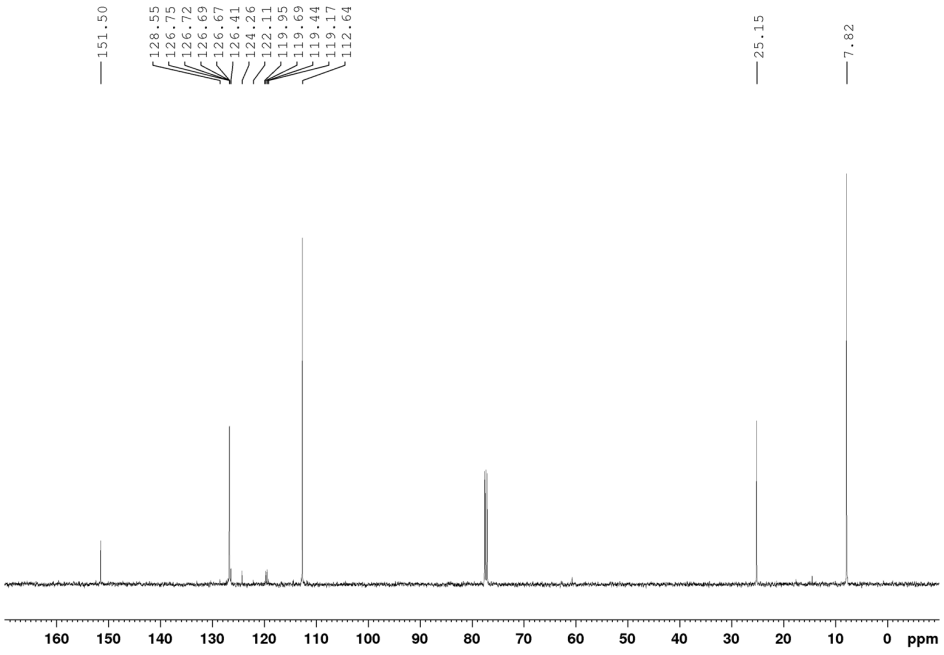

Figure A40. $^{13}C\{^{1}H\}$ NMR spectrum of *N*-cyclopropyl-4-(trifluoromethyl)aniline, **2-3e** ($CDCl_3$, 126 MHz).

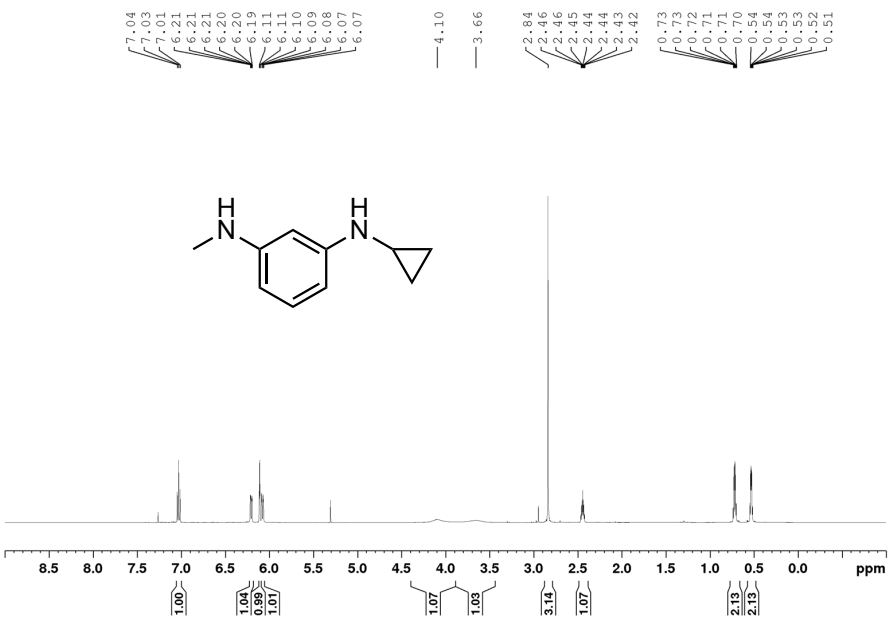

Figure A41. ^{1}H NMR spectrum of N^{1}-cyclopropyl-N^{3}-methylbenzene-1,3-diamine, **2-3f** ($CDCl_3$, 500 MHz).

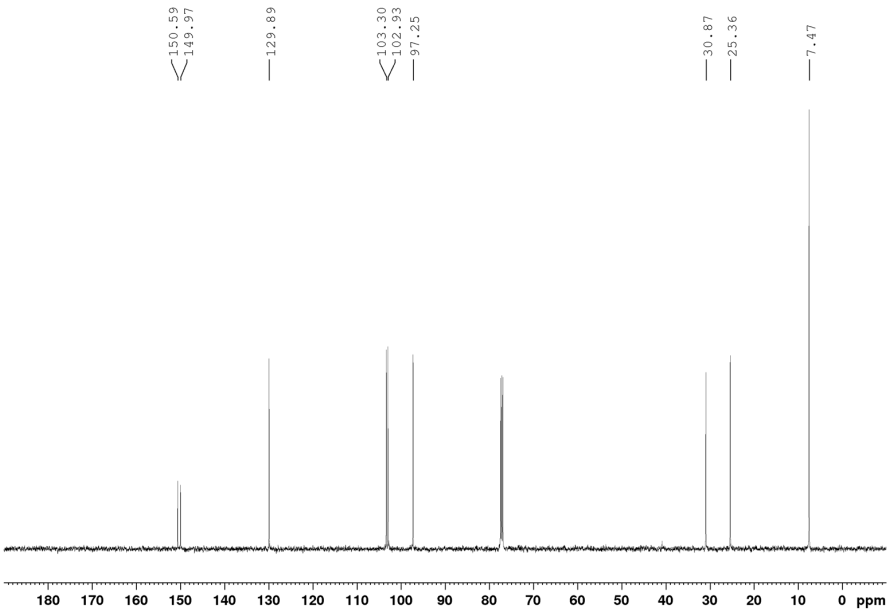

Figure A42. $^{13}C\{^{1}H\}$ NMR spectrum of N^{1}-cyclopropyl-N^{3}-methylbenzene-1,3-diamine, **2-3f** ($CDCl_3$, 126 MHz).

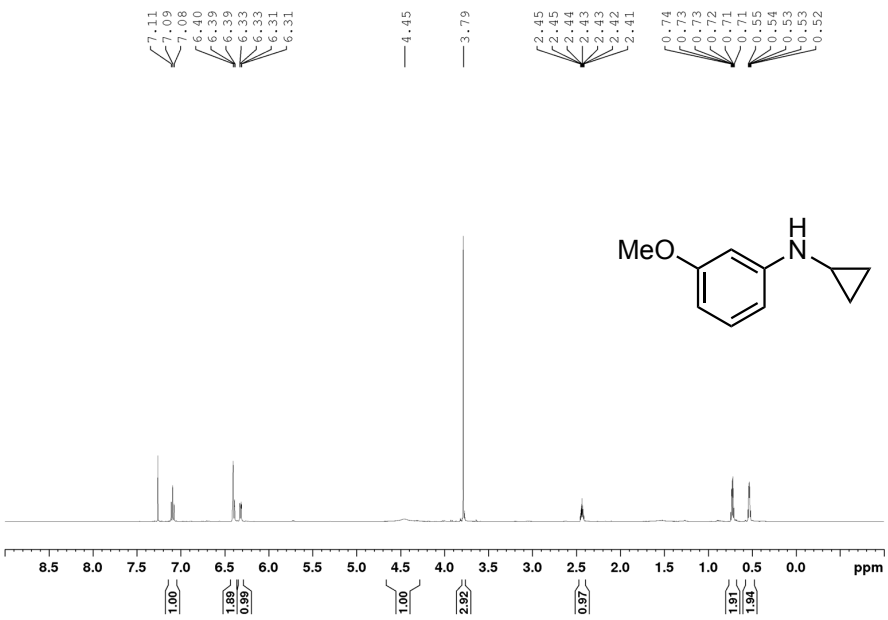

Figure A43. ^{1}H NMR spectrum of *N*-cyclopropyl-3-methoxyaniline, **2-3g** ($CDCl_3$, 500 MHz).

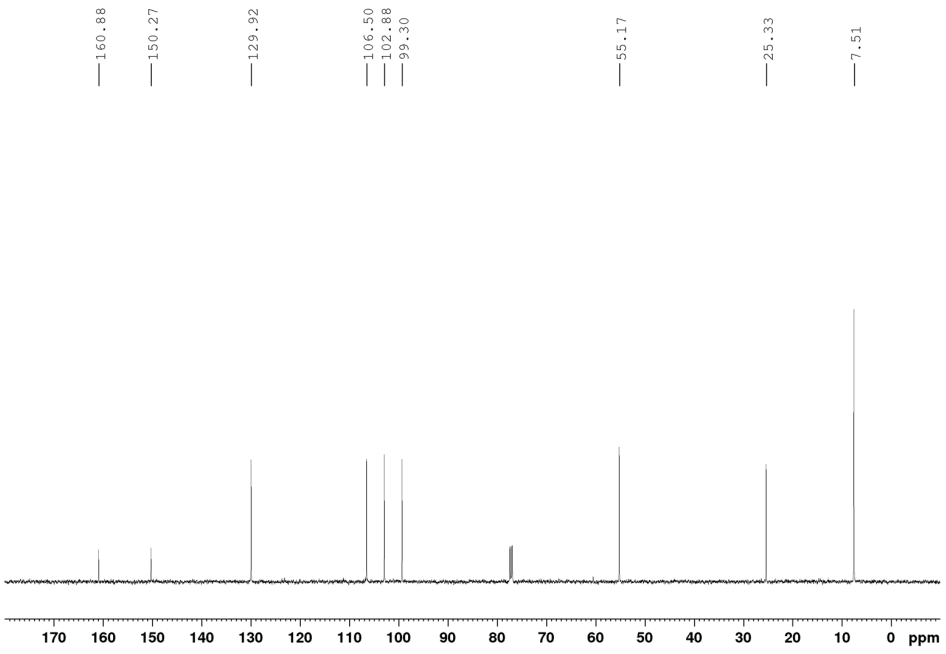

Figure A44. $^{13}C\{^{1}H\}$ NMR spectrum of *N*-cyclopropyl-3-methoxyaniline, **2-3g** ($CDCl_3$, 500 MHz).

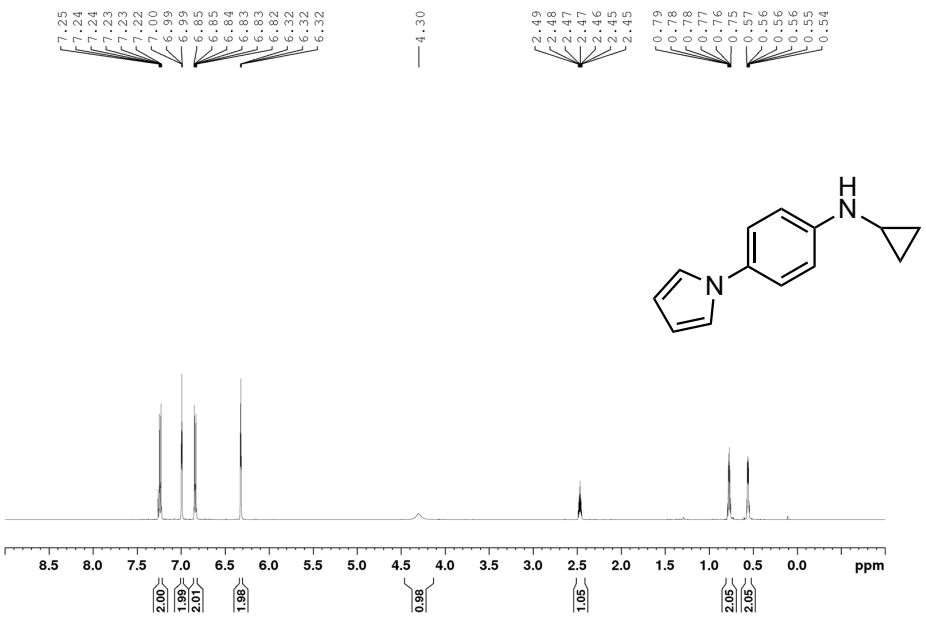

Figure A45. ^{1}H NMR spectrum of *N*-cyclopropyl-4-(1*H*-pyrrol-1-yl)aniline, **2-3h** ($CDCl_3$, 500 MHz).

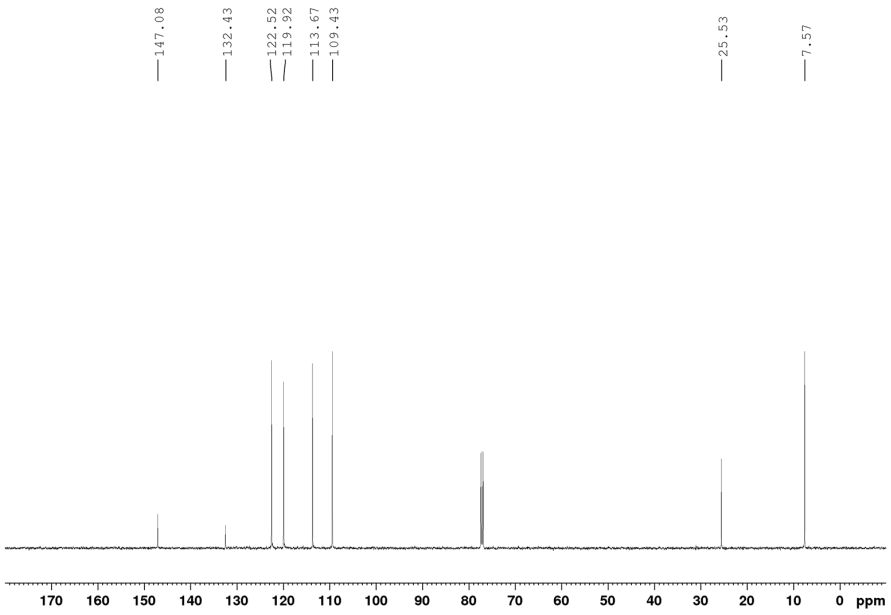

Figure A46. ^{13}C{^{1}H} NMR spectrum of *N*-cyclopropyl-4-(1*H*-pyrrol-1-yl)aniline, **2-3h** ($CDCl_3$, 126 MHz).

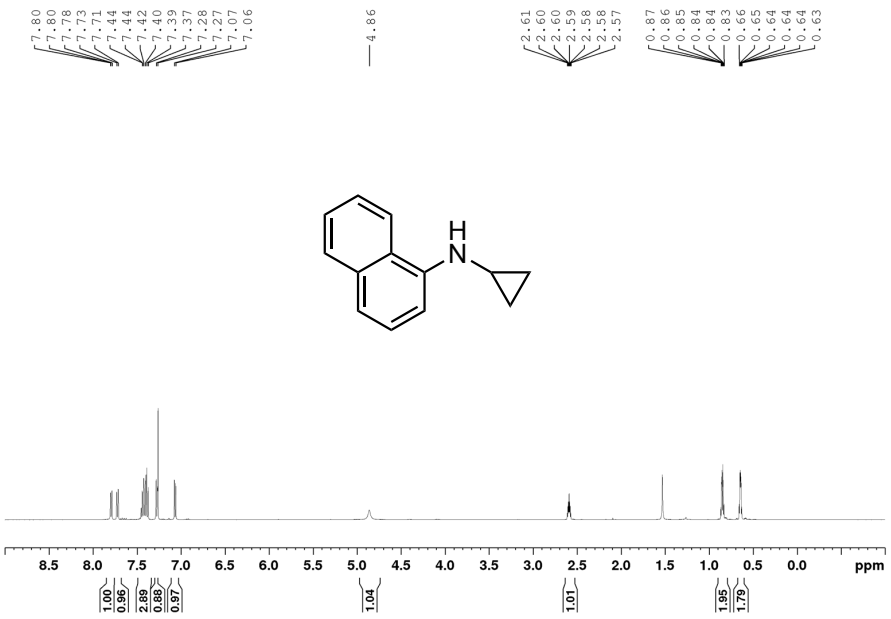

Figure A47. ^{1}H NMR spectrum of *N*-cyclopropylnaphthalen-1-amine, **2-3i** ($CDCl_3$, 500 MHz).

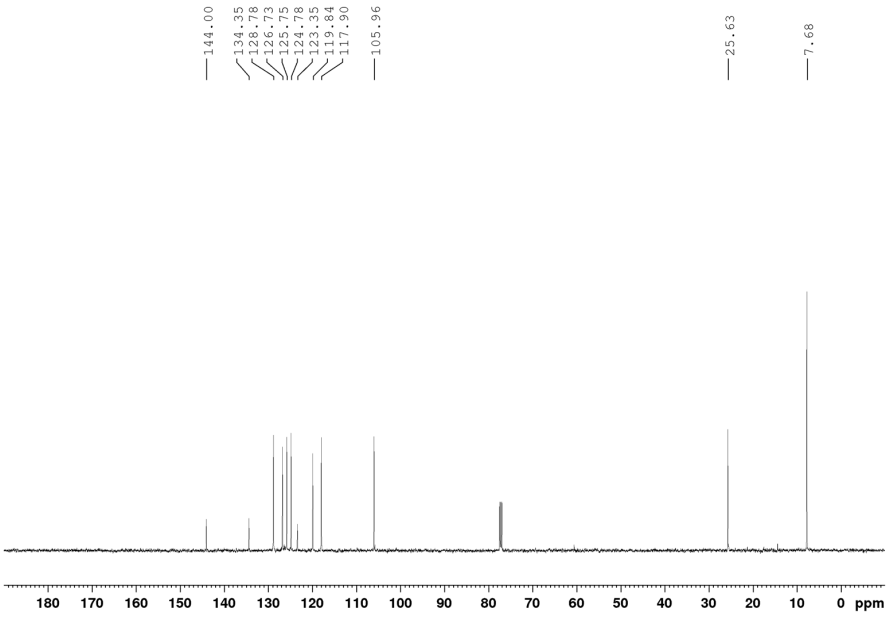

Figure A48. $^{13}C\{^{1}H\}$ NMR spectrum of *N*-cyclopropylnaphthalen-1-amine, **2-3i** ($CDCl_3$, 126 MHz).

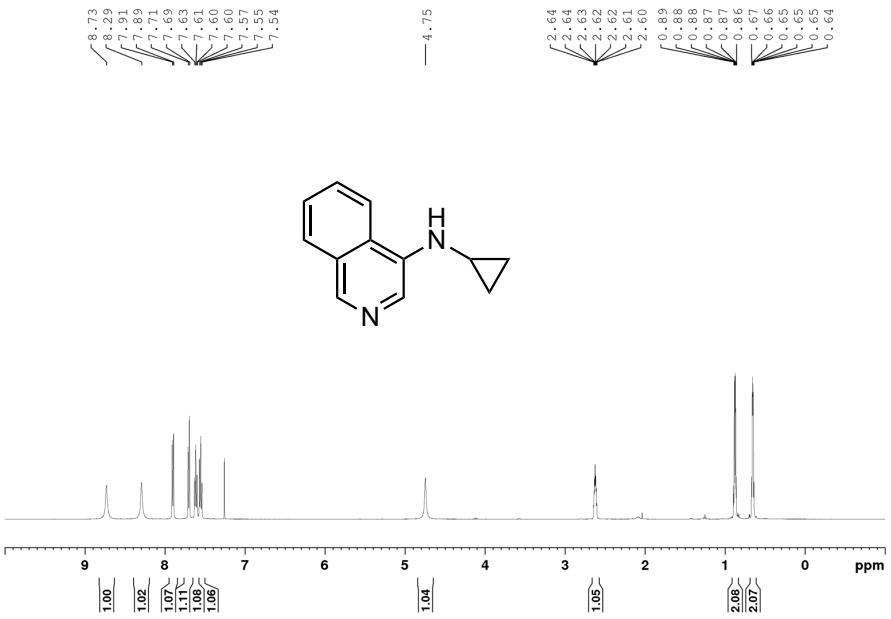

Figure A49. ^{1}H NMR spectrum of *N*-cyclopropylisoquinolin-4-amine, **2-3j** ($CDCl_3$, 500 MHz).

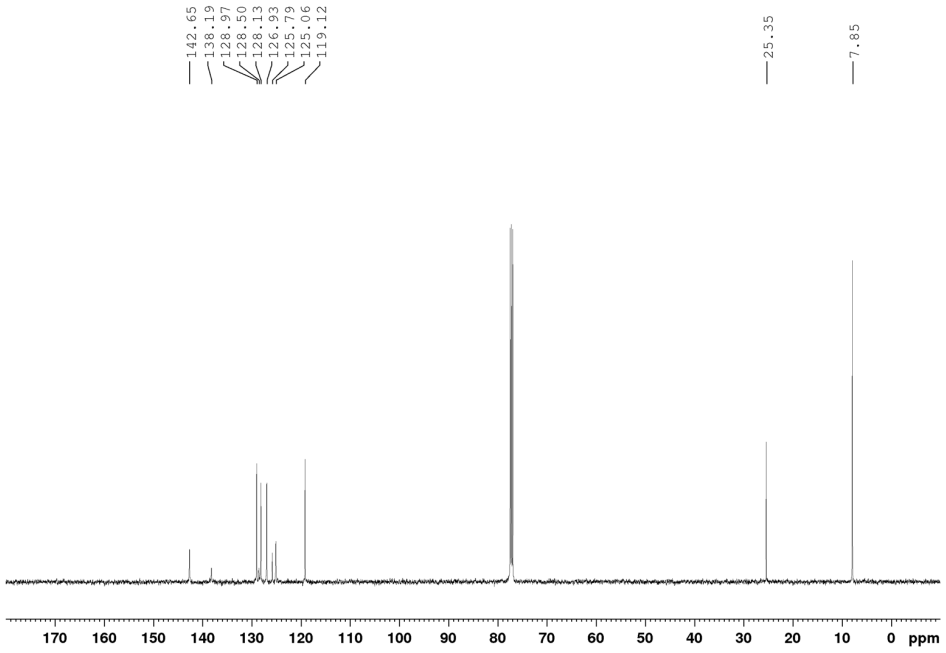

Figure A50. $^{13}C\{^{1}H\}$ NMR spectrum of *N*-cyclopropylisoquinolin-4-amine, **2-3j** ($CDCl_3$, 126 MHz).

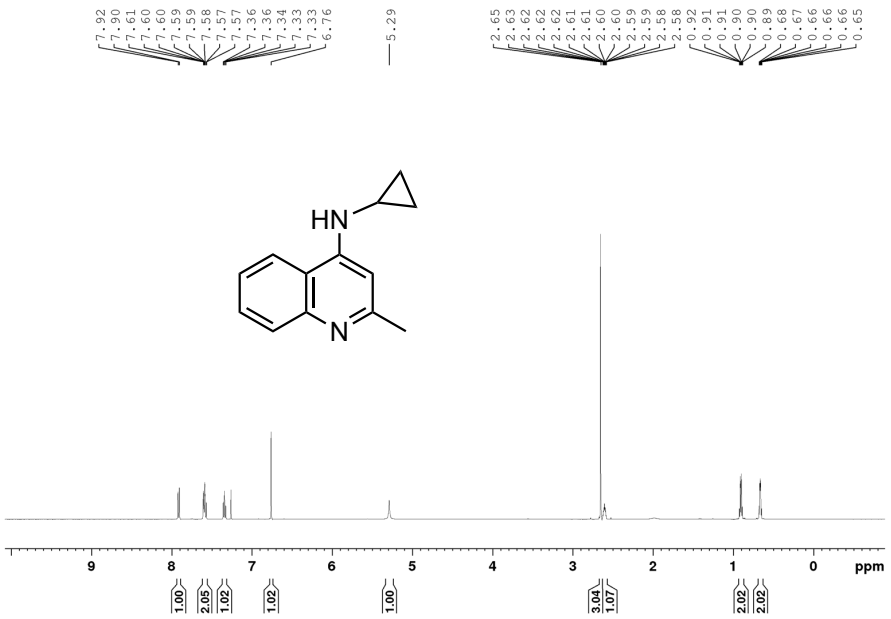

Figure A51. ^{1}H NMR spectrum of *N*-cyclopropyl-2-methylquinolin-4-amine, **2-3k** ($CDCl_3$, 500 MHz).

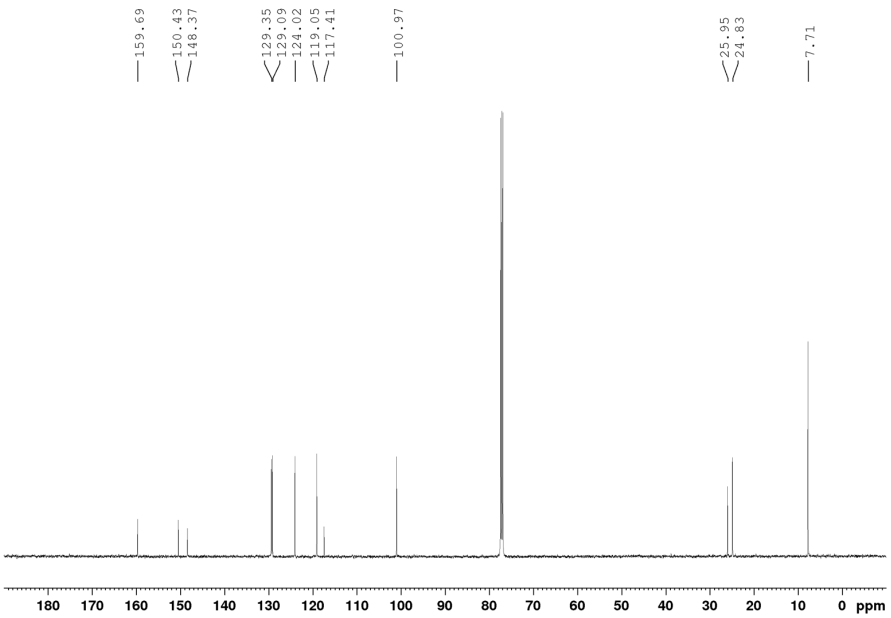

Figure A52. $^{13}C\{^{1}H\}$ NMR spectrum of *N*-cyclopropyl-2-methylquinolin-4-amine, **2-3k** ($CDCl_3$, 126 MHz).

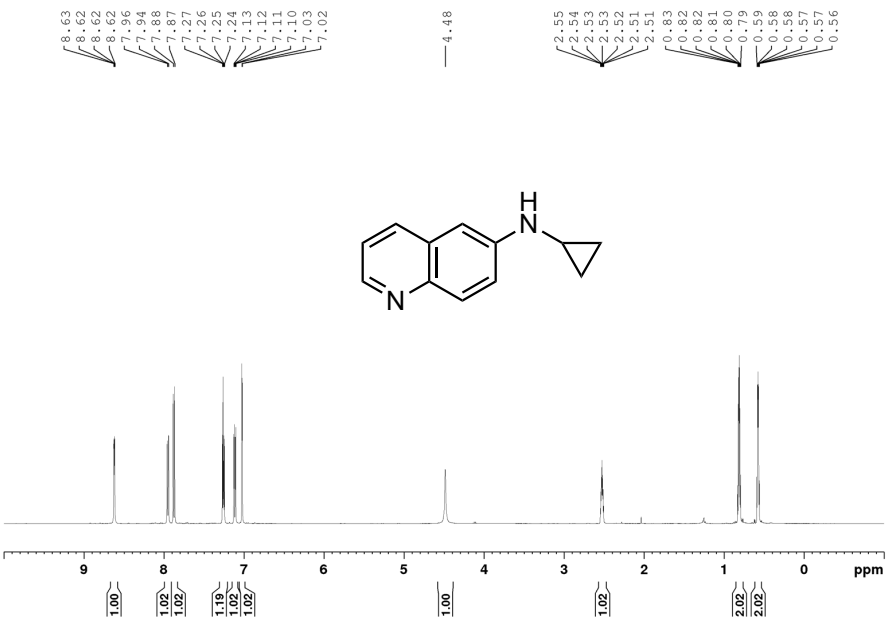

Figure A53. ^{1}H NMR spectrum of *N*-cyclopropylquinolin-6-amine, **2-3l** ($CDCl_3$, 500 MHz).

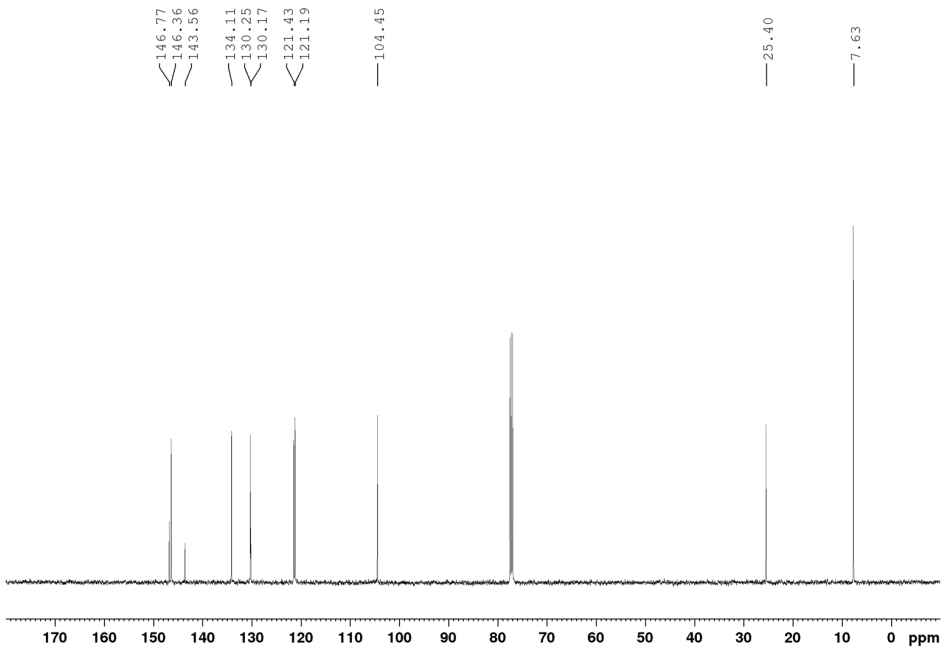

Figure A54. $^{13}C\{^{1}H\}$ NMR spectrum of *N*-cyclopropylquinolin-6-amine, **2-3l** ($CDCl_3$, 126 MHz).

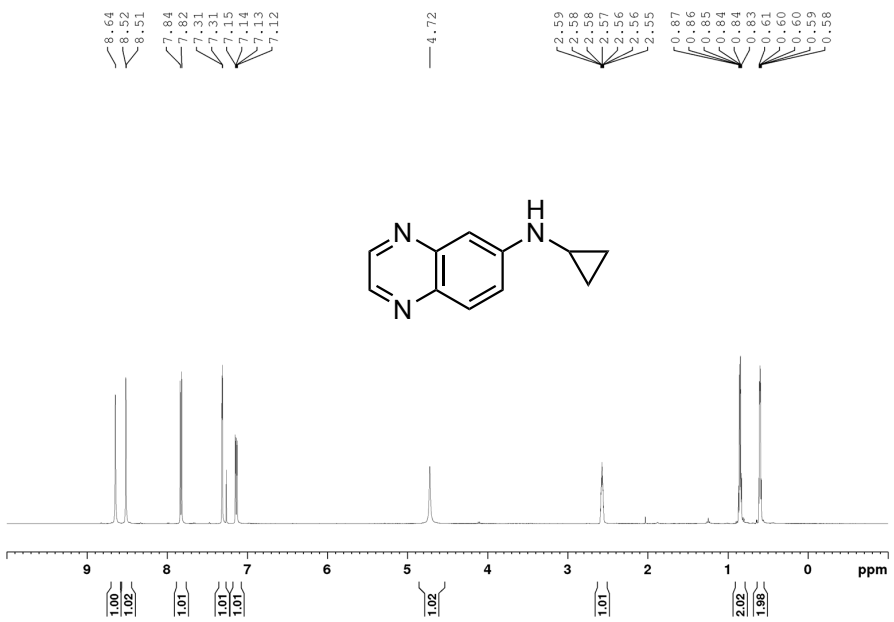

Figure A55. ^{1}H NMR spectrum of *N*-cyclopropylquinoxalin-6-amine, **2-3m** ($CDCl_3$, 500 MHz).

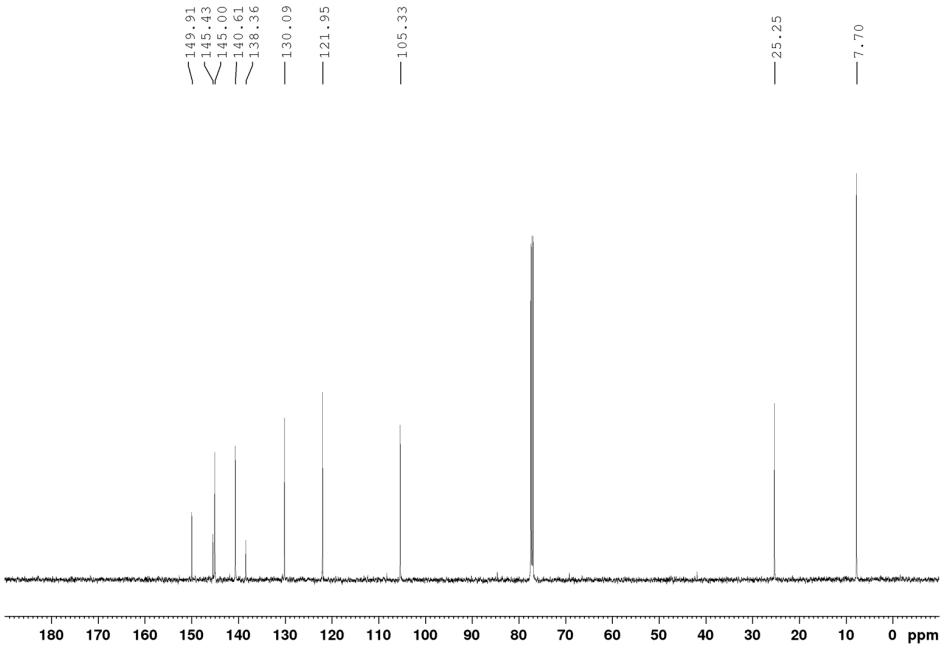

Figure A56. ^{13}C{^{1}H} NMR spectrum of *N*-cyclopropylquinoxalin-6-amine, **2-3m** ($CDCl_3$, 126 MHz).

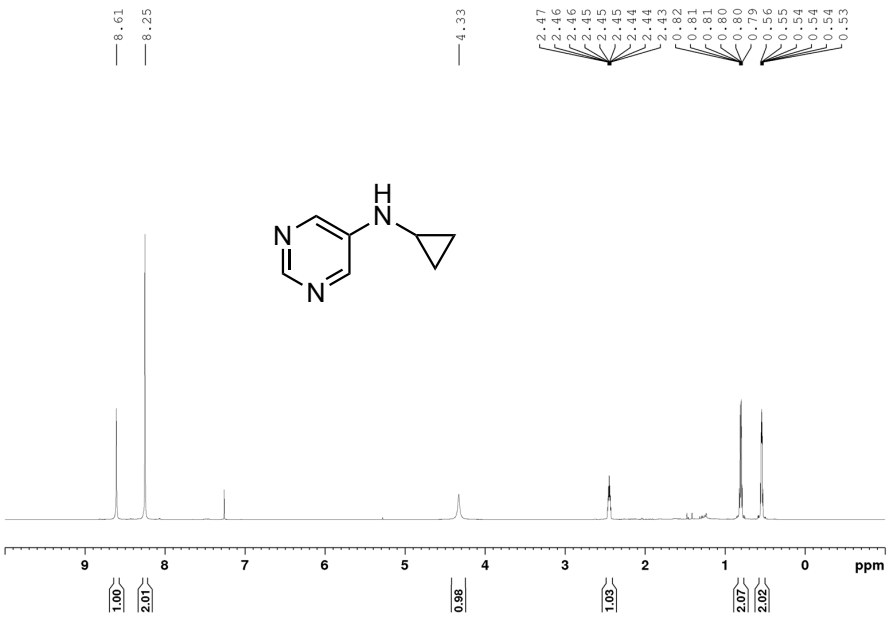

Figure A57. ^{1}H NMR spectrum of *N*-cyclopropylpyrimidin-5-amine, **2-3n** ($CDCl_3$, 500 MHz).

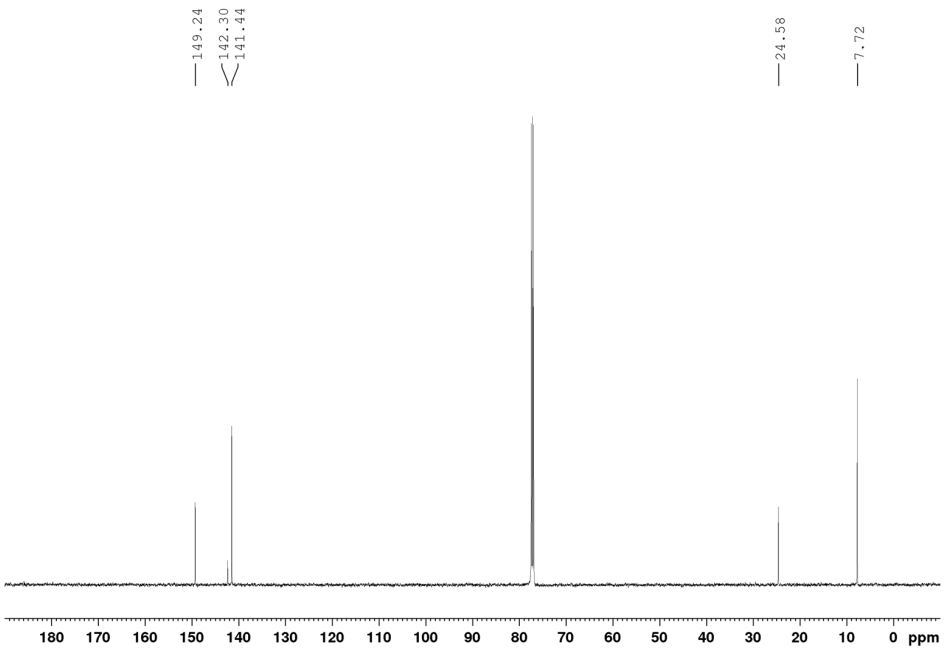

Figure A58. $^{13}C\{^{1}H\}$ NMR spectrum of *N*-cyclopropylpyrimidin-5-amine, **2-3n** ($CDCl_3$, 126 MHz).

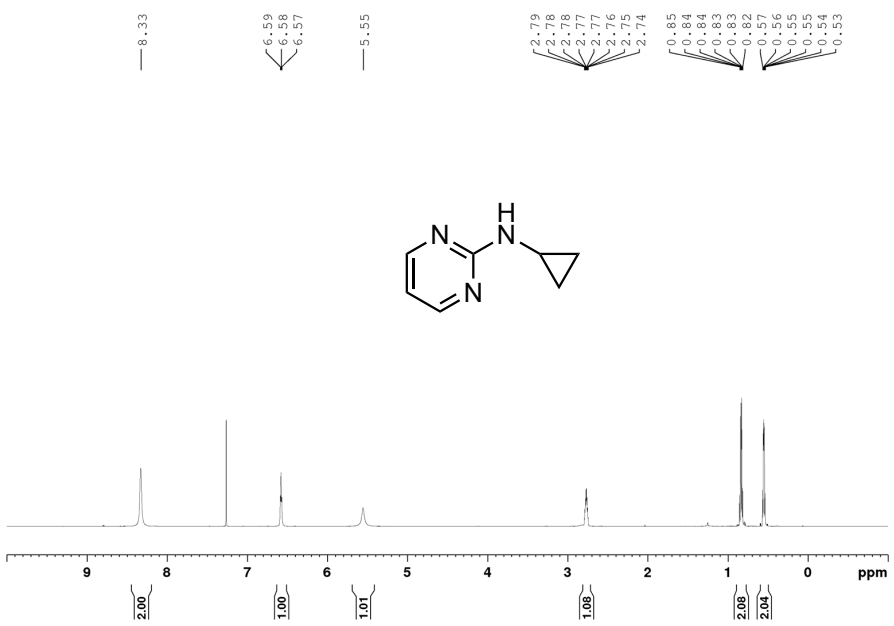

Figure A59. ^{1}H NMR spectrum of *N*-cyclopropylpyrimidin-2-amine, **2-3o** ($CDCl_3$, 500 MHz).

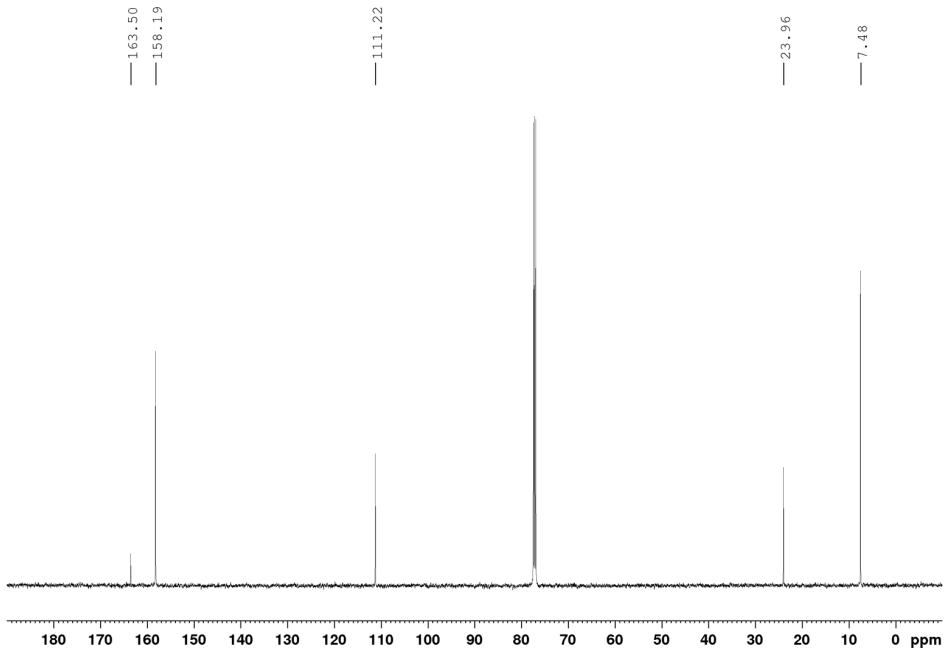

Figure A60. $^{13}C\{^{1}H\}$ NMR spectrum of *N*-cyclopropylpyrimidin-2-amine, **2-3o** ($CDCl_3$, 126 MHz).

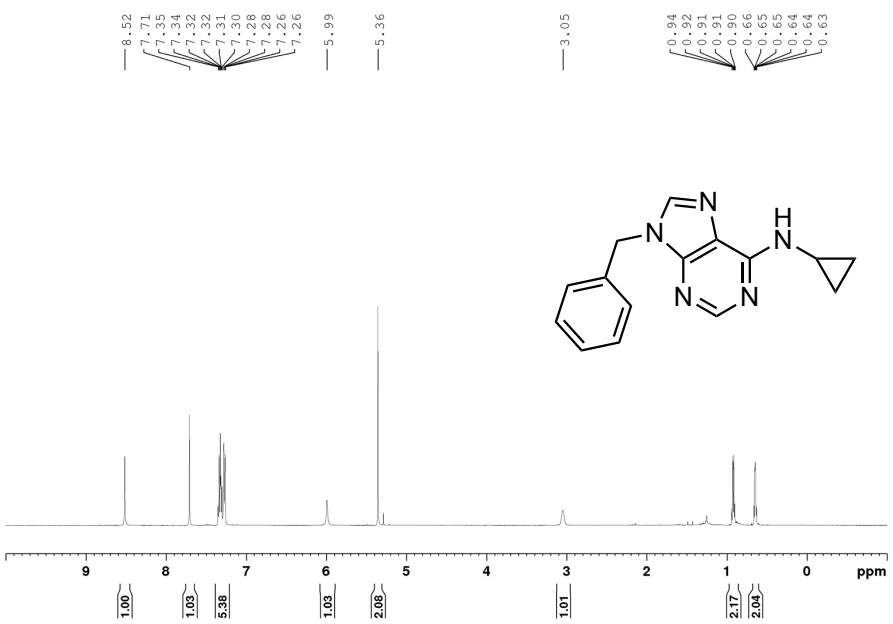

Figure A61. ^{1}H NMR spectrum of 9-benzyl-*N*-cyclopropyl-9*H*-purin-6-amine, **2-3p** ($CDCl_3$, 500 MHz).

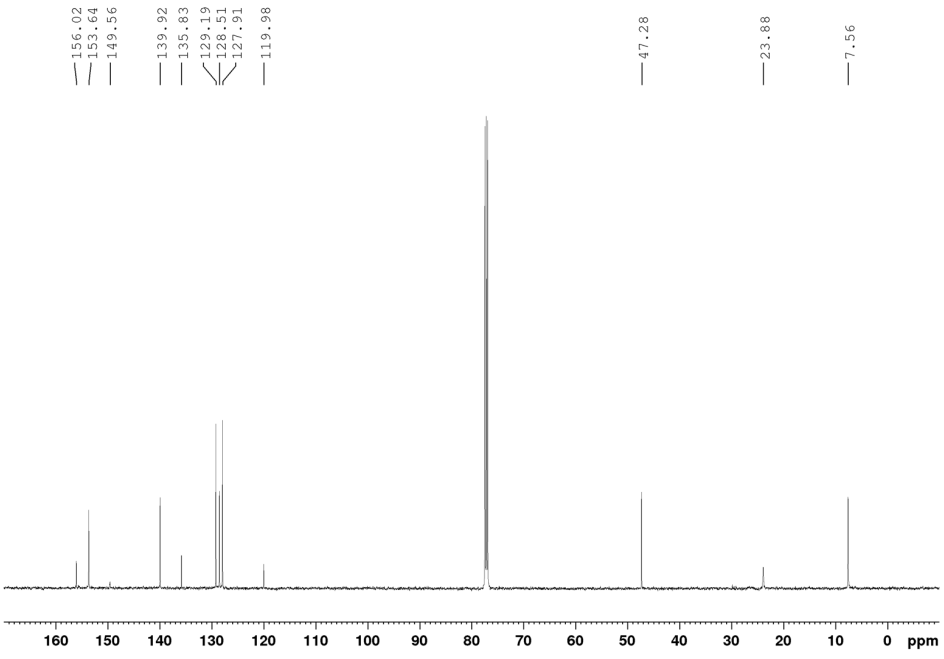

Figure A62. $^{13}C\{^{1}H\}$ NMR spectrum of 9-benzyl-*N*-cyclopropyl-9*H*-purin-6-amine, **2-3p** ($CDCl_3$, 126 MHz).

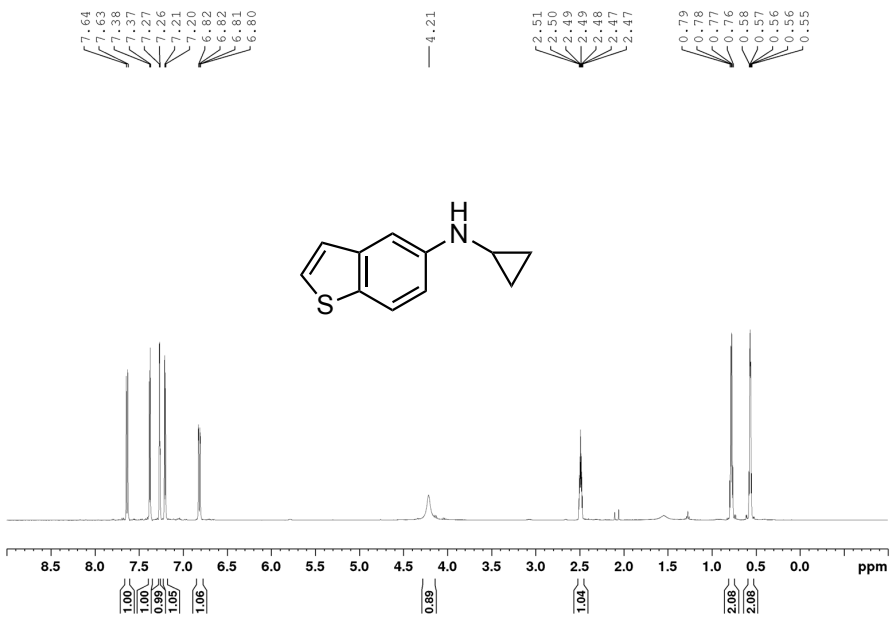

Figure A63. ^{1}H NMR spectrum of *N*-cyclopropylbenzo[*b*]thiophen-5-amine, **2-3q** ($CDCl_3$, 500 MHz).

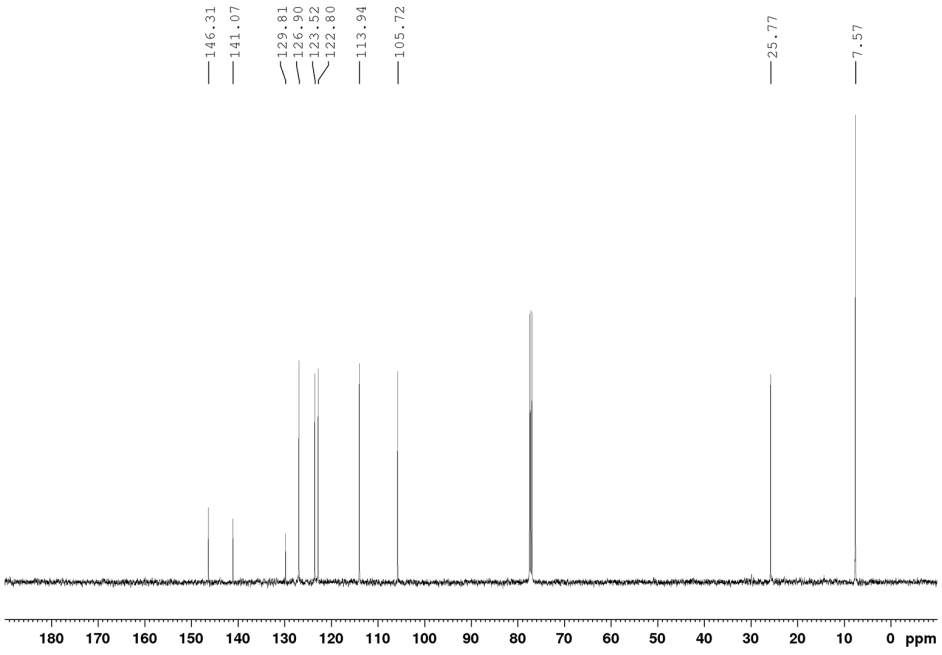

Figure A64. ^{13}C{^{1}H} NMR spectrum of *N*-cyclopropylbenzo[*b*]thiophen-5-amine, **2-3q** ($CDCl_3$, 126 MHz).

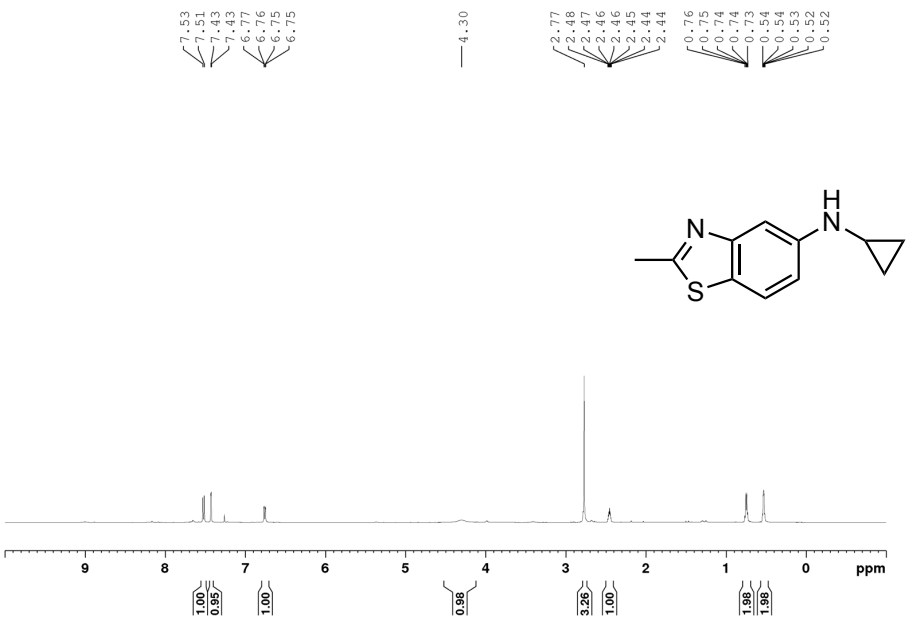

Figure A65. ^{1}H NMR spectrum of *N*-cyclopropyl-2-methylbenzo[*d*]thiazol-5-amine, **2-3r** ($CDCl_3$, 500 MHz).

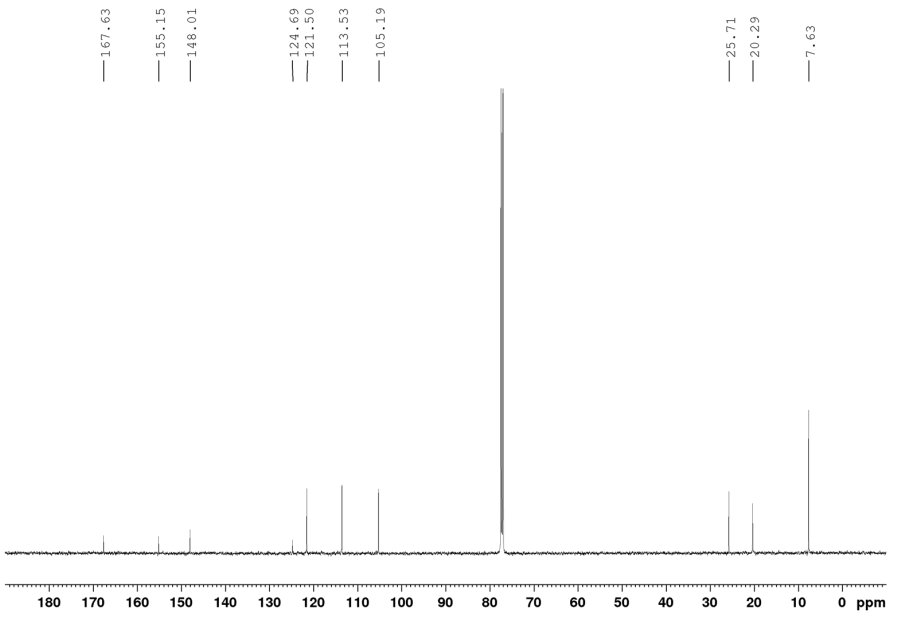

Figure A66. $^{13}C\{^{1}H\}$ NMR spectrum of *N*-cyclopropyl-2-methylbenzo[*d*]thiazol-5-amine, **2-3r** ($CDCl_3$, 128.8 MHz).

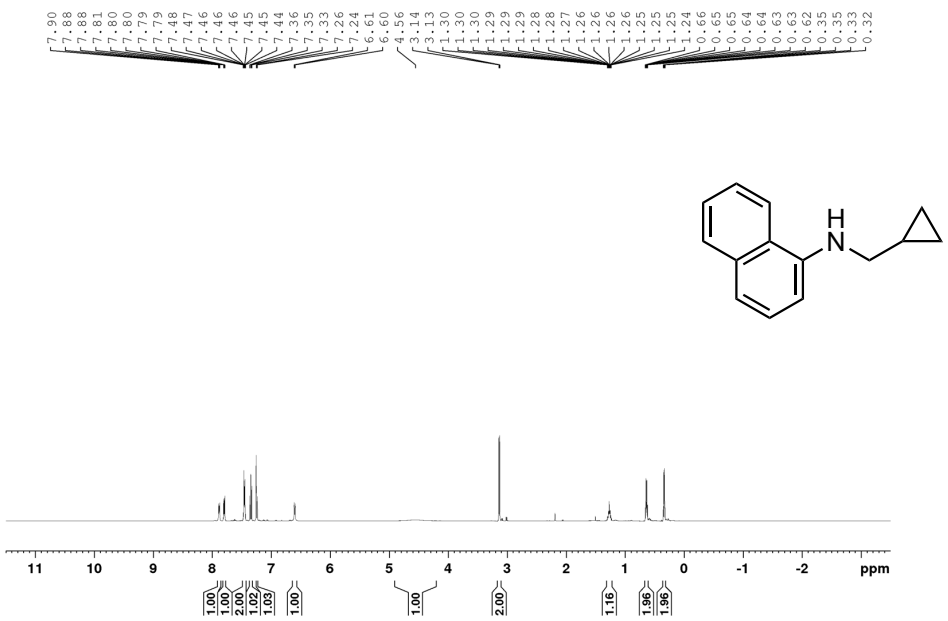

Figure A67. ^{1}H NMR spectrum of *N*-(cyclopropylmethyl)napthalen-1-amine, **2-5a** ($CDCl_3$, 500 MHz).

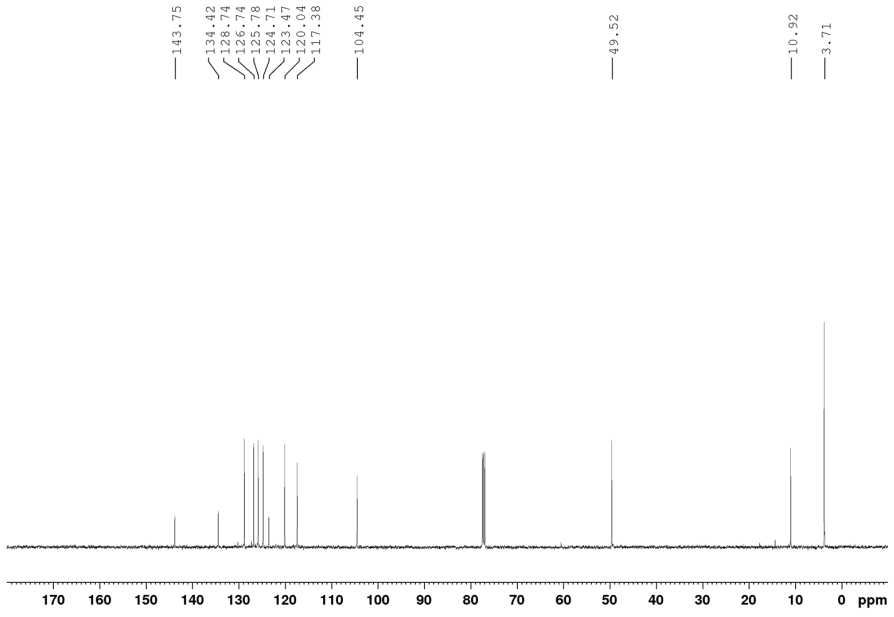

Figure A68. $^{13}C\{^{1}H\}$ NMR spectrum of *N*-(cyclopropylmethyl)napthalen-1-amine, **2-5a** ($CDCl_3$, 126 MHz).

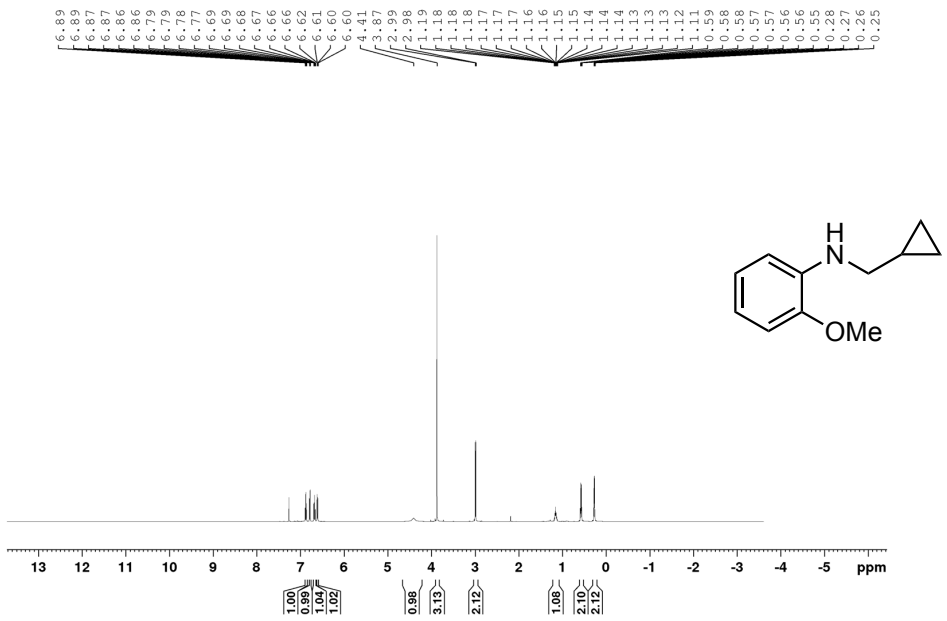

Figure A69. ^{1}H NMR spectrum of *N*-(cyclopropylmethyl)-2-methoxyaniline, **2-5b** ($CDCl_3$, 500 MHz).

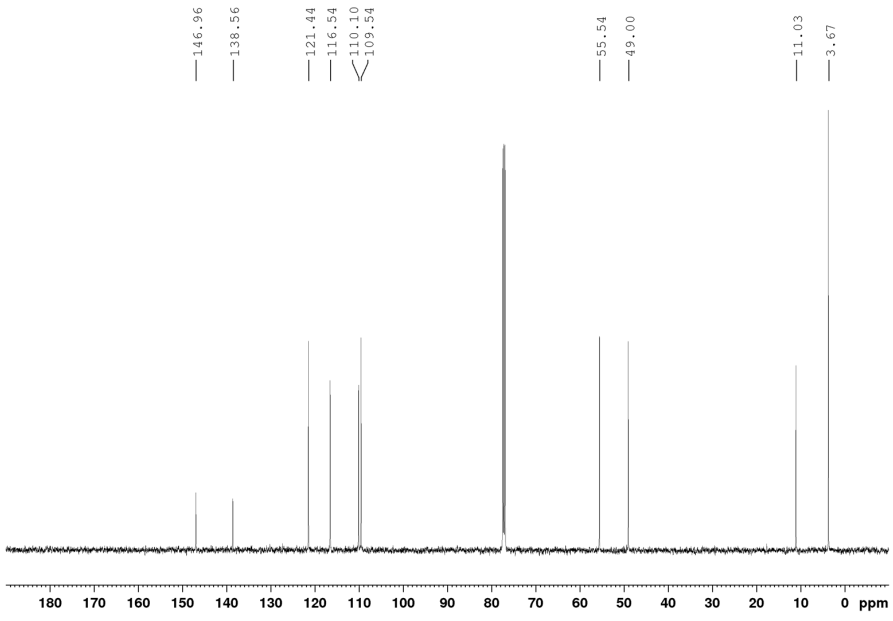

Figure A70. $^{13}C\{^{1}H\}$ NMR spectrum of *N*-(cyclopropylmethyl)-2-methoxyaniline, **2-5b** ($CDCl_3$, 126 MHz).

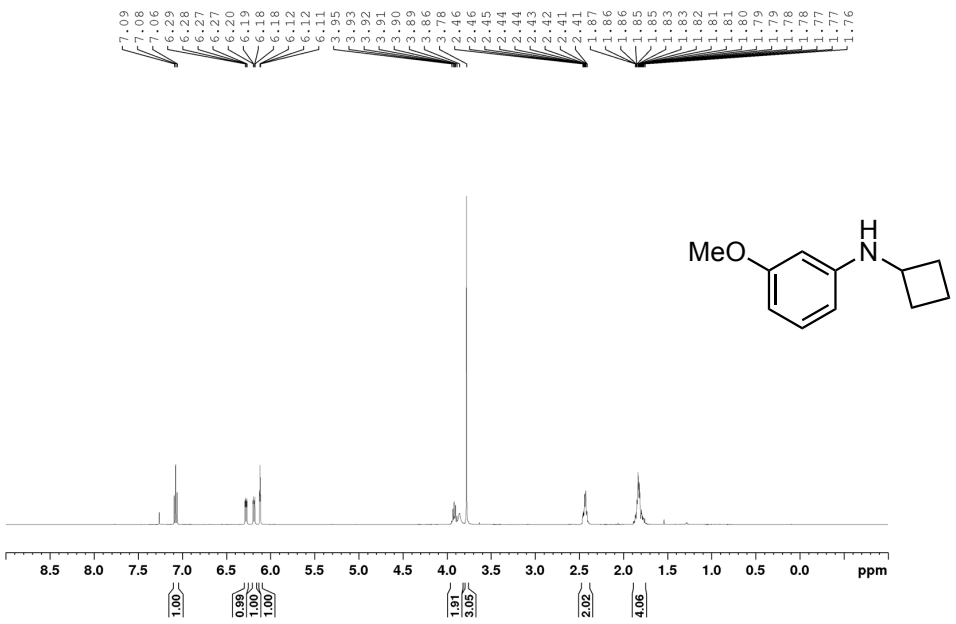

Figure A71. ^{1}H NMR spectrum of *N*-cyclobutyl-3-methoxyaniline, **2-6a** ($CDCl_3$, 500 MHz).

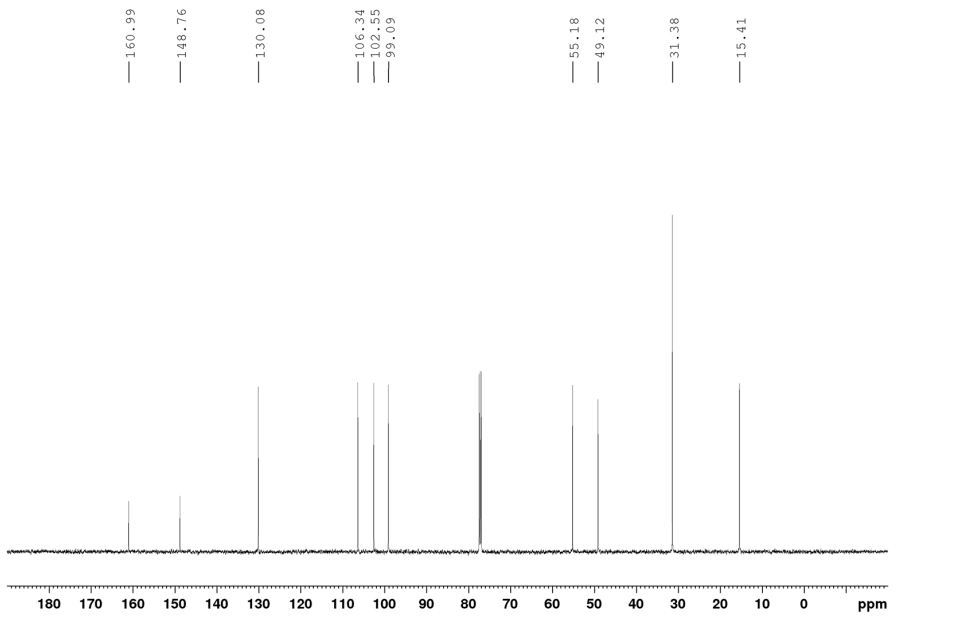

Figure A72. $^{13}C\{^{1}H\}$ NMR spectrum of *N*-cyclobutyl-3-methoxyaniline, **2-6a** ($CDCl_3$, 126 MHz).

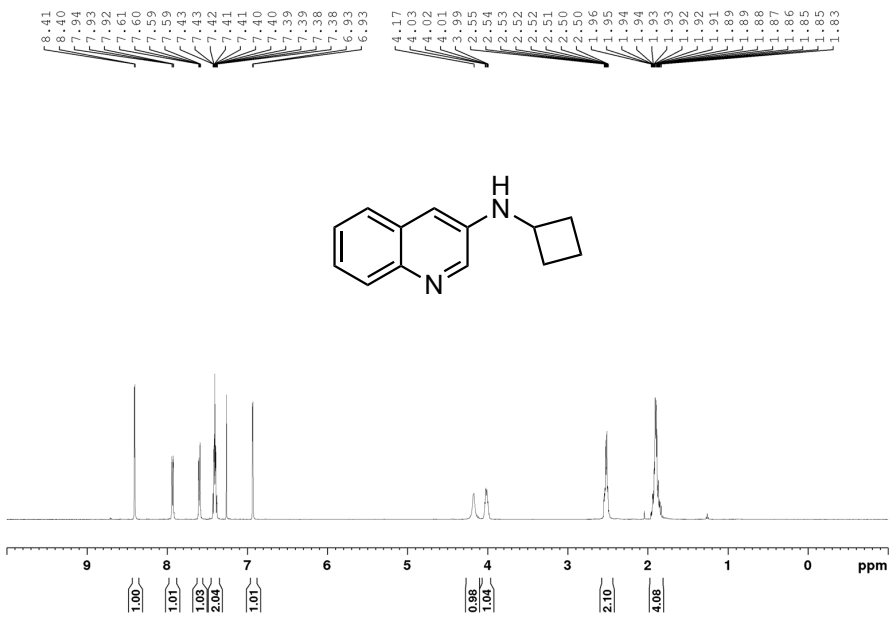

Figure A73. ^{1}H NMR spectrum of *N*-cyclobutylquinolin-3-amine, **2-6b** ($CDCl_3$, 500 MHz).

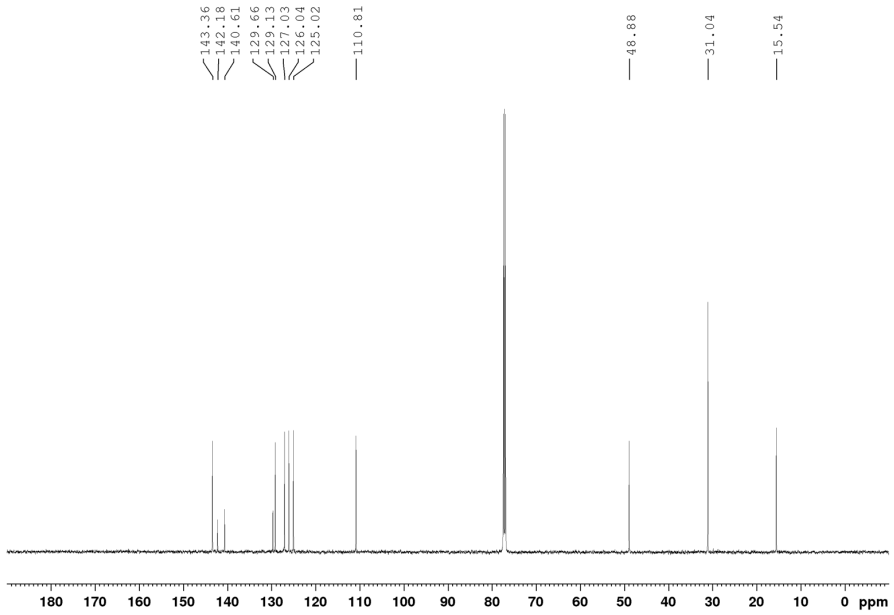

Figure A74. $^{13}C\{^{1}H\}$ NMR spectrum of *N*-cyclobutylquinolin-3-amine, **2-6b** ($CDCl_3$, 126 MHz).

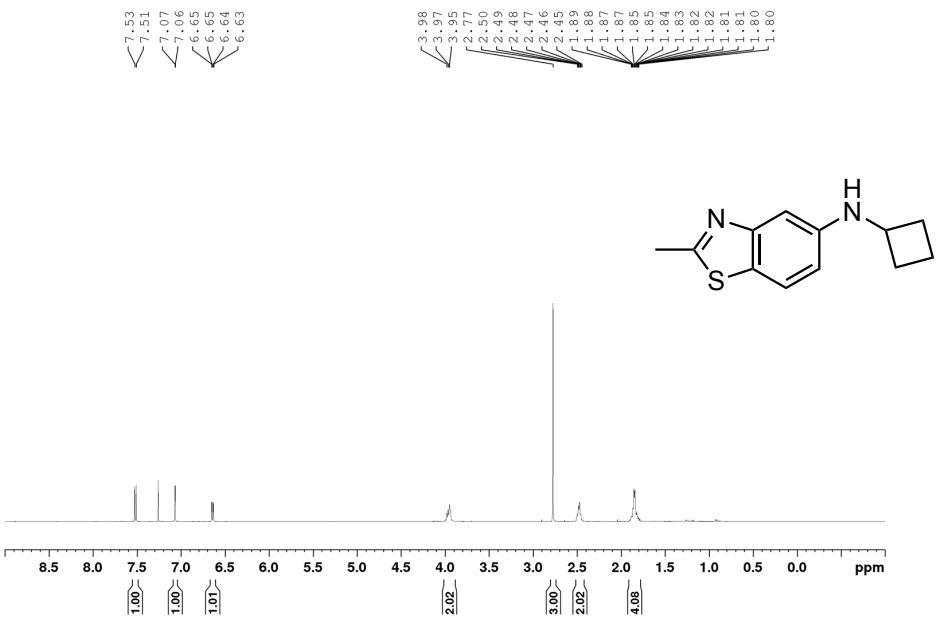

Figure A75. ^{1}H NMR spectrum of *N*-cyclobutyl-2-methylbenzo[*d*]thiazol-5-amine, **2-6c** ($CDCl_3$, 500 MHz).

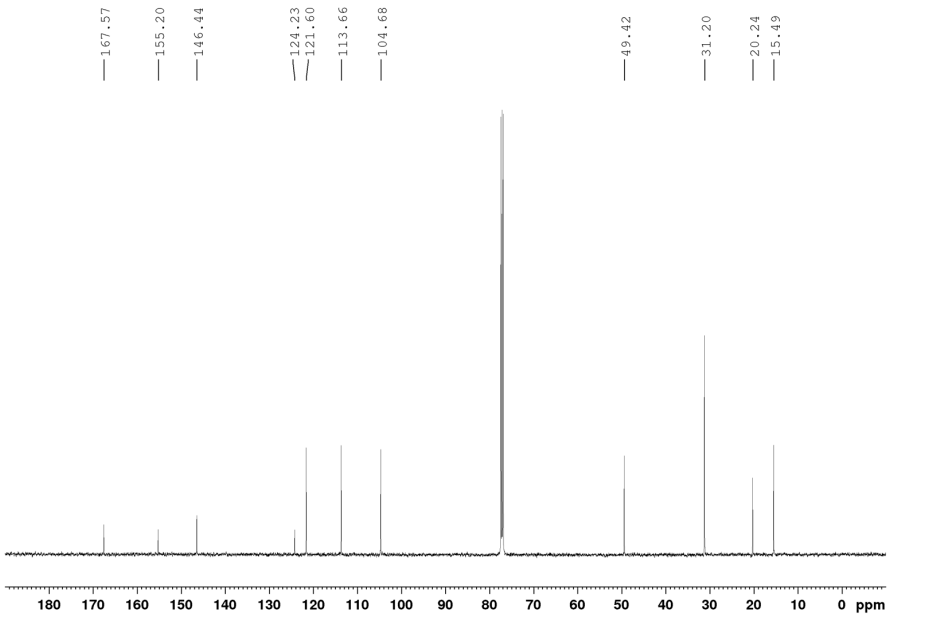

Figure A76. $^{13}C\{^{1}H\}$ NMR spectrum of *N*-cyclobutyl-2-methylbenzo[*d*]thiazol-5-amine, **2-6c** ($CDCl_3$, 126 MHz).

Appendix 4: Chapter 3 NMR Spectra

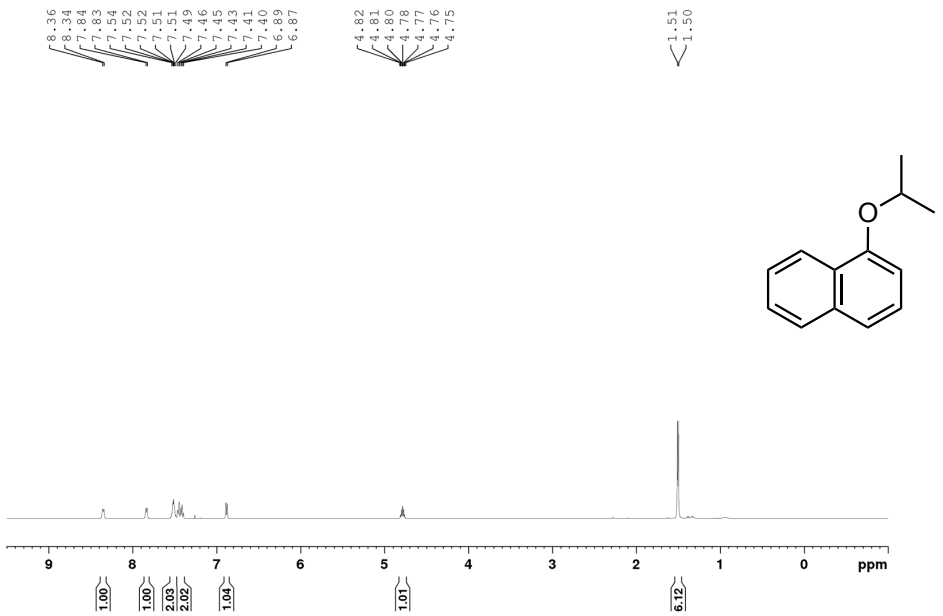

Figure A77. ^{1}H NMR spectrum of 1-isopropoxynaphthalene, **3-3a** ($CDCl_3$, 500 MHz).

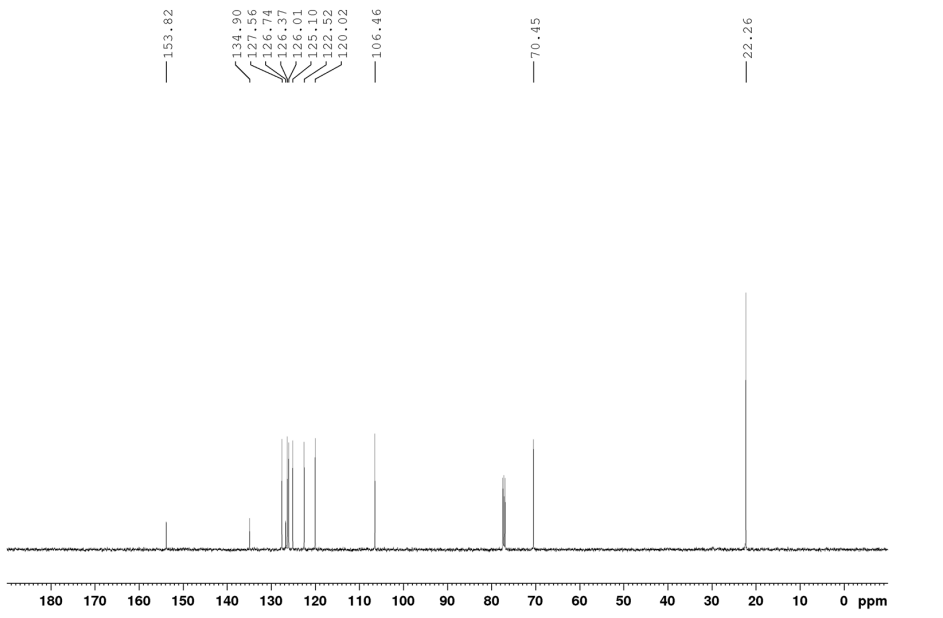

Figure A78. $^{13}C\{^{1}H\}$ NMR spectrum of 1-isopropoxynaphthalene, **3-3a** ($CDCl_3$, 126 MHz).

Figure A79. ^{1}H NMR spectrum of 2-isopropoxybenzonitrile, **3-3b** ($CDCl_3$, 500 MHz).

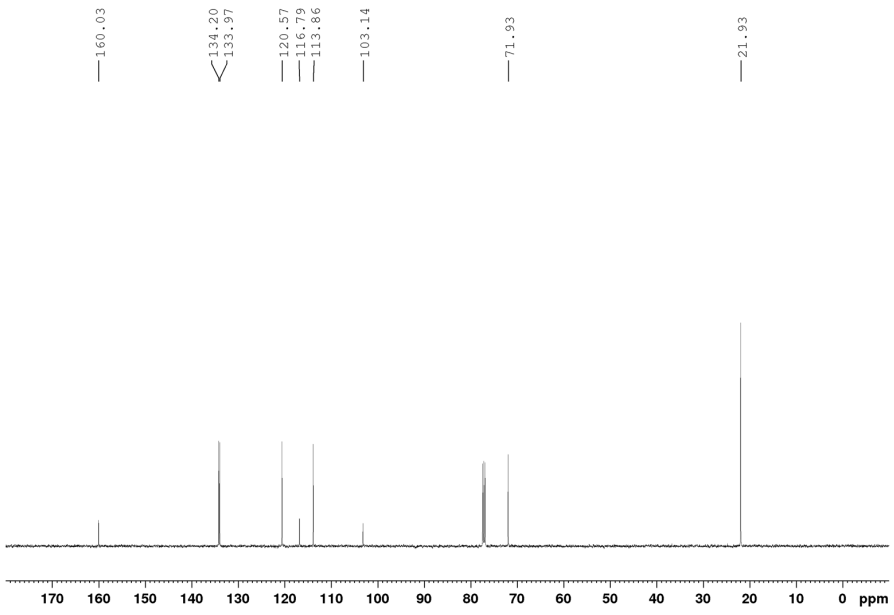

Figure A80. $^{13}C\{^{1}H\}$ NMR spectrum of 2-isopropoxybenzonitrile, **3-3b** ($CDCl_3$, 126 MHz).

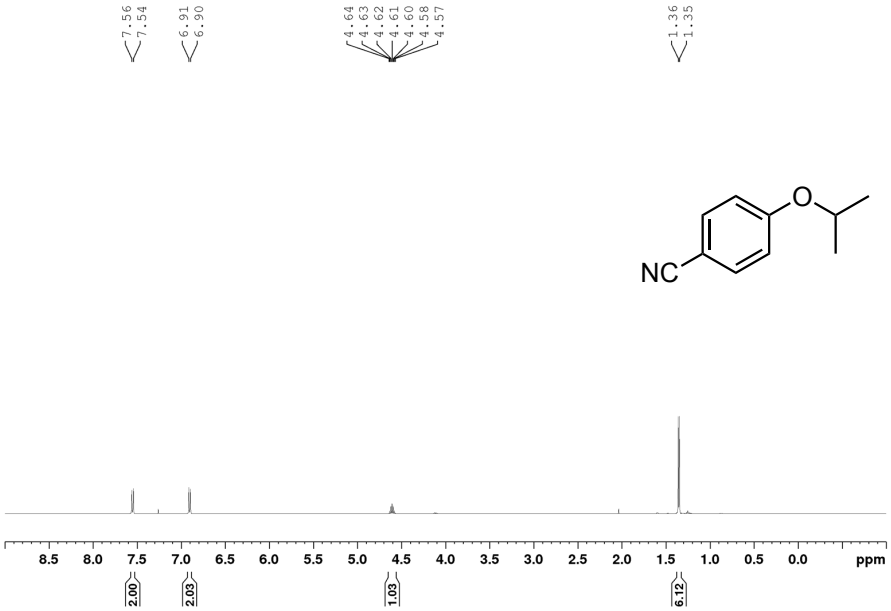

Figure A81. ^{1}H NMR spectrum of 4-isopropoxybenzonitrile, **3-3c** ($CDCl_3$, 500 MHz).

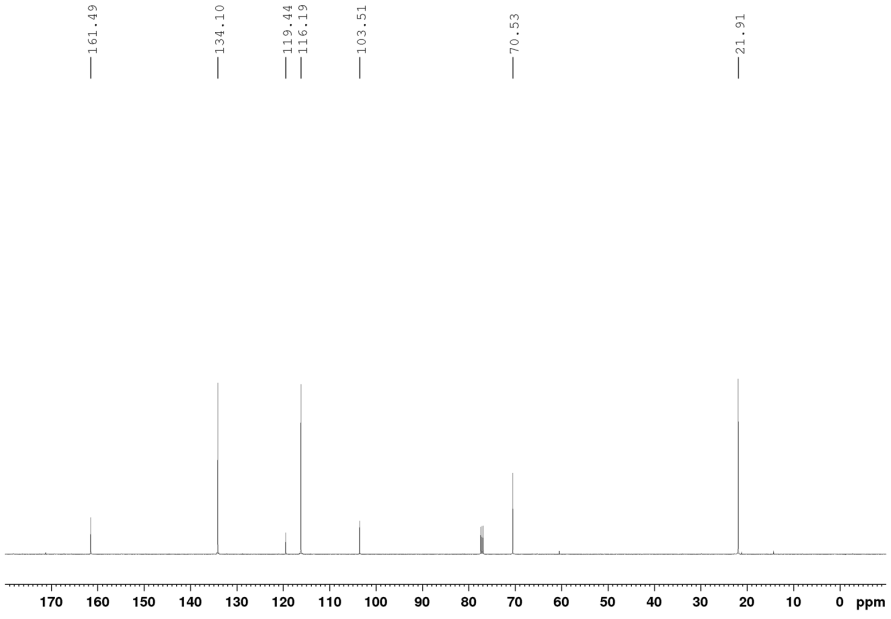

Figure A82. $^{13}C\{^{1}H\}$ NMR spectrum of 4-isopropoxybenzonitrile, **3-3c** ($CDCl_3$, 126 MHz).

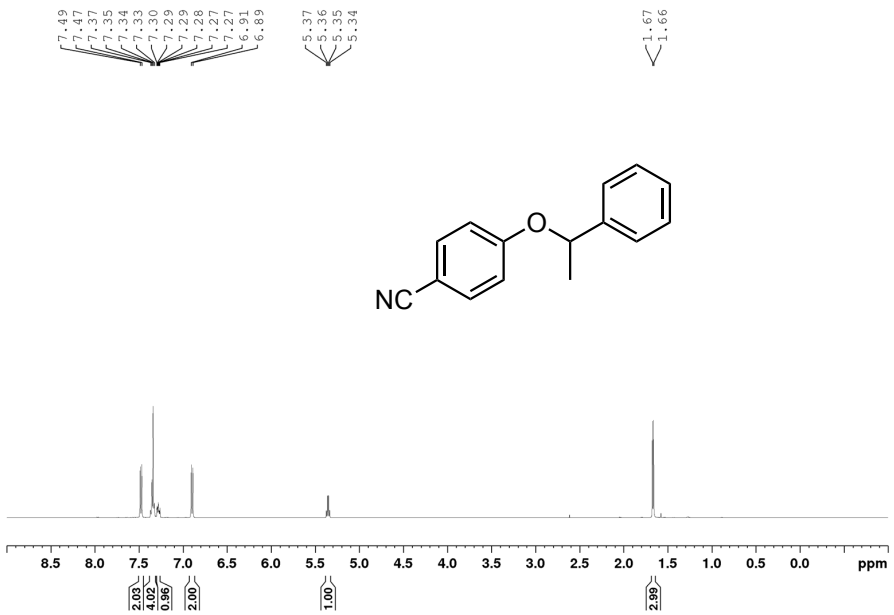

Figure A83. ^{1}H NMR spectrum of 4-(1-phenylethoxy)benzonitrile, **3-3d** ($CDCl_3$, 500 MHz).

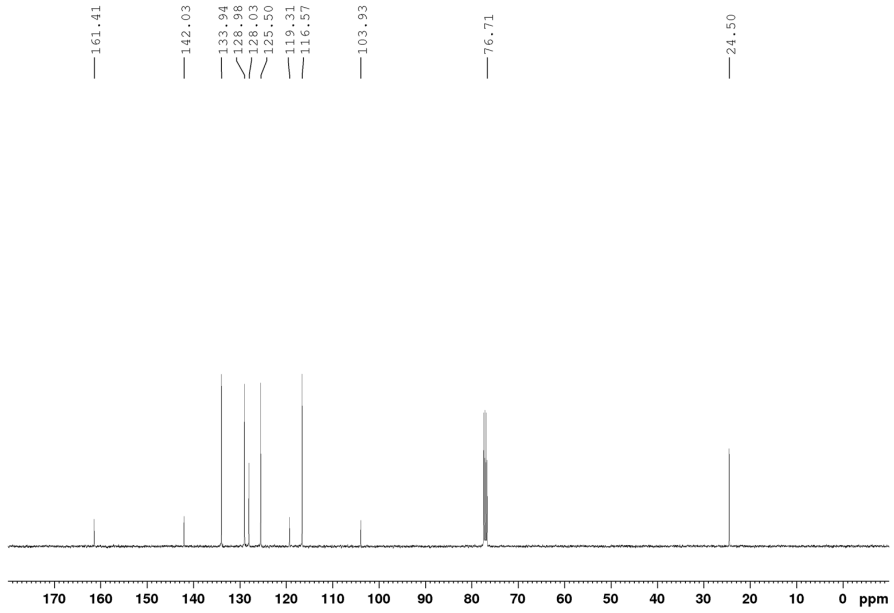

Figure A84. $^{13}C\{^{1}H\}$ NMR spectrum of 4-(1-phenylethoxy)benzonitrile, **3-3d** ($CDCl_3$, 126 MHz).

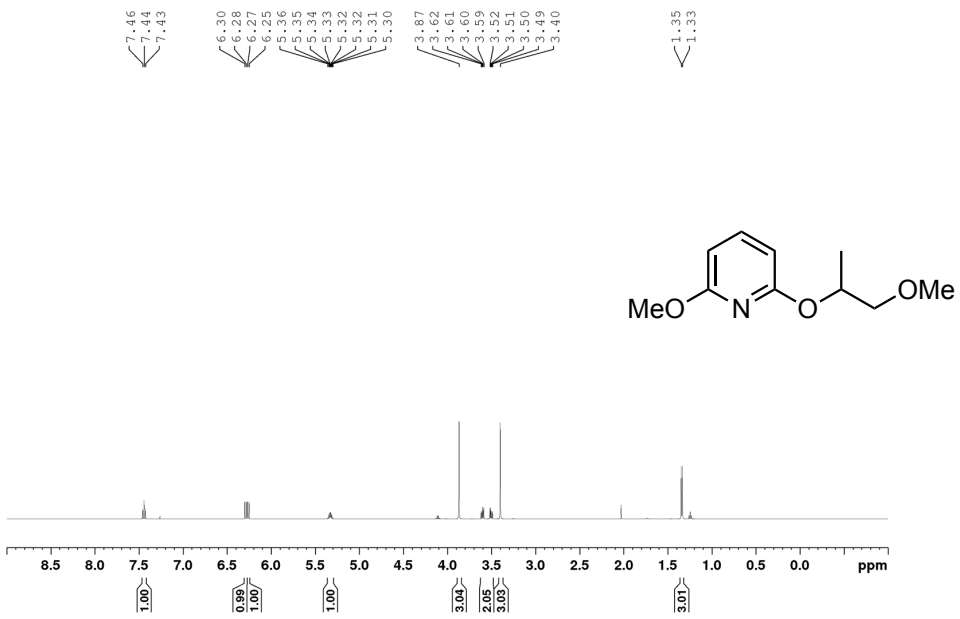

Figure A85. ^{1}H NMR spectrum of 2-methoxy-6-((1-methoxypropan-2-yl)oxy)pyridine, **3-3e** ($CDCl_3$, 500 MHz).

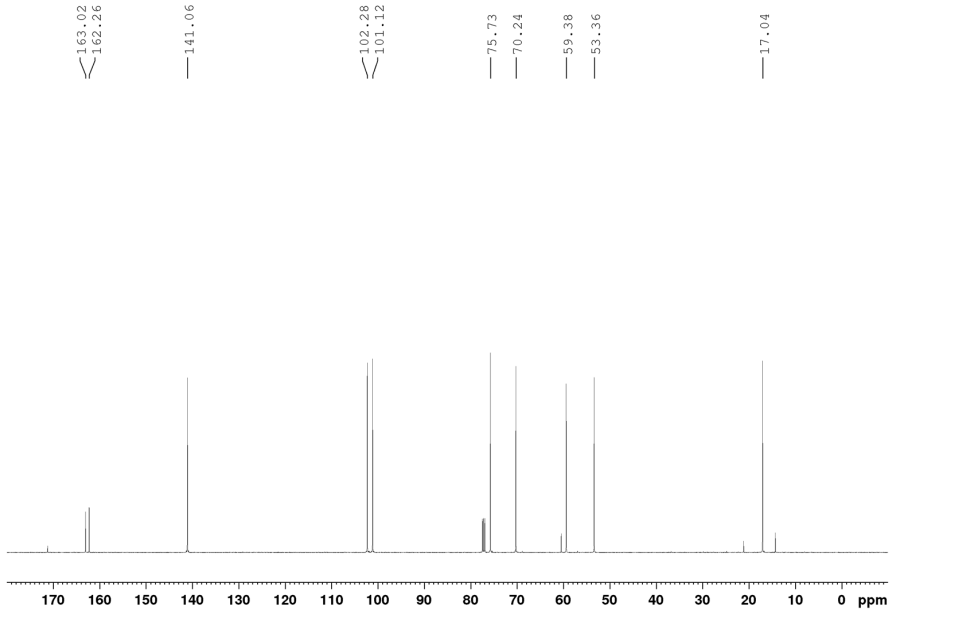

Figure A86. $^{13}C\{^{1}H\}$ NMR spectrum of 2-methoxy-6-((1-methoxypropan-2-yl)oxy)pyridine, **3-3e** ($CDCl_3$, 126 MHz).

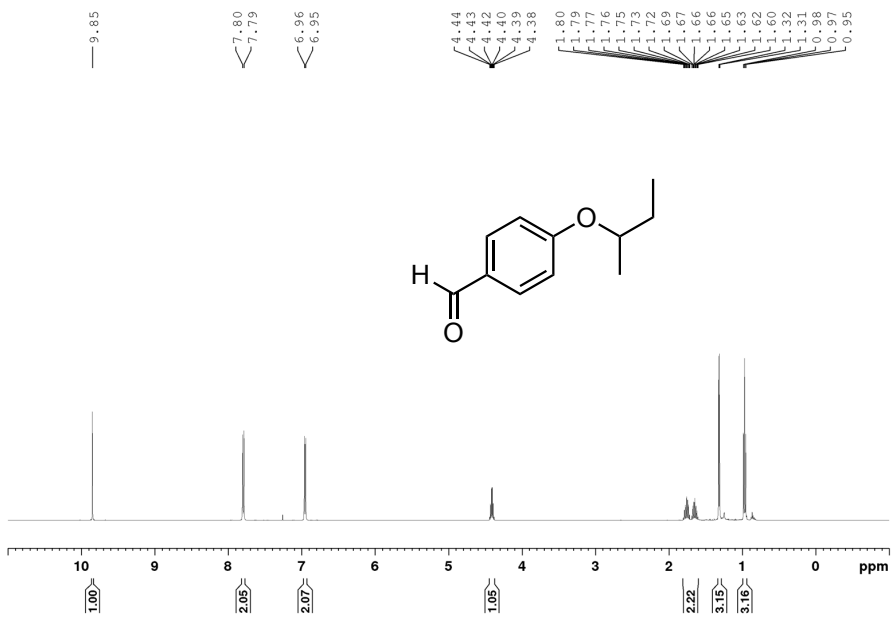

Figure A87. ^{1}H NMR spectrum of 4-(*sec*-butoxy)benzaldehyde, **3-3f** ($CDCl_3$, 500 MHz).

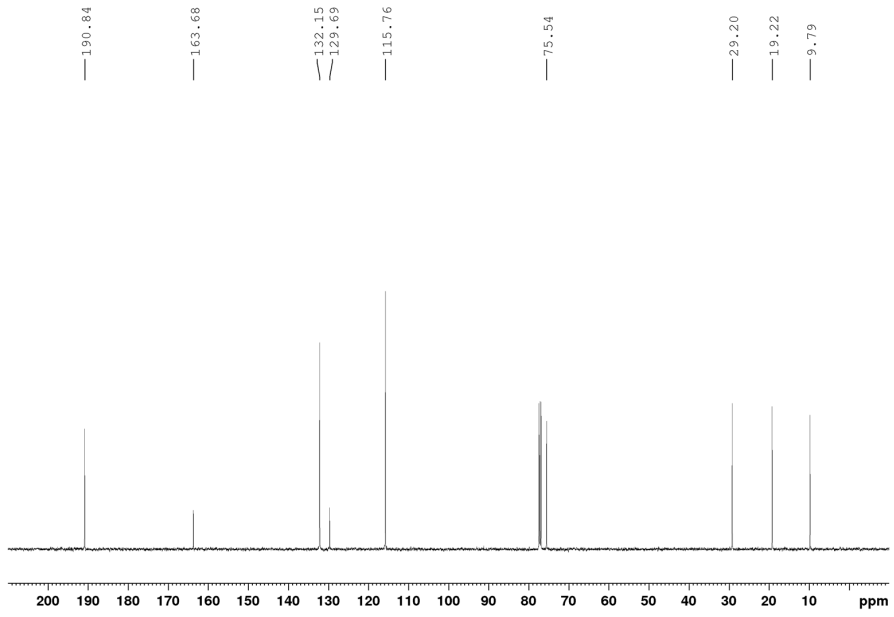

Figure A88. $^{13}C\{^{1}H\}$ NMR spectrum of 4-(*sec*-butoxy)benzaldehyde, **3-3f** ($CDCl_3$, 126 MHz).

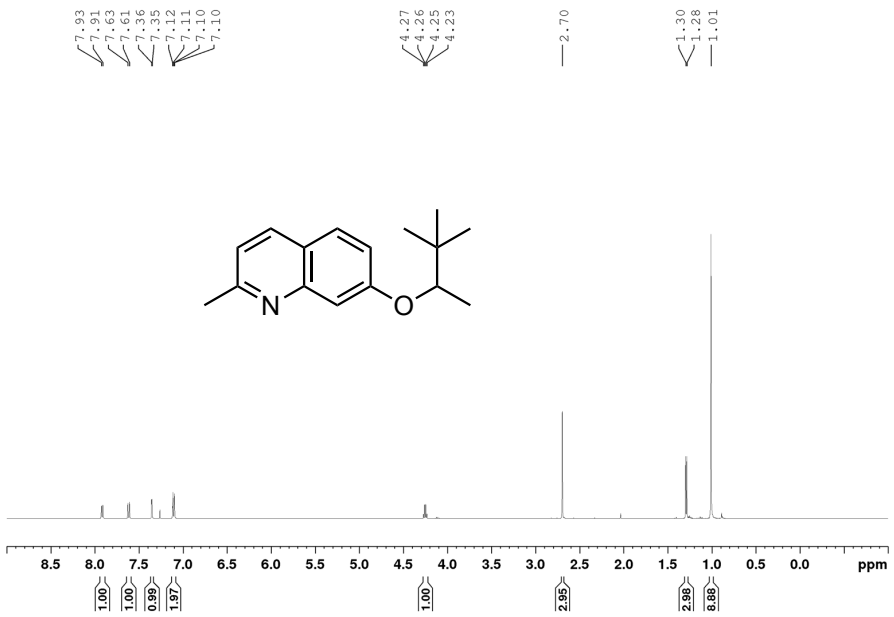

Figure A89. ^{1}H NMR spectrum of 7-((3,3-dimethylbutan-2-yl)oxy)-2-methylquinoline, **3-3g** ($CDCl_3$, 500 MHz).

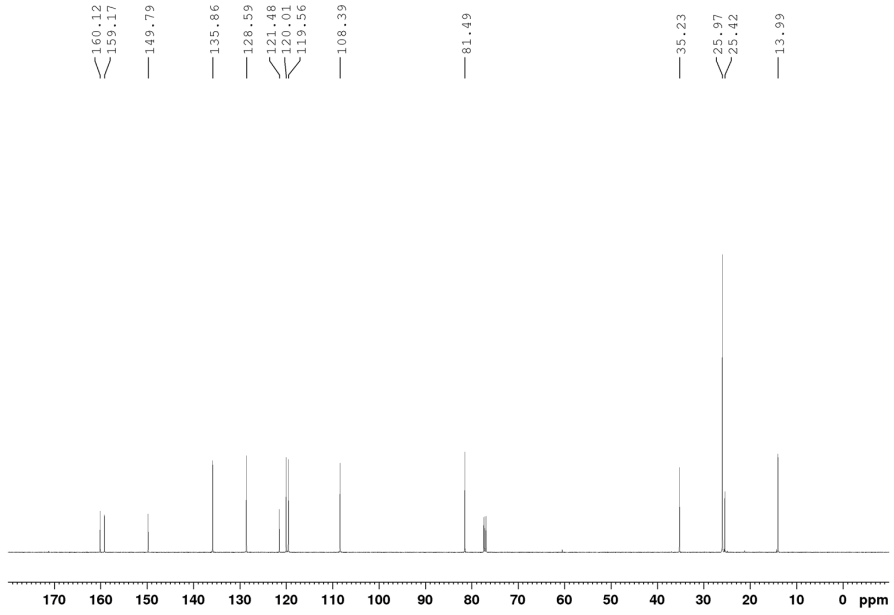

Figure A90. $^{13}C\{^{1}H\}$ NMR spectrum of 7-((3,3-dimethylbutan-2-yl)oxy)-2-methylquinoline, **3-3g** ($CDCl_3$, 126 MHz).

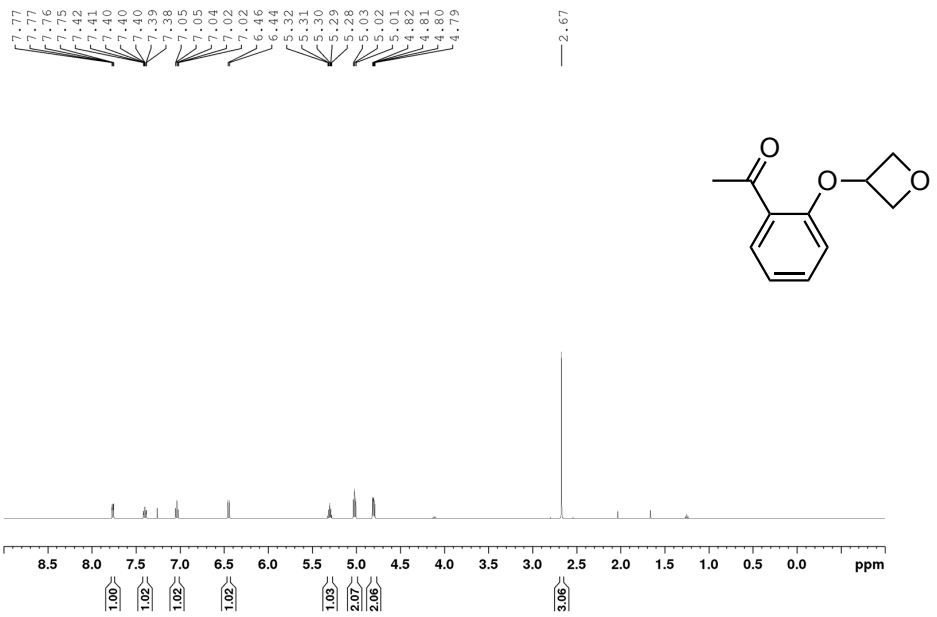

Figure A91. ^{1}H NMR spectrum of 1-(2-(oxetan-3-yloxy)phenyl)ethan-1-one, **3-3h** ($CDCl_3$, 500 MHz).

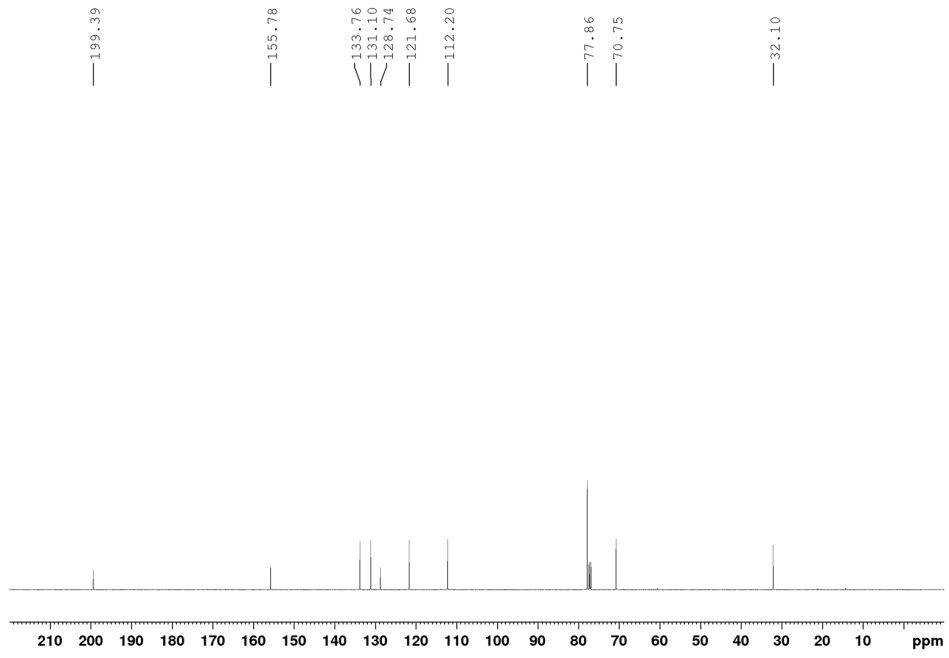

Figure A92. $^{13}C\{^{1}H\}$ NMR spectrum of 1-(2-(oxetan-3-yloxy)phenyl)ethan-1-one, **3-3h** ($CDCl_3$, 126 MHz).

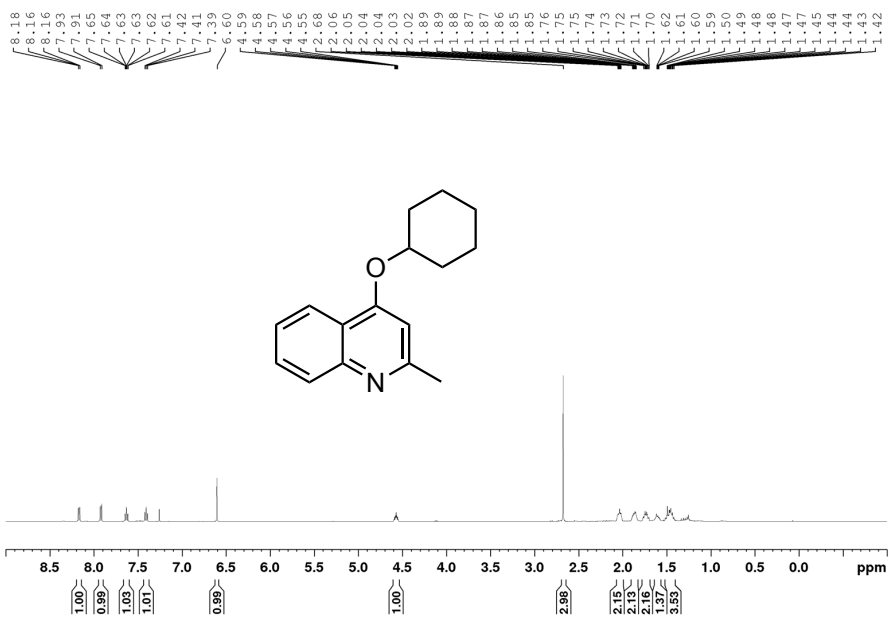

Figure A93. ^{1}H NMR spectrum of 4-(cyclohexyloxy)-2-methylquinoline, **3-3i** ($CDCl_3$, 500 MHz).

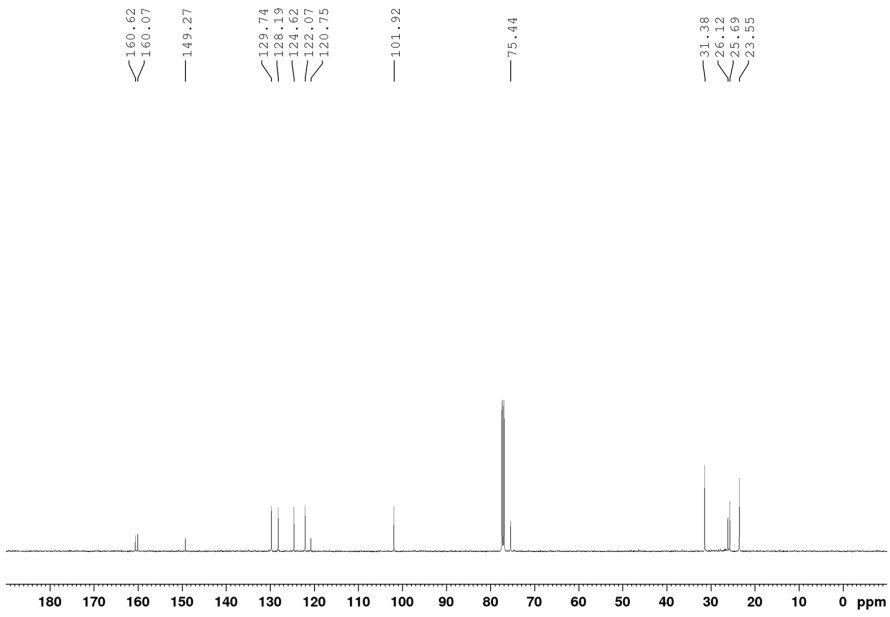

Figure A94. $^{13}C\{^{1}H\}$ NMR spectrum of 4-(cyclohexyloxy)-2-methylquinoline, **3-3i** ($CDCl_3$, 126 MHz).

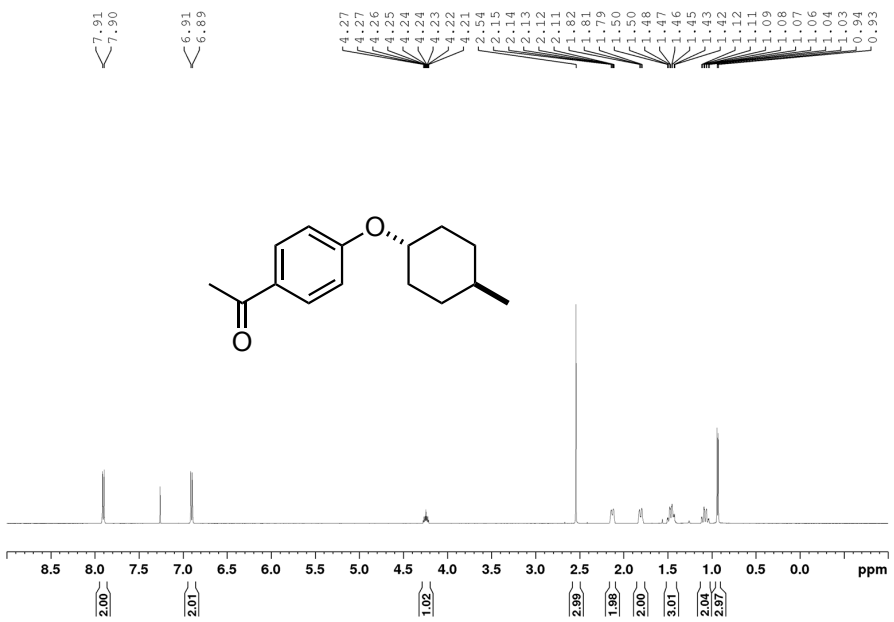

Figure A95. ^{1}H NMR spectrum of 1-(4-(((1*r*,4*r*)-4-methylcyclohexyl)oxy)phenyl)ethan-1-one, **3-3j** ($CDCl_3$, 500 MHz).

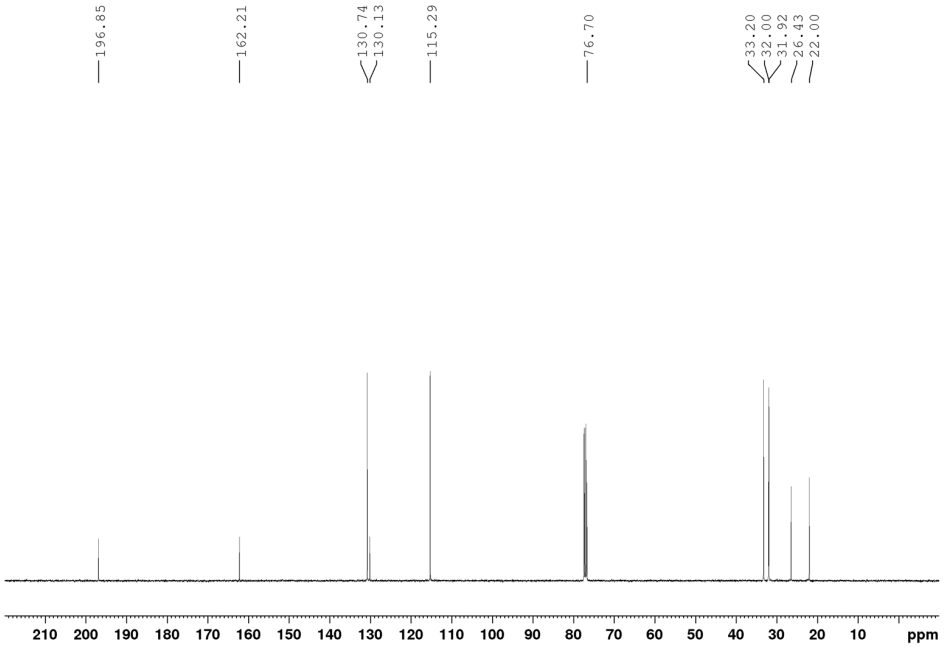

Figure A96. $^{13}C\{^{1}H\}$ NMR spectrum of 1-(4-(((1*r*,4*r*)-4-methylcyclohexyl)oxy)phenyl)ethan-1-one, **3-3j** ($CDCl_3$, 126 MHz).

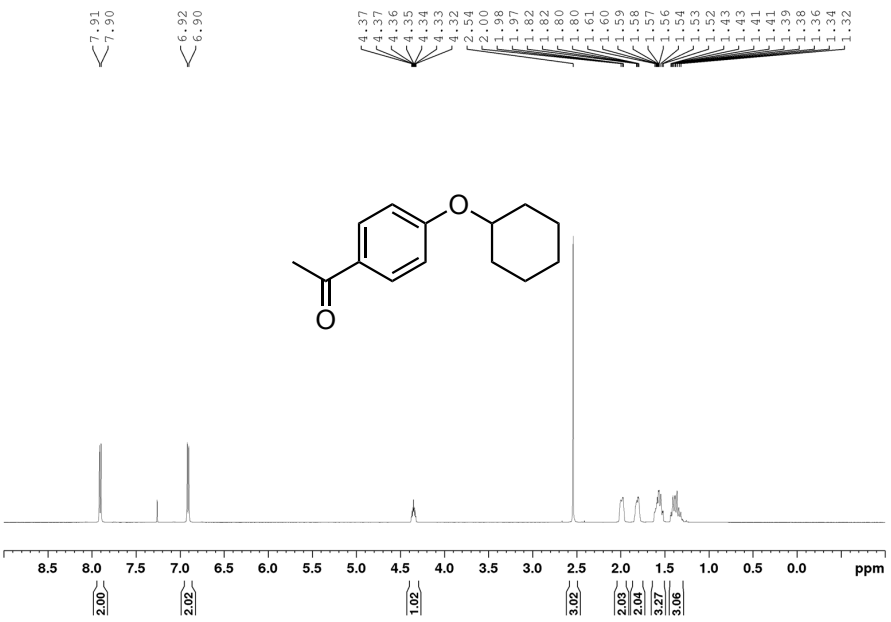

Figure A97. ^{1}H NMR spectrum of 1-(4-(cyclohexyloxy)phenyl)ethan-1-one, **3-3k** ($CDCl_3$, 500 MHz).

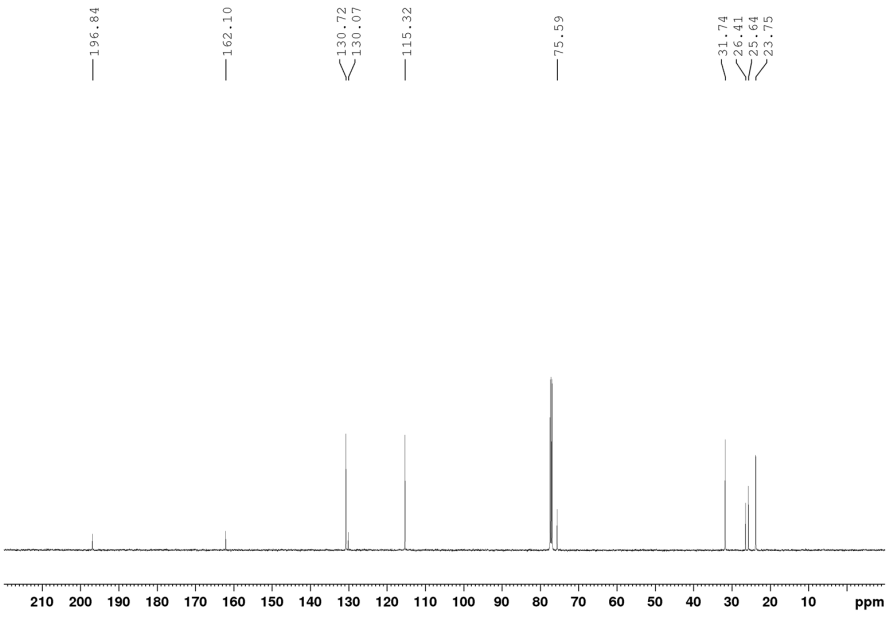

Figure A98. $^{13}C\{^{1}H\}$ NMR spectrum of 1-(4-(cyclohexyloxy)phenyl)ethan-1-one, **3-3k** ($CDCl_3$, 126 MHz).

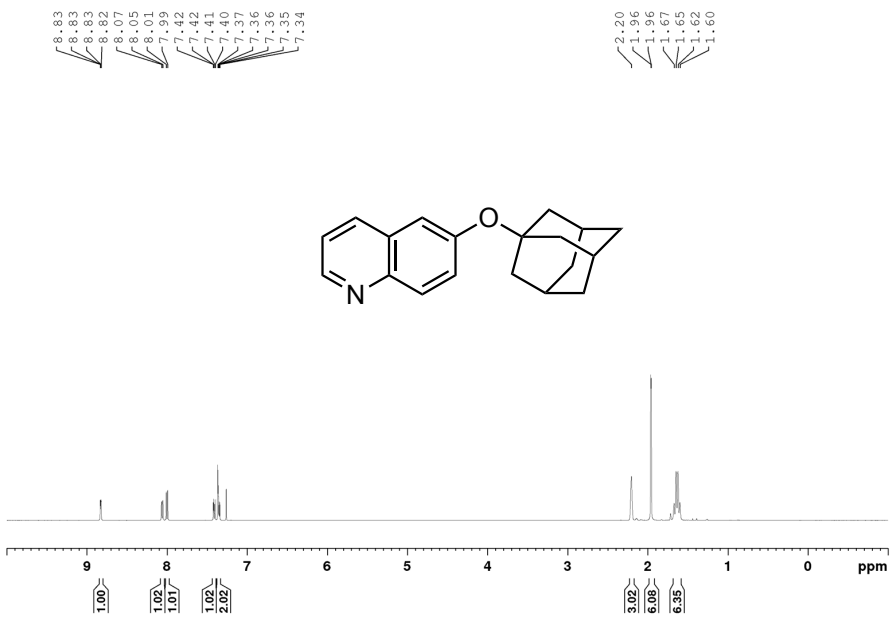

Figure A99. ^{1}H NMR spectrum of 6-((adamantan-1-yl)oxy)quinoline, **3-3l** ($CDCl_3$, 500 MHz).

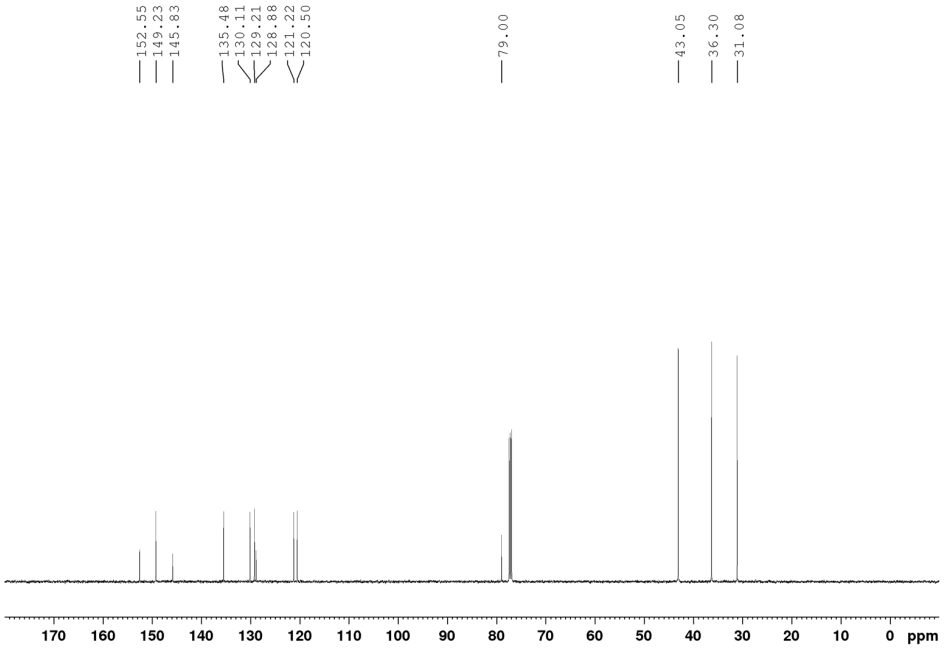

Figure A100. $^{13}C\{^{1}H\}$ NMR spectrum of 6-((adamantan-1-yl)oxy)quinoline, **3-3l** ($CDCl_3$, 126 MHz).

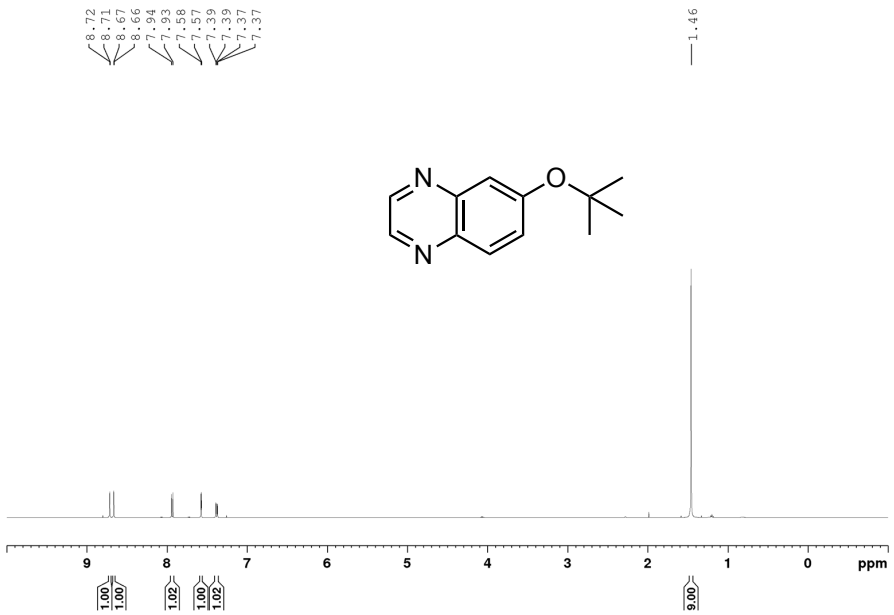

Figure A101. ^{1}H NMR spectrum of 6-(*tert*-butoxy)quinoxaline, **3-3m** ($CDCl_3$, 500 MHz).

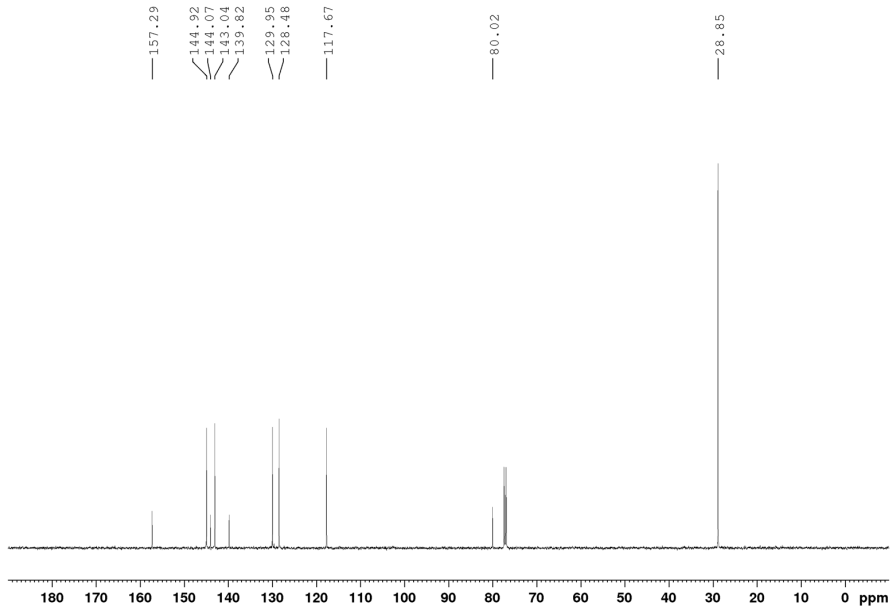

Figure A102. $^{13}C\{^{1}H\}$ NMR spectrum of 6-(*tert*-butoxy)quinoxaline, **3-3m** ($CDCl_3$, 126 MHz).

Figure A103. ^{1}H NMR spectrum of 1-((4-methylpentyl)oxy)naphthalene, **3-4a** ($CDCl_3$, 500 MHz).

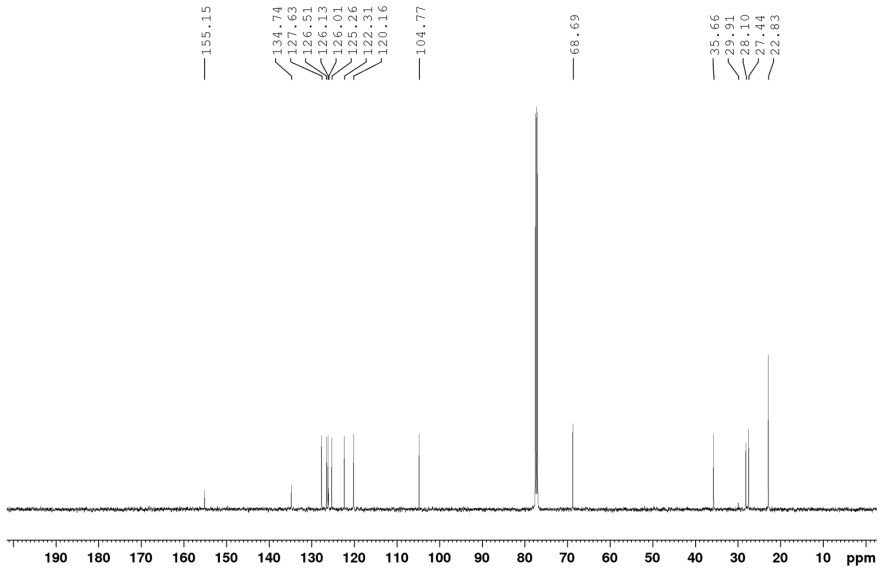

Figure A104. $^{13}C\{^{1}H\}$ NMR spectrum of 1-((4-methylpentyl)oxy)naphthalene, **3-4a** ($CDCl_3$, 126 MHz).

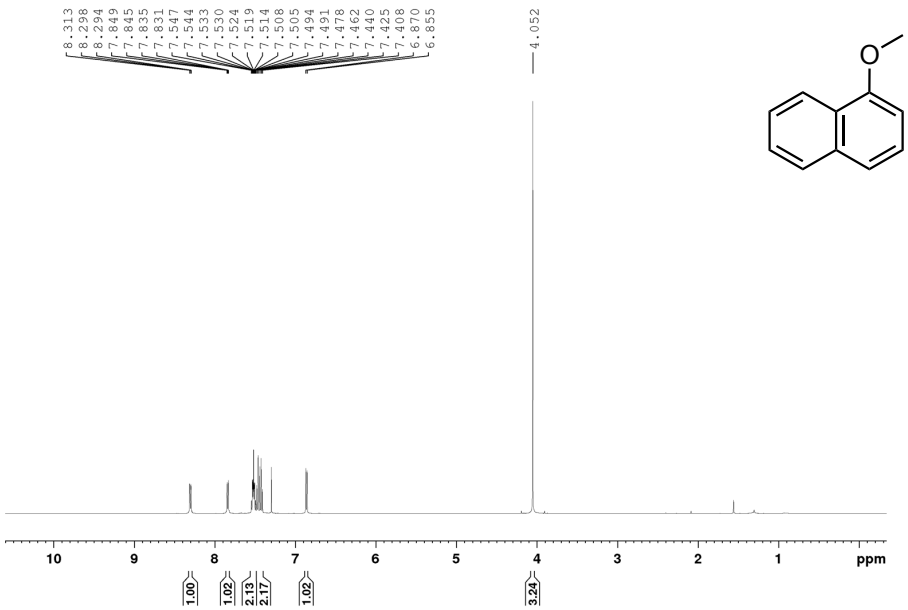

Figure A105. ^{1}H NMR spectrum of 1-methoxynaphthalene, **3-4b** ($CDCl_3$, 500 MHz).

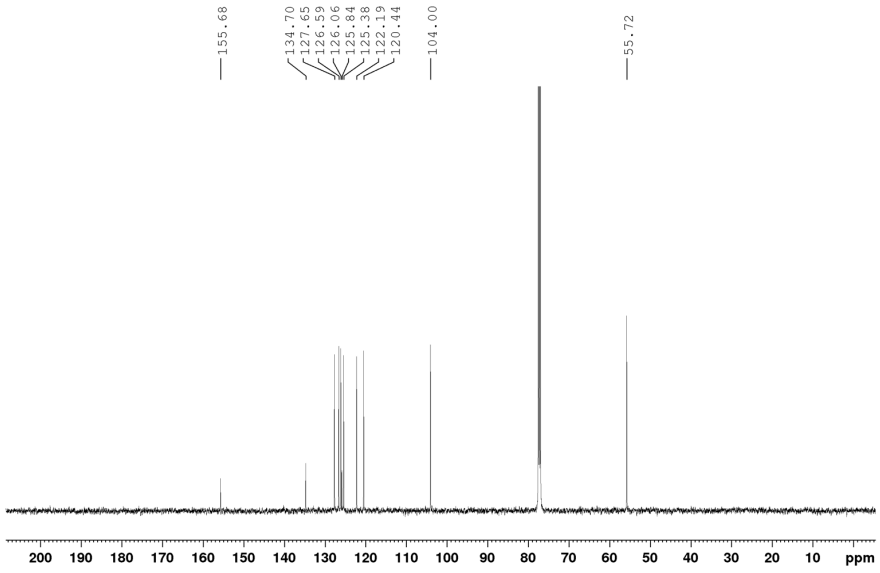

Figure A106. $^{13}C\{^{1}H\}$ NMR spectrum of 1-methoxynaphthalene, **3-4b** ($CDCl_3$, 126 MHz).

Figure A107. ^{1}H NMR spectrum of 6-methoxyquinoline, **3-4c** ($CDCl_3$, 500 MHz).

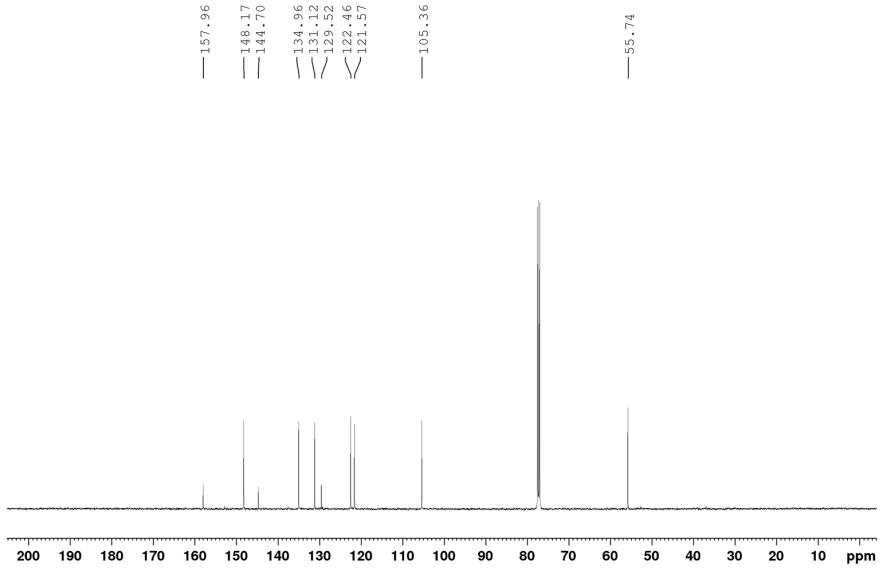

Figure A108. $^{13}C\{^{1}H\}$ NMR spectrum of 6-methoxyquinoline, **3-4c** ($CDCl_3$, 126 MHz).

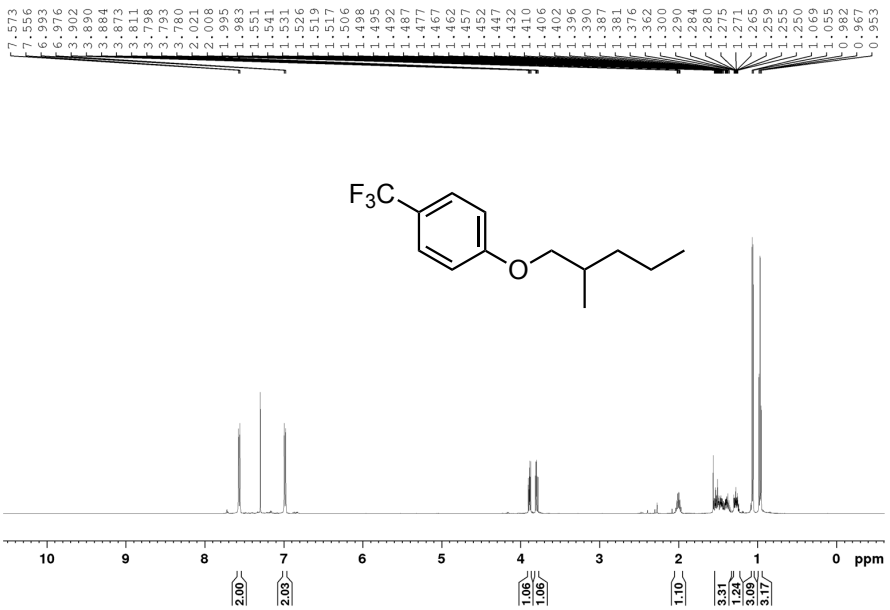

Figure A109. ^{1}H NMR spectrum of 1-((2-methylpentyl)oxy)-4-(trifluoromethyl)benzene, **3-4d** ($CDCl_3$, 500 MHz).

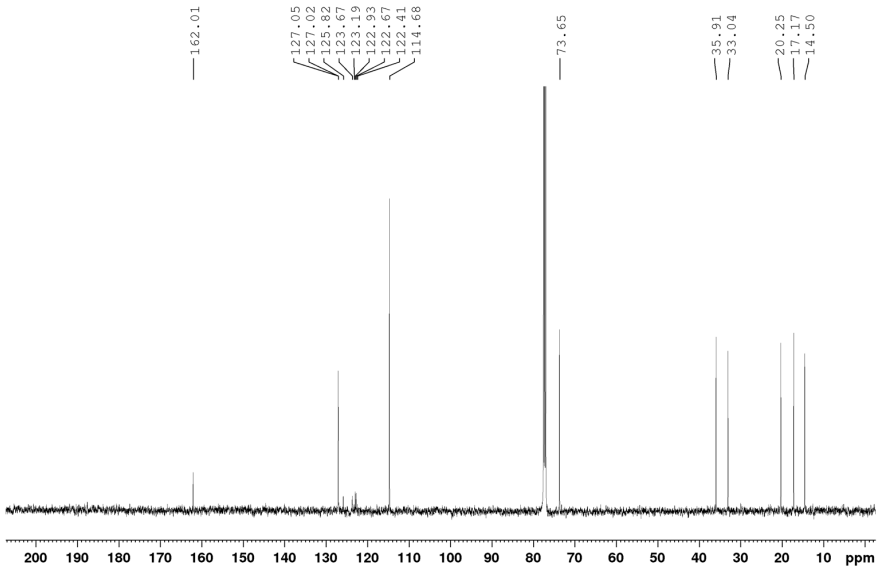

Figure A110. $^{13}C\{^{1}H\}$ NMR spectrum of 1-((2-methylpentyl)oxy)-4-(trifluoromethyl)benzene, **3-4d** ($CDCl_3$, 126 MHz).

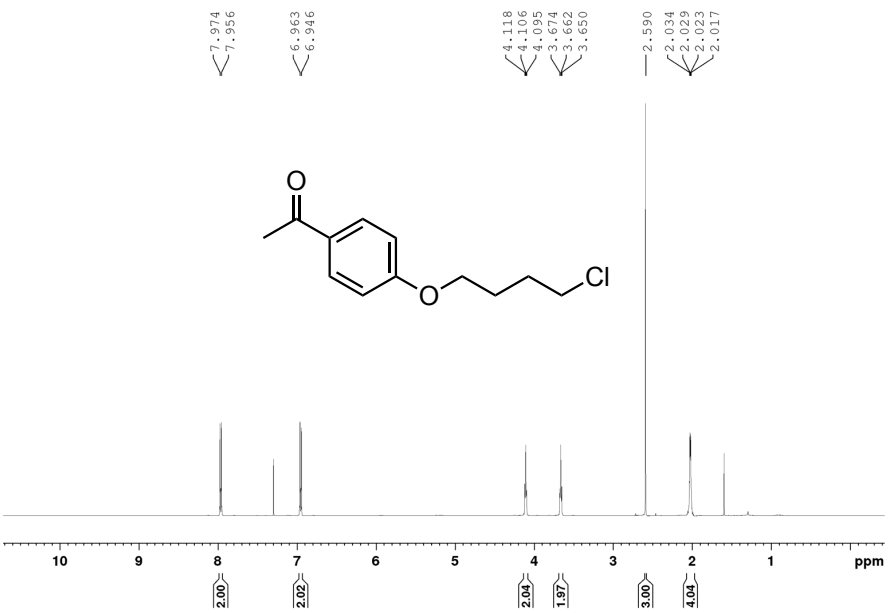

Figure A111. ^{1}H NMR spectrum of 1-(4-(4-chlorobutoxy)phenyl)ethan-1-one, **3-4e** ($CDCl_3$, 500 MHz).

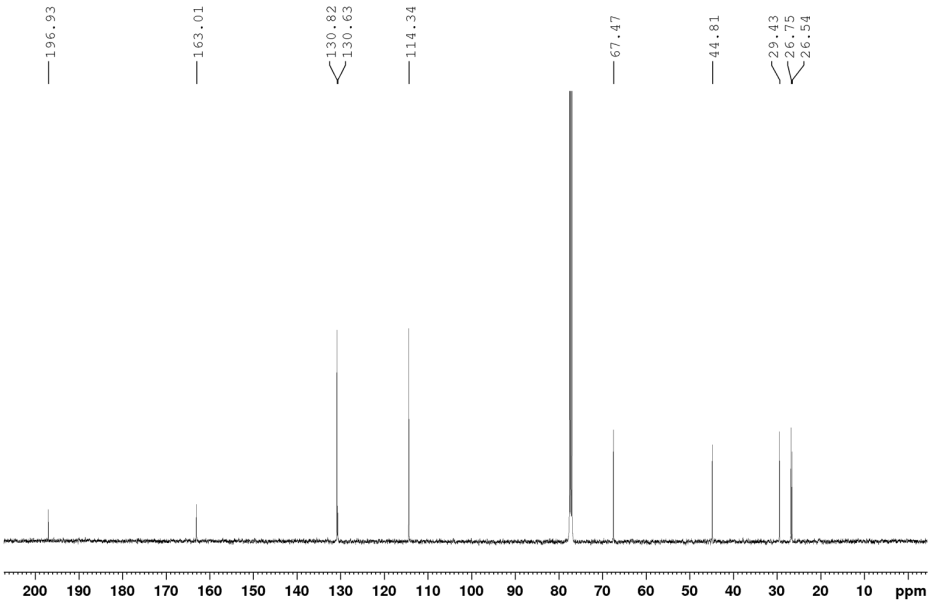

Figure A112. $^{13}C\{^{1}H\}$ NMR spectrum of 1-(4-(4-chlorobutoxy)phenyl)ethan-1-one, **3-4e** ($CDCl_3$, 126 MHz).

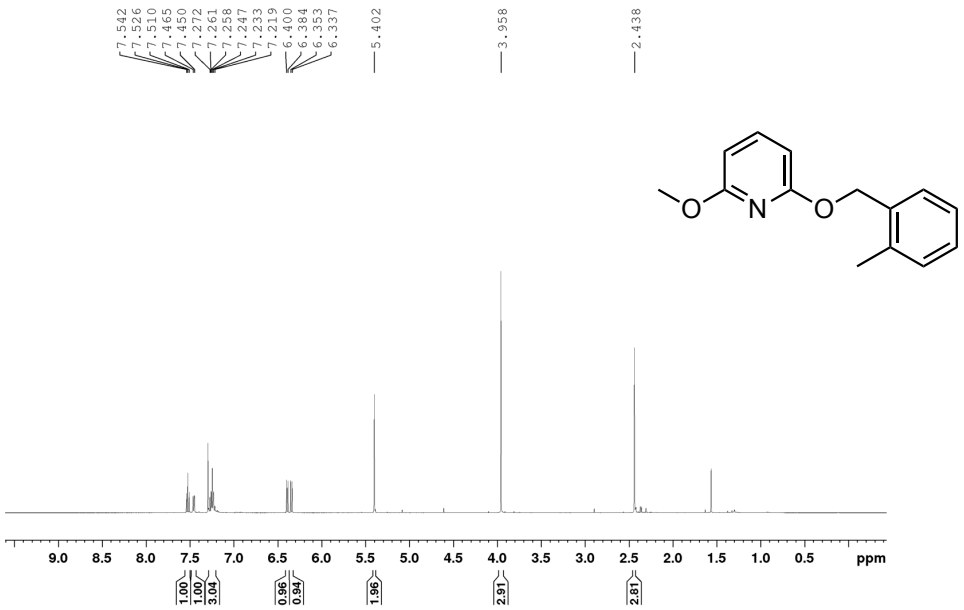

Figure A113. ^{1}H NMR spectrum of 2-methoxy-6-((2-methylbenzyl)oxy)pyridine, **3-4f** ($CDCl_3$, 500 MHz).

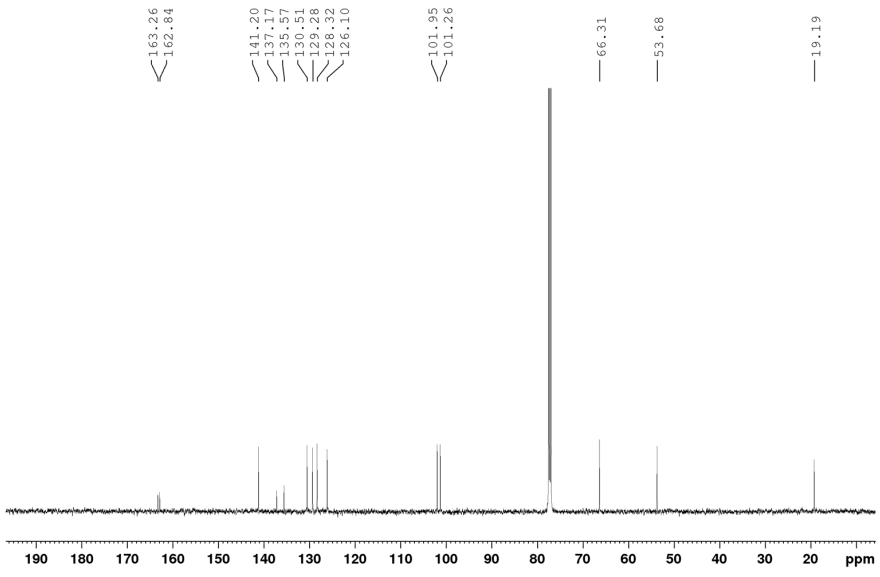

Figure A114. $^{13}C\{^{1}H\}$ NMR spectrum of 2-methoxy-6-((2-methylbenzyl)oxy)pyridine, **3-4f** ($CDCl_3$, 126 MHz).

Figure A115. ^{1}H NMR spectrum of 4-cyclopropylmethoxy-2-methylquinoline, **3-4g** ($CDCl_3$, 500 MHz).

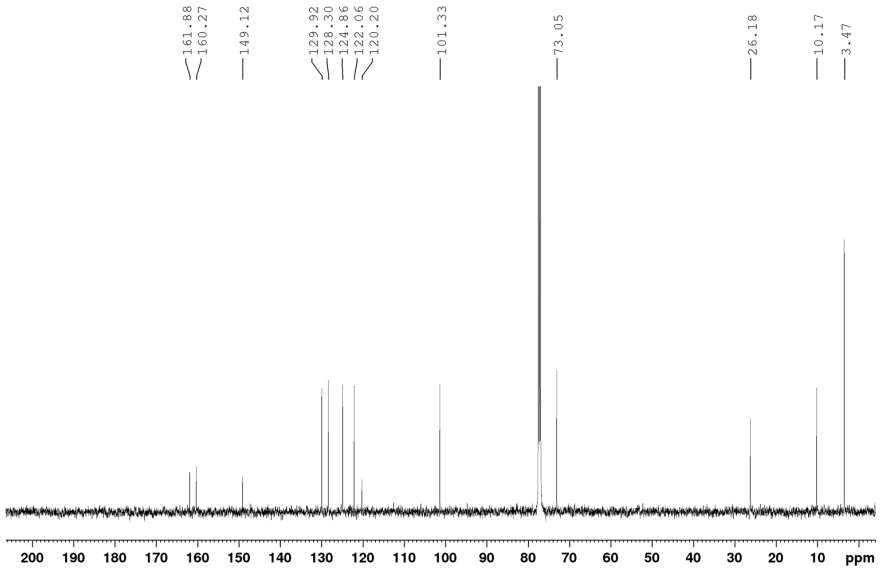

Figure A116. $^{13}C\{^{1}H\}$ NMR spectrum of 4-cyclopropylmethoxy-2-methylquinoline, **3-4g** ($CDCl_3$, 126 MHz).

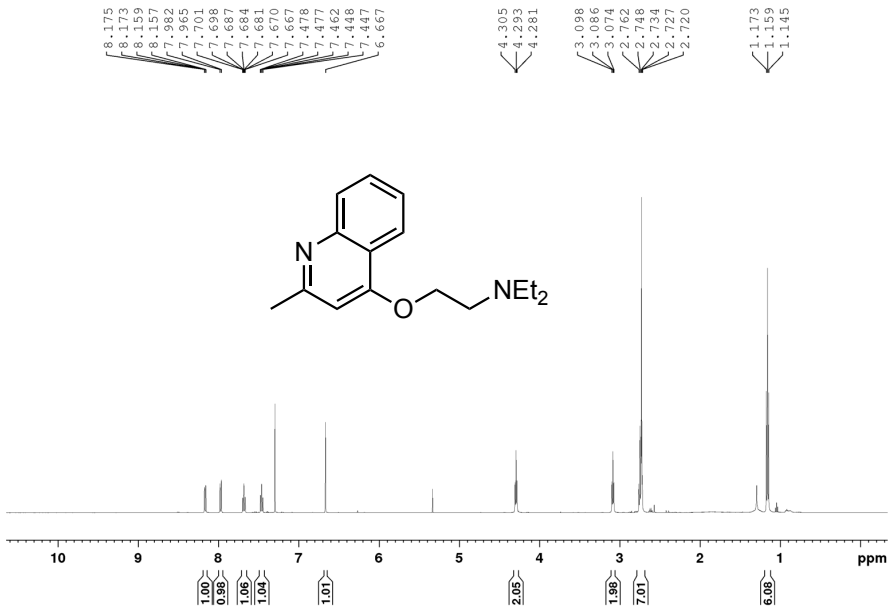

Figure A117. ^{1}H NMR spectrum of *N*,*N*-diethyl-2-((2-methylquinolin-4-yl)oxy)ethan-1-amine, **3-4h** ($CDCl_3$, 500 MHz).

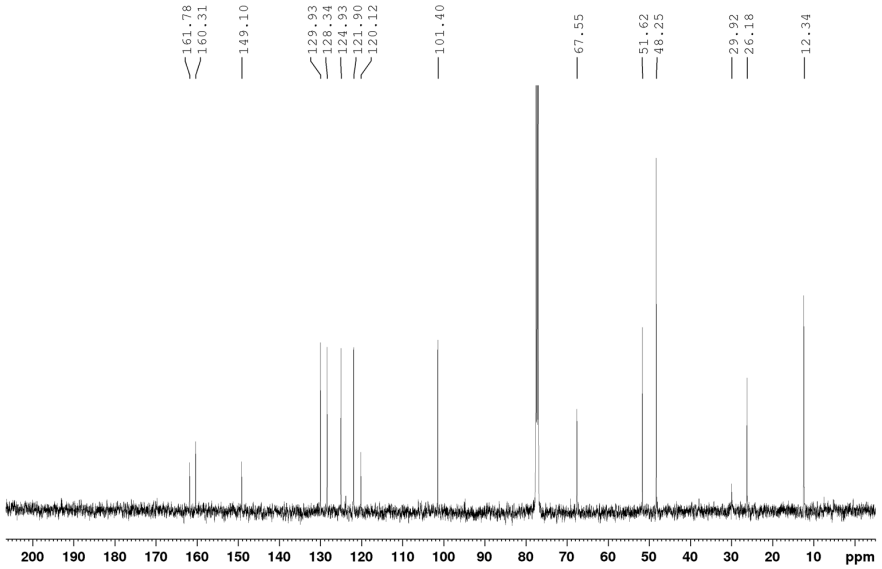

Figure A118. $^{13}C\{^{1}H\}$ NMR spectrum of *N*,*N*-diethyl-2-((2-methylquinolin-4-yl)oxy)ethan-1-amine, **3-4h** ($CDCl_3$, 126 MHz).

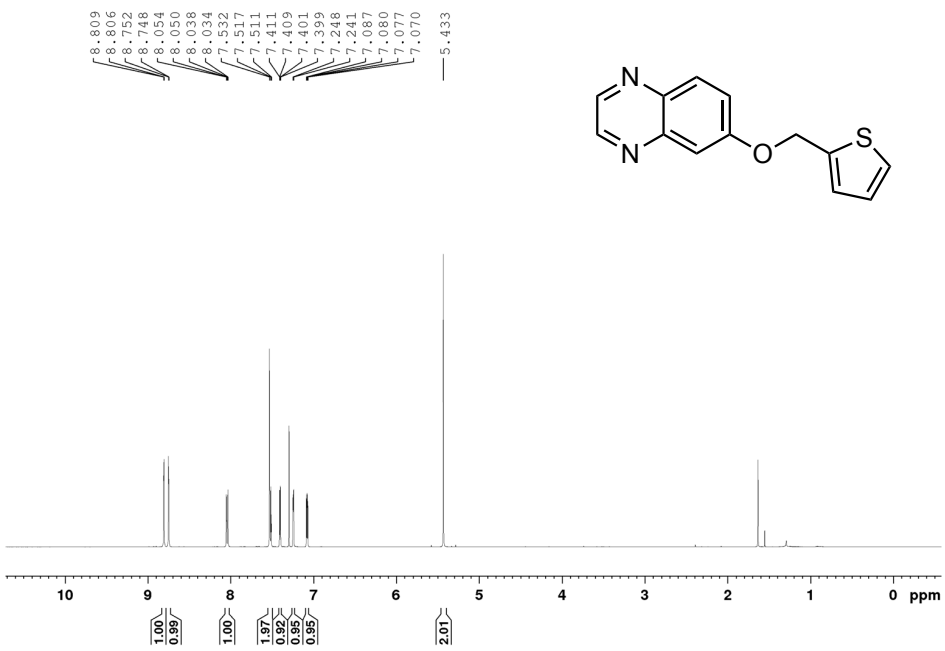

Figure A119. ^{1}H NMR spectrum of 6-(thiophen-2-ylmethoxy)quinoxaline, **3-4i** ($CDCl_3$, 500 MHz).

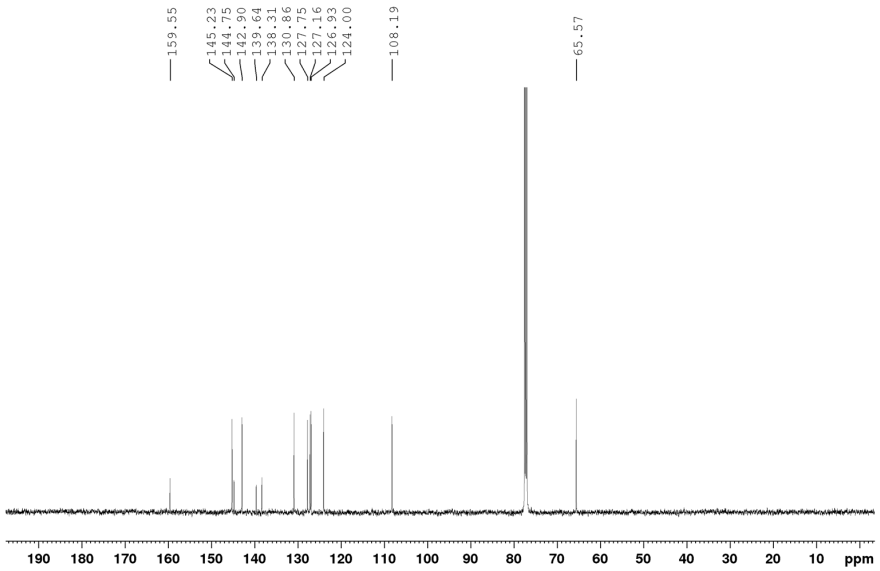

Figure A120. $^{13}C\{^{1}H\}$ NMR spectrum of 6-(thiophen-2-ylmethoxy)quinoxaline, **3-4i** ($CDCl_3$, 126 MHz).

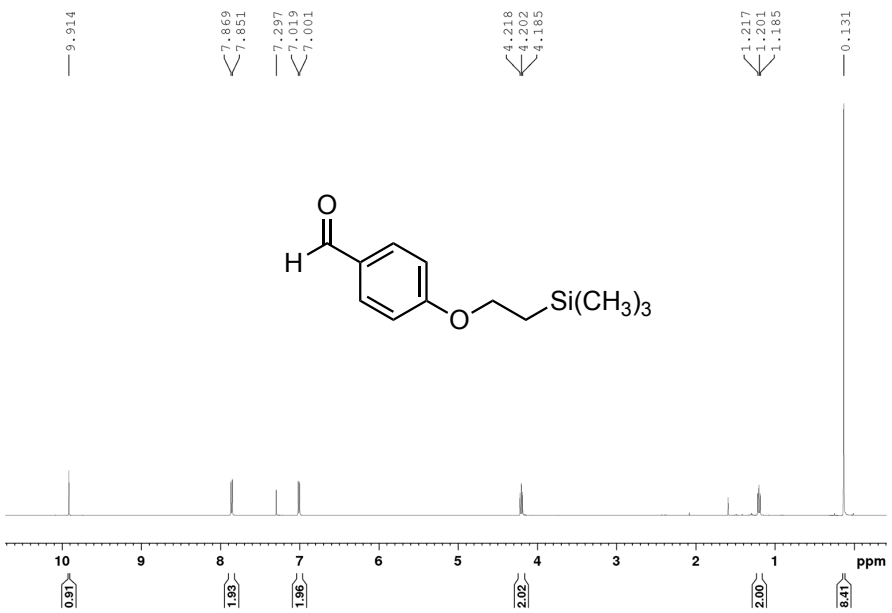

Figure A121. ^{1}H NMR spectrum of 4-(2-(trimethylsilyl)ethoxy)benzaldehyde, **3-4j** ($CDCl_3$, 500 MHz).

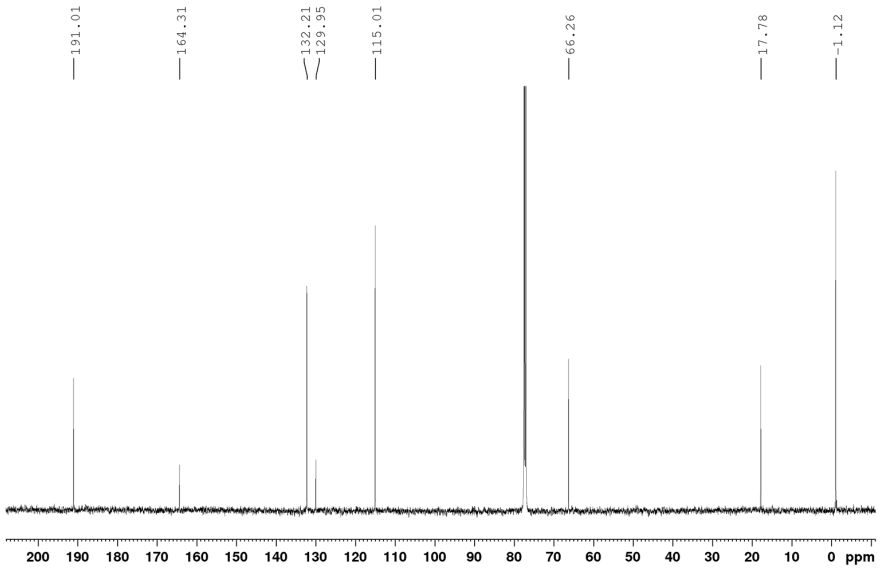

Figure A122. $^{13}C\{^{1}H\}$ NMR spectrum of 4-(2-(trimethylsilyl)ethoxy)benzaldehyde, **3-4j** ($CDCl_3$, 126 MHz).

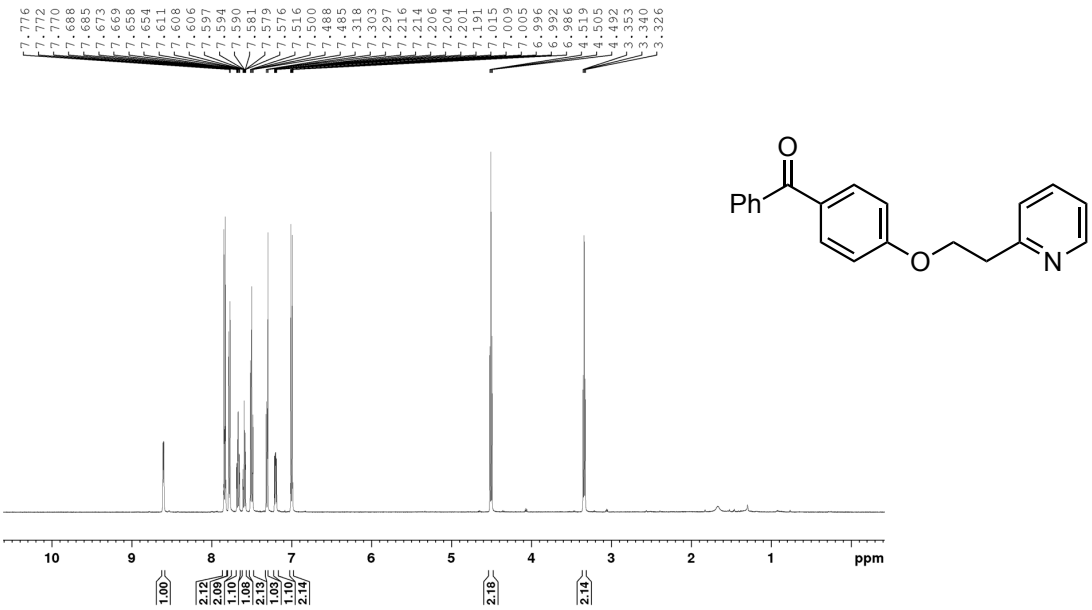

Figure A122. ^{1}H NMR spectrum of phenyl(4-(2-(pyridin-2-yl)ethoxy)-phenyl)methanone, **3-4k** ($CDCl_3$, 500 MHz).

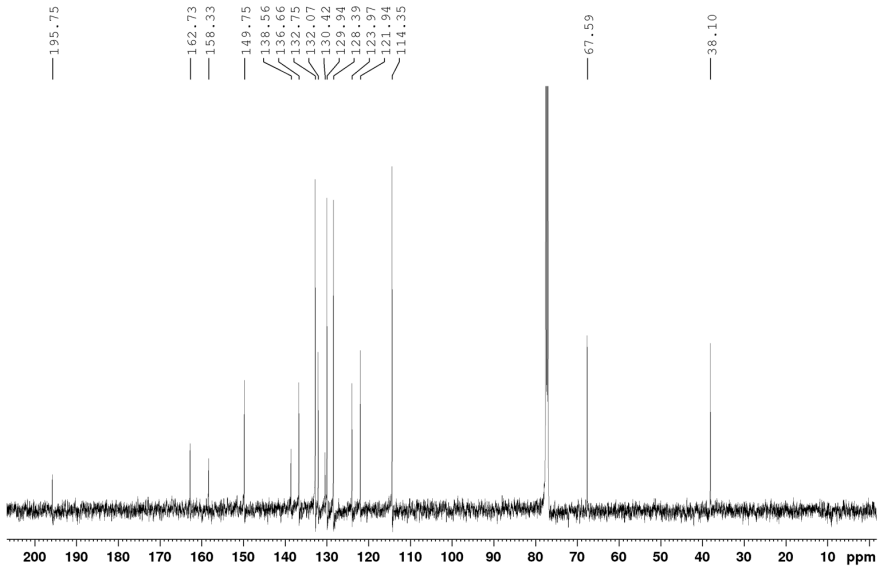

Figure A123. $^{13}C\{^{1}H\}$ NMR spectrum of phenyl(4-(2-(pyridin-2-yl)ethoxy)-phenyl)methanone, **3-4k** ($CDCl_3$, 126 MHz).

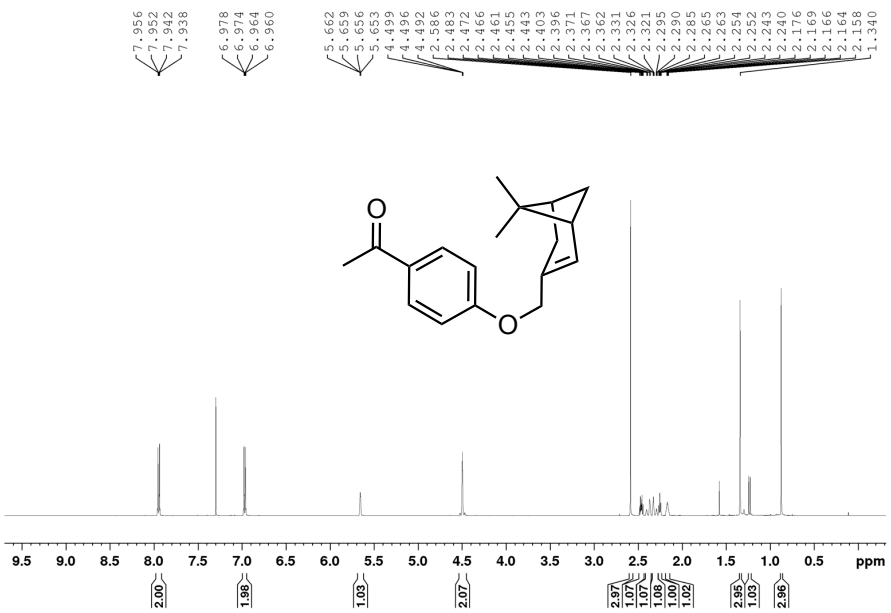

Figure A124. ^{1}H NMR spectrum of 1-[4- (6,6-dimethyl-bicyclo[3.1.1]hept-2-en-3-ylmethoxy)-phenyl]-ethanone, **3-4l** ($CDCl_3$, 500 MHz).

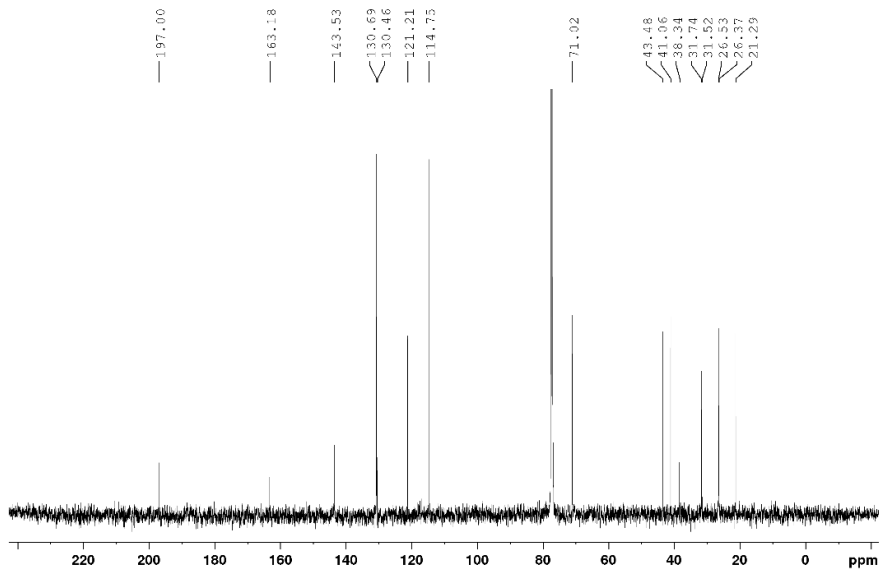

Figure A125. $^{13}C\{^{1}H\}$ NMR spectrum of 1-[4-(6,6-dimethyl-bicyclo[3.1.1]hept-2-en-3-ylmethoxy)-phenyl]-ethanone, **3-4l** ($CDCl_3$, 126 MHz).

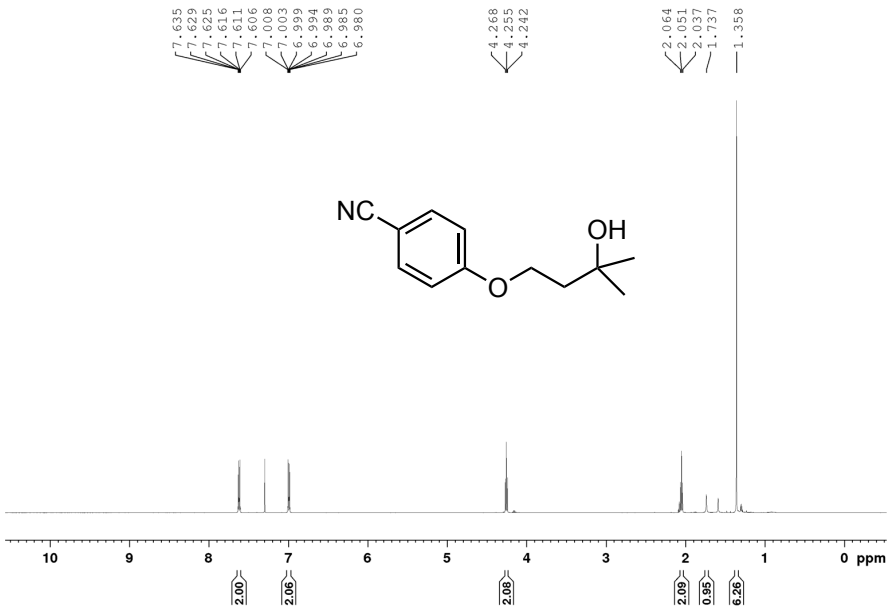

Figure A126. ^{1}H NMR spectrum of 4-(3-hydroxy-3-methylbutoxy)benzonitrile, **3-4m** ($CDCl_3$, 500 MHz).

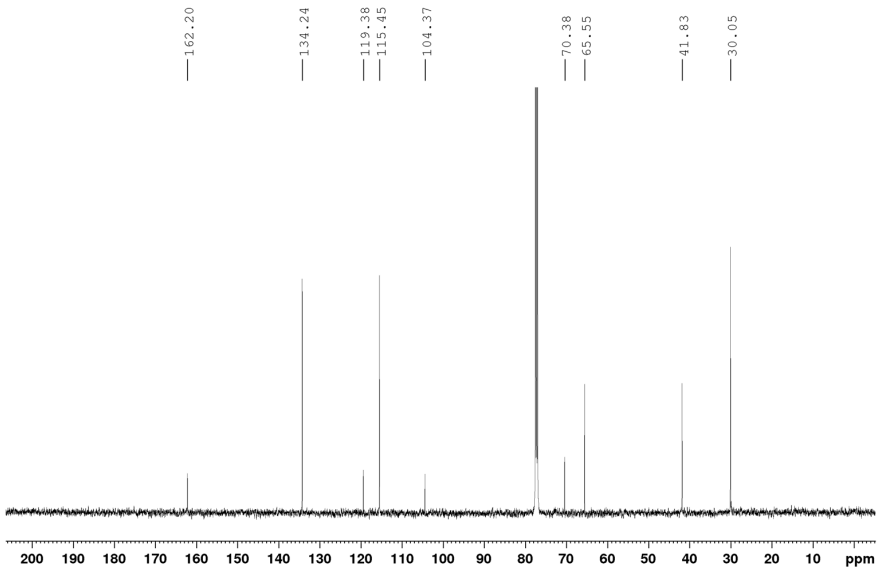

Figure A127. $^{13}C\{^{1}H\}$ NMR spectrum of 4-(3-hydroxy-3-methylbutoxy)benzonitrile, **3-4m** ($CDCl_3$, 126 MHz).

Appendix 5: Crystallographic Solution and Refinement Details for 4-C1 and 4-C2

4-C1. Crystallographic data for **4-C1** were obtained at –100(±2) °C on a Bruker D8/APEX II CCD diffractometer using Cu Kα (λ = 1.54178 Å) microfocus source radiation, employing a sample that was mounted in inert oil and transferred to a cold gas stream on the diffractometer. Programs for diffractometer operation, data collection, data reduction, and absorption correction were supplied by Bruker. Gaussian integration (face-indexed) was employed as the absorption correction method. The structure of **4-C1** was solved by use of intrinsic phasing methods and refined by use of full-matrix least-squares procedures (on F^2) with R_1 based on $F_o^2 \geq 2\sigma(F_o^2)$ and wR_2 based on all data. Anisotropic displacement parameters were employed for all the non-hydrogen atoms shown. Non-hydrogen atoms are represented by Gaussian ellipsoids at the 30% probability level. For further information, please refer to the deposited CIF (CCDC 1877193).

4-C2. Crystallographic data for **4-C2**•CH_2Cl_2 were obtained at –100(±2) °C on a Bruker D8/APEX II CCD diffractometer using Cu Kα (λ = 1.54178 Å) microfocus source radiation, employing a sample that was mounted in inert oil and transferred to a cold gas stream on the diffractometer. Programs for diffractometer operation, data collection, data reduction, and absorption correction were supplied by Bruker. Gaussian integration (face-indexed) was employed as the absorption correction method. The structure of **4-C2** was solved by use of intrinsic phasing methods and refined by use of full-matrix least-squares procedures (on F^2) with R_1 based on $F_o^2 \geq 2\sigma(F_o^2)$ and wR_2 based on all data. Positional disorder was observed for the Ni-bound *ortho*-tolyl fragment during solution and refinement. The minor component of the disordered tolyl group was restrained to have approximately the same geometry as that of the major component by use of the *SHELXL* **SAME** instruction. Further, the minor component also had a rigid bond restraint applied by use of the *SHELXL* **RIGU** instruction. Anisotropic displacement parameters were employed for all the non-hydrogen atoms shown. Non-hydrogen atoms are represented by Gaussian ellipsoids at the 30% probability level. For further information, please refer to the deposited CIF (CCDC 1877194).

Table A4. Crystallographic experimental details for **4-C1**.

A. Crystal Data	
formula	$C_{35}H_{37}ClNiO_3P_2$
formula weight	661.74
crystal dimensions (mm)	0.31 × 0.21 × 0.03
crystal system	monoclinic
space group	$P2_1/n$ (an alternate setting of $P2_1/c$ [No. 14])
unit cell parameters	
a (Å)	8.6403(3)
b (Å)	21.4171(6)
c (Å)	17.6462(5)
β (deg)	103.3756(16)
V (Å^3)	3176.86(17)
Z	4
ρ_{calcd} (g cm^{-3})	1.384
μ (mm^{-1})	2.876
B. Data Collection and Refinement Conditions	
diffractometer	Bruker D8/APEX II CCD
radiation (λ [Å])	Cu Kα (1.54178) (microfocus source)
temperature (°C)	–100
scan type	ω and ϕ scans (1.0°) (5 s exposures)
data collection 2θ limit (deg)	140.44
total data collected	20893 (-10 ≤ h ≤ 10, -26 ≤ k ≤ 26, -21 ≤ l ≤ 21)
independent reflections	6004 (R_{int} = 0.0508)
number of observed reflections (*NO*)	5518 [$F_o^2 \geq 2\sigma(F_o^2)$]
structure solution method	intrinsic phasing (*SHELXT-2014*)
refinement method	full-matrix least-squares on F^2 (*SHELXL–2016*)
absorption correction method	Gaussian integration (face-indexed)
range of transmission factors	0.9930–0.5195
data/restraints/parameters	6004 / 0 / 380
goodness-of-fit (S) [all data]	1.089
final R indices	
R_1 [$F_o^2 \geq 2\sigma(F_o^2)$]	0.0342
wR_2 [all data]	0.0872
largest difference peak and hole	0.432 and –0.446 e Å^{-3}

Table A5. Crystallographic experimental details for **4-C2•**CH_2Cl_2.

A. Crystal Data	
formula	$C_{30}H_{43}Cl_3NiO_3P_2$
formula weight	678.64
crystal dimensions (mm)	0.23 × 0.16 × 0.10
crystal system	triclinic
space group	$P\bar{1}$ (No. 2)
unit cell parameters	
a (Å)	8.0175(3)
b (Å)	10.7802(3)
c (Å)	19.1998(6)
α (deg)	89.9510(13)
β (deg)	87.4986(17)
γ (deg)	73.0233(16)
V (Å^3)	1585.50(9)
Z	2
ρ_{calcd} (g cm^{-3})	1.422
μ (mm^{-1})	4.400
B. Data Collection and Refinement Conditions	
diffractometer	Bruker D8/APEX II CCD
radiation (λ [Å])	Cu Kα (1.54178) (microfocus source)
temperature (°C)	–100
scan type	ω and ϕ scans (1.0°) (5 s exposures)
data collection 2θ limit (deg)	144.80
total data collected	11192 ($-9 \le h \le 9$, $-13 \le k \le 13$, $-23 \le l \le 23$)
independent reflections	6023 (R_{int} = 0.0261)
number of observed reflections (*NO*)	5773 [$F_o^2 \ge 2\sigma(F_o^2)$]
structure solution method	intrinsic phasing (*SHELXT-2014*)
refinement method	full-matrix least-squares on F^2 (*SHELXL–2016*)
absorption correction method	Gaussian integration (face-indexed)
range of transmission factors	0.7135–0.4899
data/restraints/parameters	6023 / 60 / 422
goodness-of-fit (S) [all data]	1.146
final R indices	
R_1 [$F_o^2 \ge 2\sigma(F_o^2)$]	0.0511
wR_2 [all data]	0.1172
largest difference peak and hole	0.950 and –0.826 e Å^{-3}

Appendix 6: Additional Catalytic Data for Chapter 4

Table A6. Temperature optimization for the nickel-catalyzed cross-coupling of **4-1a** with **4-2a**.[a]

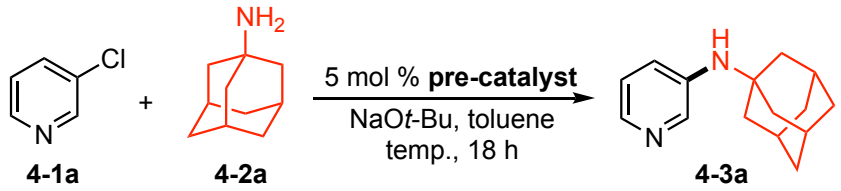

4-1a **4-2a** **4-3a**

Entry	Pre-catalyst	Temp. (°C)	Yield **4-3a** [%][b]	Remaining **4-1a** [%][b]
1	**2-C1**	110	<5	>95
2	**2-C2**	110	<5	>95
3	**3-C1**	110	<5	>95
4	**2-C3**	110	68	32
5	**2-C4**	110	<5	>95
6	**4-C1**	110	65	35
7	**4-C2**	110	27	55
8	**2-C3**	80	54	46
9	**4-C1**	80	91	9
10	**4-C1**	60	90	8
11	**4-C1**	25	73	27
12[c]	**4-C1**	60	86	13
13[d]	**4-C1**	60	77	20
14[e]	**4-C1**	60	70	29

[a]Reaction conditions: pre-catalyst (5 mol %), NaO*t*-Bu (1.5 equiv), **4-1a** (0.12 mmol, 1.0 equiv), **4-2a** (1.1 equiv), and toluene (1 mL, [ArCl] = 0.12 M) at the indicated temperature. [b]Conversions to product and remaining starting material are estimated on the basis of calibrated GC data. [c]**4-2a** (1.5 equiv). [d]Toluene (0.5 mL, [ArCl] = 0.24M). [e]**4-C1** (4 mol %).

Table A7. Temperature optimization for the nickel-catalyzed cross-coupling of **4-1b** with **4-2a**.[a]

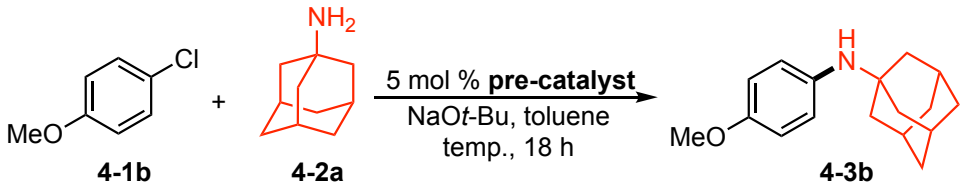

4-1b **4-2a** **4-3b**

Entry	Pre-catalyst	Temp. (°C)	Yield **4-3b** [%][b]	Remaining **4-1b** [%][b]
1	**2-C1**	110	11	89
2	**2-C2**	110	<5	>95
3	**3-C1**	110	<5	>95
4	**2-C3**	110	49	51
5	**2-C4**	110	8	89
6	**4-C1**	110	83	15
7	**4-C2**	110	27	66
8	**2-C3**	80	47	53
9	**4-C1**	80	66	28
10	**4-C1**	60	49	50
11	**4-C1**	25	9	89

[a]Reaction conditions: pre-catalyst (5 mol %), NaO*t*-Bu (1.5 equiv), **4-1b** (0.12 mmol, 1.0 equiv), **4-2a** (1.1 equiv), and toluene (1 mL, [ArCl] = 0.12 M) at the indicated temperature. [b]Conversions to product and remaining starting material are estimated on the basis of calibrated GC data.

Table A8. Temperature optimization for the nickel-catalyzed cross-coupling of **4-1c** with **4-2a**.[a]

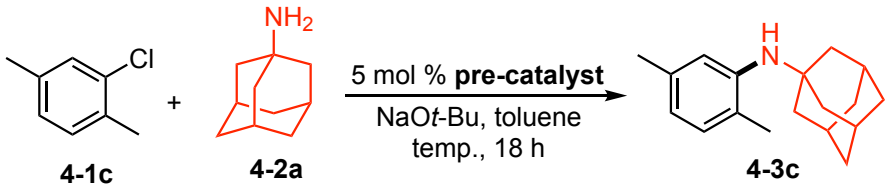

4-1c **4-2a** **4-3c**

Entry	Pre-catalyst	Temp (°C)	Yield **4-3c** [%][b]	Remaining **4-1c** [%][b]
1	**2-C1**	110	19	81
2	**2-C2**	110	<5	93
3	**3-C1**	110	<5	>95
4	**2-C3**	110	19	81
5	**2-C4**	110	6	89
6	**4-C1**	110	32	63
7	**4-C2**	110	27	67
8	**2-C3**	80	57	43
9	**4-C1**	80	49	45
10	**4-C1**	60	81	17
11	**4-C1**	25	39	56

[a]Reaction conditions: pre-catalyst (5 mol %), NaO*t*-Bu (1.5 equiv), **4-1c** (0.12 mmol, 1.0 equiv), **4-2a** (1.1 equiv), and toluene (1 mL, [ArCl] = 0.12 M) at the indicated temperature. [b]Conversions to product and remaining starting material are estimated on the basis of calibrated GC data.

Table A9. Solvent optimization for the nickel-catalyzed cross-coupling of **4-1a** with **4-2a** using **4-C1**.[a]

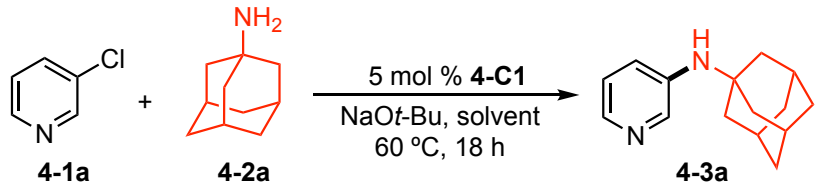

4-1a **4-2a** **4-3a**

Entry	Solvent	Yield **4-3a** [%][b]	Remaining **4-1a** [%][b]
1	toluene	90	8
2	CPME	75	25
3	1,4-dioxane	90	8
4	THF	20	74

[a]Reaction conditions: **4-C1** (5 mol %), NaO*t*-Bu (1.5 equiv), **4-1a** (0.12 mmol, 1.0 equiv), **4-2a** (1.1 equiv), and solvent (1 mL, [ArCl] = 0.12 M). [b]Conversions to product and remaining starting material are estimated on the basis of calibrated GC data.

Table A10. Solvent optimization for the nickel-catalyzed cross-coupling of **4-1b** with **4-2a** using **4-C1**.[a]

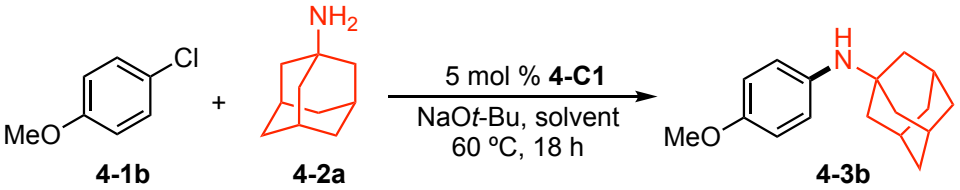

4-1b **4-2a** **4-3b**

Entry	Solvent	Yield **4-3b** [%][b]	Remaining **4-1b** [%][b]
1	toluene	49	50
2	CPME	33	62
3	1,4-dioxane	44	49
4	THF	20	74

[a]Reaction conditions: **4-C1** (5 mol %), NaO*t*-Bu (1.5 equiv), **4-1b** (0.12 mmol, 1.0 equiv), **4-2a** (1.1 equiv), and solvent (1 mL, [ArCl] = 0.12 M). [b]Conversions to product and remaining starting material are estimated on the basis of calibrated GC data.

Table A11. Base optimization for the nickel-catalyzed cross-coupling of **4-1a** with **4-2a** using **4-C1**.[a]

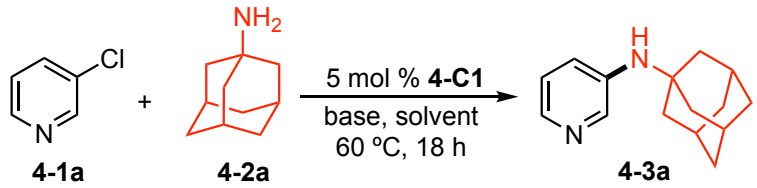

4-1a **4-2a** **4-3a**

Entry	Solvent	Base	Yield **4-3a** [%][b]	Remaining **4-1a** [%][b]
1	toluene	NaO*t*-Bu	90	8
2		LiO*t*-Bu	37	63
3		KO*t*-Bu	14	73
4		Cs_2CO_3[c]	0	>95
5		K_3PO_4[c]	0	>95
6		DBU[d]	0	>95
7	1,4-dioxane	NaO*t*-Bu	90	8
8		LiO*t*-Bu	67	33
9		KO*t*-Bu	7	86
10		Cs_2CO_3[c]	0	>95
11		K_3PO_4[c]	0	>95
12		DBU[d]	0	91

[a]Reaction conditions: **4-C1** (5 mol %), base (1.5 equiv), **4-1a** (0.12 mmol, 1.0 equiv), **4-2a** (1.1 equiv), and solvent (1 mL, [ArCl] = 0.12 M). [b]Conversions to product and remaining starting material are estimated on the basis of calibrated GC data. [c]Base (3.0 equiv). [d]Base (2.0 equiv).

Table A12. Base optimization for the nickel-catalyzed cross-coupling of **4-1b** with **4-2a** using **4-C1**.[a]

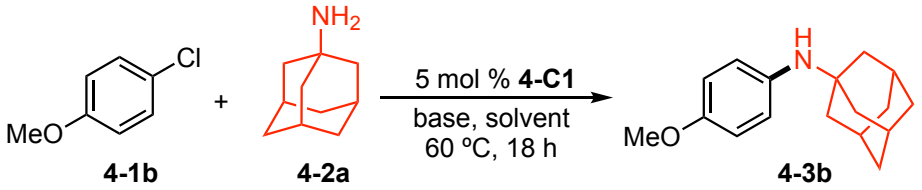

4-1b **4-2a** **4-3b**

Entry	Solvent	Base	Yield **4-3b** [%][b]	Remaining **4-1b** [%][b]
1	toluene	NaO*t*-Bu	49	50
2		LiO*t*-Bu	5	93
3		KO*t*-Bu	5	82
4		Cs_2CO_3[c]	<5	>95
5		K_3PO_4[c]	<5	>95
6		DBU[d]	<5	93
7	1,4-dioxane	NaO*t*-Bu	44	49
8		LiO*t*-Bu	46	51
9		KO*t*-Bu	<5	89
10		Cs_2CO_3[c]	<5	>95
11		K_3PO_4[c]	<5	91
12		DBU[d]	<5	95

[a]Reaction conditions: **4-C1** (5 mol %), base (1.5 equiv), **4-1b** (0.12 mmol, 1.0 equiv), **4-2a** (1.1 equiv), and solvent (1 mL, [ArCl] = 0.12 M). [b]Conversions to product and remaining starting material are estimated on the basis of calibrated GC data. [c]Base (3.0 equiv). [d]Base (2.0 equiv).

Table A13. Additional data for the pre-catalyst screen for the Ni-catalyzed cross-coupling of **9** with *tert*-butylamine (**4-2d**).[a]

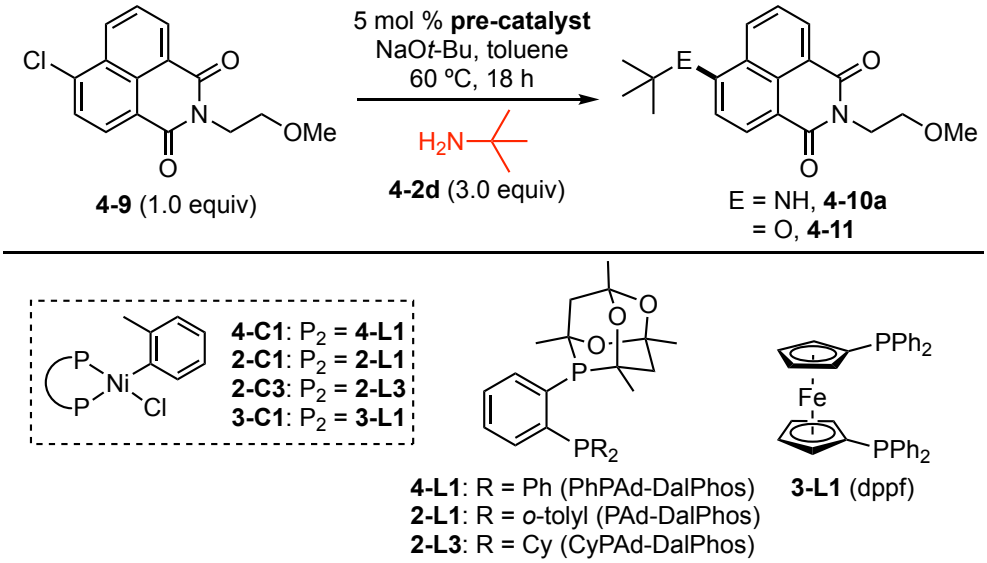

Entry	Pre-catalyst	Yield 4-**10a** (%)[b]	Remaining **4-9** (%)[b]	**4-11** (%)[b]	Other (%)[b]
1	**C1**	13	80	6	<5
2	**C2**	<5	78	18	<5
3	**C3**	<5	78	18	<5
4	**C4**	8	63	29	<5

[a]Reaction conditions: pre-catalyst (5 mol %), NaO*t*-Bu (1.5 equiv), **4-9** (0.12 mmol, 1.0 equiv), **4-2d** (3.0 equiv), and toluene (1.0 mL, [**4-9**] = 0.12 M). [b]Conversion to **4-10a** and remaining **4-9** are estimated on the basis of calibrated GC data, with the remaining mass balance attributed to the -O*t*-Bu cross-coupled product of **4-9** (**4-11**), as indicated.

Table A14. Additional data for the ligand screen and optimization for the Ni-catalyzed cross-coupling of **4-9** with *tert*-butylamine (**4-2d**).[a]

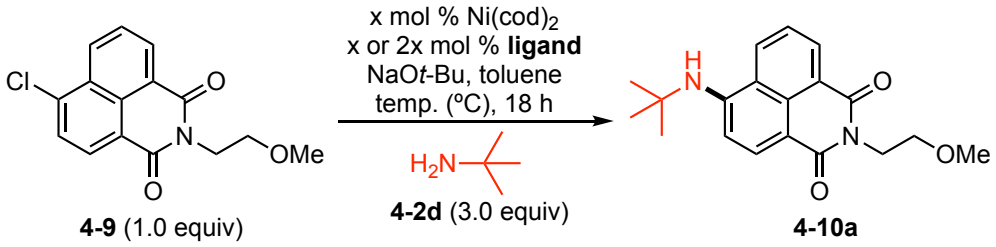

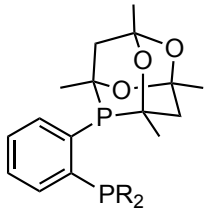

4-L1: R = Ph (PhPAd-DalPhos)
2-L1: R = *o*-tolyl (PAd-DalPhos)
2-L3: R = Cy (CyPAd-DalPhos)

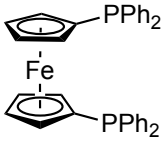

3-L1 (dppf)

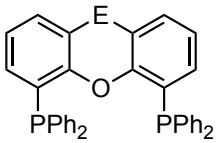

4-L3: E = $C(CH_3)_2$ (XantPhos)
4-L4: E = NH (*N*-XantPhos)
4-L5: E = nothing (DPEPhos)

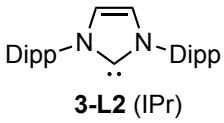

3-L2 (IPr)

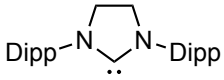

4-L6 (SIPr)

Entry	x	Ligand	Temp. (°C)	Yield **4-10a** (%)[b]	Remaining **4-9** (%)[b]	**4-11** (%)[b]	Other (%)[b]
1	10	**4-L1**	80	55	25	<5	19
2		**2-L1**		10	63	9	19
3		**2-L3**		15	55	8	21
4		**3-L1**		71	29	<5	<5
5		**4-L3**		51	23	<5	26
6		**4-L4**		68	28	<5	<5
7		**4-L5**		**>95**	<5	<5	<5
8		**3-L2**		**95**	<5	<5	<5
9		**4-L6**		71	<5	<5	38
10	5	**4-L5**	80	65	32	<5	<5
11		**3-L2**		**>95**	<5	<5	<5
12	5	**3-L2**	60	**>95**	<5	<5	<5
13		**3-L2**	25	**>95**	<5	<5	<5
14	4	**3-L2**	25	**>95**	<5	<5	<5
15	3	**3-L2**	25	83	17	<5	<5
16	5	-	25	<5	53	<5	47
17[c]	5	**3-L2**	25	<5	59	<5	42
18[c]	-	-	25	<5	47	<5	54

[a]Reaction conditions: $Ni(cod)_2$ (x mol %), ligand (x mol %; **3-L2** and **4-L6** = 2x mol %), NaO*t*-Bu (1.5 equiv), **4-9** (0.12 mmol, 1.0 equiv), **4-2d** (3.0 equiv), and toluene (1.0 mL, [**4-9**] = 0.12 M). [b]Conversion to **4-10a** and remaining **4-9** are estimated on the basis of calibrated GC data, with the remaining mass balance largely attributed to unidentified byproducts, as indicated. [c]$Ni(cod)_2$ omitted from the reaction.

Table A15. Additional ligand screen and optimization for the Ni-catalyzed cross-coupling of **4-9** with *tert*-butylamine (**4-2d**) using weak base conditions (Cs_2CO_3/1,4-dioxane).[a]

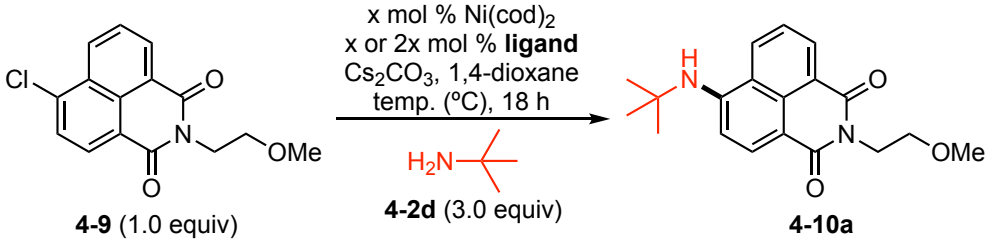

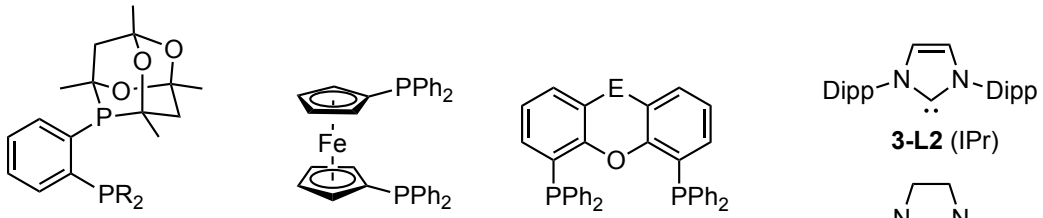

4-L1: R = Ph (PhPAd-DalPhos) **3-L1** (dppf) **4-L3**: E = $C(CH_3)_2$ (XantPhos) **3-L2** (IPr)
2-L1: R = *o*-tolyl (PAd-DalPhos) **4-L4**: E = NH (*N*-XantPhos)
2-L3: R = Cy (CyPAd-DalPhos) **4-L5**: E = nothing (DPEPhos) **4-L6** (SIPr)

Entry	x	Ligand	Temp. (ºC)	Yield **4-10a** (%)[b]	Remaining **4-9** (%)[b]	**4-11** (%)[b]	Other (%)[b]
1	10	**4-L1**	80	<5	66	<5	34
2		**2-L1**		<5	77	<5	23
3		**2-L3**		<5	61	<5	39
4		**3-L1**		<5	81	<5	18
5		**4-L3**		<5	80	<5	20
6		**4-L4**		<5	81	<5	19
7		**4-L5**		<5	74	<5	26
8		**3-L2**		**75**	18	<5	8
9		**4-L6**		49	13	<5	36
10	5	**3-L2**	80	61	33	<5	6
11		**3-L2**	60	47	44	<5	9
12[c]	10	**3-L2**	60	**93**	<5	<5	7

[a]Reaction conditions: $Ni(cod)_2$ (x mol %), ligand (x mol %; **3-L2** and **4-L6** = 2x mol %), Cs_2CO_3 (3.0 equiv), **4-9** (0.12 mmol, 1.0 equiv), **4-2d** (3.0 equiv), and 1,4-dioxane (1.0 mL, [**4-9**] = 0.12 M). [b]Conversion to **4-10a** and remaining **4-9** are estimated on the basis of calibrated GC data, with the remaining mass balance attributed to unidentified byproducts, as indicated. [c]5.0 equiv **4-2d**.

Table A16. Additional ligand screen and optimization for the Ni-catalyzed cross-coupling of **4-9** with *tert*-butylamine (**4-2d**) using alternate conditions (LiO*t*-Bu/1,4-dioxane).[a]

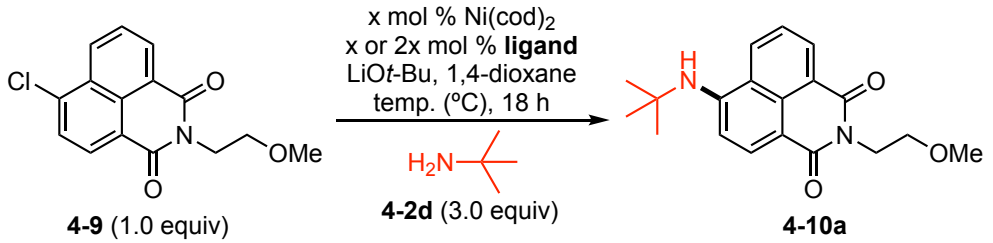

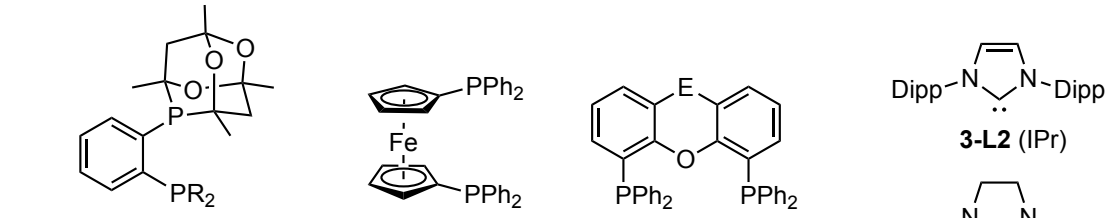

4-L1: R = Ph (PhPAd-DalPhos)
2-L1: R = *o*-tolyl (PAd-DalPhos)
2-L3: R = Cy (CyPAd-DalPhos)

3-L1 (dppf)

4-L3: E = $C(CH_3)_2$ (XantPhos)
4-L4: E = NH (*N*-XantPhos)
4-L5: E = nothing (DPEPhos)

3-L2 (IPr)

4-L6 (SIPr)

Entry	x	Ligand	Temp. (°C)	Yield **4-10a** (%)[b]	Remaining **4-9** (%)[b]	**4-11** (%)[b]	Other (%)[b]
1	10	**4-L1**	80	22	7	45	26
2		**2-L1**		22	60	<5	18
3		**2-L3**		29	51	<5	20
4		**3-L1**		**92**	<5	8	<5
5		**4-L3**		**85**	15	<5	<5
6		**4-L4**		**93**	7	<5	<5
7		**4-L5**		**>95**	<5	<5	<5
8		**3-L2**		**89**	<5	<5	11
9		**4-L6**		71	<5	<5	39
10	5	**3-L1**	80	**93**	7	<5	<5
11		**4-L3**		48	52	<5	<5
12		**4-L4**		79	21	<5	<5
13		**4-L5**		**>95**	<5	<5	<5
14		**3-L2**		**>95**	<5	<5	<5
15	5	**3-L1**	60	**93**	<5	<5	7
16		**4-L5**		**94**	<5	<5	6
17		**3-L2**		**95**	<5	<5	<5
18	5	**3-L1**	50	**>95**	<5	<5	<5
19		**4-L5**		47	53	<5	<5
20		**3-L2**		73	27	<5	<5
21	5	**3-L1**	25	**>95**	<5	5	<5

[a]Reaction conditions: $Ni(cod)_2$ (x mol %), ligand (x mol %; **3-L2** and **4-L6** = 2x mol %), LiO*t*-Bu (1.5 equiv), **4-9** (0.12 mmol, 1.0 equiv), **4-2d** (3.0 equiv), and 1,4-dioxane (1.0 mL, [**4-9**] = 0.12 M). [b]Conversion to **4-10a** and remaining **4-9** are estimated on the basis of calibrated GC data, with the remaining mass balance attributed to unidentified byproducts and/or the -O*t*-Bu cross-coupled product of **4-9** (**4-11**), as indicated.

Appendix 7: 1H NMR Spectra of the Nickel-Catalyzed Cross-Coupling of 4-9 and 4-2a Using 3-L1 and 3-L2.

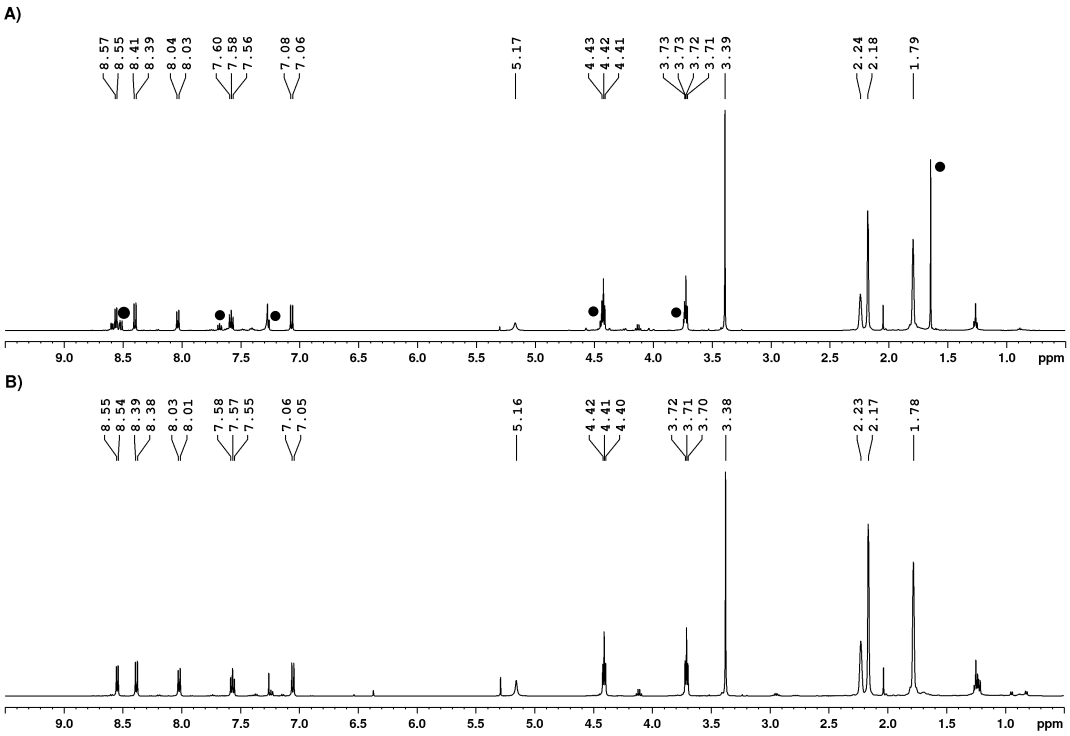

Figure A128. ^{1}H NMR spectra ($CDCl_3$, 500 MHz) of the Ni-catalyzed cross-coupling **4-9** and 1-adamantylamine (**4-2a**) using A) **3-L1** and B) **3-L2**. Circles indicate the peaks corresponding to the -O*t*-Bu cross-coupled product of **4-9** (**4-11**).

Appendix 8: Chapter 4 NMR Spectra

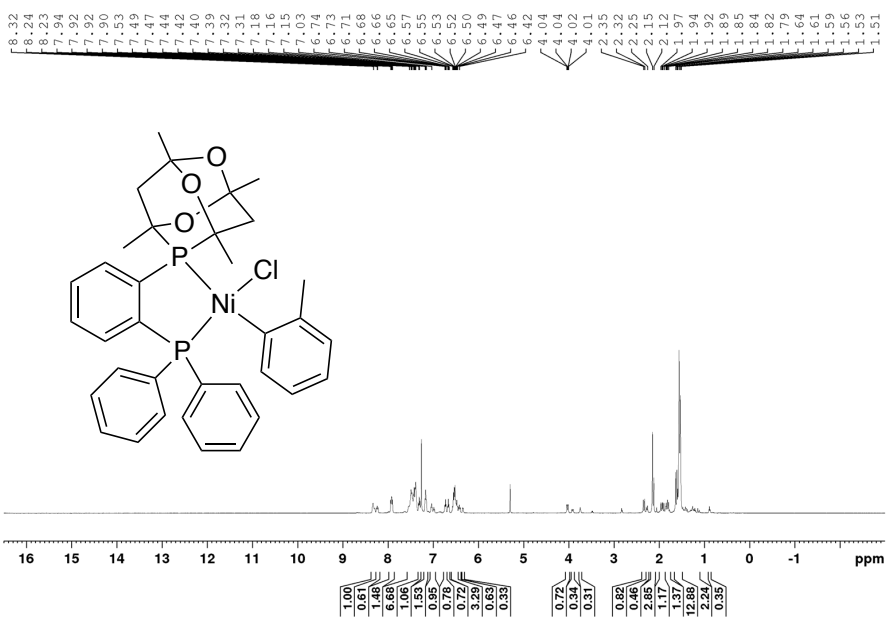

Figure A129. ^{1}H NMR spectrum of **4-C1** ($CDCl_3$, 500 MHz).

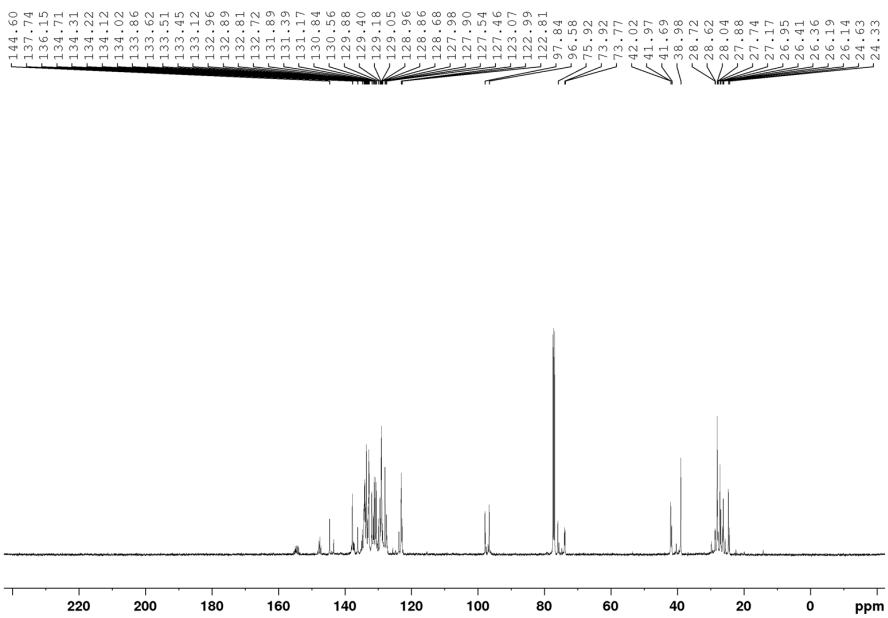

Figure A130. $^{13}C\{^{1}H\}$ NMR spectrum of **4-C1** ($CDCl_3$, 126 MHz).

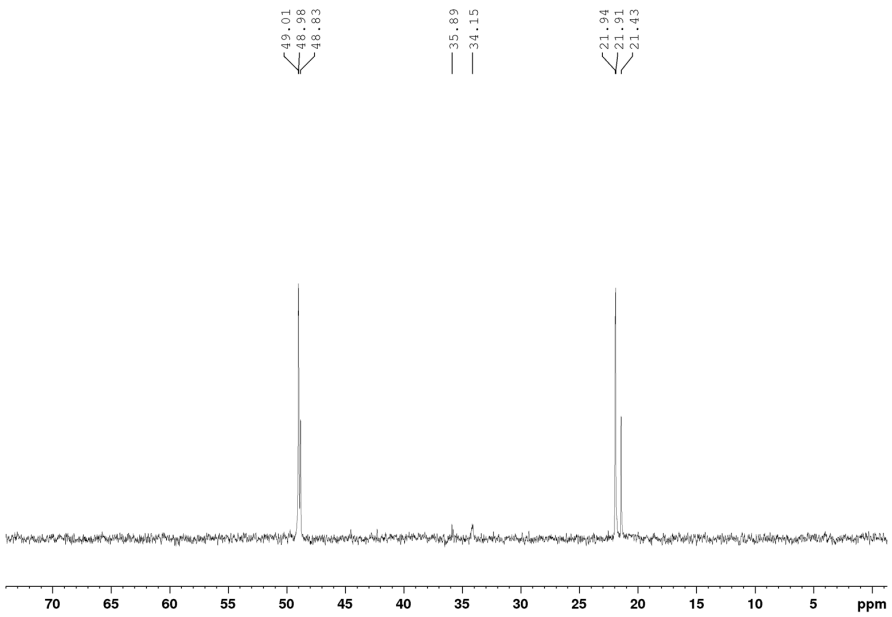

Figure A131. $^{31}P\{^{1}H\}$ NMR spectrum of **4-C1** ($CDCl_3$, 203 MHz).

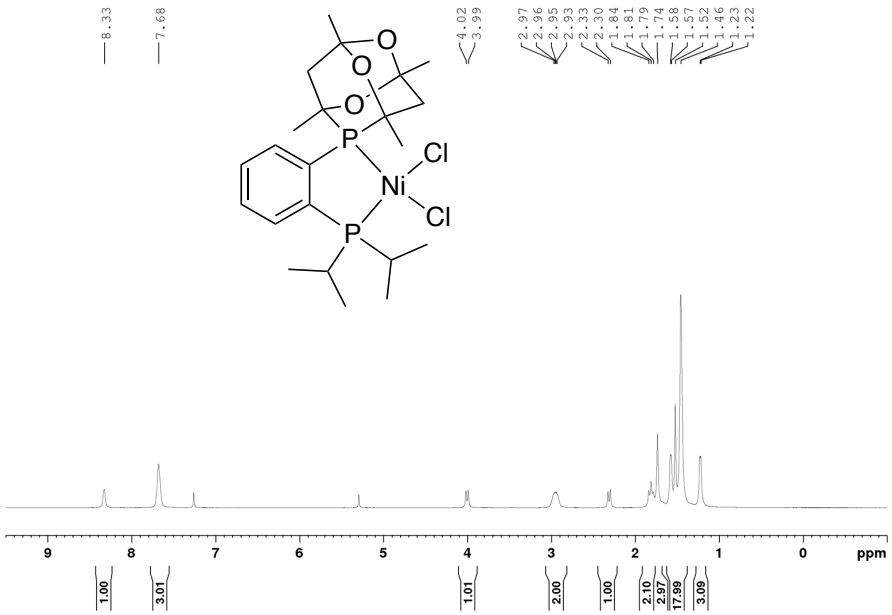

Figure A132. ^{1}H NMR spectrum of (**4-L2**)$NiCl_2$ ($CDCl_3$, 500 MHz).

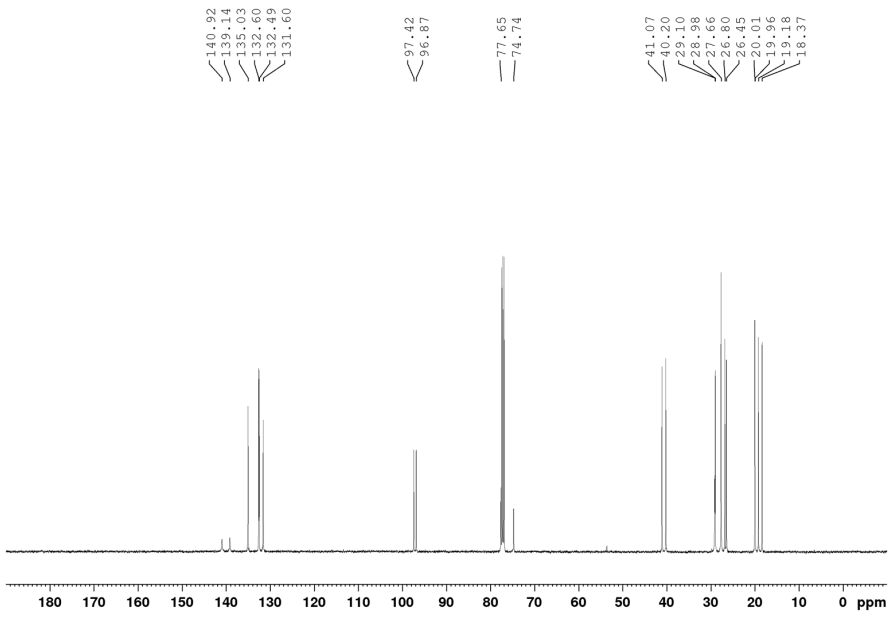

Figure A133. $^{13}C\{^{1}H\}$ NMR spectrum of (**4-L2**)$NiCl_2$ ($CDCl_3$, 126 MHz).

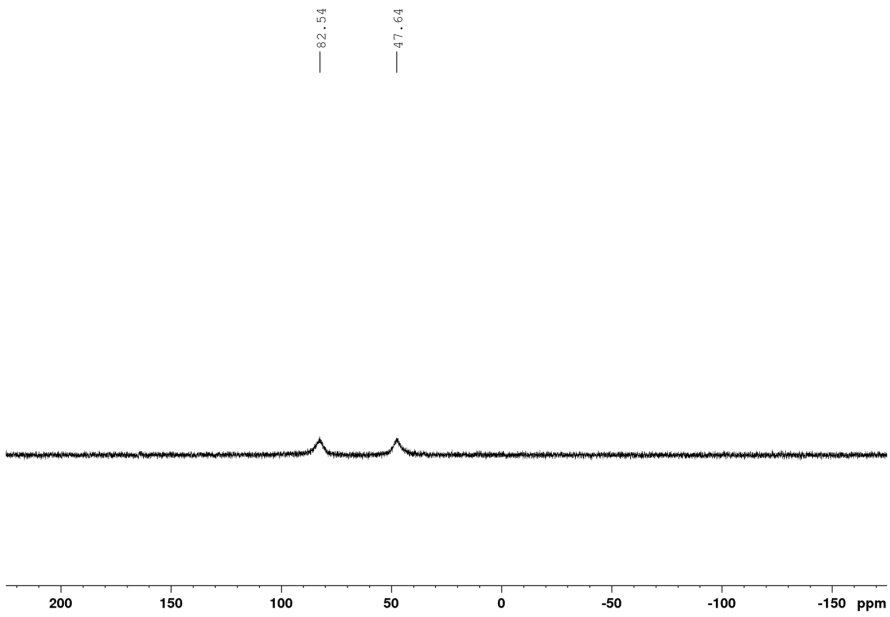

Figure A134. $^{31}P\{^{1}H\}$ NMR spectrum of (**4-L2**)$NiCl_2$ ($CDCl_3$, 203 MHz).

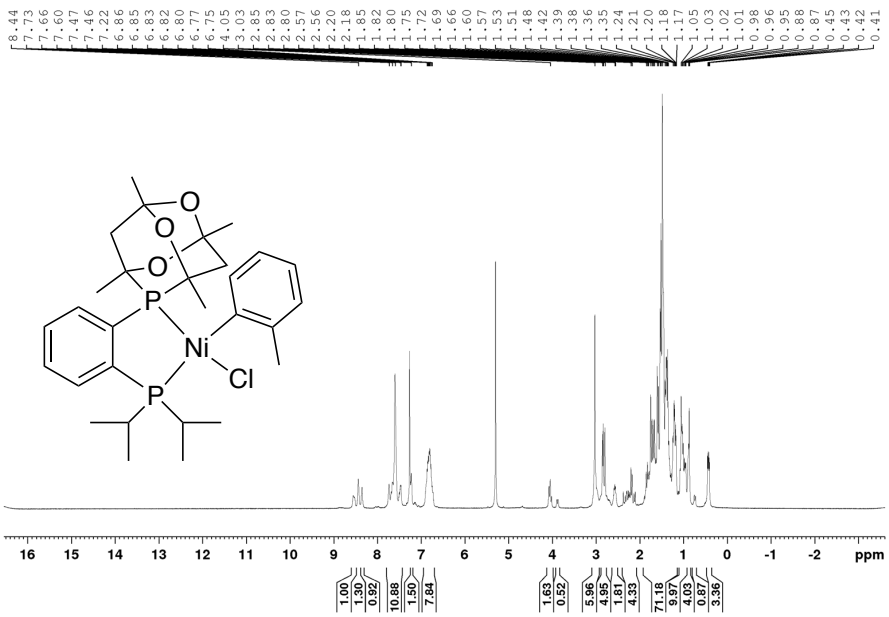

Figure A135. ^{1}H NMR spectrum of **4-C2** ($CDCl_3$, 500 MHz).

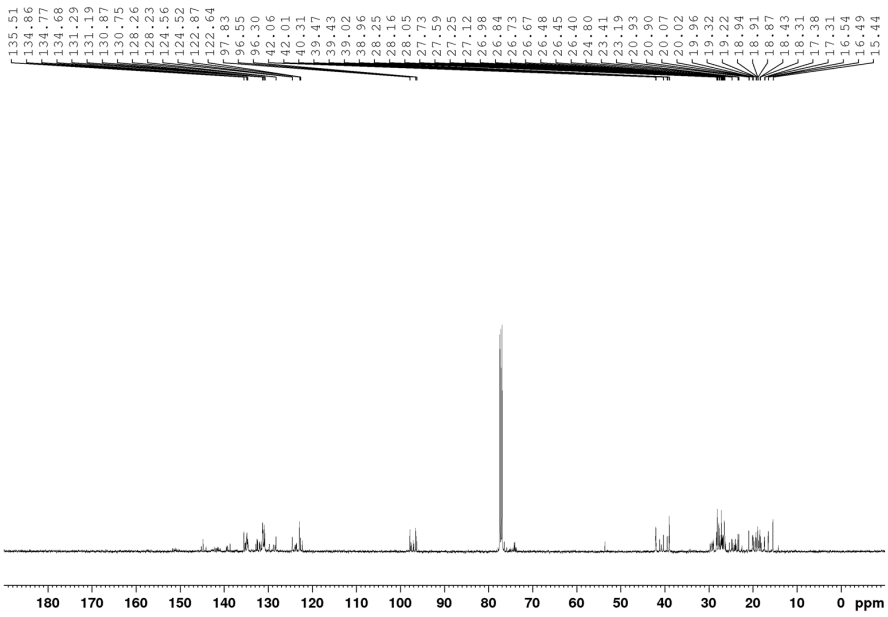

Figure A136. $^{13}C\{^{1}H\}$ NMR spectrum of **4-C2** ($CDCl_3$, 126 MHz).

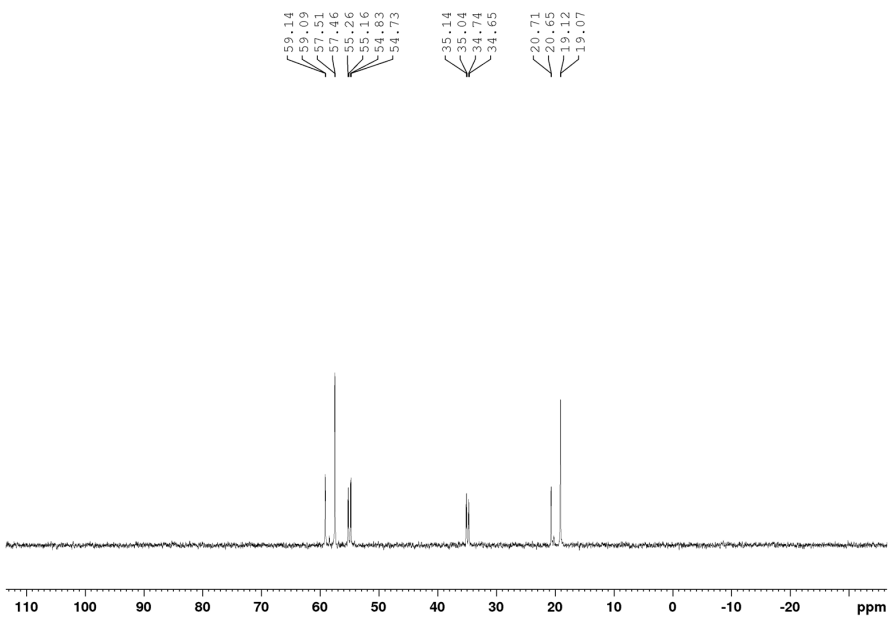

Figure A137. $^{31}P\{^{1}H\}$ NMR spectrum of **4-C2** ($CDCl_3$, 203 MHz).

Figure A138. ^{1}H NMR spectrum of *N*-(adamantan-1yl)pyridine-3-amine, **4-3a** ($CDCl_3$, 500 MHz).

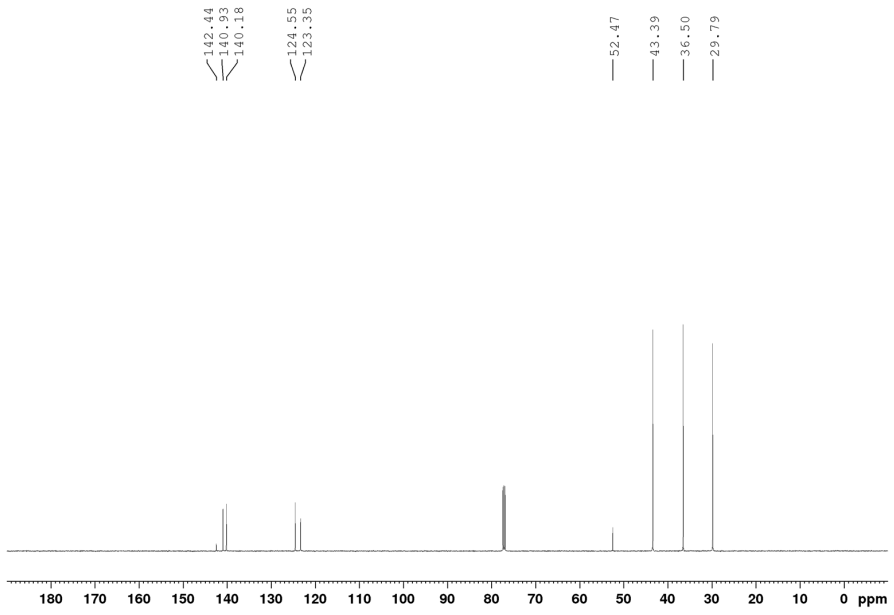

Figure A139. $^{13}C\{^{1}H\}$ NMR spectrum of *N*-(adamantan-1yl)pyridine-3-amine, **4-3a** ($CDCl_3$, 126 MHz).

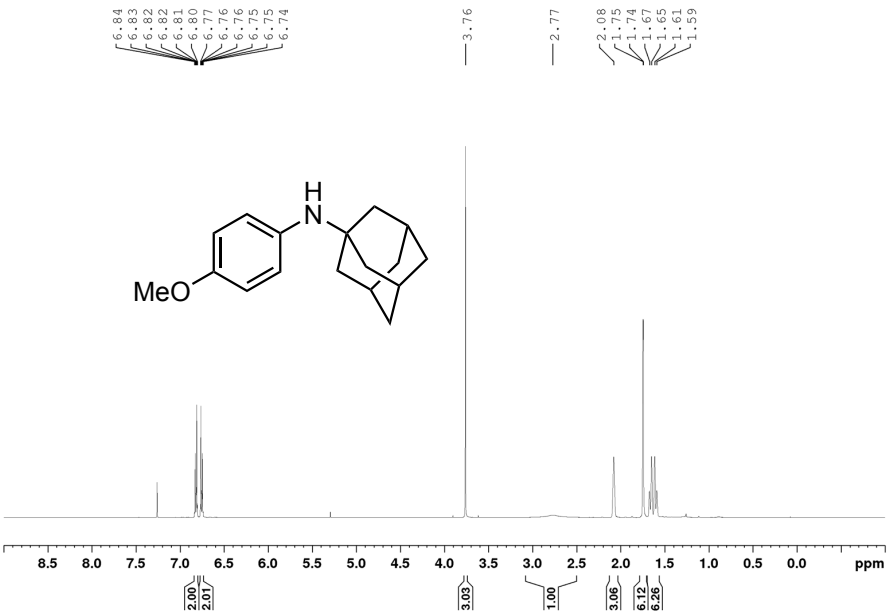

Figure A140. ^{1}H NMR spectrum of *N*-(4-methoxyphenyl)adamantan-1-amine, **4-3b** ($CDCl_3$, 500 MHz).

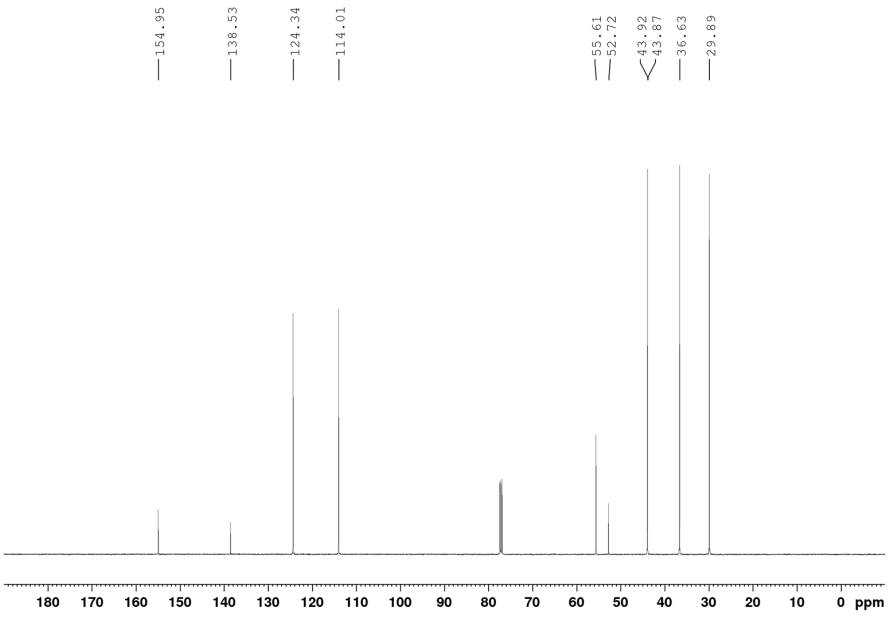

Figure A141. $^{13}C\{^{1}H\}$ NMR spectrum of *N*-(4-methoxyphenyl)adamantan-1-amine, **4-3b** ($CDCl_3$, 126 MHz).

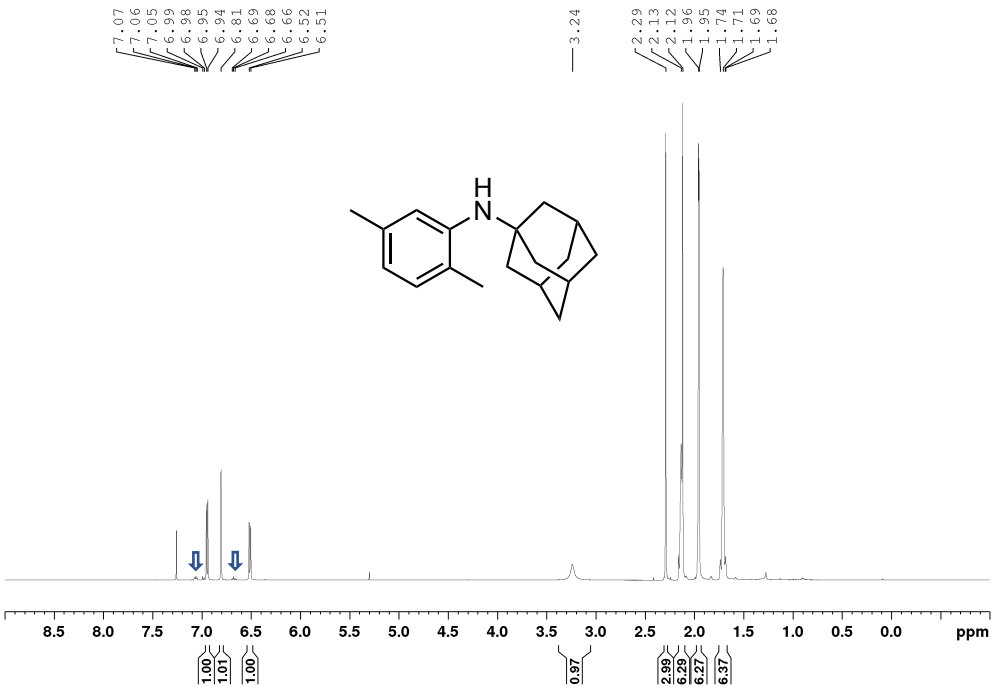

Figure A142. ^{1}H NMR spectrum of *N*-(2,5-dimethylphenyl)adamantan-1-amine, **4-3c** ($CDCl_3$, 500 MHz). (Impurity *N*-(*o*-tolyl)adamantan-1amine, **4-3c´**, is marked).

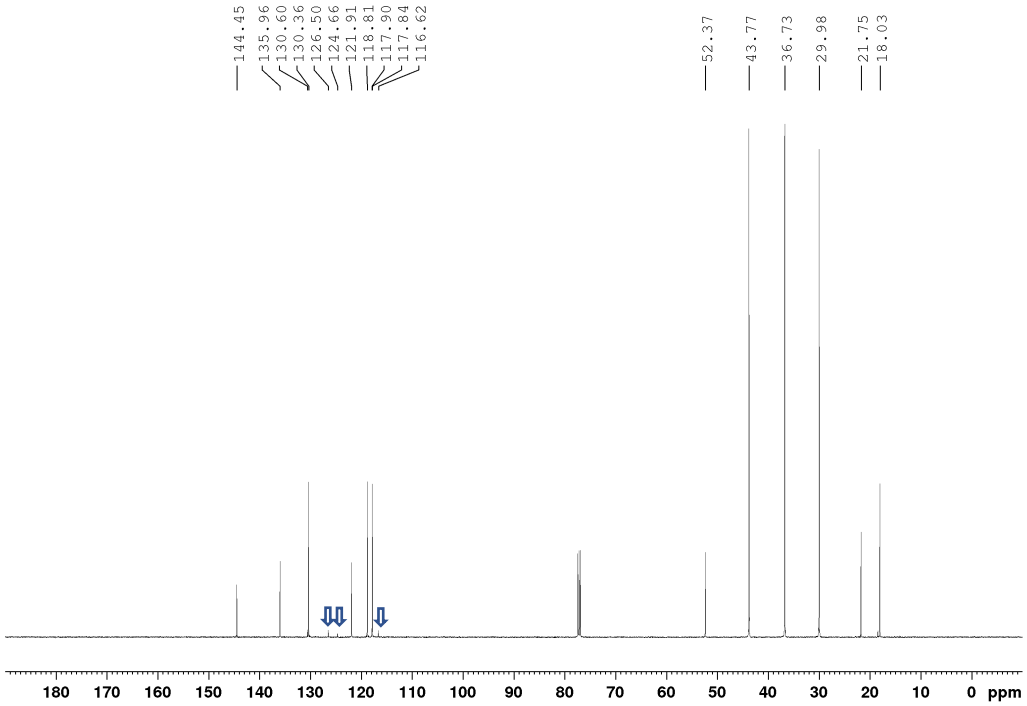

Figure A143. $^{13}C\{^{1}H\}$ NMR spectrum of *N*-(2,5-dimethylphenyl)adamantan-1-amine, **4-3c** ($CDCl_3$, 126 MHz). (Impurity *N*-(*o*-tolyl)adamantan-1amine, **4-3c´**, is marked).

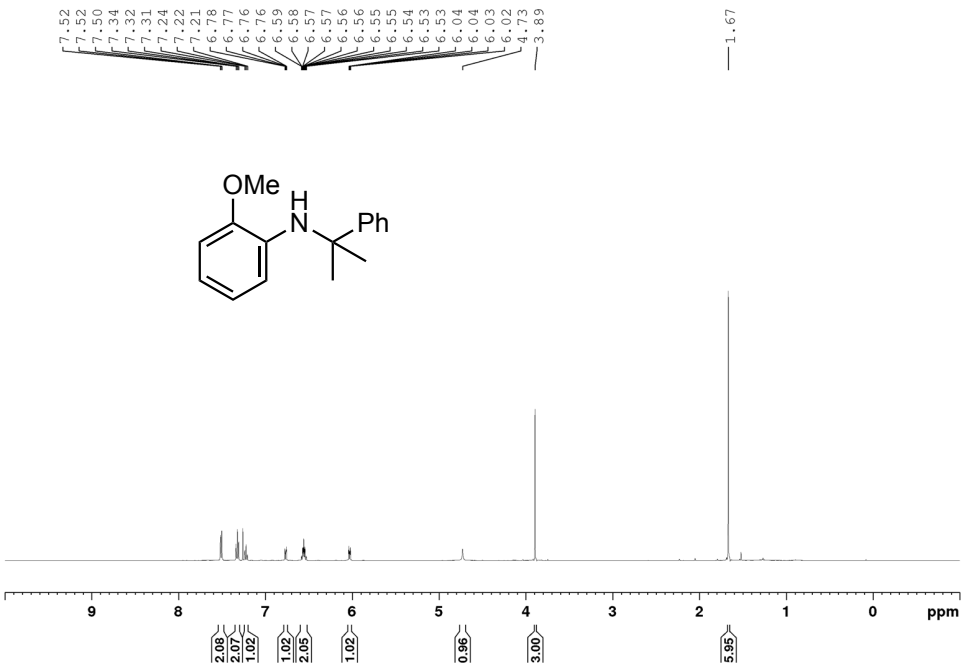

Figure A144. ^{1}H NMR spectrum of 2-methoxy-*N*-(2-phenylpropan-2-yl)aniline, **4-3d** ($CDCl_3$, 500 MHz).

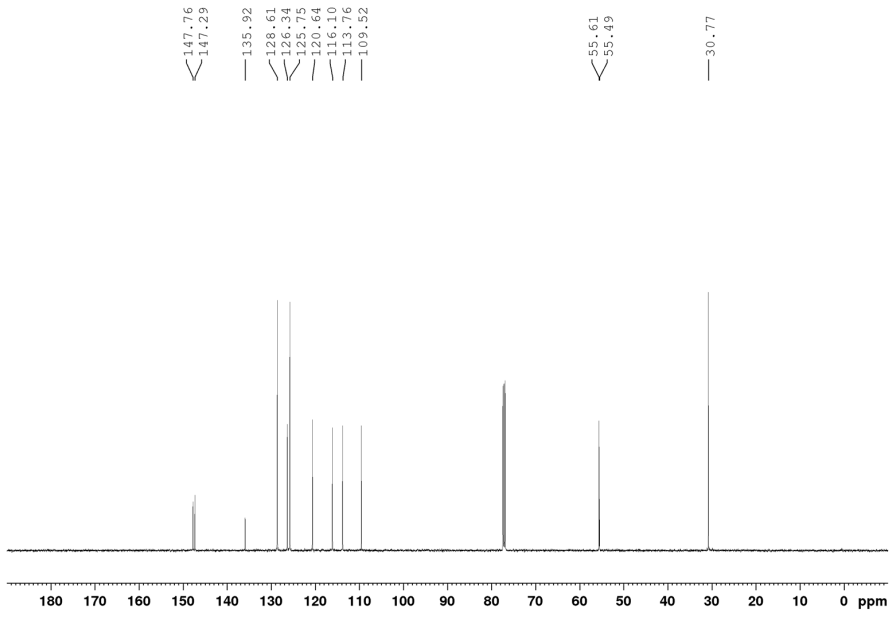

Figure A145. $^{13}C\{^{1}H\}$ NMR spectrum of 2-methoxy-*N*-(2-phenylpropan-2-yl)aniline, **4-3d** ($CDCl_3$, 126 MHz).

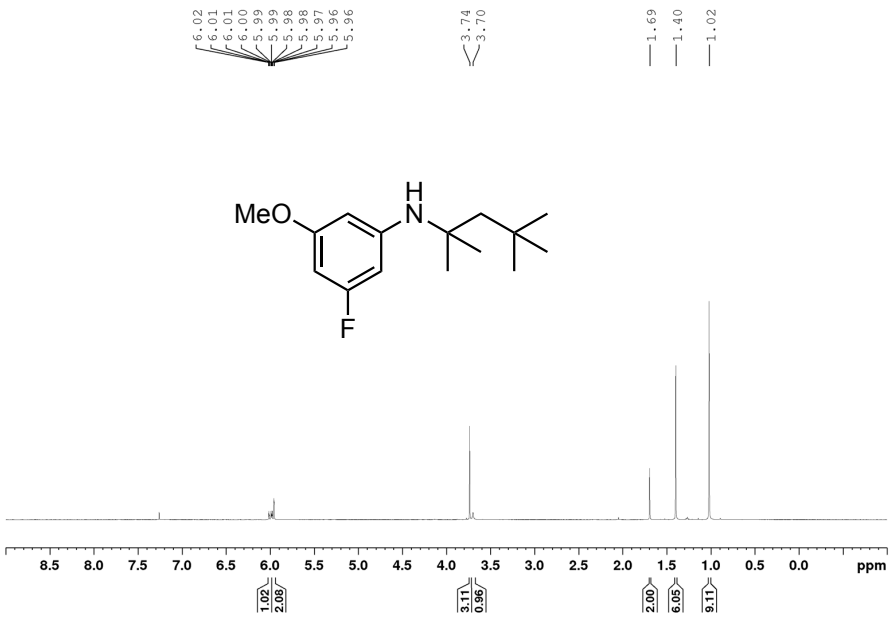

Figure A146. ^{1}H NMR spectrum of 3-fluoro-5-methoxy-*N*-(,2,4,4-trimethylpentan-2-yl)aniline, **4-3e** ($CDCl_3$, 500 MHz).

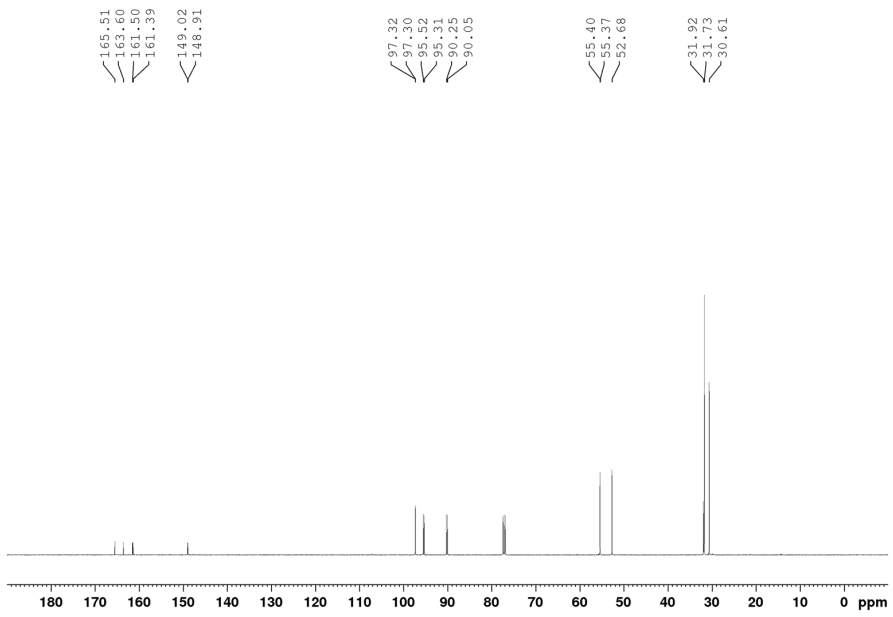

Figure A147. $^{13}C\{^{1}H\}$ NMR spectrum of 3-fluoro-5-methoxy-*N*-(,2,4,4-trimethylpentan-2-yl)aniline, **4-3e** ($CDCl_3$, 126 MHz).

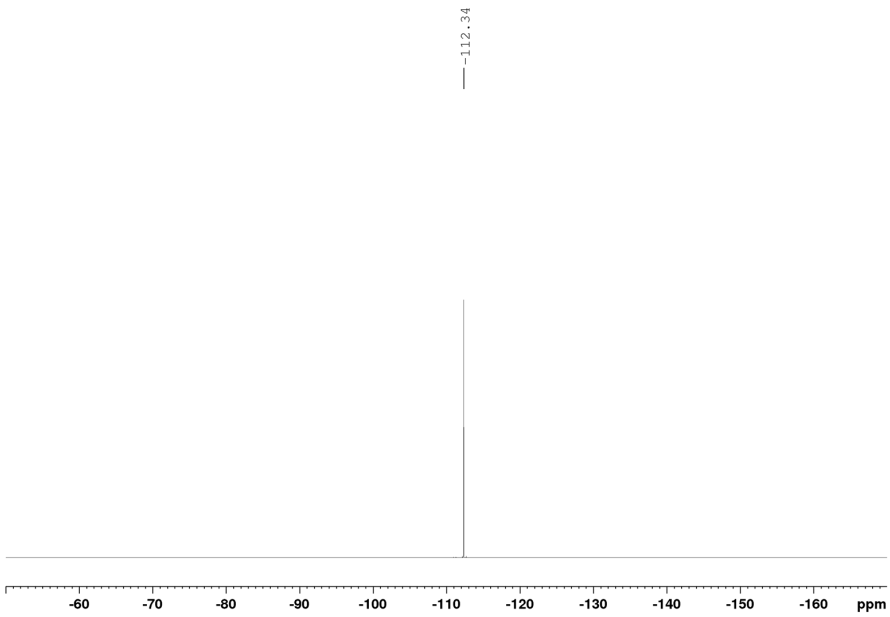

Figure A148. $^{19}F\{^{1}H\}$ NMR spectrum of 3-fluoro-5-methoxy-*N*-(,2,4,4-trimethylpentan-2-yl)aniline, **4-3e** ($CDCl_3$, 470.4 MHz).

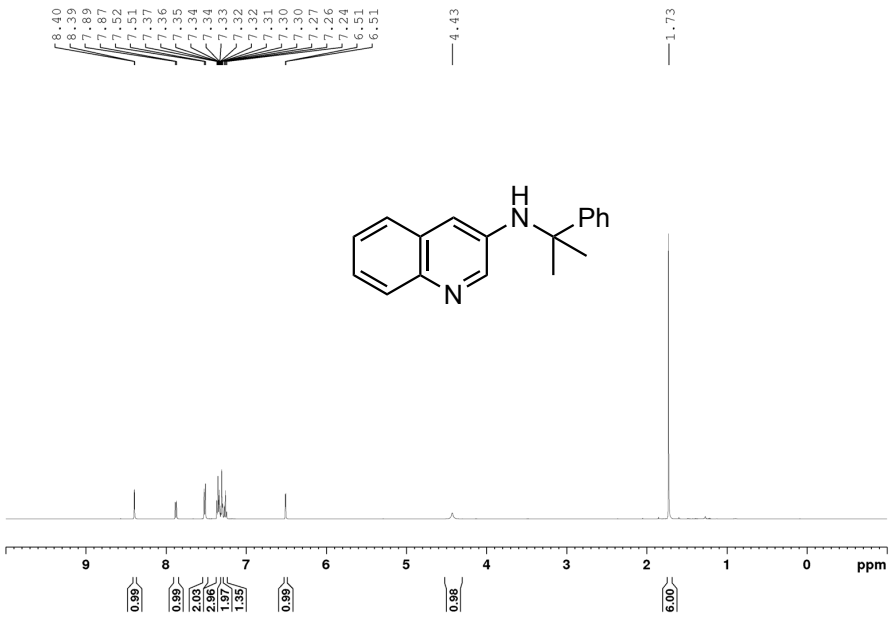

Figure A149. ^{1}H NMR spectrum of *N*-(2-phenylpropan-2-yl)quinoline-3-amine, **4-3f** ($CDCl_3$, 500 MHz).

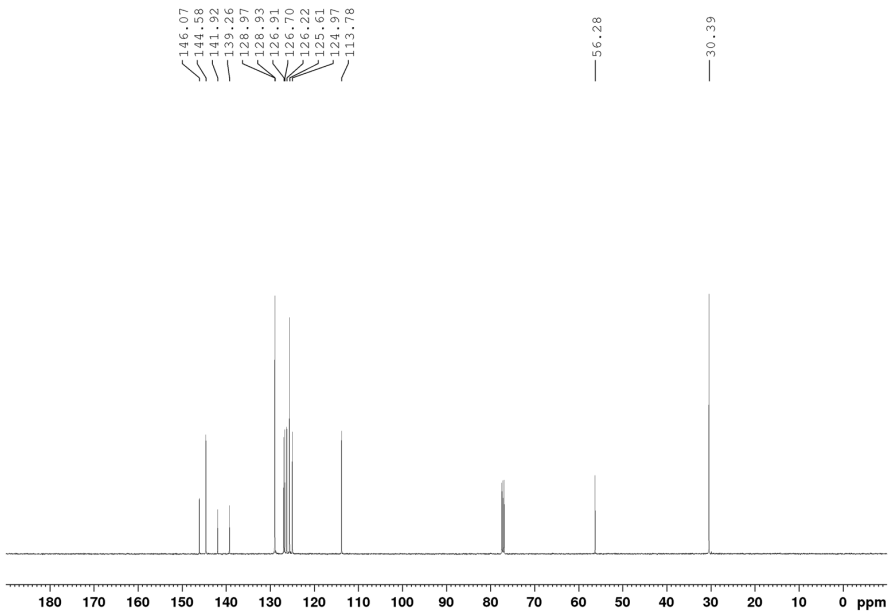

Figure A150. $^{13}C\{^{1}H\}$ NMR spectrum of *N*-(2-phenylpropan-2-yl)quinoline-3-amine, **4-3f** ($CDCl_3$, 126 MHz).

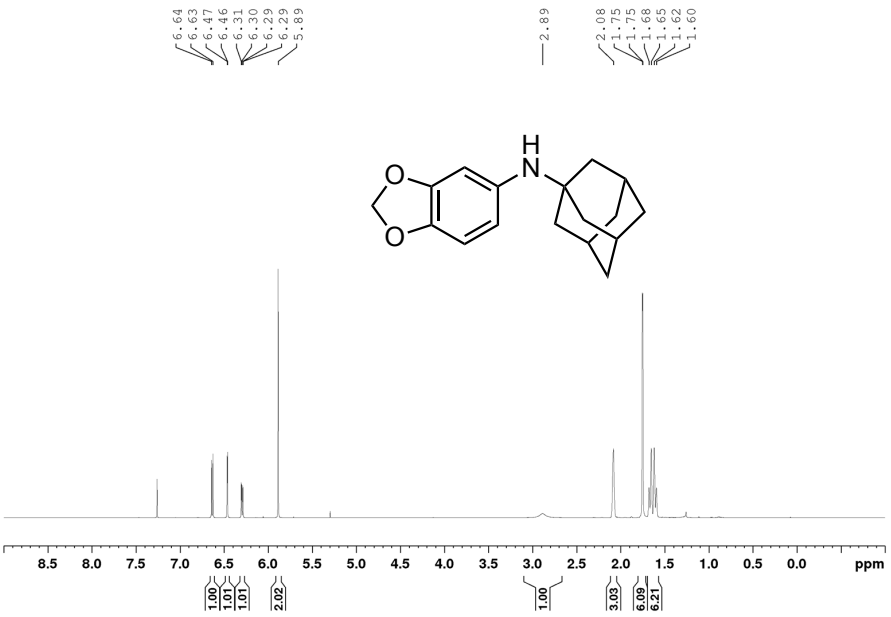

Figure A151. ^{1}H NMR spectrum of *N*-(adamantan-1-yl)benzo[*d*][1,3]dioxol-5-amine, **4-3g** ($CDCl_3$, 500 MHz).

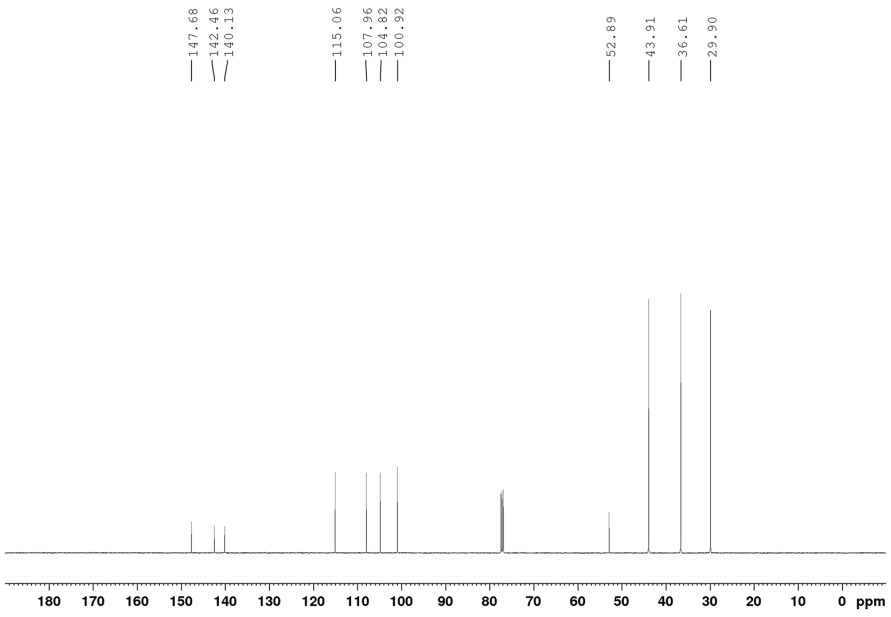

Figure A152. $^{13}C\{^{1}H\}$ NMR spectrum of *N*-(adamantan-1-yl)benzo[*d*][1,3]dioxol-5-amine, **4-3g** ($CDCl_3$, 126 MHz).

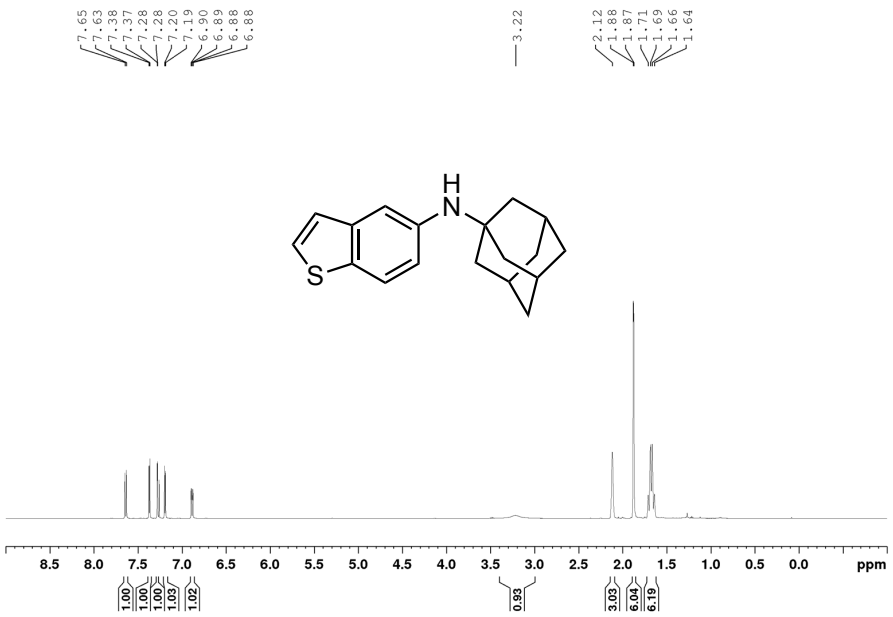

Figure A153. ^{1}H NMR spectrum of *N*-(adamantan-1-yl)benzo[*b*]thiophen-5-amine, **4-3h** ($CDCl_3$, 500 MHz).

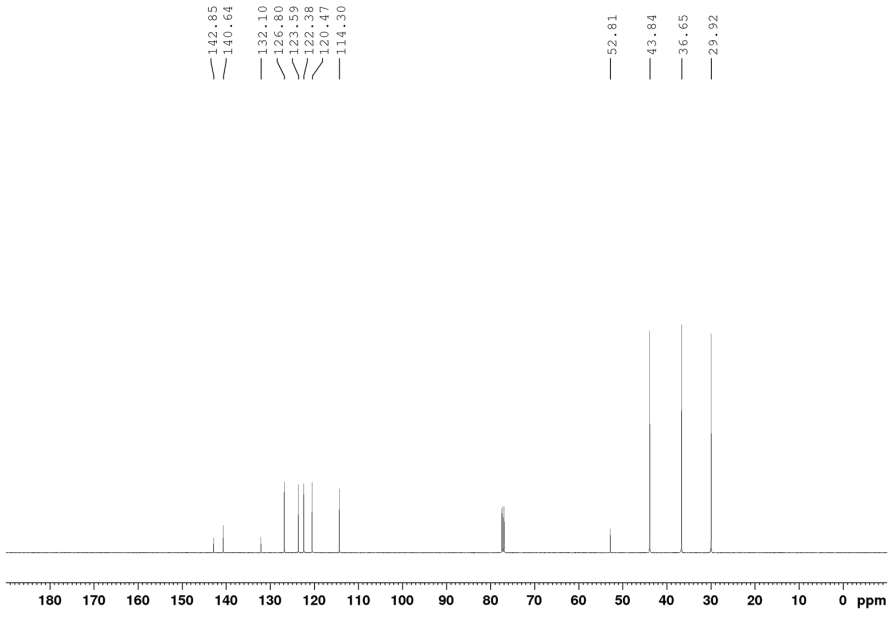

Figure A154. $^{13}C\{^{1}H\}$ NMR spectrum of *N*-(adamantan-1-yl)benzo[*b*]thiophen-5-amine, **4-3h** ($CDCl_3$, 126 MHz).

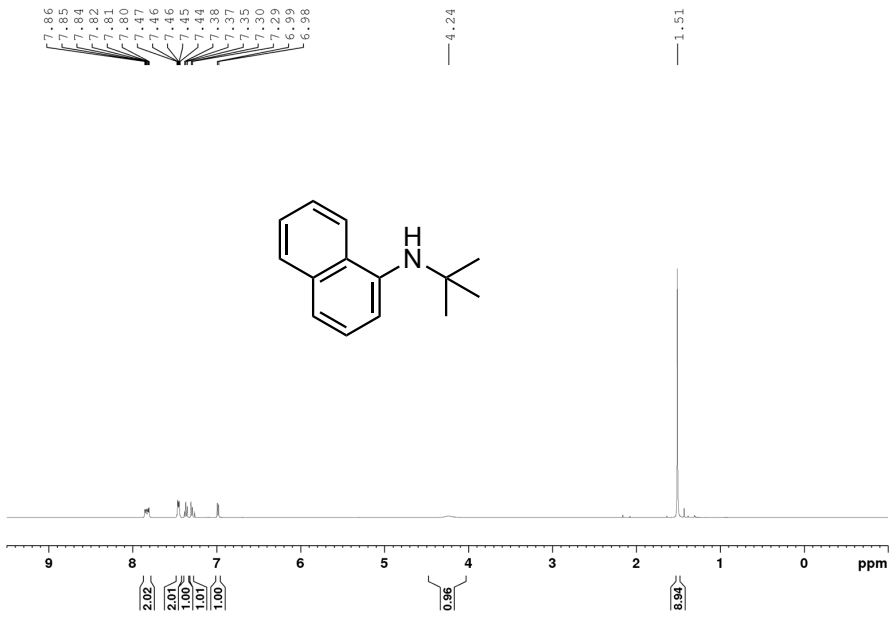

Figure A155. ^{1}H NMR spectrum of *N*-(*tert*-butyl)naphthalen-1-amine, **4-3i** ($CDCl_3$, 500 MHz).

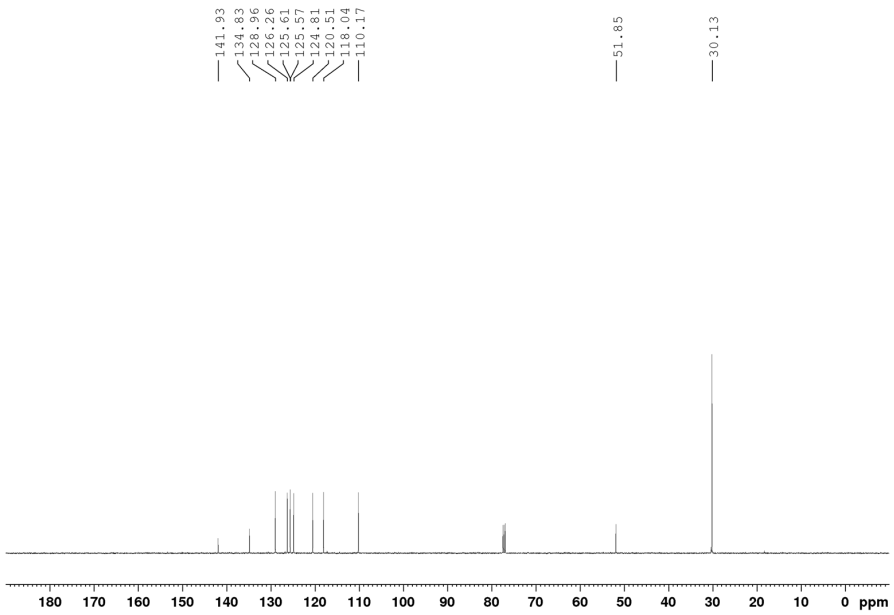

Figure A156. $^{13}C\{^{1}H\}$ NMR spectrum of *N*-(*tert*-butyl)naphthalen-1-amine, **4-3i** ($CDCl_3$, 126 MHz).

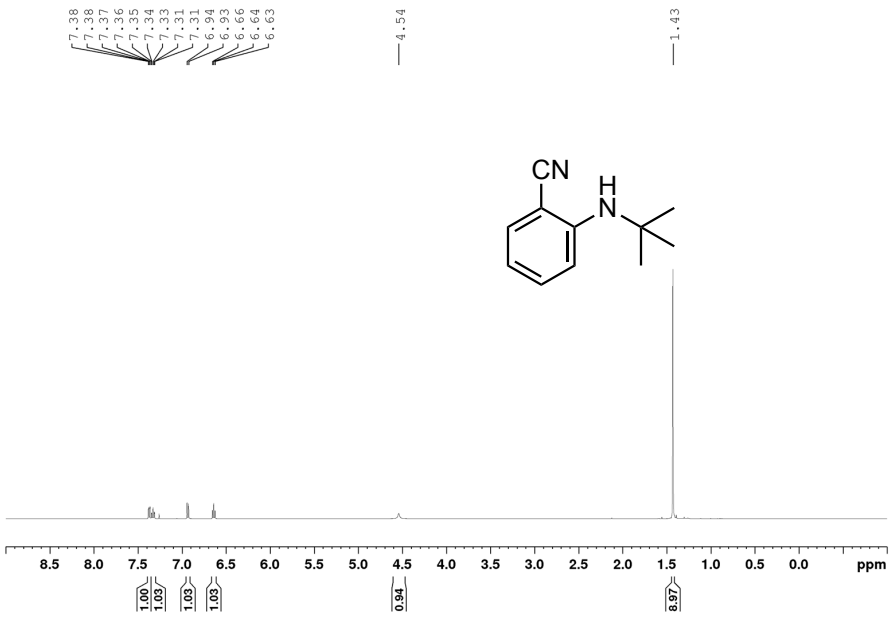

Figure A157. ^{1}H NMR spectrum of 2-(*tert*-butylamino)benzonitrile, **4-3j** ($CDCl_3$, 500 MHz).

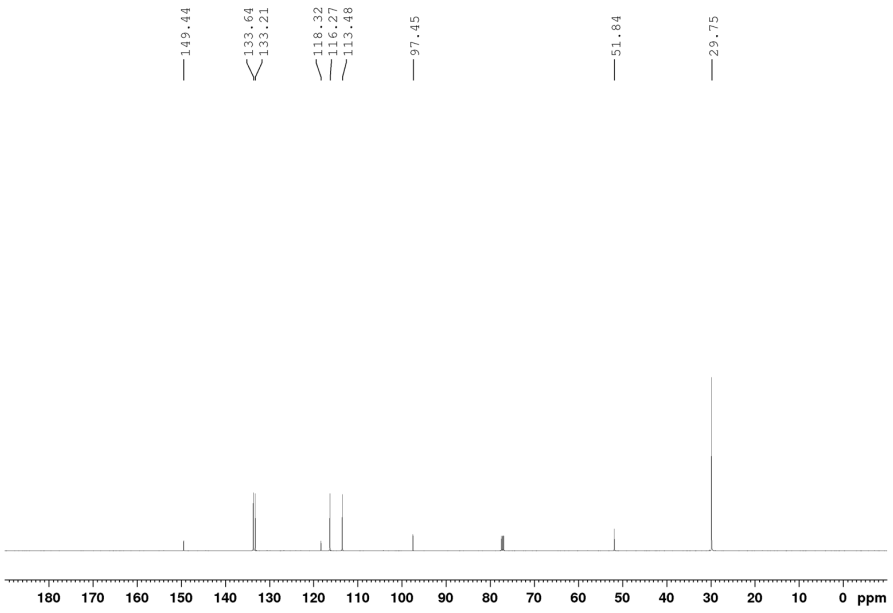

Figure A158. $^{13}C\{^{1}H\}$ NMR spectrum of 2-(*tert*-butylamino)benzonitrile, **4-3j** ($CDCl_3$, 126 MHz).

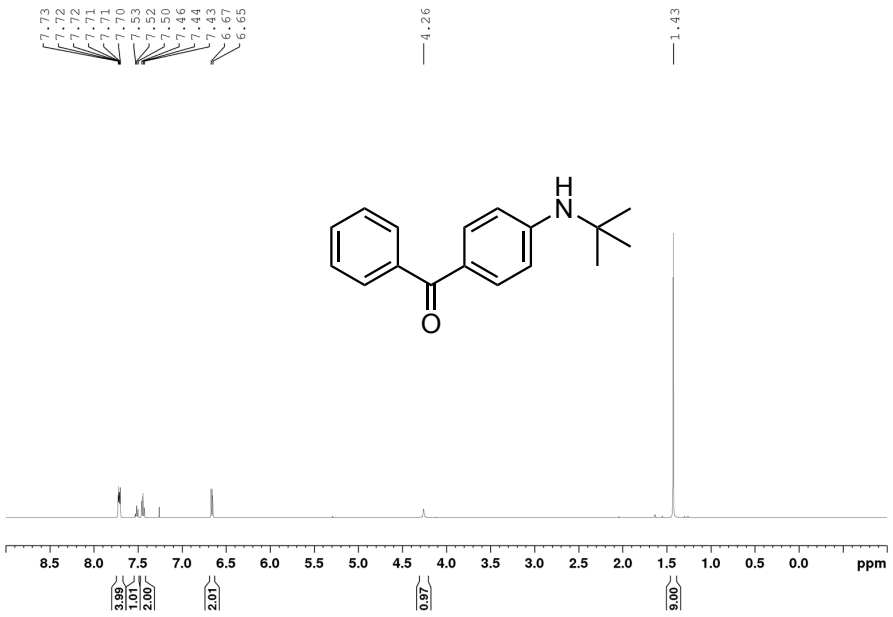

Figure A159. ^{1}H NMR spectrum of (4-(*tert*-butylamino)phenyl)(phenyl)methanone, **4-3k** ($CDCl_3$, 500 MHz).

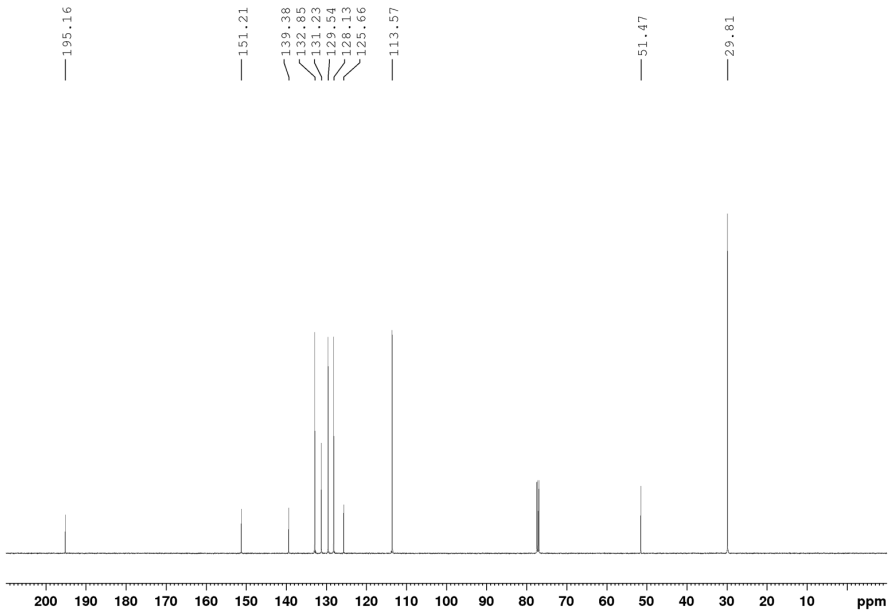

Figure A160. $^{13}C\{^{1}H\}$ NMR spectrum of (4-(*tert*-butylamino)phenyl)(phenyl)methanone, **4-3k** ($CDCl_3$, 126 MHz).

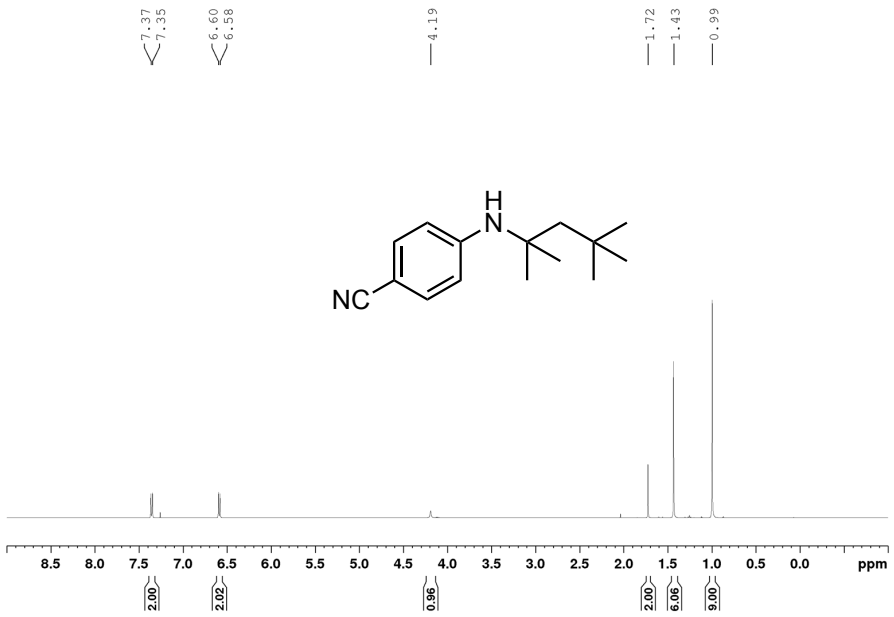

Figure A161. ^{1}H NMR spectrum of 4-((2,4,4-trimethylpentan-2-yl)amino)benzonitrile, **4-3l** ($CDCl_3$, 500 MHz).

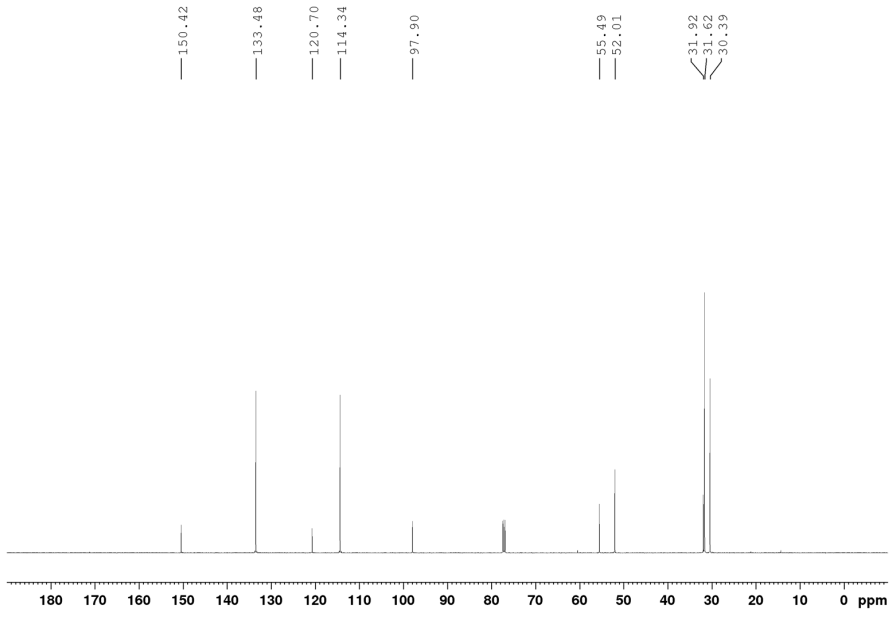

Figure A162. $^{13}C\{^{1}H\}$ NMR spectrum of 4-((2,4,4-trimethylpentan-2-yl)amino)benzonitrile, **4-3l** ($CDCl_3$, 126 MHz).

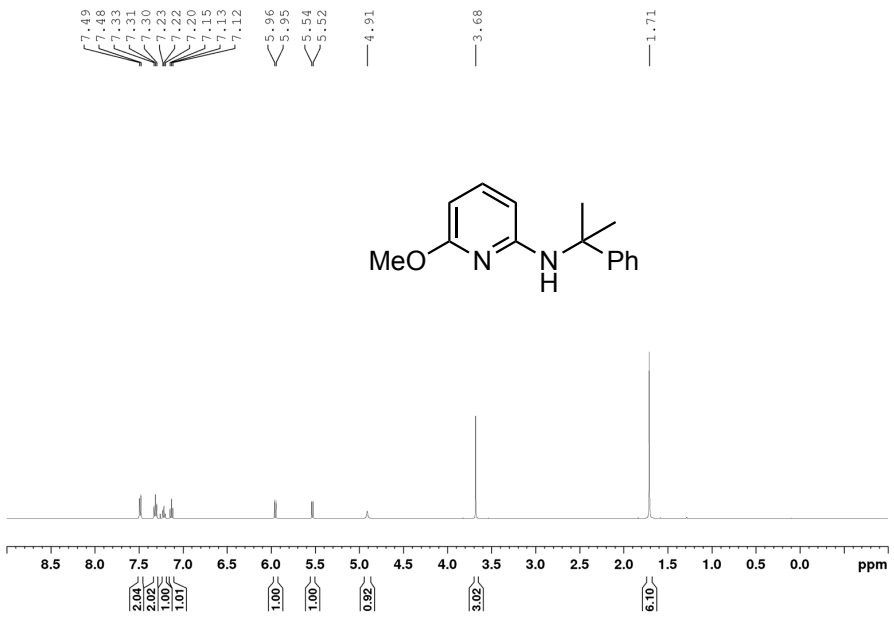

Figure A163. ^{1}H NMR spectrum of 6-methoxy-*N*-(2-phenylpropan-2-yl)pyridin-2-amine, **4-3m** ($CDCl_3$, 500 MHz).

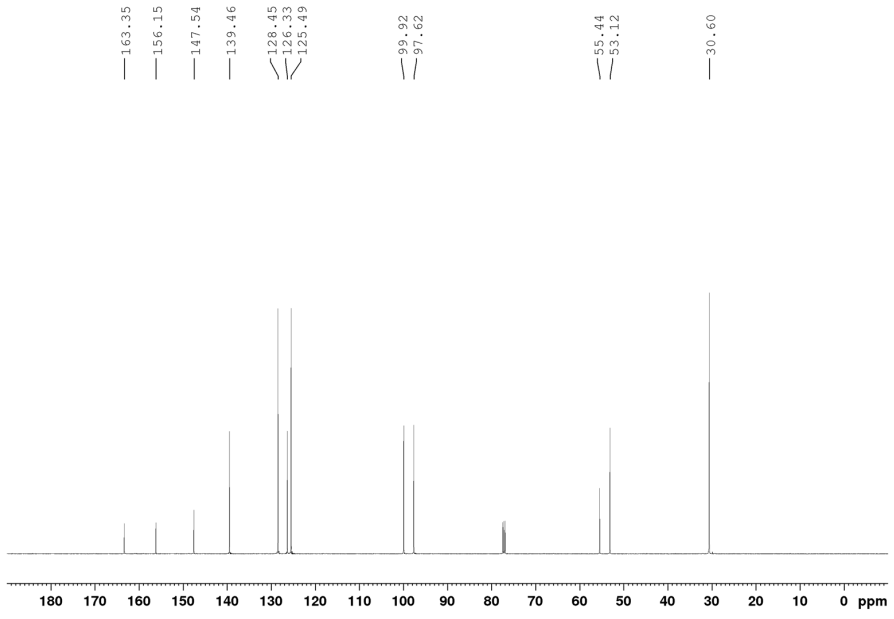

Figure A164. $^{13}C\{^{1}H\}$ NMR spectrum of 6-methoxy-*N*-(2-phenylpropan-2-yl)pyridin-2-amine, **4-3m** ($CDCl_3$, 126 MHz).

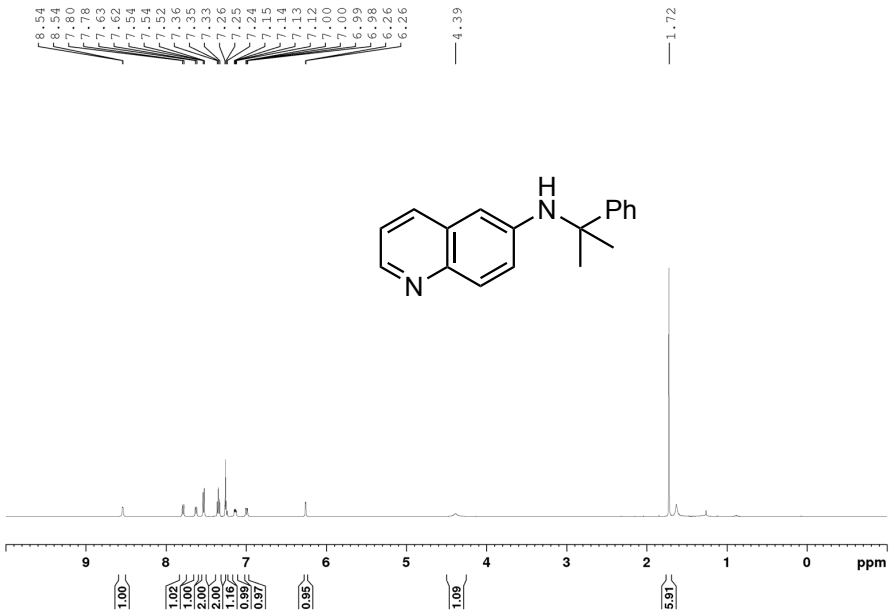

Figure A165. ^{1}H NMR spectrum of *N*-(2-phenylpropan-2-yl)quinolin-6-amine, **4-3n** ($CDCl_3$, 500 MHz).

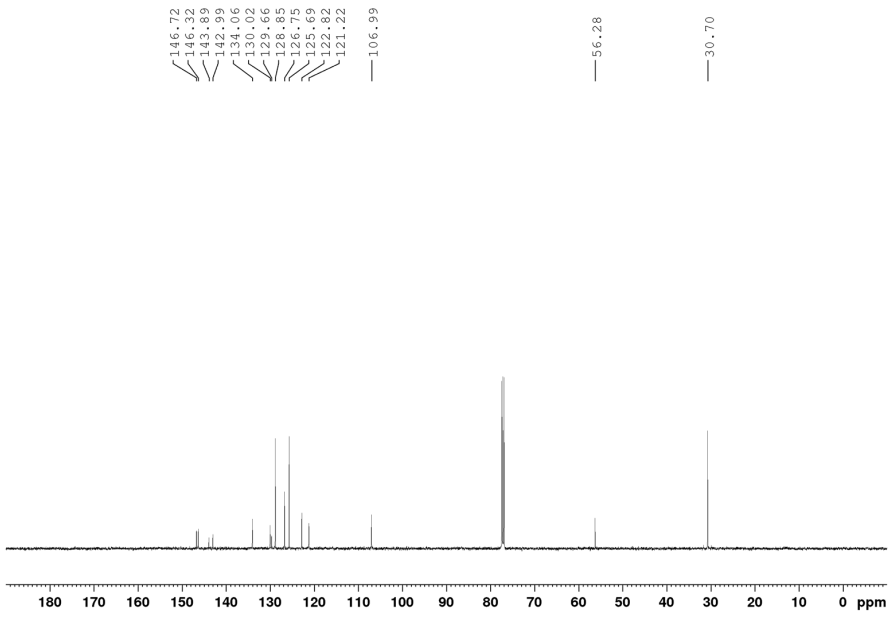

Figure A166. $^{13}C\{^{1}H\}$ NMR spectrum of *N*-(2-phenylpropan-2-yl)quinolin-6-amine, **4-3n** ($CDCl_3$, 126 MHz).

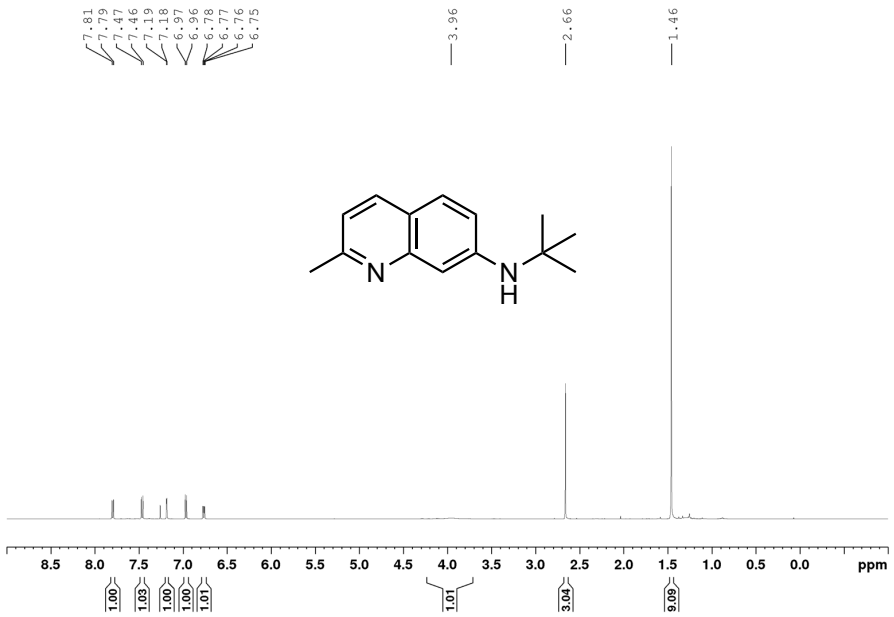

Figure A167. ^{1}H NMR spectrum of *N*-(*tert*-butyl)-2-methylquinolin-7-amine, **4-3o** ($CDCl_3$, 500 MHz).

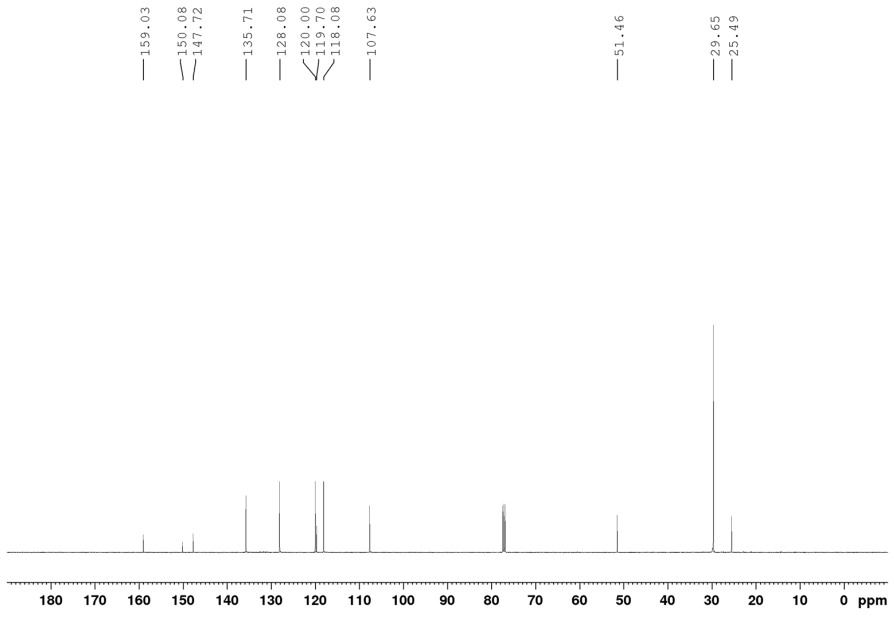

Figure A168. $^{13}C\{^{1}H\}$ NMR spectrum of *N*-(*tert*-butyl)-2-methylquinolin-7-amine, **4-3o** ($CDCl_3$, 126 MHz).

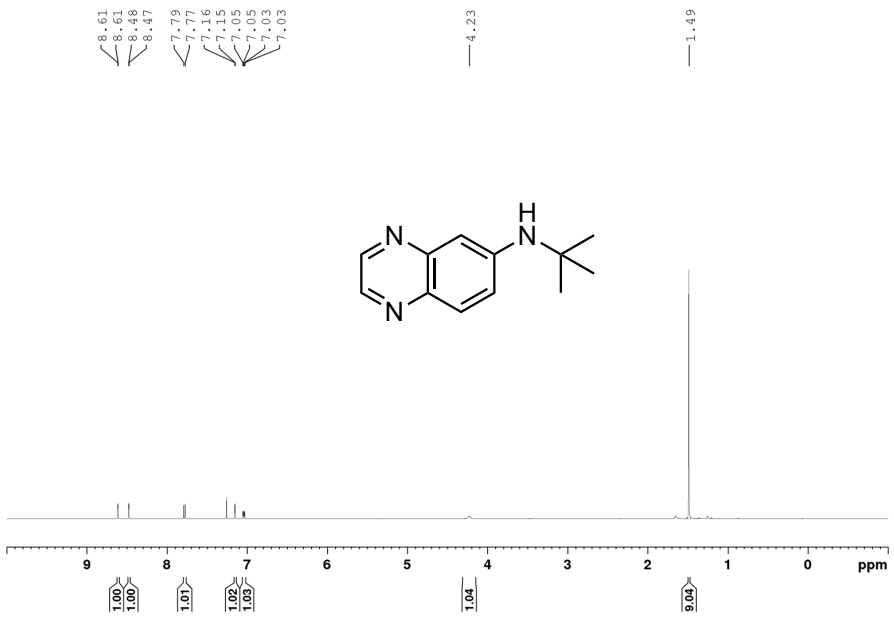

Figure A169. ^{1}H NMR spectrum of *N*-(*tert*-butyl)quinoxalin-6-amine, **4-3p** ($CDCl_3$, 500 MHz).

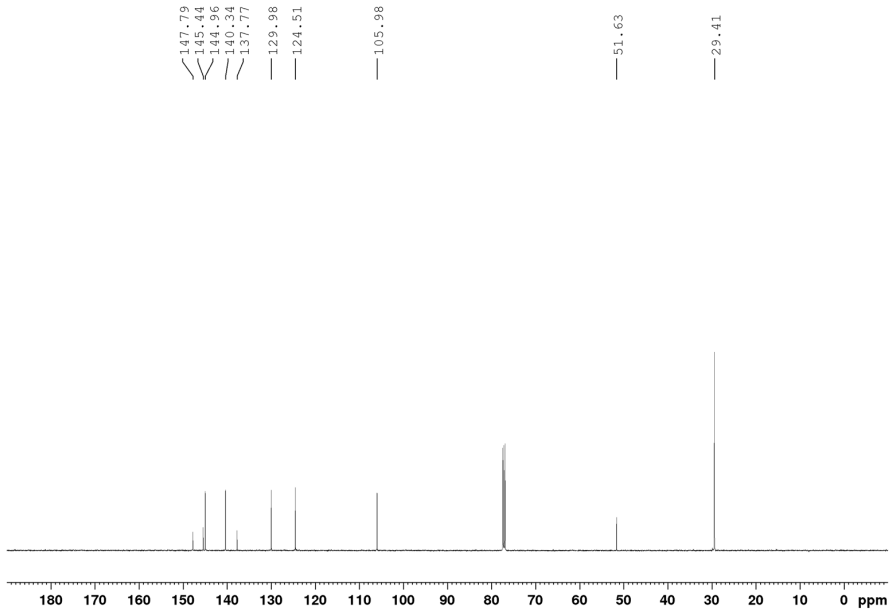

Figure A170. $^{13}C\{^{1}H\}$ NMR spectrum of *N*-(*tert*-butyl)quinoxalin-6-amine, **4-3p** ($CDCl_3$, 126 MHz).

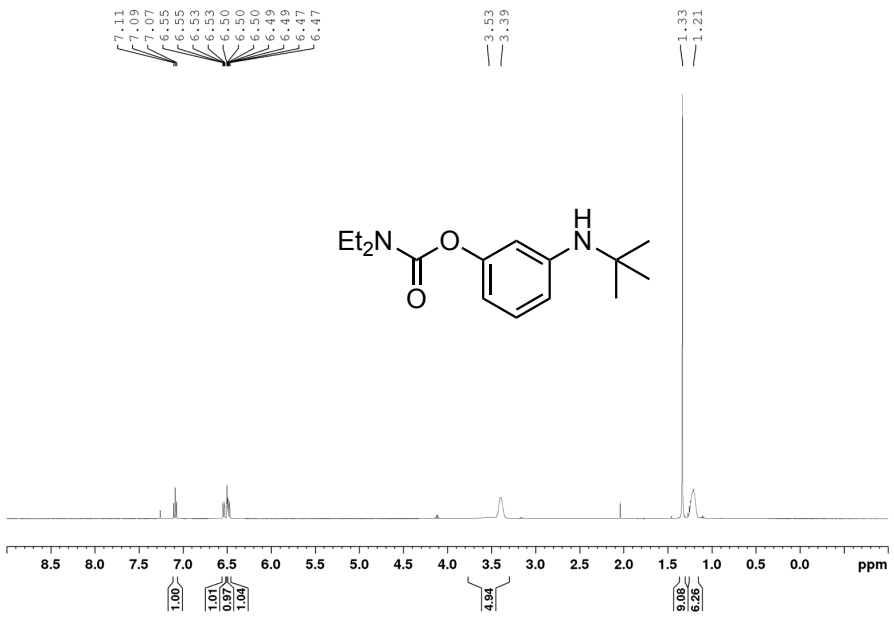

Figure A171. ^{1}H NMR spectrum 3-(*tert*-butylamino)phenyl diethylcarbamate, **4-3q** ($CDCl_3$, 500 MHz).

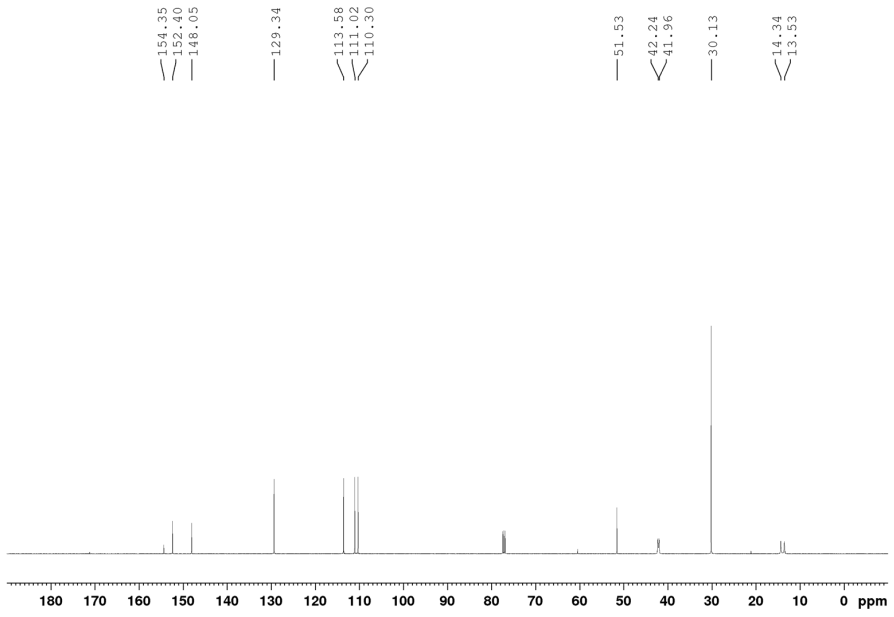

Figure A172. $^{13}C\{^{1}H\}$ NMR spectrum 3-(*tert*-butylamino)phenyl diethylcarbamate, **4-3q** ($CDCl_3$, 126 MHz).

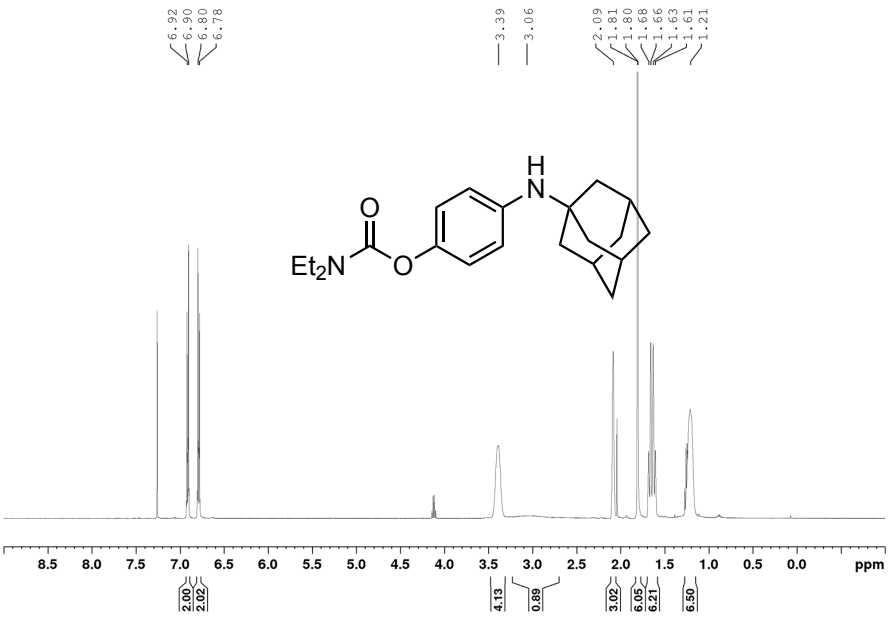

Figure A173. ^{1}H NMR spectrum 4-((adamantan-1-yl)amino)phenyl diethylcarbamate, **4-3r** ($CDCl_3$, 500 MHz).

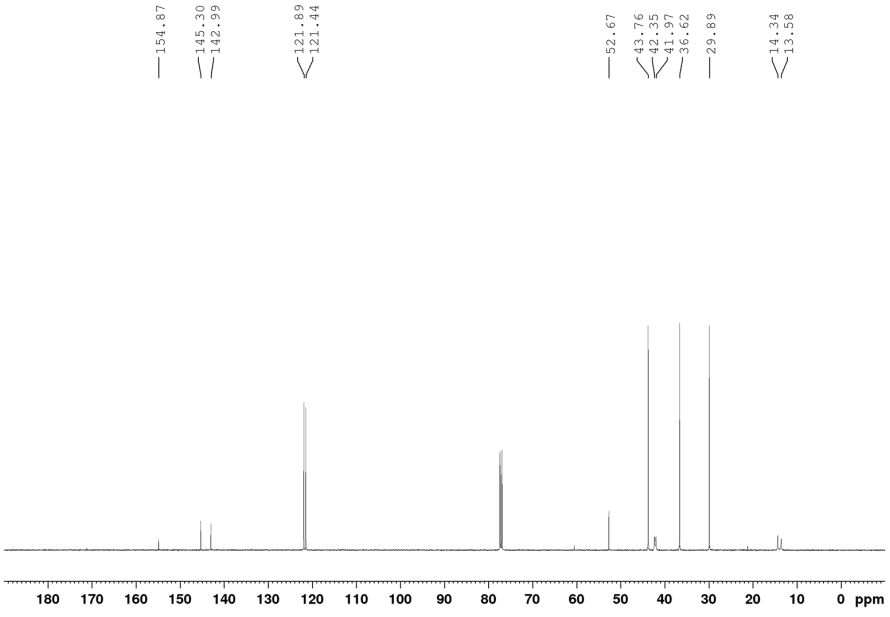

Figure A174. $^{13}C\{^{1}H\}$ NMR spectrum 4-((adamantan-1-yl)amino)phenyl diethylcarbamate, **4-3r** ($CDCl_3$, 126 MHz).

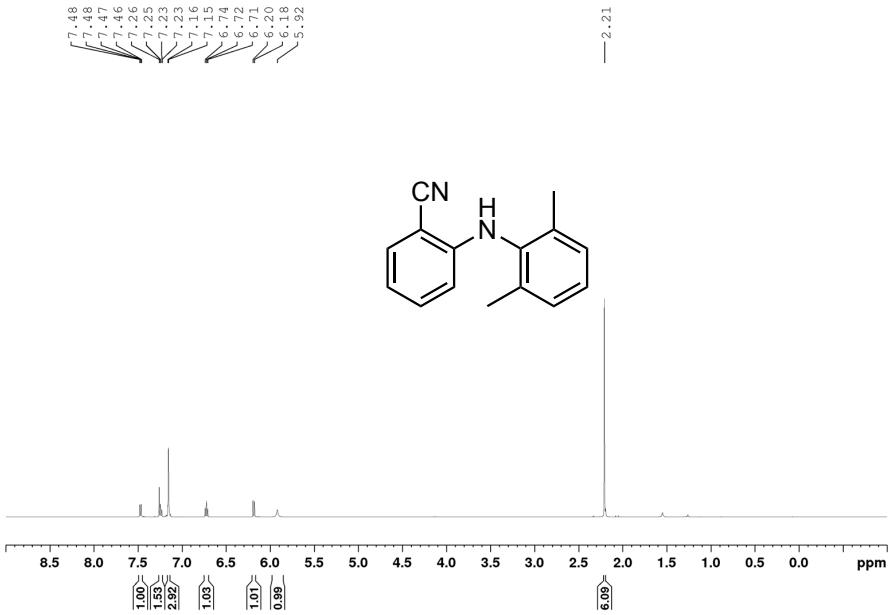

Figure A175. ^{1}H NMR spectrum 2-((2,6-dimethylphenyl)amino)benzonitrile, **4-6a** ($CDCl_3$, 500 MHz).

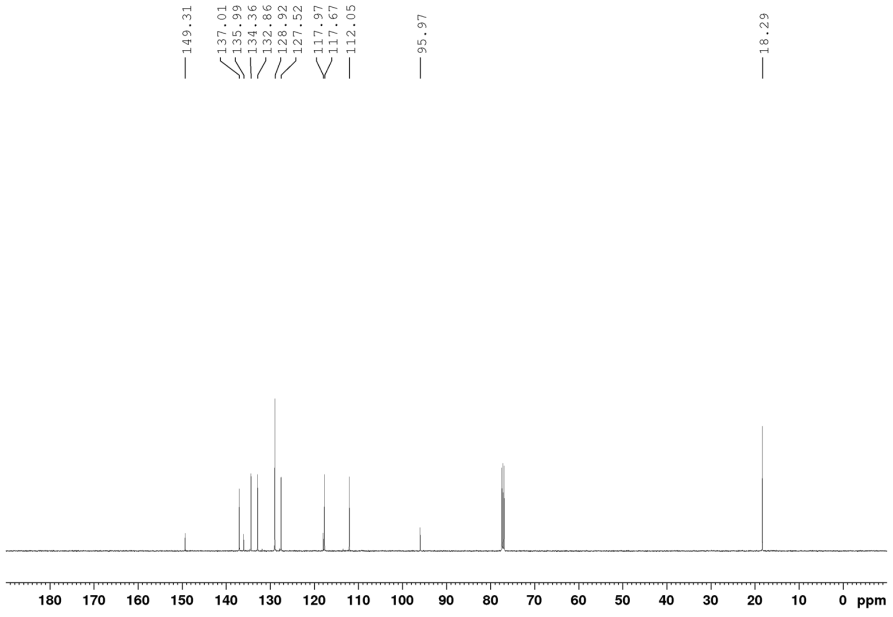

Figure A176. $^{13}C\{^{1}H\}$ NMR spectrum 2-((2,6-dimethylphenyl)amino)benzonitrile, **4-6a** ($CDCl_3$, 126 MHz).

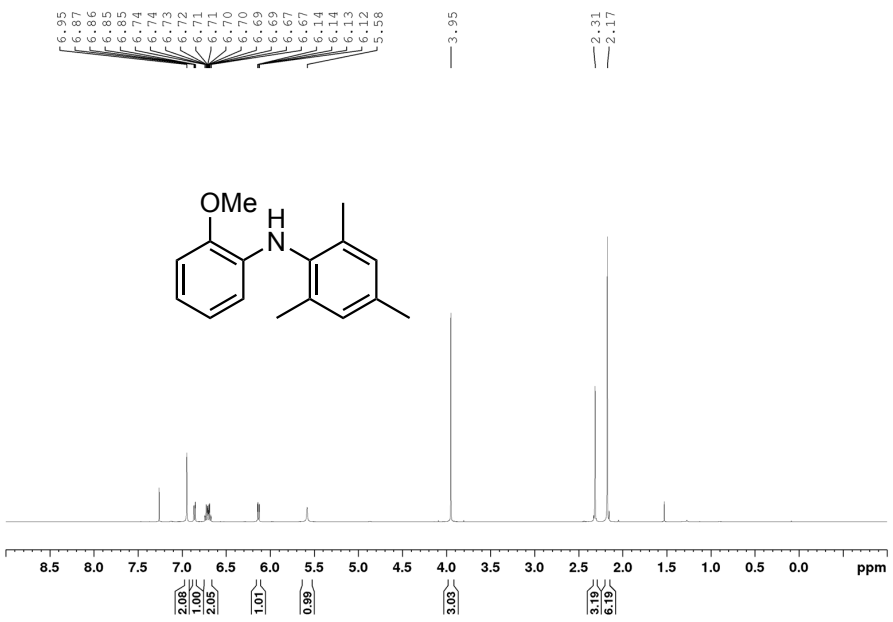

Figure A177. ^{1}H NMR spectrum *N*-(2-methoxyphenyl)-2,4,6-trimethylaniline, **4-6b** ($CDCl_3$, 500 MHz).

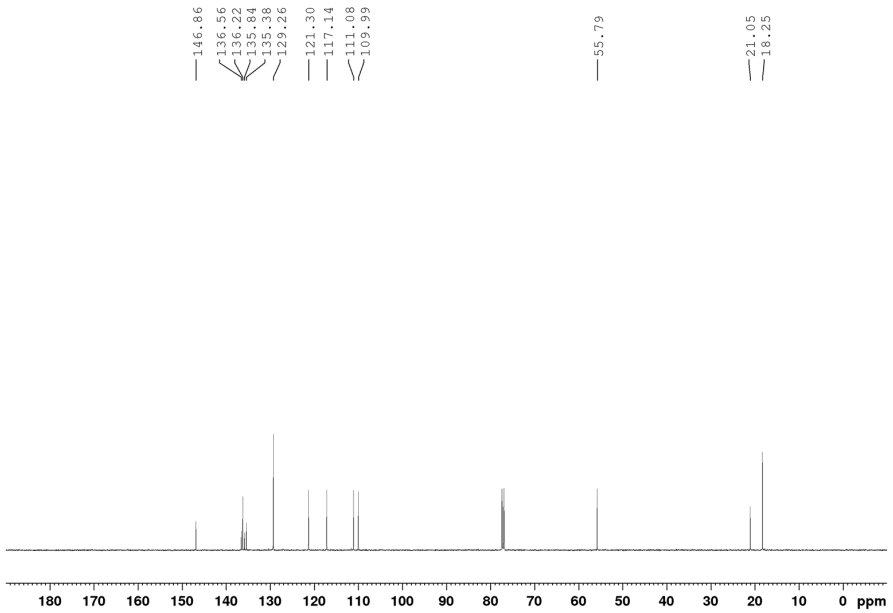

Figure A178. ^{1}H NMR spectrum *N*-(2-methoxyphenyl)-2,4,6-trimethylaniline, **4-6b** ($CDCl_3$, 126 MHz).

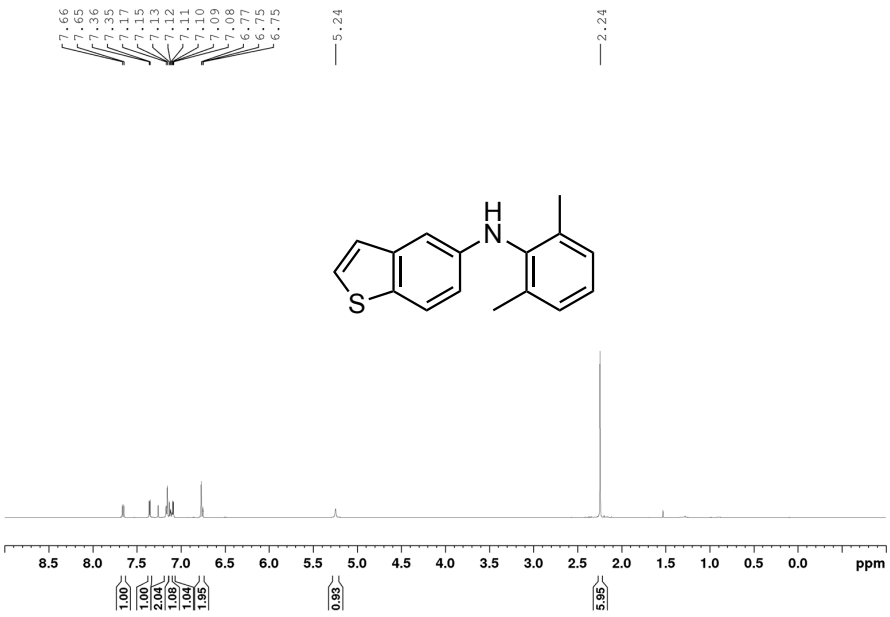

Figure A179. ^{1}H NMR spectrum *N*-(2,6-dimethylphenyl)benzo[*b*]thiophen-5-amine, **4-6c** ($CDCl_3$, 500 MHz).

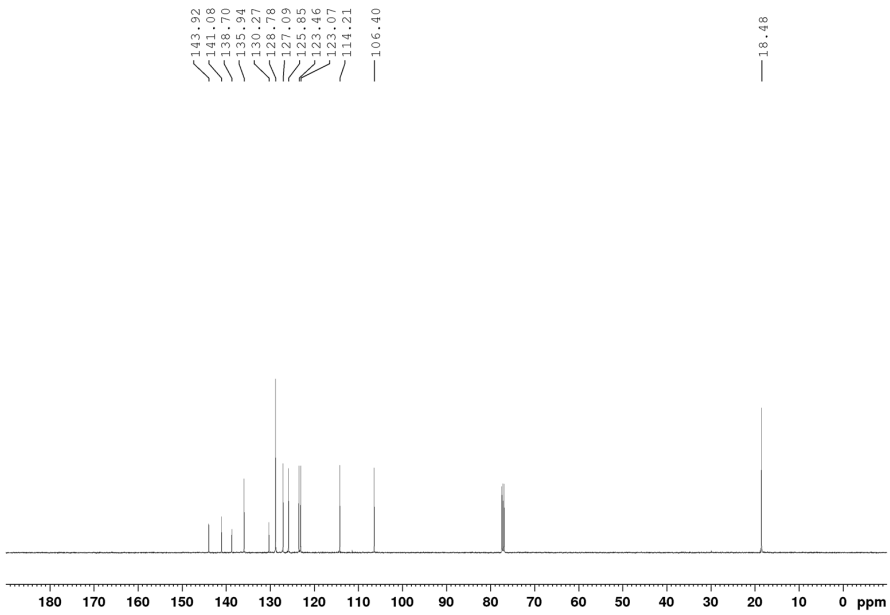

Figure A180. $^{13}C\{^{1}H\}$ NMR spectrum *N*-(2,6-dimethylphenyl)benzo[*b*]thiophen-5-amine, **4-6c** ($CDCl_3$, 126 MHz).

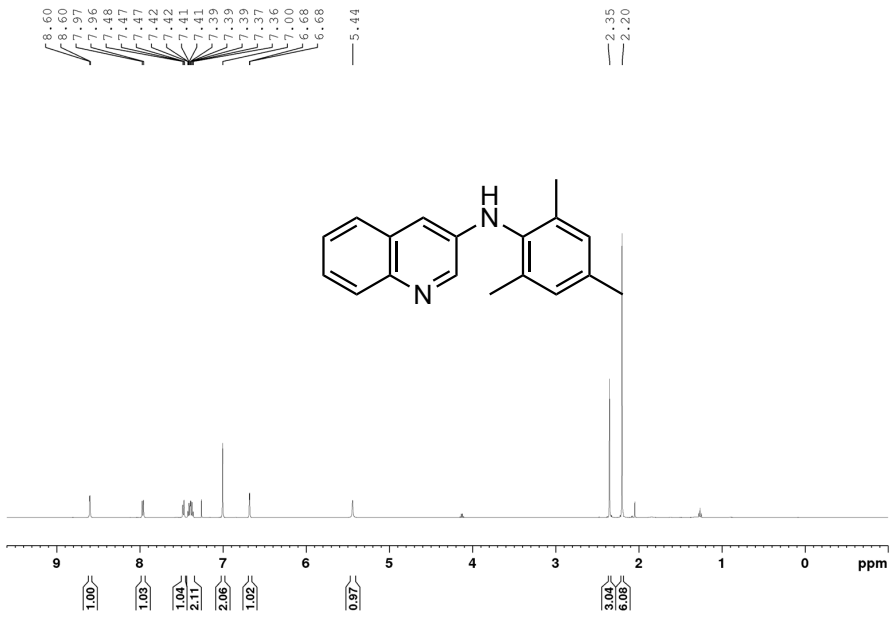

Figure A181. ^{1}H NMR spectrum *N*-mesitylquinolin-3-amine, **4-6d** ($CDCl_3$, 500 MHz).

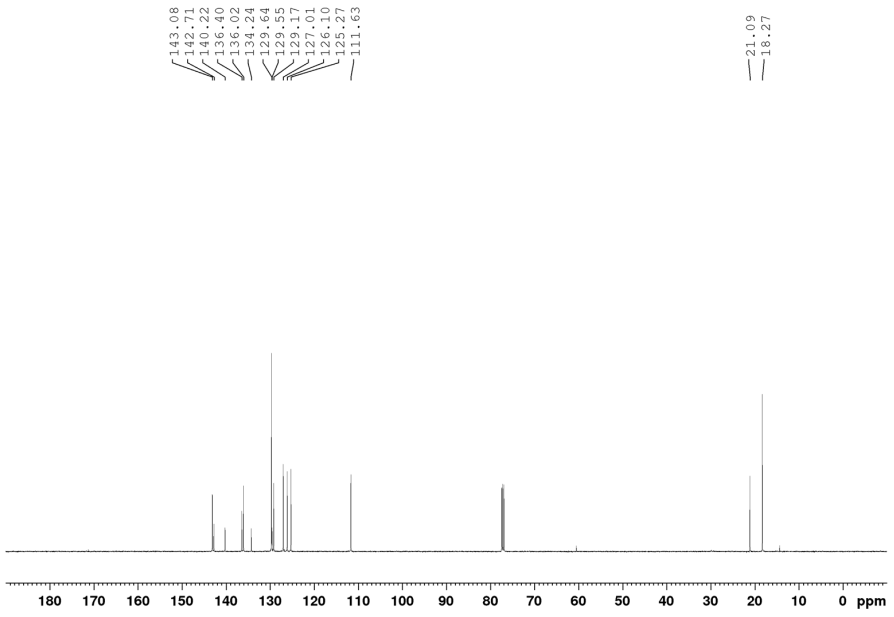

Figure A182. $^{13}C\{^{1}H\}$ NMR spectrum *N*-mesitylquinolin-3-amine, **4-6d** ($CDCl_3$, 126 MHz).

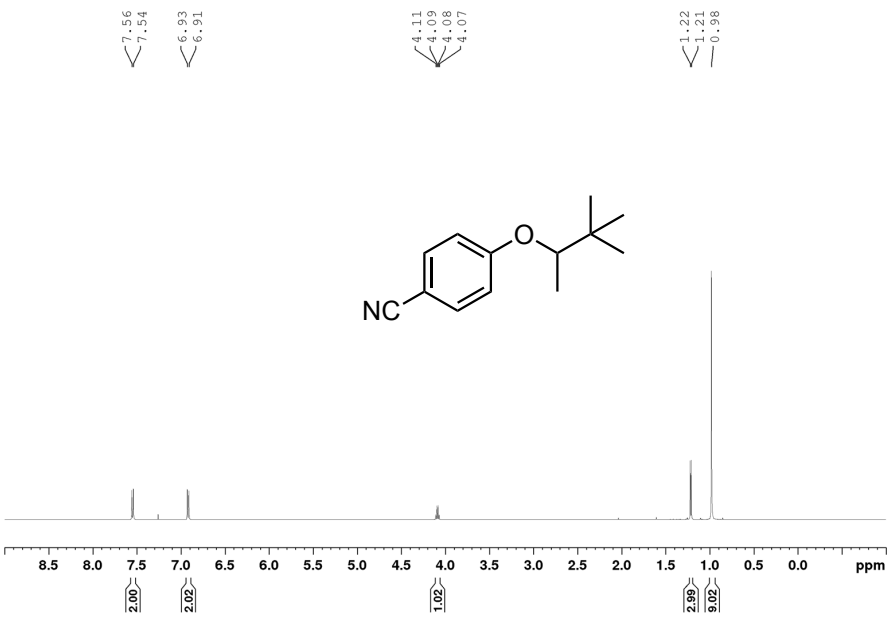

Figure A183. ^{1}H NMR spectrum 4-((3,3-dimethylbutan-2-yl)oxy)benzonitrile, **4-8a** ($CDCl_3$, 500 MHz).

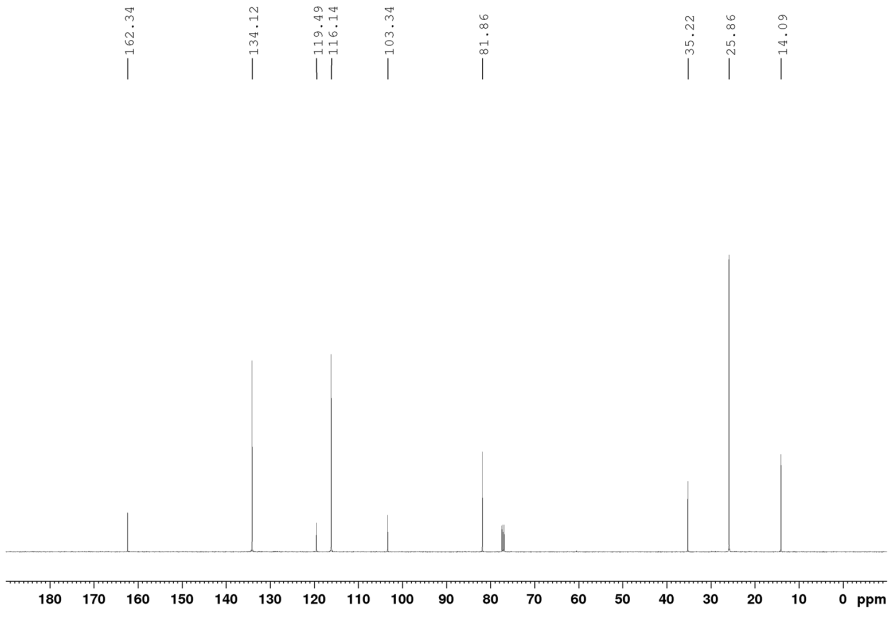

Figure A184. $^{13}C\{^{1}H\}$ NMR spectrum 4-((3,3-dimethylbutan-2-yl)oxy)benzonitrile, **4-8a** ($CDCl_3$, 126 MHz).

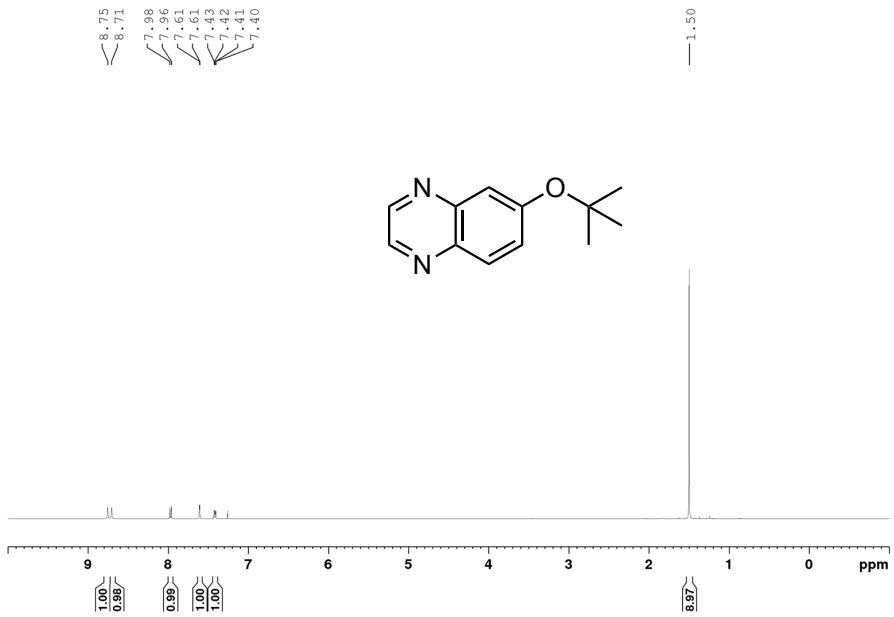

Figure A185. ^{1}H NMR spectrum 6-(*tert*-butoxy)quinoxaline, **3-3m** ($CDCl_3$, 500 MHz).

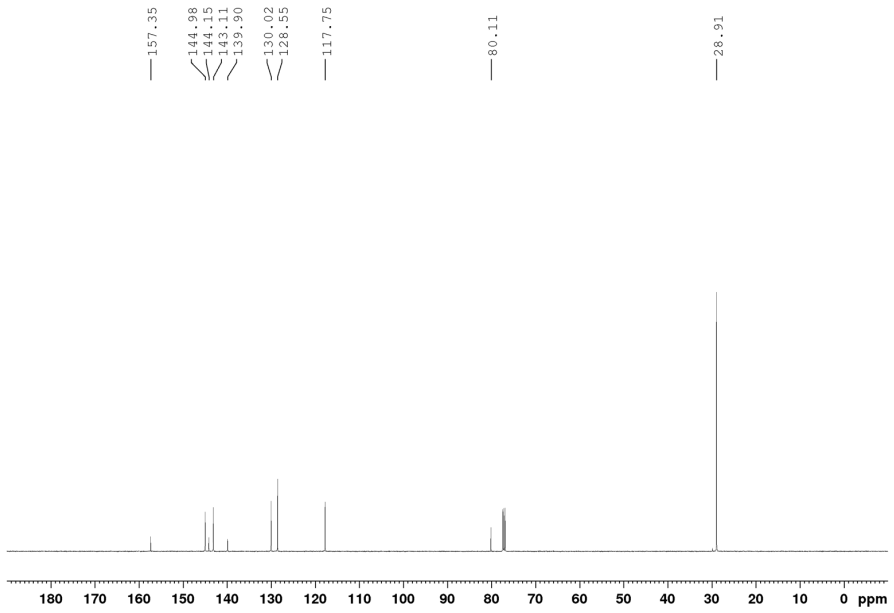

Figure A186. $^{13}C\{^{1}H\}$ NMR spectrum 6-(*tert*-butoxy)quinoxaline, **3-3m** ($CDCl_3$, 126 MHz).

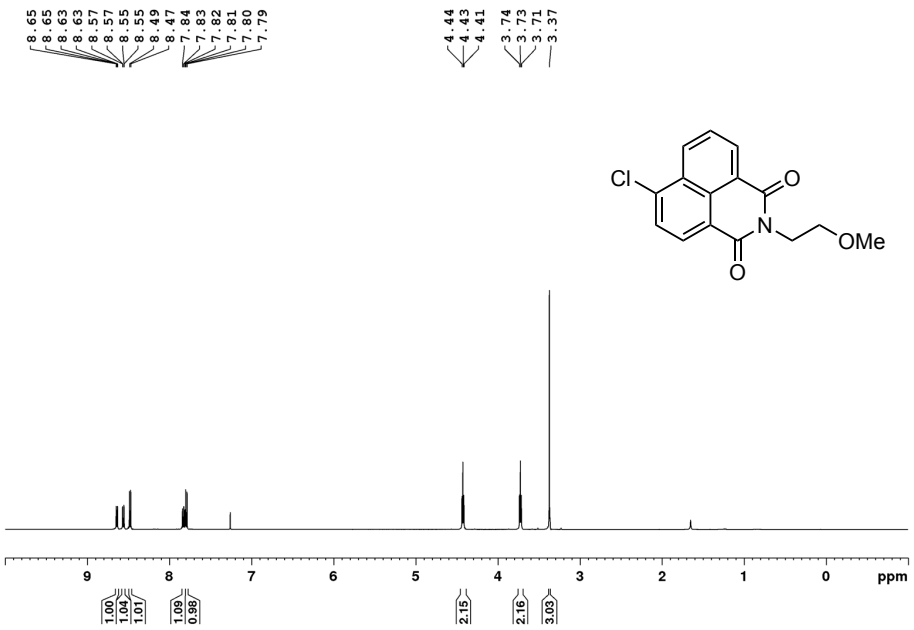

Figure A187. ^{1}H NMR spectrum of 6-chloro-2-(2-methoxyethyl)-1*H*-benzo[*de*]isoquinoline-1,3(2*H*)-dione, **4-9** ($CDCl_3$, 500 MHz).

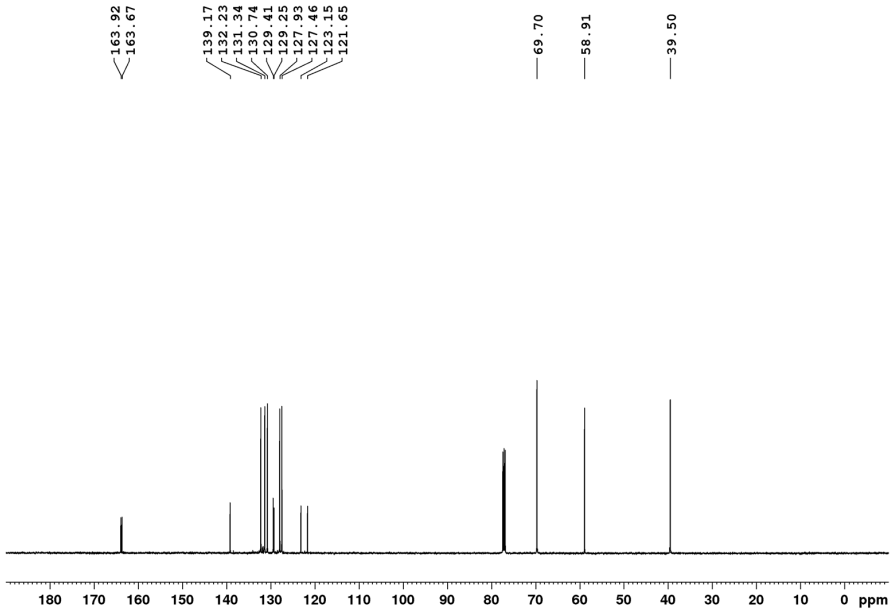

Figure A188. $^{13}C\{^{1}H\}$ NMR spectrum of 6-chloro-2-(2-methoxyethyl)-1*H*-benzo[*de*]isoquinoline-1,3(2*H*)-dione, **4-9** ($CDCl_3$, 126 MHz).

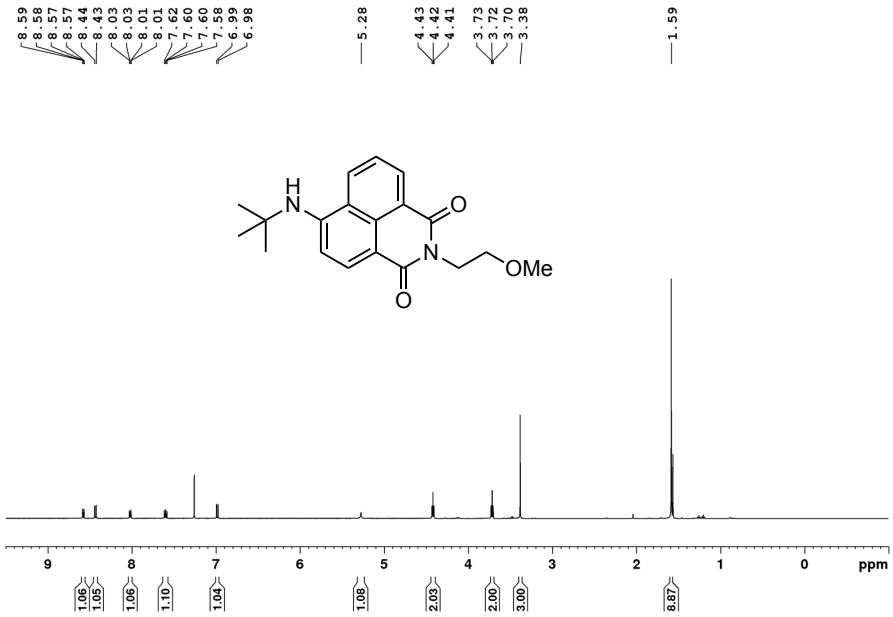

Figure A189. ^{1}H NMR spectrum of 6-(*tert*-butylamino)-2-(2-methoxyethyl)-1*H*-benzo[*de*]isoquinoline-1,3(2*H*)-dione, **4-10a** ($CDCl_3$, 500 MHz).

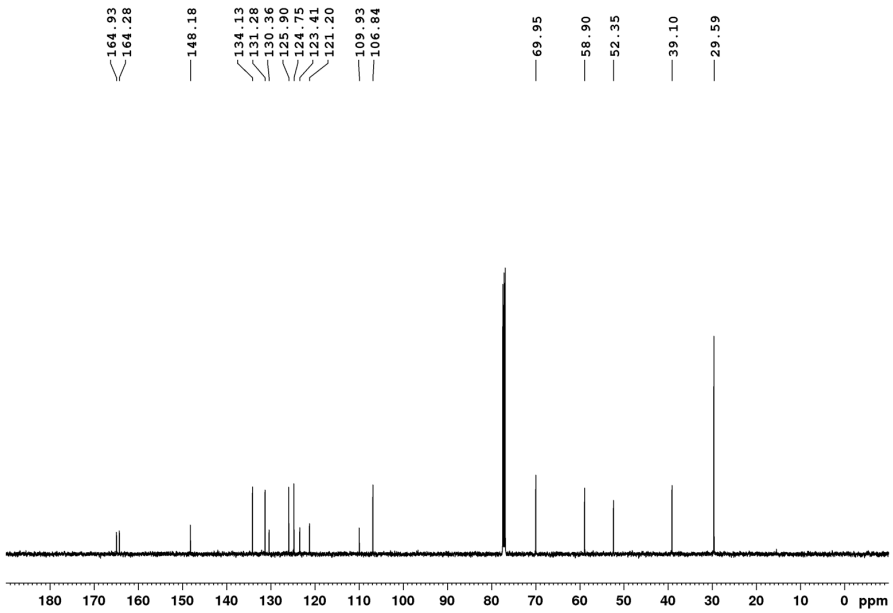

Figure A190. ^{13}C{^{1}H} NMR spectrum of 6-(*tert*-butylamino)-2-(2-methoxyethyl)-1*H*-benzo[*de*]isoquinoline-1,3(2*H*)-dione, **4-10a** ($CDCl_3$, 126 MHz).

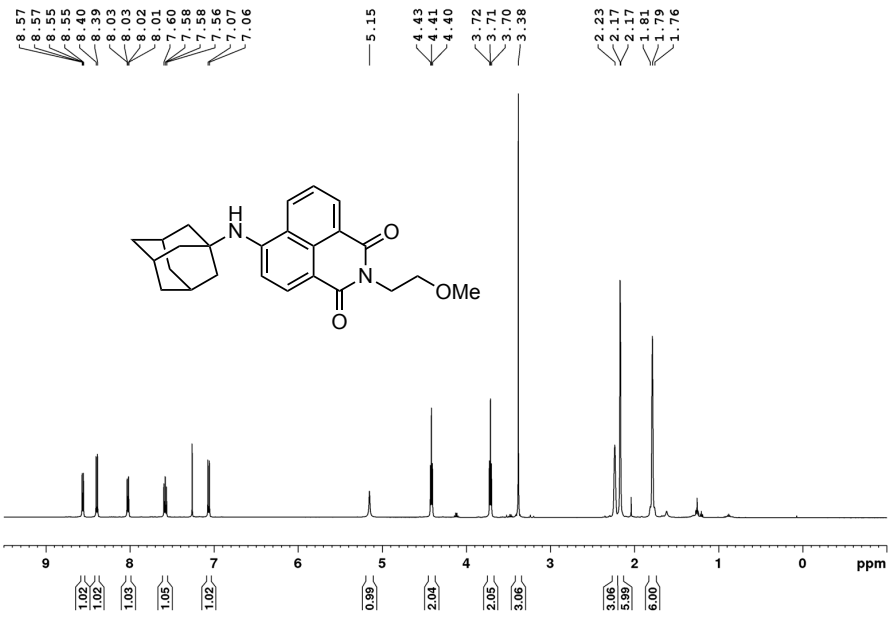

Figure A191. ^{1}H NMR spectrum of 6-(adamantan-1-ylamino)-2-(2-methoxyethyl)-1*H*-benzo[*de*]isoquinoline-1,3(2*H*)-dione, **4-10b** ($CDCl_3$, 500 MHz).

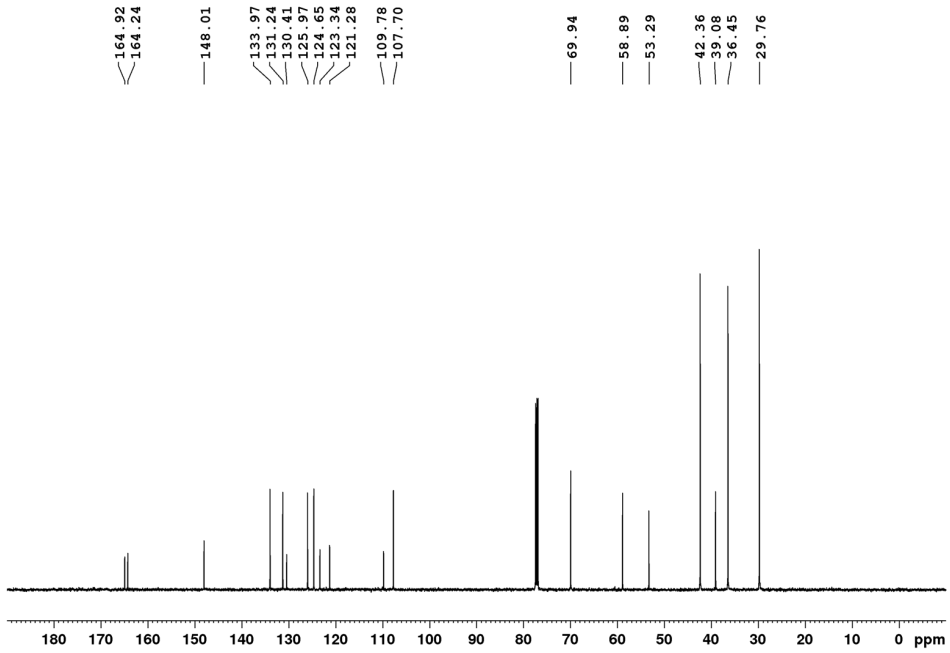

Figure A192. $^{13}C\{^{1}H\}$ NMR spectrum of 6-(adamantan-1-ylamino)-2-(2-methoxyethyl)-1*H*-benzo[*de*]isoquinoline-1,3(2*H*)-dione, **4-10b** ($CDCl_3$, 126 MHz).

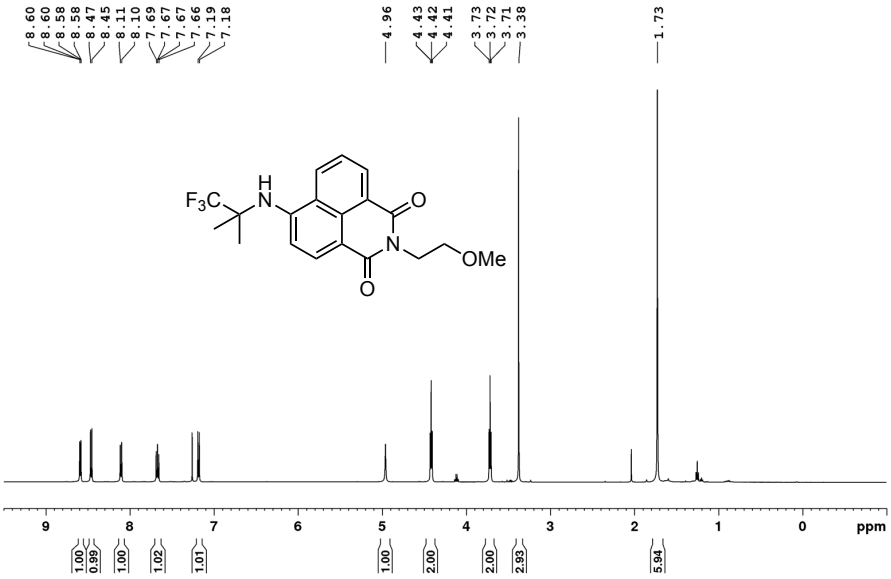

Figure A193. ^{1}H NMR spectrum of 2-(2-methoxyethyl)-6-[(1,1,1-trifluoro-2-methylpropan-2-yl)amino]-1H-benzo[*de*]isoquinoline-1,3(2*H*)-dione, **4-10c** ($CDCl_3$, 500 MHz).

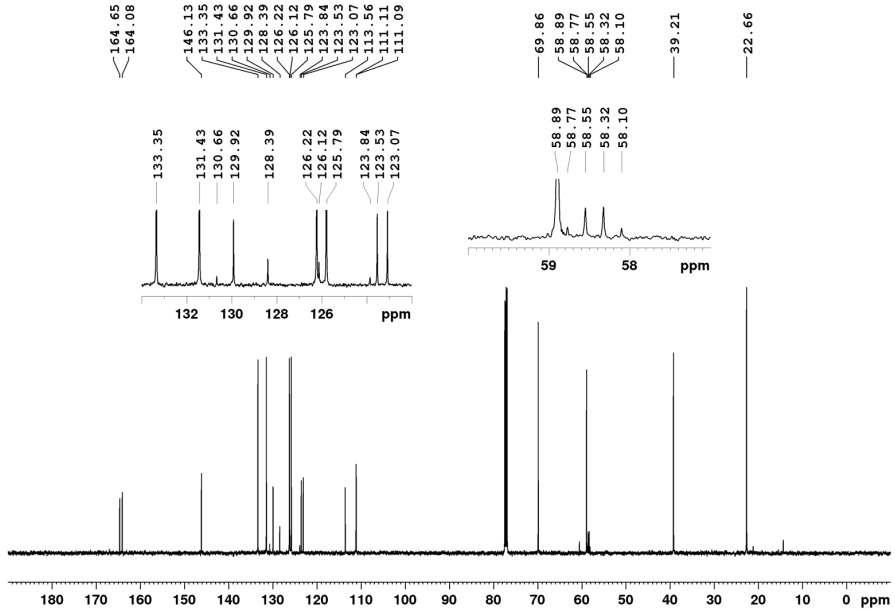

Figure A194. $^{13}C\{^{1}H\}$ NMR spectrum of 2-(2-methoxyethyl)-6-[(1,1,1-trifluoro-2-methylpropan-2-yl)amino]-1H-benzo[*de*]isoquinoline-1,3(2*H*)-dione, **4-10c** ($CDCl_3$, 126 MHz).

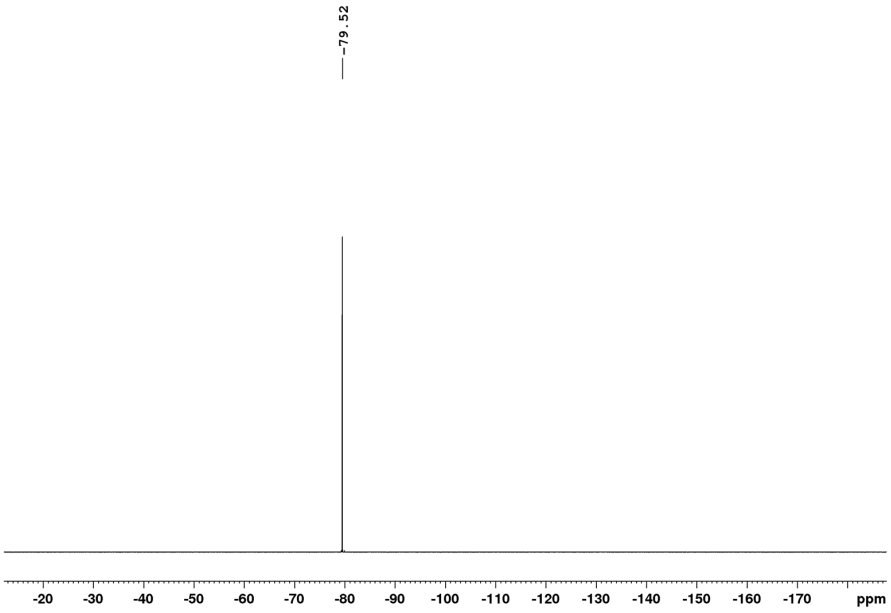

Figure A195. $^{19}F\{^{1}H\}$ NMR spectrum of 2-(2-methoxyethyl)-6-[(1,1,1-trifluoro-2-methylpropan-2-yl)amino]-1H-benzo[*de*]isoquinoline-1,3(2*H*)-dione, **4-10c** ($CDCl_3$, 470.4 MHz).

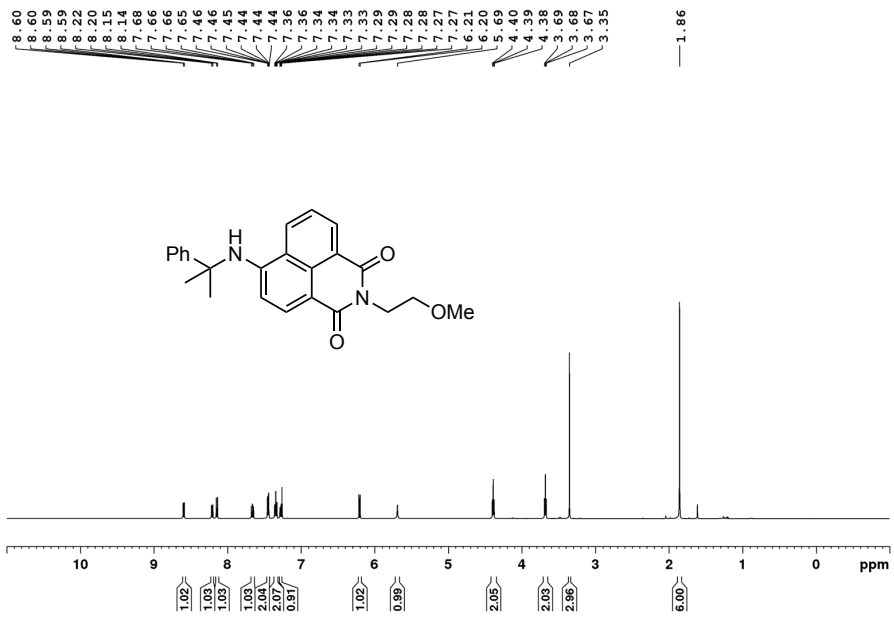

Figure A196. ^{1}H NMR spectrum of 2-(2-methoxyethyl)-6-((2-phenylpropan-2-yl)amino)-1*H*-benzo[*de*]isoquinoline-1,3(2*H*)-dione, **4-10d** ($CDCl_3$, 500 MHz).

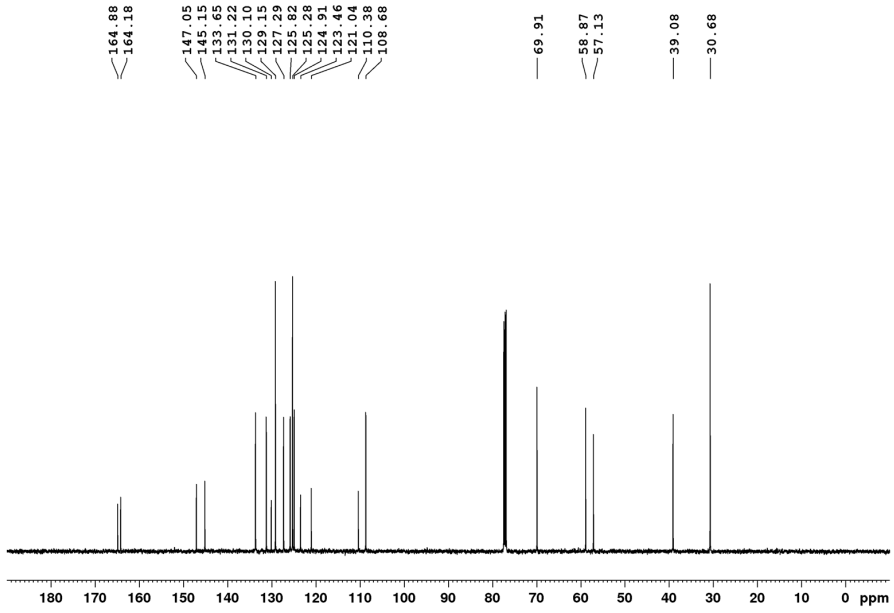

Figure A197. $^{13}C\{^{1}H\}$ NMR spectrum of 2-(2-methoxyethyl)-6-((2-phenylpropan-2-yl)amino)-1*H*-benzo[*de*]isoquinoline-1,3(2*H*)-dione, **4-10d** ($CDCl_3$, 126 MHz).

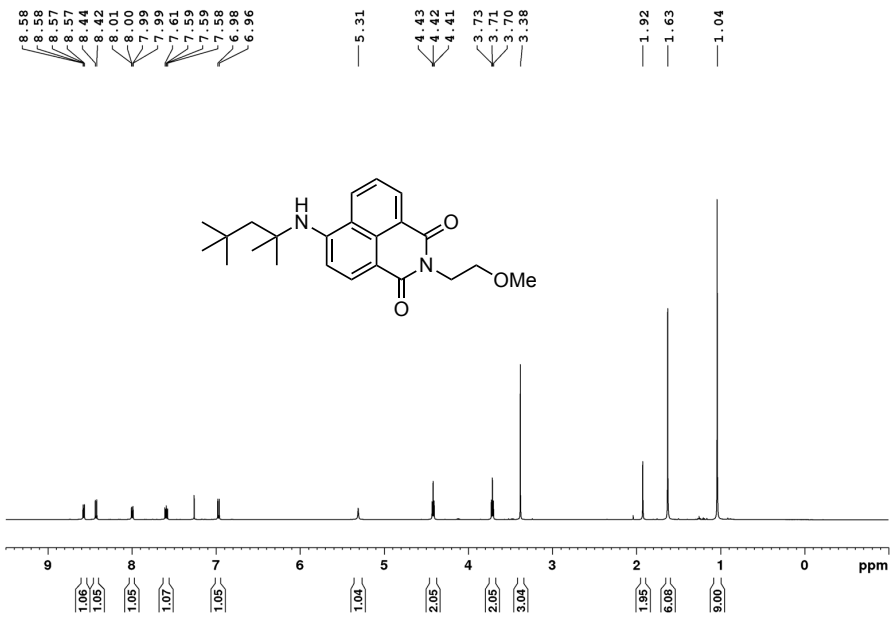

Figure A198. ^{1}H NMR spectrum of 2-(2-methoxyethyl)-6-((2,4,4-trimethylpentan-2-yl)amino)-1*H*-benzo[*de*]isoquinoline-1,3(2*H*)-dione, **4-10e** ($CDCl_3$, 500 MHz).

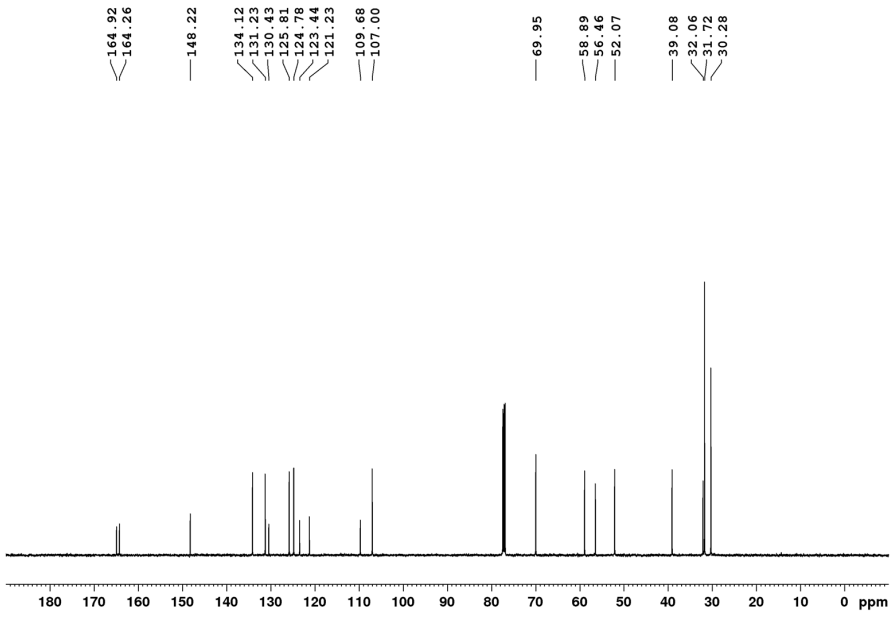

Figure A199. $^{13}C\{^{1}H\}$ NMR spectrum of 2-(2-methoxyethyl)-6-((2,4,4-trimethylpentan-2-yl)amino)-1*H*-benzo[*de*]isoquinoline-1,3(2*H*)-dione, **4-10e** ($CDCl_3$, 126 MHz).

Figure A200. ^{1}H NMR spectrum of 6-*tert*-butoxy-2-(2-methoxyethyl)-1H-benzo[*de*]isoquinoline-1,3(2*H*)-dione, **4-11** ($CDCl_3$, 500 MHz).

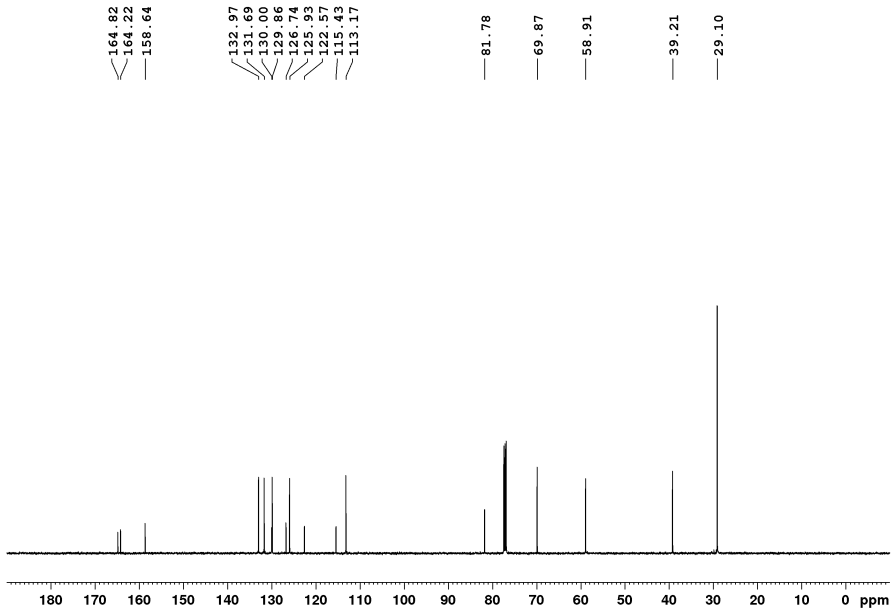

Figure A201. $^{13}C\{^{1}H\}$ NMR spectrum of 6-*tert*-butoxy-2-(2-methoxyethyl)-1H-benzo[*de*]isoquinoline-1,3(2*H*)-dione, **4-11** ($CDCl_3$, 126 MHz).

Appendix 9: Copyright Permission Letters

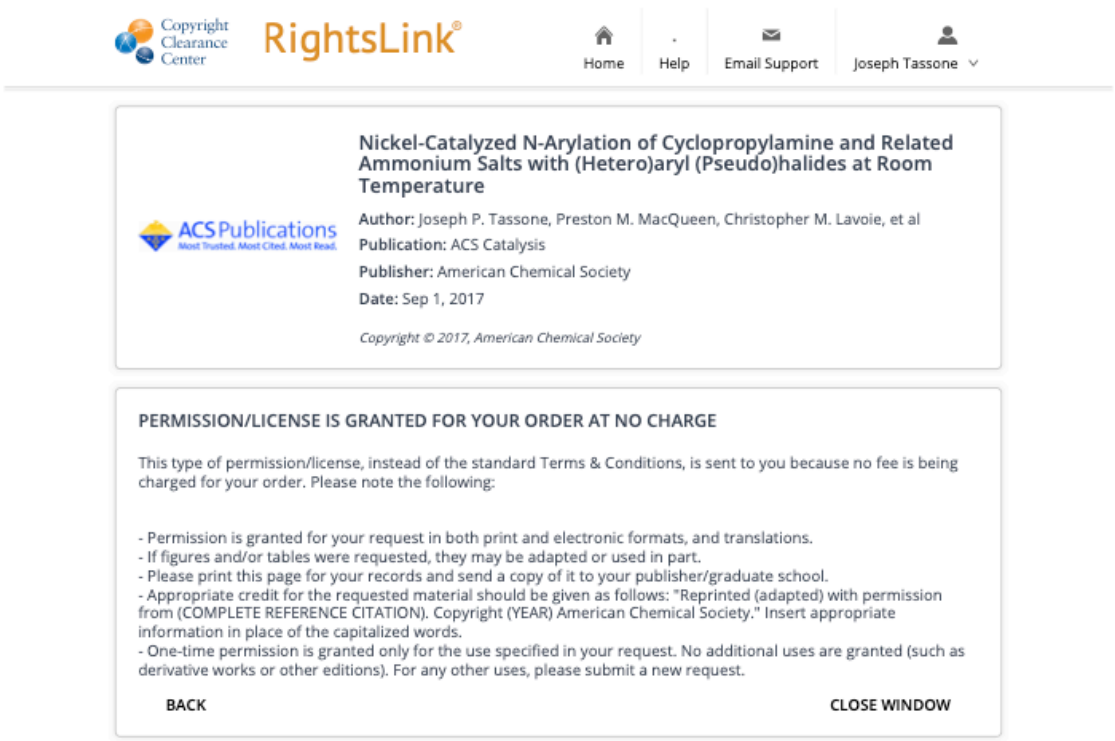

Copyright Clearance Center RightsLink®

Home Help Email Support Joseph Tassone

ACS Publications
Most Trusted. Most Cited. Most Read.

Nickel-Catalyzed N-Arylation of Cyclopropylamine and Related Ammonium Salts with (Hetero)aryl (Pseudo)halides at Room Temperature

Author: Joseph P. Tassone, Preston M. MacQueen, Christopher M. Lavoie, et al
Publication: ACS Catalysis
Publisher: American Chemical Society
Date: Sep 1, 2017

Copyright © 2017, American Chemical Society

PERMISSION/LICENSE IS GRANTED FOR YOUR ORDER AT NO CHARGE

This type of permission/license, instead of the standard Terms & Conditions, is sent to you because no fee is being charged for your order. Please note the following:

- Permission is granted for your request in both print and electronic formats, and translations.
- If figures and/or tables were requested, they may be adapted or used in part.
- Please print this page for your records and send a copy of it to your publisher/graduate school.
- Appropriate credit for the requested material should be given as follows: "Reprinted (adapted) with permission from (COMPLETE REFERENCE CITATION). Copyright (YEAR) American Chemical Society." Insert appropriate information in place of the capitalized words.
- One-time permission is granted only for the use specified in your request. No additional uses are granted (such as derivative works or other editions). For any other uses, please submit a new request.

BACK CLOSE WINDOW

JOHN WILEY AND SONS LICENSE
TERMS AND CONDITIONS

Jan 27, 2020

This Agreement between Dalhousie University -- Joseph Tassone ("You") and John Wiley and Sons ("John Wiley and Sons") consists of your license details and the terms and conditions provided by John Wiley and Sons and Copyright Clearance Center.

License Number	4757071070410
License date	Jan 27, 2020
Licensed Content Publisher	John Wiley and Sons
Licensed Content Publication	Angewandte Chemie International Edition
Licensed Content Title	PhPAd−DalPhos: Ligand−Enabled, Nickel−Catalyzed Cross−Coupling of (Hetero)aryl Electrophiles with Bulky Primary Alkylamines
Licensed Content Author	Joseph P. Tassone, Emma V. England, Preston M. MacQueen, et al
Licensed Content Date	Jan 24, 2019
Licensed Content Volume	58
Licensed Content Issue	8

Licensed Content Pages	5
Type of use	Dissertation/Thesis
Requestor type	Author of this Wiley article
Format	Print and electronic
Portion	Full article
Will you be translating?	No
Title of your thesis / dissertation	Expanding the Scope of Nickel-Catalyzed C(sp2)-N/O Cross-Coupling Reactions Using Tailored Ancillary Ligands
Expected completion date	Mar 2020
Expected size (number of pages)	300
Requestor Location	Dalhousie University 1239 Barrington Street Apartment 613 Halifax, NS B3J 1Y3 Canada Attn: Dalhousie University
Publisher Tax ID	EU826007151
Total	0.00 CAD
Terms and Conditions	